

University of Nebraska - Lincoln

DigitalCommons@University of Nebraska - Lincoln

---

Civil and Environmental Engineering Theses,  
Dissertations, and Student Research

Civil and Environmental Engineering

---

Winter 12-2021

## Modeling Watershed Sensitivity to Climate Change in Systems Affected by Discharge of Mine Tailings

Johnette C. Shockley

University of Nebraska - Lincoln, [johnette.shockley@huskers.unl.edu](mailto:johnette.shockley@huskers.unl.edu)

Follow this and additional works at: <https://digitalcommons.unl.edu/civilengdiss>



Part of the [Civil Engineering Commons](#), and the [Other Civil and Environmental Engineering Commons](#)

---

Shockley, Johnette C., "Modeling Watershed Sensitivity to Climate Change in Systems Affected by Discharge of Mine Tailings" (2021). *Civil and Environmental Engineering Theses, Dissertations, and Student Research*. 174.

<https://digitalcommons.unl.edu/civilengdiss/174>

This Article is brought to you for free and open access by the Civil and Environmental Engineering at DigitalCommons@University of Nebraska - Lincoln. It has been accepted for inclusion in Civil and Environmental Engineering Theses, Dissertations, and Student Research by an authorized administrator of DigitalCommons@University of Nebraska - Lincoln.

MODELING WATERSHED SENSITIVITY TO CLIMATE CHANGE IN SYSTEMS  
AFFECTED BY DISCHARGE OF MINE TAILINGS

by

Johnette C. Shockley

A DISSERTATION

Presented to the Faculty of

The Graduate College at the University of Nebraska

In Partial Fulfillment of Requirements

For the Degree of Doctor of Philosophy

Major: Civil Engineering

(Environmental Engineering)

Under the Supervision of Professor Shannon L. Bartelt-Hunt

Lincoln, Nebraska

December, 2021

# MODELING WATERSHED SENSITIVITY TO CLIMATE CHANGE IN SYSTEMS AFFECTED BY DISCHARGE OF MINE TAILINGS

Johnette Shockley, Ph.D.

University of Nebraska, 2021

Adviser: Dr. Shannon L. Bartelt-Hunt

For more than a century, a large volume of gold-mining tailings was deposited in Whitewood Creek and the Belle Fourche River, tributaries to the Cheyenne River in western South Dakota. Much of it still remains, and field and historical evidence indicates continued remobilization of tailings-containing alluvium in these bedrock-dominated channels. Both long-term, natural fluctuations in climate and anthropogenically driven changes can impact regional precipitation, temperature, hydrologic patterns, and ecosystem functions. Such changes have the potential to affect both the transport and distribution of arsenic-laden sediments and mechanical erosion that can undermine the stability of channel-bed and overbank material.

This study reevaluates published literature and simulates future climatic conditions with Global Change Models downscaled to hydrologic models to detect trends and determine if they differ from historical time series data or exhibit non-stationarity. Arsenic concentrations vary in solution with relatively small shifts in pH and Eh, allowing for the sorption/desorption on sediment and mobilization into the dissolved or aqueous phase. Published data suggest that the presence of competing anions are also important factors in controlling arsenic

release. Carbonates in the alluvium and locally occurring bedrock control the formation of acidic conditions.

This river system continually adjusts to historical and recent changes to achieve a “new equilibrium” from the cessation of mining discharge; geomorphic changes linked to regional continental glaciation; stream channel readjustment due to discharge velocity changes in the Oahe Reservoir; and channel instability. Knowing the relationship between streamflow and sediment transport and assessing a stream’s sediment transport capacity are important to planning and managing river corridor protection and restoration. These are also significant considerations in predicting potential exposure of contaminant sediments to human, ecological, and biological receptors.

It appears climate change may be exerting an influence on hydroclimatic variables in the Lower Cheyenne River Basin, difficult to pinpoint in a qualitative assessment. In general, water resource managers should build resiliency into their designs to adaptably account for potential future impact of climate variability.



## ACKNOWLEDGMENTS

I'd like to acknowledge my adviser, Dr. Shannon L. Bartelt-Hunt, members of my committee, and Dr. Daniel Snow for their suggestions, guidance, support, and mentoring throughout my study. Thanks to the scientists, engineers, and researchers who collected the enormous amount of data over the past 30 years in the Lower Cheyenne River Basin; I was fortunate to have their data and publications for use during my studies. Thanks to Dr. John Stamm for providing me with key information from their important research, and special thanks to him for guiding me along the plains of the Belle Fourche River, sparking my inquiry into an area where very interesting things are happening. A significant thanks to Dr. George Hunt for his insight into hydrology and sediment modeling. I'd also like to thank the members of Dr. Bartelt-Hunt's Trace Contaminants Research group, who made my time at UNL much more enjoyable. I'll always appreciate their support and friendship.

## Table of Contents

Chapter 1: Introduction	1
1.1 Overview	1
1.2 Hypothesis and Objectives	6
1.3 Physical Setting	12
1.4 Study Area General Description	15
1.4.1 Belle Fourche River	20
1.4.1.1 Geology	22
1.4.1.2 Slope Distribution	26
1.4.1.3 Land Use and Cover	28
1.4.1.4 Livestock Distribution	30
1.4.1.5 Census and Social Data	30
1.4.2 Whitewood Creek	31
1.4.3 Water Control and Diversions	34
Chapter 2: Climate Literature Review and Study Tools Used	39
2.1 Overview	39
2.2 Background	40
2.3 Summary Description of Methods	52
Chapter 3: Study Area Impacts	60
Chapter 4: Chemistry	67
4.1 Significance of Arsenic in the Study Area	67
4.2 Occurrence of Sediment and Impacts	70
Chapter 5: Sediment Mineralogy and Chemistry	84
Chapter 6: Climate Change Assessment on Hydrologic Systems	110
6.1 Methods	110
6.2 Purpose	117
6.3 Literature Review Summary	118
6.4 Current Climate and Climate Change	127
6.5 Detecting Non-stationarities	134
6.6 Historical Climatological and Geomorphic Changes	157
6.7 Temperature: Observations and Projected Trends	170
6.8 Precipitation: Observations and Projected Trends	178
6.9 Hydrologic Conditions	185
6.9.1 Observed Hydrologic Conditions	185
6.9.2 Projected Hydrologic Trends	195
6.10 Biological Impact	196
Chapter 7: Results and Discussion for Climate Change Assessment for HUC 201 10120112 – Belle Fourche River – Cheyenne River	201

Chapter 8: Summary and Recommendations

334

Appendix A

A1

## List of Figures

Figure 1.1	Locations of the watersheds within the study area	1
Figure 1.2	Initial conceptual site model for the study	10
Figure 1.3	Revised and updated conceptual site model	11
Figure 1.4	Physiographic divisions of South Dakota	12
Figure 1.5	Water resource regions in HUC-10, Missouri River Basin	14
Figure 1.6	General extent of the study area	15
Figure 1.7	Distribution of USGS stream gages in South Dakota	19
Figure 1.8	The Belle Fourche River basin in MT, WY, and SD	20
Figure 1.9	Geologic Units in HUC 10120202	23
Figure 1.10	Slope distribution percentages	27
Figure 1.11	Predominant land cover and use	29
Figure 1.12	Population distribution by Census Block FIPS Code	30
Figure 1.13	Whitewood Creek Basin with USGS gage stations	32
Figure 1.14	Confluence of Whitewood Creek and Belle Fourche River	33
Figure 1.15	Idealized schematic of study area reservoirs	36
Figure 1.16	Diagram of Belle Fourche River diversions and storage	37
Figure 2.1	History of the Keeling curve as of Sep.27, 2021	41
Figure 2.2	Graphs showing a lognormal distribution	48
Figure 2.3	Holdren illustration of shift in extremes in a warmer climate	49
Figure 3.1	Whitewood Creek effluent pre-tailings discharge cessation	60
Figure 3.2	Google Earth imagery of Homestake Mine, Aug. 20, 2013	61
Figure 3.3	Grizzly Gulch Tailings Containment Facility	62
Figure 3.4	Major mine sites in the upper reaches of Whitewood Creek	64
Figure 3.5	Total-recoverable arsenic concentrations in micrograms	66
Figure 4.1	Importance of determining fate and transport of arsenic	67
Figure 4.2	Conceptual model of metal cycling	68

Figure 4.3	Tailings-laden alluvium lining Whitewood Creek banks	72
Figure 4.4	Belle Fourche River transects and arsenic concentrations	77
Figure 4.5	Arsenic concentration decrease downstream	78
Figure 4.6	Sampling sites in Cheyenne River arm of Oahe Reservoir	82
Figure 4.7	ISS imagery showing sediment settling in study area	83
Figure 5.1	Arsenic concentrations in sediment samples	89
Figure 5.2	Belle Fourche River alluvium deposit leaching potential	90
Figure 5.3	Pierre Shale silt and clay fraction mineral composition	93
Figure 5.4	Chemical forms of metals in solid phases	97
Figure 5.5	Image of water-soluble efflorescent salts	107
Figure 6.1	Flow chart for performing climate change assessment	111
Figure 6.2	Data processing flow chart for climate model output	113
Figure 6.3	SSC hysteresis example in 1993 Mississippi River flood	124
Figure 6.4	U.S. regional boundaries and climate impacts	128
Figure 6.5	Observed precipitation trends: more rainfall, less snow	129
Figure 6.6	Decreasing snowpack in the western U.S.	130
Figure 6.7	Earlier lilac first-bloom dates indicate growing season shift	130
Figure 6.8	Earlier spring snowmelt runoff	131
Figure 6.9	Hydroclimatic trends evident in groundwater aquifers	131
Figure 6.10	Missouri River watershed streamflow trends	134
Figure 6.11	Western plains streamflow changes	140
Figure 6.12	Alterations to natural streamflow, 1980-2014	141
Figure 6.13	“Badlands” states seasonal catchments	144
Figure 6.14	Clusters of runoff regimes	145
Figure 6.15	MOPEX catchments	146
Figure 6.16	Day of peak precipitation spatial patterns	147
Figure 6.17	Day of maximum streamflow	147
Figure 6.18	Day of maximum streamflow seasonality index	148

Figure 6.19	Weather/streamflow gaging station map	152
Figure 6.20	SD annual streamflow/precipitation trends	153
Figure 6.21	Streamflow gaging station spatial distribution	156
Figure 6.22	Spatial and temporal scales	158
Figure 6.23	Stream boundaries imagery overlay	162
Figure 6.24	Estimate of glaciation extent	163
Figure 6.25	Missouri River trench anomalous upland slopes	164
Figure 6.26	Missouri River Basin after continental glaciation	166
Figure 6.27A	Belle Fourche River tributary stream bank failure	168
Figure 6.27B	Belle Fourche River tributary stream bank failure	168
Figure 6.28	Bridge project hearing notification	169
Figure 6.29	SD temperature/precipitation daily means	171
Figure 6.30	Observed and projected temperature change	173
Figure 6.31A	Cheyenne River in October	174
Figure 6.31B	Cheyenne River in January	174
Figure 6.32	Ice on the Belle Fourche River	176
Figure 6.33	Linear trends in annual precipitation, 1895-2009	179
Figure 6.34	Projected change in winter precipitation	180
Figure 6.35	Observed number of extreme precipitation events	182
Figure 6.36	Linear trends: soil moisture/annual precipitation	184
Figure 6.37	Five hydraulic subregions in South Dakota	186
Figure 6.38	Generalized surficial geology of South Dakota	187
Figure 6.39	Hydrogeologic settings for the Black Hills region	190
Figure 6.40	Schematic of hydrologic budget cycle components	191
Figure 6.41A	Basin annual runoff and precipitation relationship	192
Figure 6.41B	Basin annual runoff and precipitation relationship	192
Figure 6.42	HUC 10 observed/projected climate trends summary	195
Figure 6.43	Hydrologic-related business lines impact	196

Figure 7.1	Average monthly streamflow range and mean	210
Figure 7.2A	Mean annual max streamflow trends from 64 GCM models	211
Figure 7.2B	Statistical significance test of trend lines	212
Figure 7.3	Standard settings used in nonstationarity detection	214
Figure 7.4 to Figure 7.15	HUC 4 CHAT and NSD assessment by stream gage	216
Figure 7.16	Downscaled GCM examples for the VIC hydrologic model	324
Figure 7.17	Downscaled GCM examples for the PRMS hydrologic model	325
Figure 7.18	Hindcast and scenario for future annual VIC maxima plots	326
Figure 7.19	Hindcast and scenario for future annual PRMS maxima plots	327
Figure 7.20	Pilot analysis of 17B curves for all GCMs	328
Figure 7.21	Pilot analysis of 17B curves with daily statistic adjustments	329
Figure 7.22	Pilot GCM assessments for unadjusted runs/annual maxima	330

## List of Tables

Table 1.1	HUCs used in this study	13
Table 1.2	Cheyenne River Basin streams listed as impaired waters	17
Table 1.3	USGS gages used to perform the assessments	18
Table 2.1	GCMs and RCPs used in the USACE CHAT	54
Table 5.1	Relative mobility and availability of trace metals	96
Table 5.2	X-RD-determined mineral characteristics	101
Table 5.3	Weight percent of major oxides for samples per X-RD	102
Table 5.4	Major mineral sample characteristics per X-RD	103
Table 6.1	Non-stationarity Detection Tool methods	115
Table 6.2	MOPEX hydroclimatic indicators	143
Table 6.3	South Dakota annual streamflow trends	154
Table 6.4	South Dakota seasonal streamflow trends	155
Table 7.1	Summary of findings for gages outside study area	213
Table 7.2	Summary of findings by stream gage location	313



## Chapter 1: Introduction

### 1.1 Overview

For over a century, the Black Hills of South Dakota was the location of one of the largest gold-producing mines in the Western Hemisphere. As a result, highly contaminated sediments are deposited in and line the streams in the region today. Mining in the northern Black Hills area has impacted the Cheyenne River Basin, which contains Whitewood Creek and the Belle Fourche and Cheyenne Rivers (Figure 1.1).

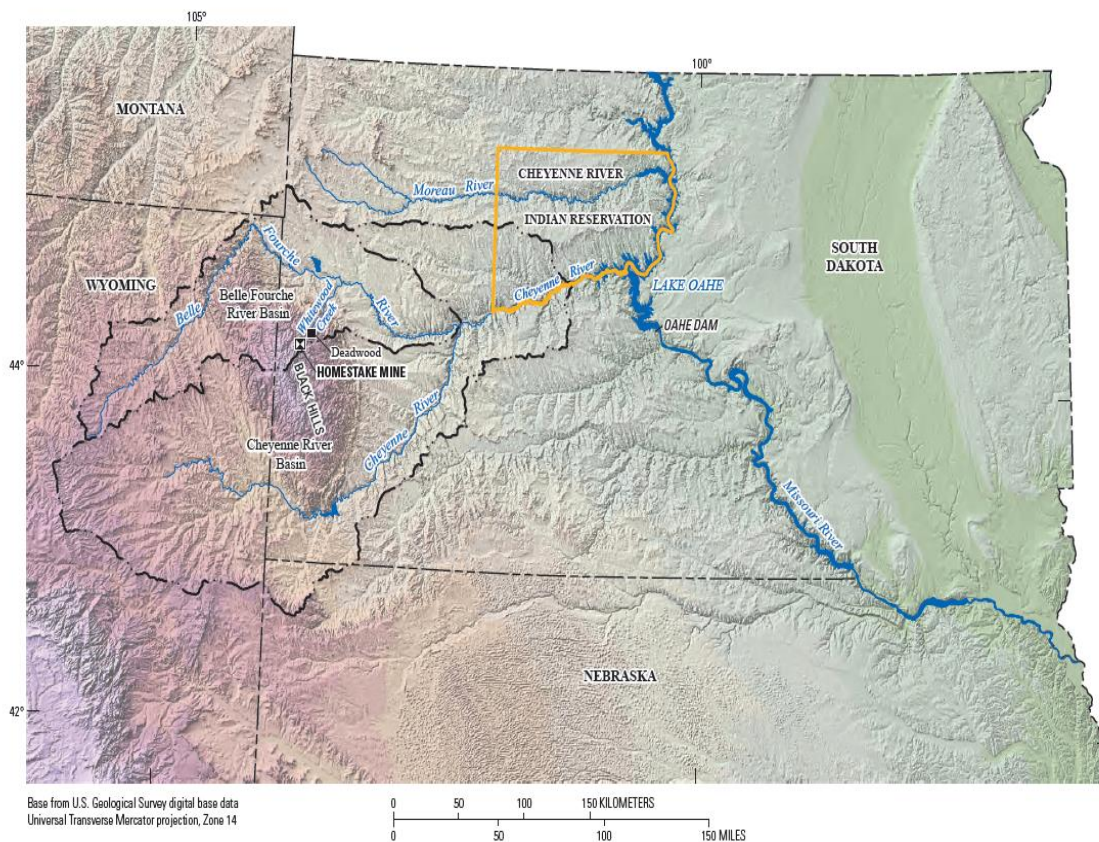


Figure 1.1. Locations of the watersheds within the study area in western South Dakota. The Whitewood Creek, Belle Fourche River and Cheyenne River System in western South Dakota comprise an area greater than 21,414 square miles (Stamm and Hoogenstratt, 2012).

Mining companies ran their operations to maximize production while minimizing costs, with little consideration given to environmental impacts. The discharge of mine wastes or “tailings” led to large-scale physical and chemical contamination of Whitewood Creek, the Belle Fourche, and Cheyenne Rivers and their adjacent alluvial floodplains. The large amount of mine tailings discharged to the streams exceeded their transport capacity, with sediment depositing on channel beds, hillslopes, and alluvial floodplains (Miller and Miller, 2007). Untreated discharge of waste materials into the Whitewood Creek stopped in 1977 with the construction of a tailings impoundment facility, but metal-enriched sediment continues to be mobilized by streamflow, especially during periods of high runoff. All sediment from these streams eventually deposits in the easternmost part of the Cheyenne River Basin – the Cheyenne River arm of the Missouri River’s Oahe Reservoir.

Naturally occurring sediment characteristics, physical properties, and chemical constituents are commonly governed by lithology of the basin, climate, topographic relief, transport energy, and hydrodynamics of the depositional environment. (Kanhaiya et al., 2017). Mining-impacted sediment continues to be a recognized as a significant source of metals (metalloid) pollution in the Lower Cheyenne River (DeVore et al., 2019). In 1971, before cessation of the tailings discharge, the U.S. Environmental Protection Agency (EPA) Office of Enforcement conducted an aerial remote sensing investigation of Whitewood Creek and the Belle Fourche and Cheyenne Rivers to locate mine tailings deposits for future field verification and sampling (U.S. EPA, 2002).

Remote sensing equipment was used to distinguish between river alluvium and mine tailings. The EPA found that older, weathered (oxidized) and fresh (non-oxidized) tailings were easily identifiable in the streambanks. At that time, mine discharges contributed 213 pounds of cyanide (CN); 240 pounds of zinc (Zn); 721 pounds of copper (Cu); 2,700 tons of suspended solids; and 9.5 tons of arsenopyrite (AsFeS) per day into Gold Run Creek, a tributary of Whitewood Creek (DENR, 2020). Numerous later investigations collected soil, sediment, and stream bottom sediment from potentially impacted locations within the watershed to verify and elucidate contaminant occurrence and transport mechanisms in the Cheyenne River basin (Goddard, 1988; Marron, 1989; Shockley, 1989). Goddard (1988) estimated that between 1900 and 1977, 75 million tons of tailings containing approximately 270,000 tons of arsenic (As) were discharged into Whitewood Creek. Mine tailings were distributed in the alluvium throughout the basin, and their presence has been confirmed as far as the Oahe Reservoir. Due to the dynamic nature of floodplains, once deposited, the mixture of naturally occurring sediment and tailings contained in floodplain sediments can be remobilized, reworked, and redistributed with their movement downstream.

Climate change refers to any major and sustained change in factors affecting the global climate system, such as surface and ocean temperatures, precipitation patterns, and other atmospheric conditions (USDA, 2019). The Intergovernmental Panel on Climate Change (IPCC) reported that climate-influenced changes may impact the amount, intensity, and frequency of

precipitation, with probable effect on the magnitude and frequency of stream flows, the intensity of floods and droughts, and water resources at local, regional, and basin-wide levels (IPCC, 2014). Changing climate may cause extreme temperature variability; changes in seasonal frost and thaws (with resulting influence on rainfall infiltration and runoff); increased precipitation or drought; high winds that increase dust; and impacts water infrastructure (U.S. Global Change Research Program (USGRCP), 2019, and the U.S. Agency for International Development (U.S. AID, 2015). The Cheyenne River Basin has likely already seen and will probably continue to experience these impacts.

The transport of sediments is intricately linked to these complex basin-wide hydrologic and geomorphic processes. Together with use of spatial patterns, parameters associated with these processes can be used to determine changes in ecological and physical variables at the regional and landscape scale (McManamay et al. 2011). Using U.S. Geological Survey (USGS) gage data, Eng et al. (2017) evaluated a suite of hydrologic metrics to describe natural flow regimes, quantify flow alterations, and provide the foundation for the development of environmental flow standards. As stream power changes with increased flows, a series of extreme precipitation events may catalyze the mobilization of tailings deposited in the alluvium of these streams from upstream sources, increasing the amount of sediments migrating downstream and eventually impacting habitats in the Cheyenne River Arm of the Oahe Reservoir, their ultimate sink. Localized high-sediment erosion may also alter the existing equilibrium in river geomorphology. A closer examination of these parameters

may offer insights to determine if variability in stream flow impacts sediments within specific river reaches within a basin, and to predict increases in sediment erosion and mobility.

Arsenic, a metalloid, occurs as arsenopyrite; arseniferous pyrite is a mineral associated with mined ore and used in this study to indicate the presence of mining contamination in river channels, floodplains, and the Oahe Reservoir. These widely distributed spatially heterogeneous sources are known to contribute to the total contaminant metal (metalloid) flux in these ephemeral streams. Most of the arsenic-laden tailings are deposited in Whitewood Creek and at its confluence with the Belle Fourche River. Alluvium along Whitewood Creek and the Belle Fourche River also has elevated levels of cadmium (Cd), chromium (Cr), cyanide, iron (Fe), manganese (Mn), mercury (Hg), silver (Ag), and zinc associated with the mined ore or the milling by-products (Goddard, 1984).

Due to the presence of carbonate geology in the region, tailings deposits in this basin do not generate the acid-leachate typically exhibited from sulfur-bearing mine tailings in other regions. Tailings deposits weather with time, resulting in chemical changes in the alluvium and alteration of the minerals into forms co-precipitated in or adsorbed on various iron- and manganese-rich clastic and authigenic minerals or mineral phases (Fe-hydroxides, Fe-oxides-coated sand, phyllosilicates, Mn, aluminum (Al) oxides, hydroxides, and authigenic pyrites). The weathering results in As-bearing Fe oxides, hydroxides, and oxyhydroxides (Fe(III) oxides) typical of phases that occur at a higher pH (8

and above) (Sø et al., 2008; Ravenscroft et al., 2009; Thi et al., 2014; Guo et al., 2014). Ground water is influenced by the mobility and spatial variability of arsenic, sediment redox boundaries, and mostly by the presence of  $\text{As}^{5+}$  (Mukherjee et al., 2007). When in solution, dissolved aqueous arsenic may enter the streams through ground water or surface water discharge, or by arsenic-laden particles entering the stream during rainfall, runoff, and erosion of riverbanks.

## **1.2 Hypothesis and Objectives**

The overall hypothesis for this study is that climate condition changes may alter existing geomorphic, hydrological, and geochemical conditions, potentially increasing the mobilization of constituents in the alluvial-deposited mine wastes and affecting water quality in these surface water systems. Historical sedimentation has already significantly impacted channel processes, alluvial aquifers, ecosystems, and fisheries. “Legacy arsenic-laden sediments in the system represent a future risk because they can be remobilized and reintroduced into the aquatic systems even following landscape amelioration” (Walter and Merits, 2008).” Despite the significant research in this region, limited information exists about the impact of changing climate on water quality, and climate change could affect the findings of previous research efforts. A need exists to assess such factors as changes in temperature, rainfall, snow cover, and spring thaw and their potential effect on sediment transport and associated chemical alterations.

To evaluate this hypothesis, this research seeks to investigate the following objectives:

- 1. *What is the impact of climate-induced hydrologic variability (primarily floods and droughts) on the stability of the alluvial deposits of mine tailings deposited in the Cheyenne River system? Do changes in stream discharge and flow impact sediment loads?***
  
- 2. *Will regional climate changes affect or modify biogeochemical and physio-chemical sediment parameters, thereby impacting arsenic concentrations that could be remobilized and released into the environment?***

The American Society for Testing and Materials describes a conceptual site model (CSM) as a representation of the watershed as an environmental system, with identification of the physical, chemical, and biological processes that control the transport of contaminants from sources through environmental media to environmental receptors (ASTM E1689–95, 2014). Typically, an initial CSM is developed, which is then refined, revised, and modified as further data become available. The CSM is routinely used and required by EPA as a systematic and iterative planning process for the collection and evaluation of environmental data (U.S. EPA, 2006). A CSM is an integral step in the development of cleanup objectives for a site and determining appropriate data quality objectives (DQOs), as it provides a basic understanding and description of what is known about site contamination and potential exposure scenarios. For this study, it assists in the understanding of the physical, chemical, hydrologic, geomorphic, and biological processes that affect contaminant transport from sources throughout the study location to potential environmental receptors.

Figure 1.2 depicts the initial CSM, first used to define research objectives and provide a preliminary representation of the proposed summary of the methods of the study to be pursued. Multiple lines of evidence then need to be evaluated to make an accurate assessment. When there is no natural reduction or degradation of chemical constituents, the ultimate remedy would be removal; however, this is not feasible due to the vast distribution of sediments throughout the basin. Formulating an effective study requires an understanding of the impacts of climate change and how, if actionable, the effects might be mitigated through intervention and management (Fischenich, 2008).

An important consideration for evaluating a watershed is to determine a conditional baseline. Borja et al. (2012) present the concept of “hindcasting,” where present conditions are compared relative to what is a pristine, unimpacted, or unaltered ecological state based on available historical information (CIS, 2003a). The biggest issue in hindcasting is scalar, both in terms of the size of the study area and the time period researched. The decisions made are critical in setting study baselines for comparing present basin/watershed conditions to a time when human impact was minimal or different from today. Both anthropogenic and natural changes in recent decades could also alter prior reference conditions, making impossible any comparison with a dataset from 50, 100, or 200 years ago (Kroencke and Reiss, 2010). While anthropogenic impacts were already significant during those first exhaustive studies of the Cheyenne River Basin about a half century ago, they differ today, complicating assessment. Borja et al. (2012) used climatic oscillations to illustrate the



complexity and challenges of hindcasting stemming from temporal changes in the values of considered indicators. Regarding climate change, Borja et al. (2012) state that hindcasting can be highly misleading when:

- (a) the causes of cyclical climate oscillations are not well established.
- (b) reference conditions are not available for the whole oscillation cycle.
- (c) the reference condition and the considered time-period are strictly identical relative to the oscillation cycle.

The CSM was used to gather initial information and then adjusted as more information became known. Specifically, the CSM was used to gain knowledge on Cheyenne River basin geomorphology and hydrology; to determine contamination sources and distribution; methods of transport; release mechanisms; exposure pathways and migration routes; and ecological, biological, and human receptors (U.S. EPA, 2011). Changing climate is regionally impacting the Cheyenne River basin. Former expectations often held that future conditions will be similar to the past, an assumption no longer valid. The hydrologic, meteorologic, and geologic processes underlying stewardship of water resources are all potentially sensitive to changes in climate. Movement is needed from a static paradigm to one that better accounts for and adapts to the dynamic, interconnected nature of physical processes.

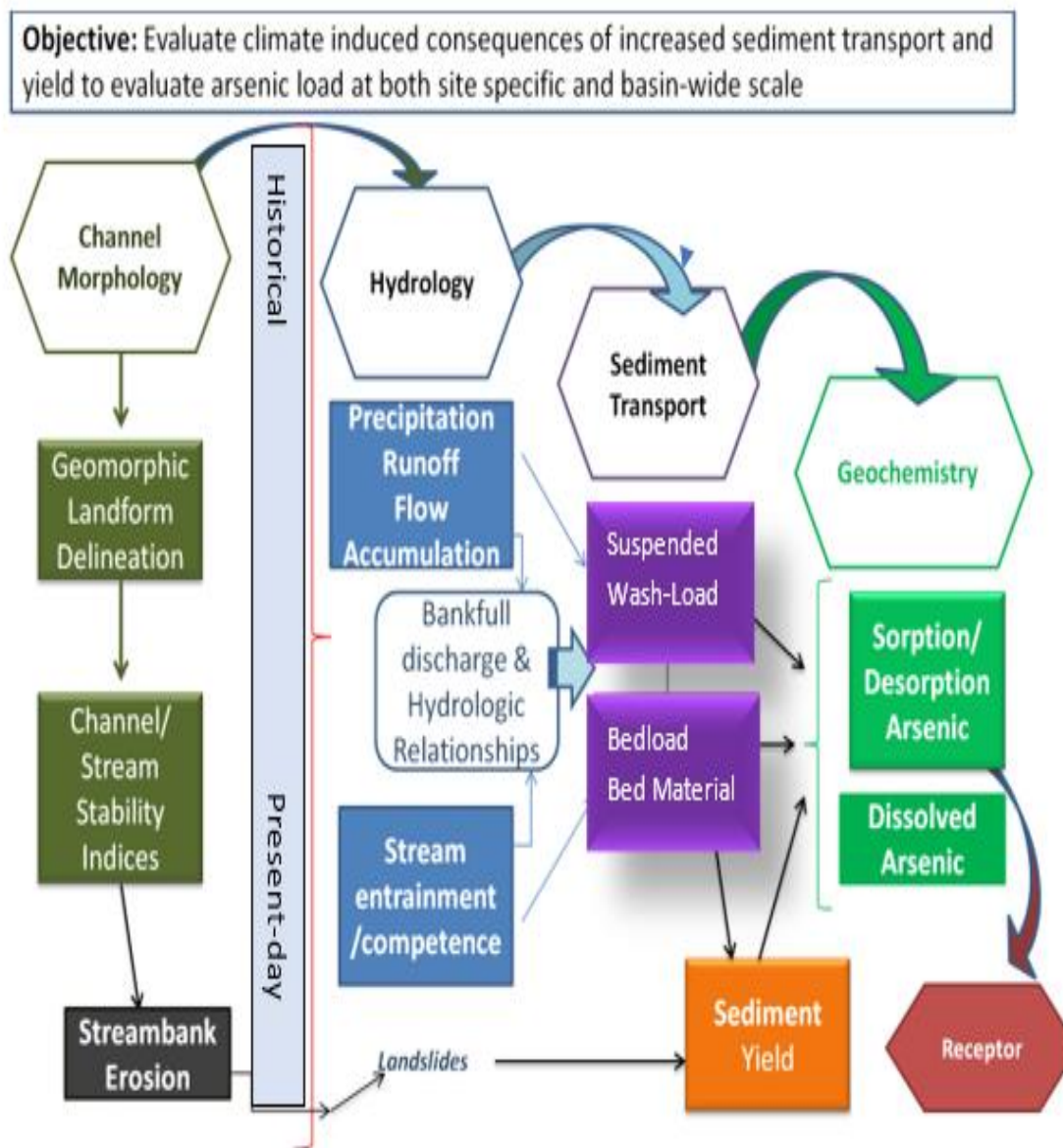


Figure 1.2. Initial CSM for the study

A primary objective of a CSM is to guide data collection by simplifying and understanding the complex system under study. The CSM in Figure 1.2 was created to initially evaluate what factors would be needed to downscale existing climate change models and what data was important to the study. Since limited

funding was available, the study relied heavily on peer-reviewed literature and readily available data. After significant study and modification, the revised CSM is presented in Figure 1.3.

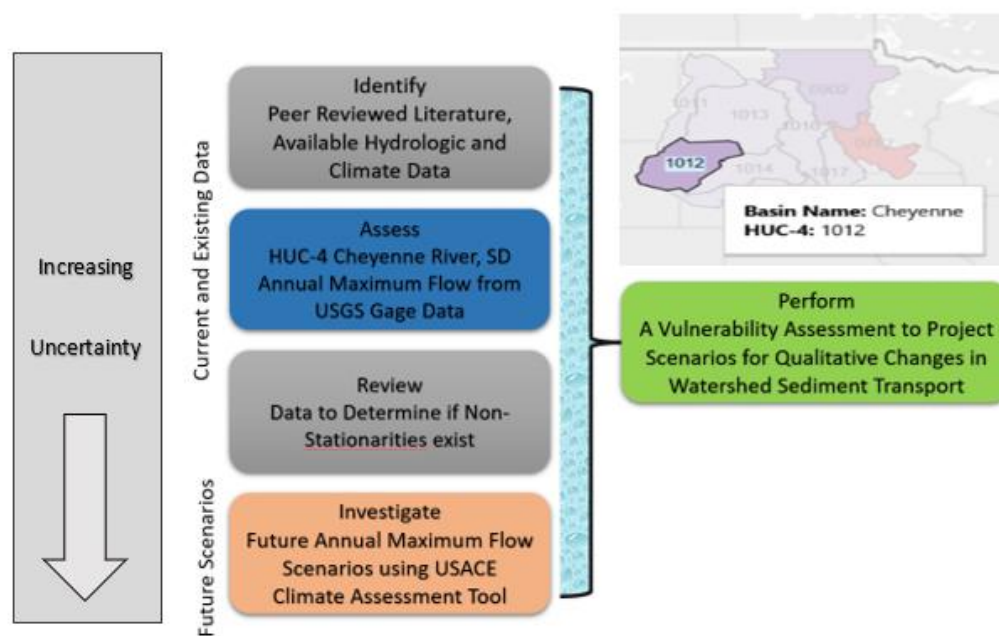


Figure 1.3. Revised and updated CSM, with the various inputs and process from observations and outcomes. USGS historical gage data is used to evaluate historical hydrological flow trends, and then used with global climate models for qualitative future annual stream discharge scenarios.

To begin addressing these issues, understanding is needed of how these stream systems are responding to impacts of both natural and anthropogenic origin. The effects of climate change on hydrologic conditions have been widely studied for impacts on streamflow magnitude, frequency (return period), timing (seasonality), and variability (averages and extremes) (Mujere and Moyce, 2009). However, linked, integrated study of stream systems and the fate and transport of diffuse (non-point) sources of mining pollution at a basin scale is needed to

identify potential mitigation strategies (Lynch et al., 2014). Many federal agencies, academic experts, nongovernmental organizations, and the private sector are working together to translate the data from climate studies into actionable science for decision-making to mitigate risk.

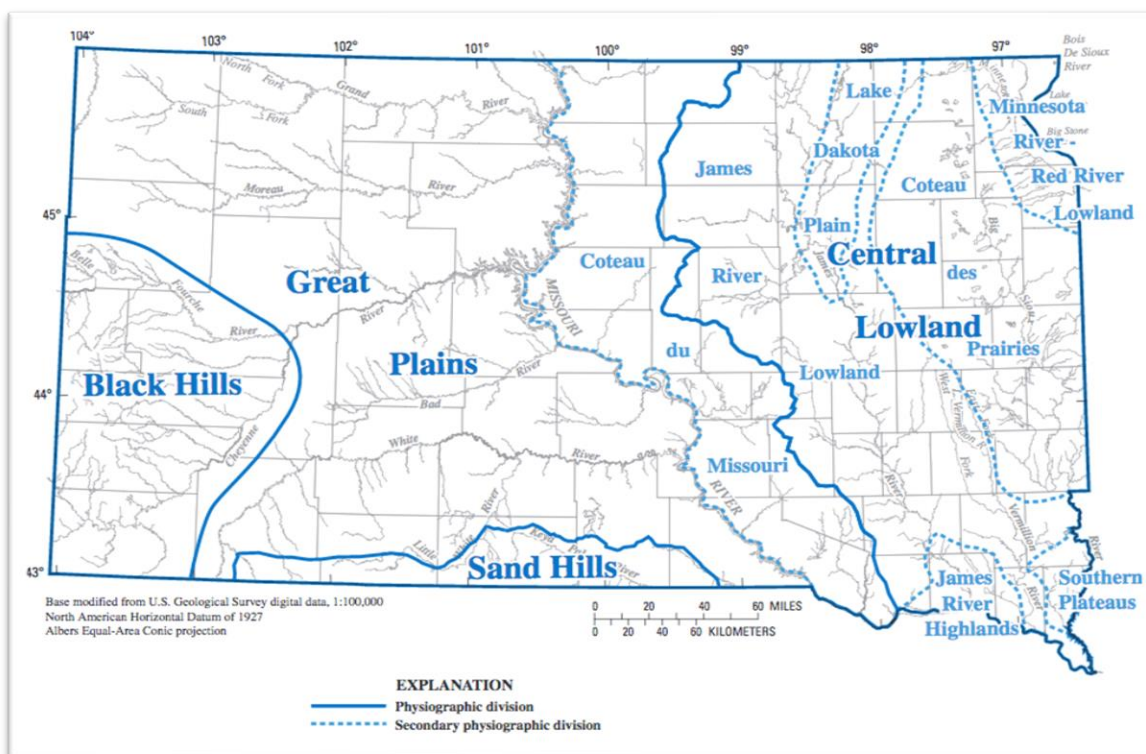


Figure 1.4. Physiographic divisions of South Dakota (Sando, Driscoll, and Parrett, 2008).

### 1.3 Physical Setting

Understanding the physical setting of a basin is integral to understanding both the natural and engineered hydrologic processes by which it is impacted. This study is located in two physiographic divisions: the Northern Great Plains Steppe (Bailey, 1995) and the Black Hills (Sando et al., 2008), which make up

most of the Northeastern Missouri River basin. Elevations range from about 3,125 feet to 1,617 feet above sea level (Figure 1.4, Sando et al., 2008), which is the “normal” maximum elevation at Oahe Reservoir on the mainstem of the Missouri River, approximately 200 miles downstream. (Roddy et al., 1991). The ecoregions in the watershed include the Black Hills Foothills; Black Hills Plateau; Black Hills Core Highlands; River Breaks; Semiarid Pierre Shale Plains; Dense Clay Prairie; and Missouri Plateau.

In a standard four-category system, the USGS uses hydrologic unit codes (HUCs) to delineate watersheds in the U.S. and Caribbean, going from largest (the drainage area of a major river) to smaller, each with its own HUC (Table 1.1). A complete list of HUCs can be found in USGS Water-Supply Paper 2294, "Hydrologic Unit Maps." (Seaber et al., 2007). The HUCs delineated for the study area are provided in Table 1.1 and Figure 1.5.

<b>2-digit HUC Region</b>	<b>4-digit Subregion</b>	<b>6-digit Basin</b>	<b>8-digit Subbasin</b>
10-Missouri	12-Cheyenne	01-Cheyenne	10120112 Lower Cheyenne River
		02-Belle Fourche	10120201 Upper Belle Fourche River
			10120202 Lower Belle Fourche River
	13-Missouri-Oahe	01- Lake Oahe	10130105 Lower Lake Oahe

Table 1.1. HUCs used in this study.

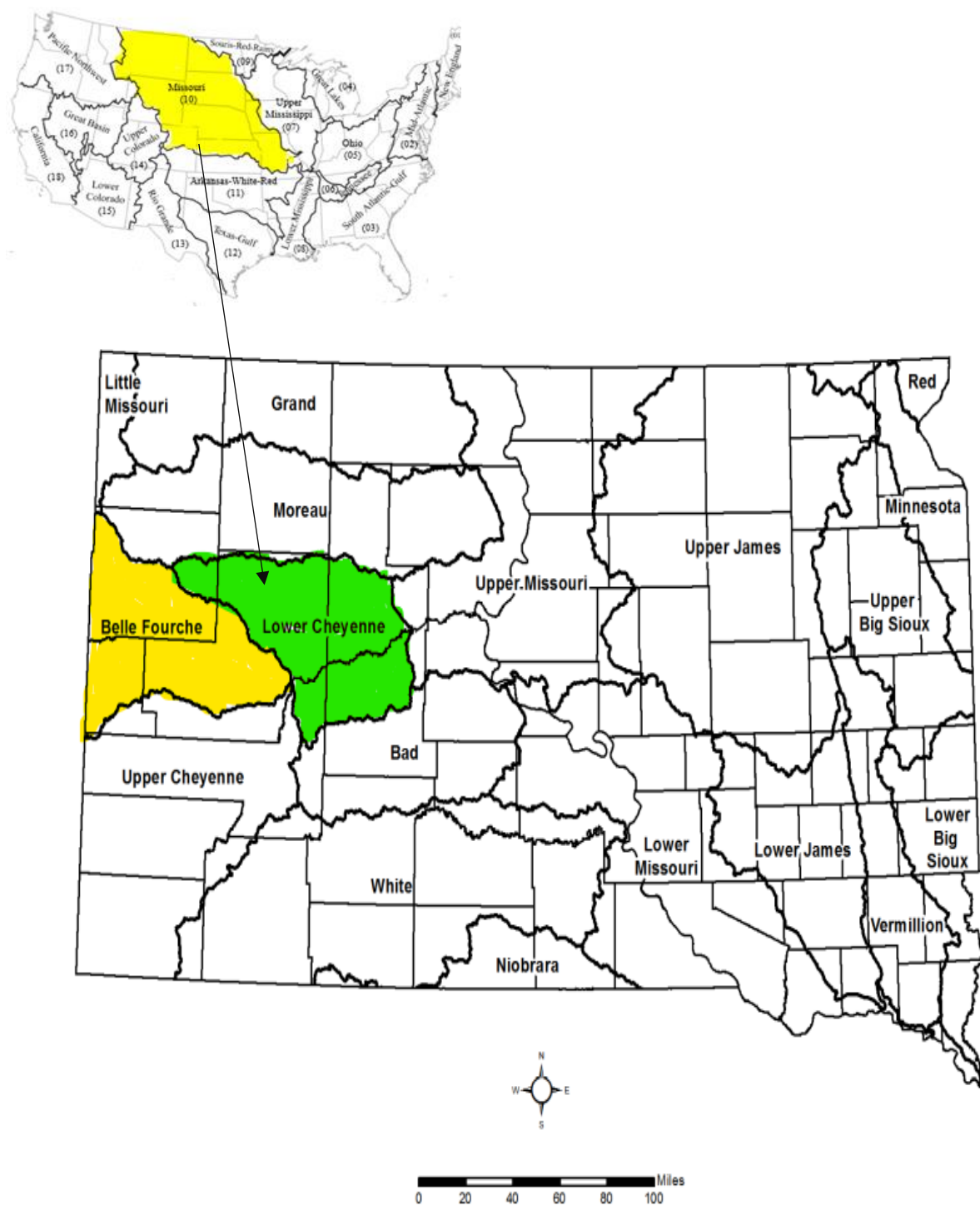


Figure 1.5. Water resource regions in South Dakota, Hydrologic Unit-10, Missouri River Basin. The study area is located in three HUCs: Lower Cheyenne River Watershed (HUC-1012012); Upper Belle Fourche (HUC-10120201); and the Lower Belle Fourche (HUC-10120202). (Modified from USACE, 2018, and DENR, 2020).



## 1.4 Study Area General Description

The study area (Figure 1.6) spans an area from the point of original tailings discharge in Whitewood Creek, to the confluence of Whitewood Creek and Belle Fourche River, into the eastern segment of the Cheyenne River Basin at the confluence of the Belle Fourche and Cheyenne Rivers, and to the confluence of the Cheyenne River and Oahe Reservoir. Contributing stream flow in the overall study area arises from 8,500 miles of streams in four states (Wyoming, Montana; South Dakota, and Nebraska), 18 counties, and a 2010 census population area of 360,000 people. EPA (2007) reported that distribution of tailings deposits, tailings-impacted soils, and the 100-year floodplain boundary of Whitewood Creek were delineated under field programs during 1991 and 1992. EPA approved the detailed maps for these boundaries in 1993 (Whitewood Development Corporation (WDC), 1994, as cited in U.S. EPA, 2007).

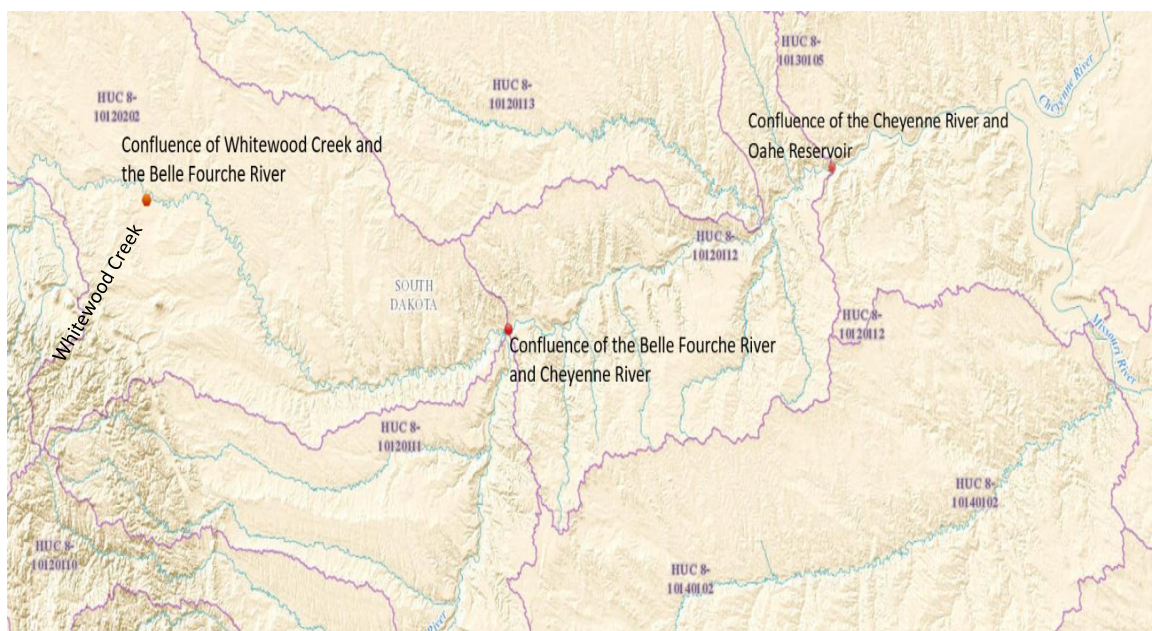


Figure 1.6. General Description and Summary of the Study area.

The study area (Figure 1.6) spans an area from the point of original tailings discharge in Whitewood Creek, to the confluence of Whitewood Creek and Belle Fourche River, into the eastern segment of the Cheyenne River Basin at the confluence of the Belle Fourche and Cheyenne Rivers, and to the confluence of the Cheyenne River and Oahe Reservoir. Contributing stream flow in the overall study area arises from 8,500 miles of streams in four states (Wyoming, Montana; South Dakota, and Nebraska), 18 counties, and a 2010 census population area of 360,000 people. EPA (2007) reported that distribution of tailings deposits, tailings-impacted soils, and the 100-year floodplain boundary of Whitewood Creek were delineated under field programs during 1991 and 1992. EPA approved the detailed maps for these boundaries in 1993 (Whitewood Development Corporation (WDC), 1994, as cited in U.S. EPA, 2007).

The Belle Fourche River and its 105 named tributaries flow through three states: Montana, Wyoming, and South Dakota. Eight counties, five in Wyoming and three in South Dakota (Butte, Lawrence, and Meade) are of interest for this study. The watershed drains to the Cheyenne River and ultimately to the Cheyenne River Arm of the Oahe Reservoir, located on the Missouri River. Prior to the installation of the Oahe Reservoir, the Belle Fourche River discharged into the Lower Cheyenne River and ultimately into the Missouri River.

Most of the streams in western South Dakota are characterized as intermittent or ephemeral (SD DENR, 2020). Once thought to be less significant than perennial streams, they have gained recognition for their ecological importance and contribution to downstream water quality, conditions of stream



habitat, and biotic integrity (SD DENR, 2020). Rivers and streams are assessed by dividing the waterbodies into segments that contain the same designated beneficial uses, water quality standards criteria, and environmental and physical influences. Each waterbody is compared to a standard applicable to the beneficial use and nutrient-related assignment. Table 1.2 gives the status of streams within the Cheyenne River Basin that are listed as impaired waters according to established Total Maximum Daily Loads (TMDLs) and Section 303(d) of the Clean Water Act.

The Cheyenne River originates in Wyoming, flows through the southern Black Hills, and enters Lake Oahe near the center of the state. The portion of the Cheyenne River basin that lies in southwestern South Dakota drains about 9,732 square miles. The diverse Cheyenne River basin includes several ecological regions, among them the mountainous Black Hills and Badlands, rangeland,

<b>Assessment Unit ID</b>	<b>Cause</b>	<b>Status</b>
SD-BF-L-Newell_01	Mercury in Fish	TMDL Completed and approved
SD-BF-R-Belle_Fourche_01	E. Coli	TMDL Completed and approved
SD-BF-R-DEADWOOD_01	E. Coli	Drafted-EPA review
SD-BF-R-WHITEWOOD_04	E. Coli	E. coli Draft-development
SD-BF-R-WHITEWOOD_06	E. Coli	IR Delist

Table 1.2: South Dakota's Revised (2018) Vision Priority Waters and Status in the Cheyenne River Basin.

irrigated cropland, and some mining areas. Cheyenne River water quality continues to be generally poor due to both natural and agricultural sources. Most of the Cheyenne River drainage basin contains highly erodible soils. The landscape contributes considerable amounts of eroded sediment during periods of heavy rainfall (DENR, 2020).

<b>USGS Gage Name (ID Number)</b>	<b>Contributing Drainage Area above Gage (mi<sup>2</sup>)</b>	<b>Period of Record Discharge</b>	<b>Period of Record Suspended Sediment</b>
<b>06436000</b> - Belle Fourche River near Fruitdale	4,520 mi <sup>2</sup>	1945 -Present	
<b>06436150</b> -Whitewood Creek above Lead	8.34 mi.	N/A (no data)	
<b>06436180</b> - Whitewood Creek above Whitewood	56.7mi <sup>2</sup>	1982-Present	
<b>06436190</b> -Whitewood Creek near Whitewood	77.5 mi <sup>2</sup>	1981-Present	
<b>06436198</b> - Whitewood Creek above Vale	102 mi <sup>2</sup>	1982-Present	
<b>06436250</b> - Belle Fourche River at Vale	Historical Data		
<b>06437000</b> - Belle Fourche River near Sturgis	5,821 mi <sup>2</sup>	1946-Present	01-Oct-1955, 30-Sep-1958
<b>06438000</b> - Belle Fourche River near Elm Springs	7,029 mi <sup>2</sup>	1928-June 1932; March 1934-present	1958-1959
<b>06423500</b> - Cheyenne River near Wasta	12,725 mi <sup>2</sup>	July 1914 to June 1915; August 1928 to June 1932; 1934-Present	
<b>06438500</b> - Cheyenne River near Plainview	21,425 mi <sup>2</sup>	1950 -Present	Limited period of record.
<b>06439300</b> - Cheyenne River at Cherry Creek	Historical data		01-Oct-1971 – 30-Sep-1976
Oahe Reservoir	Historical data		

Table 1.3. USGS gages used to perform the assessments.

Tributaries of the Cheyenne River have 45 gaging stations. The Belle Fourche River has 27, representing an average of one gaging station for every 150 and 121 mi<sup>2</sup>, respectively. Table 1.3 lists the gaging stations which provided data for this area along with periods of record (Miller and Driscoll, 1993).

Periods of records for each USGS gauge used in the study to assess climate change are detailed in Chapter 6. The distribution of long, intermediate-, and short-term stations is fairly uniform. Prior to the base period of USGS gage records, especially large annual peak flows occurred in 1920 (at the present location of USGS gage 06400500-Cheyenne River Near Hot Springs) and 1933 (at the present location of USGS gage 06439500-Cheyenne River Near Eagle Butte), both upstream of the study area on the Cheyenne River. Relatively large annual peak flows have occurred at many sites during the base period (USGS

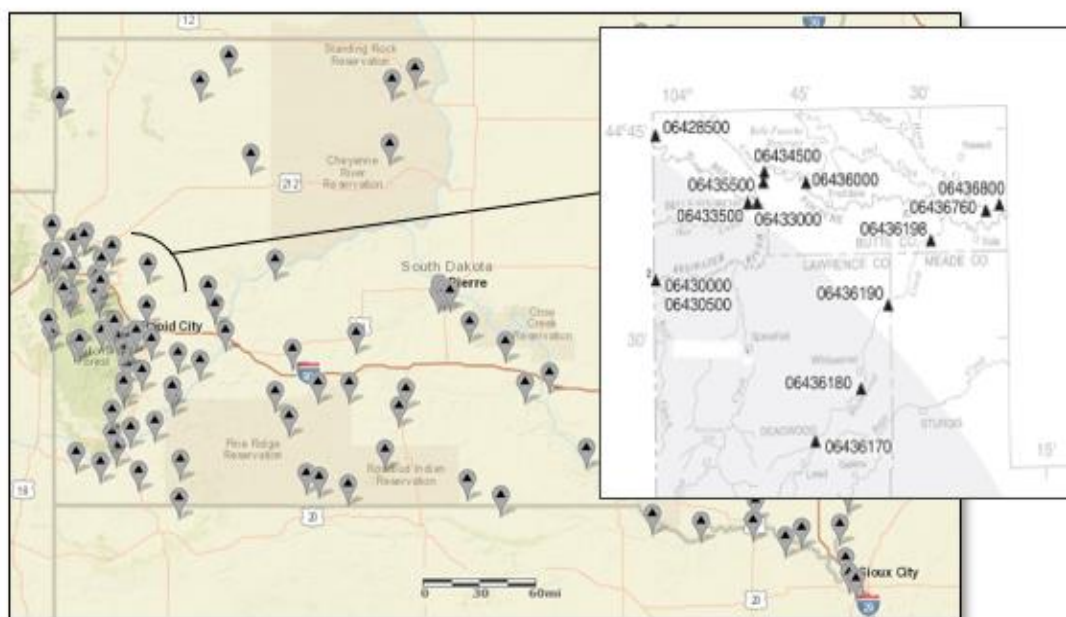


Figure 1.7. Distribution of USGS stream gages in South Dakota (modified from USGS, 2018, and Miller and Driscoll, 1993.) Triangles represent streamflow-gaging stations and their number.

South Dakota Science Center, 2018). Some of the more notable years of peak flows occurred in 1947, 1962, 1964, 1978, 1982, 1995, and 1996 (Sando et al., 2008). The density of the gaging network in the Black Hills region is the highest in South Dakota (Fig. 1.7).

### 1.4.1 The Belle Fourche River

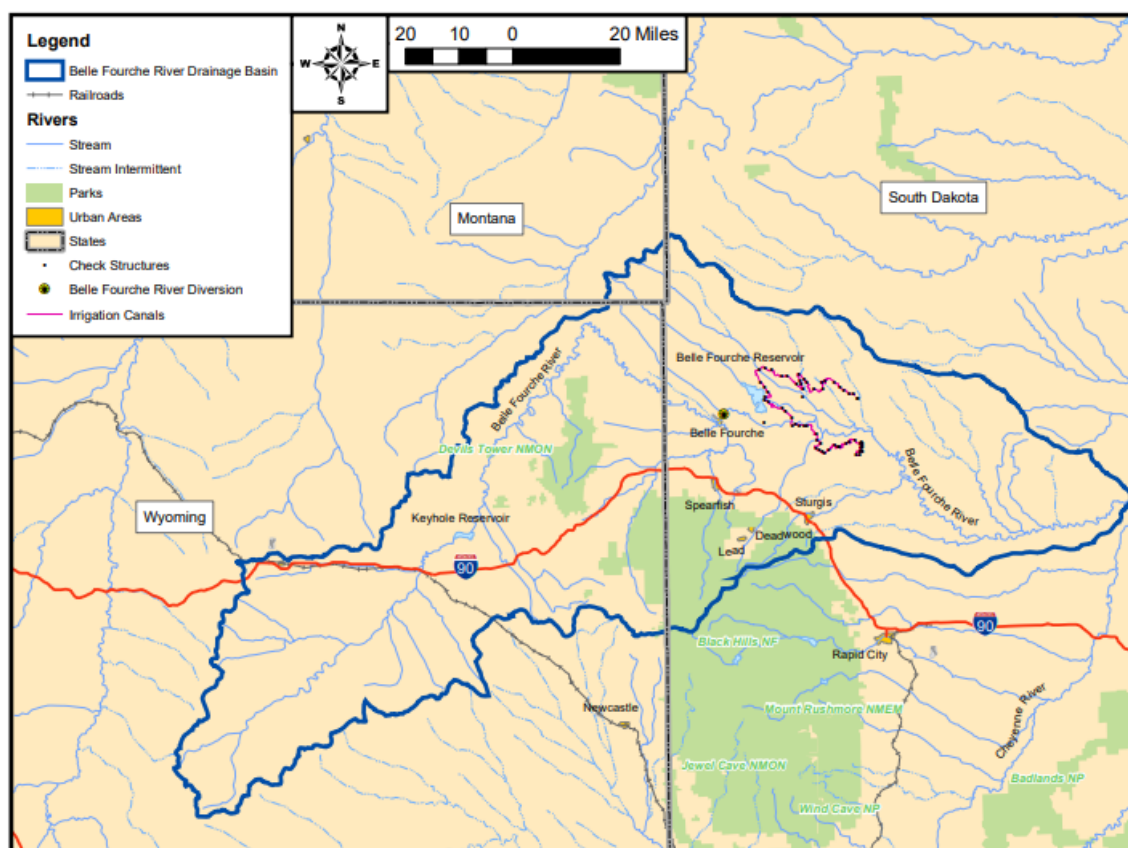


Figure 1.8. The Belle Fourche River basin in Montana, Wyoming, and South Dakota (RESPEC, 2013).

The Belle Fourche River (within HUC 10120202) (Figure 1.8), a primary area for this study, is a naturally occurring stream (RESPEC, 2013). The Belle Fourche River watershed drains portions of Butte, Lawrence, and Meade Counties in South Dakota. It encompasses approximately 2,400,000 acres (3,750 square miles) in South Dakota and includes HUCs 10120201, 10120202,

and 10120203 (SD DENR, 2018). The headwaters of the Belle Fourche River are located in Wyoming at 105.811489W longitude-43.655292N latitude, at an elevation of approximately 5,423 feet. The Belle Fourche River discharges into the Cheyenne River at 102.303211W longitude-44.435.43515N latitude, at an elevation of 2031.47 feet (USGS, 2016) in the southern portion of Meade County, SD. The river is approximately 290 miles long, with a descent of approximately 3,390 feet (USGS, 2016).

The river received runoff from agricultural operations, and the South Dakota Department of Agriculture and Environment (DENR) states that water quality in the river and its tributaries is declining due to this runoff. Land in the Belle Fourche basin is predominantly used for grazing, and there is minimal crop land. The Belle Fourche River includes five stream segments on the State 303(d) list with impairment-related TMDL waters (WWC (2), Bear Butte Creek, Horse Creek, and the Belle Fourche River) (SD DENR, 2020).

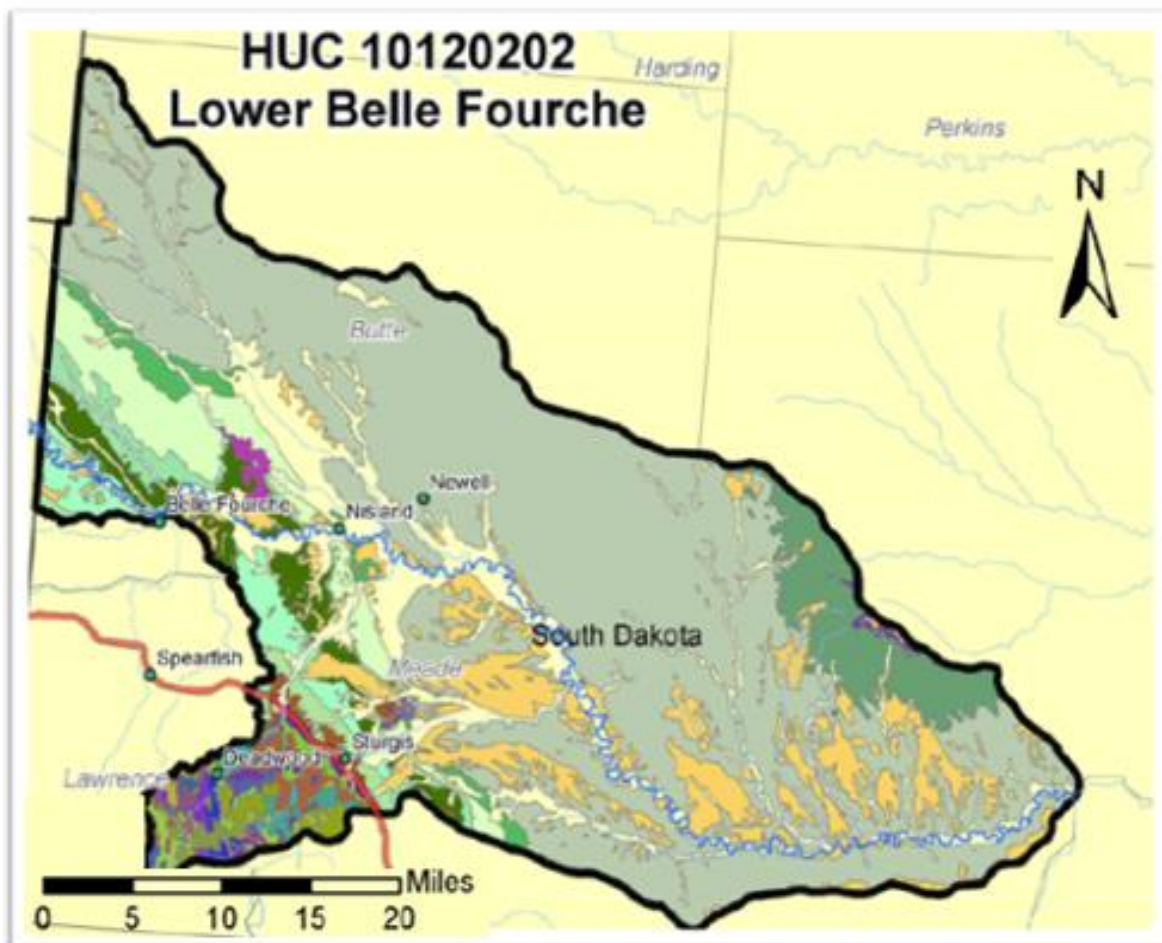
According to the Belle Fourche River Watershed Partnership Segment 9 Report (2020) the TMDLs for irrigation and return-flow, non-used irrigation water are responsible for approximately 20% of the TSS in the Belle Fourche River. The majority of the irrigated lands within the watershed are flood-irrigated. This type of irrigation results in sediments that are mobilized by three processes: (1) tail water/runoff crossing fields, (2) water in the canals and laterals, and (3) water in the intermittent streams carrying tail water/runoff to the perennial streams. Since the Belle Fourche River Watershed Partnership project began, about 20,000 to 22,000 acres have been converted to sprinkler irrigation. Rangeland

erosion contributes the remaining 5% of the TSS load. The report identified livestock as the main contributor to excess loading in the lower reach of the Belle Fourche River, with wildlife contributing approximately 3% of the load. To meet the standard for immersion recreation, E. coli loads need to be reduced to 99, 56, 21, 29, and 80%, respectively, during high, moist, midrange, dry, and low-flow conditions.

SD DENR reported that irrigation and return-flow, non-used irrigation water are responsible for approximately 20% of the total suspended solids (TSS) in the Belle Fourche River system. Much of the irrigation in the watershed is flood irrigation (SD DENR, 2014). This type of irrigation results in sediments that are mobilized by three processes: (1) tail water/runoff crossing fields; (2) water in the canals and laterals; and (3) water in the intermittent streams carrying tail water/runoff to the perennial streams within the watershed. Rangeland erosion, both natural and from land-use practices, contributes the remaining 5% of the TSS load (SD DENR, 2014).

#### **1.4.1.1 Geology**

Figure 1.9 provides a summary of the bedrock/geology in the area. Most of the bedrock is made up of Cretaceous sandstones, limestones, and marine shale. Areas of Quaternary alluvial and terrace deposits consisting of sand and gravel overlie the bedrock in the Belle Fourche and Cheyenne Rivers. Roddy et al. (1991) estimated the alluvium along the Belle Fourche River to be quite



Map Designation	Code	Major Geologic Units	Area Acres	Area %
	Kp	Pierre Shale	907,822	51
	Qal	Alluvium	249,879	14
	Qt	Terrace deposits	195,439	11
	Kfh	Fox Hills Sandstone	80,048	5
	Kc	Carlile Shale	79,655	5
	Kb	Belle Fourche Shale		3
	Kms	Mowry Shale, Newcastle Sandstone and Skull Creek Shale	42,479	2
	Kg	Greenhorn Formation	25,638	1
	Kn	Niobrara Formation	24,862	1
	Other		128,682	7
		Total	1,754,669	100

Figure 1.9. Geologic Units in HUC 10120202 (from NRCS and RESPEC, 2007).

variable, averaging 25 feet. in thickness and ranging from 0.5 to 4 miles in width. Roddy et al. (1991) state that in general, most of the area's soils are slowly drained, with good water-holding capacities, and tend to shrink and crack when dry. The shale-derived soils of the lower Cheyenne River are usually slowly drained, moderately deep, firm clays on undulating to rolling uplands. Saline alkali soils exist locally in the project area (Roddy et al., 1991).

One of the most prevalent geological formations with potential for creating temporary dams in the river is the Cretaceous Pierre Shale. The Pierre Shale outcrops on the banks of the Belle Fourche and Cheyenne River (Scully, 1975) and makes up the stream bed at many sites in the basin studied in this investigation. The cohesive properties of the Pierre shale make the bed far more resistant to scour than if it were non-cohesive. Cohesive beds are composed of several layers, each with its own shear strength. Significant scour will take place only if the shear force that the flowing water exerts on the bed exceeds the shear strength of the weakest layer. Debris flows and debris avalanches are triggered by high pore-water pressures caused by locally intense precipitation (USGS, 1987). Landslides are common in outcrops of in the Pierre Shale and controlled by discontinuities or breaks in the land surface and changes in the topographic slope. These discontinuities are avenues of water migration and contribute to the build-up of hydraulic pressures and the progressive structural deterioration and collapse of the shale material. Bruce (1968) reported that an increase in construction in areas underlain by Pierre Shale has caused it to receive greater engineering emphasis



The South Dakota Department of Agriculture and Environment (formerly South Dakota Department of Environmental Resources (DENR)) reported in 2020 that natural pollution of dissolved and suspended solids is exemplified by the erosive soils of the western South Dakota Badlands and the Missouri River basin, including the considerable exposed marine shale formations. Storm events that produce moderate-to-significant amounts of precipitation contribute to suspended sediment problems over large areas of the state, particularly in the west. E. coli concentrations also increase significantly during times of precipitation and runoff events. For the rivers and streams studied in 2018 and 2020, DENR reported that 100% of the stream miles assessed for arsenic, chromium, copper, cyanide, lead, mercury, nickel, selenium, silver, sulfate, and zinc met associated water quality standards

In its 2020 Integrated Report for Surface Water Quality Assessment, DENR reported that 22% of assessed stream miles in South Dakota fully support all assigned beneficial uses. Nonsupport in assessed streams was caused primarily by E. coli bacteria from agricultural nonpoint sources and wildlife. In order of stream miles affected, causes of impairment were E. coli, TSS; sodium adsorption ratio (salinity); dissolved oxygen; total dissolved solids; temperature; specific conductivity; and cadmium. Excluding the four Missouri River reservoirs, an estimated 30% of state lakes and reservoirs have been assessed, accounting for 67% of total lake acreage. An estimated 9% of lake acreage was considered to support all assessed beneficial uses – a decrease from 15.7% in the 2018 Integrated Report.

#### **1.4.1.2 Slope Distribution**

Earth models rely on determination of slope, a key landscape feature that contributes to the understanding of structure and functions of geomorphic, hydrologic, and terrestrial systems. Historically, hydrology was portrayed in one dimension (e.g., discharge in streams and evapotranspiration from surficial soils). Today, complex, multi-dimensional models are used to understand water movement on and below the land surface (Fan, 2019). Knowledge of regional basin slope may assist investigators in understanding regional processes, improving assessments and predictions of climate change factors which can cause geomorphic and hydrological responses to natural, global, or anthropogenic influences. Figure 1.10 provides an overview of the slope distribution percentages of the Lower Belle Fourche River HUC 101202.

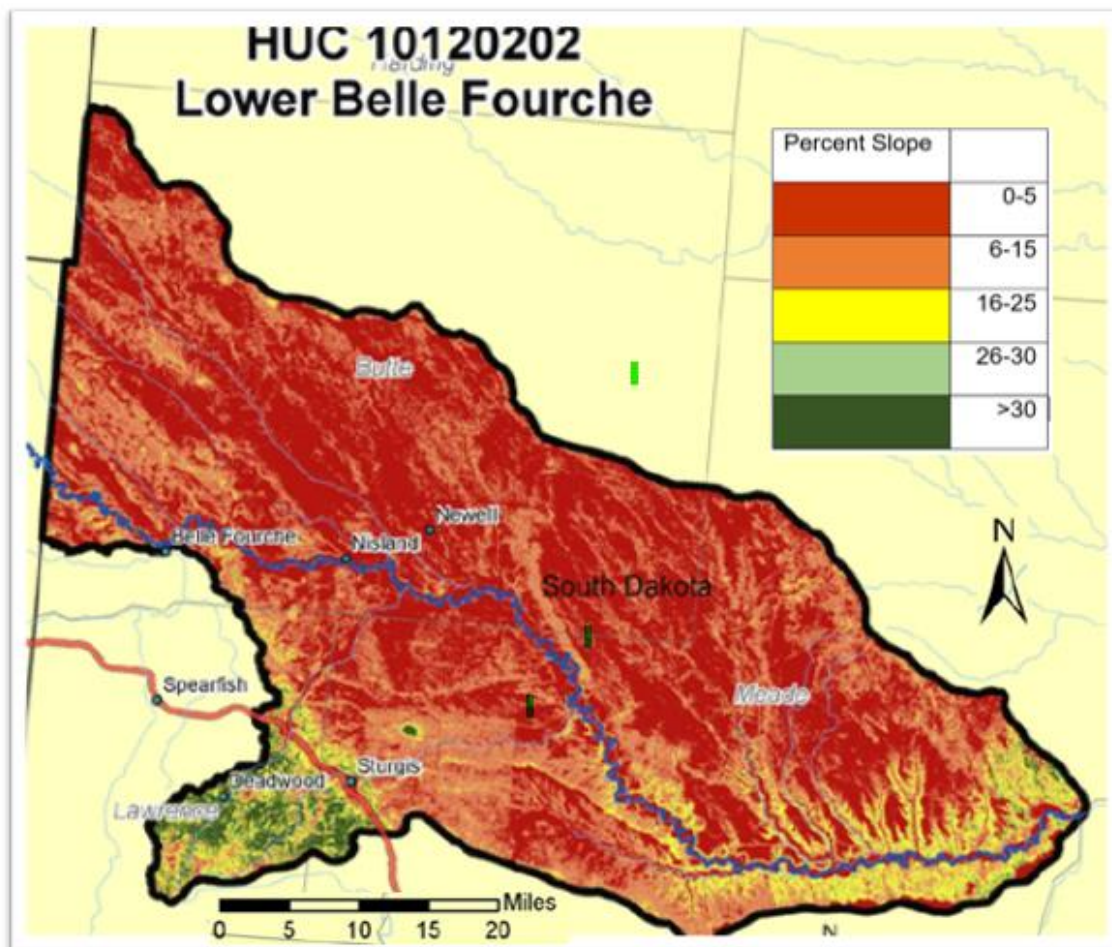


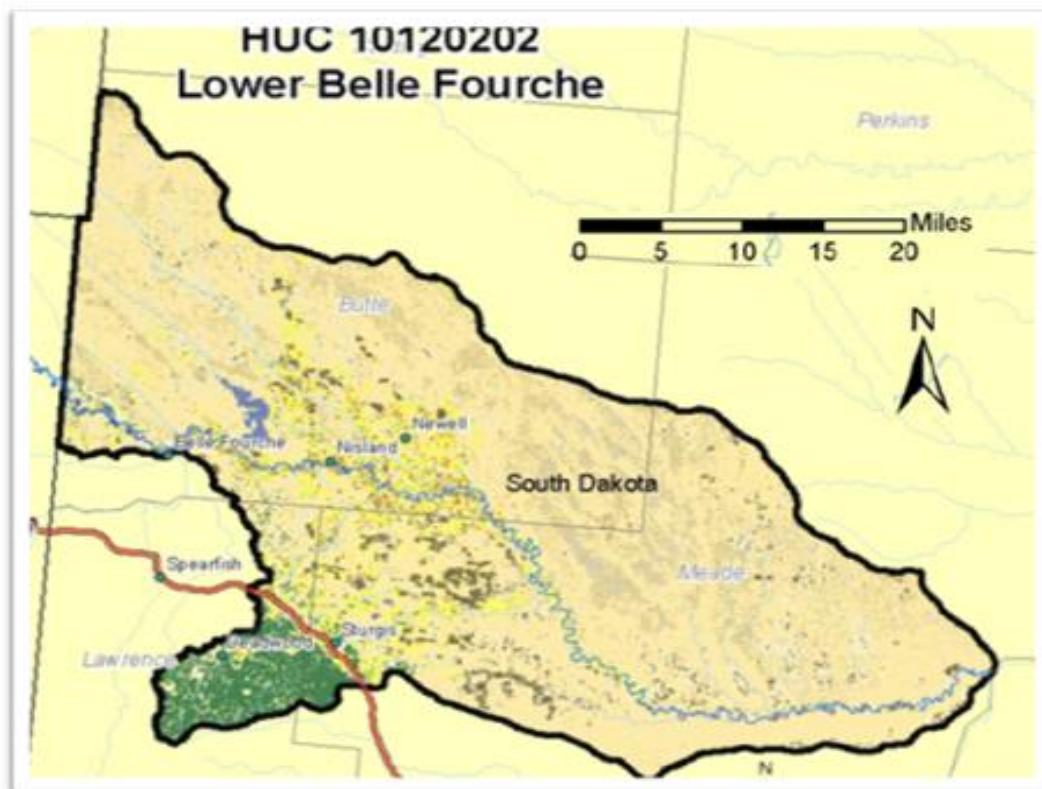
Figure 1.10. Slope distribution percentages (modified from NRCS and RESPEC, Dec., 2007).

The southwestern portion of this HUC in the Black Hills has greater than a 30% slope. The complex slope depicted in Figure 1.10 is attributed to the climate-induced historic fluvial processes which created terraces that changed the geomorphology of the region. These processes significantly altered the fluvial landscape of the Black Hills and the Belle Fourche and Cheyenne Rivers. Drivers that have historically dominated and altered the landscape are still at work today (Plumley, 1948; Hazelwood and Stetler, 2016 and 2019; Hazelwood, 2019; Zaprowski, 2001; Zaprowski et al., 2001; Stamm et al., 2013, Rahn, 1996).

Stamm et al. (2013) used slope- and age-dating of sediments to determine unique terrace levels resulting from fluvial erosion. They attribute these terraces to stream erosion from interglacial cycles that caused temperature fluctuations and precipitation changes as ice advanced and retreated during Late Quaternary continental interglacial periods. All of these events contributed to channel adjustment and changes in slope (Stamm et al., 2013).

#### **1.4.1.3 Land Use and Cover**

Eighty-four percent of the drainage area in the Belle Fourche River is watershed made-up of rangeland. Approximately 10% is cropland and the remaining areas are public land and water (SD DENR, 2005). The predominant land use within the HUC is livestock grazing on the grasslands, with the remaining areas consisting mostly of shrubland and pasture and hay land. There are 862 farms and ranches within the area, with no large residential or commercial developments. Figure 1.11 depicts the predominant land cover and use in the area.



Map Designation	NLCD Predominant Land Cover/ Land Use	Ownership					
		Private		Public		Total	
		Acres	%	Acres	%	Acres	%
	Bare Rock/Sand Clay	21,770	1	0	0	21,770	1
	Evergreen Forest	41,533	2	42,771	2	84,304	4
	Shrubland	172,484	10	24,043	2	199,527	12
	Grasslands/Herbaceous	1,003,765	58	116,391	7	1,120,156	65
	Pasture/Hay	124,637	7	0	0	124,637	7
	Row Crops	21,463	1	0	0	21,463	1
	Small Grains	62,191	4	0	0	62,191	4
	Fallow	36,683	2	0	0	36,683	2
	Woody Wetlands	36,584	2	0	0	36,584	2
	Other	29,056	2	9,406	<1	35,522	2
	Open Water					15,650	
	<b>Total</b>	<b>1,54,166</b>	<b>89</b>	<b>195,671</b>	<b>11</b>	<b>1,742,837</b>	<b>100</b>

a. "Other" includes very small acres of various land use categories.

b. Totals are approximate due to rounding. Open water is <1% of the HUC.

Figure 1.11. Predominant land cover and use (modified from NRCS and RESPEC, 2007).

### 1.4.1.4 Livestock Distribution

There are five permitted Concentrated Animal Feeding Operations (CAFOs) containing approximately 10,000 beef cattle within the Lower Belle Fourche HUC. (National Agricultural Statistics Service, 2002, cited in NRCS and RESPEC, 2007).

### 1.4.1.5 Census and Social Data

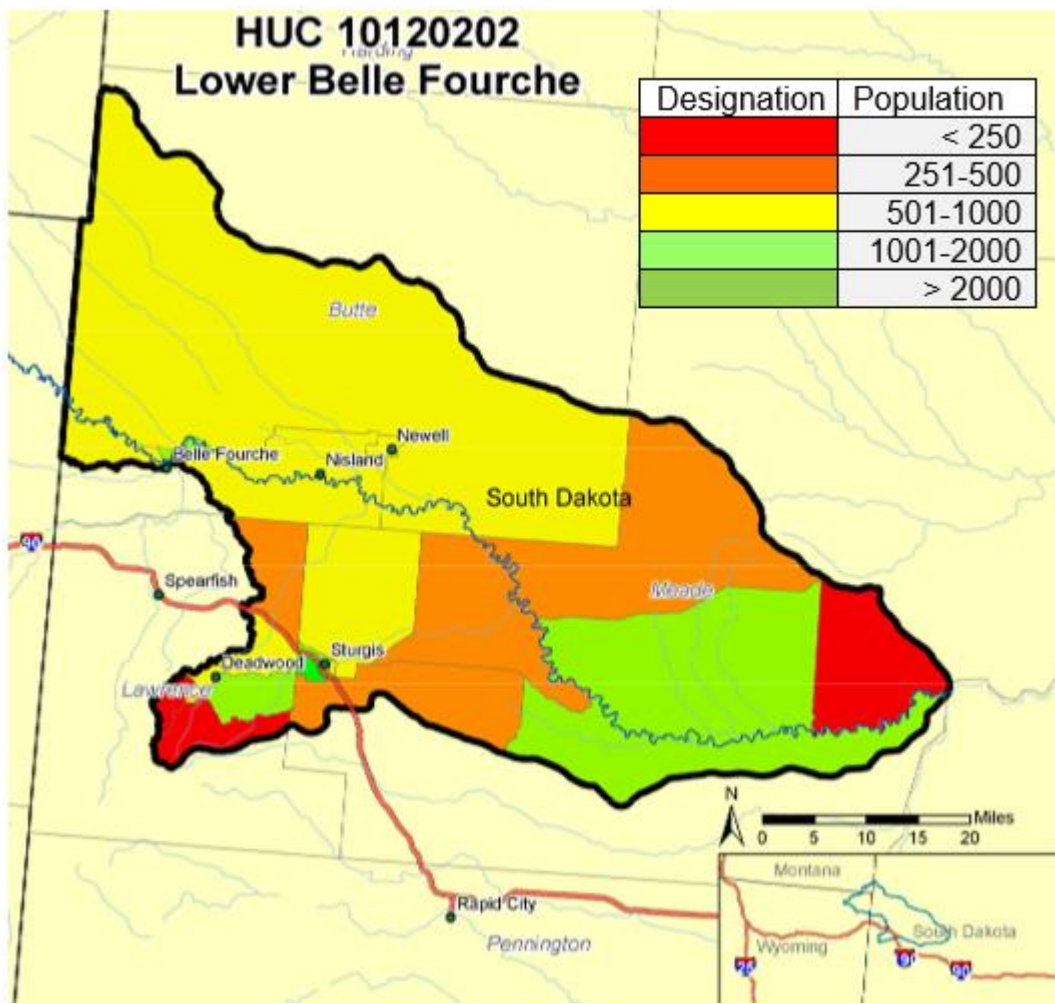


Figure 1.12. Population distribution by Census Block Federal Information Processing Standard (FIPS) Code (NRCS and RESPEC, 2007).

Based on 2000 Census data scaled to the percentage of the area within the HUC, the population of the HUC is approximately 21,359, with urban population making up more than half of the total HUC population. The population distribution by census block group and population per square mile within the HUC are shown in Figure 1.12. According to population and income statistics obtained from 2000 Census data, there are approximately 8,678 households within the HUC, with the majority earning between \$25,000 and \$50,000 per year. There are 862 farms/ranches in the HUC with 646 primary operators and 287 part-time operators (U.S. Census Bureau, 2000). Most of the farms and ranches are greater than 50 acres in size (National Agriculture Statistics Service, 2002).

#### **1.4.2 Whitewood Creek**

Whitewood Creek Basin (Figure 1.13) is located in the northwest portion of HUC 10120202, within the ponderosa pine woodland and savannah grasses of the Black Hills region, a distinct vegetation community. The remaining watershed area can generally be described as largely prairie grassland and sagebrush steppe. Whitewood Creek is a perennial, snow-fed tributary of the Belle Fourche River and occupies the northwest portion of the study basin. Whitewood Creek originates in the northern Black Hills at approximately 1,700 meters elevation and is a moderate gradient stream with well-developed riparian areas. It has a drainage area of approximately 40 mi.<sup>2</sup> at Lead, S.D., and approximately 104 mi<sup>2</sup> near its mouth. The steep slope of the Whitewood Creek Basin helped facilitate the conveyance of the mine-tailings discharge at Gold Run. Between the towns of Lead and Whitewood, the Whitewood Creek Basin has a steep V-shaped



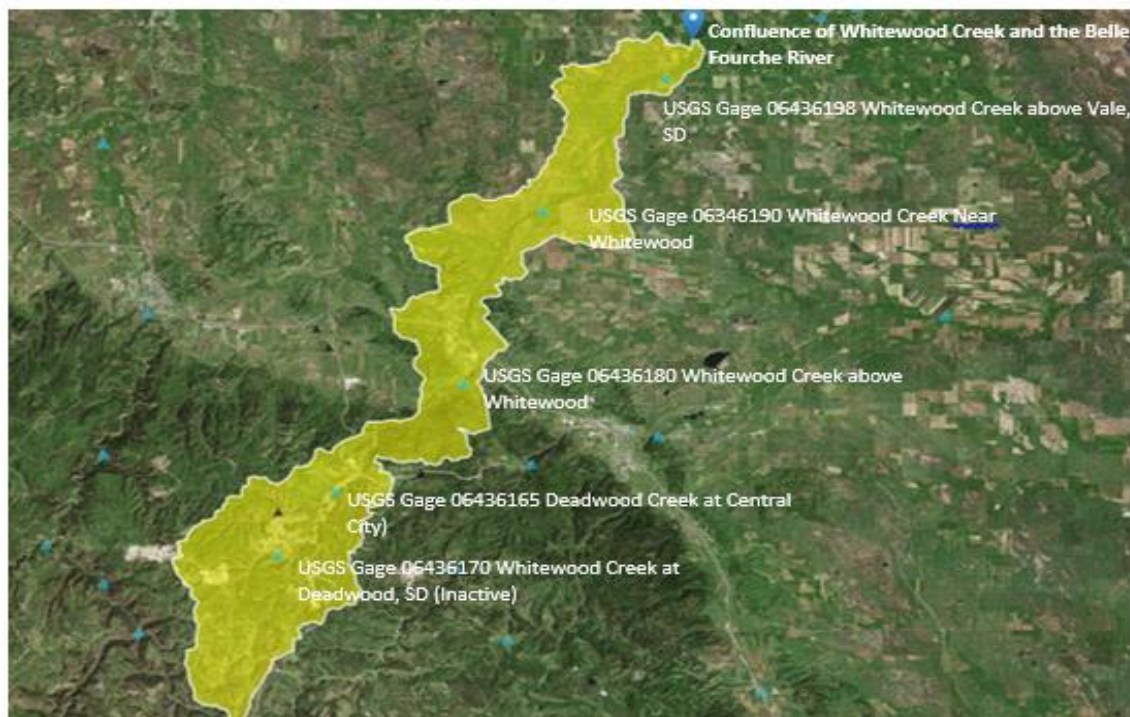


Figure 1.13. Whitewood Creek Basin with USGS gage stations (USGS Streamstats, 2018).

channel, with an average gradient of 0.0016 (Marron, 1992), which is deeply incised into predominately metamorphosed crystalline bedrock. (U.S. EPA, 1990). The lack of an established floodplain in this reach inhibited a suitable depositional environment, contributing to the transport of tailings further downstream. Downstream from the town of Whitewood, Whitewood Creek has an alluvial floodplain and an average gradient of 0.0086. Much of the channel along this lower reach is incised into alluvium and bedrock. Downstream of the town of Whitewood, Whitewood Creek and the Belle Fourche River flow through a gently hilly region primarily used for livestock grazing and agriculture (U.S. EPA, 1997). Figure 1.14 shows the confluence of Whitewood Creek and the Belle Fourche River





Figure 1.14. Google Earth imagery from Oct. 1, 2016. The red point indicates the confluence of Whitewood Creek and Belle Fourche River at 44.6402N latitude-103.4614W longitude. Channel width on the Belle Fourche River is represented by the green line upstream from its confluence with Whitewood Creek. Channel width at that point is approximately 100 feet. Notice that the channel characteristics change, indicating a more braided channel consistent with an increase in sediment load. Stream width decreases by about half, to approximately 50 feet.

Fox Consultants, Inc. (1984) stated that before the start of tailings discharge, Whitewood Creek was a small stream with insufficient capacity to move large quantities of sediment. To adjust for the conveyance of the vast tonnages of tailings sediments into the stream, the stream length of the stream channel diminished, primarily through meander abandonment, thereby increasing the stream gradient and the stream's sediment-carrying capacity (Fox

Consultants, Inc., 1984). These abandoned meanders eventually filled with tailings and natural alluvium. Successive layers of these tailings sediments were deposited in overbank areas, particularly during periods of ice jamming. As the meanders were being abandoned, the stream began a period of downcutting along the course of the present channel. Downcutting was limited by resistant coarse alluvial deposits and by shale outcrops that form the streambed in many places. As a result, Whitewood Creek became a braided channel with shifting small bars and small, unstable islands (Fox Consultants, Inc., 1984).

### **1.4.3 Water Control and Diversions**

Dams built across rivers and streams create reservoirs that impound water for many purposes, including water supply, maintenance of wildlife habitat, flood control, and recreation. The 2,565 dams in South Dakota (USACE, National Inventory of Dams, 2012) play an important role in and are a key component of environmental, hydrologic, ecological, and faunal change in the Cheyenne River Basin within the Missouri River drainage system. These dams and their associated reservoirs were also built for multiple intended uses, including hydropower generation, water supply, flood storage, and recreation. However, reservoirs also intercept and reduce discharge stream flow, causing fluvial sediment to settle and store behind the dam, and the resulting changes to stream sediment have both upstream and downstream consequences. Some of the potential downstream impacts are the increased erosion degradation of the stream bed (channel incision) and the reduction or loss of fluvial features such as mid-channel and transverse bars, which are important to the ecological function

of certain species due to loss of fluvial riparian habitat. The most significant upstream impact is the loss of storage volume in the reservoir. Additional environmental impacts may also result from temperature changes within water in the reservoir, retention of dissolved constituents (Thurman and Fallon, 1995), or leaching of chemicals from contaminated sediments into the reservoir.

USACE (1999 and 2005) performed studies to estimate the extent of sediment accumulation in the reach of the Cheyenne River influenced by Lake Oahe. The Cheyenne River drains a 26,000 mi.<sup>2</sup> area west of the Missouri River, and eventually flows into Lake Oahe approximately 40 miles upstream of the Oahe Dam. These studies provide estimates and quantification of sediment delivered to the reservoir over time (USACE, 1999). Several large hydrologic structures influence flows in the Belle Fourche and Cheyenne Rivers (Figure 1.15). The most significant are the Oahe Dam; the Belle Fourche Reclamation Project, a system of dams and canals used for irrigation; and the Keyhole Dam. Oahe Dam, the largest of these projects, is located on the Missouri River's Oahe Reservoir in Hughes County, SD. Completed in 1958, it is owned and operated by the U.S. Army Corps of Engineers, Northwestern Division, Omaha District (project I.D. 100592). Average monthly Oahe Reservoir pool elevation since 1967 has ranged from between 1,581.9 and 1,619.2 feet, with an average of 1,604.8 feet (USACE, 1999). USACE (2018) lists Oahe Reservoir's primary purposes as debris and flood control, hydroelectric power generation, irrigation, and navigation.

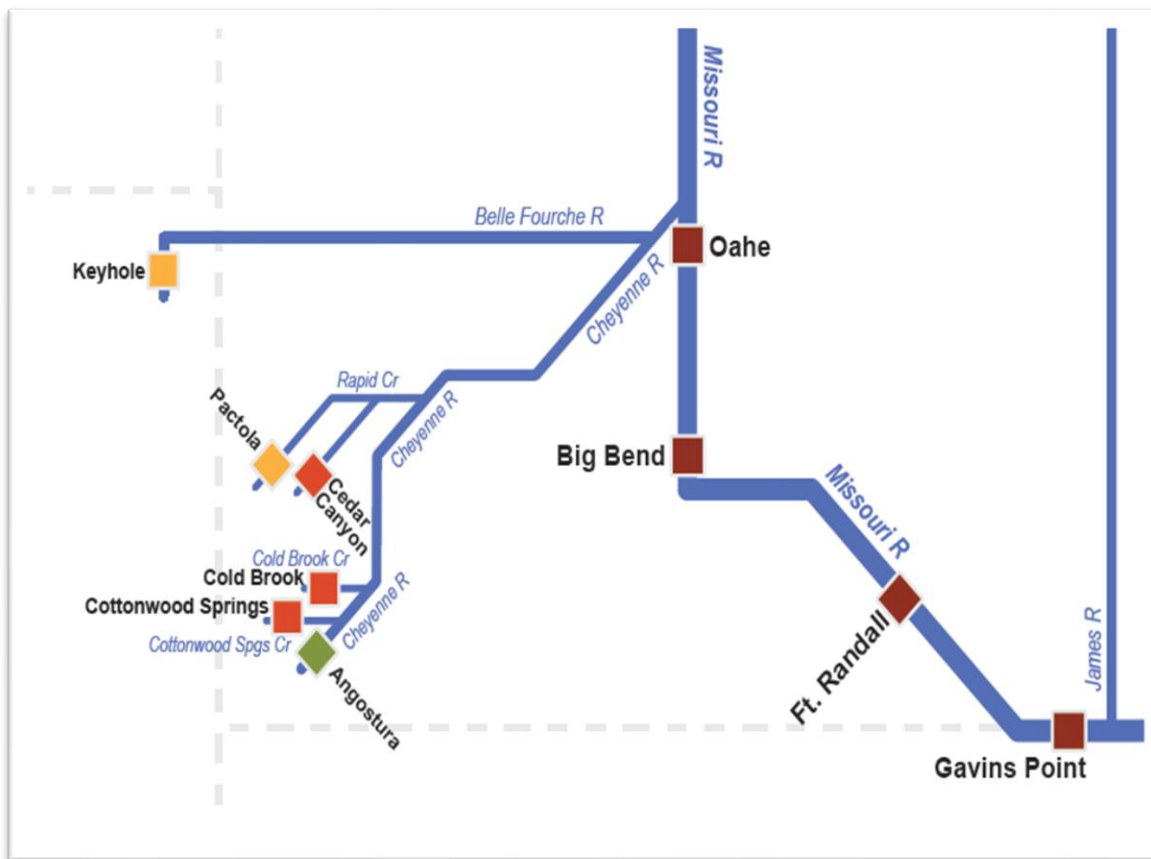


Figure 1.15. Schematic showing idealized model of reservoirs impacting discharges in the Belle Fourche and Cheyenne River (modified from USACE personal communication, 2014).

Completed in 1914, the Belle Fourche Reclamation Project (Figure 1.16) is the second oldest Bureau of Reclamation project in the nation, providing most of the region's irrigation water. It provides about 120,000 acre-feet of water used during the May-September irrigation season. During this period, irrigation drainage comprises most of the streamflow of the Belle Fourche River downstream of the project. In addition, a small amount of irrigation drainage water leaks from this network of unlined canals and drains to recharge

groundwater. A portion of this shallow groundwater moves laterally downgradient into and through the alluvium along major streams, accounting for a large percentage of the base streamflow during the rest of the year (Roddy et al., 1991).

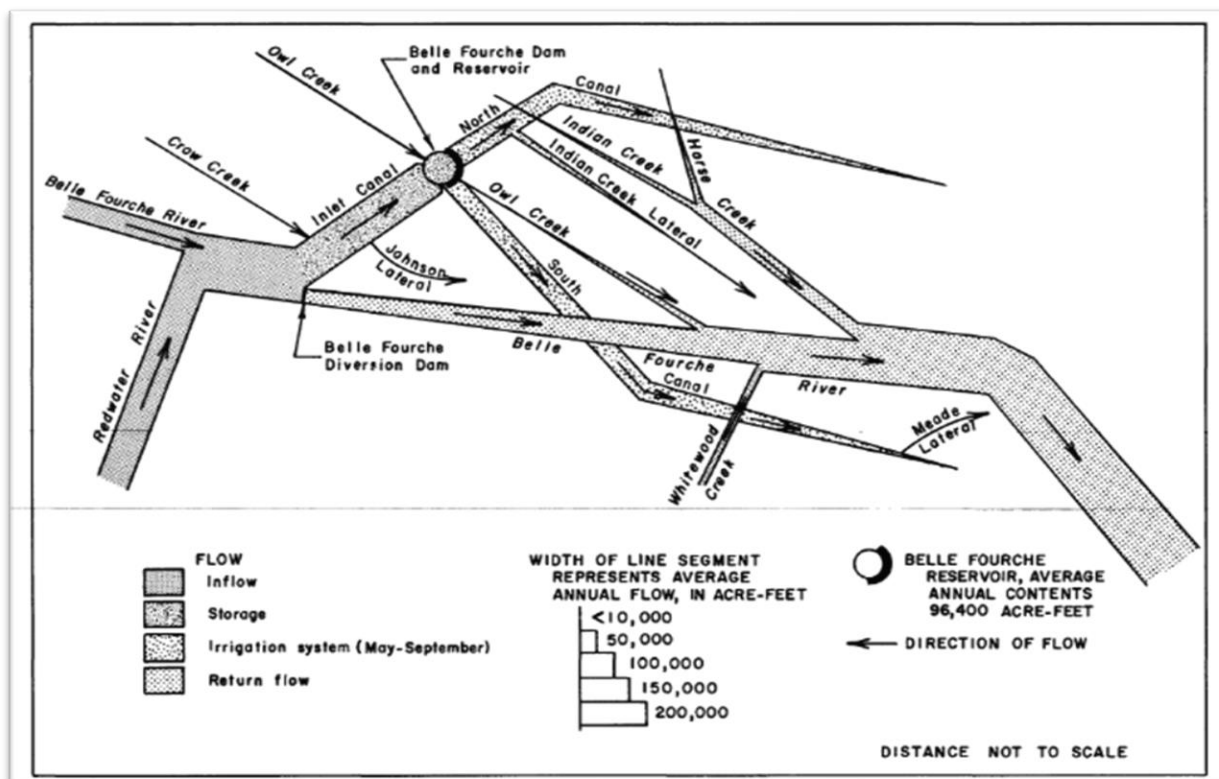


Figure 1.16. Schematic diagram showing diversions, storage, and movement of surface water in the Belle Fourche study area (Roddy et al., 1991).

The Keyhole Reservoir is an earthen dam located in Crook County, Wyoming, on the Belle Fourche River, 146 miles upstream from the Belle Fourche Diversion Dam, part of the Belle Fourche Reclamation Project. Operated by the Bureau of Reclamation for flood control (Roddy et al., 1991), it is used primarily for flood control and storage for riverside irrigation in Wyoming and South Dakota. The Belle Fourche River is generally free flowing except for the input from Keyhole Reservoir.

Belle Fourche River flows also are affected by a diversion to Belle Fourche Reservoir, an off-stream reservoir east of the City of Belle Fourche (and also part of the Belle Fourche Reclamation Project). The diversion canal (inlet canal), completed in 1914, has a capacity of about 1,500 ft<sup>3</sup>/s. The effect of this diversion can be substantial for many peak flows at USGS gage 06436000, Belle Fourche River near Fruitdale, located about five miles downstream. This gage is used to represent background conditions in the study area. Effects from these dams become relatively minor, however, for other stations progressively farther downstream (Roddy et al., 1991). One of the dams most prominent to the study area is the privately owned Grizzly Gulch Tailings Dam, part of the Grizzly Gulch tailings impoundment facility. Completed in 1977, this earthen, 380-ft. high, 2,000-ft. long, structure is located in Lawrence County, SD, near the town of Pluma, close to the former Homestake mining site, at 103.73W longitude-44.333N latitude. It has a maximum storage capacity of more than 20,000 acre-feet (USACE, National Inventory of Dams, 2018)

## Chapter 2: Climate Literature Review and Study Tools Used

### 2.1 Overview

This study will provide an analysis of the Earth's climate system and how the Cheyenne River Basin is affected. Climate change is caused by changes in external factors, called forcings, that may lead to either warming (positive) or cooling (negative). Climate forcings can be classified as either natural or anthropogenic and are also referred to as climate drivers. Natural climate drivers include changes in the sun's energy output, regular changes in Earth's orbital cycle, and volcanic eruptions that eject light-reflecting particles into the upper atmosphere. Examples of anthropogenic forcings include emissions of heat-trapping gases (greenhouse gases (GHG)), land-use changes, increasing atmospheric emissions from human-induced wildfires, and aerosol production and use.

Water quality is affected by changes in stream flow regimes, which are subject to climate change impacts. For this study, observed trends were compared to values reported in peer-reviewed literature and data available about the Cheyenne River Basin. Various climate trajectories are demonstrated by different Representative Concentration Pathway (RCP) forcing scenarios. An RCP is a greenhouse gas (not emissions) trajectory adopted by the IPCC (2014). RCPs — originally RCP2.6, RCP4.5, RCP6, and RCP8.5 — are labelled after a possible range of atmospheric radiative forcings values in the year 2100 (2.6, 4.5, 6, and 8.5 W/m<sup>2</sup>, respectively). The RCPs depict trajectories using tools to downscale climate data from GCMs. (A description of each RCP will be

discussed later in this study.) Although not comprehensive, results provide insight into future studies and climate impacts research in the Cheyenne River Basin. Downscaling global climate change studies to regional watersheds, especially in the context of water quality and ecological impacts, still involves considerable uncertainty. By the use of available tools, this study will provide qualitative insights into the variability in spatial downscaled data when applied to hydrologic systems.

## **2.2 Background**

Global climate change is one of many challenges to the nation's water resources and supporting infrastructure. Water resource managers must make decisions that rely on assumptions about future supplies, demands, weather, climate, and operational constraints at varying space and time scales. It is therefore important to collect, measure, and evaluate climate data over time, as analysis of climate change's impact requires exploration of time-series data. Many governments, academic, and industry organizations have developed tools and web applications to explore hydrologic and climatic time-series data to evaluate and address these impacts on the resources they manage. Atmospheric greenhouse gases include water vapor, CO<sub>2</sub>, methane, and nitrous oxide that can absorb infrared radiation and trap heat (IPCC, 2019). Anthropogenic forcings that increase the concentration of CO<sub>2</sub> and other greenhouse gases are reported to contribute to temperature increases and the creation of a radiative energy imbalance (Kunkel et al., 2013). Anthropogenic



forcing is also reported to increase atmospheric moisture and transport of moisture into storms (Ponce, 2021).

As of Sep. 27, 2021, the latest CO<sub>2</sub> reading was reported by the University of California, San Diego (UCSD) Scripps Institute of Oceanography as 412.97 ppm (UCSD, Scripps Institute of Oceanography, 2021) – an increase from 310 ppm when Dr. Charles Keeling started measuring atmospheric CO<sub>2</sub> in 1956 (UCSD, Scripps Institute of Oceanography, 2013) (Figure 2.1). The upslope depicted in this graph of the Earth's atmospheric CO<sub>2</sub> concentration does not show an equilibrium condition where variables do not change. If the atmosphere is considered as a fluid, at equilibrium the CO<sub>2</sub> concentration would not change with time (Mathinsight.org, 2021).

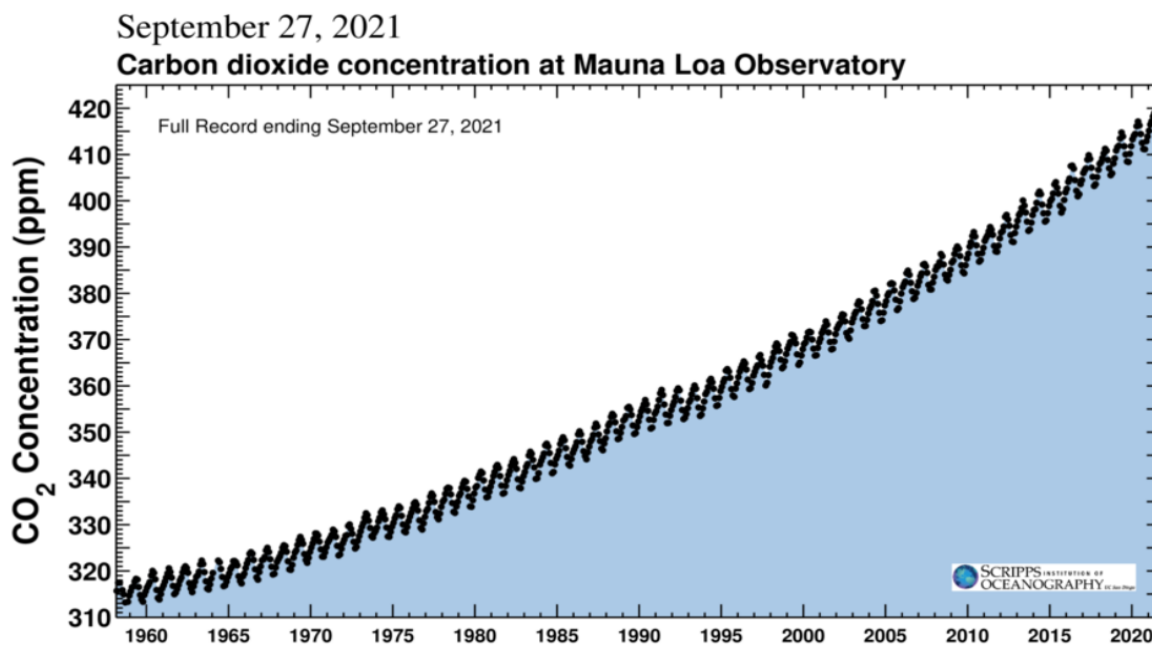


Figure 2.1. History of the Keeling curve as of Sep.27, 2021 (UCSD-Scripps Institute of Oceanography.

[http://bluemoon.ucsd.edu/co2\\_400/mlo\\_full\\_record.pdf](http://bluemoon.ucsd.edu/co2_400/mlo_full_record.pdf)

The IPCC attributes three-fourths of the present atmospheric CO<sub>2</sub> increase to anthropogenic emissions from the burning of fossil fuels, with a small contribution from cement production (2018 IPCC Working Group I: The Scientific Basis: Executive Summary on CO<sub>2</sub> Concentration Trends and Budgets). It further states that on average,  $5.4 \pm 0.3$  Pentagrams (one billion metric tons) of carbon per year (PgC/yr) were emitted during 1980 to 1989, and  $6.3 \pm 0.4$  PgC/yr during 1990 to 1999 (IPCC, 2018). The IPCC (2018) reported that land use change (e.g., deforestation, erosion of agricultural soils, overgrazing, firewood and charcoal production, coastal erosion, etc.) is responsible for the rest of the emissions. Coastal erosion is attributed to storm surges and sea level rise. IPCC figures showed the rate of increase of atmospheric CO<sub>2</sub> content as  $3.3 \pm 0.1$  PgC/yr from 1980 to 1989, and  $3.2 \pm 0.1$  PgC/yr from 1990 to 1999. The IPCC (2019) further reported that these rates are less than the emissions because some of the emitted CO<sub>2</sub> dissolves into the oceans, is taken up by plants, or accumulated in soils as part of the global carbon cycle.

In their model simulations, Allen, and Ingram (2002) state that while the exact climate of 2050 cannot be predicted or the weather inferred on a particular day, the relative likelihood of different long-term trends can be predicted given the observations and physical understanding available today. With CO<sub>2</sub> expected to continue to dominate climate change in the 21<sup>st</sup> century, they focused their study on the impact of anthropogenic carbon dioxide. Allen and Ingram (2002) state that the global-mean temperature response to an increase in CO<sub>2</sub> is controlled largely by three basic properties of the climate system:

(a) The strength of atmospheric and surface feedbacks, which determine the so-called “climate sensitivity” (equilibrium warming on doubling CO<sub>2</sub>);

b) the effective heat capacity of the fraction of the oceans in contact with the atmosphere on short (sub- to inter-annual) timescales; and

(c) how heat export to the ocean depths depends on recent changes at the surface. They further provide evidence which, although regionally specific, identifies a trend that with increasing atmospheric CO<sub>2</sub>, there is also an increase in global-mean precipitation.

Both Allen and Ingram (2002) and Evans (2021) note, however, that the regression between precipitation and temperature does not pass through the origin, resulting in a negative offset and an absolute mean precipitation change per degree of warming slightly less than the increase in the extremes.

The IPCC and other sources used Global Climate Models (GCMs) to assess the impact of the increasing amount of CO<sub>2</sub> and other greenhouse gases by determining land/ocean/atmosphere interactions through different scenarios. GCMs are the primary tools used for projecting future conditions of transient atmospheric circulation variables that are an effect of previously unseen CO<sub>2</sub> levels. The GCMs based on physical algorithms developed with 100-kilometer grids over the Earth are useful tools for assessing anthropogenic CO<sub>2</sub> emissions and their effects on temperature, precipitation, and evaporation at large scales (Samuels et al., 2010; National Research Council, 1995).

Integrating assessments of global climate change with relevant decision-making requires the use of appropriate spatial scale to the levels where specific

actions may be taken. Accordingly, GCMs should be downscaled to watersheds or regions as necessary (Wilbanks and Kates, 1999; O'Brien et al., 2004).

However, due to their large scale, GCMs tend to lack specificity at fine temporal and spatial resolutions, making them less useful for studies in smaller areas over shorter periods of time. This limitation is revealed by inconsistencies between observed climate data and GCM hindcasts. To offset these inconsistencies, climate scientists frequently apply statistical transforms to better fit model outputs to observed data. These adjustments make GCM projections more precise; by applying the same transform to model forecasts, adjusted outputs better align with expected trends at a given location.

Despite these improvements from transform consistency, significant uncertainties may still be introduced by the post-processing required to extract applicable outputs (for example, stream flow data). USACE (2016) addressed these limitations by using an alternate method to obtain projected flows, where statistical transforms directly adjust hydrologic model hindcast data to match observed flow data at a given location. For a given location, assessments can be performed to compare various models and transformations to identify the best approach, using the adjusted model to forecast plausible hydrologic behavior.

Since hydrologic models cannot forecast future climate changes, the challenge is how to pair climate and hydrological models. With large-scale GCMs generally less reliable for analysis of surface and groundwater water balances in regional river basins, the leading tools for these analytical purposes are usually hydrological and agricultural models, used to support water policy, management,

and design decisions (Samuels et al., 2010). These models are often valid for a particular watershed — geographically much smaller in size than the climate model — and usually calibrated with local historical trends of streamflow or groundwater flow.

Climate variability is a crucial factor to assess due to the closely related and influencing effect climate has on stream discharge and sediment transport. Increasing temperatures and variation in precipitation patterns could also alter streamflow, potentially increasing streamflow intermittency and impacting the ecosystem. (Jager and Olden, 2012). Owens (2005) compared climate records and anthropogenic activities to estimate trends in fine-grained sediment fluxes (transport or deposition rates) and found they provide the best explanation of patterns in sediment fluxes. Owens (2005) evaluated many temporal and scaling effects, magnitude-frequency, elevation, hillslope coupling, and floodplain and channel storage effects, and also determined that regional patterns in fine-grained sediment fluxes can be attributed to fluctuations caused by decadal phenomena such as El Niño and the Southern Oscillation. (El Niño is an irregularly recurring flow of unusually warm surface waters from the Pacific Ocean toward and along the South American west coast that disrupts typical regional and global weather patterns. The Southern Oscillation is a periodic seesaw fluctuation in sea-level atmospheric pressures over the southern Pacific and Indian Oceans believed to be linked to El Niño.)

Downton et al. (2005) state that climate changes are likely to change the characteristics of precipitation (e.g., intensity, duration, frequency, amounts).

They recommend that observations from radar, sensors, and satellite be improved and incorporated within models to gain additional insight into the characteristics that influence GCM and hydrologic model results. Wang (2018) and Evans (2021) present evidence that precipitation extremes are increasing in recent years. All investigators refer to the Clausius-Clapeyron relationship, an equation which relates the equilibrium condition between atmospheric temperature and saturation water vapor pressure. For each degree of warming, the atmosphere can hold approximately 7% per degree of Celsius more water vapor before saturation occurs (Trenberth et al., 2003). Evans (2021) presents findings that extreme rain events occur when the atmosphere is close to saturation. Prein et al. (2017) report that in the U.S., extreme precipitation is increasing along with temperature in moist, energy-limited environments, and decreasing abruptly in dry, moisture-limited environments.

Climate change has shifted the climatological baseline and range about which a natural seasonal climate variability occurs. Helsel et al. (2020) report that data analyzed by water resources scientists often have the following characteristics:

- (a) A lower bound of zero, with negative values rarely possible.
- (b) While some variables can take on negative values, such as hydraulic heads measured against some datum, temperatures, or flows in situations where flow reversals are possible (for example, backwater from a larger river or from tidal waters), in most cases hydrologic variables have a lower bound of zero.

(c) The presence of outliers, observations that are considerably higher or lower than the vast majority of the data. High outliers (such as flood discharges that are vastly larger than typical annual floods) are more common in water resources than low outliers

(d) Positive skewness, which is typically a result of the properties listed in points (a) and (b) above.

Skewness can be expected when the values that are farthest from the center of the distribution occur primarily on one side of the center rather than on both sides. An example of a positive-skewed distribution, which is often a good representation of the population of some hydrologic variables, is the lognormal distribution (Figure 2.2)

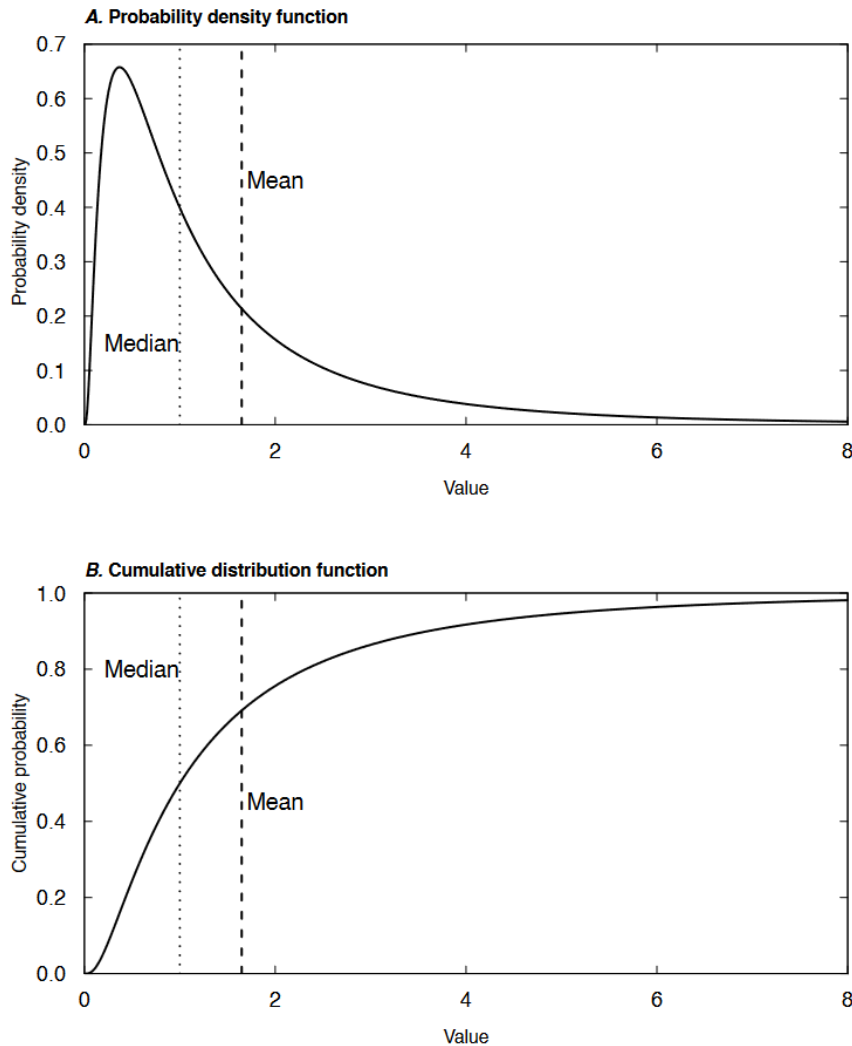


Figure 2.2. Graphs showing a lognormal distribution. A shows the probability density function of a lognormal distribution, showing the location of the population mean and median. B shows the cumulative distribution function (CDF) of the same lognormal distribution (Helsel et al., 2020).

Holdren (2019) (Figure 2.3) also presents how a modest increase in average temperature can shift the extremes of the normally distributed variables.



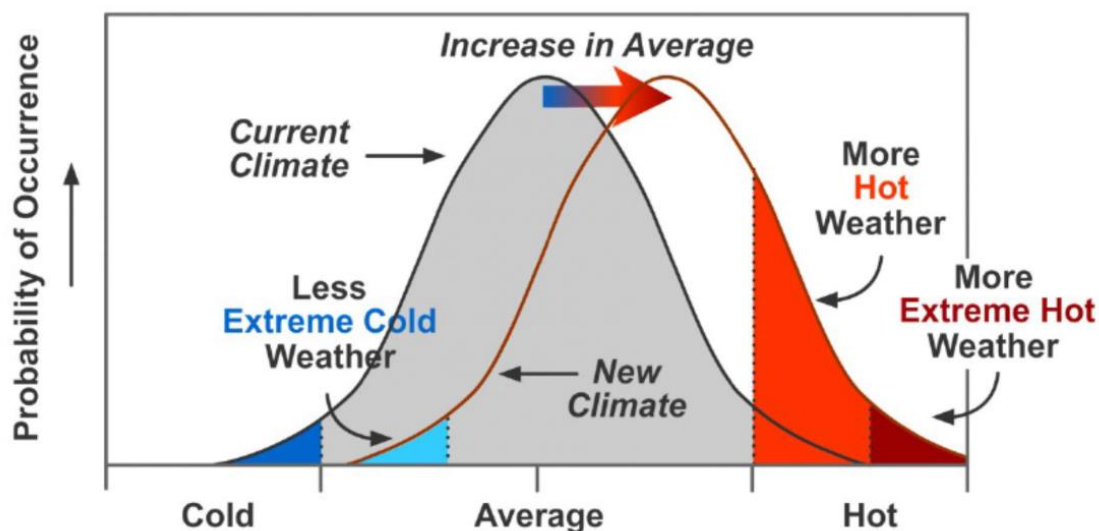


Figure 2.3. Holdren's illustration of the shift in extremes in a warmer climate. For example, once-improbably high temperatures can now occur more frequently. The accentuation of extremes accompanying small changes in the average occurs with any normally distributed variables.

This is important to water managers, scientists, and engineers because many of the calculations necessary to manage, allocate, or design infrastructure associated with fluvial systems rely on assumptions of stationary climatic baselines and a fixed range of natural variability, as captured in the historic hydrologic record. These assumptions may no longer be appropriate for long-term projections of risk. Using the depiction in Figure 2.3, a warming climate is expected to lead to increasing rainfall intensities which can result in increases and flooding and the lengthening of dry spells between rainfall events, shifting the tail of the distribution, with resulting stressors on infrastructure (Ivancic and Shaw, 2016).

With observed and projected precipitation changes, the need exists to improve information for applications and models to estimate regional probable maximum precipitation (PMP), the greatest accumulation of precipitation

meteorologically possible for an area during a given duration. PMP calculations form the basis for many model simulations and scientific and engineering applications such as the design of civil engineering works (Kunkel et al., 2013). With projected changes to climate conditions, events such as 100-year floods (those that currently have a 1% chance of occurring in any given year) are likely to become more common (USGS, 2021; Mallakpour et al., 2019). Future extreme events may exacerbate flooding and stress existing flood control infrastructure, necessitating revisions to design standards for flood infrastructure and a reevaluation of floodplains. Floodplain management and mitigation of flooding are currently left largely to local governments and cities and are thus reliant on local funding and resources for successful implementation. Mallakpour et al. (2019) stated that while the potential effects of more variable and extreme precipitation on infrastructure are obvious, the precise links between specific events and their resulting damage are uncertain as most infrastructure is exposed to both climatic and non-climatic man-made stressors whose effects are difficult to separate without a high degree of monitoring.

In his 2007 book “The Black Swan: The Impact of the Highly Improbable,” Nassim Nicholas Taleb defines black swans as rare and unpredictable outlier events that have extreme impact. He examines the tendency of people to find simplistic after-the-fact explanations for these events. Referencing Taleb in his 2015 article “Black Swans and Pink Flamingos,” Frank Hoffman defines pink flamingos as “known knowns” – widely understood but not acted upon due to organizational cultures and decision-making structures.

Both of these concepts are important in the context of climate change and its physical manifestations in hydrologic systems. Hydrologists and engineers both rely on continual updating of the body of knowledge from multiple disciplines, with application to the planning, design, construction, and operations supporting water allocation and infrastructure. Further study and refinement of hydrological systems should include use not only of historical records but verified hydrologic, meteorologic, agronomic, and ecological data which incorporate reported extreme events (outliers such as floods, significant rainfall events, and droughts) that have increased in recent years. The expectation in science and engineering is that the state of the art/practice continually evolves and is inherently self-correcting as new data, information, and knowledge become available (Pilkey and Ritchie, 2020). However, when it comes to water, the past is not always the best guide for the present, much less for the future. Pew, 2019, wrote: “Over the past century, impact of dams, pipes and pumps has upended the natural movement and storage of water between the land, sea, and air that sustain life. Serious threats now require new thinking,” as climate change has introduced an additional complicating factor (Pew, 2019). But as engineers and scientists increase their understanding of climate change, they will also be able to more accurately account for, reduce, and mitigate associated risk (Pilkey and Ritchie, 2020).

Evidence suggests that these former black swan-type climatically extreme occurrences are becoming part of a new norm. No longer the outliers they once were, they should now merit interpretation as pink flamingos. However, Taleb’s

observation of a human tendency for rationalized responses to these events likely remains valid, especially when faced with the increased cost of building extreme weather event-resilient infrastructure, and associated political ramifications.

Pilkey and Ritchie (2020) state that the current practice of GCMs and their scenarios of GHG emissions through the end of the 21st century are grounded in outdated portrayals of the recent past. Because climate models depend on these scenarios to project future climate behavior, Pilkey and Ritchie say they provide a misleading basis both for developing a scientific evidence base and for informing climate policy discussions. Increasing knowledge will allow stakeholders to understand what impacts they may encounter and begin to incorporate projections to increase their knowledge into basin-wide planning processes. Bill Gates (2021) succinctly summarized that “a little is a lot” due to the profound effect that changing the average global temperature just a few degrees Celsius can have on the physical environment. Carlisle and Wolock et al. (2019) present a similar concept in an ecological context called the “Goldilocks Principle,” which applies to the relation between high-flow streamflow variability and ecosystems: Just the right amount of annual variation is required to maintain ecological health.

### **2.3 Summary Description of Methods**

Changes attributed to natural forcings have always produced climate change and variability throughout the Earth’s history; only recently have anthropogenic forcings significantly affected its climate system. Chapter 6 will present the results and discussions of use of these tools for the study, including

information from the literature, model chains, and modeled projections for study area temperature, precipitation, and area runoff, starting with outputs from the GCM ensembles used in the Coupled Model Intercomparison Project, Phase 5 (CMIP5) (Table 2.1). USACE statistical downscaling techniques (USACE, 2011) and publicly available tools used in this study are can be accessed at [https://www.usace.army.mil/corpsclimate/Public\\_Tools\\_Dev\\_by\\_USACE/Climate-Impacted\\_Hydrology.aspx](https://www.usace.army.mil/corpsclimate/Public_Tools_Dev_by_USACE/Climate-Impacted_Hydrology.aspx). Large-scale Global Climate Model (GCM) data (Table 2.1) was used to dynamically extrapolate the effects of large-scale climate processes to a regional or local scale on the Cheyenne River Basin, SD. These tools transform climate model outputs into statistically refined products that are more appropriate for use as input to regional or local climate impacts studies. These GCM outputs were downscaled using the Bias Correction and Spatial Disaggregation (BCSD) method (Wood et al., 2004). Monthly BCSD outputs drove the Variable Infiltration Capacity (VIC) hydrologic model (Liang et al., 1996) and the Precipitation-Runoff Modeling System (PRMS), a “deterministic, distributed-parameter, physical process-based” modeling system developed to evaluate the response of various combinations of climate and land use on streamflow and general watershed hydrology (USGS, 2021). These tools use area hydrologic model outputs based on annual maximum monthly flow. The downscaled climatology and projected hydrology data produced by USACE (2016) and used in this tool are available online at <https://gdo-dcp.ucllnl.org> Results from this analysis are provided in Chapter 6.

	GCM Name	Modeling Center	RCP used in CHAT
1	ACCESS 1-0	CSIRO-BOM	4.5, 8.5
2	BCC-CSM1-1	BCC	2.6, 4.5, 6.0, 8.5
3	BCC-CSM1-1-1M	BCC	4.5, 8.5
4	CanESM2	CCCma	2.6, 4.5, 8.5
5	CCSM4	NCAR	2.6, 4.5, 6.0, 8.5
6	CESM1-BGC	NSF-DOE-NCAR	4.5, 8.5
7	CESM1-CAM5	NSF-DOE-NCAR	2.6, 4.5, 6.0, 8.5
8	CMCC-CM	CMMC	4.5, 8.5
9	CNRM-CM5	CNRM-CERFACS	4.5, 8.5
10	CSIRO-CM5	CSIRO-QCCE	2.6, 4.5, 6.0, 8.5
11	FGOALS-g2	LASG-CESS	2.6, 4.5, 8.5
12	FIO-ESM	FIO	2.6, 4.5, 6.0, 8.5
13	GFDL-CM3	NOAA-GFDL	2.6, 4.5, 6.0, 8.5
14	GFDL-ESM2G	NOAA-GFDL	2.6, 4.5, 6.0, 8.5
15	GFDL-ESM2M	NOAA-GFDL	2.6, 4.5, 6.0, 8.5
16	GISS-E2-H-CC	NASA-GISS	4.5
17	GISS-E2-R-CC	NASA-GISS	4.5
18	GISS-E2-R	NASA-GISS	2.6, 4.5, 6.0, 8.5
19	HadGEM2-AO	NIMR-KMA	2.6, 4.5, 6.0, 8.5
20	HadGEM2-CC	MOHC	4.5, 8.5
21	HadGEM2-ES	MOHC	2.6, 4.5, 6.0, 8.5
22	INMCM4	INM	4.5, 8.5
23	IPSL-CM5A-LR	IPSL	4.5, 8.5
24	IPSL-CM5A-MR	IPSL	2.6, 4.5, 6.0, 8.5
25	MIROC-ESM	MIROC	2.6, 4.5, 6.0, 8.5
26	MIROC5	MIROC	2.6, 4.5, 6.0, 8.5
27	MPI-ESM-LR	MPI-M	2.6, 4.5, 8.5
28	MPI-ESM-MR	MPI-M	2.6, 4.5, 8.5
29	MRI-CGSME	MRI	2.6, 4.5, 8.5
30	NorESM1-M	NCC	2.6, 4.5, 6.0, 8.5

Table 2.1. GCMs and RCPs used in the Coupled Model Intercomparison Project, Phase 5 (CMIP5), for modeling future hydrologic scenarios with the USACE CHAT tool.

The USACE Climate Hydrology Assessment Tool (CHAT) used in this study was designed to access existing (historic) stream gage data for projecting future climate scenarios by developing standardized, repeatable analytical results using consistent information (USACE, 2016). This tool steps users through a

process of developing information for reporting hydrologic data, including trend detection in observed maximum daily and annual flow. The CHAT was used to determine if the resulting data could be applied to evaluate potential effects on erosion and sediment transport and loads, which are generally correlated with variability and changes in stream flow discharge. Three representative RCPs, representing a low-to-high 21<sup>st</sup> century emissions scenario, were used in the creation of 81 sets of statistically downscaled climate projections for the Cheyenne River Basin. These scenarios (NOAA, 2021) were:

(a) RCP 2.6 Scenario – A scenario in which temperatures would peak by mid-century and then decline to the end of the 21<sup>st</sup> century.

(b) RCP 4.5 Scenario – Referred to as the “stabilization” scenario, meaning that by the year 2100, radiative forcing levels will remain steady at 4.5 W/m<sup>2</sup>, resulting in a moderate overall increase in temperature.

(c) RCP 6.0 Scenario – Uses a high greenhouse gas emission rate and is a stabilization scenario where total radiative forcing stabilizes after 2100 through use of a range of technologies and strategies for reducing GHG emissions. 6.0 W/m<sup>2</sup> refers to the radiative forcing reached by 2100.

(d) RCP 8.5 Scenario – The highest emissions scenario and would result in the largest increases in temperature.

Another tool employed was the USACE Non-stationarity Detection Tool, developed to address the need for multiple types of analytical methods for time series data analysis (USACE, 2019). The Non-stationarity Detection Tool enables a deeper analysis of trend measurement and seasonality, using multiple

regression techniques and statistical methods to identify and define patterns. It was used on stream gage data for multiple sites in the Cheyenne River Basin for the purpose of using statistical tests to evaluate the presence of change points in the data. Non-stationarity analysis is essential to confirming the statistical validity of datasets of physical processes being evaluated. It is used for the important function of differentiating between smooth and abrupt changes in the dataset (IPCC, 2013). This application enables users to visualize and select the most appropriate time series model for a given dataset (Olson et al., 2019).

USACE's Non-stationarity Detection Tool (Friedman et al., 2016) was used to aid in identifying continuous periods of statistically homogenous (stationary) annual instantaneous peak streamflow datasets that can be used for further hydrologic analysis. This tool enables users to conduct monotonic trend analyses on the identified subsets of stationary flow records. It was used to perform a series of statistical tests to assess the stationarity of annual instantaneous peak streamflow data series at USGS streamflow gage sites in the study area with more than 30 years of annual instantaneous peak streamflow records that ideally contained no discontinuities in the peak streamflow. (If the period of record contains significant discontinuities, or if it has been reduced by the user to less than 30 years of data, detected non-stationarities may be inaccurate.) Output from the tool identifies discontinuities, allowing the user to better judge the appropriateness of the data input for the evaluation. Stream gages previously shown in Table 1.3 were evaluated through Water Year 2014.



Analytical results were then applied to future scenarios and potential for sediment transport.

GCMs lack effectiveness at fine temporal and spatial resolutions. This limitation is revealed by inconsistencies between observed climate data and GCM hindcasts. Climate scientists frequently apply statistical transforms to better fit model outputs to observed data. These adjustments make GCM projections more precise. By applying the same transform to model forecasts, adjusted outputs better align with expected trends at a given location. While these outputs resemble the traditional inputs for hydrologic models, there are significant uncertainties introduced by the post-processing required to extract applicable outputs (e.g., stream flows). To address these limitations, USACE tested a prototype method to obtain projected flows, where statistical transforms directly adjust hydrologic model hindcast data to match observed flow data in a given location. This prototype method was used in this study at select stream gages with minimal anthropogenic influence in western South Dakota. The two hydrologic models (VIC and PRMS) and statistical transforms were used to gain qualitative results useful in adjusting models and developing future tools to better assess hydrologic conditions related to climate change.

The goal of regionally downscaling climate models is to develop alternative likely future scenarios, thus enabling consideration of policies that can be effective despite uncertainties and ignorance (Pilkey and Ritchie, 2020). Hirsch et al. (2010) developed changes to methods related to the analysis of long-term surface water flow and water quality. They identified novel approaches

to better describe and understand trends in hydrology and water quality, exploiting technological advances such as the increase in computer and remote sensing capabilities, new methods of exploratory data analysis, and the application of statistical graphics. As an example, scientists can use data from multiple disciplines (stream features; land use; water use, wastewater discharge; diversions; reservoir storage). A current example is the National Water Model (Cohen, Praskievicz, and Maidment, 2018), which allows water managers to use statistical methods, machine learning, and comprehensive models and simulations to improve understanding of streams and rivers. Eng et al. (2013) and Allen and Ingram (2002) (<http://www.climateprediction.net>) predict the near-term achievability of objective, probabilistic forecasts of regional hydrologic changes several orders of magnitude greater than those in use today. Novel approaches using multi-discipline distributed computer processors, models, and datasets will diminish uncertainty, improve scenarios, and help develop more realistic applications. (Allen and Ingram, 2002).

Long-term, natural fluctuations in climate or anthropogenically driven climate change can alter regional precipitation, temperature, and hydrology patterns. This is specifically relevant to hydrology as the assumptions of stationary climatic baselines and a fixed range of natural variability, as captured in the historic hydrologic record, may no longer be appropriate for long-term hydrologic projections. This study seeks to provide qualitative information which can be used to determine how hydrologic variables would respond to climate

change. The results of this qualitative assessment can be used to inform and increase the resilience of existing and proposed projects in the watershed

Natural processes, human activity, and shifts in climate variability are reshaping land surfaces at various rates and scales (Parker et al., 1997), and Schumm (2005) attributes climate as a primary controlling factor in determining river hydrology and type. Chapter 6 will briefly summarize how regional climatic changes on a geologic time scale impact the geomorphology of the South Dakota streams and influence on sediment transport. Within the basin, Stamm et al. (2013) attribute regional geomorphic changes in the Belle Fourche and Cheyenne River to post-continental glacial isostatic tilting. Marron (1992) expressed a vital connection of the routing of sediment through the watershed system and its relationship to basin geomorphology. Jaeger and Olden (2012) confirm the concept of hydrological connectivity, a water-mediated transfer of matter, energy, and/or organisms within or between elements of a typical hydrologic cycle. In addition, Fausch et al. (2002) state the need for understanding geomorphic stream patterns and the effects of runoff and streamflow filled with sediment and debris.

### Chapter 3: Study Area Impacts

Although Homestake Mining Company (later acquired by Barrick Gold Corporation in 2002) (Barrick Gold Corporation, 2001) discontinued the use of mercury in its gold recovery process in December 1970, EPA sampling in 1971 revealed that effluents discharged into Whitewood Creek still contained an estimated 1.1 kg of mercury/day resulting from leaching of ore (Figure 3.1). Walter et al. (1973) identified mercury in fish over 300 miles from the mine discharge site in the Cheyenne River arm of the Oahe Reservoir, attributable to tailings from the Homestake mill at Lead. Even after tailings discharge stopped, a large amount of oxidized and unoxidized metal-containing and arsenic-laden tailings remain on and in the banks and floodplains of Whitewood Creek and the Belle Fourche River (Stach et al., 1978).



Figure 3.1. Flow in Whitewood Creek near the bridge pier immediately downstream from effluent discharge before cessation of tailings discharge in 1977. (Sharples and Sharples, 1986.)

The impacts of restoration programs in the basin are minor compared to the magnitude of impact that mining had on the physical and ecological functions in this watershed. Hemond and Benoit (1988) refer to the cumulative effects on water quality functions that cannot be predicted from the sum of the effects of each individual impact.



Figure 3.2. Homestake Mine, former open cut, Lead, SD, on Aug. 20, 2013; 44.360417N latitude-103.762762W longitude. (Google Earth, 2016; imagery date is Sep. 20, 2013).

Because water quality functions result from the interaction of many individual distinct physical and chemical mechanisms, the nature of each individual process must be considered (Hemond and Benoit, 1988). While impossible to mitigate to the pristine conditions present before significant anthropogenic disturbance, progress has been made. In Dec, 1977, Homestake



completed the construction of the Grizzly Gulch Tailings Impoundment Facility (Figure 2.3). When fully operational, it diverted the discharge of tailings to Whitewood Creek. (Goddard, 1987; USGS Toxics Program, 2013).



Figure 3.3. Grizzly Gulch Tailings Containment Facility, Lead, SD.

In response to many studies in the basin, the EPA designated an 18-mile segment of Whitewood Creek as a Superfund site (Durken et al., 1988). In 1990, partial removal of mine tailings and stabilization measures were initiated. By 1994, the potentially responsible party (PRP), the Homestake Mining Company, had completed cleanup of the mine tailings, including removal and replacement of contaminated soil from 16 residences (U.S. EPA, 2014). Remedial construction along multiple sites on Whitewood Creek was completed in March 1993, and it was delisted from the EPA National Priority List in Aug. 1996 (U.S. EPA, 2014). In 1999, the Water Resources Development Act (WRDA) as

amended in 2000, required a study of sediment contamination in the Cheyenne River “no later than 10 years after the date of enactment” to “take appropriate remedial action to eliminate any public health and environmental risk posed by the contaminated sediment” (33 U.S.C 2352, WRDA, 2000). Homestake Mine closed in 2002 after 126 years of operation. Following its closure, site restoration occurred for several years, including the demolition of the mill buildings and the reclamation of mine dumps and tailings disposal areas (Mining History Association, 2016). Remedial actions did not include areas impacted with mine tailings along the Belle Fourche and Cheyenne Rivers (Figure 3.4). The EPA continues to monitor institutional controls on the site because contaminated sediments still remain (U.S. EPA, 2016).

Strawberry Creek, a small creek near Deadwood, has been impacted by historic mining activity and associated acid drainage (SD DENR, 2020). One of the contributing sources of impairment was Brohm Mining Corporation’s Gilt Edge Mine. In 1999, Brohm’s parent company, Dakota Mining, declared bankruptcy, and the state of South Dakota took over water treatment. In 2000, the site was listed as a Superfund Site. Remediation activities at Gilt Edge Mine are contracted by EPA to HydroGeoLogic, Inc. Successful remediation efforts enabled the delisting of copper, low pH, and zinc as impairment causes in 2010; however, Strawberry Creek continues to be noncompliant for chronic cadmium levels. A cadmium TMDL was approved for Strawberry Creek in April 2010. DENR (2020) reports that several parts of Whitewood Creek near Lead are noncompliant for E. coli; sources of the high bacteria count are likely aging septic

and sewer systems, the combined sewer overflow in Lead, and wildlife and livestock. A surface water discharge permit has been issued to the city of Lead for the combined sewer overflow, requiring compliance with EPA's related minimum controls. The city of Lead is engaged in efforts to separate its sewer

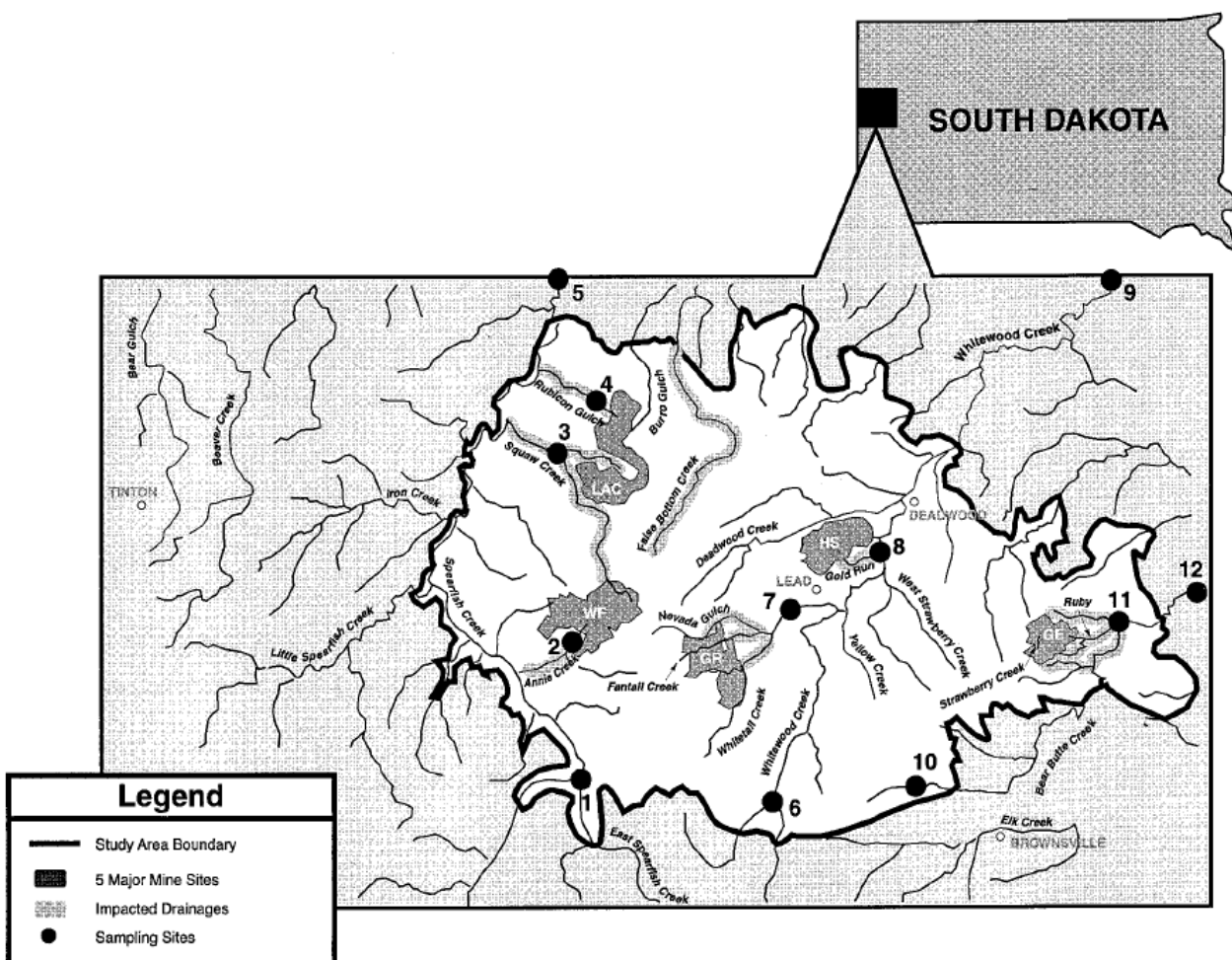


Figure 3.4. Major mine sites in the upper reaches of Whitewood Creek. Most were open-pit operations using cyanide leaching for treatment of low-grade ores. May et al. determined that there continues to be evidence of elevated metal levels in both water and sediment, with the potential of hazardous exposure of biological resources to contaminants even after mitigation and remediation. Study objective was to ascertain whether area streams in the vicinity of these give large-scale gold mines (LAC Resources (LAC); Homestake (HS); Wharf (WF); Golden Reward (GR); and Gilt Edge (GE)) have been impacted (modified from May et al., 2001)



systems, to eliminate this combined overflow. TMDLs are also being developed for the impacted segments of Whitewood Creek. An implementation project has been ongoing since 2004 to address water quality of the Belle Fourche River and tributaries, with efforts mostly focused on irrigation practices to reduce TSS and grazing management practices to reduce bacteria. The Belle Fourche River continues to remain non-supporting for TSS; however, a TMDL was approved in 2005. Fecal coliform and E. coli TMDLs have also been approved for two segments of the Belle Fourche River (DENR, 2020). The EPA continues to advocate for mine waste remediation as a tool to reduce exposure and prioritize proximity and erosion of waste to the surface water, especially where there is visual evidence or a high potential for mine waste to erode into surface water (U.S. EPA, 2013). Mine wastes originally discharged into Whitewood Creek contained heavy metals including arsenic, cadmium, copper, silver, mercury, and/or cyanide, all impacting groundwater, surface water, and/or soils. Total-recoverable-arsenic concentrations at study area sampling sites are shown in Figure 3.5.

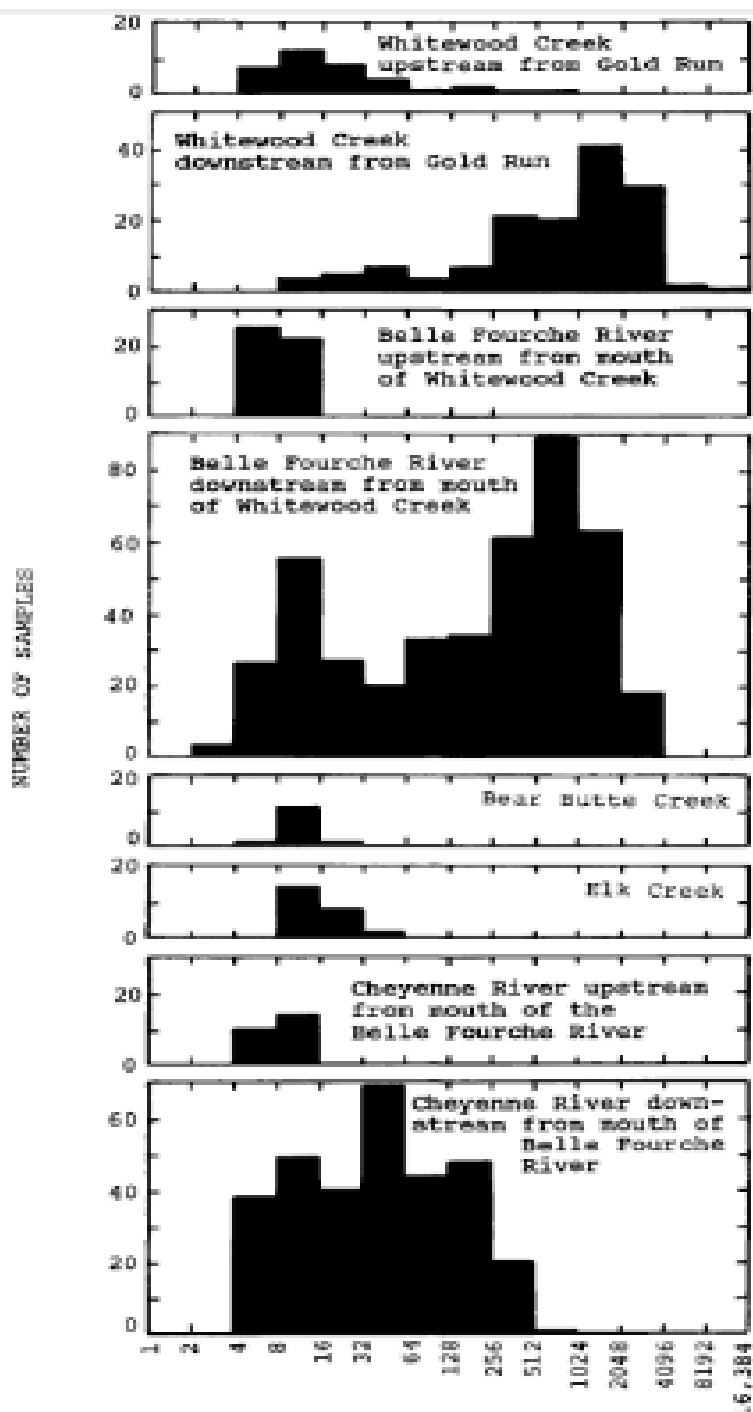


Figure 3.5. Total-Recoverable-Arsenic Concentrations in micrograms/grams displayed as frequency distributions of total-recoverable-arsenic concentrations in sediment samples collected from the flood plains along Whitewood Creek, the Belle Fourche River, Bear Butte and Elk Creeks, and the Cheyenne River (Goddard, 1987).

## Chapter 4: Chemistry

### 4.1 Significance of Arsenic in the Study Area

Arsenic is the primary contaminant of concern, with concentrations in sediment recently reported as high as 600 mg/kg (U.S. EPA, Region 8, 2014). Per the Agency for Toxic Substances and Disease Registry's (ATSDR) toxicological profile, the presence of arsenic fate and transport is an important environmental and public health concern and should be assessed to prevent or reduce exposure (Figure 4.1).

#### **Why is it important to conduct studies to determine fate and transport of arsenic?**

- Arsenic cannot be destroyed in the environment. It can only change its form or become attached to or separated from particles.*
- Arsenic attached to very small particles may stay in the air for many days and travel long distances.*
- Arsenic in soil may be transported by wind or in runoff or may leach into the subsurface soil. Rain and snow remove arsenic dust particles from the air. Arsenic is largely immobile in agricultural soils; therefore, it tends to concentrate and remain in upper soil layers indefinitely.*
- Many common arsenic compounds can dissolve in water. Most of the arsenic in water will ultimately end up in soil or sediment. Transport and partitioning of arsenic in water depends upon its chemical form. Soluble forms move with the water and may be carried long distances. Arsenic may be adsorbed from water onto sediments or soils.*

Figure 4.1. Arsenic in the environment: the importance of arsenic fate and transport studies (ATSDR, 2011).

The U.S. Department of Health and Human Services released a document entitled “Report on Carcinogens” which indicated that arsenic and inorganic arsenic compounds are known to be human carcinogens (U.S. Dept. of HHS, National Toxicology Program, 2016), and also stressing the importance of understanding how and when arsenic may be released from sediments into the environment. Figure 4.2 provides a conceptual model of sediment metal cycling in a hydrological environment (modified from Lynch, et.al, 2017.)

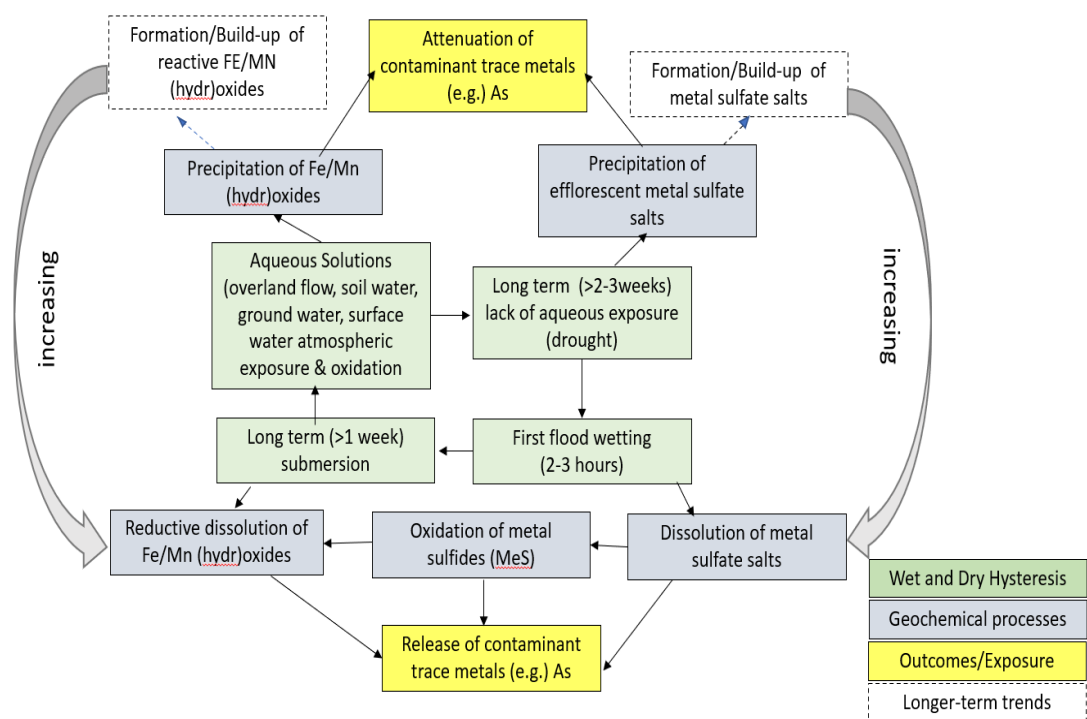


Figure 4.2. Conceptual model of metal cycling showing the hydrological stages in wet and dry cycle and key geochemical mechanisms (modified from Lynch et al., 2017).

The toxicity of arsenic depends on its binding form (Bissen and Frimmel, 2003). Recently published literature also indicates that arsenic may also be an endocrine disruptor. Having a unique mechanism, arsenic appears to act

differently than other endocrine known disrupters such as pesticides. According to Hamilton (2006):

Arsenic does not activate receptors, as some endocrine disruptors do, by mimicking the natural hormone, nor does it block the ability of the normal hormones to activate their specific receptor, as most other endocrine disruptors do. Nor does it affect the ability of the hormone-activated receptor to move to the nucleus of the cell or to bind to DNA to initiate gene expression. Yet, somehow arsenic still strongly affects the ability of these hormone-activated receptors to regulate gene expression (Hamilton, 2006).

Hamilton, a toxicologist at Dartmouth College, found that exposure to very low concentrations of arsenic disrupts the function of the glucocorticoid receptor, a steroid hormone receptor that regulates a wide range of biological processes (Hamilton, 2006). Arsenic appears to suppress the ability of this critical receptor to respond to its normal hormone signal (Hamilton, 2006). At very low doses (in the range of 5-50 ppb), arsenic enhances hormone-stimulated gene expression by two-to-three-fold. At slightly higher doses (in the range of 50-200 ppb, commonly reported in groundwater from wells completed in the mined tailings), arsenic has the exact opposite effect, strongly and almost completely inhibiting hormone-stimulated gene expression by these receptors. This non-conventional dose-response suggests that arsenic might have vastly different biological effects at the lower and higher doses (Hamilton, 2006). Both processes are impacted in the environmentally relevant, and intimately tied to a narrow range

of pH and Eh that exists in the basin which influences arsenic binding and release from mining wastes. through absorption and desorption by chemical, physical, and biological mechanisms (National Technology Program, 2016).

EPA's non-enforceable maximum contaminant level goal (MCLG) for arsenic is zero. EPA has set this level of protection based on the best available science to prevent potential health problems. Based on the MCLG, in 2002, EPA set an enforceable regulation for arsenic, called a maximum contaminant level (MCL), at 0.010 mg/L or 10 parts per billion (ppb) (U.S. EPA, 2002). South Dakota drinking water standards for arsenic follow EPA standards. There are no arsenic water standards for private wells. The National Institute of Environmental Health Sciences (NIEHS) has found that arsenic and inorganic arsenic compounds, even at low levels, can interfere with the body's endocrine system (NIEHS, 2016). In several cell culture and animal models, arsenic has been found to function as an endocrine disruptor, which may underlie many of its health effects (Munoz et al., 2015; Andres et al., 2007).

#### **4.2 Occurrence of Sediment and Impacts**

Tailings contain a mixture of metals, metalloids, and iron sulfides in the mineral forms of pyrites, pyrrohotites, marcasite, and arsenopyrite that were associated with the mined ore (Goddard, 1989). These minerals can oxidize, causing a slow rate of dissolution with decadal impacts. The first system-wide studies of the Whitewood Creek area were conducted in the 1960s by the South Dakota Department of Health (Bergeland, 1976). In 1974-75, the EPA (U.S. EPA 1990) reported that about 50 Holstein cattle in a dairy operation located adjacent

to Whitewood Creek had died of unknown causes. The South Dakota State University Veterinary Department study identified the cause of death as arsenic toxicosis from consumption of corn silage contaminated by accidental incorporation of arsenic-bearing mining wastes with fodder during silo-filling operations (South Dakota Department of Health, 1960).

EPA's Office of Enforcement conducted an investigation in 1971 using aerial remote sensing over Whitewood Creek and the Belle Fourche and Cheyenne Rivers to document their courses and for locating mine tailings deposits for sampling (U.S. EPA, 2002) (Figure 4.3). The remote sensing equipment distinguished between river alluvium and oxidized tailings, with fresh (dark, non-oxidized) tailings easily identified. Unfortunately, after multiple EPA searches of its archives, only the narrative descriptions were found but not the imagery for this comprehensive survey. Multiple previous investigations had identified locations of tailings stored in floodplain sediments (Marron, 1989; Shockley, 1989; Chadima, 2018, personal communication). From the late 1800s until 1977, metallic mercury was used in a mercury amalgamation process to recover gold in the northern Black Hills. Mercury concentrations identified in the 1970s were also a primary catalyst to initiate further basin-wide



Figure 4.3. Iron-stained tailings-laden alluvium lining the banks of Whitewood Creek (Rapid City Journal, 2017)

until 1977, metallic mercury was used in a mercury amalgamation process to recover gold in the northern Black Hills. Mercury concentrations identified in the early 1970s were also a primary catalyst to initiate further basin-wide investigative studies. In 1971, EPA reported 0.1 to 0.5 pounds per day of mercury transported in the Belle Fourche River during periods of low flow. (U.S. EPA, 1971). Hesse et al. (1975) cited an EPA report which revealed that 12-40 pounds of metallic mercury per day had been discharged into the basin since the mine's inception. A sediment sample from the Cheyenne River contained 0.83



parts per million (ppm) of mercury, reflecting the previously heavy use of mercury in the gold extraction process.

Wentz et al. (2014) stated that gold ore deposits were finely ground, elemental mercury was added to amalgamate the gold, and heat was applied to the mixture which vaporized the mercury, which was condensed and recovered for reuse. Placer deposits were flushed through sluice boxes to separate the heavier gold particles from the lighter sand and gravel. Elemental mercury was added to the bottom of the sluice boxes to facilitate the separation, and the gold-mercury amalgam was collected and heated to isolate the gold and recover the mercury. However, mercury recovery from gold mining operations was notoriously inefficient (Wentz et al. 2014).

The mercury component of historical tailings discharge will continue to be released into the aquatic ecosystem or indirectly through emissions to the atmosphere, dispersing this pollutant throughout the basin. Homestake Mine discontinued the use of mercury in its mining operations at EPA's request (Hesse et al., 1975). However, in 1975, five years after this discontinuation, 1.1 kg (2.5 lbs.) of mercury per day was still being leached from stockpiled ore. Hesse et al. (1975) sampled 22 species of birds from the contaminated watershed at three sites on the Cheyenne River and another site on the Belle Fourche River upstream from the confluence of the Belle Fourche and Cheyenne Rivers. Elevated mercury levels were found in the birds with fish as their food source, such as the double-crested cormorant. Levels in non-fish-eating birds were lower, but the mean residues were significantly higher than the mean levels of

control birds. Hesse et al. (1975) found mercury accumulations occurred in the livers of fish-eating birds and the kidneys of non-fish eaters. Mercury residues were compared to muscle-liver, muscle-kidney, and liver-kidney tissue combinations. The study identified a significant correlation ( $P < 0.01$ ) in all three combinations of the animal species examined. The mercury residues found in the Cheyenne River birds were higher than levels previously demonstrated to harm reproduction in certain species of birds. The study indicated that methylmercury is a highly stable organic compound which accumulates primarily in the liver and kidneys and is not rapidly excreted, thus accumulating in the muscles of birds tested. During this study period, five of six piscivorous species were found to have accumulated higher residues in the liver, and 10 of 116 non-fish-eating species had higher kidney mercury levels, indicating that several forms of mercury were in the food chains.

Hesse et al. (1975) cited a 1971 Jernelov and Lann study which implied that a bacterial-mediated process can methylate inorganic mercury in the intestines and in the slime on the outside of the fish. This suggests that all the mercury in fish was in the methylated form and also transferred to the birds in this form. With the identification of mercury in fish over 300 miles from the mine, the U.S. Fish and Wildlife Service (USFWS, 1985) conducted a study at two locations in the Cheyenne River Basin: the first on four species of fish, three species of birds, and sediments on Foster Bay, located at the confluence of the lower Cheyenne River and Oahe Reservoir; and at the second at the Highway 34 Bridge on the Belle Fourche River. Both were sampled because of their "known

history of problem some mercury levels.” (USFWS, 1985). USFWS reported a considerable difference in the mercury content of the livers from birds with different food sources. No mercury was detected in the livers of cliff swallows which have a primary diet of flying insects. Three of eight examined killdeer, which feed mostly on upland grasses and sometimes shorelands, had detectable levels of mercury. The mercury level was highest in the livers of the spotted sandpiper, which feeds on invertebrates along the water’s edge. Levels varied from 0.11 to 5.1 ppm. The EPA threshold for criteria of mercury in fish-tissue is 0.3 ppm (Wentz et al. 2014). USFWS (1985) also reported that great blue herons, with a diet primarily of aquatic life both on and off the river, had liver mercury levels of 0.69 to 2.0 ppm, with a mean of 1.2 ppm. The cormorant, a high-level food-chain predator on fish, had the highest levels with a range of 0.38 to 36.00, with a mean concentration of 9.2 ppm. USFWS (1985) noted that the mercury and selenium content of livers of adult cormorants was significantly higher than in juvenile birds. The report stated that the juveniles are presumed to have accumulated their levels from a local source, but the same assumption cannot necessarily be made with the adult birds.

In 2013-14, The South Dakota Department of Health (SDDOH) sampled three sites in the Cheyenne River Basin: Lake Oahe (Minneconjou Bay), the Belle Fourche River (Willow Creek to Alkali Creek), and the Cheyenne River in both Pennington and Fall River County. It reported that all fish species and sizes tested safe (below acceptable limits). Wentz et al. (2014) state that environmental mercury concentrations began to decrease when mercury use

began to decline in response to 1970s-era legislation to reduce mercury discharge to the air and water. Concentrations decreased in fish during the 1970-1980s but showed no widespread trends during the 1990-2000s (Wentz et al., 2014).

To fully understand patterns of tailings dispersal within the basin, the position of the channel when mining was at its peak needs to be considered. Sediment cycled through the fluvial system during this time contained metals in concentrations that far exceeded those observed in currently active sediments, since mining waste was discharged directly into the river in large quantities. Areas of floodplain close to the mining-era channel still contain high metal concentrations. Several published articles provide clear pictures of tailings dispersal patterns in the floodplain. Depth profiles are available for each of the sites investigated in detail by Marron (1987, 1988, 1989, 1992); Horowitz and Elrick, 1988; Goddard, 1989; Stamm et al., 2012 and 2013; Pfeifle et al., 2018; and DeVore et al., 2019. Figure 4.4 shows transects and arsenic concentrations along the banks of the Belle Fourche River, while Figure 4.5 depicts how arsenic concentrations decrease downstream due to dilutional effects.

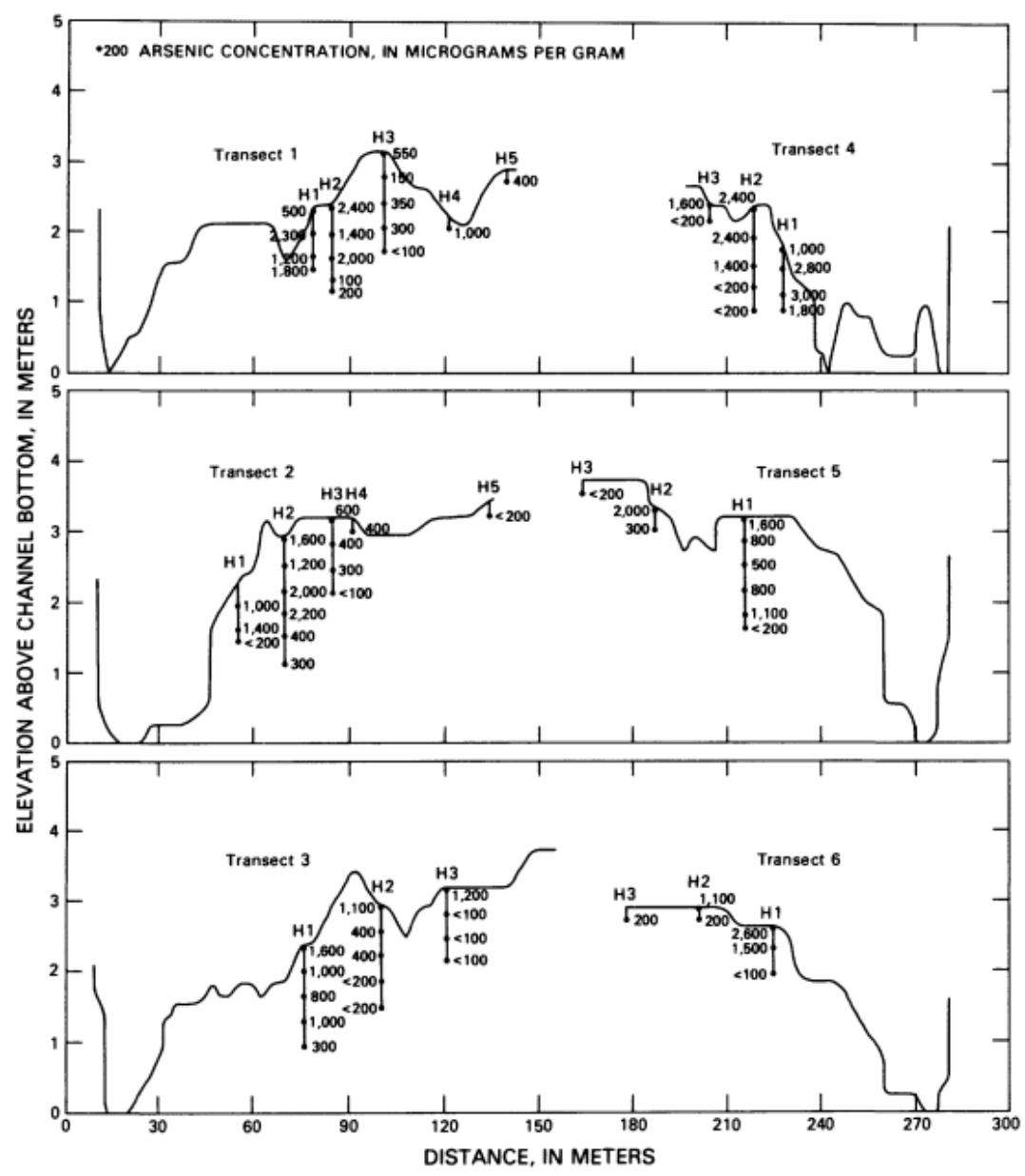


Figure 4.4. Site "C", one of nine transect profiles, auger-hole locations, depths, and arsenic concentrations of sediment samples along the banks of Whitewood Creek and the Belle Fourche River. (Marron, 1988.)

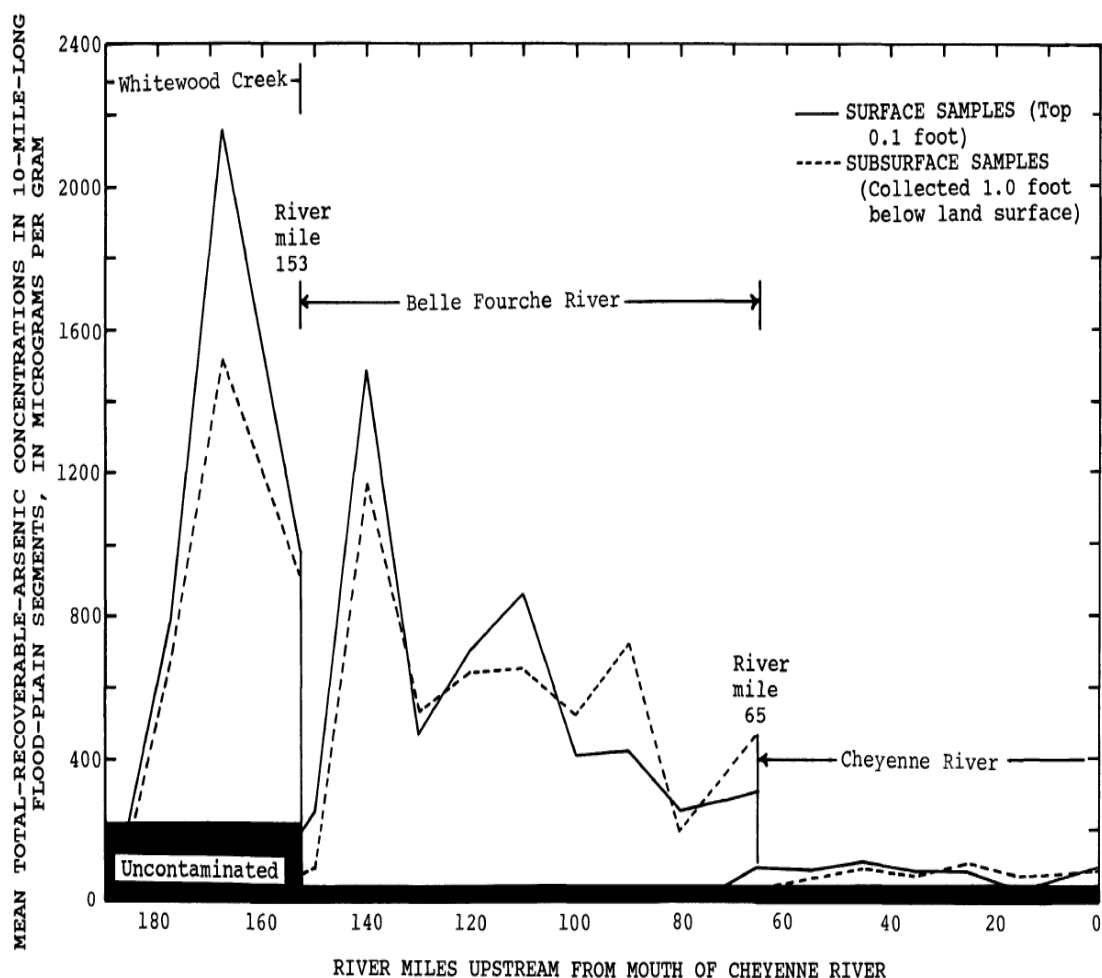


Figure 4.5. Mean total-recoverable arsenic concentrations in surface and subsurface sediment samples collected from the flood plains of Whitewood Creek and the Belle Fourche and Cheyenne Rivers. Arsenic concentrations decrease downstream due to dilutional effects. (Shockley and Goddard, 1989).

Fluvial sediment has been significantly impacted by dams in the study area. Dams built across rivers and streams create reservoirs that impound water for a range of purposes. South Dakota has 2,565 dams (USACE National Inventory of Dams, 2012), many of which play an important role in and are a key component of environmental, hydrologic, ecological, and faunal change in the Cheyenne River and within the Missouri River drainage system. Along with their

resulting reservoirs, they have multiple intended uses, including hydropower generation, water supply, flood control, maintenance of wildlife habitat, and recreation. However, reservoirs also intercept and reduce discharge stream flow-rates, resulting in the settling and storage of fluvial sediment. The change of sediment in the stream may have both upstream and downstream consequences. Some of the potential downstream impacts are the increased erosion of the stream bed (channel incision) and the reduction or loss of fluvial features such as mid-channel and transverse bars, which are important to the ecological function of certain species by the loss of fluvial riparian habitat. The most significant upstream impact is the loss of storage volume in the reservoir. Additional environmental impacts may also result from the increase in temperature of the water in the reservoir, retention of dissolved constituents (Thurman and Fallon, 1995), or leaching of chemicals from contaminated sediments into the reservoir. USACE (1999 and 2005) performed studies to estimate the extent of sediment accumulation in the reach of the Cheyenne River influenced by Lake Oahe (USACE, 1999). The Cheyenne River, drains approximately 26,000 square miles on the west side of the Missouri River and eventually flows into Lake Oahe approximately forty miles of upstream of the Oahe Dam. The study provides estimates and quantification of sediment delivered to the reservoir over time (USACE, 1999).

Flows of the Belle Fourche River also are affected by a diversion to Belle Fourche Reservoir, which is an off-stream reservoir east of Belle Fourche. The diversion canal (Inlet Canal) was completed in June 1914 and has a capacity of

about 1,500 ft<sup>3</sup>/s. The effect of this diversion can be substantial for many peak flows at station 06436000 (map number 105), which is about 5 miles downstream. Effects become relatively minor, however, for other stations progressively farther downstream (Roddy et al., 1991).

The Grizzly Gulch tailings dam figures heavily in this study. Durken et al. (1998) reported that several studies conducted to monitor the adequacy of spent ore neutralization within the tailings impoundment area showed that the neutralization requirements for spent ore have been protective of the environment. However, the Sanford Underground Research Facility (SURF) indicated in a 2013 press release that leachate water from the tailings impounded at Grizzly Gulch contains trace amounts of ammonia. (The SURF, which today occupies the site of the former Homestake mine, has a water treatment plant that also treats water from Grizzly Gulch.)

To determine the maximum reach of tailing concentrations and distributions in the sediment, and to establish a history of trace element deposition from mining-related discharges, Horowitz et al. (1988) took core samples of bottom sediments in the Cheyenne River arm of Lake Oahe (Figure 4.5, with amplifying imagery at Figure 4.6). Core subsamples were analyzed to determine the sediment chemistry, and it was reported that the sedimentation rates in the river arm appear to be event-dominated and rapid, on the order of 6-7 cm per year. Their study postulated that if significant deposition began in the river arm with the opening of the Oahe Dam in 1958, at least two meters of



sediment had been deposited at the time of their study conducted in 1988. Their sedimentation rate measurements are consistent with those of USACE (1999).

The near-surface cored sediments taken by Horowitz et al. had chemical properties similar to the rest of the Cheyenne River bedrock's Cretaceous Pierre Shale, except for arsenic and mercury. Core samples were found to be enriched with both arsenic and mercury compared to levels found in surrounding bedrock. They postulated that the arsenopyrite and mercury were associated with mine tailings transported to the site. In addition, Goddard (1987) reported that sediments containing iron and manganese hydroxides from weathered tailings deposited along the stream banks were also mobilized and deposited along with the unaltered mine tailings. Horowitz et al.(1988) indicated that the post-depositional arsenic appears to be relatively immobile once deposited. Concern exists that an extreme discharge event could scour the deposits, or dredging could remobilize the sediments.

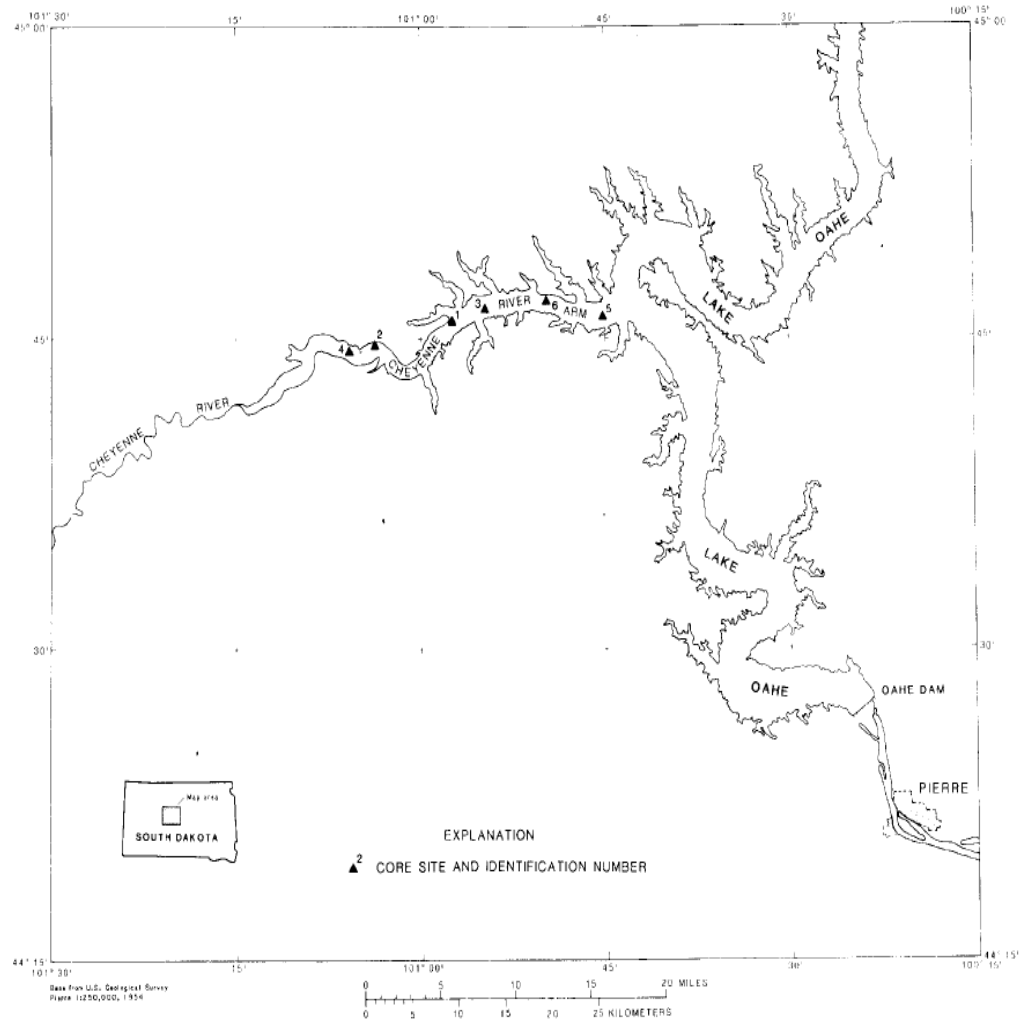


Figure 4.6. Sites of core samples taken in the Cheyenne River arm of Oahe Reservoir (Horowitz et al., 1988).



ISS006E52932

Figure 4.7. Imagery from the International Space Station showing sediment settling as the Cheyenne River discharges into the Cheyenne River arm of the Oahe Reservoir (NASA, 2003).

## Chapter 5: Sediment Mineralogy and Chemistry

Sediment is influenced by a range of physical, chemical, and biological processes all synergistically operating with each other. Sediments adjacent the active stream channel may be subject to more rigorous physical and chemical variations (redox, Eh, pH) caused by river flow, brought about through bioturbation (Kuwabara et al., 1989; Linge, 2008), infiltration and exfiltration of river and ground water through the hyporheic zone (Bencala, 2000; Eggleton, and Thomas, 2004; Caetano et al., 2003; Krause et al., 2011), and reoccurring episodes of repeated exposure and submergence of river bank sediments during floods and droughts (Lynch et al., 2014, Du Laing et al., 2009, Nordstrom, 2009). Pollutant concentrations are typically higher in sediments than in the dissolved phase, and riverine sediment fluxes are dominated by fluvial transported sediments and those physically entering the active channel through mechanical means. Horowitz (1991) and Macklin (1992) found that once a sediment enters a stream, its behavior is not static. Physical erosion of bed sediments can result in transport further downstream. Due to the dynamic nature of floodplains, once deposited, streambank sediments can remobilize, creating more surface area for chemical alteration and bioavailability of contaminants. To provide insight into distribution of tailings in floodplain surface sediments, Stamm et al. (2012 and 2013), DeVore et al. (2019), and Pfeifle et al. (2018) performed studies of floodplain sediments, identifying large gaps in the spatial coverage of geochemical data.

Diffuse sources of pollution can arise from surface-water runoff from tailings (Cherry, et. al, 1986), through inputs of contaminated sub-surface water from the hyporheic zone (Gandy et al., 2007) and from remobilization of arsenic previously deposited contaminated overbank sediment (Gomez and Marron, 1991; Marron, 1989; Marron, 1992). Bencala (2000) refers to the hyporheic zone as a stream/sediment interface or membrane. He describes it as a continuum of interfaces connecting stream water with soil water, root-zone water, riparian (ground) water, quick-flow, delayed-flow, and macropore flow which includes the stream's base flow. Harvey and Bencala (1993) state that these interfaces play the most significant role in the study of in-stream dynamics of solutes, nutrients, and metals.

The uptake, release, and mobility of arsenic compounds in sediment depends on the sediment's size, physical properties, mineralogy, ability to weather, and chemistry. Sediments, whether suspended in water or stored in the river banks, are influenced by changes in temperature, pH, occurrence of oxidation–reduction reactions, precipitation–dissolution, adsorption–desorption, and the chemical composition of the water, especially the presence of competing anions. Conditions that favor the release of arsenic to ground water include the presence of iron oxide and sulfide mineralogy. The mobility of arsenic compounds in sediment is dependent on the type, amount, mineralogy, of adsorbing sediment/soil constituents, the pH value, and the redox potential (Bissen and Frimmel, 2003). Arsenic is influenced by compounds of Fe, Mn, Al, Ca, and Mg, natural organic matter, and clay minerals. Other anions compete

with arsenic anions for adsorption sites on soil constituents and influence the mobility of arsenic compounds. DeVore et al. (2019) found that sediment reaction with bicarbonate and phosphate can result in the release of considerable As to solution due to competitive ion displacement. This finding is important given the alkaline nature of surface waters in the Cheyenne River Basin and the relevance of phosphate as a proxy to evaluate the effect of nutrient inputs into the watershed resulting from livestock and agricultural activities.

Arsenic associated with the mined ore is the primary chemical of concern within alluvium sediments in the Lower Cheyenne River system. Historically, due to the lack of waste treatment and sustainable management practices, metal-bearing slags and unprocessed mine-tailings waste were dumped directly into the streams and are still potentially a source of contamination. As previously reported, because of the diffuse nature of the contaminant source and in-stream transport, metal contaminants can be deposited in particulate and form on riverbanks and floodplains several hundreds of miles from their original points of discharge (Horowitz et al., 1988 and 1989). Thousands of tons of tailings-laden sediments are stored along river banks and floodplains in the Lower Cheyenne River Basin (Marron, 1987; Shockley, 1989; Wuolo, 1986; McKallip et al., 1989). Post-mining contaminated alluvial sediments buried deep within floodplains may remain in “long-term” storage and unavailable for uptake by organisms and plants. Mining alluvial deposits and associated constituents can remain in the sediment for hundreds of years (Stamm, and Hoogenstratt, 2012), potentially posing a long term-threat to streams and potential receptors (Kuwabara and

Fuller, 2003 and 2004; and Kuwabara, et. al, 1989). It is clear that the Cheyenne River system has been highly impacted by anthropogenic influences, with conditions found today very different from those before mining in the Black Hills.

Bed sediment samples in streams typically reflect the geochemical “footprint” of the upstream drainage geochemistry since it originates from upstream erosion and local bedrock and soils. However, in impacted streams, trace element and metal pollution from authigenic sources is also affected by geochemical signatures from mining and smelting industries, since the two are often superimposed (Swennen and Van Der Sluys, 1998). As a result, sampling locations should be adjusted to determine “background” concentrations. Arsenic in surface water is derived primarily from the natural weathering of soils and rocks and from the discharge of ground water, with associated normal background concentrations. However, detectable arsenic concentrations at the levels present in Whitewood Creek and the Belle Fourche River are uncommon in the Lower-Cheyenne River Basin streams. The data for thousands of water, sediment, and biological samples collected for analysis by the USGS from 1960-2018 under the USGS Toxics Study Program are available for several stream gage sites along the Whitewood Creek and Belle Fourche River (some shown in Table 1.3). Goddard (1989) compared natural, uncontaminated-sediment samples with contaminated-sediment samples and identified arsenic as the most anomalous trace constituent. Uncontaminated-sediment samples had a mean arsenic concentration of 9.2 ug/g (micrograms per gram); arsenic concentrations were 1,920 ug/g.in contaminated-samples. Although most of the sulfide minerals

exposed and present in sediment weathered to secondary oxides and hydroxides, arsenic concentrations as much as 11,000 ug/g have been reported in the study area (Goddard, 1989). Figure 5.1 shows arsenic concentrations measured in these collected sediment samples.

Alluvium not directly adjacent the stream is impacted by infiltrating rainfall and locally occurring ground water. As they are not in direct contact with the active stream channel, these deposits are of lower environmental risk (Marron, 1987). However, in a study from 1975-1978, the South Dakota Geological Survey and the USGS reported arsenic groundwater concentrations ranging from 2.5 to 1,530 ug/L in areas containing significant tailings deposits (Stach et al., 1978). Pfeifle (2011) conducted a two-week study in which he analyzed for As and Fe speciation to determine sediment redox chemistry. He found that sites along the Belle Fourche River had the greatest concentration of As in pore water (2,570 ppb) and sediment (1,010 ppm).

The alluvium which lines the stream banks is also a source of and sink for arsenic-bearing sediment. Tailings deposited by the stream are prevalent in the stream itself, its banks, and alluvium and remnant channels. Figure 5.2 highlights areas of alluvium present in the Lower Belle Fourche River that may contain arsenic-laden sediments.



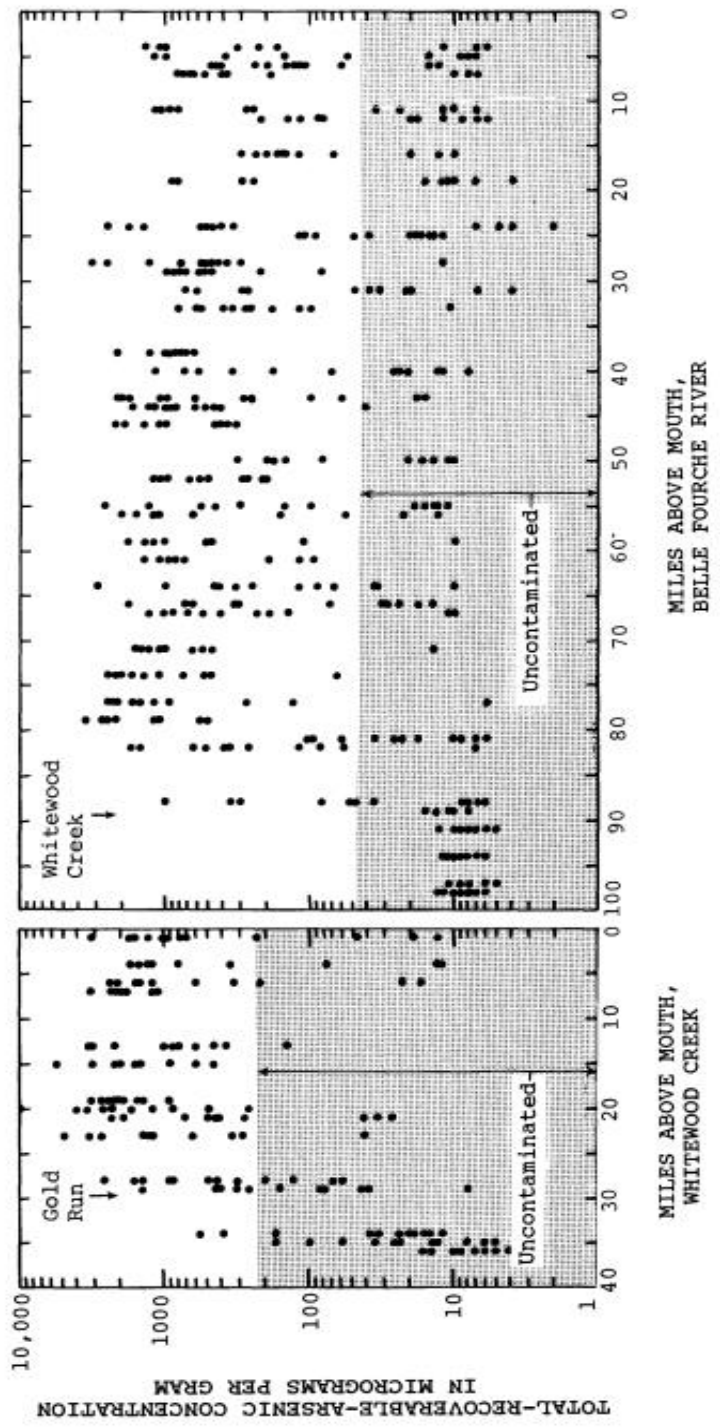


Figure 5.1. Arsenic concentrations measured in sediment samples collected from the flood plains along Whitewood Creek and the Belle Fourche River (Goddard, 1989).

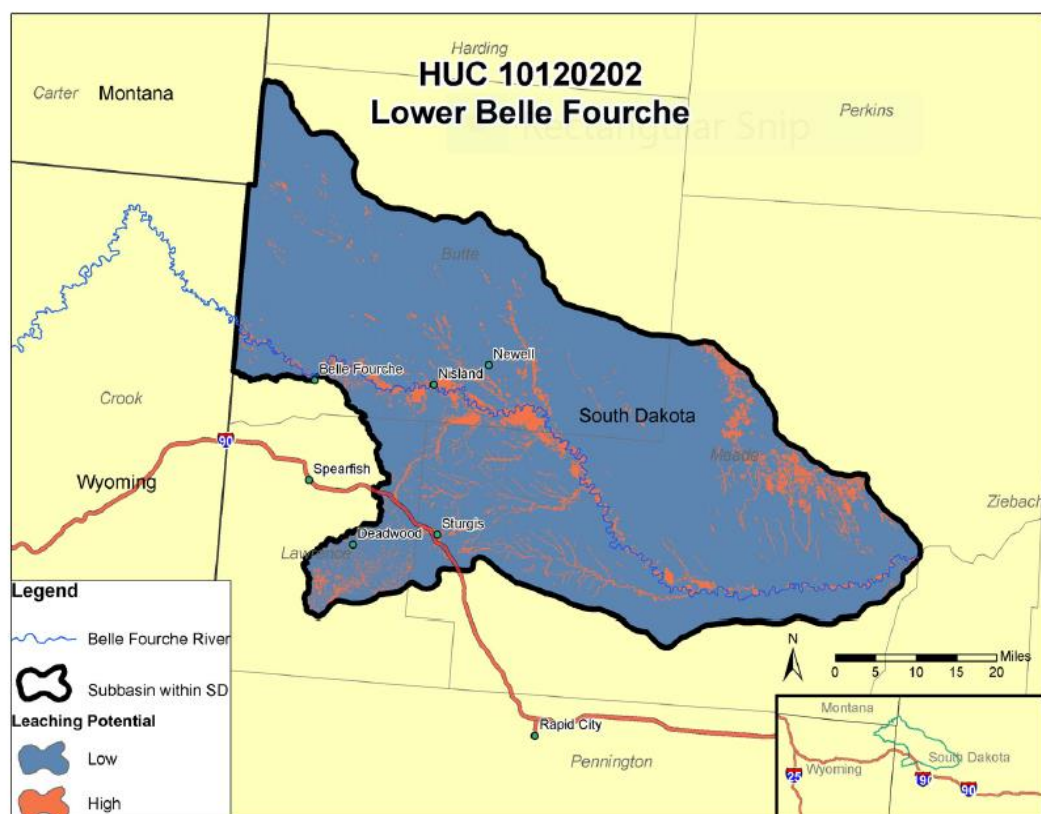


Figure 5.2. Alluvium deposits along the Belle Fourche River with their leaching potential.

Under the Comprehensive Environmental Response and Liability Act (CERCLA), EPA is required to conduct five-year reviews along the remediated stretch of Whitewood Creek. Surface soils at remediated residences in this area are required to be visually inspected after a 50-year or greater flood event (WDC, 2003). This is to ensure that should contaminated materials be redistributed during flooding, residential soil concentrations remain below the 100-ppm arsenic residential soil action level. If inspections indicate reoccurrence of contamination, the PRP must conduct soil sampling. If results indicate

recontamination, contaminated sites require remediation within a year per U.S. EPA's project selected remedy (WDC, 2003, and U.S. EPA, 2007).

Hyporheic zone soils with shallow aquifers are considered vulnerable for contaminate leaching. Saturated hydraulic conductivity ( $K_{sat}$ ), expressed in micrometers per second, refers to the ease with which pores in a saturated soil transmit water. Soils with a  $K_{sat}$  value of greater than 10 micrometers per second and with slopes less than 6% are considered to have a high leaching risk (USDA, 1993). Many areas within the Lower Belle Fourche HUC with high leaching potential (Figure 5.2) are composed predominantly of unconsolidated deposits of alluvial materials in the stream channels. (Not all alluvial deposits represented in Figure 5.2 contain tailings deposits.)

Solid sediment particles can be composed of organic or inorganic mineral fragments containing trace elements derived from soils, rocks, and debris of biological activity with which the water has come in contact. Physical factors of sediment include grain size, specific gravity, exposed surface area, surface charge, bulk density, and cation exchange capacity (CEC), all of which may play a role in its fate and transport. Each of these geochemical properties can be significantly impacted by chemical, geomorphological, meteorological, and hydrological events. Geological factors contributing to spatial variability in erosion and sediments are topography, soil type, composition, and water detention capacity (amount of water trapped in the pores of the soil). Physical chemical factors can vary both locally and regionally, and include pH, CEC, redox reactions, buffering capacity, and hydrolysis. Thomas et al. (2017) provide

an excellent summary of mineralogical and chemical characteristics of mined waste and the weathering processes they encounter. Ollson et al. (2016) found that different mined materials may have order-of-magnitude differences (30-47,000 mg kg<sup>-1</sup>), each having statistically dissimilar arsenic and bio-accessibility values.

The major-ion chemistry of Whitewood Creek and the Belle Fourche and Cheyenne Rivers is controlled by the underlying geologic formations through which they flow. Whitewood Creek flows through “the geologic time-scale,” starting in Precambrian crystalline igneous and metamorphic, Paleozoic sedimentary, and Cretaceous marine sedimentary rocks, then progressively encountering younger geologic formations as it flows from the Black Hills to the plains. Whitewood Creek crosses outcrops of the carbonaceous “Dakota” Madison limestone. The water in its upstream reach is a calcium bicarbonate type consistent with water in contact with carbonate rocks (Driscoll et al., 2002). As Whitewood Creek flows out of the Black Hills, its major-ion chemistry is impacted by the Permian and Triassic Spearfish formation, a unit that contains abundant gypsum. As it continues to flow, it is impacted by the shale that underlies the downstream reach of Whitewood Creek and the Belle Fourche and Cheyenne Rivers.

In their study of the Pierre Shale (prominent bedrock in the Belle Fourche and Cheyenne Rivers), Rolfe and Hadley (1964) identified that the weathered profile of the Pierre Shale is dominated by mica in both the silt and clay fractions. Montmorillonite occurs only in the upper 16 inches of the clay fraction (Figure

5.2). Quartz dominates both size fractions at the surface but decreases with depth. Vermiculite occurs throughout in fairly strong amounts in the silt fraction but varies from weak-to-moderate in the clay. Kaolin content of the silt fraction is dominant at the surface and decreases thereafter. Its content in the clay fraction is moderate in the upper layers and weak in the lower. The feldspar content of the silt fraction is prominent throughout the 21-inch profile of Figure 5.3, but that of the clay fraction is weak, except for the 5-8-inch fraction.



Figure 5.3. Mineral composition of the silt and clay fraction of the weathered profile in the Pierre Shale. (Rolfe and Hadley, 1964).

Hadley and Rolfe (1955) demonstrated what they termed “mineralogical winnowing” – a change in the mineralogical composition of the silt and clay fractions of the transported material as it passes from upland slopes into the stream channel. They also identified a change in the textural composition of the material finer than 1.0 mm as it moves from upland slope into the stream

channel. The weathered material is sorted en route to stream channels; the texture is finer and there are fewer kinds of minerals when it reaches the stream channel.

The interactions of metal cations with clays include adsorption by ion exchange, precipitation as hydroxides or hydrous oxides on clay surfaces, and adsorption as complex species. Arsenic is in the same group or column on the periodic table as phosphate. Arai et al. (2005) indicate that its interactions with calcium ions, amorphous hydroxides of  $\text{Fe}^{3+}$  and  $\text{Al}^{3+}$ , and amorphous allophane are likely more important than adsorption by clay minerals in affecting its solubility at near-neutral pH.

Identified vermiculites or degraded micas are present in the outcrops of weathered Pierre Shale. This process, called potassium fixation, will occur with other ions of similar diameter to about the same extent. Hadley and Rolfe (1955) also reported this phenomenon in the Pierre Shale, attributing the occurrence to the “potassification” or reconstitution of degraded micas between outcrop and stream, or to alteration of vermiculites to montmorillonites.

Given rivers' and streams' dynamic nature, arsenic concentrations will vary with time, season, and location. Concentrations of arsenic within the sediment vary with pH value, the redox potential, and the presences of adsorbents such as oxides, hydroxides of  $\text{Fe(III)}$ ,  $\text{Al(III)}$ ,  $\text{Mn (III/IV)}$ , humic substances, and clay minerals (Bissen and Frimmel, 2003). To determine concentrations in the environment, models of adsorption and desorption should be used to determine environmental fate and exposure. Water quality criteria,

based on results of laboratory batch tests, are assumed to represent toxicity thresholds in pore water (Besser et al., 1997). Besser et al. propose a concept called the sediment quality criteria, or "SQC," which provides an estimate of contaminant concentrations in sediment which are protective of sediment-dwelling organisms. They used the analogy of the  $K(OC)$ , which represents the octanol water partitioning coefficients, to determine behavior of individual organic compounds described by DiToro et al. (1991). Although direct measurement of concentrations of nonpolar organics in pore water is often difficult, pore water concentrations can be modeled by assuming the compounds making up or adsorbed to sediments partition between sediment and pore water. This is because no single sediment component controls metal bioavailability across the range of sediment environments that may be encountered in natural systems like rivers (Besser et al., 1977). The most widely used approach to model metal bioavailability in sediments impacted by mining is based on the tendency of many toxic metals (Cd, Cu, Pb, Ni, and Zn) and metalloids such as arsenic to form highly insoluble metal sulfides in the presence of acid-volatile sulfide (AVS). Metals are predicted to be unavailable, and sediments non-toxic, if the molar sum of the concentrations of metals is less than the molar concentration of AVS (Ankley et al., 1996). Besser et al.'s model defines a conservative "no-effect" condition, rather than a true sediment quality criteria or potential concentration available for exposure. The model does not consider the sorption of metals to sediment components other than AVS, notably organic carbon and hydrous metal oxides. An alternative approach based on direct measurement of metals in

pore water is limited by difficulties of defining and analyzing bioavailable forms of aqueous metals. Table 5.1 depicts relative mobility and availability of trace metals, while Figure 5.4 shows the chemical formulas of metals in solid phases.

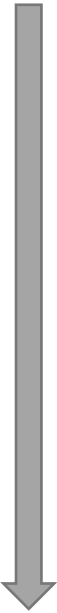
Metal species and association	Mobility	Solubility	
Disordered amorphous sulfides, iron oxides	High	High solubility	
Exchangeable (dissolved) cations	High. Changes in major cationic composition (e.g., estuarine environment may cause a release due to ion exchange).		
Metals associated with Fe-Mn oxides	Medium. Changes in redox conditions may cause a release but some metals precipitate if sulfide mineral present is insoluble		
Metals associated with organic matter	Medium/High. With time, decomposition/oxidation of organic matter occurs		
Metals associated with sulfide minerals	Strongly dependent on environmental conditions. Under oxygen-rich conditions, oxidation of sulfide minerals leads to release of metals.		
Metals fixed in crystalline phase	Low. Only available after weathering or decomposition		Low Solubility

Table 5.1. Relative mobility and availability of trace metals (modified from Salomons, 1995, and USGS download (<https://pubs.usgs.gov/of/1995/ofr-95-0831/CHAP2.pdf>)).



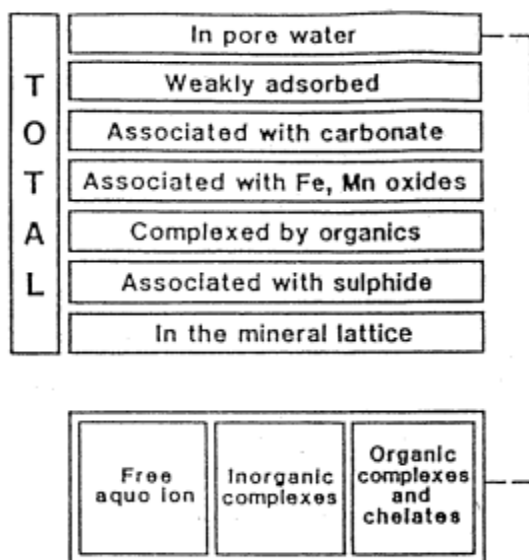


Figure 2. The chemical forms of metals in solid phases. Modified from Gunn and others (1988).

Figure 5.4. The chemical forms of metals in solid phases (modified from Gunn et al., 1988, and Salomons, 1995).

Clay particles have both a size classification (typically being less than 2  $\mu\text{m}$  in diameter) and a functional classification that describe their chemical/mineral constituents. Soils and sediments in natural systems have varying proportions of clay material containing clay-mineral components (usually the phyllosilicates), as well as non-clay-mineral material that may include a variety of substances such as iron and aluminum oxides and hydroxides, quartz, amorphous silica, carbonates, and feldspar. The types of clays found are related to the parent geologic material, climate, topography, and vegetation. From field inspection, clays play a more prominent role in the lower reaches of the Cheyenne River.

Allison and Allison (2005) surveyed data in the literature for 13 metals to characterize the sorption distribution coefficient  $K_d$  in soil, sediment, and suspended matter. They define the metal partition coefficient  $K_d$  (sorption distribution coefficient) is the ratio of sorbed metal concentration (expressed in mg metal per Kg sorbing material) to the dissolved metal concentration (expressed in mg metal per L of solution at equilibrium). Twelve metals exhibited a progression of decreasing affinity for sorption material in the order: suspended matter > sediment > soil. In other words, comparison of mean  $K_d$  values for particular metals showed the result that:  $K_d$  Suspended Particle Matter (SPM) >  $K_d$ ,Sediment >  $K_d$ ,Soil. In two other cases where at least two of the  $K_d$  types could be characterized from the literature data, both followed this same pattern. In addition, a somewhat consistent progression in  $K_d$  magnitude for metals within the three natural media was noted. For the best represented metals, the following patterns of decreasing  $K_d$  were observed (based on ordering the mean  $K_d$  values from highest to lowest magnitude for each medium):

Soils: Pb > CrIII > Hg > As > Zn = Ni > Cd > Cu > Ag > Co

Sediment: Pb > Hg > CrIII > Cu > Ni > Zn > Cd > Ag > Co > As

SPM: Pb > Hg > CrIII = Zn > Ag > Cu = Cd = Co > Ni > As

Allison and Allison (2005) noted similarities in shuffling of the magnitude of  $K_d$  ordering among these media-types, with obvious inconsistency in the progression of  $K_d$  magnitude is for As. They attribute this to the activity of the affinity of these metals (metalloids) due to their unique characteristics in reaction

to their sorbing surfaces. Multiple adsorption surfaces are present in all of these materials. The consistency of affinity relationships among these metals suggests that the distribution of  $K_d$  is partly due to characteristics unique to the metals themselves and partly due to characteristics associated with the sorbing surfaces. Regardless of the reason, Allison and Allison (2005) stated that it is feasible to exploit these trends to provide an estimate of  $K_d$  for a given metal in one medium if its value in another medium is available.

To characterize tailings distributed throughout the lower Cheyenne River Basin, Wuolo, (1983) contracted with the South Dakota School of Mines and Technology Mining Experiment Station to conduct quantitative x-ray diffraction (X-RD) analysis of freeze-dried samples of both pre-and post-mining alluvium from Whitewood Creek. These samples were representative of the composition of tailings deposited throughout the system. Wuolo, (1983) indicated that in most stream bank exposures, the pre-mining and post-mining alluvial boundary was a very distinct oxidized, iron-stained boundary. Results are summarized in Table 5.2. One analysis was performed on freeze-dried samples of pre-mining alluvium (AC-1), and three on post-mining alluvial samples (TC-1, TC-2, and TC-3). Wuolo (1983) found that the major constituent in tailings is quartz, which made up from 50 to 65% of the samples. The minerals chlorite, gruenerite, and hematite are also gangue constituents in the gold ore at Homestake Mine, and important in distinguishing post- from pre-mining alluvium. X-RD highlighted that the pre-mining alluvial sample contained a much higher illite, kaolinite, and calcite (minerals not typically associated with the originally mined ore) content

than the post-mining samples. kaolinite, and calcite (minerals not typically associated with the originally mined ore) content than the post-mining samples. X-RD results from DeVore et al. (2019) found similar mineralogical results. DeVore et al. also conducted batch experiments indicating the release of As(v) was at least 10-times higher after reaching mine waste solids with phosphate, compared to the experiments with bicarbonate. with bicarbonate (Table 5.4). Their results indicate that considerable release of As was observed after reaction with the bicarbonate solution, which has important implications for the water quality conditions in the Cheyenne River Basin. Though As can be released by changes in associate iron minerology, and reductive solution. DeVore et al. (2019) suggest that the mobilization of AS can be affected by phosphate and, to some extent, bicarbonate by competitive ion replacement.

XRD Reported in Wuolo, 1986		Weight %	Variance ±%	Weight %	Variance ±%	Weight %	Variance ±%	Weight %	Variance ±%
Mineral	Chemical Formula								
Illite	(Al,Mg,Fe) <sub>4</sub> O <sub>1</sub>	11	1.4	-	2.6	0.36	-	-	-
Grunerite	Fe <sub>7</sub> Si <sub>8</sub> O <sub>22</sub> (OH) <sub>2</sub>	-	-	2.3	0.31	4.4	0.57	4.6	0.57
Chlorite	(Mg,Fe) <sub>3</sub> (Si,Al) <sub>4</sub> O <sub>10</sub> (OH) <sub>2</sub> ·(Mg,Fe) <sub>3</sub> (OH) <sub>6</sub>	-	-	3.7	0.67	12	1.9	11	1.8
Jarosite <sup>1</sup>	Pb-Jarosite: Pb <sub>0.5</sub> Fe <sub>3</sub> (SO <sub>4</sub> ) <sub>2</sub> (OH) <sub>6</sub> K-Jarosite: KFe <sub>3</sub> (SO <sub>4</sub> ) <sub>2</sub> (OH) <sub>6</sub> H-Jarosite: (H <sub>3</sub> O) <sup>+</sup> Fe <sub>3</sub> (SO <sub>4</sub> ) <sub>2</sub> (OH) <sub>6</sub>	0.45	0.06	-	-	0.94	0.13	2.5	0.32
Quartz	SiO <sub>2</sub>	52	4.3	64	3.8	56	2.7	5.0	2.9
Oligoclase and Anorthite	(NaAlSi <sub>3</sub> O <sub>8</sub> )	4.3	0.58	2.7	0.38	1.9	0.36	2.1	0.28
Dolomite	CaMg(CO <sub>3</sub> ) <sub>2</sub>	12	1.7	0.5	0.08	0.49	0.08	-	-
Hematite	Fe <sub>2</sub> O <sub>3</sub>	-	-	2.1	0.46	0.72	0.16	1.7	0.36
Limonite (amorphous)	FeO(OH)·nH <sub>2</sub> O	3.1	2.8	16	2.2	22	2.5	2.0	2.6
Gypsum	CaSO <sub>4</sub> ·2H <sub>2</sub> O	0.58	0.12	0.45	0.09	-	-	3.0	0.57
Orthoclase	KAlSi <sub>3</sub> O <sub>8</sub>	5.7	1.9	7.9	2.5	-	-	0.9	0.33
Kaolinite	Al <sub>2</sub> Si <sub>2</sub> O <sub>5</sub> (OH) <sub>4</sub>	3.5	0.93	-	-	-	-	-	-
Muscovite	Al <sub>2</sub> Si <sub>2</sub> O <sub>5</sub> (OH) <sub>4</sub>	-	-	-	-	-	-	4.4	0.59
Calcite	CaCO <sub>3</sub>	7.7	4.1	-	-	-	-	-	-
<b>Total</b>		<b>100.63</b>		<b>99.7</b>		<b>101.1</b>		<b>100.2</b>	

1-Formula not specified, mineral variations from Thomas, et al., 2017.  
2-Samples AC-1 Taken on alluvium without tailings. Samples TC-1, TC-2 and TC-3, alluvium contains tailings.

Table 5.2. Weight percentage and variance of major minerals for samples determined by X-RD (after Wuolo, 1986).

Oxide	AC-1 Weight %	TC-1 Weight %	TC-2 Weight %	TC-3 Weight %
SiO <sub>2</sub>	65	73	64	60
Al <sub>2</sub> O <sub>3</sub>	6.7	3.4	4.2	4.9
Na <sub>2</sub> O	0.64	0.43	0.23	0.36
K <sub>2</sub> O	1.6	1.0	0.24	0.63
CoO	8.1	0.53	0.42	1.3
FeO	0.45	1.4	3.3	3.3
Fe <sub>2</sub> O <sub>3</sub>	3.2	15	18.7	19
MgO	2.6	1.0	3	2.8
H <sub>2</sub> O	1.9	2.8	4.7	5.2
CO <sub>2</sub>	8.9	0.23	0.23	0.02
SO <sub>3</sub>	0.41	0.2	0.3	2.2
MnO	0.13	0.12	0.36	0.35
TiO <sub>2</sub>	0.06	0.02	0.04	0.04
PbO	0	0	0	0
NiO	0.01	0	0	0
CuO	0	0	0	0
V <sub>2</sub> O <sub>3</sub>	0	0	0	0
P <sub>2</sub> O <sub>5</sub>	0.1	0.05	0.06	0.06
Cr <sub>2</sub> O <sub>3</sub>	0	0	0	0.03
As <sub>2</sub> O <sub>3</sub>	0	0	0	0
MnO <sub>2</sub>	0	0	0	0
BaO	0	0.01	0	0.02
SrO	0	0	0	0
Li <sub>2</sub> O	0	0	0	0.01
ZnO	0	0	0	0
<b>Total</b>	<b><u>99.8</u></b>	<b><u>99.19</u></b>	<b><u>99.78</u></b>	<b><u>100.22</u></b>

Table 5.3. Weight percentages of major oxides for samples as determined by X-RD (Wuolo, 1986).

Results from the X-RD analysis identified several mineral assemblages associated with ore. Not surprisingly, hematite, amorphous limonite (FeO(OH)·nH<sub>2</sub>O), jarosite (KFe<sup>3+</sup><sub>3</sub>(OH)<sub>6</sub>(SO<sub>4</sub>)<sub>2</sub>), barium, lithium, and chromium oxides were identified in the post-mining samples. Weight percentage of

amorphous limonite is very high in the post-mining alluvium samples (16-22%) compared to limonite percentages in the AC-1 pre-mining sample (3.1%).

The dominance of ferric oxide in post-mining alluvium is further demonstrated by the weigh percentage of oxides in Table 5.3. In the post-mining alluvium samples, the range of Fe<sub>2</sub>O<sub>3</sub> was between 15 and 19% of all oxides but only 3.2% by weight in the pre-mining alluvium. Manganese oxides were also only present in very low percentages. As<sub>2</sub>O<sub>3</sub> was either absent or in amounts too minute to detect for any of the samples. Mineral forms of sulfides such as arsenopyrite were not readily identified in the X-RD scans in low concentrations. Aluminum oxides were relatively high (6-7%) in the pre-mining samples, which can probably be attributed to occurrences in kaolinite and illite rather than an amorphous alluvium coating.

<b>XRD Reported in DeVore et al., 2019</b>		<b>WWC<sup>3</sup></b>	<b>DR<sup>4</sup></b>
<b>Quartz</b>	SiO <sub>2</sub>	77%	<u>75%</u>
<b>Gypsum</b>	CaSO <sub>4</sub> · 2H <sub>2</sub> O	4%	ND
<b>Biotite</b>	K(Mg,Fe) <sub>3</sub> (AlSi <sub>3</sub> O <sub>10</sub> )(F,OH) <sub>2</sub>	7%	7%
<b>Chlorite</b>	(Mg,Fe) <sub>3</sub> (Si,Al) <sub>4</sub> O <sub>10</sub> (OH) <sub>2</sub> · (Mg,Fe) <sub>3</sub> (OH) <sub>6</sub>	6%	6%
<b>Calcite</b>	CaCO <sub>3</sub>	-	2%
<b>Feldspa</b>	(Cation Not Specified) AlSi <sub>3</sub> O <sub>8</sub>	4%	8%
<b>Grunerit</b>	Fe <sub>7</sub> Si <sub>8</sub> O <sub>22</sub> (OH) <sub>2</sub>	<u>2%</u>	<u>2%</u>
<u>3-WWC-Whitewood Creek</u>			<u>100%</u>
<u>4-DR-Deal Ranch (Cheyenne River)</u>			

<b>Total As mg kg-1</b>	2040	235
% Mobilized with HCO <sub>3</sub>	0%	1.30%
% Mobilized with PO <sub>4</sub> <sup>-3</sup>	4.90%	33%
% Mobilized with DI Control	0.00%	0.70%

Table 5.4. Weight percentage and variance of major minerals for samples determined by X-RD (DeVore et al., 2019).

Similar findings were identified by DeVore et al. (2019) and Root et al. (2005). Studying tailings in the semi-arid region at the Iron King Mine and Humboldt Smelter, a Superfund site in central Arizona, Root et al. identified distinct redox gradients in the top 0.5 meters of the tailings and the mineral assemblage. This indicates progressive transformation of ferrous iron sulfides to ferrihydrite and gypsum, which, in turn, weather to form schwertmannite and then jarosite, accompanied by a progressive decrease in pH (7.3–2.3). Root et al. (2015) indicate that arsenic from arsenopyrite oxidation forms complexes on ferrihydrite and binds within jarosite in iron sulfide mine tailings. Similar redox gradients are common throughout the alluvial tailings deposits along Whitewood Creek and the Belle Fourche and Cheyenne Rivers. This is consistent with the findings of Horowitz et al. (1988) in their analysis of cores from the Cheyenne River arm of the Oahe Reservoir.

After analyzing iron precipitated as a mixture of Fe sulfide and an Fe(III)-oxide phase, O'Day (2010) found that with aging, these mixtures formed poorly crystalline hematite. Precipitates were initially amorphous to X-RD and became more crystalline with aging for end members, but the rate of transformation of Fe sulfides and oxides from amorphous to crystalline was generally much slower (weeks to months) when As was present in solution. O'Day (2010) characterized precipitation products by synchrotron X-ray absorption spectroscopy (XAS) at aging times up to a month. O'Day indicated that the local structure around Fe or As was indicative of the final solid products after 210 days of aging. These data suggest that small (perhaps nano-to-micro-meter sized) particles are



nucleating on short time scales consistent with overall thermodynamic stability, but that ripening to long-range crystallographic ordering are inhibited when both Fe and As are present in solution.

Although written in the context of bioaccessibility, Thomas et al. (2017) provide a comprehensive summary of changing conditions of tailings-contaminated sites over time. These sites exhibit similar conditions and have similar mineralogy, chemistry, and molecular processes related to the presence of toxic metal(loid)s in secondary and tertiary weathering products (prevalent in the oxic near-surface of the tailings). They found that the natural oxidative process of weathering that occurs in the decades following tailings deposition decreased the bio-accessibility of the arsenic and lead present. They identified the molecular processes controlling these observations, and report that oxidative weathering decreased the bioaccessibility of As and Pb by adsorption and coprecipitation with ferric iron, including the formation of secondary precipitates such as jarosite, capable of sequestering As and Pb. Conversely, Zn bioaccessibility did increase with weathering extent, as its release was found to be governed by oxygen and pH-dependent mineral stability. By revealing molecular mechanisms controlling contaminant bioaccessibility, the results of these experiments should inform measures to limit contaminant bioaccessibility at similar tailings sites.

Horowitz et al. (1988) analyzed surfaces of the high-arsenic-containing samples by X-RD and scanning electron microscopy (SEM). They could not identify any specific arsenic-bearing phases but found quartz, plagioclase,

feldspar, calcite, and various clay minerals. This finding was confirmed both by SEM and an energy-dispersive X-ray (EDAX) analysis system, implying that no specific arsenic-bearing phase exists in the sample; that the arsenic bearing phases were so diffuse as to be undetectable with these methods; and that arsenic is held in a non-crystalline form undetectable by X-RD or SEM-EDAX techniques. With additional processing, Horowitz et al. (1988) identified high-arsenic bearing size fractions, that were found to be quite fine-grained (4-32  $\mu\text{m}$ ), which revealed both well-crystallized arsenopyrite and amorphous ("framboidal") iron-sulfide low in arsenic (100ppm). Using thermodynamic calculations for interstitial water present in the reducing environment in the cores, Horowitz et al. (1988) presumed that the arsenic was detrital (transported) rather than of an authigenic origin in the sediment column. They also postulated that only ~470 mg of the mineral arsenopyrite in one kilogram of sediment with no other arsenic-bearing source could account for all of the arsenic sample from Core 5 (sampling site shown in Figure 4.6). Horowitz et al. (1988) also found detectable levels of arsenic associated with iron and manganese oxide coatings of sediment grains. Their SEM-EDAX analysis also found octahedral pyrite grains, which are normally associated with hydrothermal deposits and not likely to be formed in place or authigenically. Horowitz et al. (1988) summarized that transport of As into Lake Oahe occurs in association with Fe- and Mn-Oxides, and arsenopyrite As transport appears to be dominated by arsenopyrite "whose apparent provenance" is the Whitewood Creek-Belle Fourche River system.

Taken together, these data suggest that the bioaccessibility and lability of metal(loid)s are altered by mineral weathering, which results in both the downward migration of metal(loid)s to the redox boundary, as well as the precipitation of metal salts at the surface (Root, 2015). Water-soluble efflorescent salts often form on alluvial tailings in the Cheyenne River Basin during dry periods. They are hydrated magnesium sodium sulfate salts accumulated from soil-moisture evaporation, around alluvial seeps. These salts contain heavy metals such as Cu, Ni, Zn, As, and Se. Once inundated with streamflow, they quickly dissolve in the water. (Shockley, 1989, and Roddy et al., 1991).



Figure 5.5. Water-soluble efflorescent salts (Cottonwood Productions, 1986).

Substantial portions of the near-surface sediment exhibited arsenic concentrations similar to bed sediment levels previously reported for the Cretaceous Pierre Shale, which makes up the bedrock in the Cheyenne River bed. The exceptions were concentrations of arsenic and mercury. Study results indicated that As was the only element which appears enriched in the core samples compared to surface sediment levels (Horowitz et al., 1988). The distributions of mercury and arsenic were highly variable, ranging from 0.02 to 0.62 ppm for mercury and 6 to 260 ppm for arsenic. Horowitz et al. (1988) identified well-crystallized arsenopyrite found in high-As bearing strata from two cores. It was probably transported in that form from reducing sediment-storage sites in the banks or floodplains of Whitewood Creek and the Belle Fourche River. Arsenopyrite had not oxidized due to the reducing conditions in the sediment column of the Cheyenne River arm. Some As may also be transported in association with Fe- and Mn-oxides and -hydroxides, remobilized under the reducing conditions in the river arm, and then re-precipitated in authigenic sulfide phases. After deposition, sediments were not oxidized; however, reducing conditions exhibited in the sediment column at 2-3 cm were not significant enough to produce conditions that would differentiate Fe and Mn in the sediment column. Deposited in its mineral crystallized form as arsenopyrite, Horowitz et al. (1988) postulated it was transported from mine tailings deposited upstream of this studied reach. Goddard (1987) also reported that in sediments containing Fe and Mn-oxides, hydroxides were also mobilized and deposited along with the unaltered mine tailings. In either case, Horowitz et al. (1988), indicated that the

post-depositional As appears to be relatively immobile in the sediment column.

There would be reason for concern only if a significant discharge event occurred to remobilize the sediments, or if activity took place to remove the sediment from the channel.

## **Chapter 6: Climate Change Assessment for Hydrologic Systems**

### **6.1 Methods**

Climate change impacts on the hydrology of the Cheyenne River Basin are considered in accordance with the USACE Engineering Construction Bulletin (ECB) 2018-14, “Guidance for Incorporating Climate Change Impacts to Inland Hydrology in Civil Works Studies, Designs and Projects (USACE, 2020),” and USACE Engineering Technical Letter (ETL) 1100-2-3, “Guidance for Detection of Non-stationarities in Annual Maximum Discharges (USACE, 2017 and Friedman et al., 2016).” This assessment is performed to interpret and use climate change information for hydrologic analysis through a qualitative assessment of potential climate change threats and impacts relevant for a broad hydrologic analysis being performed. As indicated in Figure 6.1, qualitative analysis includes consideration of both past (observed) changes and potential future (projected) changes to applicable hydrologic inputs. This analysis uses a weight-of-evidence-based approach to make a qualitative assessment of climate change impacts in the Cheyenne River Basin.

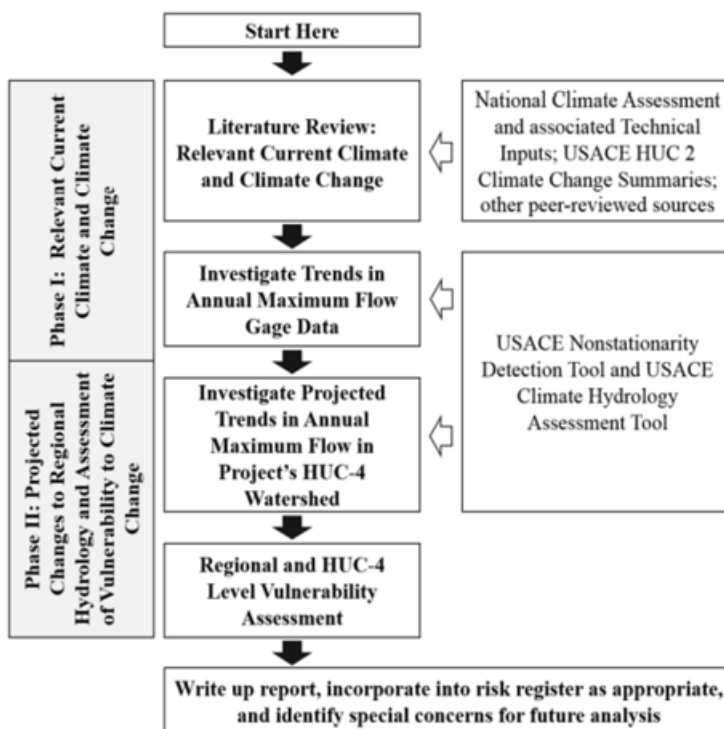


Figure 6.1. Flow chart for performing climate change point assessment (USACE, 2016).

USACE (2021) states that the techniques required to obtain the data for the statistical analysis can be cumbersome, and that the multiple steps required could introduce errors and uncertainty that might adversely affect the results. Refinement of the tools is an iterative, evolving process. Developers work across the community to continually improve methods and available data, and to update tools with the advancement of new methods and techniques as they are discovered and made available. The methods defined by ECB 2018-14 in performing this climate change assessment include:

1. A literature review.

2. An investigation of trends in annual maximum flow in cubic feet per second (cfs), and changes in gage heights in feet at USGS gages.

a. This investigation includes trend detection of observed annual peak instantaneous streamflow in selected watersheds to obtain data for the desired USGS gage. Historical streamflow is presented by water year to develop a trend line, its equation, and a qualitative indication of significance.

b. Based on historical data, projected annual maximum monthly flow range is projected through the year 2100. The range of 93 calculations (32 GCMs and multiple associated RCPs; Table 2.1) to project a qualitative annual maximum monthly flow. The range of projections is generated and displayed with its calculated mean. A trend of annual maximum monthly flow models by water year is developed, with a trend line, its equation, and a qualitative indication of significance. The trend line continues with a projection into the future for the selected HUC-4 (Cheyenne River Basin), along with the equation of the line and its indication of significance.

3. Use of the CHAT (Figure 6.2), which displays simulated historical and projected future climate-changed hydrology (annual maximum of average monthly streamflow) for the selected watershed. CHAT uses the GCM output from the CMIP5, which was created with the Localized Constructed Analogs (LOCA) method of empirical-statistical downscaling (Pierce et al., 2014). The temporal resolution of the modeled hydrologic data is daily and spans the years 1950-2099 (1950-2005 are simulated historical years and 2006-2099 are



projected years). Additional details about the CMIP5-LOCA dataset and spatial downscaling method are documented in Vano et al. (2020), Livneh et al. (2013 and 2015) and online at <http://loca.ucsd.edu/>. Downscaled GCM outputs for temperature, precipitation, and areal runoff for RCPs 4.5 and 8.5 drove the VIC hydrologic model (Liang et al., 1996). VIC outputs routed runoff for 32,824 stream segments, denoted by segment ID number. Modeled hydrology projections used in this study are available at: <https://gdo.dcp.ucllnl.org/>. A subset of 2,517 terminal downstream segment IDs were identified as indicative of cumulative flow. In most cases, these matched up 1-to-1 with the 2,112 HUC8s in the U.S. HUCs with more than one segment, the largest total flow was chosen for use in the model. Output in the default units of cubic meters per second ( $\text{m}^3 \text{sec}^{-1}$ ) were converted to cfs. Model projection data were aggregated to the monthly level by adding up the routed runoff for all days per month. Then, the annual maximum of those monthly values per water year was compared between model runs per HUC8. The minimum, maximum, and mean of those annual maximum monthly flows are plotted on a graph of Model Projected Streamflow. The mean is shown in the Modeled Streamflow Trend illustration.

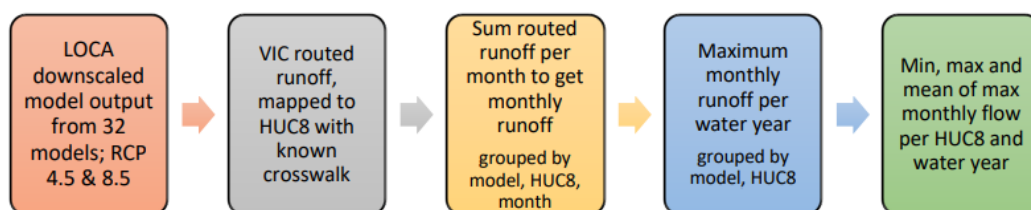


Figure 6.2. Data processing flow for climate model output (USACE, 2020).

4. Detection of Non-stationarities in Observed Peak Streamflow. The Non-stationarity Detection Tool was developed in conjunction with USACE ETL 1100-2-3, Guidance for Detection of Non-stationarities in Annual Maximum Discharges, to detect non-stationarities in maximum annual flow time series. The tool is a mainstay in assessment of the stationarity of all streamflow records analyzed in support of hydrologic analysis. The Non-stationarity Detection Tool enables the user to apply a series of statistical tests to assess the stationarity of annual instantaneous peak streamflow and stream gage stage data series at any USGS gage site with more than 30 years of flow record through Water Year 2014-2020. The tool is intended to aid practitioners in identifying continuous periods of statistically homogenous (stationary) datasets that can be adopted for further hydrologic analysis (USACE, 2021; <https://climate.sec.usace.army.mil/nsd/>). The web tool detects non-stationarities in the historical record to help the user segment the record into flow datasets whose statistical properties can be considered stationary. The tool also allows users to conduct monotonic trend analysis on the resulting subsets of stationary flow records identified. The web tool facilitates direct access to annual maximum streamflow datasets; does not require the user to have specialized software or a background in advanced statistical analysis; provides consistent, repeatable analytical results that support peer review processes; and allows for consistent updates over time. This functionality is contained within three different means:

- Non-stationarity Detector – The Non-stationarity Detector tool uses the different statistical methods in Table 6.1 to detect the presence of both abrupt and smooth non-stationarities in the period of record.
- Trend Analysis – The Trend Analysis sheet displays the results from four different statistical methods for trend analysis.
- Method Explorer – Within the Method Explorer, a user can select any of the twelve non-stationarity detection methods to view independently of the other statistical tests.

Abbreviation	Statistical Method	Type of Statistically Significant Change Being Detected
CVM	Cramer-von-Mises	Distribution
KS	Kolmogorov-Smirnov	Distribution
LP	Lepage	Distribution
END	Energy Divisive	Distribution
LW	Lombard Wilcoxon	Mean
PT	Pettitt	Mean
MW	Mann-Whitney	Mean
BAY	Bayesian	Mean
LM	Lombard Mood	Variance
MD	Mood	Variance
SLM	Smooth Lombard Mood	Smooth/Gradual Change in Variance
SLW	Smooth Lombard Wilcoxon	Smooth/Gradual Change in Mean

Table 6.1. Twelve non-stationarity detection methods within the Non-stationarity Detection Tool.

5. Use of the USACE pilot model comparison tool to evaluate basin-specific climate change by RCP emission scenarios for 30 projections of annual maximum monthly flow with the CMIP-5 GCM (presented in Table 2.1) and the four RCPs discussed in Chapter 1. Results provide an ensemble for gage sites with a publicly available, long-term (1915–2011), hydrologically consistent dataset for the conterminous United States, intended to aid in studies of water and energy exchange at the land surface (Livneh et al., 2013). Monthly Bias

Corrected Spatial Disaggregation (BCSD) outputs drove the VIC hydrologic model (Liang et al., 1996) and the Precipitation-Runoff Modeling System (PRMS), a “deterministic, distributed-parameter, physical process-based” modeling system developed to evaluate the response of various combinations of climate and land use on streamflow and general watershed hydrology (USGS, 2021). These tools use area hydrologic model outputs based on annual maximum monthly flow. The downscaled climatology and projected hydrology data produced by USACE (2016) and used in this tool are available online at <https://gdo-dcp.ucllnl>. Results from this analysis are provided later in this report. The ensemble method was used with projections from multiple GCMs using raw data and calculated flow duration curves. This pilot tool uses recorded historical data from daily or annual maximum discharge rates to inform current and future scenarios of GCMs. The data from GCM projections are then downscaled and routed into the hydrologic models VIC and PRMS with 0.01 quantile steps with multiple quantile mapping strategies, including:

- None- Raw Data
- Non-robust Quantiles (QUANT)
- Parametric Transformation (PTF)
- Robust Quantiles (RQUANT)
- Smoothing Splines (SSPLIN)
- And comparison metrics including:
  - Mean Error
  - Root Mean Squared Error
  - Percent Bias
  - Modified Agreement Index

This tool, still in a developmental stage, provides some insight to improve process understanding and develop additional modeling capabilities.

## 6.2 Purpose

The analysis was conducted to determine if a changing climate's impact can be assessed with regard to existing flood risks, ecosystem sustainment, and engineered projects in the basin system using published data in the Cheyenne River Watershed HUC 4 located within the larger Missouri River Basin HUC 10 (Table 1.1). This study also seeks to provide qualitative information that can be useful in considering potential directions to be taken to assess the impacts from climate change.

This study's initial step is a qualitative assessment to determine the relevance of climate change in the study area. The long-term, hydrologically consistent datasets that were used form the basis for initially evaluating response of hydrologic parameters to changing climatic conditions. Results of the analysis are compared to historical data and the available literature.

The USACE Recent US Climate Change and Hydrology literature applicable to USACE's missions document provides a summary of the best, recent climate literature for the U.S. by region (USACE, 2015). Additional publications containing information on assessments within the Basin were also reviewed and included in this assessment when relevant. Qualitative climate change assessment was then conducted using USACE ECB 2018-14 (USACE, 2020) and ETL 1100-2-3. This assessment included both a literature review and analysis of data from USGS gages within the Cheyenne River Basin and its tributaries. The study area was previously discussed in depth characterized in Chapter 1. Datasets publicly available on the web were also used to perform

analyses. They were input into available climate assessment tools used to estimate projected trends in specific locations and also in climate projection scenarios a basin scale. Tools from other federal agencies were also evaluated, with their results compared to results from the tools and methods from the USACE.

### **6.3 Literature Review Summary**

Chapter two's literature review summarized peer-reviewed science about natural and anthropogenic climate trends in the study region. It does not attempt to identify the causes of climate change (e.g., natural or anthropogenic sources). This chapter's literature review is hydrologically oriented. A synthesis of authoritative, publicly available sources and historical data was evaluated and summarized to identify and address significant hydrologic-related impacts of climate variables. Observed climate data are used to assess historical climate trends. Climate literature from other federal agencies, academia, and peer-reviewed literature sources was also used, with citations and references in the bibliography.

GCMs of the Earth's thermodynamic system are used to model projected future precipitation and temperature (USACE, 2015). GCMs have substantial uncertainty associated with their estimates; however, these computer models represent the best available science to predict trends in climate (USACE, 2015)

Engineers and scientists track, record, and develop methods from historical records, including an allowance to account for uncertainty and to

provide results useful for the planning, design, construction, and operation of the water control facilities at a site or within the basin. Most engineering and hydrologic projects are implemented to accommodate the range of regional or localized natural climatic and hydrologic variability of flow in the river, with the intent of meeting a defined purpose (USGS, 2021, NOAA, 2021). If data are not available, or where observed records are limited and detailed analytical or dynamic representations of physical processes are not available, engineering design factors are incorporated to provide a margin for uncertainty for the range of conditions, using engineering hydrologic or hydraulic algorithms and models (NAS, 2013). Safe, cost-effective water infrastructure design depends on the employment of effective methodologies to conduct hydrologic assessments of factors including frequency of events, sensitivity to changes, and adaptive capacity (ability to plan or mitigate a response). Accuracy of discharge measurements and estimation of hydrologic trends influence the accuracy of an engineered design, and are important parts of any climate change hydrologic study or watershed climate change assessment (McCuen and Galloway, 2010).

C.S. Holling (1973) used the term “resilience” to help understand the non-linear dynamics or hysteresis of natural systems. Many models are not suited for measuring resilience. Lebel et al. (2006) state that to understand a natural system’s resilience in adapting to climate change, a systems approach should be taken to identify the external or internal origins contributions and the adaptive capacity of the entire system. Understanding of resilience is also useful as a context for looking at how systems can shift from relatively stable states toward

increasing instability, or to an entirely different state altogether. Holling and Meffe (1996) describe two common types of resilience in ecological systems: equilibrium (engineering) resilience and ecosystem (ecological) resilience. The first represents an effort to simplify and maintain systems at a steady state where resilience is measured as a function of the ability of the system to return to an equilibrium condition after a perturbation or shock. The second term, “ecological resilience,” is the amount of disturbance an ecosystem can withstand or stay constant without changing processes and structures, or the time it takes to return to a stable state following a disturbance. Carpenter et al. (2001) define resilience as the magnitude of disturbance a system can tolerate before it changes its structure in response to the variables and processes that control its behavior. Carpenter et al. (2001) use the mathematical concepts of state space (essentially, the set of all possible configurations of a system) and domain of attraction, or DoA (essentially, some starting point in state space for convergence to equilibrium), as part of their definition. They state that a system’s ability to move toward a point of stable equilibrium within a DoA, is related to slowly changing variables or disturbance regimes which control the DoA’s boundaries, or the frequency of events that could push the system across the DoA. If, forced by external drivers, a system is subject to a magnitude of disturbance beyond which it can tolerate, it will move to a different region of state space controlled by a different set of processes.

An example of resilience in the Cheyenne River Basin is its assimilative capacity of carbonate minerals in the mine tailings, stream alluvium, and



carboniferous shale bedrock, which prevents sulfide-derived acid generation (“acid mine drainage (AMD)”) in mining tailings. AMD is commonly found at other mined sites (Marron, 1988). Goddard (1989) reported that carbonate minerals, also common in the mined ore, are rare in the contaminated sediment samples collected as part of his late 1980s study. Calcite was detected in only six of 46 samples, and siderite and dolomite were each detected only once. These results differ from those reported by Cherry et al. (1986), who detected calcite in five of nine samples, siderite in four, and dolomite in four. Both the rarity of carbonate minerals in the contaminated-sediment samples analyzed during Goddard’s study, and the contrasting data with Cherry et al.’s may be attributable to the different locations from which the sample groups were collected. The samples analyzed in the Goddard study were collected from trenches in streamside deposits and from cores obtained from thin deposits on the flood plain along the Belle Fourche River – places where the carbonate had already been utilized. Almost all the samples for the Goddard study were collected at depths of less than five feet from the land surface and many were from areas that were inundated yearly by the Belle Fourche River. Goddard (1989) indicated that calcite and other soluble carbonate minerals may have been removed by solution, a process that would be hastened by acids produced during sulfide-mineral oxidation.

Hysteresis is a common phenomenon in which a physical system’s response to an external influence depends not only on the present magnitude of that influence but also on the system’s previous history. Examples of hysteresis

include biological diurnal systems and seasonal systems. In hydrology, it can be used as a model to describe system component processes such as river discharge, soil moisture tension, solute concentrations, and suspended sediment concentrations. Hysteresis in river discharge occurs during unsteady flow when the water surface slope changes due to either rapidly rising or rapidly falling water levels in a channel control reach. An understanding of hysteresis can be helpful in determining hydrological system processes. Suspended sediment concentrations generally show clockwise, or positive, hysteresis loops. Suspended sediment concentrations on the rising limb of a storm hydrograph are higher than those measured at equivalent flows on the falling limb, so sediment concentrations typically reach their maximum before the hydrograph peak (Figure 6.3). Among other factors, this effect is caused by sediment depletion in the channel system or the increased portion of the baseflow during the recession limb. But counterclockwise hysteresis can also occur (Kumar, 2011) due to such factors as bank collapse or sediment originating from distant sources (Baca, 2008).

Even though many assessments rely on historical hydrologic data, the assumption that current and future climate conditions will resemble the recent past is no longer valid. Recent evidence shows that in some places, climate change is shifting historical natural climatic conditions, with significant impact (Reidmiller et al., 2018).

Horowitz (2006) presented an important conclusion worthy of consideration when studying suspended sediment concentrations during the

1993 flood in the Missouri and Mississippi Basins (Figure 6.3). The results from his study indicate that the factors/processes affecting SSC and SSC-associated constituents that occurred in the upper part of the system may not be reflected in the lower part of the system for decades. He used the following equation:

Suspended sediment flux (tonnes day<sup>-1</sup>) = [Q(ft<sup>3</sup> s<sup>-1</sup>)] [SSC(mg L<sup>-1</sup>)] [0.00245]  
 where: Q = daily mean discharge and SSC = daily suspended sediment concentration.

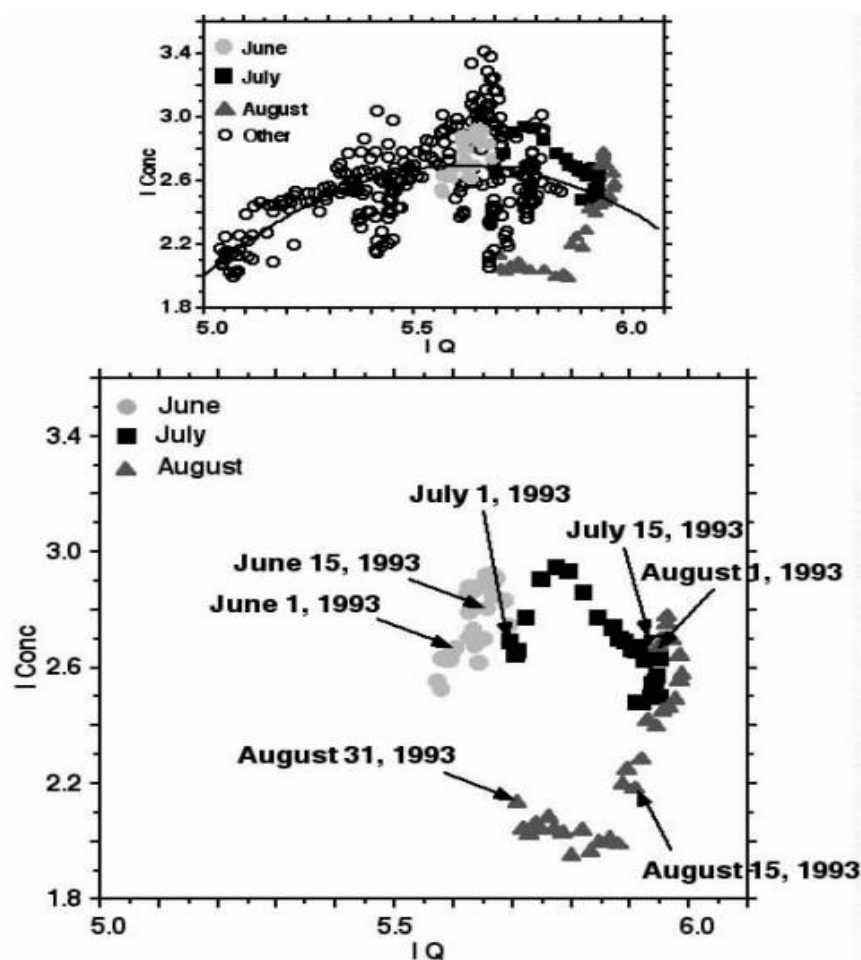


Figure 6.3. Sediment rating curve (upper) and hysteresis example (lower) of suspended sediment concentrations during the 1993 flood for the Mississippi River at Thebes (Horowitz, 2006). The horizontal axes (IQ) are the log of the discharge and the vertical axes (I Conc) are the log of the concentration of suspended sediment.

Note that the unit of discharge is non-metric, but fluxes were converted to metric units (tonnes) through the use of an appropriate constant (0.00245), previously reported in Porterfield (1977). Therefore, Horowitz (2006) was able to calculate annual suspended sediment fluxes using daily mean SSC estimates presented in Figure 6.3. Daily fluxes were calculated and then added together for the period of interest.

As stated in *Engineering Within Ecological Constraints*, National Academy of Engineering: “The expectations placed on engineers shift with the cultural evolution of societies in which they practice. When the cumulative impacts of humans were small, the environmental implications of engineering designs were of less concern. Now that the impact of humans has reached a global scale, there is a growing concern about environmental implications of engineering designs; a new set of constraints has become important to engineers” (Schultz, ed., 1996). These include considerations for water resource planning; design; construction; operation and maintenance; flood control; navigation; water supply; drought; irrigation; recreation; and support of ecological communities. A complicating factor is the “low adaptive capacity of many governments and economic systems to rapidly adapt to these changes” (Busby et al., 2011).

Strong resilience usually enables protection or sustainability of a status quo, a desirable property of a system. Resilience is typically viewed as a positive; however, based on Carpenter et al.’s definition, that is not always the case. It can be undesirable if it leads social and ecological degradation by not protecting the systems we want to maintain. Dornelles et al. (2020) addressed

“the resilience of undesired (social) system states,” with undesirable resilience negatively “having a central role in the pursuit of sustainable human-nature relations.” Undesirable resilient properties, such as bureaucratic inertia or narrowly self-interested behavior by politically, economically, or socially powerful entities, can create or can maintain an undesirable social or ecosystem regime by being a barrier to the transformation needed for sustainability (Glaser et al., 2018). Carpenter et al. (2001) addressed the importance of moving in a positive environmental and social direction by achieving sustainability through removal of the mechanisms that hinder needed transformation. Desirable resilience is linked to the capacity to effect transformation needed for sustainability. “Weakening undesirable resilience at multiple levels is needed to move toward sustainable human-nature relations from the local to the global level” (Dornelles et al., 2020).

A classic example of challenges stemming from a complex interplay of systemic hydrological, climatological, anthropogenic, engineering, and sociopolitical factors is presented in the management of the Colorado River, which provides water for tens of millions and enables agriculture in a desert environment. To establish the appropriations and water law for the river, water managers used the historical flow records during a period where it was particularly “wet” (Luminultra, 2019). Once regional precipitation amounts returned to an “average” or climatological baseline “equilibrium,” over-allocation became a serious, growing issue, as the river did not have enough water to meet competing demands. A 1944 treaty between the U.S, and Mexico guaranteed

Mexico 1.5-million-acre feet of river water per year, not enough for present-day needs. But the ability to provide even that amount has been stressed by hydroelectric dams (most notably Hoover Dam) and reservoirs which intercept and store natural flow, reducing flow downstream. The large surface areas of these reservoirs (most notably Lake Mead and Lake Powell) also increase surface evaporation, further lowering the amount of water for all uses. Prolonged drought in the region has exacerbated the problem, raising questions about whether the drought is cyclical or if dry conditions are the new normal, with the available supply of surface water reduced indefinitely. The Colorado River is now governed by the Colorado River Compact, (Luminultra, 2019) which prioritizes water allotments in its basin based on over 100 court case decisions, statutes, regulations, international treaties, and interstate agreements that together comprise what is recognized as the “Law of the River” (Garrick et al., 2008). A current challenge in the allocation of Colorado River water is establishing effective management and planning strategies for a dynamic system of high uncertainty. More advanced technological tools will need to be brought to bear to effectively address the complexities associated with the Colorado River’s governance (Garrick et al., 2008).

For use in determining the effects of increasing GHG concentrations on climate, GCMs are created based on physical laws of thermodynamic and mathematical equations, with various terms for radiation and latent heat. These equations are the basis of programmed computer simulations for 4-dimensional atmospheric conditions which include ocean general circulation, sea ice, and

land-surface components (IPCC, 2007), and aid in predicting climate change impacts on a global scale.

Tung and Wong (2016) state that uncertainty cannot be avoided in the application of hydrologic/hydraulic models because the models involve idealizations of the reality, and the values of model inputs/parameters cannot be quantified with absolute accuracy. While data collection provides water managers with a means to manage uncertainty, it doesn't eliminate it. In this study, emphasis is placed on the importance of using available data and tools to aid in baseline evaluations, and to improve the thought and decision-making process as it is applied to preparing for future climate conditions.

#### **6.4 Current Climate and Climate Change**

The study area falls within the boundaries of the Northern Great Plains (Figure 6.4), an area subject to changing climatic conditions that include flooding, drought, rising temperatures, and spread of invasive species (Reidmiller et al., 2018).

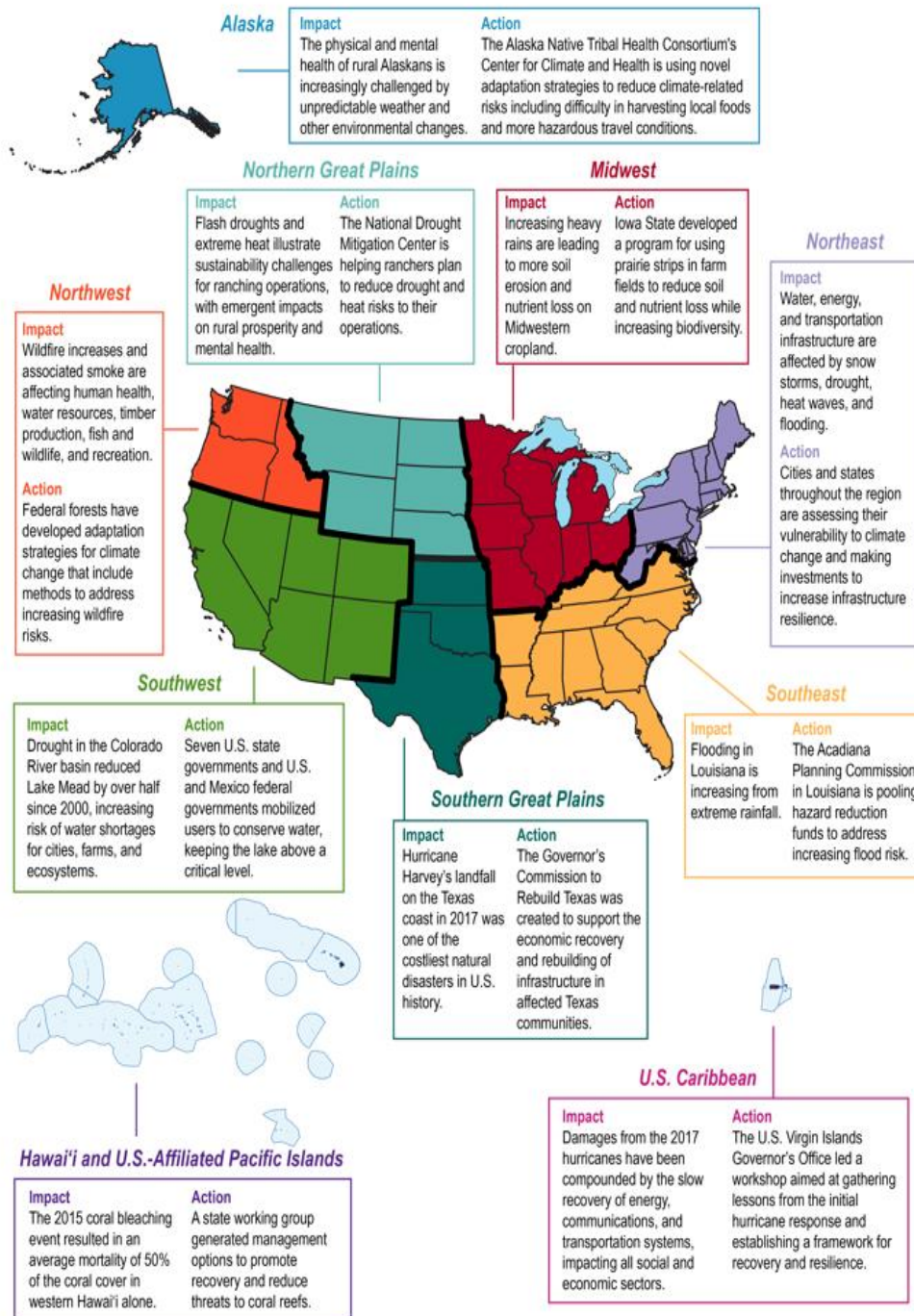


Figure 6.4. U.S. regional boundaries and climate impacts, per the Fourth National Climate Assessment. The dramatic elevation change in the Northern Great Plains change contributes to the diversity in geographical, ecological, and climatological variability across the region. (Reidmiller et al., 2018).



From monitoring watersheds, researchers report the trends in observable hydroclimatic changes depicted in Figures 6.5-6.9. Figure 6.5 shows that precipitation is changing, occurring less as snowfall and more as rain. Figure 6.6 indicates shows decreasing snowpack in the western United States. Figure 6.7 depicts earlier first-bloom dates of lilacs, indicating a shift in the growing season, and Figure 6.8 indicates the earlier onset of spring snowmelt runoff. These hydroclimatic trends are also evident in groundwater aquifers (Figure 6.9).

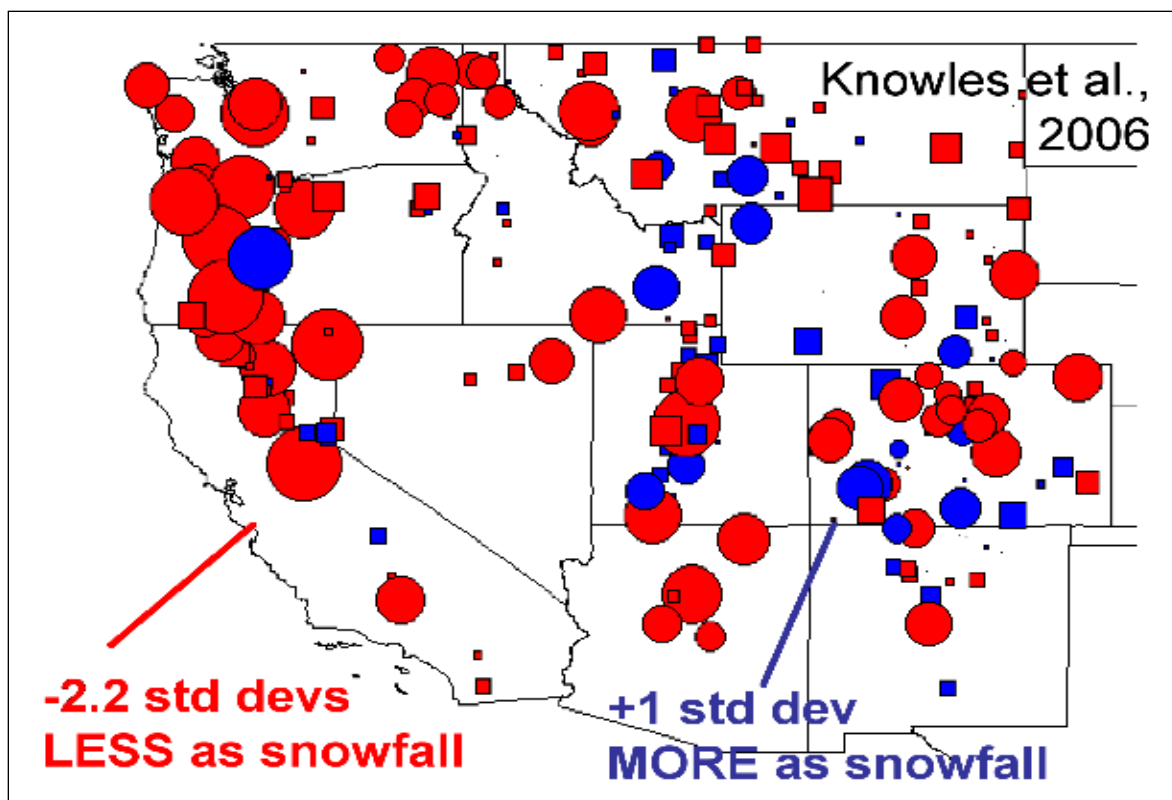


Figure 6.5. Observed: Less snow/more rain. Diagram from Knowles et al. (2006) represents observed precipitation trends in western basins

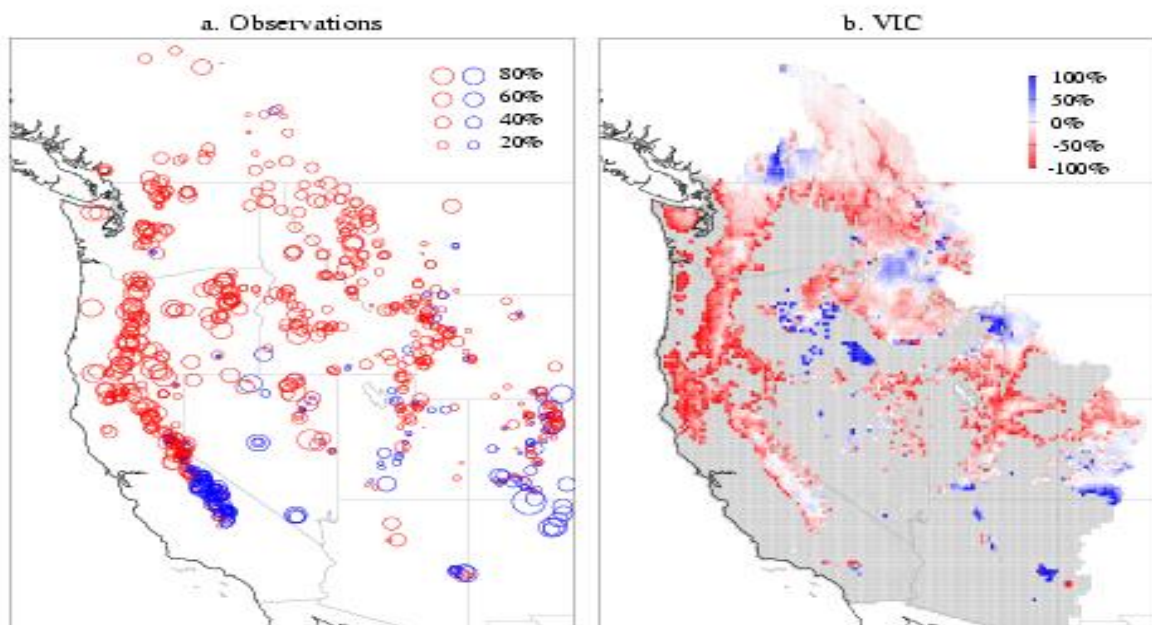


Figure 6.6. Observed: Less spring snowpack. (Trends are for the period 1950-1997 on April 1; snow-water content at western snow courses (Mote, 2003).

SHADES: TRENDS OF BEGIN DATE OF GROWING SEASON, 1950-99, FROM TEMPERATURES  
 DOTS: TRENDS IN LILAC FIRST-BLOOM DATES (Sites with 20+ yrs of record)

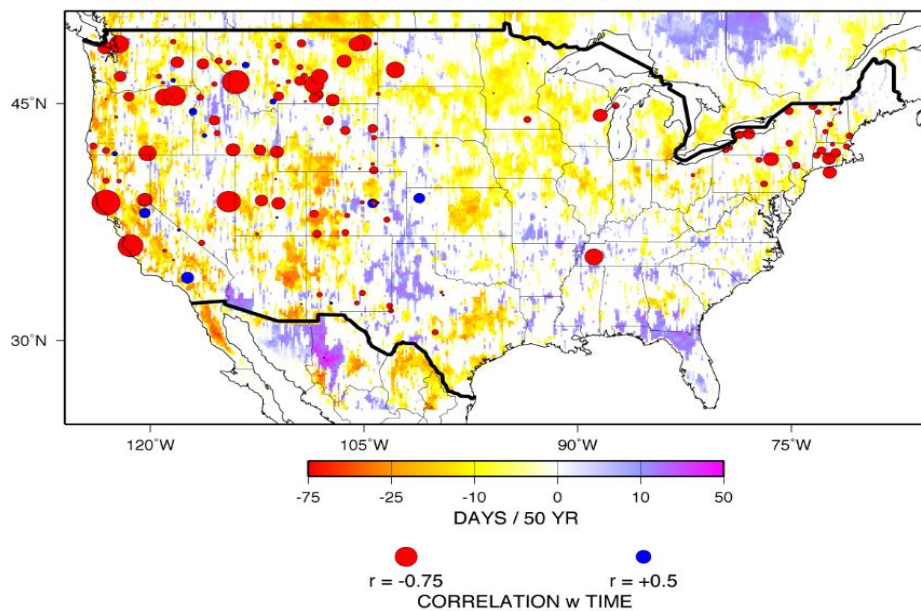


Figure 6.7: Observed: Earlier first-bloom dates of lilacs, indicating a shift in the growing season (Cayan et al., 2001).

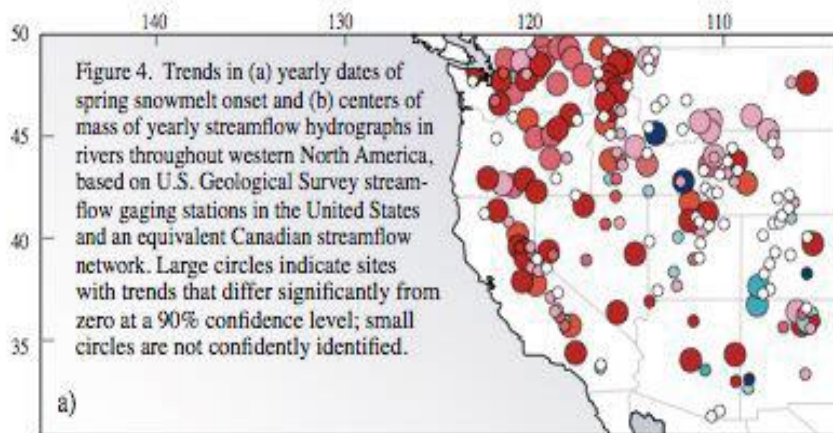


Figure 6.8. Earlier spring snowmelt runoff: Trends in yearly dates of spring snowmelt onset in annual streamflow hydrographs for rivers in the western North America based on USGS stream gages (Norton et al., 2014).

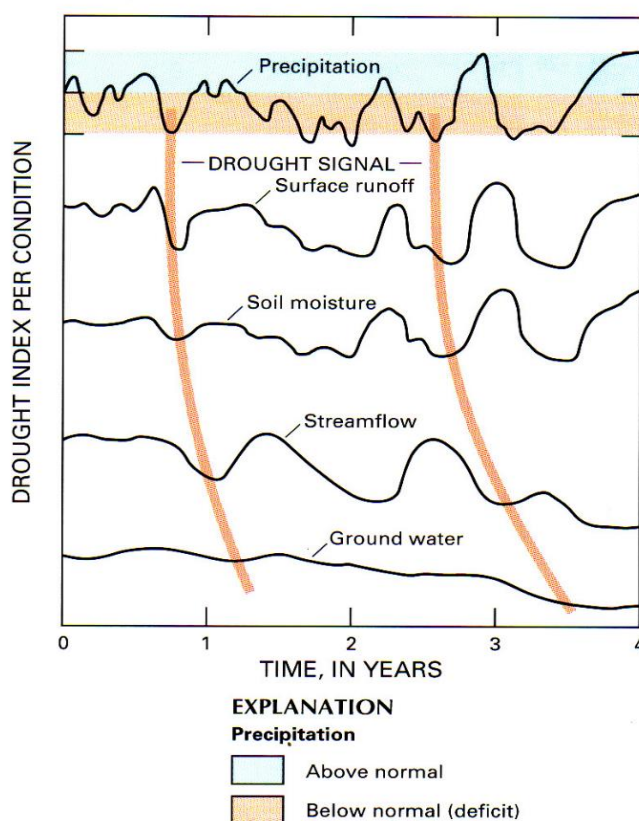


Figure 6.9. Aquifers respond preferentially to lowest frequency climatic variations. This means that aquifers may express climate trends disproportionately (Changnon, 1987).

Too much or too little water, overall changes in distribution, and changes in snowpack and snowmelt are all indicative of more overall variability. Rainfall, runoff, and subsequent flow in rivers in any single year can vary above or below a long-term human-identified trend due to substantial natural variability (Huntington et al.,2018).

McCabe and Wolock (2020) evaluated multi-year (1900-2014) hydroclimatic droughts and “pluvials” (rain or wet-periods) across the conterminous United States using time series of water-year runoff for 2,109 hydrologic units (HUs). Recurring periods were identified by their characteristic events including frequency, duration, and severity. This study incorporated an analysis using gridded tree-ring reconstructions of the Palmer Drought Severity Index (PDSI) for the years 1475-2005, to place the drought and pluvial characteristics determined in the context of multi-century climate variability using water year runoff data for 1900-2014. These runoff results indicated that most drought events occurred before about 1970, with most pluvial periods occurring in following years. They attributed this change in the frequencies of drought and pluvial events around 1970 to an increase in fall (Oct. Dec.) precipitation across much of the central United States after that time. In addition, the duration and severity of droughts and pluvials identified using runoff for 1900-2014 generally were not significantly different from the drought and pluvial characteristics identified using the PDSI for 1475-2005. The duration and severity of droughts and pluvials identified for the 1900-2014 period generally were not significantly

different from the drought and pluvial characteristics identified for the 1475-2005 period.

Villarini et al. (2009) and Milly et al. (2002) examined temporal changes in flood peak distributions based on some of the longest records in the United States. Their study identified an ambiguous nature of temporal trends in flood records and raised questions about the assumption of stationarity. They stated that distinction between man-made influences and natural variability is difficult to discern, and that detection of an increase in great-flood frequency and attributions of increases in great-flood frequency to “radiatively induced climate change are tentative” (Villarini et al., 2009). Physical processes associated with flood production and statistical procedures that are used to infer distributional properties of flood series can impose major limitations on attempts to infer temporal changes in flood peak distributions. In the majority of studies in the literature, inferences are based on records that go back less than 100 years. Norton et al. (2014) report an upward trend in observed streamflow in the study area, shown in Figure 6.10..

The IPCC (2014) reported that in general, rising temperatures from climate change will amplify existing climate-related risks to people, ecosystems, and infrastructure. Disruptions to the planetary energy balance can increase temperatures and affect components of the moisture budget, leading to changes in the water content of the atmosphere, amounts of clouds, and precipitation rates. The IPCC (2014) stated that small changes in atmospheric temperature have had significant impact on Earth processes. The Earth has warmed by

about 0.6 degrees Celsius over the last century, and the IPCC projects a further increase of 1.0–3.5 degrees Celsius by the year 2100

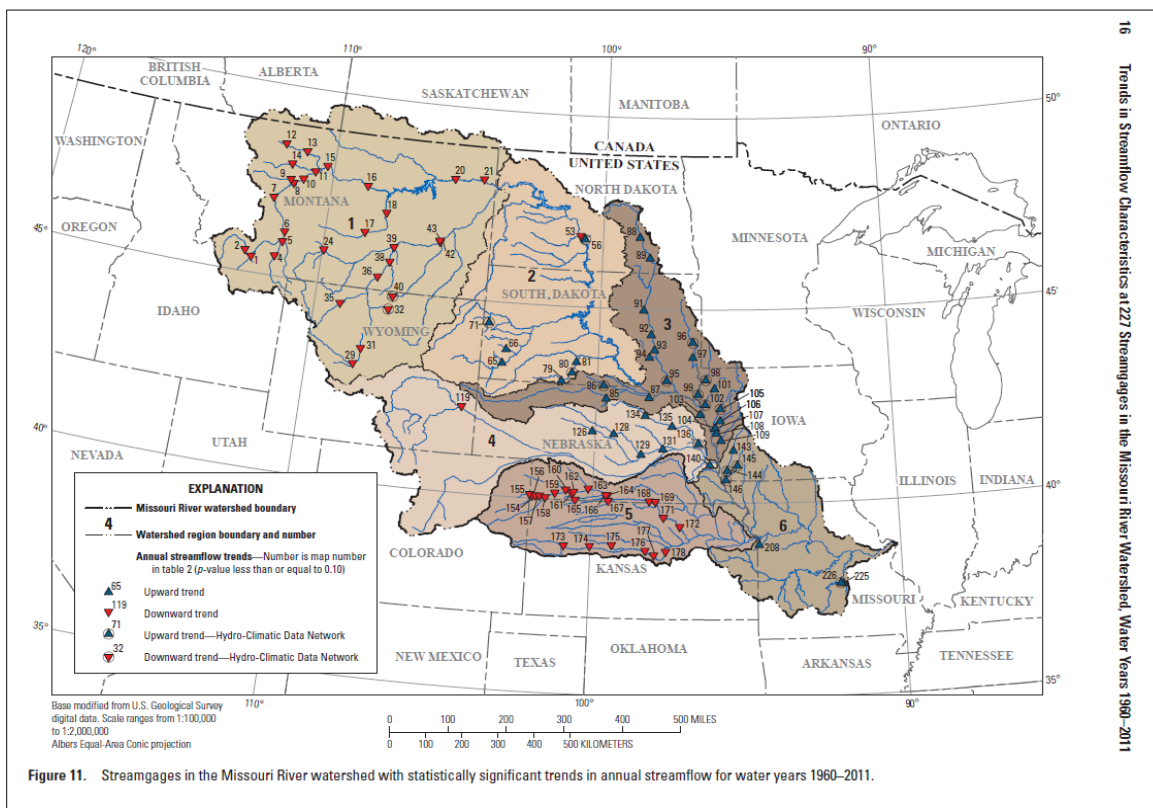


Figure 6.10. USGS stream gages in the Missouri River watershed with statistically significant trends in annual streamflow for water years 1960-2011 (Norton et al., 2014). Gages in South Dakota show an upward trend.

## 6.5 Detecting Non-stationarities

Milly et al. (2008) examined the concept of stationarity in looking holistically at hydrologic time series data as it applies to watersheds. Stationarity essentially means that the statistical properties of time-series data do not change over time. A stochastic process used in mathematics and statistics to evaluate



data, it is based on the assumption that an unconditional joint probability distribution does not change, and parameters such as mean and variance are constant through time (Wikipedia, 2017).

Milly et al. (2008) further describe hydrologic stationarity as a statistical term based on the assumption that the statistical characteristics of hydrologic time series data remain constant. This enables the use of well-accepted statistical methods in water resources planning and design. The “operational” assumption of hydrologic stationarity is used extensively in hydrologic time series data by water resource planners, scientists, and engineers who rely on the observed record to predict future conditions.

Matalas (2017) holds that stationarity implies the future will be statistically indistinguishable from the past, and that operational assumption of hydrologic stationarity has been accepted on the grounds that historical records do not exhibit strong indications of non-stationarity, where the statistical characteristics of hydrologic data series would not be constant. Factors do exist that can potentially lead to non-stationarity in hydrometeorological records, such as climate change or modifications in watersheds such as diversions or dams. However, when conducting flood flow analysis, engineers and scientists are not affected by climatic trends or cycles and climatic time invariance (Matalas, 2017).

The concept of stationarity is a fundamental assumption underlying hydrologic analysis and design, as shown by U.S. Interagency Advisory Committee on Water (ACWI) Data Bulletin 17-B, “Guidelines for determining

flood flow frequency.” First published in 1982, it has guided flood-frequency analysis in the United States for nearly four decades. Stationarity was assumed in its development. However, consideration is being given to modifying this document to reflect knowledge gains about both hydrology and statistical methods since it was first published. An ACWI working group formed to consider possible updates “in light of advances in our understanding and methods” recently made “modest proposed changes” as a starting point. (Cohn et al., 2019)

Iacobellis and Fiorentino, (2000) performed a statistical analysis to improve knowledge of the climatic and geomorphologic processes for calculating the probability distribution of floods. The probability is controlled by the expected values of some quantiles; for example, contributing area and soil moisture conditions, the high randomness of which is significant at the localized event scale only. Tung and Wong (2016) had found that the maximum water surface elevation and peak discharge obtained from their model responses are generally most affected by the rainfall characteristics (i.e., rainfall amount and rainfall profile), but recognized that other model input parameters play a significant role depending on the locations of interest in the river basin. They conclude that a need exists for deeper knowledge of conditions at which a certain mechanism tends to prevail at the basin scale; that further research is needed about the spatial variability of rainfall; and that field experiments aimed at better understanding the physical processes underlying flood generation processes



should be conducted, with particular attention to the role played by the long-term climate and degree of vegetation of the basin. (Tung and Wong, 2016).

In the Cheyenne River study area, flows of many streams are impacted by and regulated to some extent by impoundments or diversions (Sando et al., 2008). In some cases, peak-flow characteristics largely are unaffected, especially where regulation consists of minor diversions for irrigation or water supply. However, effects are large for some streams that are regulated by large on-stream reservoirs or by substantial diversion to off-stream storage (Sando et al., 2008). In some cases, peak-flow characteristics largely are unaffected, especially where regulation consists of minor diversions for irrigation or water supply. However, effects are large for some streams that are regulated by large on-stream reservoirs or by substantial diversion to off-stream storage (Sando et al., 2008). Regulating structures and diversions with potential to affect peak-flow characteristics and associated data from stream gages include the Angostura Dam on the Cheyenne River and the Keyhole Dam and irrigation diversion canals for the Belle Fourche River. For this study, stream gage impacts are listed individually with each gage assessed.

Statistical methods have been developed to detect both abrupt and gradual changes in hydrologic processes, which can occur either quickly or gradually depending on the characteristics of the factors affecting the relevant physical processes. Due to limitations in current understanding, USACE ETL 1100-2-3 does not apply to detection of the potential presence of Long-Term

Persistence (LTP) in the discharge time series that are related to oscillations in climate regime over a wide range of temporal scales.

The IPCC (2002) recognizes precipitation as one of the key climate variables of impact, indicating that an understanding of its distribution is essential to understanding climatic extremes. With increased GHG, increases in extreme precipitation greater than in the mean have been reported in many climate models, both on global and regional scales. Allen and Ingram (2002) state that the overall climate response to increasing atmospheric concentrations of GHG may prove much simpler and more predictable than the chaos of short-term weather.

Streamflow modification can impair more than ecosystem health. McCabe and Wolock (2020) found that biological communities were increasingly likely to be impaired (defined as having lost a statistically significant number of species) in streams with flows most different from natural conditions. When modified, many characteristics of streamflow were related to impaired biological communities, including the magnitude, duration, frequency, annual variability (year-to-year fluctuation of flows), and daily flow fluctuations (Carlisle et al., 2015).

For example, Greene (accessed 2021) describes an apparent shift to a new regime that appears resilient but is not necessarily desirable. As new vegetation and animals invade environments, the native ecosystems will be replaced, shrink or disappear. As a result, many of the ecosystem services societies benefit from will change. Green provides an example of a fluvial

geomorphic response in the Missouri River where cottonwood tree regeneration is decreasing in the river's riparian zone. Mainstem dams on the Missouri River reduce sediment transport downstream; as a result, the floods that previously formed new shallow-water habitat and wet the alluvial sediments for cottonwood germination rarely occur. Furthermore, the altered sediment transport downstream from the dam resulted in degradation of the channel bed as the river system establishes a new equilibrium. As the riverbed lowers, the water table drops, decreasing riparian zone soil moisture. The loss of cottonwoods habitat is providing conditions for a different species, red cedar, to move in. Compared to cottonwoods, red cedar prefers drier soils and sediments and does not survive well in frequently flooded areas. With the dams decreasing flooding and soil moisture within the study area, red cedar easily invades the riparian zone.

Many studies in the literature have sought to determine impacts on a regional scale. In a 2019 report for the USGS and EPA, Carlisle et al. (2019) compiled data from 599 USGS stream gaging sites to research how land and water management is impacting streamflow (Figure 6.11).

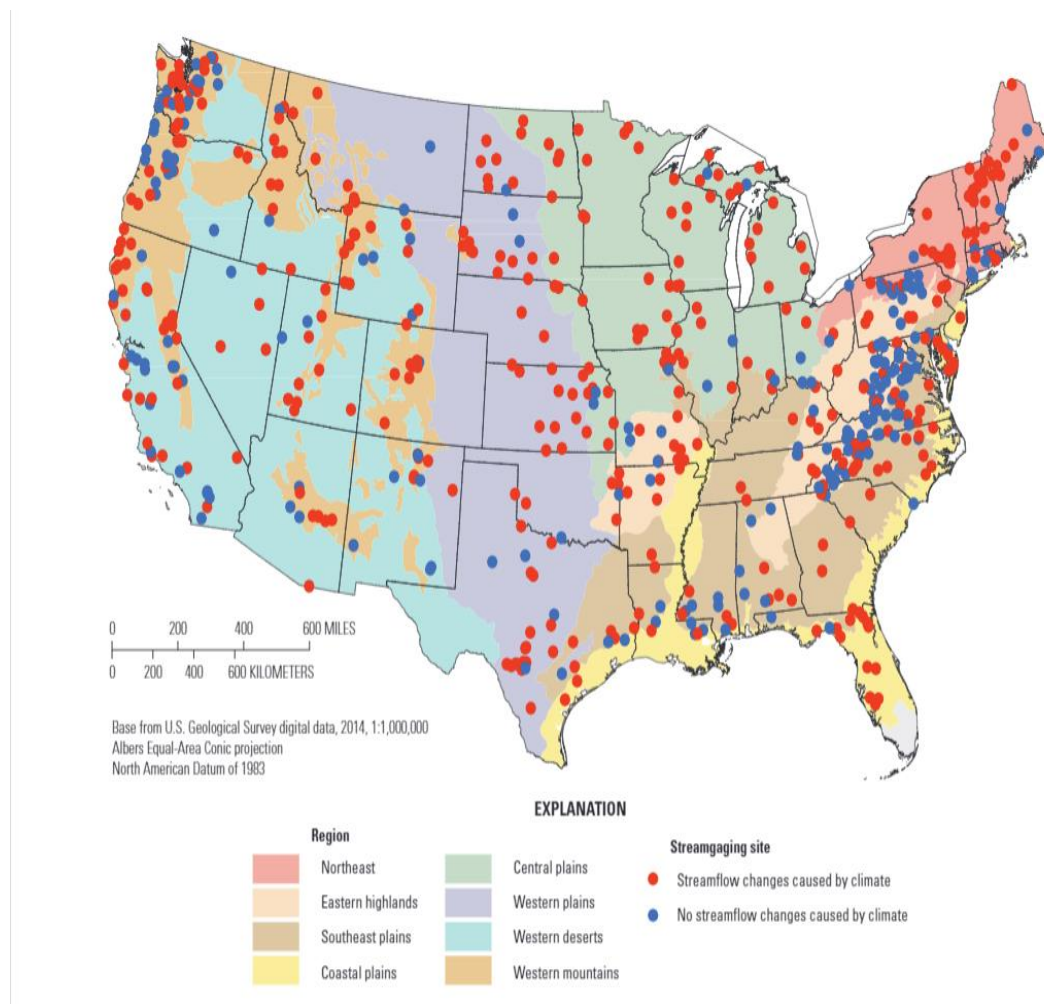


Figure 6.11. Carlisle et al. (2019) visually summarize the climate-impacted streamflow changes within the Western plains. This figure highlights general trends in precipitation and air temperature over the last half century which have likely had major impacts on streamflow in parts of the U.S.

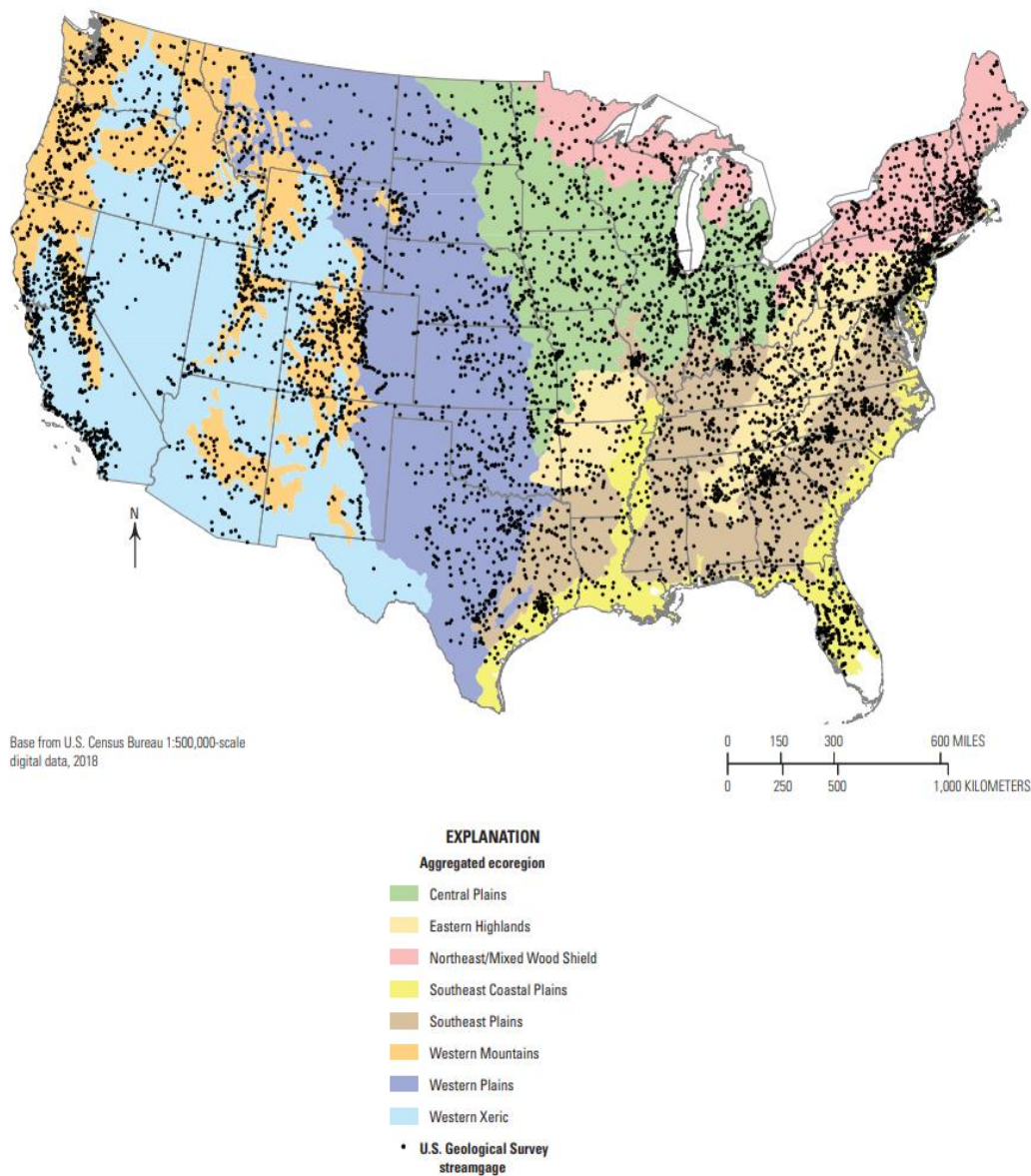


Figure 6.12. Eng et al. (2019) characterized the severity and extent of alterations to natural streamflow regimes from 1980–2014 based on hydrologic metrics at 3,355 USGS stream gages.

Eng et.al. (2019) (Figure 6.12) used 12 hydrologic metrics with known relevance to aquatic ecosystem health were used to characterize the streamflow regime. Alterations to the 12 hydrologic metrics were quantified by taking ratios of the metrics calculated from observed daily streamflow records divided by the

same metrics predicted for natural conditions by random forest statistical models. Some level of streamflow alteration (diminishment or inflation of hydrologic metrics) compared to natural conditions was indicated at about 80 % of the assessed stream gages across the conterminous United States. The severity of alteration differed among ecoregions because of differences in dominant land and water management practices. When considered over the period 1980–2014, climate variability generally played a minor role in the alteration of streamflows across the United States compared to the effects of land and water management.

Coopersmith et al. (2014) studied four simple hydroclimatic indicators (Table 6.2) with the Model Parameter Experiment (MOPEX) data set over a 55-year period using clusters of similarly behaved regional watershed catchments in the continental United States to determine if there were any statistically significant hydrological changes. The MOPEX data set takes into account the decadal climatic cycles known to characterize differences in climatic variability within the U.S. They identified temporal shifts in precipitation and runoff regime curves that differ from region to region and presented the data as a qualitative proxy of a preview of future catchment conditions. Their study found that the Midwest and Rocky Mountains seem to demonstrate more frequent but less intense storms after 1980. Coopersmith et al.'s 2014 study indicates that the climate of the continental U.S. is such that the seasonal variation of energy (and temperature) is relatively uniform across the country. The timing of precipitation is effectively a measure of the phase difference between the seasonality of precipitation and potential evaporation. On the other hand, the timing of the

Similarity Indices	Description	Codes Regime behavior indicator	In South Dakota Study Area
Seasonality index	Quantifies the strength of seasonal variability of precipitation within the year- and answers the question: is precipitation uniform or periodic?	L = "Low Seasonality", $S < 0.25$ I = "Intermediate Seasonality", $0.25 < S < 0.5$ X = "Extreme Seasonality", $0.5 < S$	X = "Extreme Seasonality", $0.5 < S$  0.52-0.58
Aridity index	First order, determines the annual water balance,	V = "Very-Humid", $E_p/P < 0.5$ H = "Humid", $0.5 < E_p/P < 0.75$ T = "Temperate", $0.75 < E_p/P < 1.2$ S = "Somewhat Arid", $1.2 < E_p/P < 2$ A = "Arid", $2 < E_p/P$	A= Arid $2 < E_p/P$  2.23-3.06
The timing (mean date) of runoff peak within the year.	(Especially in relation to precipitation and potential evaporation) capture the mechanisms of storage (in soil water or snow storage) and release (in terms of subsurface drainage or snowmelt).	Q =Max runoff during summer months. Early June through August. F = "Fall/Hurricane season". Generally, in September/October. Uncommon (TX and FL). M = "Melt", Spring melt, usually at a peak in April, May, or early June. C = "Cold runoff", max runoff occurring from early February to before April. D = "December", max runoff during December/January or early February.	C = "Cold runoff", max runoff occurring from early February to before April
The timing (mean date) of precipitation peak within the year.	The timing of precipitation is effectively a measure of the phase difference between the seasonality of precipitation and potential evaporation.	J = "June", Max rainfall occurs in early or mid-summer (not necessarily in June). W = "Winter", Max rainfall occurs in winter (mid-February or March). B = "Blizzard", Max rainfall in late November (to mid-February). P = "Printemps", Max rainfall during spring.	J= 143-171 Day of Max Precipitation

Table 6.2. Coopersmith et al. (2014) hydroclimatic indicators.

runoff peak (especially in relation to precipitation and potential evaporation) captures the mechanisms of storage (in soil water or snow storage) and release (in terms of subsurface drainage or snowmelt).

Coopersmith et al. (2012 and 2014) used an algorithm with four indices to form a classification tree and associated basin catchment classes, and characterized the hydrological response in un-gaged basins to show similarity. They examined the similarities across climate and landscape gradients to gain insight into the physical controls on regional patterns related to regional flow duration curves. A focus of their efforts was identifying factors of catchment regime behavior that leave major imprints on the shape of the flow duration curves, especially slope. The northern Midwestern “badlands” (XACJ, Figure 6.13) are made up of five extremely arid catchments in Nebraska and North and South Dakota.

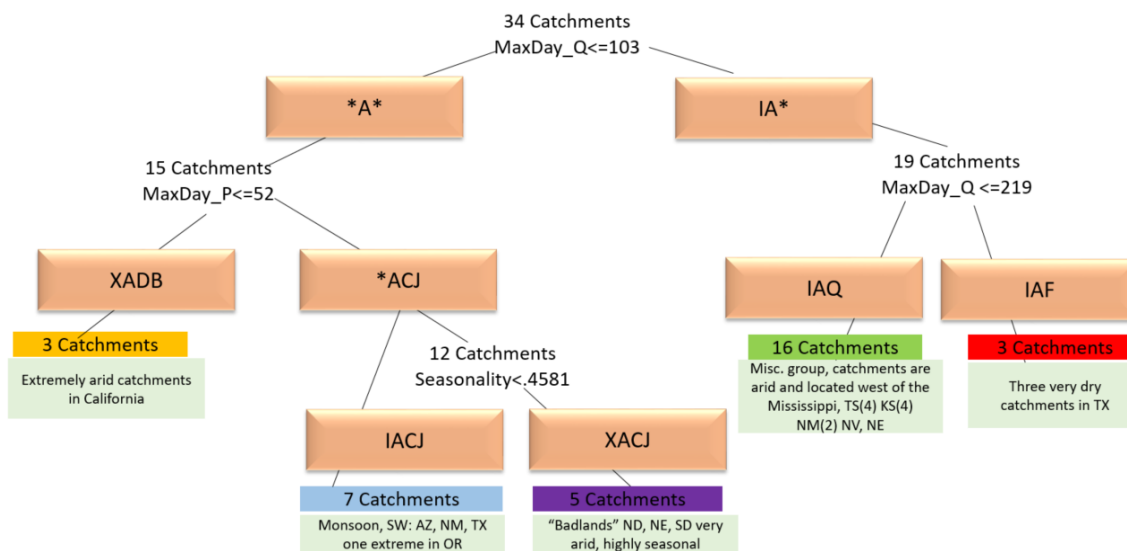


Figure 6.13. The catchments from the Coopersmith et al. (2014) study.



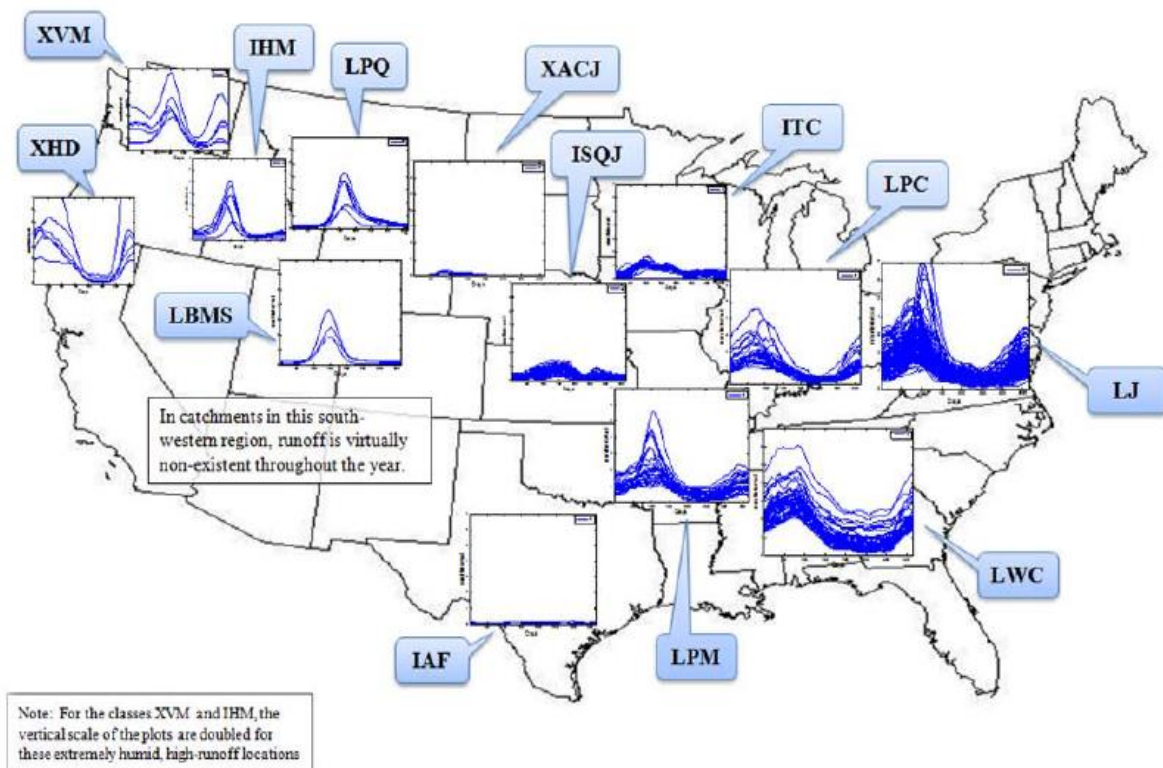


Figure 6.14. Clusters of runoff regimes (Coopersmith et al., 2014).

Figures 6.14 through 6.18 depict key results of the Coopersmith et al. (2014) study to develop a hydroclimatic classification system that divides the U.S. into clusters of similarly behaved watersheds based on evaluation of over 400 basins.

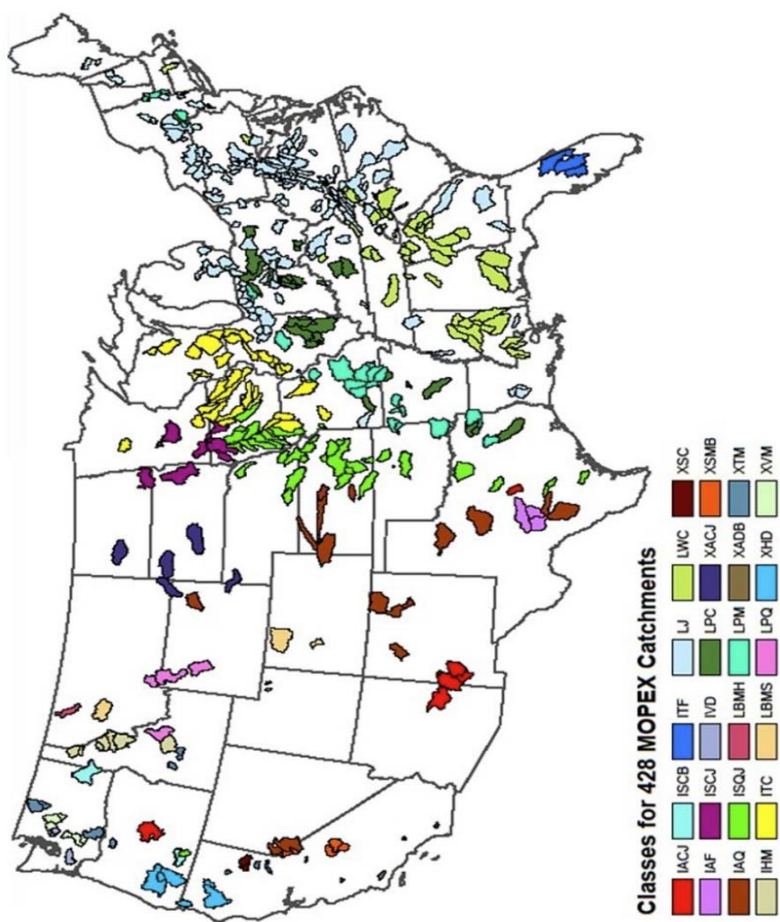


Figure 6.15. Classes for 428 MOPEX Catchments described by (Coopersmith et al., 2012 and 2014).

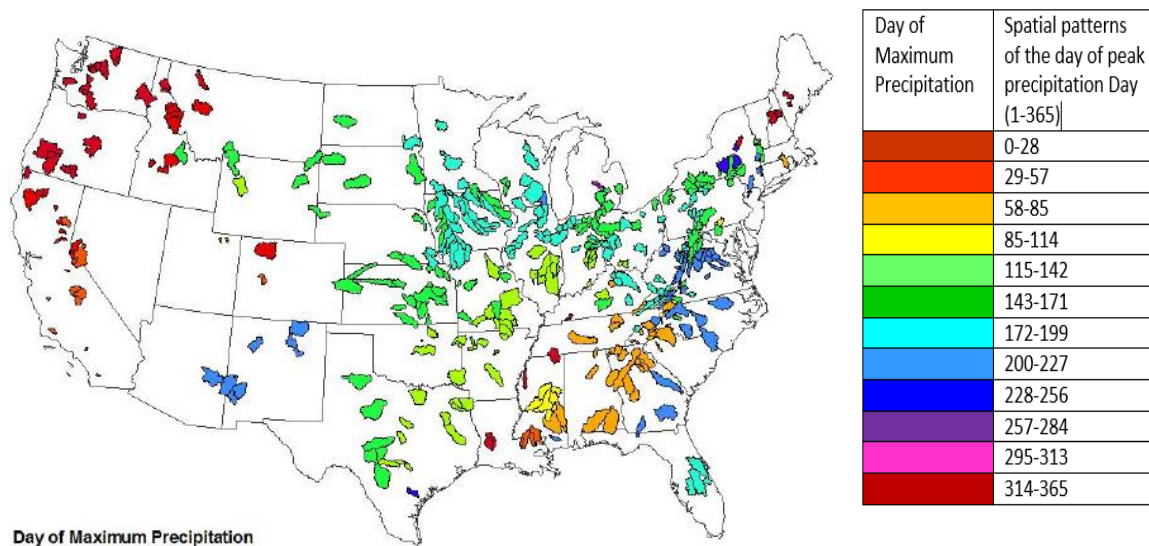


Figure 6.16. Spatial patterns of the day of peak precipitation, 1-365 (Coopersmith et al., 2012).

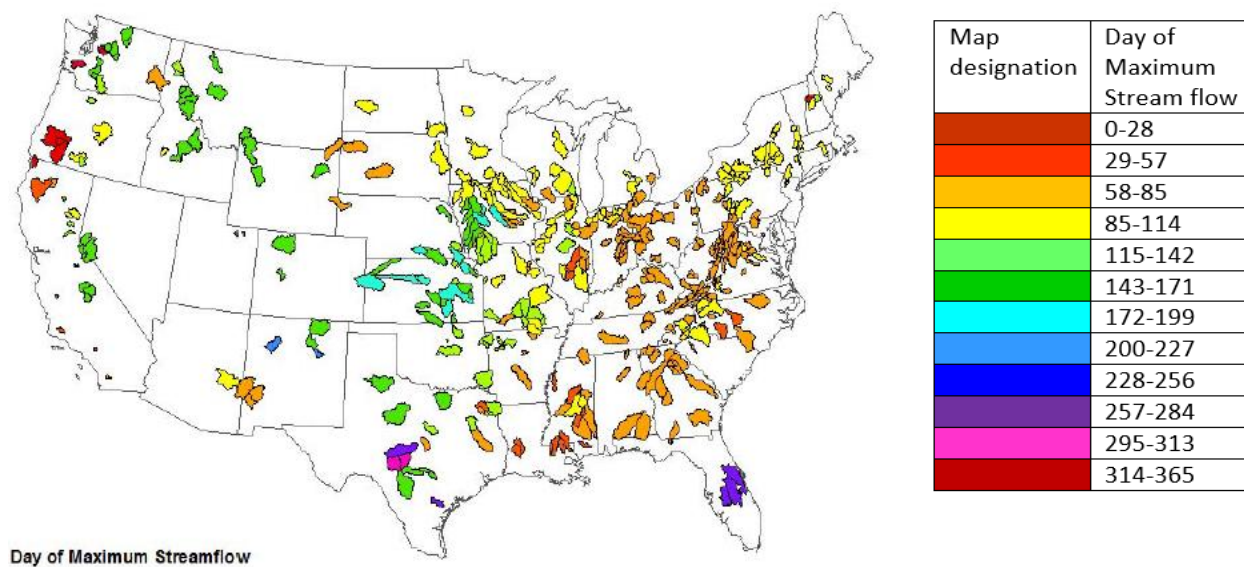


Figure 6.17. Day of maximum streamflow, 1-365 (Coopersmith et al., 2012).

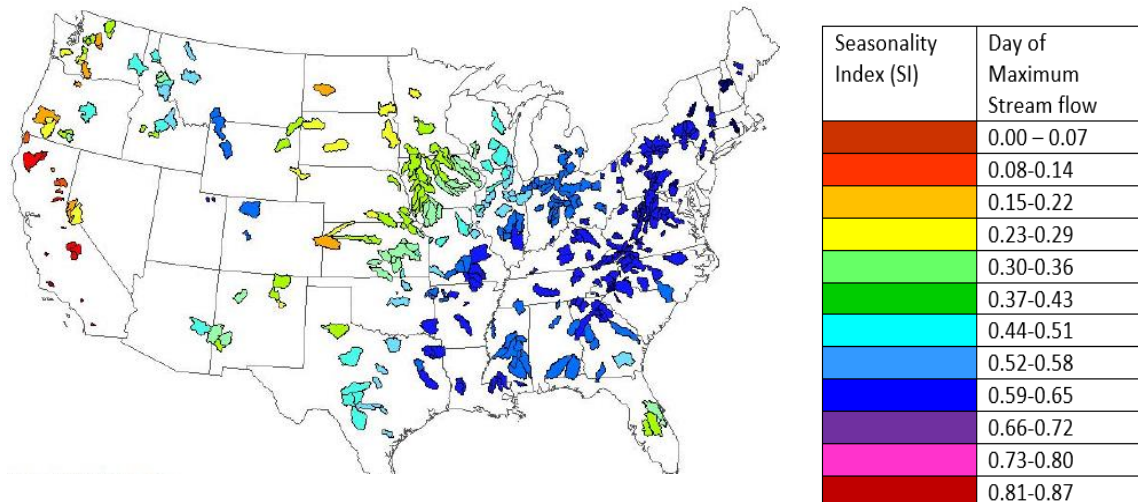


Figure 6.18. Spatial distribution of the seasonality index for maximum streamflow (Coopersmith et al., 2012).

Archfield et al. (2013) also present the concept of a hydro-ecological stream classification by grouping streams by their similar hydrologic responses, aquatic habitat, and ecological flow targets. Archfield et al. (2013) use seven fundamental daily streamflow statistics (FDSS) rather than winnowing down an uncorrelated subset from 200 or more ecologically relevant streamflow statistics (ERSS) commonly used in hydro-ecological classification studies. This new classification approach has the additional advantages of overcoming some of the subjectivity associated with the selection of the classification variables and providing a set of robust continental-scale classes of US stream gages. Use of this set of gages may provide new insight if used to downscale climate models.

Patceg (2006) identified areas of rapid change within stream segment reaches in the Cheyenne River Watershed. The study established 48 sites in the

Cheyenne River Basin and its tributaries to compare and determine classification and assessment of physical habitat to TSS using criteria from the South Dakota Dept. of Environment and Natural Resources and the EPA's Environmental Monitoring and Assessment Program (EMAP). The evaluation included the Belle Fourche River near Elm Springs and the Cheyenne River near Belle Fourche confluence. Patceg (2006) also incorporated Rosgen's (1994) geomorphic classification model and Schumm's (1977) five-stage channel evolution model to classify each site from the stream gradient from the upper portions of the basin down to its outlet. The sites were categorized on channel types, vegetation types, and physical habitat classifications grouping those sites with similar characteristics. Patceg (2006) used a Kruskal-Wallis statistical test to identify those sites with the greatest variability. A spatial description of the watershed was used to identify areas recommended for further monitoring, laying the foundation for a detailed sampling plan focused on areas identified as contributing to impairment, for development of TMDL reports for impaired stream segments. Morlok (2010) measured physical habitat and geomorphic parameters at 64 sites and compared them with suspended sediment loadings in the Cheyenne River to determine if the sediment in the Cheyenne River is from natural sources. Morlok (2010) later conducted a principal component analysis (with results summarized in a "PCI Index") to define regions with similar habitat characteristics and estimate suspended sediment loading at 14 sites in the Cheyenne River Watershed. His findings led to a recommendation that a site-

specific standard based on natural background can be applied to the Cheyenne River.

Building on Patceg et al.'s 2006's study, Morlok (2010) measured physical habitat parameters at 64 sites and compared them with estimated suspended sediment loads at those 14 Cheyenne River Watershed sites. This comparison was used to determine if the sediment in the Cheyenne River is from natural sources, for evaluation of a watershed-based standard for TSS. His principal component analysis was conducted to describe physical habitat variability in the watershed using metrics calculated from the habitat data and to define regions with similar habitat characteristics. Morlok (2010) looked at the effects of bedrock recorded as a substrate parameter to understand which method more accurately represented the geomorphic characteristics at a site. The sediment load from the Badlands region impacted the physical habitat in the Cheyenne River. The Belle Fourche River constituted 48 % of the flow of the Cheyenne River but carried relatively lower sediment loadings, which increased the erosional power of the Cheyenne River.

This addition of erosional power was reflected by the PCI Index values at the sites of Cheyenne River near Deep Creek and Cheyenne River near Four Corners Bridge. In addition, a relationship between the PCI Index and suspended sediment loadings at monitored sites on the main stem of the Cheyenne River indicated that physical habitat parameters were correlated with sediment load. Sediment loading estimates from before 1990 and then from 2007 to 2009 were compared at the sites of Rapid Creek near Farmingdale, Belle

Fourche River near Elm Springs, and Cheyenne River near Plainview; these comparisons indicated that suspended sediment loadings did not increase at these sites. Morlok (2020) grouped together two sites, one on the Belle Fourche River near Elm Springs and another on the Cheyenne River near the Bell Fourche River confluence, into one region because he was unable to determine if they were anomalous or if they represented another entirely distinct watershed/water quality region.

Kibria et al. (2016) also conducted an analysis of streamflow trends and responses to climate variability and land cover changes in South Dakota. They evaluated trends in high, moderate, and low streamflow conditions from USGS streamflow gaging stations for the period 1951–2013 for 18 selected watersheds in South Dakota using a modified Mann-Kendall test. These 18 gaging stations were selected based on their period of record and their precipitation trends. Twenty-one weather stations located within 20 kilometers of the streamflow gaging stations were also evaluated for the same study period with the assumption that they accurately represented precipitation in the study watersheds, regardless of their proximity to the stream. Kibria et al.'s study indicated "mixed patterns," with seven of the 18 stream gaging stations showing a significantly increasing trend, nine showing a slightly increasing trends, and two showing a decreasing trend for annual streamflow. Of the four stream gaging stations in the study area vicinity, three showed increasing streamflow trends, and none showed significant trends in rainfall. Figures 6.19, 6.20, and 6.21 and Tables 6.4 and 6.5 depict the key data from the Kibria et al. (2016) study

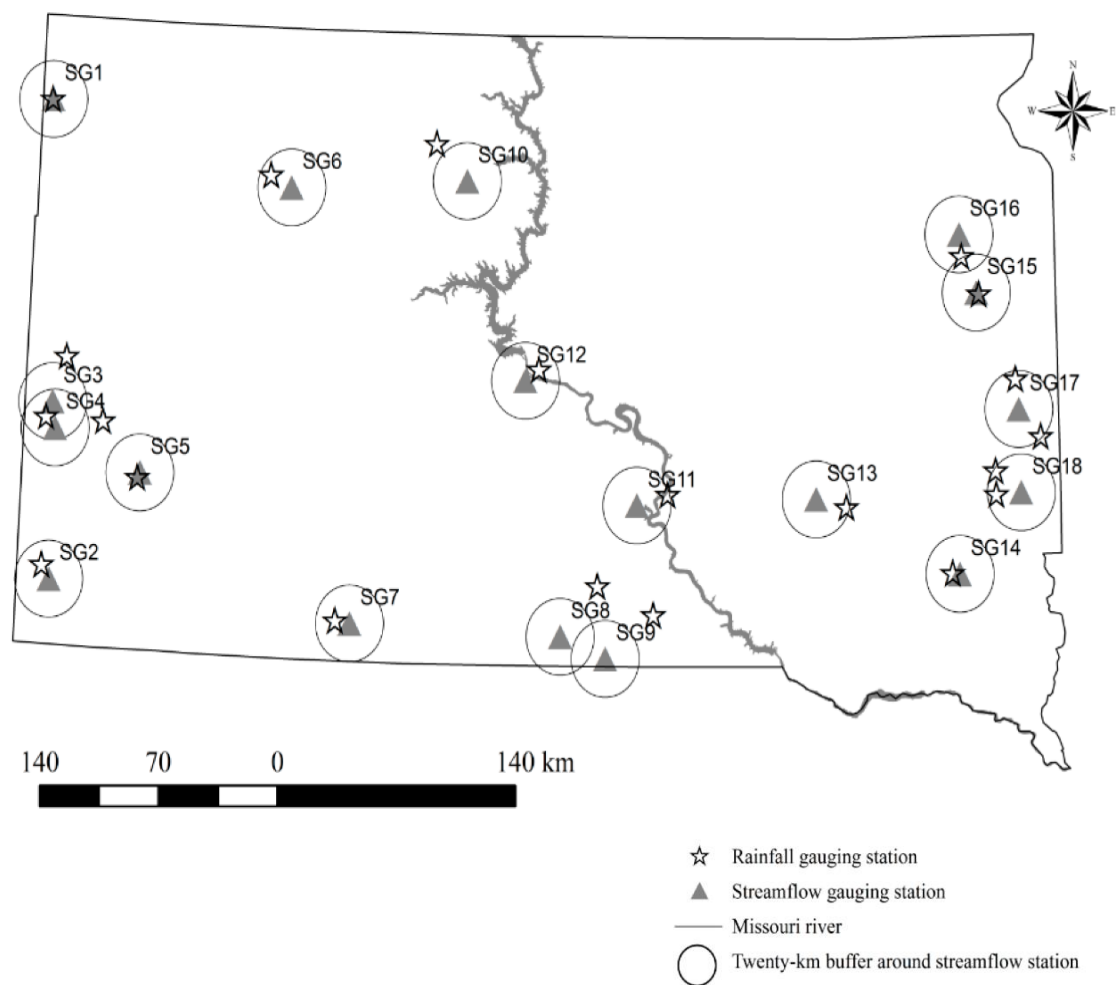


Figure 6.19. Weather/streamflow gaging station map (Kibria et al., 2016).



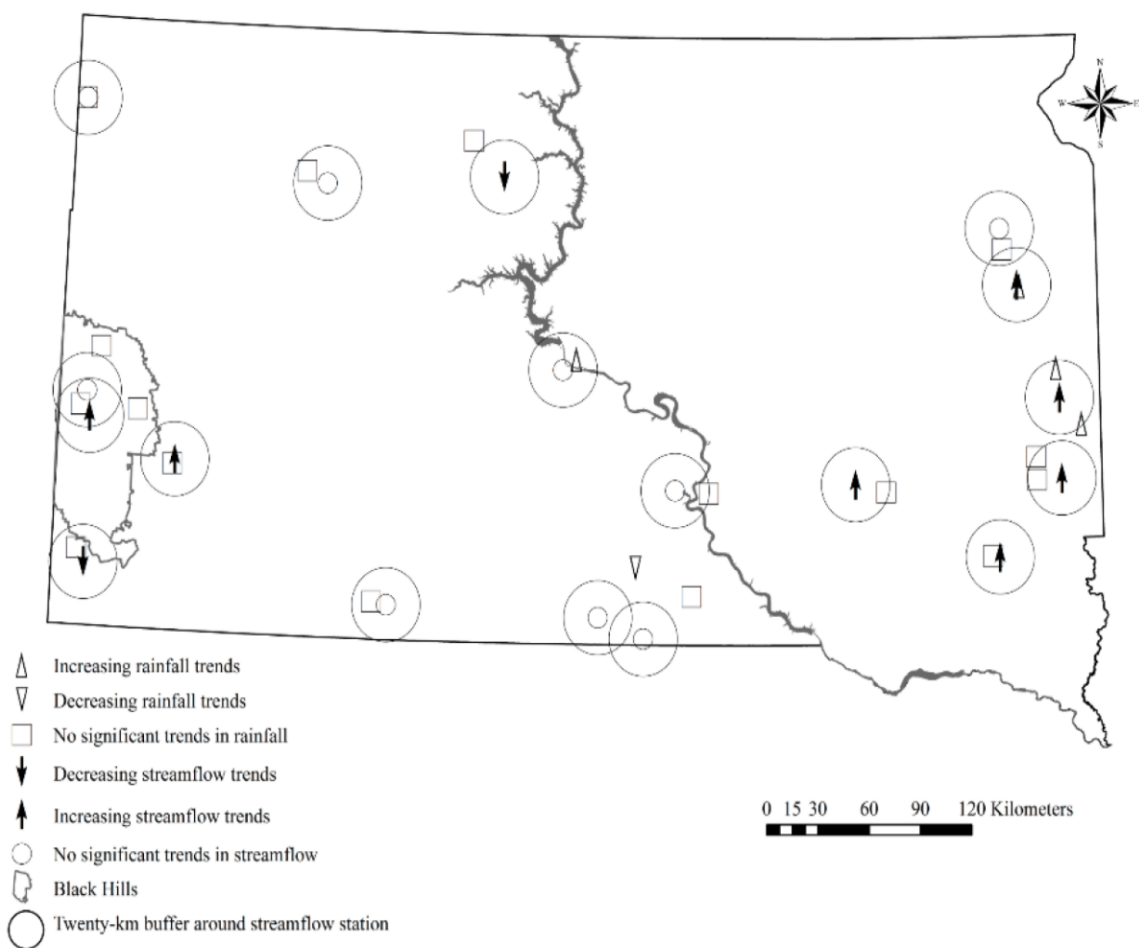


Figure 6.20. Trends in annual streamflow and precipitation in South Dakota (Kibria et al., 2016).

USGS Station Number	USGS Station Name	Annual Stream flow	One-Day Min (Low Flow)	Seven-Day Min (Low Flow)	One-day Max (High Flow)	Seven Day Max (High Flow)	Median Daily (Flow)	Daily Average (Flow)
06359500	Moreau River Near Faith	1.2 (0.20) [0.09]	1.5 (0.12)	1.6 (0.11)	0.8 (0.42)	0.9 (0.32)	<b>1.7</b> <b>(0.08)</b>	1.3 (0.20)
06395000	Cheyenne River at Edgemont	<b>-2.1</b> <b>(0.04)</b> <b>[-0.03]</b>	<b>2.4</b> <b>(0.01)</b>	<b>2.3</b> <b>(0.01)</b>	<b>-2.7</b> <b>(0.01)</b>	<b>-2.2</b> <b>(0.02)</b>	<b>1.8</b> <b>(0.07)</b>	<b>-2.0</b> <b>(0.04)</b>
06409000	Castle Creek Above Deerfield	<b>1.8</b> <b>(0.08)</b> <b>[0.41]</b>	1.5 (0.12)	1.6 (0.11)	1.9 (0.05)	1.6 (0.09)	1.8 (0.07)	1.8 (0.08)
06441500	Bad River Near Ft. Pierre	-0.05 (0.62) [-0.03]	1.1 (0.25)	<b>1.9</b> <b>(0.05)</b>	-0.9 (0.33)	0.01 (0.91)	-0.5 (0.64)	-0.5 (0.62)
06452000	White River Near Oacoma	0.9 (0.35) [0.08]	1.1 (0.26)	1.0 (0.29)	0.6 (0.54)	0.1 (0.97)	1.5 (0.13)	0.9 (0.35)
06406000	Battle Creek at Hermosa	<b>1.7</b> <b>(0.9)</b> <b>[0.23]</b>	<b>2.5</b> <b>(0.01)</b>	<b>2.4</b> <b>(0.01)</b>	-0.1 (0.93)	0.9 (0.35)	<b>2.0</b> <b>(0.04)</b>	<b>1.7</b> <b>(0.095)</b>
06360500	Moreau River Near Whitehorse	<b>-3.9</b> <b>((&lt;0.10</b> <b>)</b> <b>[-0.21]</b>	<b>1.8</b> <b>(0.07)</b>	1.6 (0.01)	0.4 (0.66)	0.1 (0.91)	-2.5 (0.01)	-3.9 (<0.10)
06334500	Little Missouri River at Camp Crook	-0.3 (0.73) [-0.4]	1.4 (0.16)	1.5 (0.12)	-0.6 (0.52)	-0.4 (0.72)	-0.7 (0.51)	-0.3 (0.73)
06447500	Little White River Near Martin	0.7 (0.46) [0.07]	1.4 (0.16)	1.2 (0.20)	<b>-2.0</b> <b>(0.04)</b>	-1.6 (0.12)	1.1 (0.29)	0.7 (0.46)
06408700	Rhodes Fork Near Rochford	0.20 (0.82) [0.46]	0.2 (0.82)	0.3 (0.73)	0.2 (0.85)	0.001 (1.00)	0.2 (0.81)	0.2 (0.85)

Table 6.3. Annual trends and trend magnitudes of streamflow in South Dakota. Modified Mann-Kendal Z-value (p-value) and [Magnitude, mm/year] are shown. Values in bold represent statistically significant trends at the 90% confidence level. Rows in gray indicate sites in the Black Hills (Kibria et al., 2016).

USGS Station Number	USGS Station Name	Fall	Spring	Summer	Winter
06359500	Moreau River Near Faith	<b>2.67</b> <b>(0.01)</b> <b>[0.004]</b>	1.27 (0.20) [0.15]	0.17 (0.86) [0.001]	<b>2.60</b> <b>(0.01)</b> <b>[0.06]</b>
06395000	Cheyenne River at Edgemont	<b>1.72</b> <b>(0.09)</b> <b>[0.001]</b>	1.38 (0.17) [0.002]	-1.99 (0.05) [-0.008]	2.17 (0.03) [0.002]
06409000	Castle Creek Above Deerfield	0.48 (0.63) [0.002]	0.91 (0.36) [[0.003]]	0.92 (0.36) [[0.0025]]	0.26 (0.79) [[0.001]]
06441500	Bad River Near Ft. Pierre	0.32 (0.75) [0.0001]	-0.50 (0.62) [-0.004]	-0.97 (0.33) [-0.007]	0.82 (0.41) [[0.001]
06452000	White River Near Oacoma	1.69 (0.09) [0.011]	0.84 (0.39) [[0.016]	0.50 (0.62) [[0.006]	1.94 (0.05) [0.013]
06406000	Battle Creek at Hermosa	2.3 (0.02) [0.055]	1.72 (0.08) [0.172]	1.76 (0.08) [0.106]	2.09 (0.04) [0.007]
06360500	Moreau River Near Whitehorse	2.00 (0.05) [0.056]]	1.58 (0.11) [[0.048]	1.50 (0.13) [[0.037]	2.48 (0.01) [0.047]
06334500	Little Missouri River at Camp Crook	0.39 (0.69) [[0.0013]	-0.46 (0.64) [-0.015]	-1.12 (0.26) [-0.017]	0.70 (0.48) [[0.001]
06447500	Little White River Near Martin	1.25 (0.21) [0.008]	1.11 (0.27) [[0.023]	0.14 (0.89) [[0.003]	1.97 (0.05) [0.027]
06408700	Rhodes Fork Near Rochford	-0.10 (0.99) [-0.001]	0.33 (0.74) [0.134]	0.23 (0.82) [[0.059]	0.36 (0.72) [[0.164]

Table 6.4. Seasonal trends and trend magnitudes of streamflow in South Dakota. Modified Mann-Kendal Z-value, (p-value) and [magnitude, mm/year] are shown. Values in bold represent statistically significant trends at the 90% confidence level (Kibria et al., 2016).

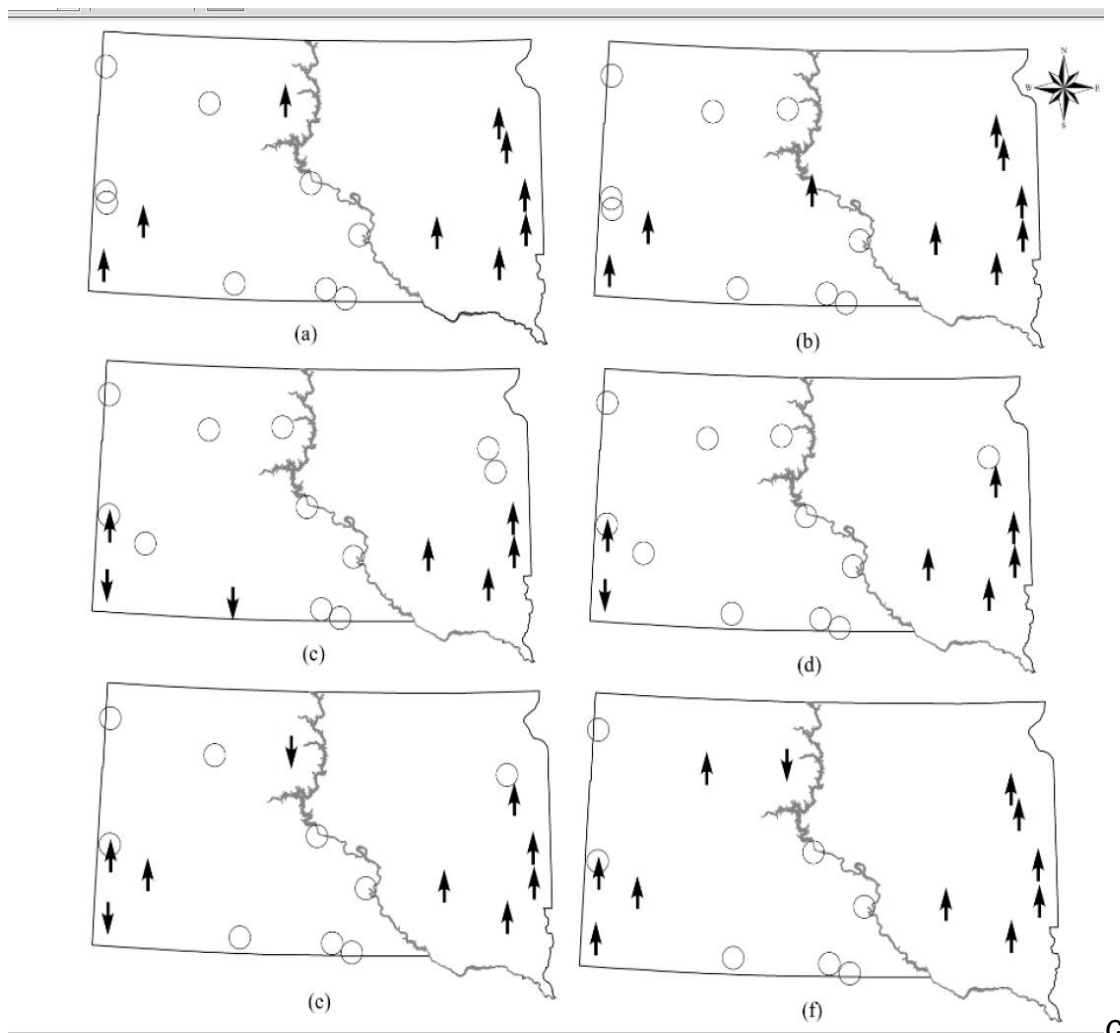


Figure 6.21. Spatial distribution of streamflow gaging stations with statistical significance and no trends in (a) one-day minimum flow; (b) seven-day minimum flow, (c) one-day maximum flow; and (d) seven-day maximum flow; (e) daily average flow; and (f) mean daily flow (Kibria et al., 2016).

The USGS's National Climate Change Viewer (NCCV) is accessible at:

[https://www2.usgs.gov/landresources/lcs/nccv/maca2/maca2\\_watersheds.html](https://www2.usgs.gov/landresources/lcs/nccv/maca2/maca2_watersheds.html).

It allows the user to identify observed and projected climate trends for a desired watershed or county. To model projected climate trends, the USGS uses CMIP5 climate data and a simple water balance model. An automated report for the climate characteristics of the Cheyenne River Basin was generated using the

NCCV USGS summary tool. Data are provided in Appendix A. In general, the data agree with other findings mentioned previously, showing trends of warmer temperatures, similar or higher precipitation, lower snow water equivalent, lower soil water storage, and higher evaporative deficit. Runoff trends vary by season but are less clear.

## **6.6 Historical Climatological and Geomorphic Changes**

The Cheyenne River Basin has undergone significant changes across both geologic and recent time scales. Causes of these changes and resulting adjustment to sediment loads in the streams include:

- Anthropogenic impacts (mining, changes in base level due to construction of dams, canals and streamflow diversions)
- Changes in land use, variation in discharge (i.e., flood events)
- Mass wasting
- Base level changes
- Stream capture events
- Regional uplift
- Glacial isostatic rebound
- Climatic changes.

Despite the many studies in this region, detailed information on the evolution of its geomorphology at a basin-wide scale is limited. An increased understanding of these changes may give insight into the driving forces behind basin landscape evolution, which may increase the understanding of the basin-wide, large-scale driving factors that contribute to erosion and sediment movement.

Hydrogeomorphic processes in the Lower Cheyenne River Basin have created many channel adjustments due to a wide variety of factors (e.g., sediments, bank and channel erosion, floods, landslides) upstream from the

Oahe Reservoir. The direction and magnitude of these adjustments vary with local and regional geologic lithology as well as channel shape at both a reach and basin scale.

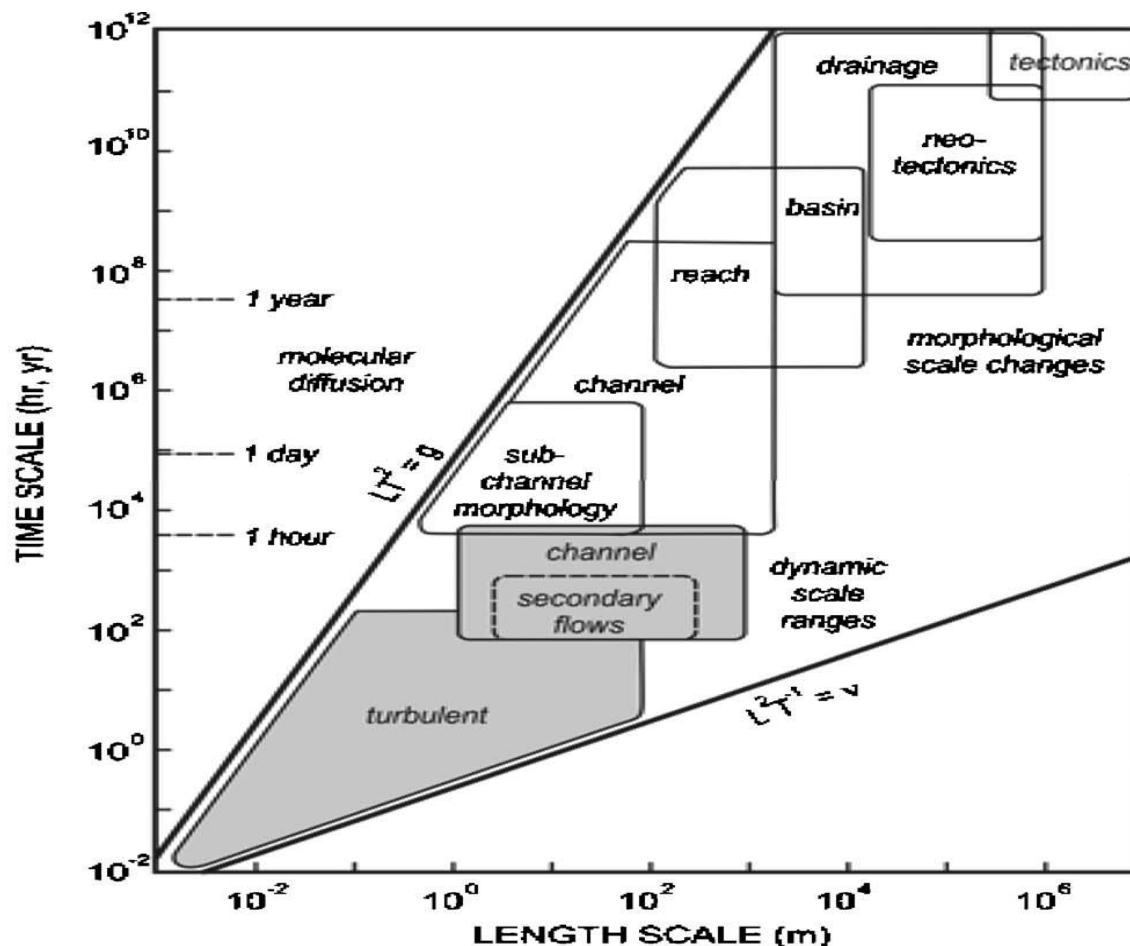


Figure 6.22. Illustration of spatial and temporal scales (adapted from O'Connor and Costa, 1959). Total work (shaded area) is identical for the events, but the scale of channel change is greater for the high-magnitude event.

Specific watershed issues should be approached by determining the appropriate scale for the resolution of the questions and problems being addressed. Scalar conditions are important factors that must be considered when

interpreting relevant interplay of these factors (Figure 6.26). Hydrogeomorphic processes in the Cheyenne River Basin have created many channel adjustments due to a wide variety of factors (e.g., sediments, bank and channel erosion, floods, landslides, increases in sediment volume) upstream from the Oahe Reservoir. The direction and magnitude of these adjustments vary with local and regional geologic lithology, as well as channel shape, at both a reach and basin scale.

In the mid-20<sup>th</sup> century, six large dams were constructed on the Missouri River's mainstem in Montana, North Dakota, and South Dakota. These projects, along with changes to land cover and land use across the basin, had substantial influence on the Missouri River's form, dynamics, and sediment regime. Current volumes of sediment transported into Louisiana by the Missouri and Mississippi rivers average roughly 145 million metric tons per year (Meade and Moody, 2009). The magnitude and patterns of streamflow and sediment supply of Whitewood Creek and the Belle Fourche and Cheyenne Rivers have been heavily impacted by the operation of Oahe Dam since filling of the Oahe Reservoir began in 1962. Before the elimination of discharge of tailings, large volumes of tailings containing fine sediment were deposited in Whitewood Creek and the Belle Fourche River, resulting in an increase in the number and size of sandbars in lower Whitewood Creek and in the Belle Fourche River downstream from its confluence with Whitewood Creek.

In addition to the impact of the mainstem dams, changes initiated by bank stabilization and channelization projects have had a variety of effects on the

Missouri River's sediment regime. For example, the river channel immediately downstream of both mainstem and tributary dams has degraded and lowered because of erosive forces of clear-water releases from the dams. As the Missouri's hydrology became increasingly controlled, the river basin's sediment regime (including such processes as sediment erosion, transport, and deposition) also was changed dramatically. While something of an oversimplification, water discharge and sediment chemistry under low-flow conditions in fluvial systems tend to be dominated by point sources and groundwater discharge into the stream; under high-flow conditions, both are dominated by nonpoint sources. Evidence shows that regardless of river basin size or area, fluxes of suspended sediment and sediment-associated chemical constituents area are dominated by high-flow events. (Horowitz, 2008; 2013) and Hirsch et al. (2010).

Distinct linkages between suspended sediment concentration (SSC) and/or sediment-associated chemical constituents and water discharge have been observed that appear to be somewhat counterintuitive. Under low-flow conditions, SSCs ( $\text{mg l}^{-1}$ ) tend to be low and dominated by fine-grained material, while sediment-associated chemical concentrations ( $\text{mg kg}^{-1}$ ) tend to be high as a result of the grain-size effect (Horowitz, 2008; 2013). This is opposite under high-flow conditions, where SSCs ( $\text{mg l}^{-1}$ ) are usually greater and coarser, and sediment-associated chemical concentrations ( $\text{mg kg}^{-1}$ ) usually low – again as a result of the grain-size effect (Horowitz, 2008; 2013). Despite the lower sediment-associated constituent concentrations associated with high flows, their fluxes usually increase because the effects of the lower concentrations are



compensated for by the higher discharges and increased SSCs (Horowitz, 2008; 2013).

The evolution of geospatial tools over the last decade has given hydrologists and engineers the capability to evaluate topography and relationships between hydrography, hydrology, and geomorphology. Parameters such as slope angle and slope aspect can help hydrologists to analyze hydrological processes and topographic structure and shape. Grams et al. (2013) employed an approach to link morphodynamic response with sediment mass balance in the Colorado River. They indicate that spatially propagated error varies depending on the spatial scale of interest. Because an increasing number of studies use high-resolution topographic data for geomorphic monitoring, increased interest in understanding and quantifying uncertainty in these data sets has identified several uncertainties with measuring sediment in streams. Grams et al. (2013) list several examples, which include: 1) Five-percent-level biases which can be introduced in discharge measurements made with mechanical current meters through inappropriate characterization of near-bank velocities or the shape of velocity profiles; 2) Biases which can be introduced into discharge measurements made with acoustic-Doppler current profilers through application of incorrect edge coefficients. extrapolation of the measured velocity profiles to the bed or water surface, or incorrect compensation of moving-bed effects.

For this investigation, NHDPlus (National Hydrology Dataset Plus) was evaluated for use in identifying general channel gradients, knick-points, or

potential areas in the basin that warranted more focused study. These areas may be of interest in view of potential climate change impacts on them. Multiple attempts were made to try to detect the center line slope of the river with little success. Figure 6.23 identifies the discrepancies from use of this data set, which at 10 meters resolution lacked the resolution to obtain meaningful results.

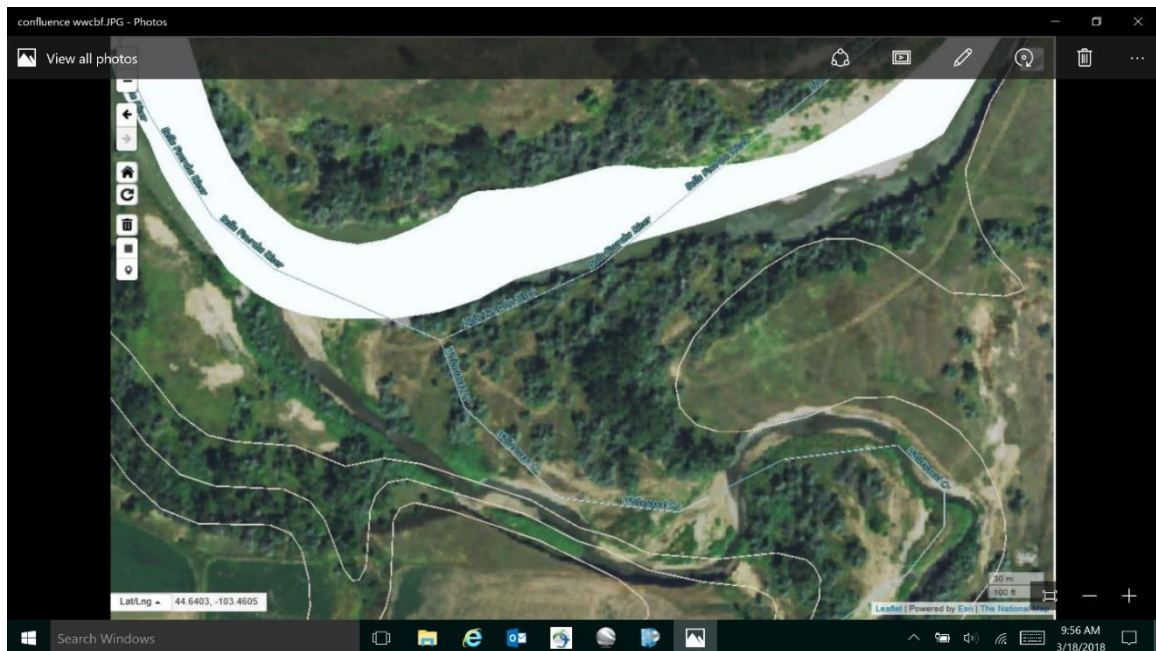


Figure 6.23. Screen shot of an overlay of the stream boundaries over imagery of the confluence of Whitewood Creek and the Belle Fourche River. The National Map maintained by USGS was used along with the NHD to determine if stream elevation could be used to obtain stream slope data. As evident in this figure, the two data sets were not rectified, creating an inaccurate representation of the existing streams.

One of the most impactful historic events in the Missouri River Basin was the presence of continental ice sheets in the Pleistocene Epoch about 14,000 years ago. Continental glaciation transformed and rerouted river systems in the region.

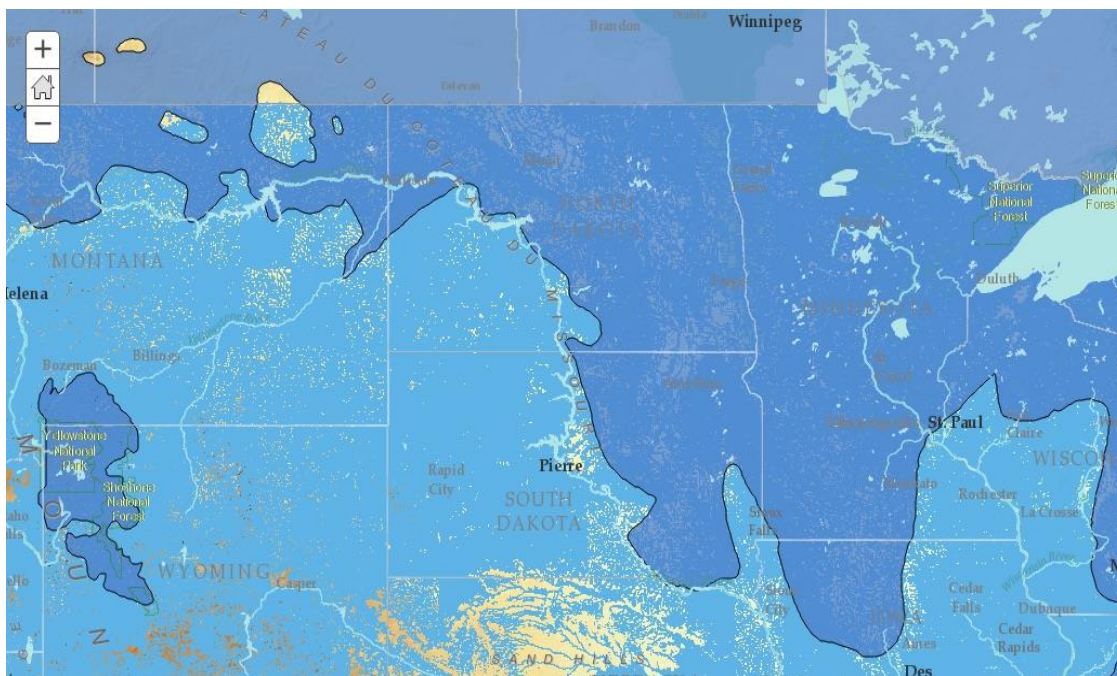


Figure 6.24. A depiction of the best estimate of the most recent North American glacial extent (Dyke, 2014).

The Missouri River owes its present course through South Dakota to continental glacial rearrangement. Before continental glaciation, the rivers in South Dakota had a very different drainage pattern. J.E. Todd conducting the pioneering studies of the Missouri River after many reconnaissance studies in the western U.S. in the early 20<sup>th</sup> century (Todd, 1914 and 1923). He identified that “east of the Missouri is of eastward-trending valleys partly filled with drift and containing no through-flowing streams.” He inferred that these eastward-trending valleys represented parts of major preglacial drainage that had been overwhelmed by ice advancing from the northeast that was partly choked with glacial deposits of gravels, sands, and till (clays). Todd (1914 and 1923) postulated that the current James River lowland in eastern South Dakota was cut by a large river made by five western streams combined, and that this river

flowed north to the region of Hudson Bay. He considered the Missouri to have formed along the margin of the blockading ice sheet, and the west-to-east-flowing streams detoured around the ice, rerouting into the current Missouri River (Figure 6.24).

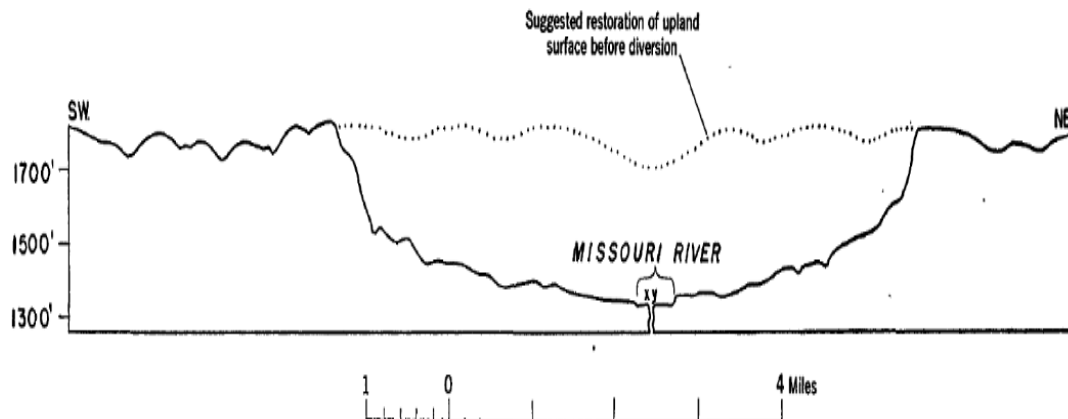


Figure 6.25. Anomalous upland slopes adjacent the Missouri River trench. The profile is located north of Chamberlain, SD. The dotted line (inferred) suggests a possible restoration of the upland surface prior to glacial diversion. (Flint, 1955).

Flint (1955) inferred that ponding of the ancient, pre-diversional valleys by the encroaching continental ice sheet may have resulted in sediment deposition. However, little evidence of these deposits survived, as they were washed away by the western tributaries to the Missouri. In this erosion, lacustrine sediments would have been washed away very soon. Except in the vicinity of the glacier, these sediments would have consisted mostly of clay derived from the underlying Pierre Shale.

Plumley (1948) mapped terraces originating from streams emanating eastward from the Black Hills. Attributing the terrace levels to periodic pauses of Pleistocene glaciation in eastern South Dakota, he said the terraces probably correlate with the last glacial stage in eastern South Dakota. He inferred that their origin may be due to downstream blocking by Pleistocene continental ice sheets on what is now the Missouri River, approximately 200 miles to the east. Plumley (1948) reported that active downcutting adjustment was still taking place along stream reaches near the Belle Fourche and Cheyenne South Fork Rivers.

Continental glaciers blocked the flow of northeasterly flowing streams, causing them to reroute and discharge into the Missouri River. Streams in the region had drained from west to east prior to the advance of Pleistocene glaciers (Hoagstrom, 2006). After the continental glaciers receded, the floodplains dynamically “coevolved” with their channels. Belmont (2011) recognized that both are integral components of “the same system dictating the conveyance and routing of water and sediment within a river system.” (Belmont, 2011) and Zaprowski (2001) each used knick-point migration to identify natural geomorphic changes to the streams in the Black Hills. They connected knick-points with glacial climatic changes that caused base levels to change, indicating that the occurrence of glaciers has been underappreciated in terms of their ability, over very long-time spans and large areas (and even outside those areas directly impacted by glaciation) to integrate drainages and modify landscapes. Darton (1909) noted that the Belle Fourche River “truncated” (captured the flow of) a major tributary of the Little Missouri River.

Confirming this phenomenon, Stamm et al. (2013) provided evidence about the stream piracy which substantially affected the region's geomorphic evolution, including that of the Cheyenne and Belle Fourche Rivers. (Stream piracy is an event in which water from one stream is captured by another stream with a lower base level.) Stamm et al. (2013) proposed that Black Hills stream piracy substantially affected the geomorphic evolution of the Missouri River watershed and drainages within, including the Little Missouri, Cheyenne, Belle Fourche, Bad, and White Rivers. The ancestral Cheyenne River eroded headward in an angular pattern around the eastern and southern Black Hills and pirated the headwaters of the ancestral Bad and White Rivers after 660ka. The headwaters of the ancestral Little Missouri River were pirated by the ancestral Belle Fourche River. All of these factors are “relatively recent” in geologic

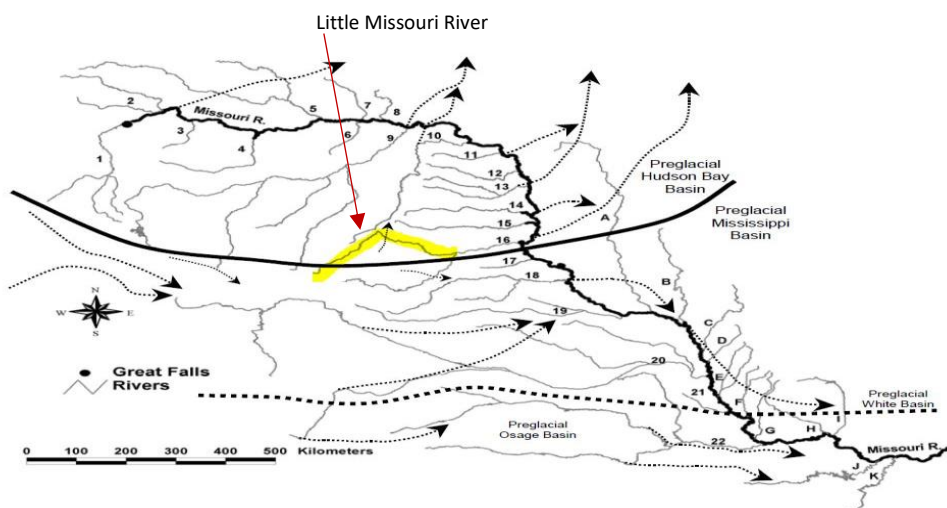


Figure 6.26. The Missouri River Basin after continental glaciation. The Belle Fourche River is highlighted in yellow (Modified from Hoagstrom, 2006). Although the study region was not significantly impacted by the presence of continental glaciation, streams in the basin continue to adjust to the geologic changes brought on by the glacially induced formation of the Missouri River.

timescales and may play an important role in regional channel adjustment and resulting sediment generation, as regional basin baselines are still adjusting

Stamm et al. (2013) used optically stimulated luminescence (OSL) dating techniques to estimate the age of terraces within the study area to the time of the piracy event at ~22-21ka. The geomorphic evolution of the Cheyenne and Belle Fourche Rivers is also expressed by regionally recognized "strath" terraces that include, from oldest to youngest, the Sturgis, Bear Butte, and Farmingdale terraces. Radiocarbon and OSL dates from fluvial deposits on these terraces indicate incision to the level of the Bear Butte terrace by ~63ka, to the level of the Farmingdale terrace at ~40ka, and to the level of the modern channel after ~12-9ka. Hypothesized causes of incision are the onset of a colder climate during the middle Wisconsinan glaciation and the transition to the full-glacial climate of the late-Wisconsinan. Lower Cheyenne River incision during the Holocene Epoch is as much as ~80m and is three to four times the magnitude of incision at ~63ka and ~40ka. The magnitude of incision during the Holocene might be due to a combined effect of three geomorphic processes acting in concert: glacial isostatic rebound in lower reaches (~40m), a change from glacial to interglacial climate, and adjustments to increased watershed area resulting from piracy of the ancestral headwaters of the Little Missouri River. Understanding the existing terraces in the study area in relation to the existing stream channel provides insight into the regional changes that are occurring in geomorphic conditions and streamflow.



Figure 6.27A. Stream bank erosion is widespread along Bear Butte Creek, a tributary of the Belle Fourche River, from effects of physical processes within the basin. Massive amounts of bank sediments can be deposited in the channel by



landslide activity, which may significantly impact the sediment transport capacity of the existing channel, resulting in aggradation and increases in the channel elevation and modification of the channel slope.

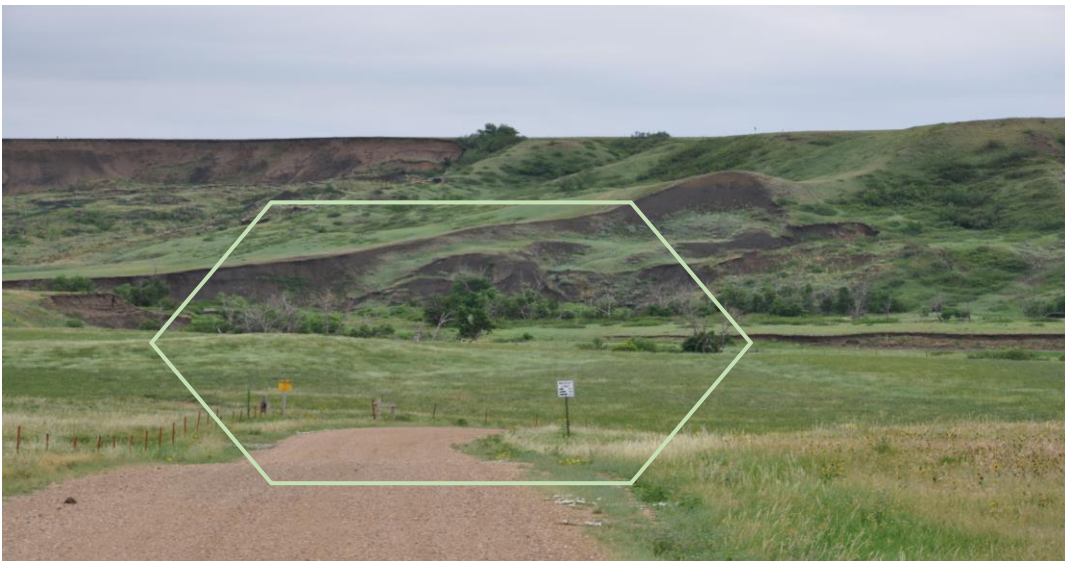


Figure 6.27B. Another look at the effects of widespread stream bank erosion in Bear Butte Creek, a tributary of the Belle Fourche River. Although no mining-contaminated alluvium is present at these sites, tailings containing alluvium occurring as overbank deposits can collapse, providing a significant supply of sediment with storm-related events.





Public Meeting/  
Open House

June 28, 2012

PROJECT P 0034(143)44 PCN 02AB  
MEADE COUNTY

SD 34 Bridges Located 6.0, 9.4, 17.6 & 19.5  
Miles NE of SD79

Bridge Replacements & Approach Grading  
Bridge Erosion Protection

The South Dakota Department of Transportation provides services without regard to race, color, gender, religion, national origin, age or disability, according to the provisions contained in SDCL 20-13, Title VI of the Civil Rights Act of 1964, the Rehabilitation Act of 1973, as amended, the Americans With Disabilities Act of 1990 and Executive Order 12898, Federal Actions to Address Environmental Justice in Minority Populations and Low-Income Populations, 1994.

Any person who has questions concerning this policy or who believes they have been discriminated against should contact the Department's Civil Rights Office at 605-773-3540.



Project Location



Figure 6.28. Public hearing notice about design of a new bridge reflects local concern about infrastructure degradation from channel bed erosion in the area.

As early as the 1950s, Louis Peltier recognized the relationship between climate as an agent of erosion and geomorphology of streams, stating that “even changes in climate (mean annual temperature and rainfall) would become recognizable in the landscape.” Climate change effects on surface water include magnitude, frequency (return period), timing (seasonality), variability (averages and extremes), and direction of predicted changes of flow (Mujere and Moyce, 2018). Although the potential impacts of climate change on water supply have received much attention, relatively little is known about climatic effects on regional water quality.

## 6.7 Temperature: Observations and Projected Trends

The Fourth National Climate Assessment group reported in 2017 that observed temperature in the United States has increased 1.3-1.9 degrees Fahrenheit since 1895, with the largest proportion of this increase occurring since 1970 (Melillo et al., 2014). Much of the warming occurred in recent decades; since 1991, temperatures rose 1.0-1.8 degrees Fahrenheit over most of the United States relative to temperatures during the period 1901-1960. Paleo-temperature evidence shows that recent decades to be the warmest of the past 1,500 years (*medium confidence*).

Due to its location in the center of the North American continent, far from the moderating effects of the oceans, and the range of forest and grassland biomes in the state, South Dakota experiences a wide range of temperature extremes. Average January temperatures range from less than 12 degrees Fahrenheit in northeast South Dakota to more than 24 in the southwest, with average July temperatures ranging from less than 64 in the Black Hills to more than 75 in the south-central part of the state. Temperatures of 100 degrees or more occur nearly every year (Frankson et al., 2017). Figure 6.22 depicts annual daily mean climate data from the NOAA-CIRES Climate Diagnostic Center for maximum and minimum temperature and precipitation.

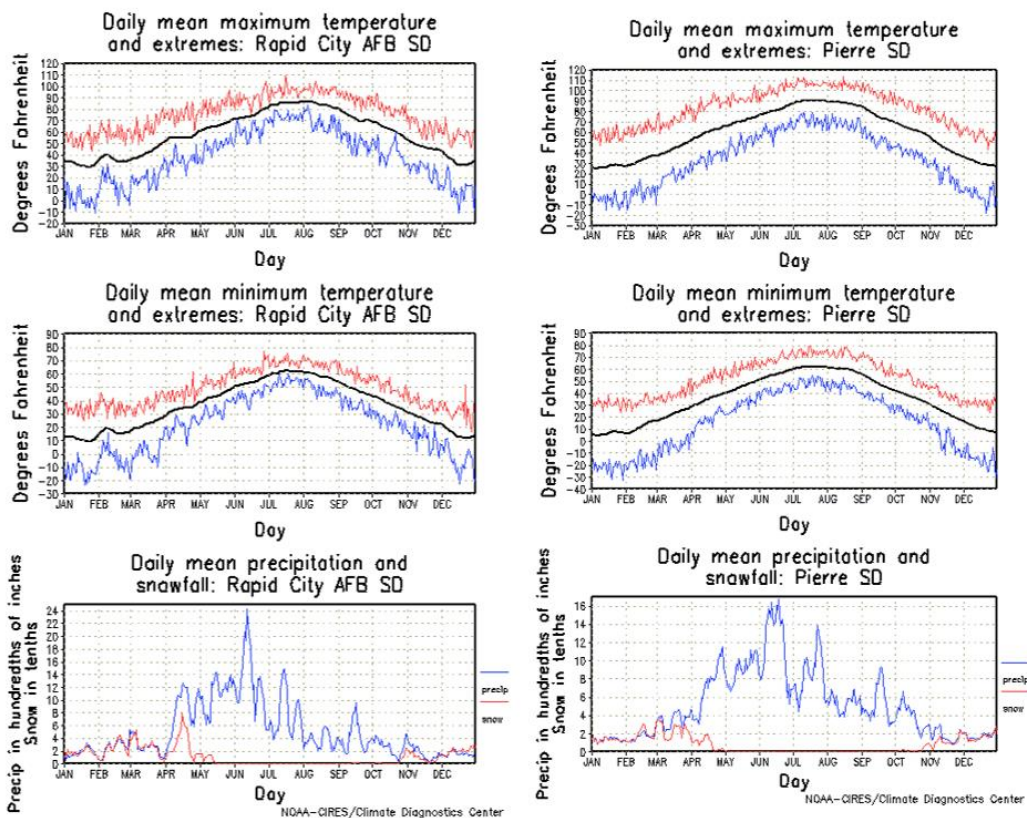


Figure 6.29. Daily means for temperature/precipitation. (NOAA CIRES (Cooperative Institute for Research in Environmental Sciences)/Climate Diagnostic Center).

The numbers in Figure 6.22 represent minimum, maximum, and mean temperature and precipitation based on records from 1961 to 1990 for both the west (Rapid City) and (Pierre) on the east side of the basin. NOAA-CIRES characterizes the study basin's climate as semiarid and continental, with wide temperature ranges, low relative humidity, high evapotranspiration, frequent high winds, relatively low amounts of precipitation, long winters, and warm summers. Based on data for Meade County, SD, the growing season ranges from 115 to 130 days, with the average last killing frost in mid-May and the first killing frost in

late-Sep (NDSU, 2018). The growing season in the upper reaches of Whitewood Creek at higher elevations in the Black Hills is shorter than those on the eastern plains. From 1991-2011, the average frost-free season nationally was ten days longer relative to an earlier 1901-1960 period (Melillo et al., 2014). USACE (2015) identified an apparent small shift in seasons in the Missouri River region by examining historical data from over 22,000 stations across the U.S., obtained from the National Climate Data Center with periods of record extending through 2010. The findings indicate that for the Missouri River region, spring onset is occurring at least a few days earlier for the period 2001-2010 than it did during an earlier baseline reference decade of 1951-1960.

Frankson et al. (2017) report an increase of approximately 2°F in South Dakota since beginning of the 20th century (Figure 6.31). Temperatures in the 2000s have been warmer than any other historical period, except for the 1930s Dust Bowl era, when poor land management practices likely worsened already-hot summer temperatures. Warming is reported to be occurring mostly in the winter and spring; summers have not warmed much in South Dakota, a trend in keeping with much of the Great Plains and Midwest

Figure 6.30 depicts projected changes in temperature for 2006–2100 from GCMs showing two possible futures: one in which GHG emissions continue to increase (higher emissions) and another in which GHG emissions increase at a slower rate (lower emissions). Temperatures in South Dakota (orange line) have risen almost 2°F since the beginning of the 20th century. Shading indicates the range of annual temperatures from the set of models. Observed temperatures

are generally within the envelope of model simulations of the historical period (gray shading). Historically unprecedented warming is projected during the 21<sup>st</sup> century. Less warming is expected under a lower emissions future (the coldest years being about 2°F warmer than the long-term average; green shading), and more warming under a higher emissions future (the hottest years being about 16°F warmer than the long-term average; red shading).

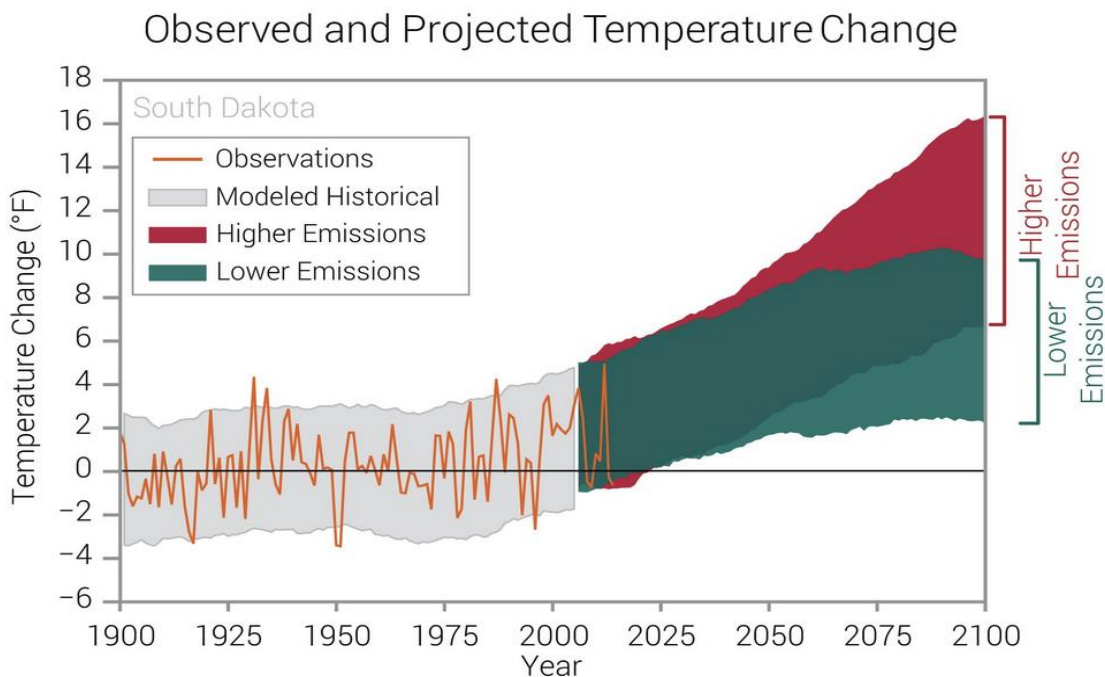


Figure 6.30. Observed and Projected Temperature Change ((CICS-NC (Cooperative Institute for Climate and Satellites—North Carolina) and NOAA NCEI (National Centers for Environmental Information) in Frankson et al., 2017).

Winter imparts unique seasonal climatic and hydrologic changes that affect river channels, discharge, and sediment transport (Figures 6.24 A and B). Ice formation can occur when the average daily temperature is at or below freezing. Ice cover thickens throughout the winter and is dependent on such



variables as water surface width, channel curvature, freeze-up stage, and ice competence.

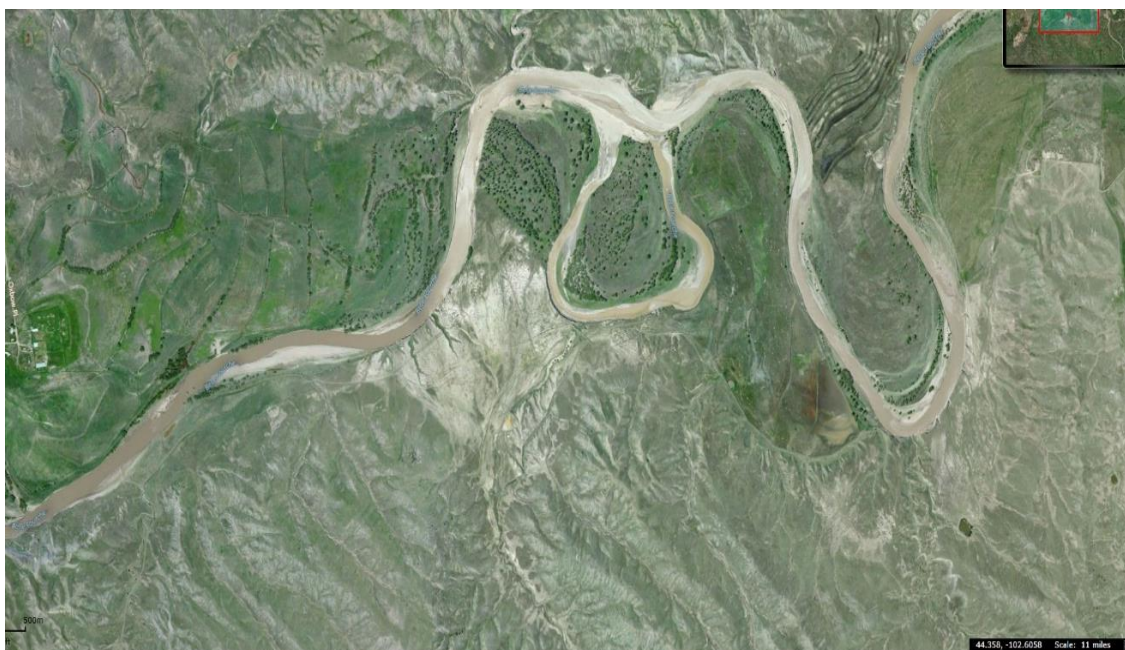


Figure 6.31A. The Cheyenne River, 44.358N latitude-102.6058W longitude, Oct. 2014 (DigitalGlobe, 2015).



Figure 6.31B. The Cheyenne River, same location, Jan. 2015. Icing is constricting flow through the channel meander (DigitalGlobe, 2015).

Stewart et al. (2005) present a statistical analysis covering changes in the timing of snowmelt and streamflow across western mountainous states from 1948 to 2002. Results show trends in both earlier onset of the snowmelt pulse and earlier CT timing (center of mass of the annual flow). Although the overall average streamflow at most locations remained similar, the snowmelt season started 10 to 30 days earlier than during the 1948-2002 period of analysis.

Hains and Zabilansky (2004) conducted real-time monitoring of river bed elevation and made extensive bathymetry measurements on the Mississippi, Missouri, and White River (just south of the Belle Fourche and Cheyenne River). Their studies found the sediment-transport processes under icing conditions to be significantly different than what was predicted using existing conventional sediment transport equations.

Daly (2011) describes four distinct phases of freeze-up conditions:

- (a) Pre-freeze up open water with no or minimal amount of ice.
- (b) Freeze up – stationary ice is forming which may impact the river stage.
- (c) Ice smoothing – overall hydraulic resistance of the ice cover is declining.

He attributes this to the smoothing of the underside of the ice cover through melting and/or deposition of transported frazil ice along the bottom of the ice cover. During this state, which can last 90 or more days, the stage slowly drops back to the pre-freeze up open water levels.

- (d) Melting of ice and return to open water.



Figure 6.32. Ice on the Belle Fourche River, Jan. 15, 2017, at 44.3725N Latitude-102.9509W Longitude (Digital Globe, 2017).

Predicting how the ice cover of a river is going to break up as a result of increased runoff is crucial to such concerns as environmental impact assessment of climatic and hydrologic changes, emergency flood warning and mitigation, and winter hydro-power production. Zabilansky et al. (2002) indicated that river ice potentially influences the alluvial channel morphology because it affects the prevailing conditions of the stream discharge, alluvial sediment availability, and channel banks. They suggest that it is common knowledge that ice cover affects the vertical and lateral distribution of flow in a channel, but less well known is how river ice influences the flow's capacity to entrain bed sediment (incorporate it into fluid flow), transport alluvial sediment and maintain the geotechnical stability of channel banks flanking the flow. This seasonal influence creates a hysteresis with the annual occurrence of winter weather.

Ice begins to form and builds up to cover up to 100 % of the stream once there has been enough time with temperatures below freezing; it then breaks up



once temperatures rise above freezing long enough for it to thaw (Murphy et al., 2006). Once ice is broken up, it can result in river ice jams that when released may cause extreme flood events, impacting the stream's sediment transport capacity. River ice can damage structures such as bridges and piers by buckling or lifting from broken-ice accumulations, and by bed scour from the hydraulic effects of flowing waves of water and ice (Neill, ed., 1973). Ice accumulation may also contribute to increased scour by altering flow velocities and turbulence near the riverbed. Ice scour can occur from moving ice during the period of ice breakup, when it can shear off sediment or pull vegetation out of a stream channel bed or banks. As for any river in cold regions, the riverbanks of the lower Cheyenne and Belle Fourche Rivers are subject to freeze–thaw and freeze–sublimation weakening. Freeze–thaw weakening potentially influences riverbank erosion and may impact channel morphology as well. Freeze–sublimation weakening will deteriorate the exposed faces of riverbanks. The soils comprising the riverbanks contain enough silts and fine sands to make them prone to both forms of weakening. The east–west orientation of the average axis of the reach may create differences in erosion rates, because riverbanks facing south receive greater insulation than do north-facing banks. The extent to which the ice-related weakening influences rates of riverbank recession has yet to be determined (Zabilansky et al., 2002).

## 6.8 Precipitation: Observations and Projected Trends

The National Climate Assessment provides information about projected future precipitation at global, national, and regional scales (USGCRP, 2018, and Shafer et al. (2014). On a global scale, climate models show consistent projections of future increases in precipitation for northern climates under a range of greenhouse gas (GHG) emissions scenarios (Melillo et al., 2014). In addition to increases in annual precipitation, the frequency of storm events with heavy precipitation events is expected to increase relative to current conditions (Melillo et al., 2014), leading to increased runoff and flooding which can reduce water quality and increase soil erosion

A 2011 study by McRoberts and Nielsen-Gammon used a new continuous and homogenous data set to perform precipitation trend analyses for sub-basins across the United States. The extended data period used for the analysis was 1895-2009. Linear positive trends in annual precipitation were identified for most of the U.S, including the Missouri River Region (Figure 6.33) except for Montana, which showed a slight decreasing trend. The trend in annual precipitation indicates a change on the order of -5 to 15% per century depending upon location.

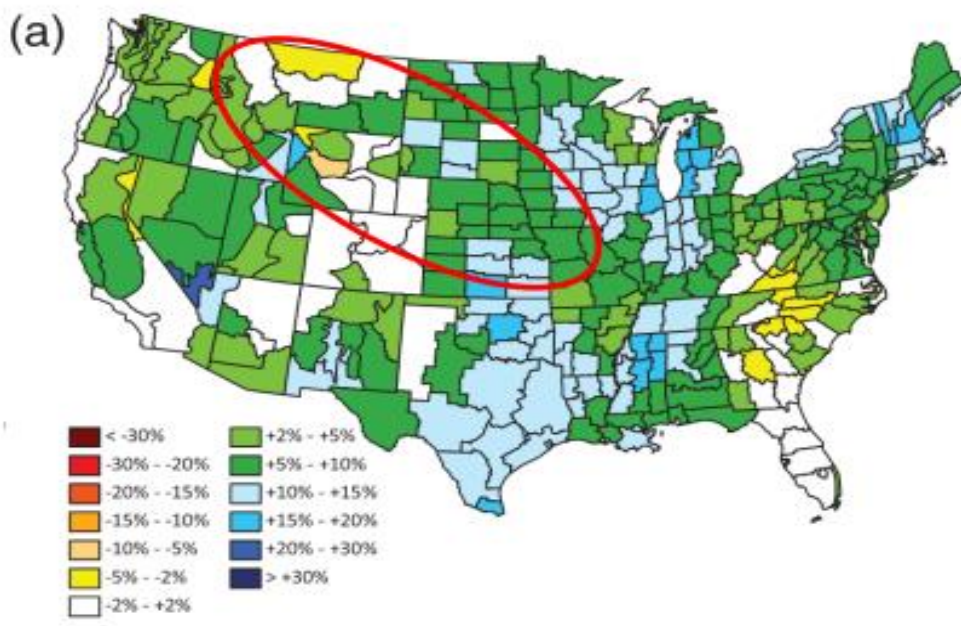


Figure 6.33. Linear trends in annual precipitation, 1895-2009. The Missouri River Region is within the red oval (McRoberts and Nielsen-Gammon, 2011).

Changes in extreme precipitation events recorded in recent historical data have been the object of a number of studies, with studies of extreme events focusing mainly on their intensity, frequency, and duration. Wang and Zhang (2008) used recent historical data and downscaled GCMs to investigate changes in extreme precipitation across North America, focusing specifically on changes in the frequency of the 20-year maximum daily precipitation event. They looked at both historical trends in observed data and trends in future projections, and found statistically increases in the frequency of the 20-year maximum precipitation event across the lower portion of the Missouri River Region for the period 1977 to 1999 as compared to the period 1949-1976. Wang and Zhang (2008) quantified an increase in frequency of ~33-50% for this area. For the

upper portion of the Missouri River Region, they identified a decreasing frequency of the 20-year storm event in the range of -33%.

For winter precipitation, Frankson et al. (2017) project a > 15% increase in the study region (Figure 6.34), which is consistent with the upward trend reported by McRoberts and Nielsen-Gammon, 2011).

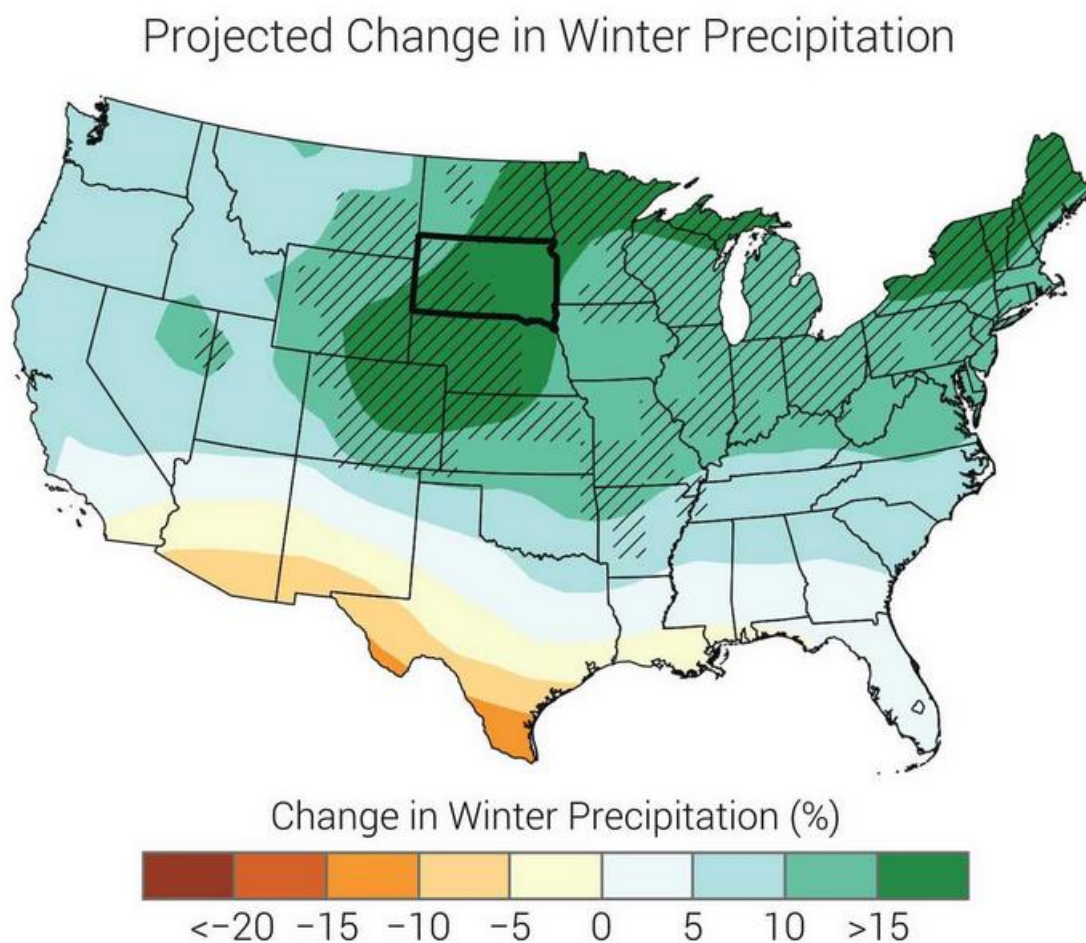


Figure 6.34. Projected changes in winter precipitation (%) for the middle of the 21<sup>st</sup> century compared to the late 20<sup>th</sup> century, under a higher emissions pathway. The diagonal lines (which cover the study region) represent areas where the majority of climate models indicate a statistically significant change. Winter precipitation is projected to increase by 10-20% (Frankson et al., 2017).

Along with temperature data, Figure 6.29 previously showed annual daily mean rain and snowfall data for Pierre and Rapid City, SD, which is near the study area. In the Northern Great Plains, snowfall is highly variable from year to year. For example, the annual snowfall totals at Menno, SD, have varied from about 10 inches (in the winters of 1986–87 and 1999–2000) to nearly 70 inches (winters of 1959–60 and 1983–84). South Dakota's northern location and proximity to the typical U.S. winter storm track makes it highly susceptible to the usual impacts of winter storm systems, including heavy snows. In any given year, the probability of a blizzard occurring somewhere in the state is greater than 50 %.

The Black Hills significantly influence the weather in the Cheyenne River Basin, its high-elevation topography playing a large part in the convection, initiation, and evolution of weather systems producing precipitation (Klimowski et al., 1996). Klimowski et al. (1996) report that a large majority (77%) of the squall lines, bow echoes, and high wind events in western South Dakota were initiated within 100 miles of "significant topography" (i.e., the Black Hills), and most (56%) were initiated within 50 miles of the change in elevation. One of the study area's most significant flood events occurred on June 9-10, 1972, with a death toll of 234, mostly in Rapid City (USACE, 1972). Over 15 inches of rain fell in six hours just northwest of Rapid City, causing Rapid Creek, a subwatershed in the Cheyenne River Basin, to flood. During this event, the average six-hour rainfall over 1,000 square miles in the region was 6.7 inches. Peak discharges in Rapid Creek were 50,000 cfs, compared to a previous recorded maximum peak

discharge of record of 3,300 cfs in 1962 (USACE, 1972). Ironically, the Rapid City flood took place during a period of fewer-than-average extreme precipitation events. (Figure 6.35).

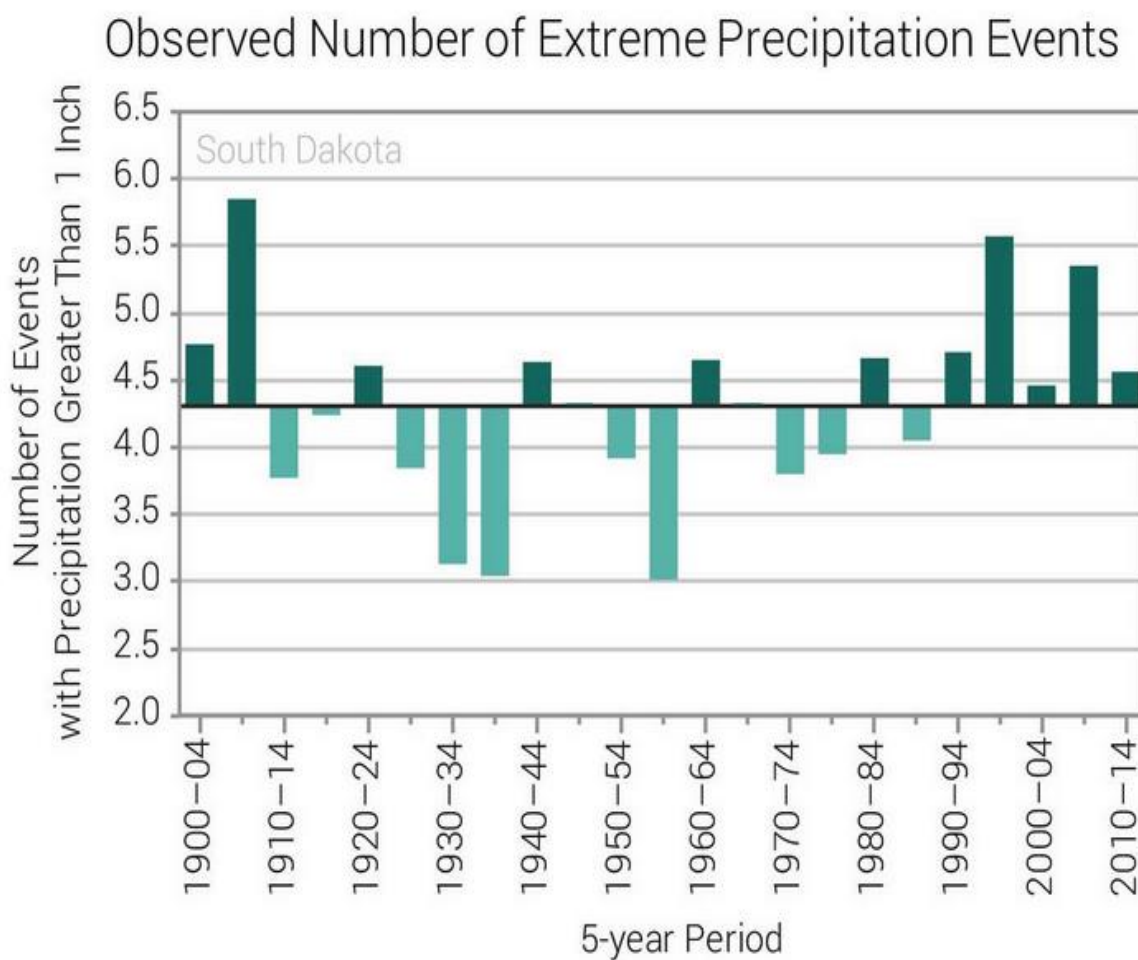


Figure 6.35. Observed number of extreme precipitation events (annual number of days with more than an inch of precipitation for 1900-2014, averaged over 5-year periods. Values are averages from 32 long-term reporting sites. Since 1990, South Dakota has experienced an above average number of these events. The dark horizontal line is the long-term average of 4.3 days per year over this 115-year period (CICS-NC and NOAA NCEI).

Although there is consensus about temperature increases, less certainty exists about probable impacts on water quality from changes in regional

precipitation—especially the impacts from changes in extreme events, which need to be considered. New designs may be required for power and water supply systems, and urban drainage and treatment systems may have to incorporate design features resilient to climate change effects (Whitehead et al. (2009). New operational procedures may also be needed, with major possible implications for water quality monitoring protocols, environmental standards, and compliance and reporting (Crane et al., 2005). However, it is also possible that current water quality standards are sufficiently robust to cope with climatic change, especially considering their evolution from wide-ranging toxicity studies (Crane et al., 2005).

For heavy rainfalls, runoff and solid material transportation are the main consequences. For countries in the temperate zone, climate change will decrease the number of rainy days but increase the average volume of each rainfall event (Brunetti et al., 2001; Bates et al., 2008). As a consequence, drought–rewetting cycles may impact water quality as these cycles enhance decomposition and flushing of organic matter into streams (Evans et al., 2005). The presence of water is the primary catalyst for sediment transport or chemical interaction; as precipitation increases, the rate of chemical reactions will vary directly with rainfall. (In accordance with the Arrhenius equation, there is also a general tendency for the rate of a chemical reaction to increase with temperature (Laidler, 1984)).

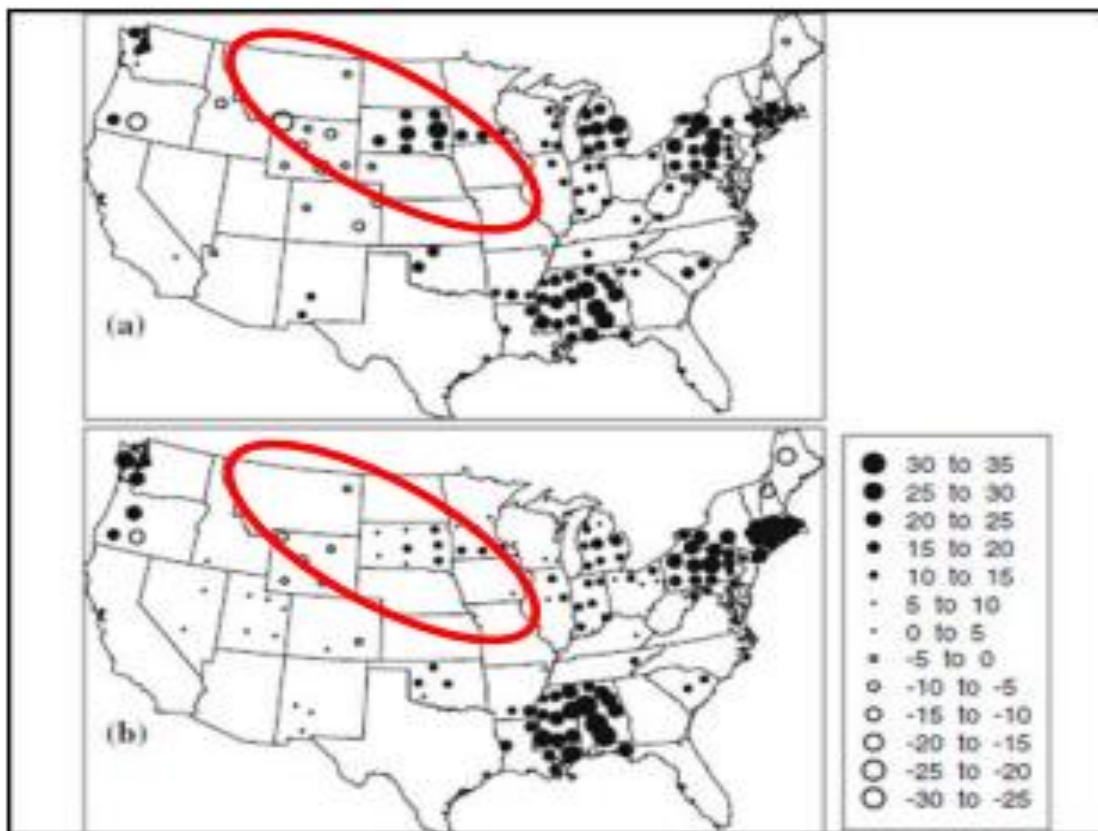


Figure 6.36. Statistically significant linear trends in (a) soil moisture index (unitless) and (b) annual precipitation (cm) for the continental U.S., 1895-2006. The Missouri River Region is within the red oval (Grundstein, 2009).

Multiple researchers have noted increasing trends in total annual precipitation in recent historical records for the lower Missouri River Region, with decreasing trends for the region's upper portion. Grundstein (2009) identified statistically significant (95% confidence interval) positive linear trends for the period of 1895-2006 in both annual precipitation and the soil moisture index for multiple sites within South Dakota. However, slightly decreasing trends were observed in the upper portion of the Missouri River Region, including Montana and Wyoming (Figure 6.36). Soil moisture is a function of both supply



(precipitation) and demand (evapotranspiration (ET)), which makes it “an effective proxy” for both precipitation and ET. The upper portion of the region was found to have a slightly decreasing trend in ET while the lower portion was observed to have a slightly increasing trend (Grundstein, 2009).

## 6.9 Hydrologic Conditions

### 6.9.1 Observed Hydrologic Conditions

In addition to Chapter 1’s descriptions of the Whitewood Creek/Belle Fourche and Cheyenne Rivers study area, three published USGS reports provide excellent summaries of the observed hydrologic conditions in both the Black Hills (Whitewood Creek and Belle Fourche River) and Great Plains regions (Cheyenne River):

- *Hydrologic Conditions and Budgets for the Black Hills of South Dakota, Through Water Year 1998* (2001) by Daniel G. Driscoll and Janet M. Carter
- *Peak-flow frequency estimates based on data through water year 2001 for selected streamflow-gaging stations in South Dakota: U.S. Geological Survey Scientific Investigations Report 2008–5104* (2008) by Steven K. Sando, Daniel G. Driscoll, and Charles Parrett
- *Flood-frequency analyses from paleoflood investigations for Spring, Rapid, Box Elder, and Elk Creeks, Black Hills, western South Dakota: U.S. Geological Survey Scientific Investigations Report 2011–5131* (2011) by Tessa M. Harden, Jim E. O’Connor, Daniel G. Driscoll, and John F. Stamm

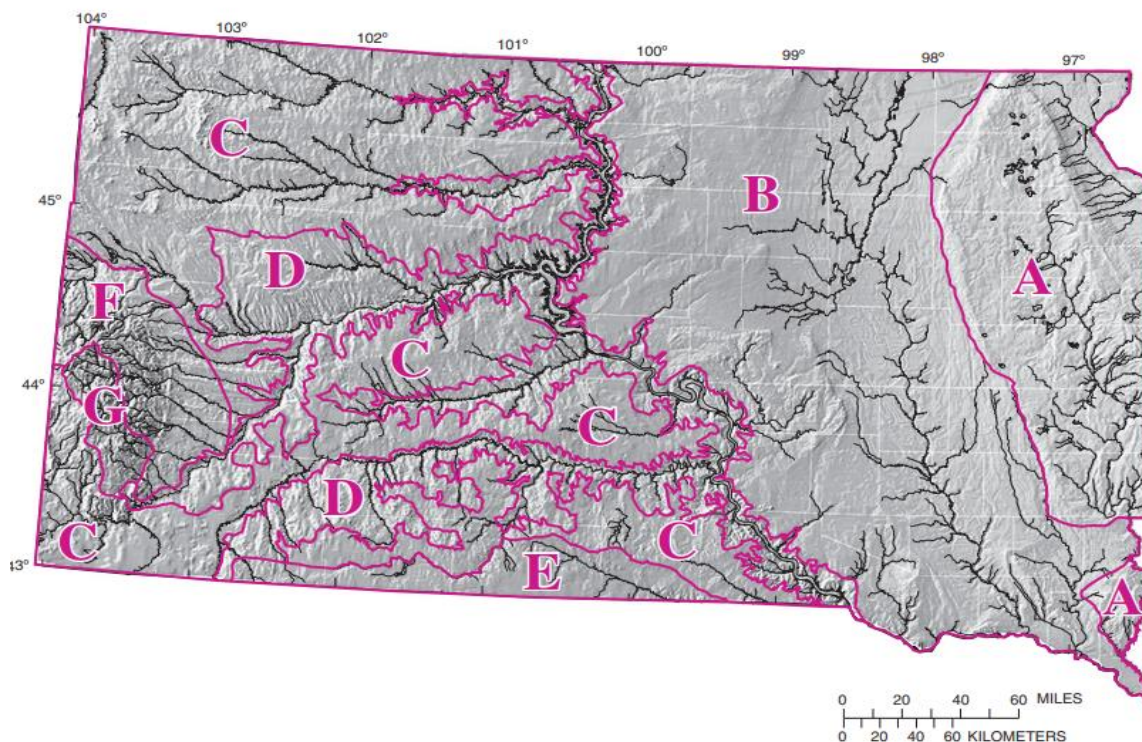


Figure 6.37. Five hydraulic subregions in western South Dakota. Subregions C and D (Belle Fourche and Cheyenne River) and F (Whitewood Creek) comprise the study area (Sando, 1998)

Sando (1998) and Sando et al. (2008) identified seven hydrologic subregions within South Dakota for statewide regionalization of peak-flow characteristics; selection of the subregions was substantially influenced by the primary and secondary physiographic subdivisions shown in Figure 6.37 (Sando, 1998; Sando et al., 2008). Land-surface altitudes range from about 1,000 feet (ft) above National Geodetic Vertical Datum of 1929 (NGVD 29) in the northeastern part of the State to more than 7,000 ft above NGVD 29 in some parts of the Black Hills. The largest relief occurs in the Black Hills, where topography is relatively steep in many locations and general altitudes drop to about 3,000 to 4,000 ft above NGVD 29 in surrounding areas.

Black Hills geology is highly variable and complex, and there are unique and distinct effects on annual peak flows based on the geology of the stream location (Martin et al., 2004, in Sando et al., 2008) (Figure 6.38).

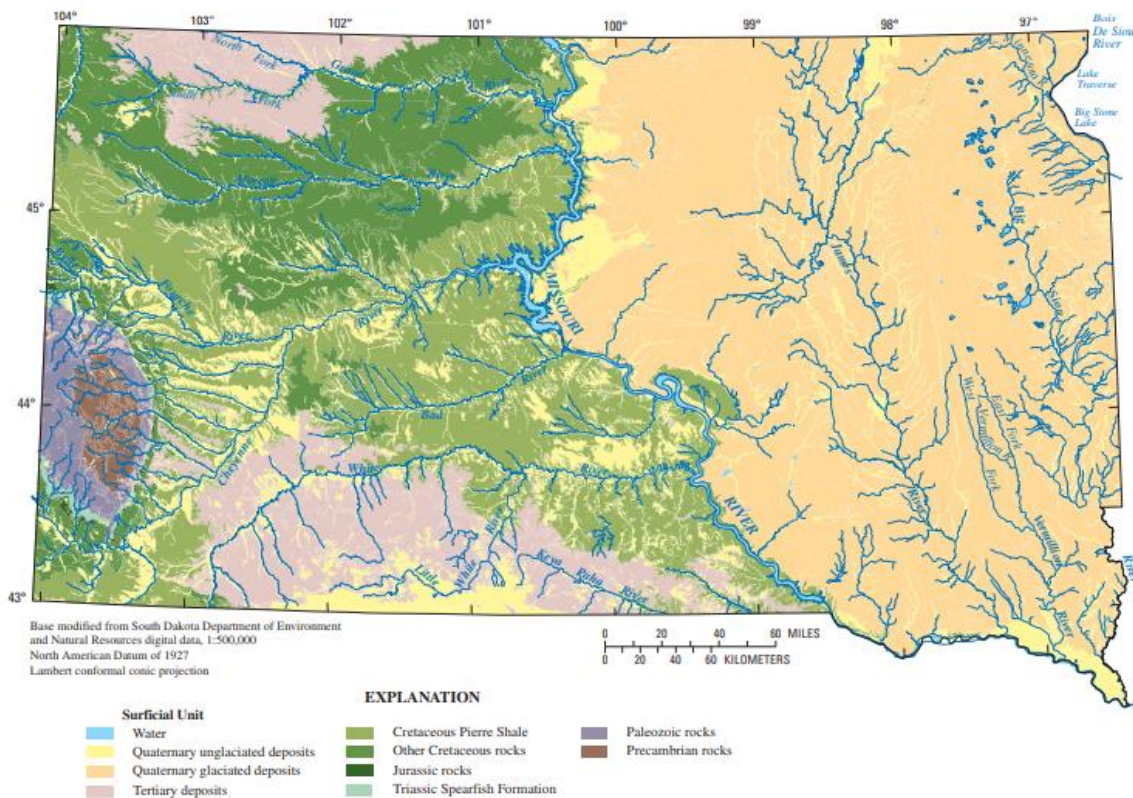


Figure 6.38. Generalized surficial geology of South Dakota (in Sando, 2008; modified from Martin et al., 2004).

Driscoll and Carter (2001) provide a detailed description of the hydrology the Black Hills region, which is included the Cheyenne River Basin. The Cretaceous-age Pierre Shale (Figure 6.38) is the dominant geologic outcrop in western South Dakota, and small outcrops of this formation also occur in a corridor just east of the Missouri River. The soils associated with the Pierre Shale are rich in clay and have low infiltration capacity. Many outcrops of the

Pierre Shale support little vegetative cover along the “breaks” of the Missouri River and along several other of its major tributaries, which results in particularly high peak-flow potential. Similar river breaks also occur in various other geologic outcrops throughout western South Dakota. Sando et al. (2008) included such areas as a separate subregion in regionalizing statewide peak-flow characteristics, noting larger uncertainties in peak-flow frequency estimates for these areas. The common occurrence of clays and siltstones in outcrops of several other Cretaceous formations (Figure 6.37 areas designated as C and D) can result in relatively high peak-flow potential in other relatively large parts of western South Dakota. The “Badlands” area (Figure 6.37 “C”), located predominantly within the White River, Cheyenne, and Bad River Basins, has highly erodible clay soils which represent outcrops of the Tertiary-age White River Group.

Harden et al. (2011) presented a detailed hydraulic analysis and paleo flood chronology using the USACE HEC-RAS hydraulic model based on a digital (5-ft. contour interval) topographic coverage to estimate peak-flow magnitudes for paleofloods along lower Rapid Creek. This is a commonly used alternative procedure to extend records. Calibration of the hydraulic model was accomplished by using surveyed elevations for 1972 highwater evidence within the reach and calibrated with the 1972 peak-flow value of 31,200 ft<sup>3</sup> /s for stream gage 06412500, Rapid Creek above Canyon Lake. Projections were generated by coupling GCMs with macro-scale hydrologic models. Harden et al. (2011) found their study procedures effective for addressing bias resulting from

nonrepresentative climatic conditions during several specific periods, and for reducing inconsistencies among multiple gaging stations along common stream channels with different periods of record. Using the procedures from this study, and coupling GCM projections with macro-scale hydrologic models, could be an improved way to assess all inland waterways, as it might enable better prediction of the impact from increased precipitation and flow in streams from climate change.

Four hydrogeologic settings are represented in Figure 6.39. The “limestone headwater” setting occurs within outcrops of the Mississippian-age Madison Limestone and the Pennsylvanian- and Permian-age Minnelusa Formation within the “Limestone Plateau” area along the South Dakota/ Wyoming border. The Loss zone and Artesian spring hydrogeologic settings are part of The Madison Limestone and Minnelusa Formation physiographic divisions shown in Figure 6.39



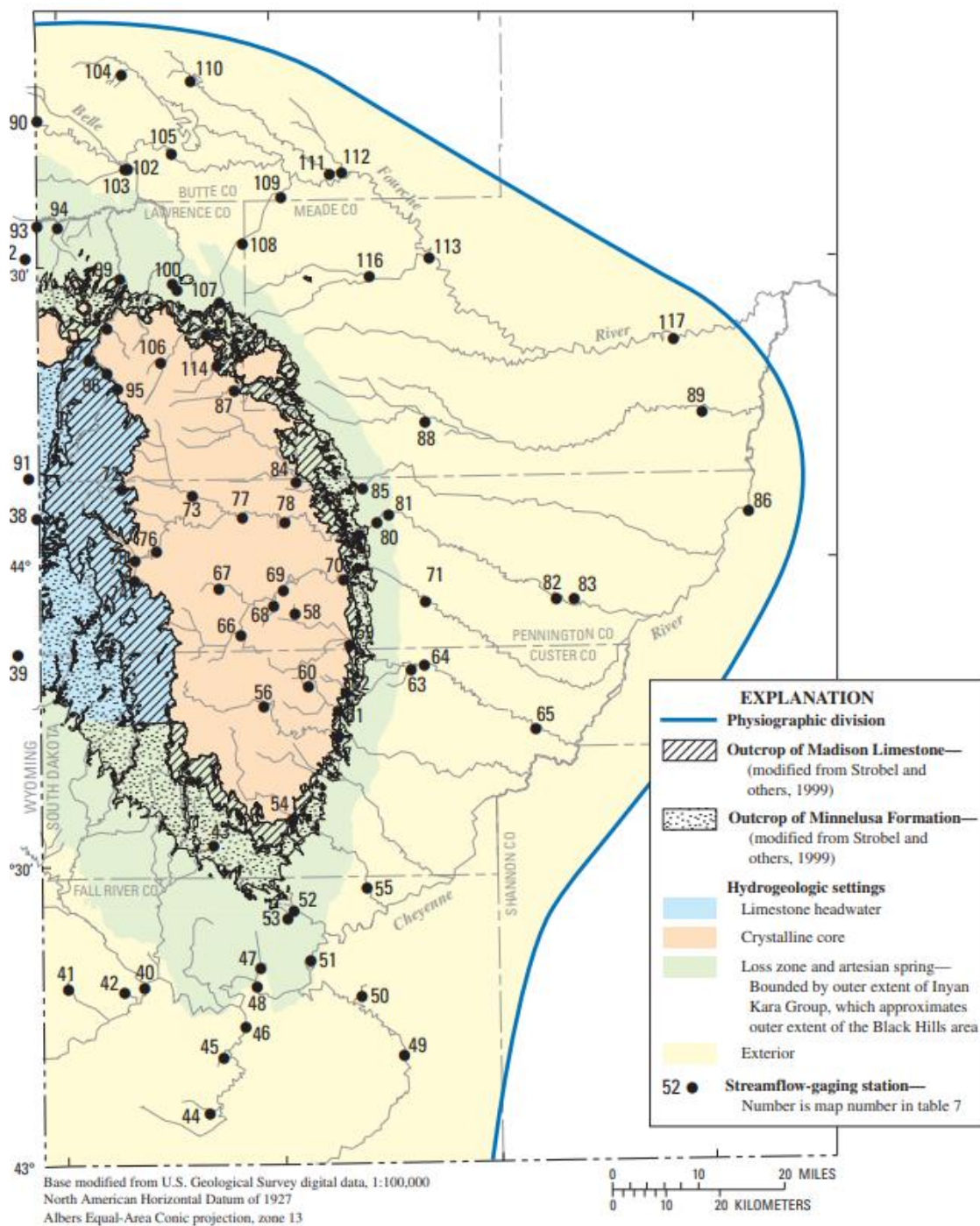


Figure 6.39. Hydrogeologic settings for the Black Hills region (modified from Driscoll and Carter, 2001, in Sando et al., 2008). Whitewood Creek is located in the northeast section of the Black Hills; USGS stream flow gages designated as sites 108-113 and 117 are located in the study area.

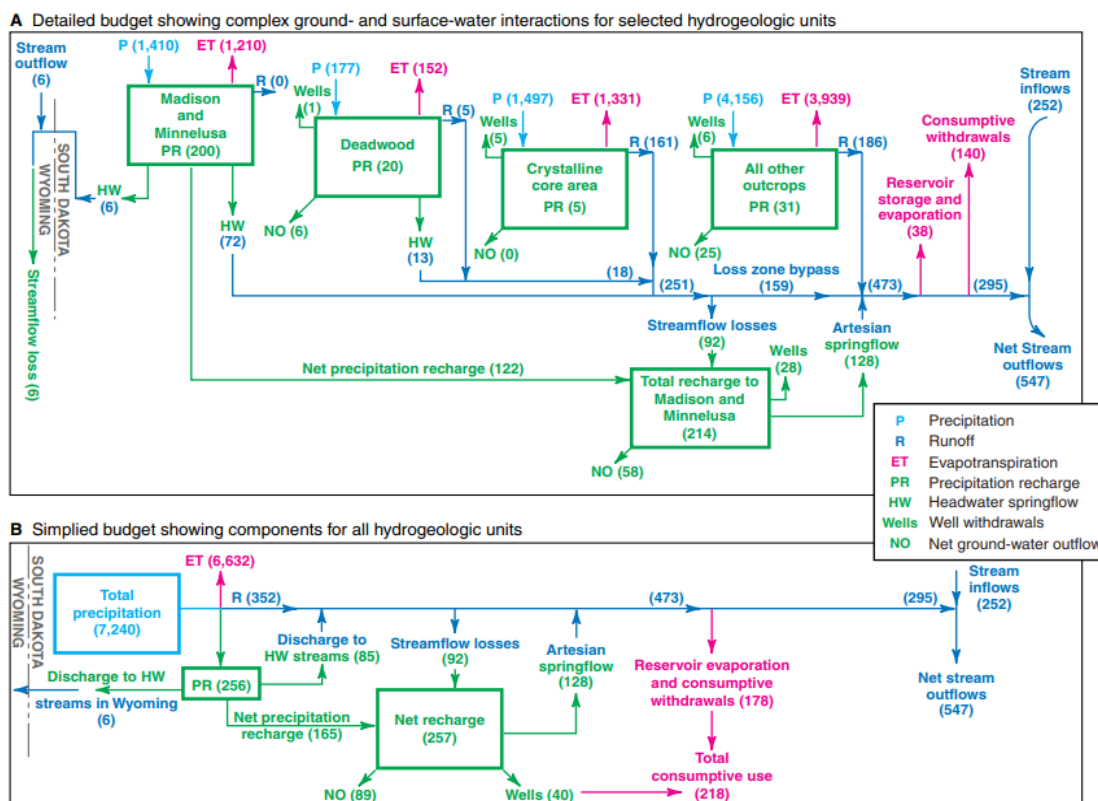
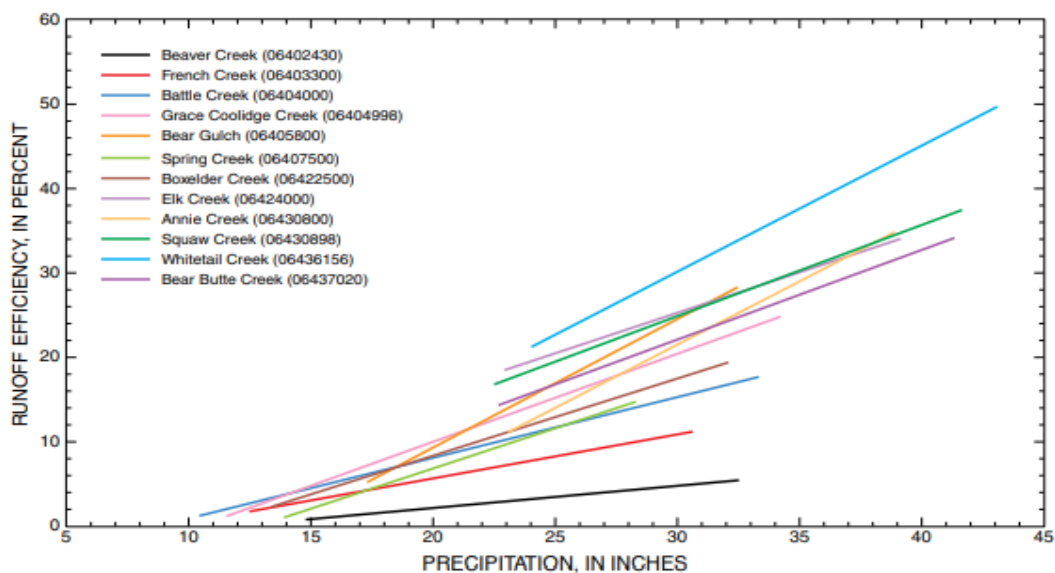
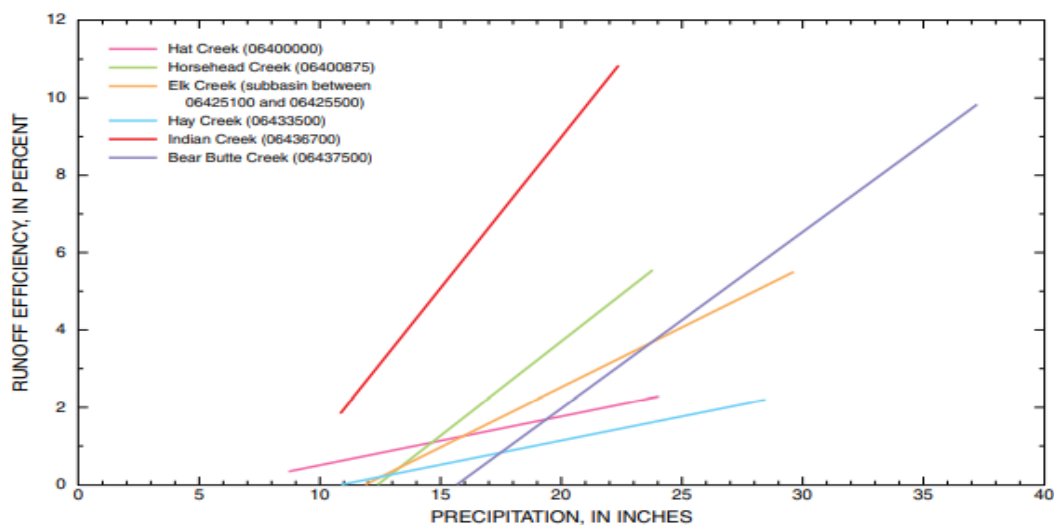


Figure 6.40. This schematic diagram shows the average hydrologic budget components for the study area for water years 1950-1998 (Driscoll and Carter, 2001), demonstrating the complexity of the hydrologic budget component in the Black Hills. Perennial streamflow in this area typically occurs only where large springs exist around the periphery of the Limestone Plateau, and direct runoff is uncommon.

Peak-flow characteristics are affected by a wide variety of hydrogeologic conditions in South Dakota. Figures 6.41A and B show the runoff efficiencies of streams within the depicted basins. (While the study area watersheds are not included, these figures are representative of the region at large.) “A” shows the runoff efficiency for precipitation for streams within Figure 6.39’s hydrogeologic setting of the Black Hills “Crystalline core,” and “B” for the “Exterior” (Figure 6.39). Figures 6.41A and B show that the variation in the runoff efficiency

increases with increasing annual precipitation, and that basins with higher precipitation generally have higher efficiencies. Given increasingly large precipitation, runoff efficiencies would eventually approach 100 percent as annual evapotranspiration is increasingly exceeded.



Figures 6.41A (top) and B (bottom). A shows the relationship between annual runoff efficiency and precipitation for basins within the Black Hills crystalline core; B shows the relationship between annual runoff efficiency and precipitation for exterior basins(those outside of the Black Hills uplift) (Driscoll and Carter, 2001).



Peak-flow characteristics have changed substantially for many rivers in South Dakota because of reservoir construction (Sando, 1998). Thousands of relatively small reservoirs (locally referred to as “stock reservoirs” or “stock dams”) exist in all the major river basins in South Dakota. Sando et al. (2008) references a study by Culler and Peterson (1953) who reported a large reduction in annual runoff for the Cheyenne River that they attributed to the cumulative impact from the construction of numerous stock reservoirs before 1944. Mean annual runoff for the Cheyenne River near Hot Springs (Station 06400500) was 497,200 acre-feet during 1915–20, compared with 101,300 acre-ft (0.22 in. per unit area) during 1944–50. Mean annual precipitation in the drainage basin for the same periods was estimated at 17.66 and 17.42 inches per year, respectively.

Although there are major reductions in annual runoff due to these stock reservoirs, changes in peak-flow characteristics resulting from stock reservoir presence are likely to be highly variable and transient. Small peak flows can be entirely contained by stock reservoirs in some drainages, and virtually all peak flows might be attenuated to at least some extent. However, effects on larger peak flows might be relatively small, especially during flow events when reservoirs are already at or near capacity. Peak flows can also be increased by stock reservoir failures, which can happen often as visually evidenced by numerous failed stock reservoirs throughout the state. Although an important parameter for water use, Sando et al. (2008) did not make an attempt to account for potential changes resulting from stock reservoir construction because (1)

accounting for such changes would be generally infeasible and (2) peak-flow records for most gaging stations largely post-date primary periods of stock reservoir construction.

Sando et al. (2008) indicated that all of South Dakota experiences both short- and long-term drought conditions, with the drought potential generally increasing in a westerly direction across the state as it naturally becomes more semi-arid. Sando et al. (2008) indicate that progressive depletion of vegetative cover during prolonged multiyear drought periods might contribute to increased peak-flow potential, especially in western South Dakota. One of the worst droughts in the state's history was that of the 1930s Dust Bowl-era, with extremely dry conditions made worse by the extreme heat (Frankson et al., 2017). Not only was 1936 the driest summer on record, with only 3.54 inches of precipitation (more than 4.5 inches below the long-term average), but it was also the hottest summer on record, with an average temperature of 76.4°F, 6.8°F above the long-term average. During the recent drought of 2012, South Dakota experienced its driest July–Sep. period on record, receiving only 2.86 inches of precipitation. Even without drought, extreme heat waves alone can be problematic: In 2011, unusually hot and humid conditions in South Dakota caused the deaths of at least 1,700 head of cattle died (Frankson et al., 2017).

### 6.9.2 Projected Hydrologic Trends

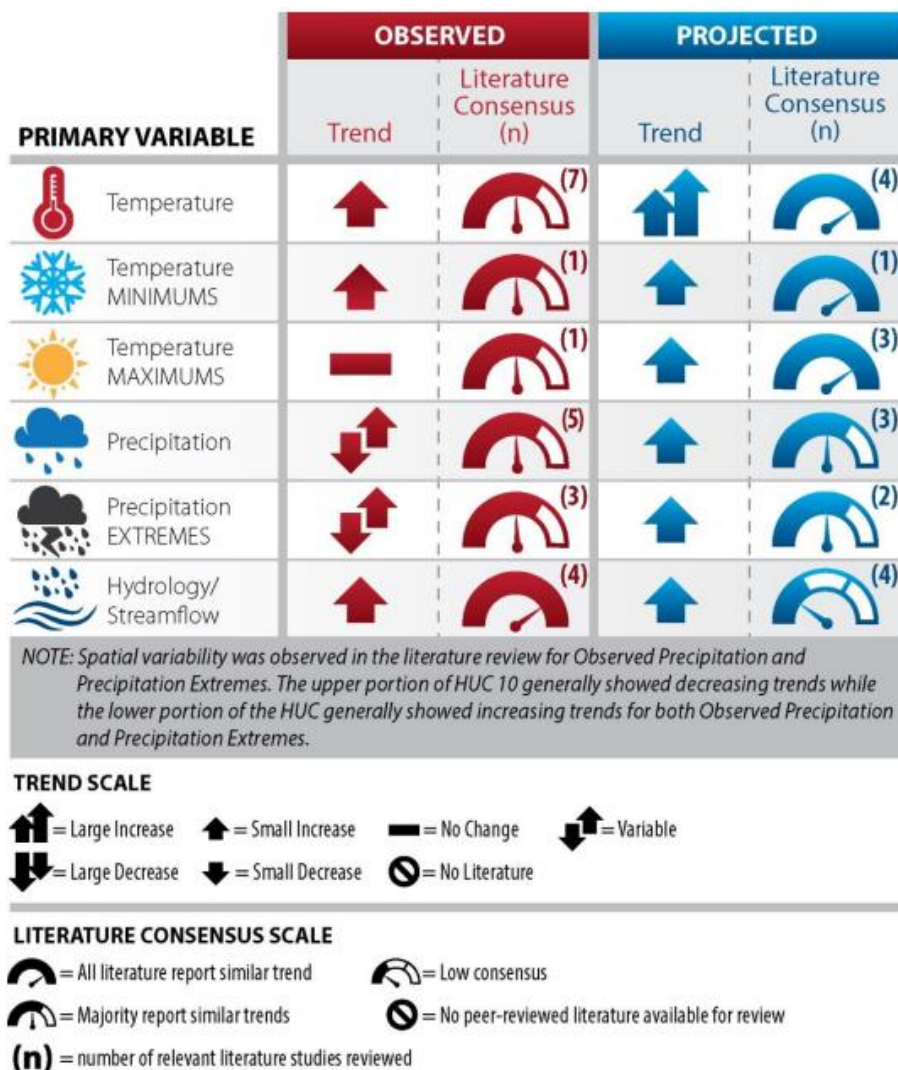






















Figure 6.42. Summary matrix of observed and projected climate trends and literary consensus for the Missouri River, HUC 10 (USACE, 2015).

CLIMATE VARIABLE	VULNERABILITY
 Increased Ambient Temperatures	<p>Increased ambient air temperatures throughout the century, and over the next century are expected to create the following vulnerabilities on the business lines in the region:</p> <ul style="list-style-type: none"> <li>• Loss of vegetation from increased periods of drought and reduced streamflows may have impacts on vegetation within the region, which is important for sediment stabilization in the watershed. Loss of non-drought resistant vegetation may result in an increase in sediment loading, potentially causing geomorphic changes in the tributaries to the river system.</li> <li>• Decrease in flows may result from periods of drought has implications for maintain water levels in the rivers; however hydrological models show little concenseous on streamflow.</li> <li>• Risk of wildfires during hot and dry conditions may cause an increased risk of wildfires, especially in heavily forested and dry areas. Flora and fauna that are not drought resistant can also be impacted by longer drought conditions, which may reduce opportunities for recreational wildlife viewing.</li> </ul> <p><b>BUSINESS LINES IMPACTED:</b>       </p>
 Increased Maximum Temperatures	<p>Air temperatures are expected to increase 4-8°C in the latter half of the 21st century, especially in the summer months. This is expected to create the following vulnerabilities on business lines in the region:</p> <ul style="list-style-type: none"> <li>• Increased water temperatures leading to water quality concerns, particularly for the dissolved oxygen (DO) levels, growth of nuisance algal blooms and influence wildlife and supporting food supplies.</li> <li>• Increased evapotranspiration.</li> <li>• Human health risk increases from extended heat waves, impacting recreational visitors and increasing the need for emergency management.</li> </ul> <p><b>BUSINESS LINES IMPACTED:</b>   </p>
 Increased Annual Precipitation	<p>By the middle of the century, annual precipitation is expected to increase in the region which are expected to influence the following vulnerabilities on business lines in the region:</p> <ul style="list-style-type: none"> <li>• Times of increased streamflows and runoff, which may carry pollutants to receiving water bodies, decreasing water quality.</li> <li>• Increased erosion with subsequent changes in sediment accumulation rates and creating water quality concerns.</li> <li>• Increased flooding, which may have negative consequences for all infrastructure, habitats, and people in the area.</li> </ul> <p><b>BUSINESS LINES IMPACTED:</b>       </p>

*NOTE: The Regulatory and Military Program business lines may be impacted by all climate variables*



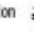

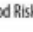

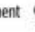
 = Navigation  
  = Flood Risk Management  
  = Ecosystem Restoration  
  = Hydropower  
  = Recreation  
  = Water Supply  
  = Emergency Management

Figure 6.43. Summary of projected climate trends and impacts on hydrologic-related business lines (USACE, 2015).

Detailed summaries and discussion of climate projections for this study are presented in Chapter 7.

### 6.10 Biological Impact

Climate change impacts on water quality can result in direct or indirect impacts on physical and chemical properties of streams. Physical impacts could include temperature; fire; changes in amount, duration, and frequency of surface-water discharge; and mixing of waterbodies in rivers and lakes. Chemical

changes could include increased nutrient concentrations, water color, solubility, and decreased oxygen content. Biology would be affected as well, with biologically mediated changes including alteration of species, species populations, and harmful algal blooms (Mujere and Moyce, 2018). Other biological changes could include changes in populations of benthic macroinvertebrates from changes in their metabolic processes, or indirectly through alteration of their habitat, from pathogenic microorganisms, or even the extinction of organisms sensitive to these changes.

An increase in solar irradiation could also alter water quality, especially characteristics of natural organic matter in freshwater systems, both by warming and ultraviolet (UV) radiation. In aquatic systems, a harmful increase in photolysis (decomposition or separation of molecules from of light or UV radiation) could occur from deeper penetration of damaging UV radiation (Soh et al., 2008). Phototransformation might also be a potentially serious effect since exposure to light or UV radiation can cause photoreactive chemicals in the water such as pharmaceuticals to become “transformation products” harmful to aquatic life (Canonica et al., 2008).

Delpla et al. (2009) identify several transformations or effects from water temperature increase, including dissolution, solubilization, complexation, degradation, and evaporation. Increased water temperature leads both to increased concentration of dissolved substances in water and decreased concentration of dissolved gases. For dissolved oxygen in water, oxygen concentrations decrease almost 10 % for every three-degree increase in

temperature (10 mg/L at 15°C) – identified as a serious problem for aquatic ecosystem health in all IPCC scenarios where air temperature is estimated to increase between 1.8 and 4.0°C by the end of the 21st century (Bates et al., 2008).

Warmer air temperatures exert considerable control over numerous aquatic ecosystem processes, including lake and river ice dynamics. Changes to these processes can have significant implications for harmful algal blooms and the community structure, with temperature affecting such ecological processes as ecosystem metabolism and nutrient cycling. Jurgens (1968) used macroinvertebrates to define the extent of pollution in Black Hills Streams, as they can reveal the viability of the community, are somewhat static, and can be used to represent intermittent pollution. In the Black Hills, the establishment of *Didymosphenia geminata* (*D. geminata*) has been associated with significant changes in stream ecosystems in several creeks. The presence of this organism in streams is influenced by water chemistry (phosphorous, iron, nutrients), flow regime, light availability (stream canopy), or combinations of these factors (James et al., 2014). They found that stream reaches with steeper gradients likely experience increased water velocities during flood events, giving them a greater propensity for bed scouring. *D. geminata* blooms were absent in Spearfish and Whitewood creeks, which have greater stream gradients at 1.10% and 1.34%, respectively. Laverly (2013) suggests that climate-induced shifts in environmental conditions that favor increases in nuisance algal blooms merit further investigation as a potential explanation of recent blooms.

Kuwabara et al. (1989 and 1990), studying periphyton abundance in Whitewood Creek, identified that benthic flora represent a significant arsenic pool that may episodically affect water-column concentrations of arsenic. Their study found that chemical interactions involving arsenic and phosphorus between biota and the overlying water may significantly affect arsenic transport and distribution. They reported growth of periphyton biomass between Late May and July at two sites (Whitewood Creek above Vale and the Sheeler Seep located just above the confluence of Whitewood Creek with the Belle Fourche River), that exhibited both a rapid and significant accumulation of arsenic. Results indicated that temperature effects on algal growth rates may contribute to a downstream increase in algal abundance. They also reported increasing algal abundance due to the increase in macronutrients downstream of the Lead-Deadwood water-treatment plant effluent, from ground water inputs, and irrigation runoff from fertilized land. Inferring the importance of temperature and community structure during the summer, Kuwabara et al. (1989 and 1990) raised a number of complex questions about the modeling of periphyton effects on stream transport of arsenic.

Newman et al. (1999) used a rapid bioassessment technique for benthic macroinvertebrates and amphibians to study the health of Whitewood Creek compared to other adjacent, unimpacted watershed streams in the Black Hills. They found that the invertebrate community may be impacted by contaminants leached from mine tailings by spring floodwaters. The low number of invertebrates, brown trout, and white suckers in Whitewood Creek, and its low

stream assessment score, indicate stressful conditions compared to reference streams, especially in May. The assessment score for Whitewood Creek in the spring was 44 % of the average for the reference streams, placing it in the biological condition category of "moderately impaired" (Newman et al., 1999). Their study identified the most likely stressors as toxins (e.g., arsenic, copper, mercury) from mine tailings in the riparian zone.

The abundant pine forests of the Black Hills also play an important role in maintaining its watershed quality. Bunkers et al. (1999) used dendrochronology techniques to study drought history in the Black Hills by using tree rings taken by coring in 1992 from a single ponderosa pine tree that was over 700 years old. Their study's intent was to examine historic climatic patterns from the 13th through most of the 20th century, as inferred from ring widths of trees. Because of its location on a steep rocky slope, the tree survived fires and other "damaging agents" (Bunkers et al., 1999). The analysis indicated previous occurrence of both wet and dry spells of longer duration and magnitude than even the Dust Bowl drought, which ranked fourth in severity in their chronology study dating back to 1600. They also stated that if broader evidence supports the single tree record, the 1930s drought may be of even less significance. These results can be combined with the recorded historic hydrologic records to improve climate change simulations.



## **Chapter 7: Results and Discussion for Climate Change Assessment for HUC 10120112 – Belle Fourche River – Cheyenne River**

USACE created tools to assist in conducting a qualitative analysis of the climate and hydrology relevant to past (observed) changes as well as projected, future (modeled) changes. These tools can be useful in for incorporating considerations about future conditions into projects and programs associated with climate change related to hydrologic inputs. The tools are iterative, evolving when incremental improvements are identified. During the timeframe of these assessments, many tools released as version 1.0 were modified with the release of Version 2.0 in Oct. 2021.

USACE (2015) reports little consensus in the recent literature about the projected trend in stream flow over time in the Missouri River Basin (HUC 10). Trend direction is dependent on the selection of GCM models used for temperature and precipitation, the emission scenario, and the hydrologic model used. Uncertainty is large in these hydrologic models. Based on the literature review conducted for this study, hydrologic variables important to conditions in the Cheyenne River Basin may be impacted by climate change. Perturbations include an increase in air temperature along with intensity, duration, and frequency of precipitation and resulting stream discharge. These changes could lead to modifications in duration and magnitude of peak runoff events and droughts. It is therefore appropriate to investigate the potential impacts of global climate change in the Cheyenne River Basin.

Tools base impacts on a 100-year planning horizon because most current climate model data sets typically end at 2099 or 2100 (USACE, 2020). Global Climate Model (GCM) output from the Climate Model Intercomparison Project, Phase 5 (CMIP5) and modeled hydrology projections used in climate assessments are available at: <https://gdo.dcp.ucllnl.org/>. Model output was created with the Localized Constructed Analogs (LOCA) method of empirical-statistical downscaling (Pierce et al., 2014). The temporal resolution of the modeled hydrologic data is daily, spanning 1950-2099, where period 1950-2005 is simulated historical years and the period 2006-2099 projected years. Additional details about the dataset and spatial downscaling method are documented in Vano et al. (2020), Livneh et al. (2013, 2015), and online at <http://loca.ucsd.edu/>. Downscaled GCM outputs for temperature, precipitation, and areal runoff for Representative Concentration Pathways (RCPs) 4.5 and 8.5 drove the Variable Infiltration Capacity hydrologic model (VIC; Liang et al., 1996). VIC outputs routed runoff for 32,824 stream segments, denoted by Segment ID number. A subset of 2,517 terminal downstream segment IDs were identified as indicative of cumulative flow. In most cases, these matched up 1-to-1 with the 2,112 HUC8s in the U.S. In the event where there was more than one segment within a HUC8, the segment with the largest total flow was chosen. Output in the default units of cubic meters per second was converted to cubic feet per second. Model projection data were aggregated to the monthly level by adding up the routed runoff for all days per month. Then, the annual maximum of those monthly values per water year was compared between model runs per HUC8.

The minimum, maximum, and mean of those annual maximum monthly flows are plotted against water years. The data shown are historical gage data of observed instantaneous maximum streamflow per water year. A trendline of this data is also shown. The regression line, R-squared, and p-value (t-test, Mann-Kendall and Spearman Rank Order) appear with the Figure in association with the trend line.

The observed instantaneous streamflow for the containing the project area within HUC 8 Belle Fourche and Cheyenne is projected to increase with time and has statistical significance. The average and range denoting the variation in these figures result from the 64 combinations of GCM+RCP projections, with the default year of 2000 separating where emissions were held constant (1950-1999) and where the projected pathway of emissions is being applied (2000-2099). The projected stream flows have a large amount of uncertainty. This uncertainty is shown visually in the spread of flow results for the HUC8 presented in Figure 7.1. Uncertainty is introduced with each step of generation of the data set generation including the boundary conditions used in the GCMs for producing projections of temperature and precipitation; the RCPs selected for the modeling; the downscaling method used to convert the global results to regional HUC 8 scale results; and the uncertainties in the hydrologic model used to generate the stream flow.

The Climate Hydrology Assessment Tool (CHAT) Version 1.0, was used to develop first-order trends for annual peak flows at gages in the study basin (Table 1), and is available online at:

[http://corpsmapu.usace.army.mil/cm\\_apex/f?p=313:2:0::NO](http://corpsmapu.usace.army.mil/cm_apex/f?p=313:2:0::NO). Version 1.0 of the CHAT generates a p-value for the linear regression; a smaller p-value would indicate greater statistical significance. Although there is no recommended threshold for statistical significance, typically 0.05 is used as a value associated with a 5% risk of a Type 1 error or false positive. Version 1.0 uses historic data sets from annual discharge from USGS stream gages in the selected watershed for assessment. Using the CHAT Version 1.0, regression lines for two stage/gage height records of the 8 gages were found to be statistically significant: 06436190 at Whitewood Creek Above Vale, SD, and 06438500 Cheyenne River Near Plainview, SD. The results for all other stream gages assessed with the CHAT did not show any statistically significant trends. Figures 7.4 through 7.15 provide the graph of CHAT version 1.0 results, along with a map of the USGS gage and its available data on the USGS Water Data website at: <https://dashboard.waterdata.usgs.gov/app/nwd/?region=lower48&aoi=default>.

Recognizing the need for improvement, USACE developed CHAT Version 2.0, released in late Oct. 2021 at <https://climate.sec.usace.army.mil/chat>. This version features data from CMIP-5, carbon emission scenarios from RCP 4.5 and 8.5, and analysis at the HUC-8 level. The CHAT performs an evaluation of the annual-maximum of the average monthly runoff (i.e., streamflow). Maximum of average monthly runoff was taken over the hydrologic year called the “water year”. Monthly means were calculated by averaging the daily runoff. The inter-model range across 64 CMIP-5 models (i.e., 32 models + 2 RCPs) is displayed for annual-max of average monthly runoff (i.e., the inter-model minimum, mean,

and maximum). CHAT version 2.0 displays simulated historical and projected future climate-changed hydrology (annual maximum of average monthly streamflow) for the selected watershed. These values are displayed and analyzed in two ways: 1) the inter-model, inter-scenario range of streamflow values; and 2) the trends in the inter-model, inter-scenario mean streamflow values. USACE also released a Version 2.0 of the NSD tool with updated interface; results are the same as those in Version 1.0. Tables 1 and 2 summarize the annual peak instantaneous streamflow and stage/gage height trend results.

Using CHAT version 1.0. with stream gages within the impacted study area, none had regression (trend) lines that were statistically significant (Figures 7.4.-7.15). Due to this finding, stream gages adjacent the impacted watershed were then assessed. These gages are listed in Table 2; some are of similar size and with conditions comparable to Whitewood Creek and the Belle Fourche and Cheyenne Rivers. Most of these gages are in rural watersheds and all are impacted by regulated flow. Many of the stream gages assessed in western South Dakota but outside of the Cheyenne River Basin study area have periods of record less than 15 years and are therefore too short to use in a climate assessment where 30 years is required for some of the tools. Figures 7.4 through 7.15 show the results from the Climate Hydrology Assessment Tool (CHAT) Version 1.0; analytical results from gages using historical and annual instantaneous peak streamflow (cfs) data; gage height/stage (ft) data; and identification of non-stationarities from the non-stationarity detection tool. Figure

3 provides a listing of settings for the Version 2.0 NSD assessment (available at: <https://climate.sec.usace.army.mil/nsd/>). A copy of the peak-flow frequency estimate curves for each stream gage from Sando et al. (2008) was included for each stream gage for comparison of existing conditions. The periods of record used for each gage in this analysis were determined with input from the non-stationarity detection tool and are summarized Table 1 and in the Figures 7.4-7.15 for each gage. These analyses can be very useful in considering future conditions in the basin study area and the potential direction of climate change.

A major obstacle in quantifying any change in discharge is the limited availability of hydrologic data exhibiting “natural conditions” – i.e., those from monitoring sites that have not been substantially altered by human influence (diversions, dams, agricultural, water use). All gages in the study area were found to have been affected by anthropogenic activity. Also, to determine if there were any regional trends, basins adjacent the study area were also assessed. Using Version 1.0 of the CHAT, 13 of the 62 gages in the region exhibited trend lines that were statistically significant; they are reported in Table 7.2. Those with trend lines exhibiting statistically significant results are highlighted in gray. No determination was made at sites outside of the study area about whether they are impacted by regulated flow.

In this study, an assessment was made about the likelihood of different long-term trends given the existing data, physical observations, and understanding available today. Long-term statistical significance of a trend in discharge measurements is questionable. This can be important in a study if it

uses a Bulletin 17C analysis or calibration events that are not recent. Stationarity assumes that the statistical characteristics of hydrologic time series data are constant through time, a fundamental assumption for many statistical processes in hydrology. However, this analysis and recent scientific evidence shows that climate change and human modifications to some watersheds are undermining this assumption.

Non stationarities identified need site-specific interpretation and knowledge of local conditions, which may not be identifiable simply by using the tool. Many gages in the region did not have the amount of long-term data free from conditions that impact flow, (i.e., land use change indicators), which challenges the ability to perform long term trend analysis. It was difficult to quantify impacts from regulated flows, so determining impact exclusively from climate change proved to be inconclusive. Although no statistically significant trends were identified, test of non-stationarity were performed to identify any consistent patterns. The stationarity of the flow record within stream gages in the Cheyenne River Basin is assessed by applying a series of eleven nonparametric statistical tests and one Bayesian, parametric statistical test to the observed peak flow record. All change points detected by the tool are considered statistically significant. The relative strength of a detected non-stationarity is evaluated using criteria of consensus, robustness, and magnitude. The results of the statistical tests are shown in Figures for each stream gage (Figures 7.4 to 7.15). All assessments conducted identified non-stationarities in eight different years (1960-1963; 1972; 1977; 1980-1982; 1983-1984; 1993; 2005-2007; and 2012-

2014) (Table 7.1). In comparison with the South Dakota data from drought.gov site, these dates are consistent with periods of drought in South Dakota (1977; 1981; 2005-2007; 2012-2014), which may explain the non-stationarities detected.

The relative strength of each non-stationarity is determined by considering the level of consensus between different statistical tests targeted at detecting the same type of non-stationarity (variance/standard deviation, mean, distribution) in the flow data series. If consensus is not found for a given year or a short period of time, it is reasonable to discount the non-stationarity. According to the USACE NSD Tool User Guide, if the various abrupt statistical methods detect statistically significant non-stationarities within five years of one another, the user should combine those non-stationarities to be representative of a single non-stationarity in the flow record (USACE, 2016). Consequently, the non-stationarity detected in sequential years may be combined with the results from the other tests. Three different statistical tests indicate a change in the distribution in 1981 at Cheyenne River Near Plainview, Gage 06438500, due to missing data points. According to USGS gage records, because of drought conditions, no flow was recorded in 1981 at stream gage 06438000, Belle Fourche River Near Elm Springs. Non-stationarities were detected, and by evaluation were due to lack of data collected or reported; snow/ice impacts; changes in stream discharge trends when the gage recorded peak events, or periods when the gaged watershed changed from a drought condition to a trend more representative of an average condition of streamflow. In some instances, the length of record at many stream gages was not suitable to determine long-term trends, or the data set had missing data or



lacked statistical significance. The large intervening drainage area between the Belle Fourche Reservoir and gages on the Belle Fourche River in this study lessened the effects of dam operation, so the gages downstream from the reservoir were analyzed. Detected change points are likely due to effects of anthropogenic climate change, long-term natural fluctuations in climate, and/or changes to the hydrologic properties of the basin (such as land use changes, changes in channel geomorphology, changes in land cover, etc.). Downscaling global climate change studies to regional watersheds, especially in the context of water quality and ecological impacts, involves considerable uncertainty

### Annual Max of Average Monthly Streamflow: Range and Mean

#### HUC 10120112 - Belle Fourche River-Cheyenne River

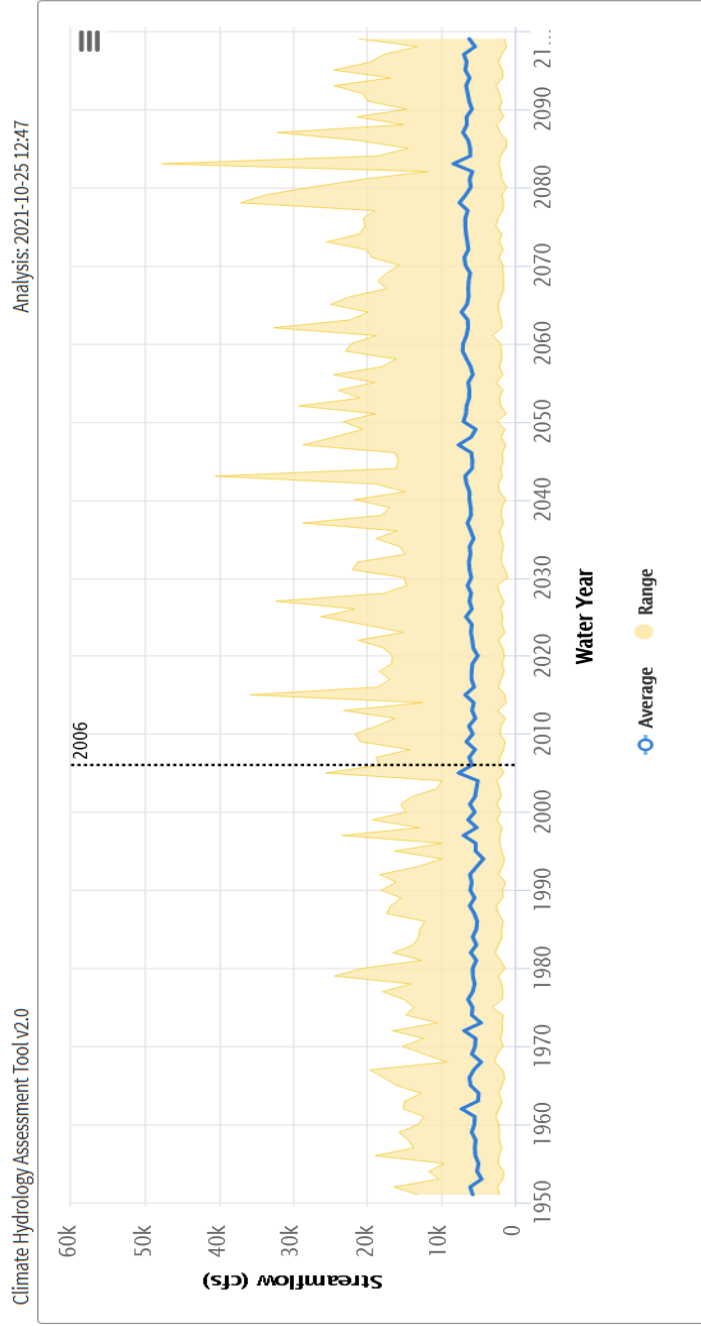


Figure 7.1. The Modeled Streamflow (CHAT version 2.0) provides an assessment of climate-changed hydrology CMIP-5 Data downscaled the Belle Fourche River-Cheyenne River HUC-8 watershed. The range of 64 GCM/RCP projections of annual of average maximum monthly flow is shown in yellow. The mean of the 64 GCM projections of annual maximum of average monthly streamflow is shown in blue. Simulated flows are

## Trends in Mean Annual Max of Average Monthly Streamflow from 64 Climate-Changed Hydrology Models

### HUC 10120112 - Belle Fourche River-Cheyenne River

Climate Hydrology Assessment Tool v2.0

Analysis: 2021-10-25 12:47

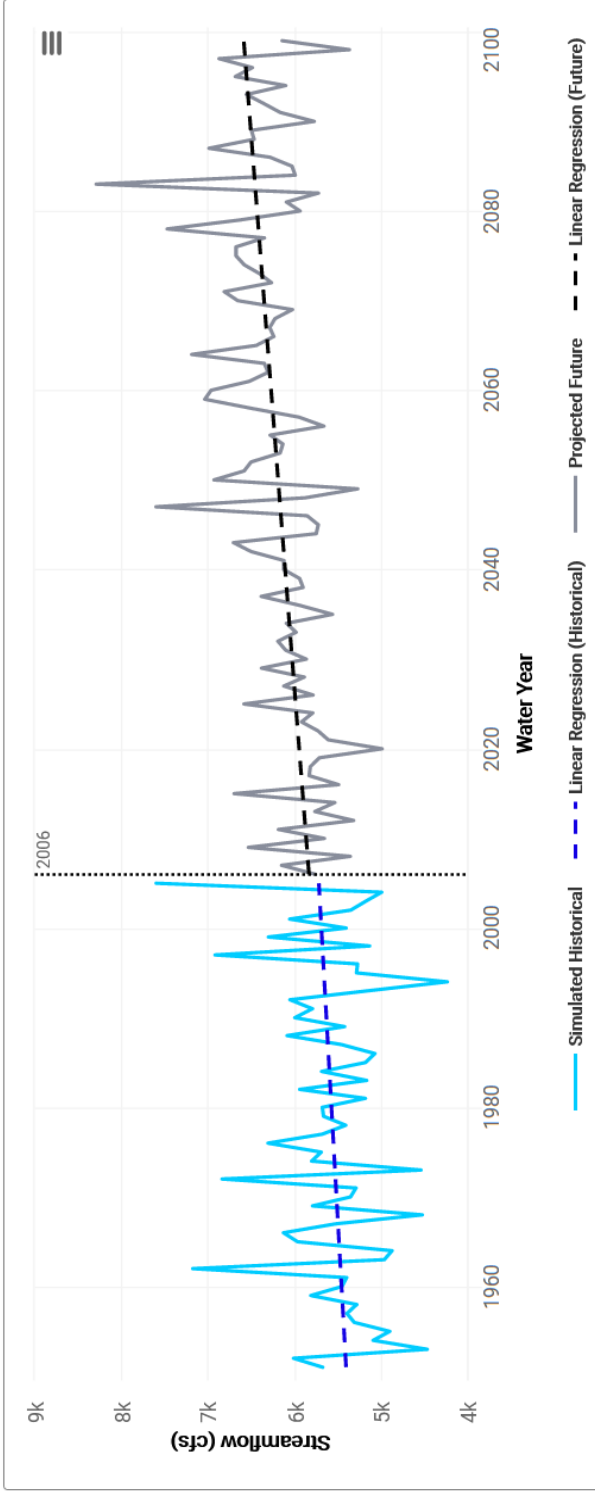


Figure 7.2A. Modeled Streamflow Trend. The graph shows a trendline of simulated historical data (1951-2005) and a projected future data (2006-2100) using CHAT Version 2.0. A line chart in the center contains multiple time-bound tracking, --Simulated Historical, Linear Regression (Historical), Projected Future and Linear Regression (Future). The regression line  $R^2$  and p-values are calculated and presented in Figure 7.2.b. which presents statistical significance tests for historical simulated and projected future periods associated with this graph (USACE, 2020).

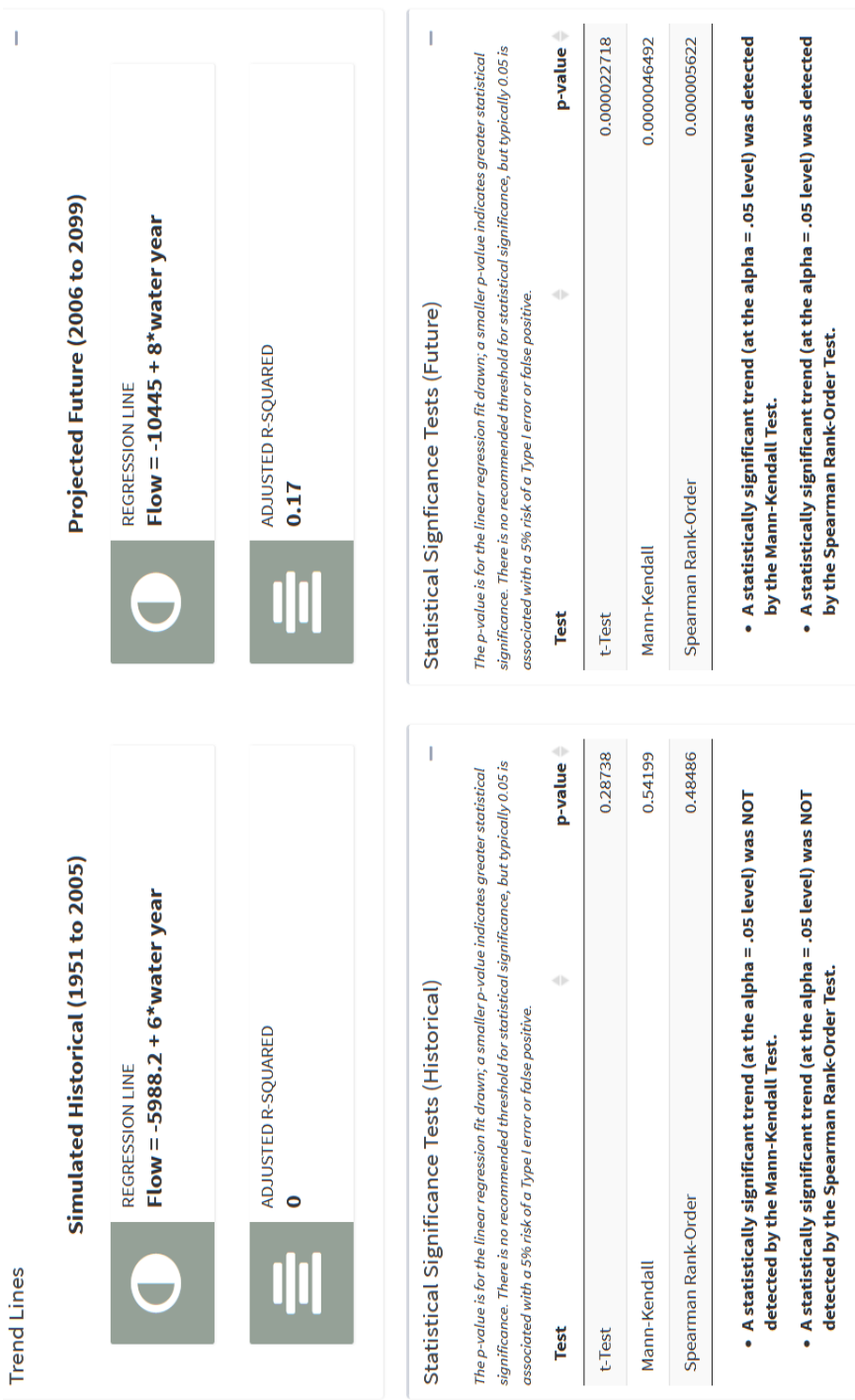


Figure 7.2B. Statistical significance of graph presented in Figure 7.2 using hydrologically simulated and routed statistically aggregated CMIP 5 GCM outputs at the HUC 8 watershed level described in USACE, 2020. Statistically significant trend was not identified in historical simulated flow for the period 1951-2005. A statistically significant increasing trend for the mean annual maximum of average monthly streamflow was identified in the projected future for HUC 10120112 For the Belle Fourche River-Cheyenne River.

USGS Gage Site	Period of Record	Impacted Flow Diversions, Reservoirs	Trend* Analysis	Number NSD identified	Cramer-von-Mises:	Kolmogoro v-Smirnov	LePage	Energy Divisive Method	Lombard Wilcoxon	Pettitt	Mann-Whitney	Bayesian	Lombard Mood	Smooth Lombard Mood	Smooth Lombard Wilcoxon
06436000 Belle Fourche River Near Fruitdale, SD <i>Missing Values 1959-1960</i>	1946-2020	Yes	No	IPS-2 Stage-2				1977							1946-1949
06436180 Whitehead Creek Above Whitehead, SD	1983-2020	No	No	IPS-0 Stage-0											
06436190 Whitehead Creek Near Whitehead, SD	1982-2020	Yes	No	IPS-0 Stage-0											
06436198 Whitehead Creek Above Vale, SD	1982-2020	Yes	IPS-No Stage-Yes	IPS-0 Stage-0											
06427000 Belle Fourche River Near Sturgis, SD	1946-2020	Yes	No	IPS-2 Stage-3				1982 1982					1993 1993, 1994		
Elm Springs, SD <i>*missing data points 1932-1934</i>	1929-2019	Yes	No	IPS-1 Stage-1									2006 2006		2005-2007
06438500 Cheyenne River Near Plainview, SD <i>*missing data points 1981-1995</i>	1951-2020	Yes	IPS No Stage-Yes	IPS-1 Stage-6	1981	1981	1981		1980	1981	1981				
06439300 Cheyenne River at Cherry Creek <i>Not in study area-adjacent basins</i>	1961-1994	Records Not available	No	IPS-0 Stage-0											
06431500 Spearfish Creek at Spearfish	1947-2020	Yes	IPS No Stage-Yes	IPS-5 Stage-5	1984, 1983 1984, 1983			1983 1977			1984, 1993 1984, 1993				1960-1963
06452000 White River Near Oscoma	1929-2020	No	IPS- No Stage-Yes	IPS-2 Stage-2				1982 1972					2017 2017		
06447000 White River Near Kadoka <i>missing data 1992-1994</i>	1942-2020	No	No	IPS-2 Stage-3				1972 1984							2016-2018
06441500 Bad River Near Ft. Pierre <i>missing data 1932-1934/IPS</i>	1950-2014	No	No	IPS-0 Stage 3											

Bayesian Change-point Test Not Applied, Assumption of Normality Not Met on any assessment.  
 \*Trend: "No" means a statistically significant trend (at the alpha = .05 level) was NOT detected by the Mann-Kendall Test.  
 "No" means a statistically significant trend (at the alpha = .05 level) was NOT detected by the Spearman Rank-Order Test.  
 \* For all Trend Analysis Plot of Maximum Annual Flow/Height with Slope Fits (Traditional and Sen's Slope).  
 IPS-Instantaneous Peak Streamflow  
 Stage-gage height  
 Blank values signify NSD not detected

Table 7.1. Summary of assessment findings by stream gage location. Although not represented in this Table, a statistically significant trend was identified in projected future mean annual maximum average streamflow presented in Figure 7.2.a.

## Configure Testing Parameters



The below parameters are described in the Nonstationarity Detection Tool User Guide. Engineering judgment is required if parameters other than the default are used

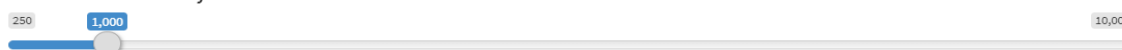
For more information, please review the NSD Tool User Guide.

For these parameters, larger values will decrease the sensitivity of these tests, resulting in fewer nonstationarities detected.

#### CPM Methods Burn-In Period



#### CPM Methods Sensitivity



#### Bayesian Posterior Threshold



#### Energy Divisive Method Sensitivity



For these parameters, smaller values will decrease the sensitivity of these tests, resulting in fewer nonstationarities detected.

#### Pettitt Sensitivity



#### Bayesian Prior Likelihood



#### Lombard Smooth Methods Sensitivity

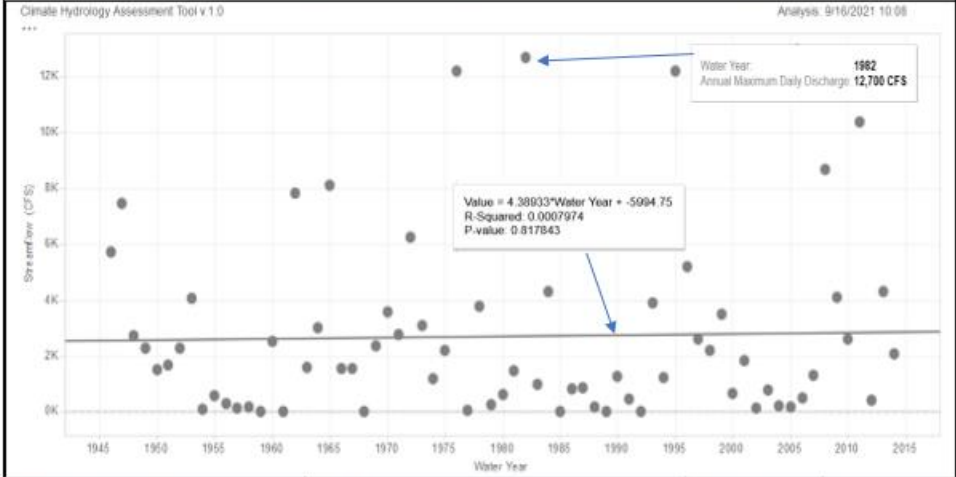
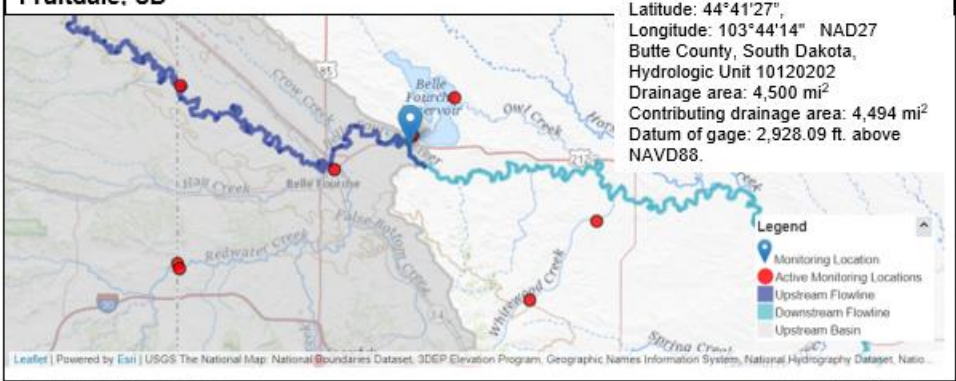


Figure 7.3. The standard settings used in the NSD tool for all USGS streamflow gage sites. USGS streamflow gage sites available for assessment within this application include locations where there are discontinuities in USGS peak flow data collection throughout the period of record and gages with short records.

In general, a minimum of 30 years of continuous streamflow measurements must be available before this application should be used to detect non-stationarities in flow records (USACE, 2020, and Friedman et al., 2018). Figures 7.4 -7.15 present a summary of assessment results by USGS gage listed in order of their presentation in Table 7.1. Each of the figures provides a map location of the USGS gage and results of analysis with Version 1.0 of the CHAT. CHAT generates a plot of water year against streamflow (the equation of the regression indicating a trend, as well as its  $R^2$  and p-value) and the highest

reported streamflow value for the period of record assessed. Also presented is the list of USGS parameter types available, data type, and range of reported values. Trends identified in graphs of annual peak streamflow and stage-gage height and their analysis are presented at each gage. An assessment using CHAT version 2.0 follows, with an assessment of the Version 2.0 of the Non-stationarity tool assessment. If non-stationarity was detected, a separate graph depicting it is presented by the method used for its identification. The figures also provide a copy of the peak-flow frequency estimate curves for the stream gage from Sando et al. (2008) for comparison.

**Figure 7.4 HUC 4 CHAT Assessment 06436000-SBFS2- Belle Fourche River Near Fruitdale, SD**



USGS Parameter Group	Data Types	Start Date	End Date
Information	Water-quality	1981-10-07	2002-11-13
Inorganics, Major, Metals	Water-quality	1983-01-05	2002-11-13
Inorganics, Major, Non-metals	Water-quality	1983-01-05	2002-11-13
Inorganics, Minor, Non-metals	Water-quality	1983-01-05	2002-11-13
Inorganics, Minor, metals	Water-quality	1983-01-05	2002-11-13
Physical	Daily Values, Unit Values, Water-quality	1945-11-01	2021-09-16
Sediment	Water-quality	1983-04-21	1984-07-10
n/a	Peak Measurements	1946-06-01	2020-05-17
n/a	Site Visits	1946-06-02	2021-06-24
n/a	USGS Annual Water Data Reports Site	2006-01-01	2020-01-01



### Nonstationarities Detected using Maximum Annual Flow

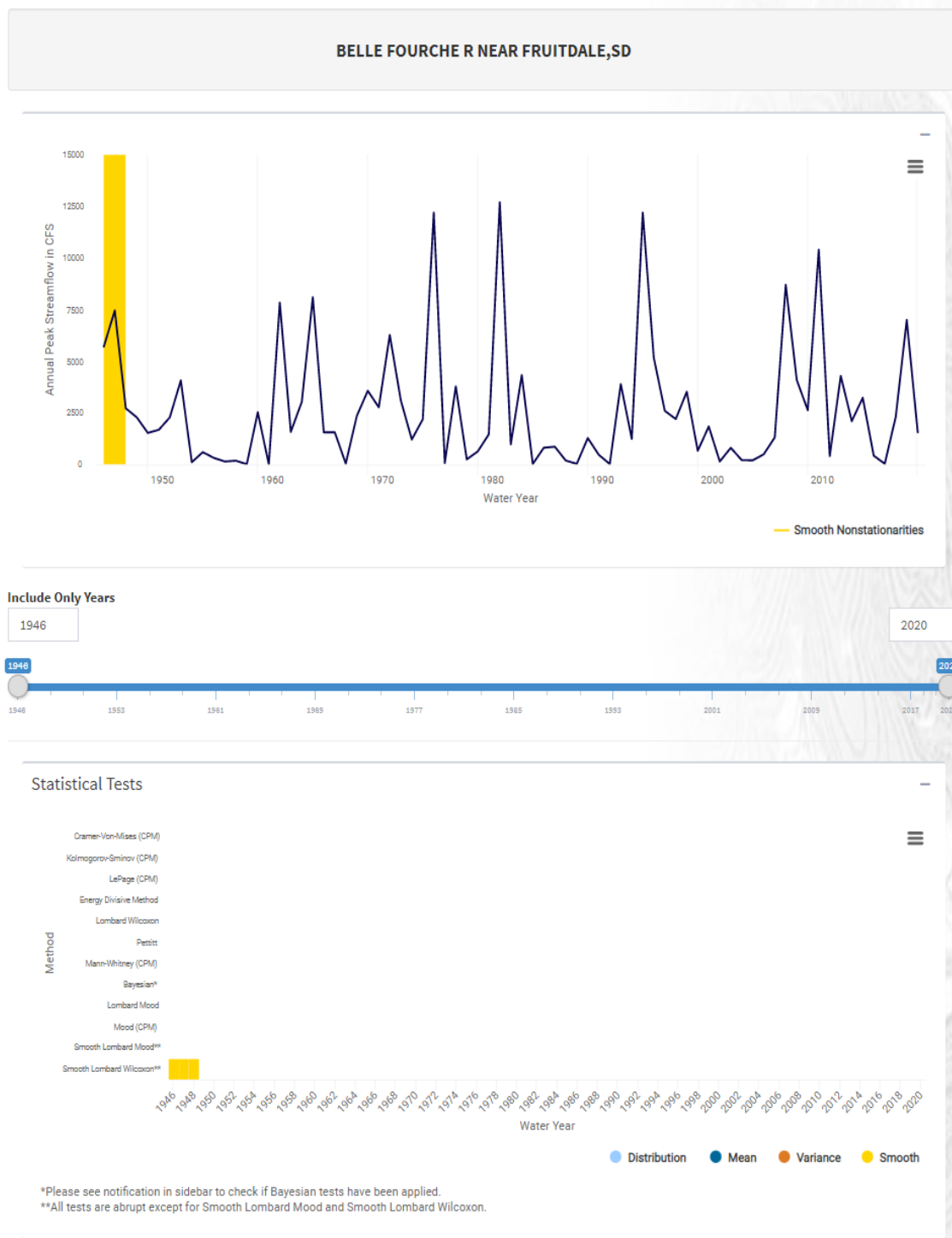


Figure 7.4.1. USGS Gage 06436000-Belle Fourche River Near Fruitdale, non-stationarities identified for Instantaneous Peak Streamflow (IPS) using annual peak streamflow in cfs, for years 1946-2020 using NSD tool version 2.0. The Bayesian Changeoint Test was not applied as the assumption of normality was not met. A Smooth Lombard Wilcoxon was identified for the years 1946-1948.

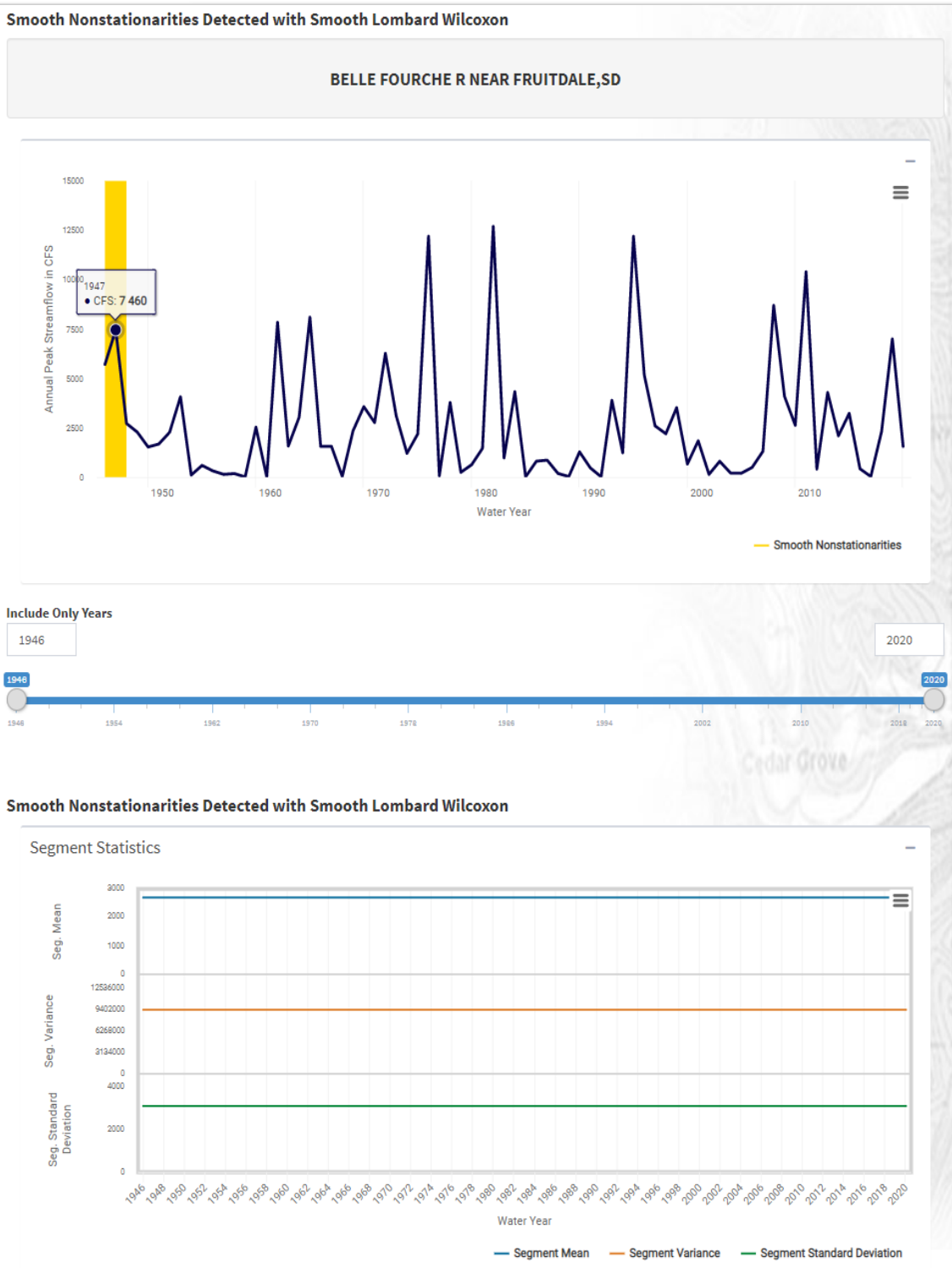


Figure 7.4.2. USGS Gage 06436000-Belle Fourche River Near Fruitdale, non-stationarities identified for Instantaneous Peak Streamflow (IPS) using annual peak streamflow in cfs, for years 1946-2020 using NSD tool version 2.0. A Smooth Lombard Wilcoxon was identified for the years 1946-1948.

Plot of Maximum Annual Flow/Height with Slope Fits (Traditional and Sen's Slope)

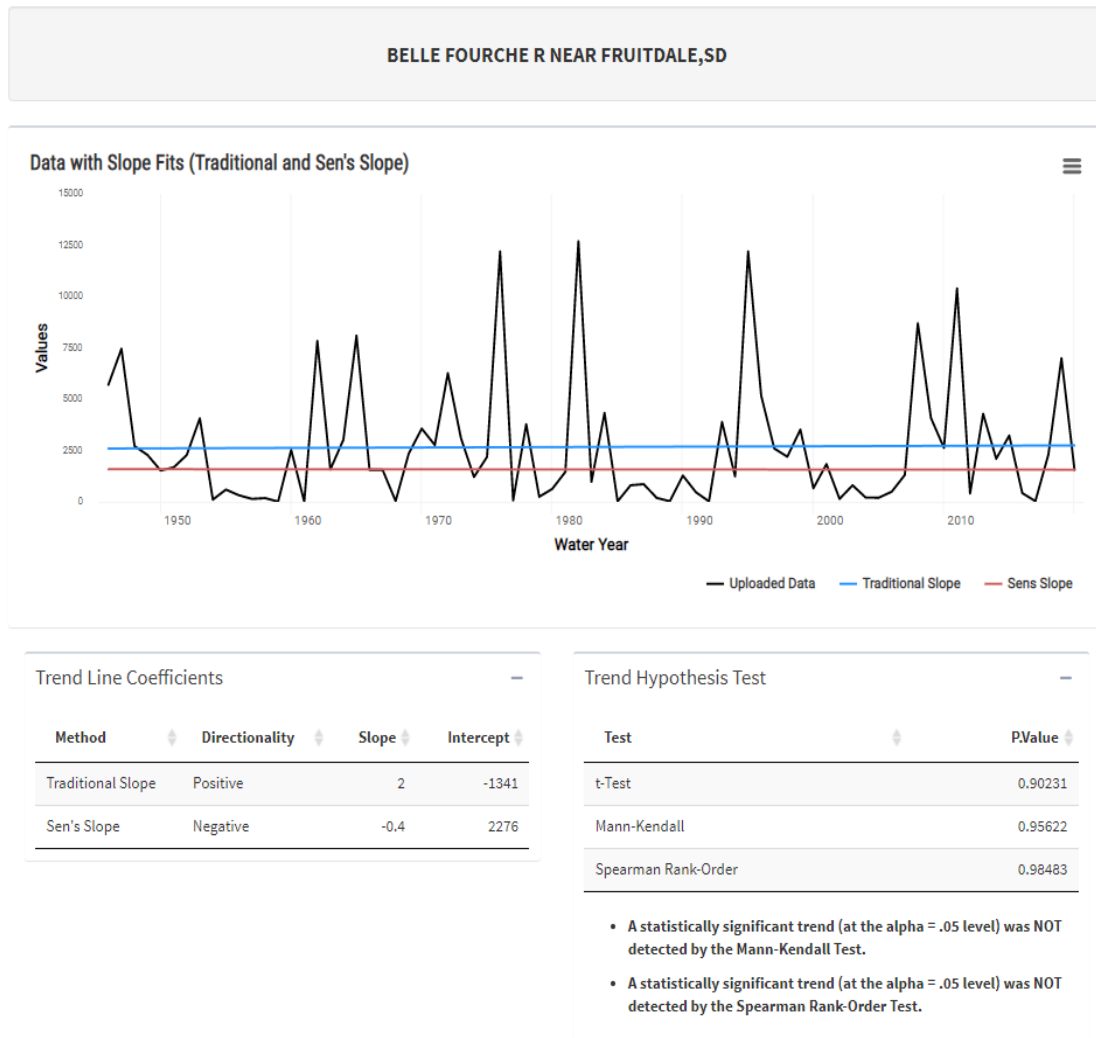


Figure 7.4.3. USGS Gage 06436000-Belle Fourche River Near Fruitdale, plot of maximum annual flow (cfs) with slope fits (Traditional and Sen's Slope). No statistically significant trends (at the alpha = 0.05 level) were detected using the Mann-Kendall or the Spearman Rank-Order tests for the period 1946-2020.

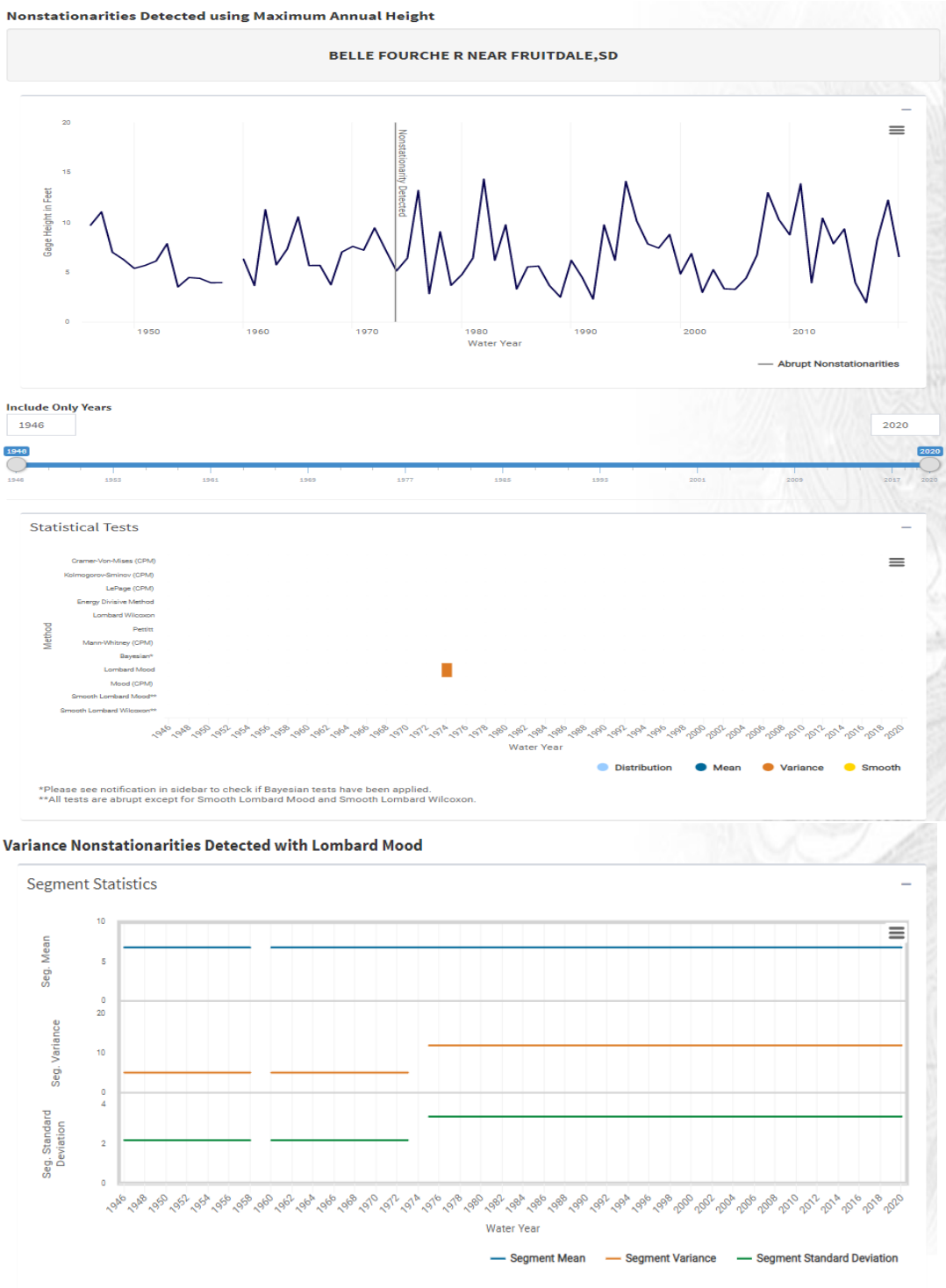


Figure 7.4.4. USGS Gage 06436000-Belle Fourche River Near Fruitdale, non-stationarities identified for gage/stage height (ft.) for years 1946-2020. A variance non stationarity was detected with the Lombard Mood method for the year 1974. The Bayesian Changepoint Test was not applied as the assumption of normality was not met.

### Plot of Maximum Annual Flow/Height with Slope Fits (Traditional and Sen's Slope)

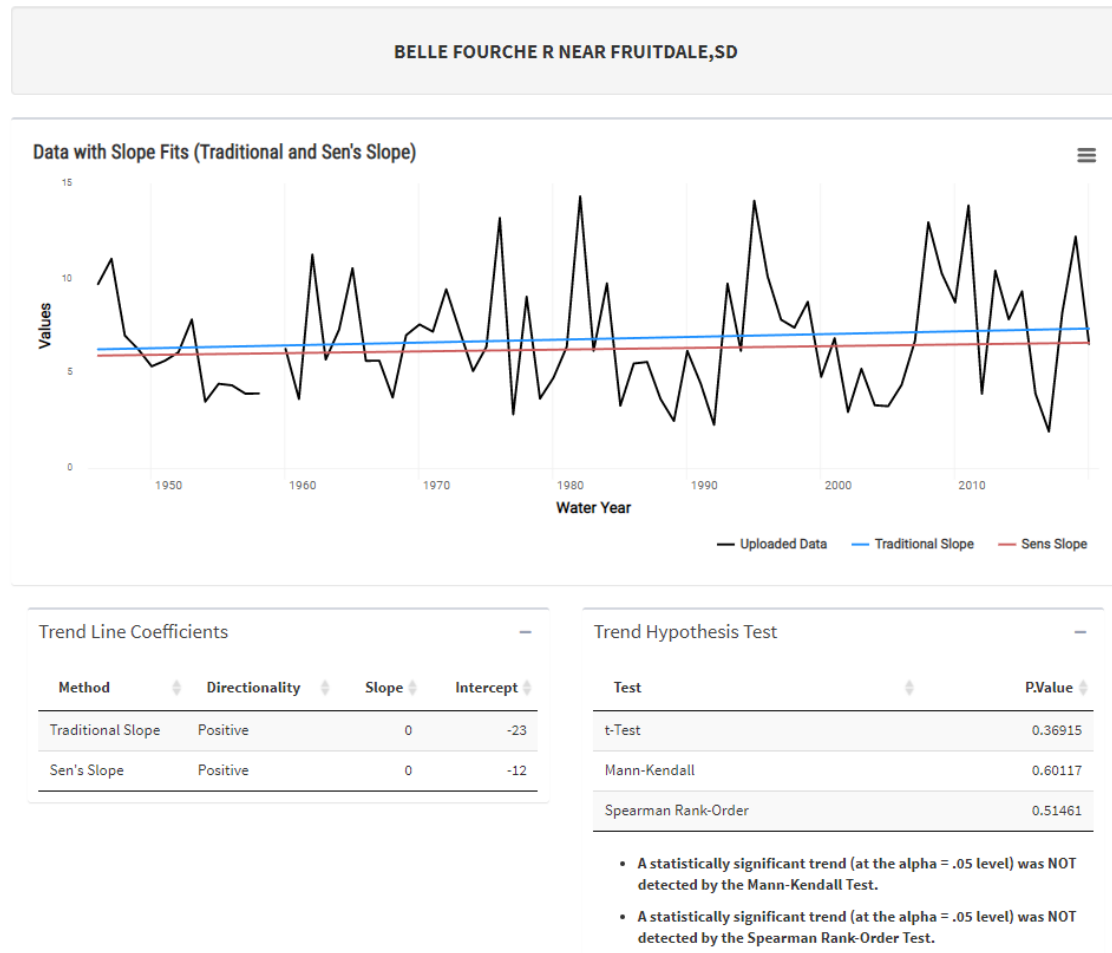


Figure 7.4.5. USGS Gage 06436000-Belle Fourche River Near Fruitdale, plot of gage/stage height (ft.) with slope fits (Traditional and Sen's Slope). No statistically significant trends (at the alpha = 0.05 level) were detected using the Mann-Kendall or the Spearman Rank-Order tests for the period 1946-2020.

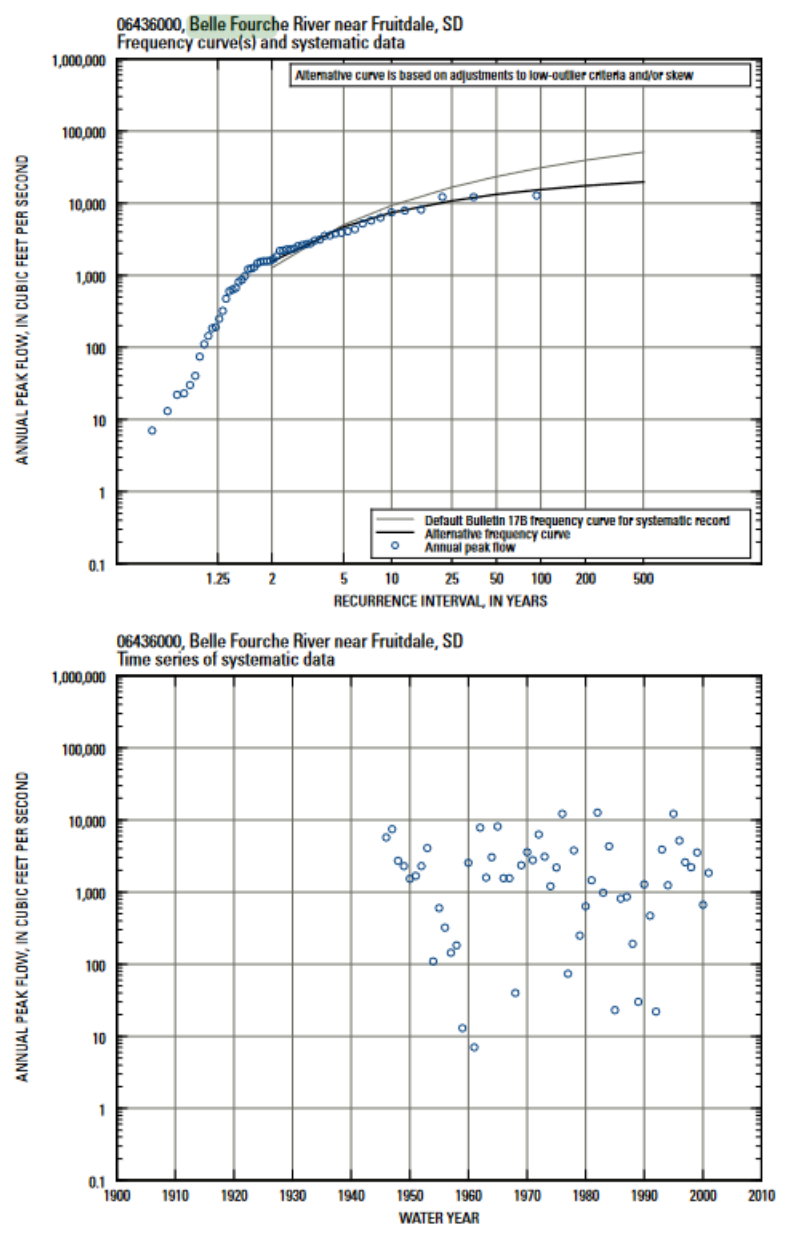
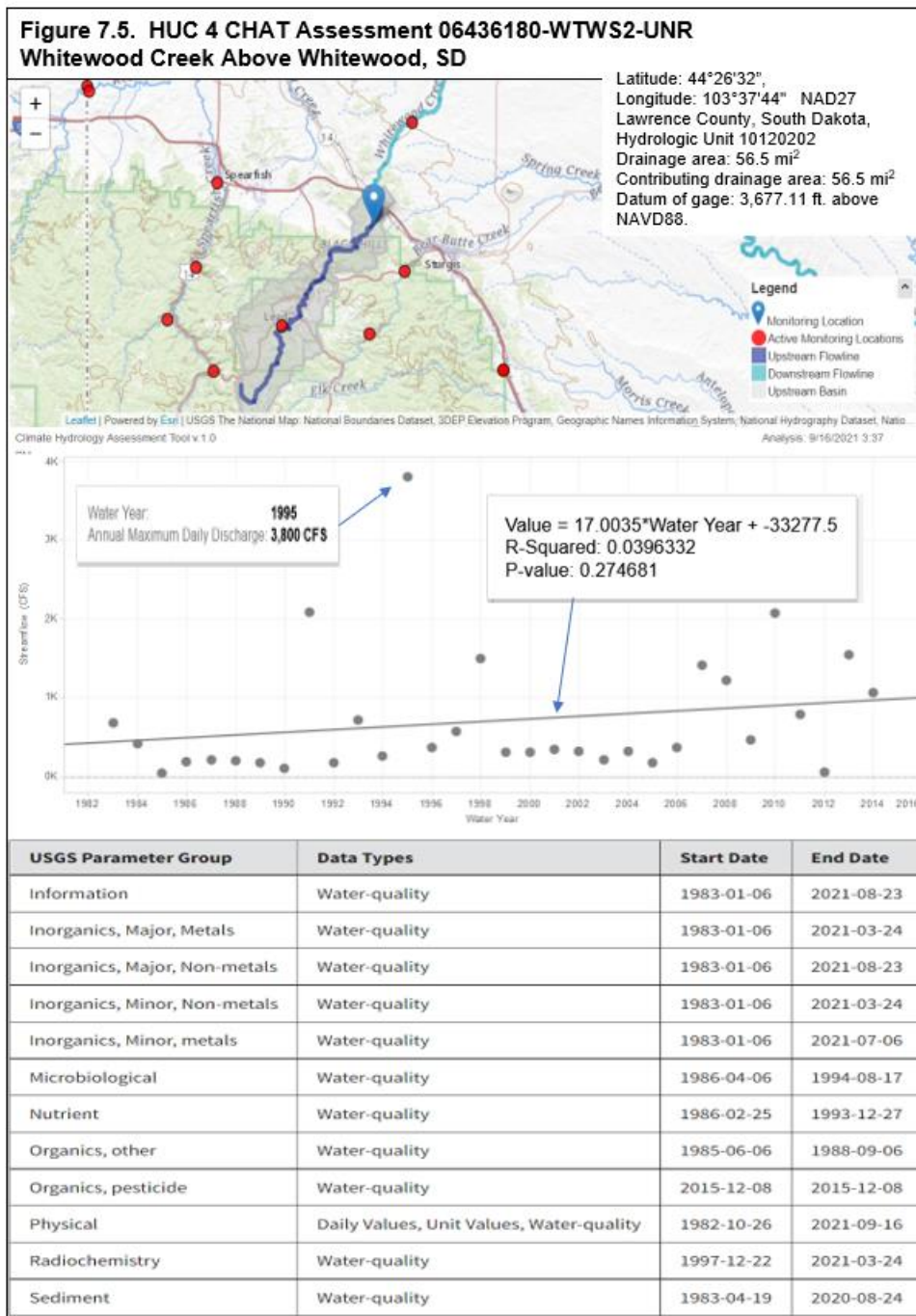


Figure 7.4.6. Peak-flow information for USGS gage station 06436000, Belle Fourche River near Fruitdale, SD (Sando et al., 2008).

Figure 7.5. USGS Gage 06436180 Whitewood Creek Above Whitewood, SD



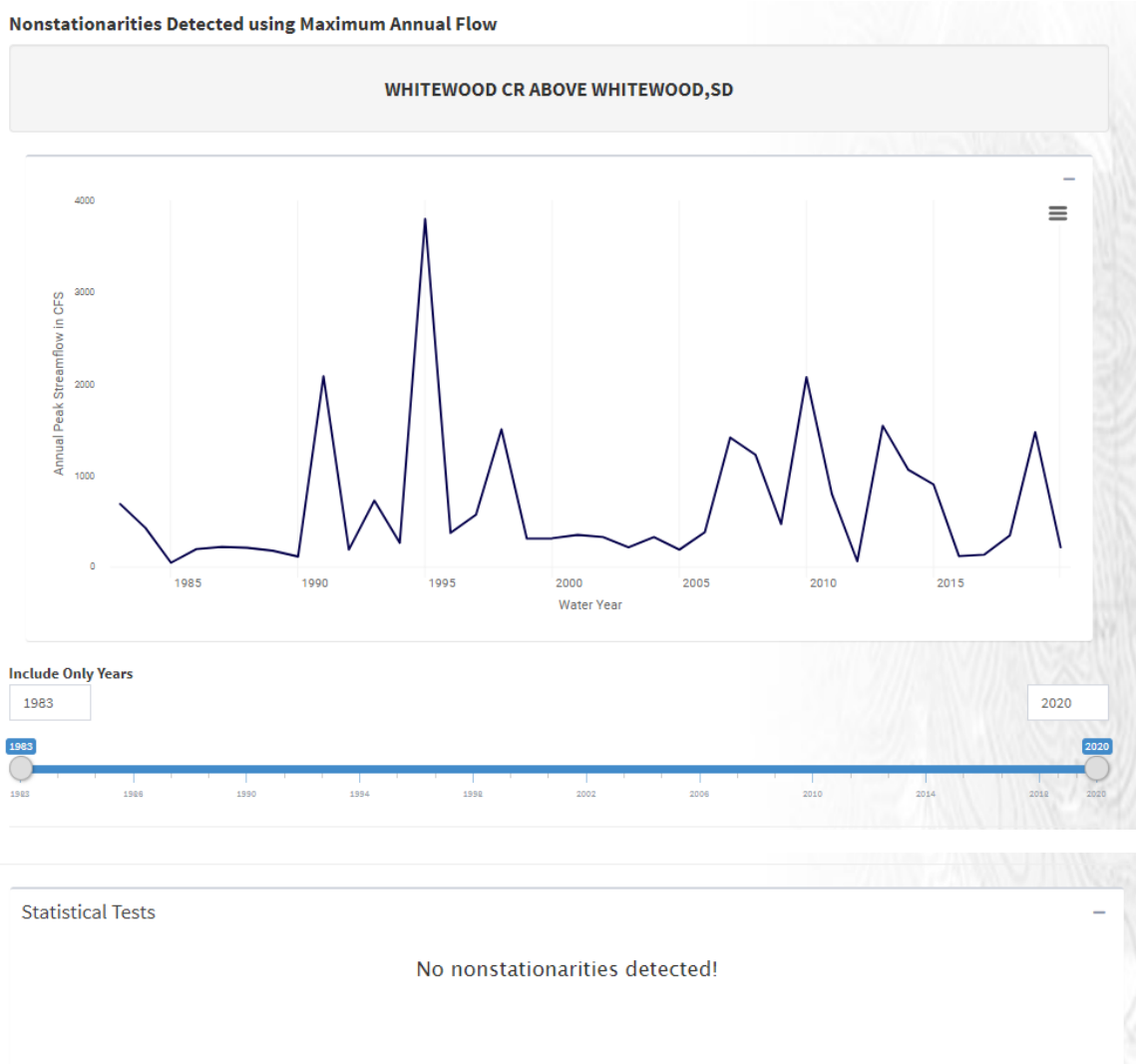


Figure 7.5.1. USGS Gage 06436180-Whitewood Creek Above Whitewood, SD, no non-stationarities identified for instantaneous peak streamflow for the period 1982-2020 using annual peak streamflow in cfs, using NSD tool version 2.0. The Bayesian Changepoint Test was not applied as the assumption of normality was not met.



Plot of Maximum Annual Flow/Height with Slope Fits (Traditional and Sen's Slope)

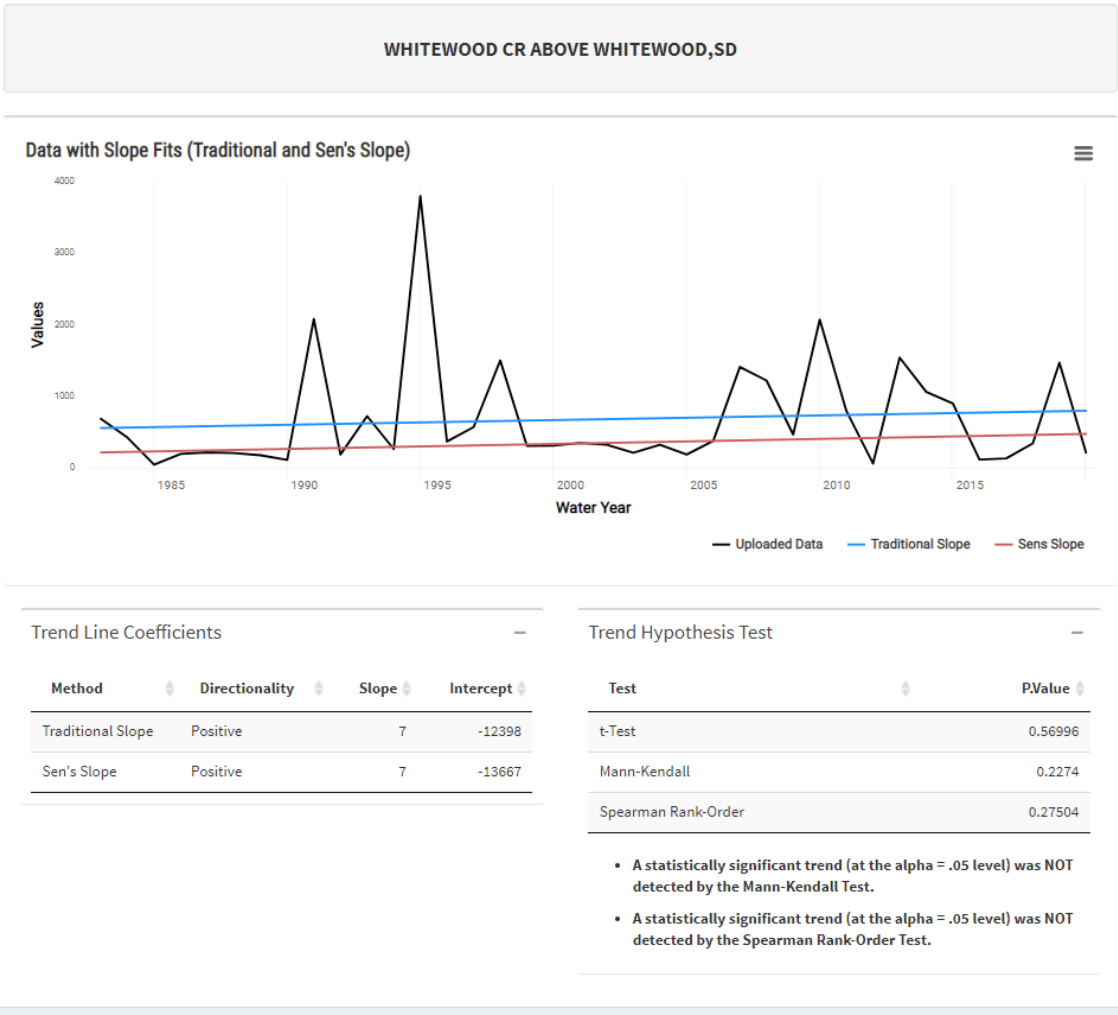


Figure 7.5.2. USGS Gage 06436180-Whitewood Creek Above Whitewood, SD, plot of maximum peak flow (ft.) with slope fits (Traditional and Sen's Slope). No statistically significant trends (at the alpha = 0.05 level) were detected using the Mann-Kendall or the Spearman Rank-Order tests for the period 1983-2020.

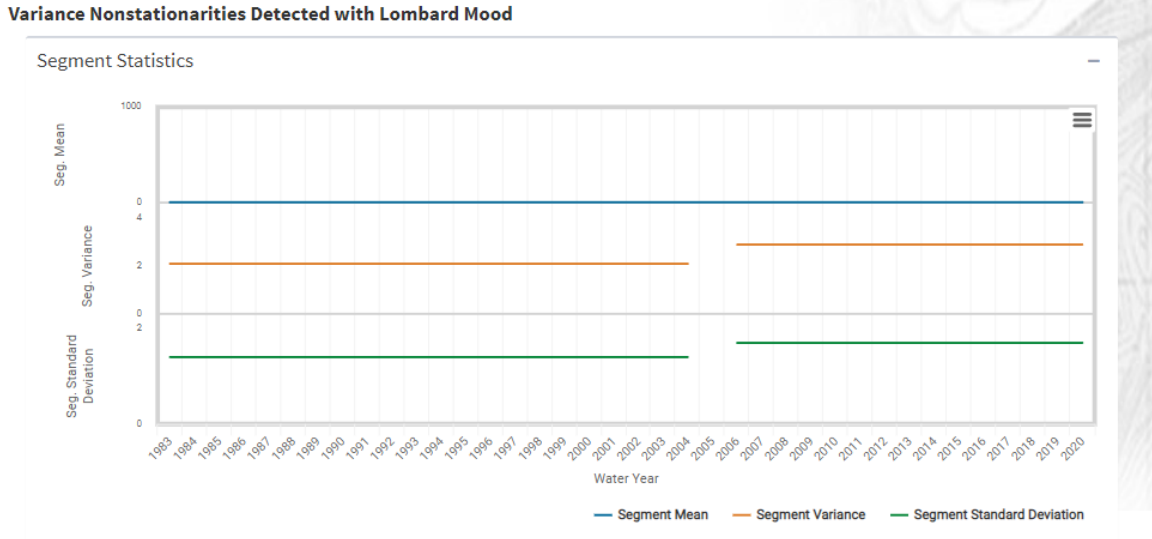
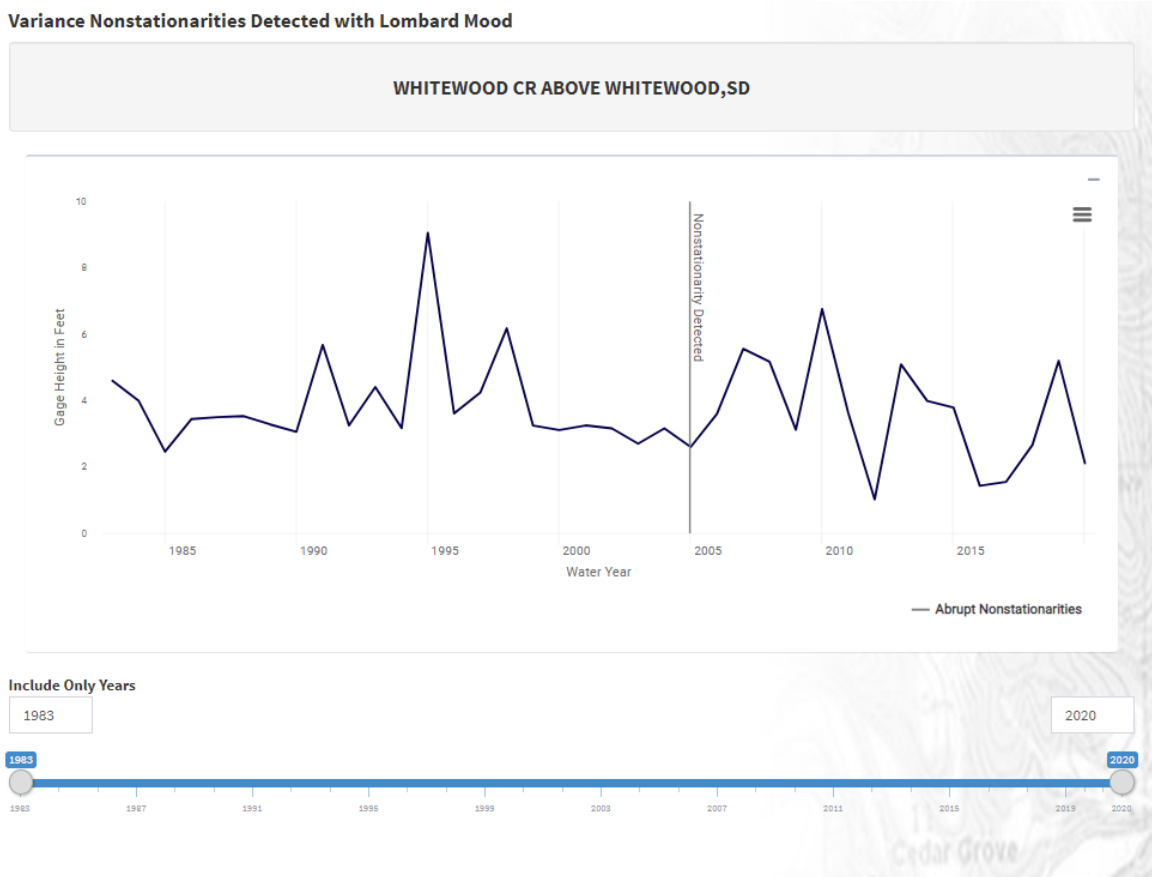


Figure 7.5.3. USGS Gage 06436180-Whitewood Creek Above Whitewood, SD, one segment variance non-stationarity was identified for stage/gage height (ft.) by the Lombard Mood for 2005 for the period 1983-2020 using NSD tool version 2.0. In 1983-2004 segment variance was 2.1, and 2006-2020 was 2.9, The segment standard deviation was 1.4 to 1.7, respectively. The Bayesian Changepoint Test was not applied as the assumption of normality was not met.

## Plot of Maximum Annual Flow/Height with Slope Fits (Traditional and Sen's Slope)

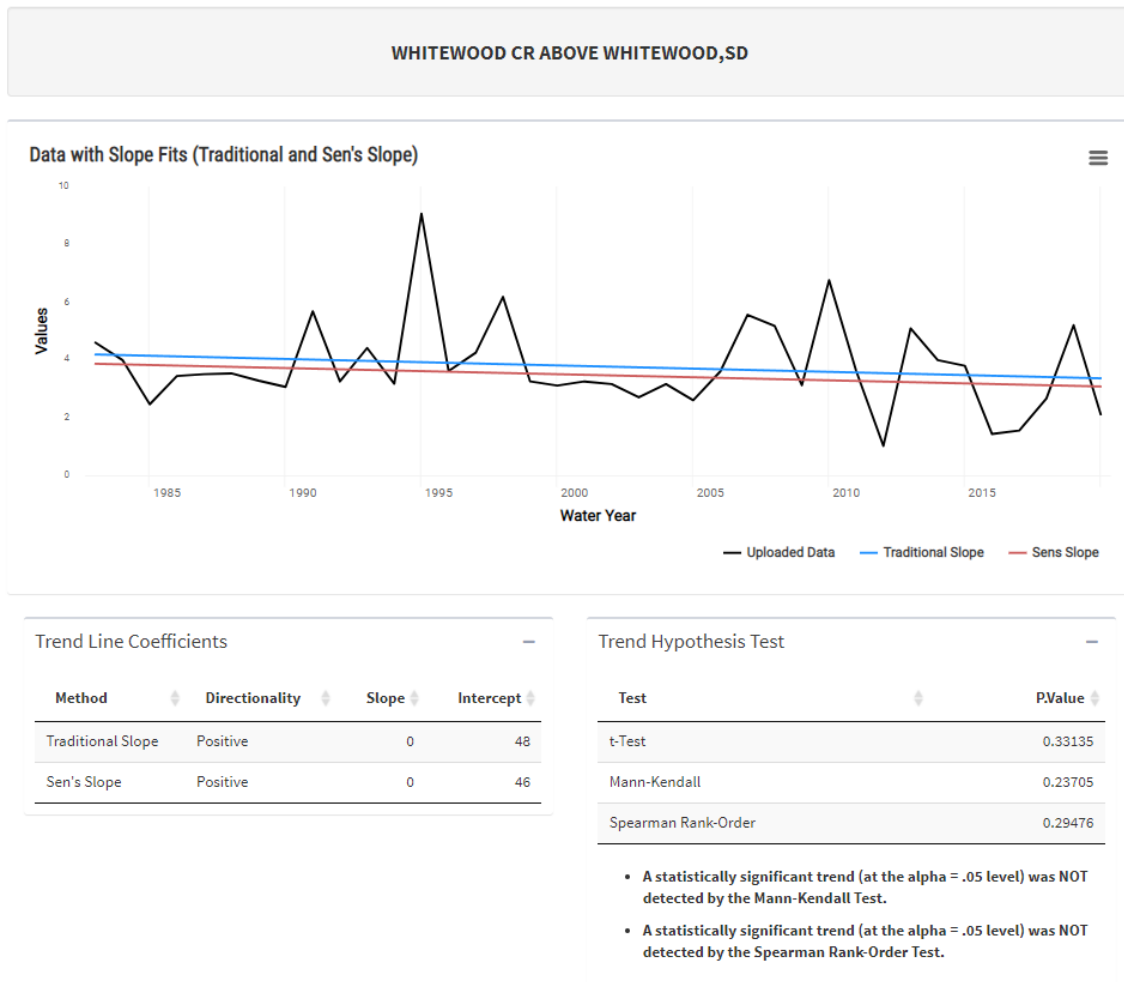


Figure 7.5.4. USGS Gage 06436180-Whitewood Creek Above Whitewood, SD, plot of gage/stage height (ft.) with slope fits (Traditional and Sen's Slope). No statistically significant trends (at the alpha = 0.05 level) were detected using the Mann-Kendall or the Spearman Rank-Order tests for the period 1983-2020.

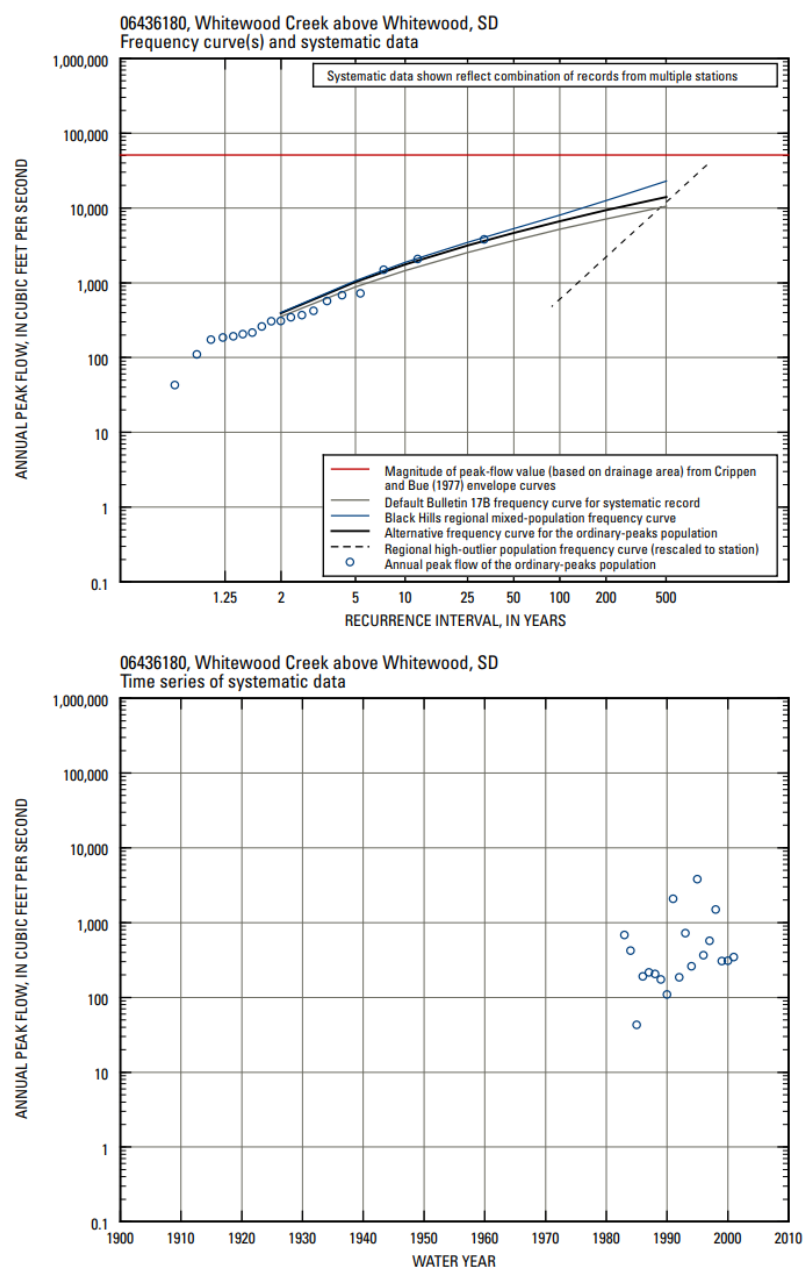
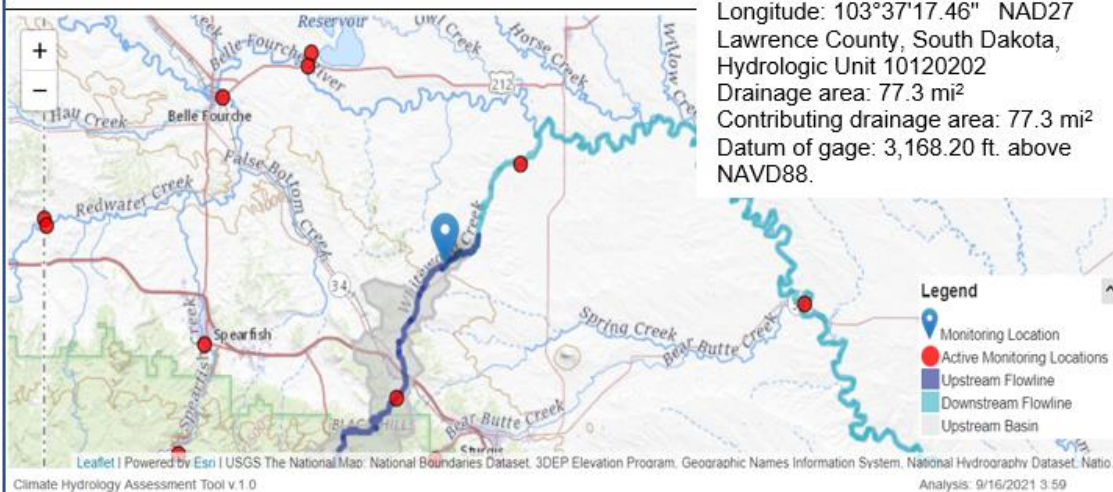


Figure 7.5.5. Peak-flow information for USGS gage station 06436180, Whitewood Creek Above Whitewood, SD (Sando et al., 2008).

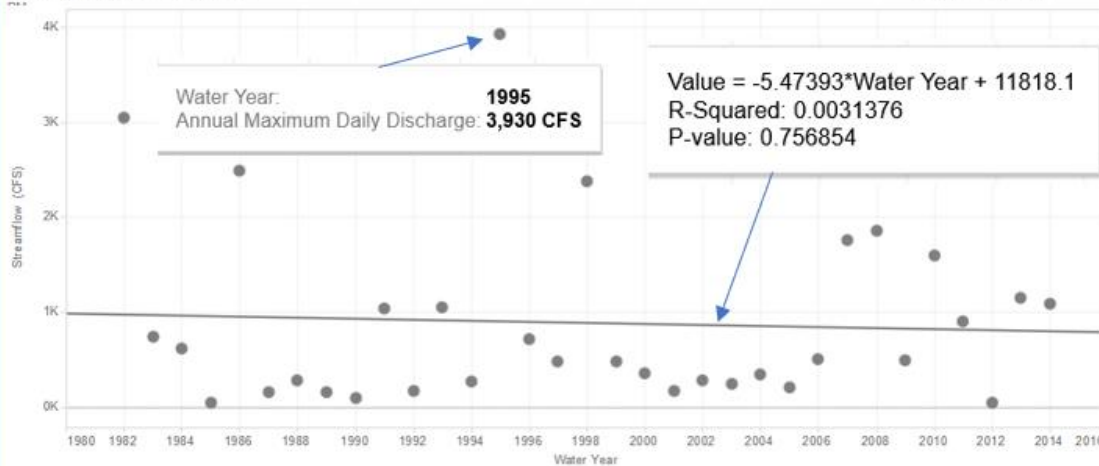
**Figure 7.6. HUC 4 CHAT Assessment 06436190-WNWS2-UNR  
Whitewood Creek Near Whitewood, SD**

Latitude: 44°32'30",  
Longitude: 103°37'17.46" NAD27  
Lawrence County, South Dakota,  
Hydrologic Unit 10120202  
Drainage area: 77.3 mi<sup>2</sup>  
Contributing drainage area: 77.3 mi<sup>2</sup>  
Datum of gage: 3,168.20 ft. above  
NAVD88.



Climate Hydrology Assessment Tool v.1.0

Analysis: 9/16/2021 3:59



USGS Parameter Group	Data Types	Start Date	End Date
Information	Water-quality	1981-11-06	1992-09-01
Inorganics, Major, Metals	Water-quality	1983-01-06	1984-08-07
Inorganics, Major, Non-metals	Water-quality	1983-01-06	1984-08-07
Inorganics, Minor, Non-metals	Water-quality	1983-01-06	1984-08-07
Inorganics, Minor, metals	Water-quality	1983-01-06	1984-08-07
Physical	Daily Values, Unit Values, Water-quality	1981-09-22	2021-09-16
Sediment	Water-quality	1983-04-19	1984-08-07
n/a	Peak Measurements	1982-05-20	2020-04-28
n/a	Site Visits	1981-11-06	2021-09-08
n/a	USGS Annual Water Data Reports Site	2006-01-01	2020-01-01

Nonstationarities Detected using Maximum Annual Flow

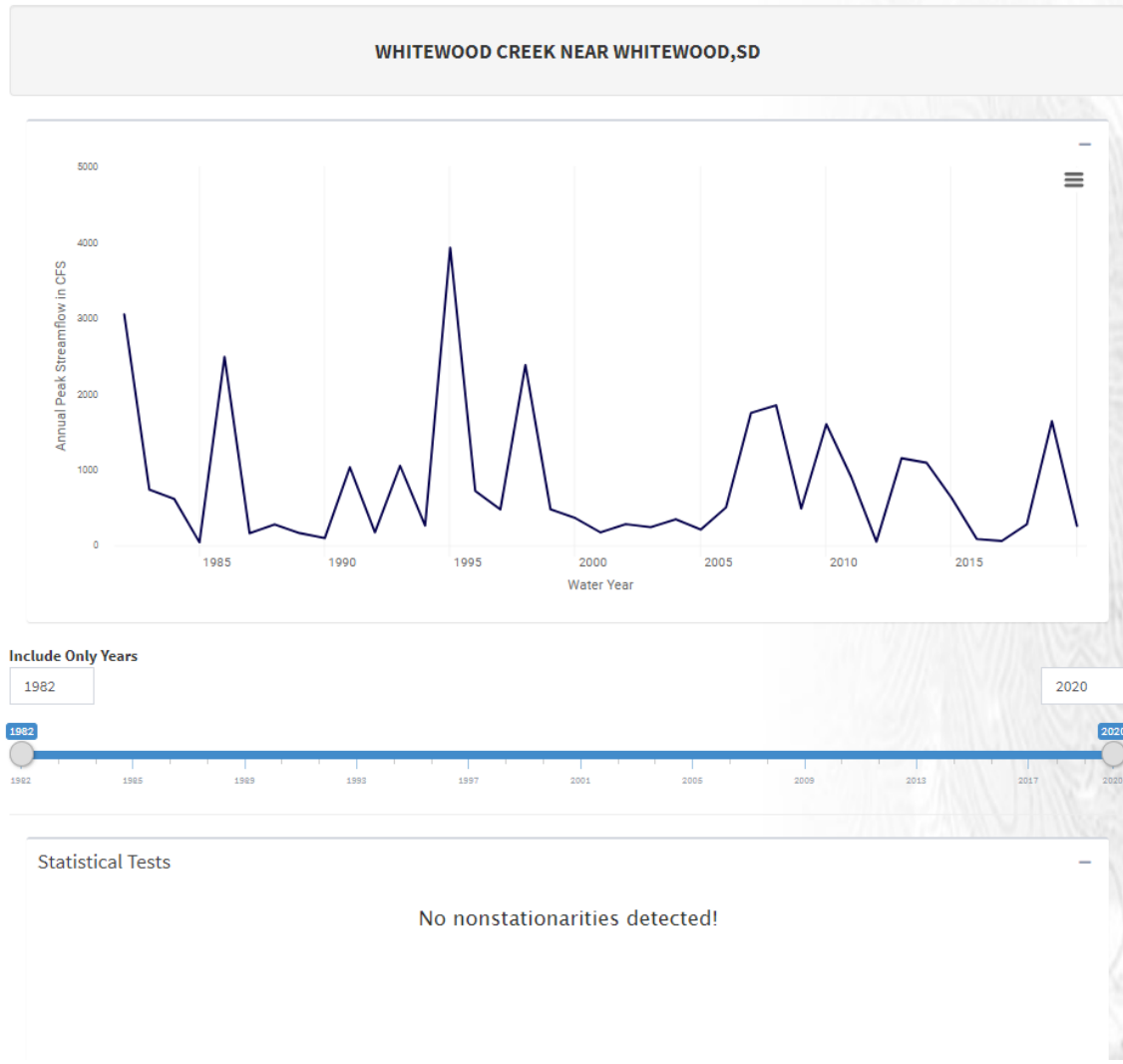


Figure 7.6.1. USGS Gage 06436190, Whitewood Creek Near Whitewood, SD non-stationarities identified for Instantaneous Peak Streamflow (IPS) using annual peak streamflow in cfs, for years 1982-2020 using NSD tool version 2.0. The Bayesian Changepoint Test was not applied as the assumption of normality was not met. No non-stationarities were detected.

Plot of Maximum Annual Flow/Height with Slope Fits (Traditional and Sen's Slope)

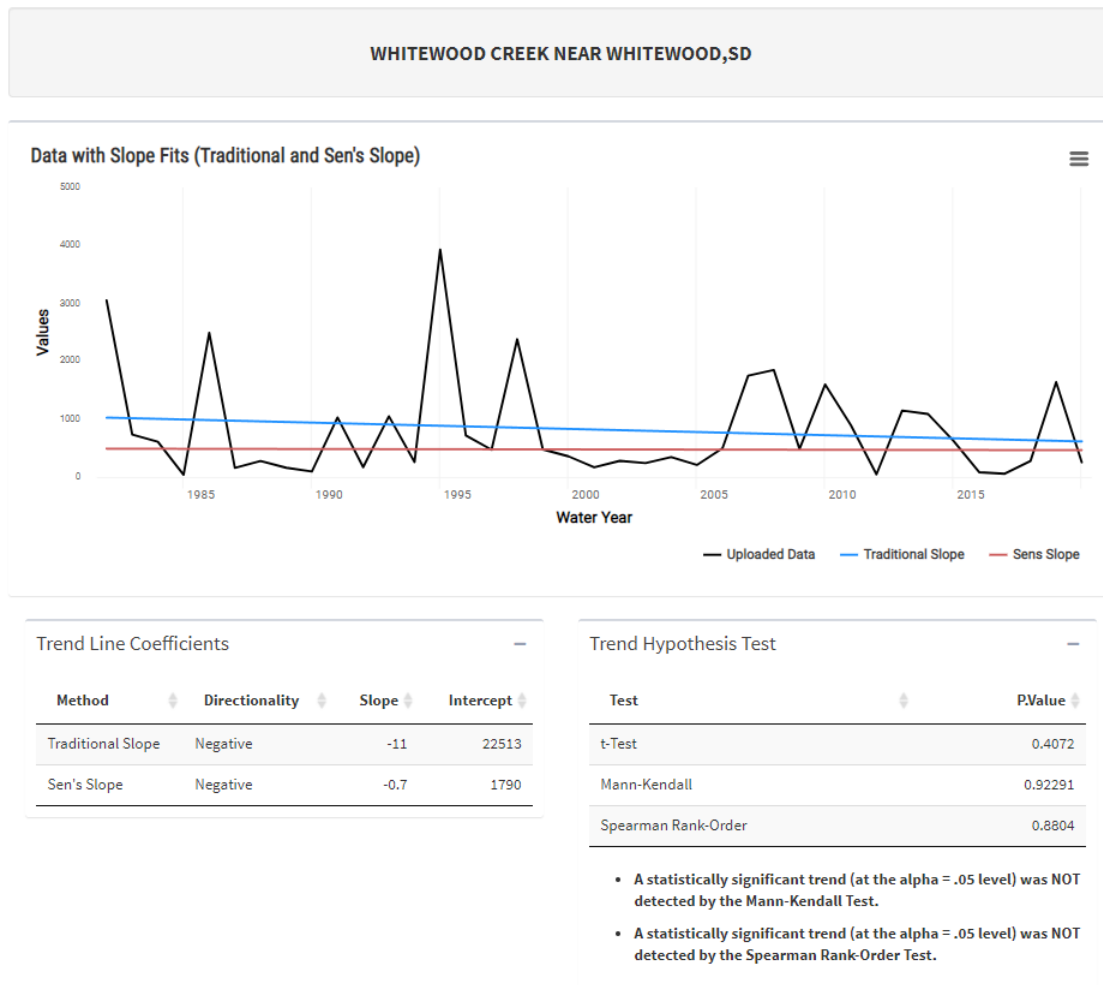
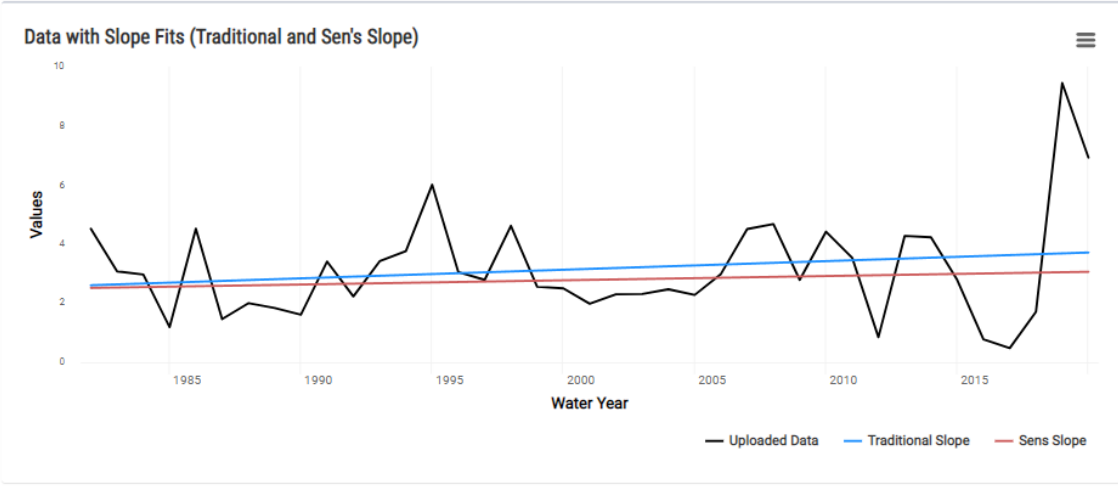


Figure 7.6.2. USGS Gage 06436190, Whitewood Creek Near Whitewood, SD plot of annual maximum flow (cfs) with slope fits (Traditional and Sen's Slope). No statistically significant trends (at the alpha = 0.05 level) were detected using the Mann-Kendall or the Spearman Rank-Order tests for the period 1982-2020.

Plot of Maximum Annual Flow/Height with Slope Fits (Traditional and Sen's Slope)

WHITEWOOD CREEK NEAR WHITEWOOD,SD



Method	Directionality	Slope	Intercept
Traditional Slope	Positive	0	-55
Sen's Slope	Positive	0	-26

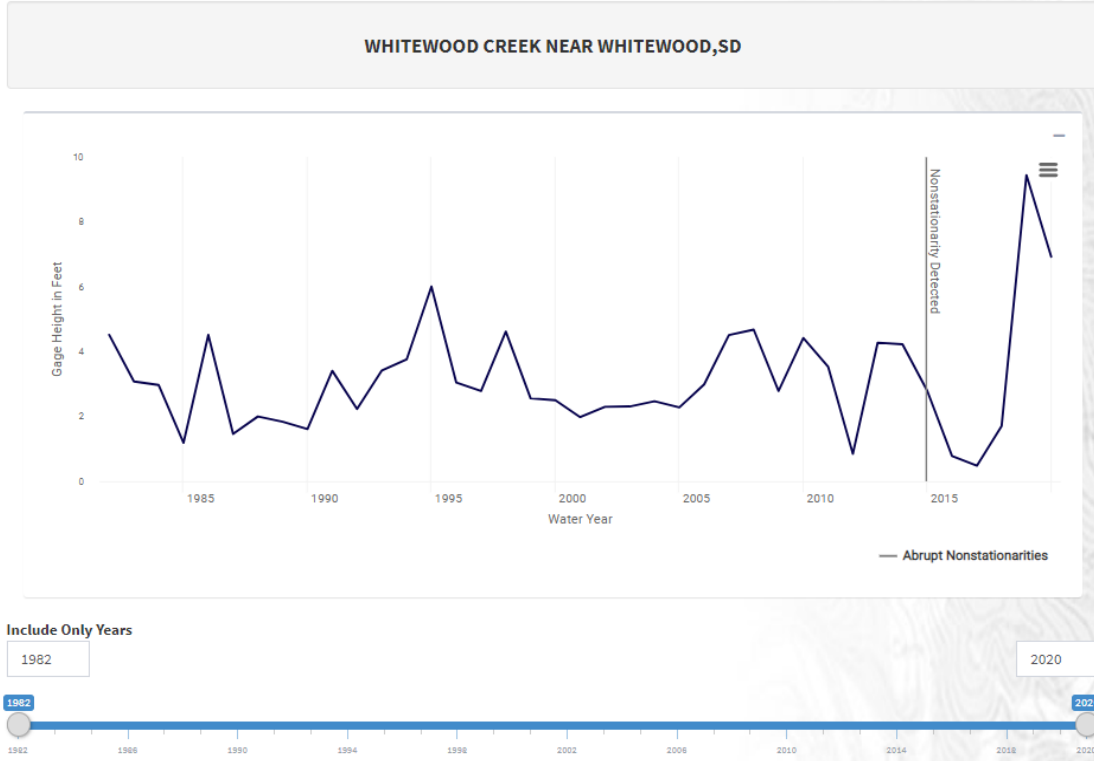
Test	PValue
t-Test	0.24453
Mann-Kendall	0.64563
Spearman Rank-Order	0.67799

- A statistically significant trend (at the alpha = .05 level) was NOT detected by the Mann-Kendall Test.
- A statistically significant trend (at the alpha = .05 level) was NOT detected by the Spearman Rank-Order Test.

Figure 7.6.3. USGS Gage 06436190, Whitewood Creek Near Whitewood, SD plot of gage/stage height (ft.) with slope fits (Traditional and Sen's Slope). No statistically significant trends (at the alpha = 0.05 level) were detected using the Mann-Kendall or the Spearman Rank-Order tests for the period 1982-2020.



Variance Nonstationarities Detected with Mood (CPM)



Variance Nonstationarities Detected with Mood (CPM)

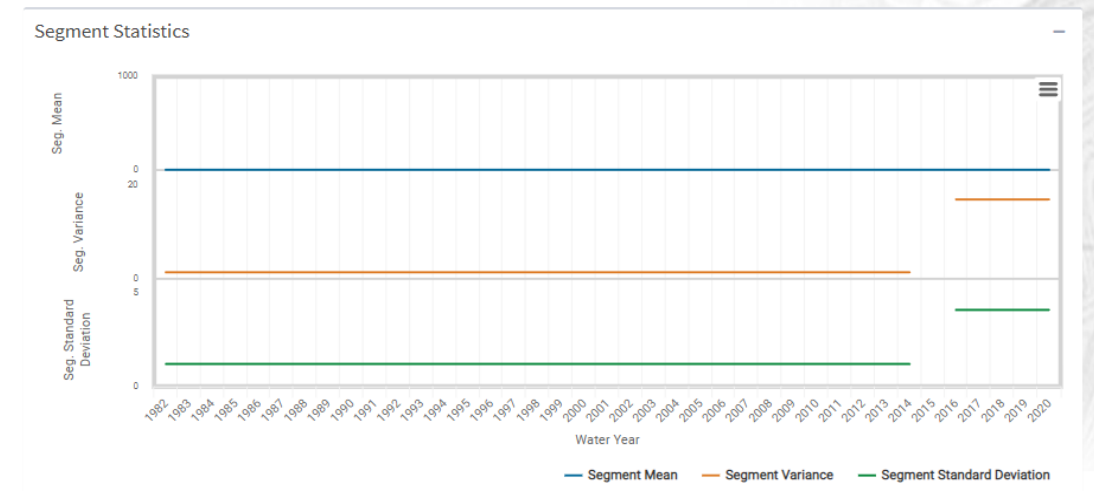
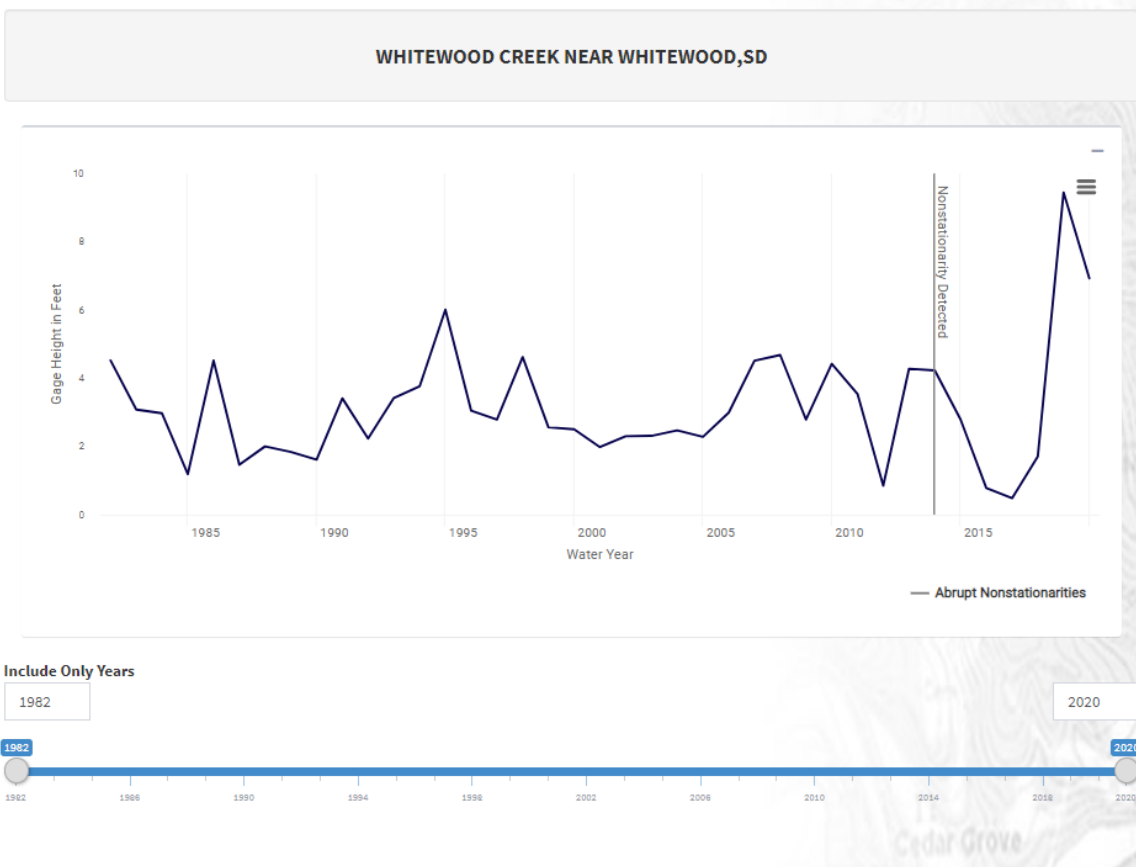


Figure 7.6.4. USGS Gage 06436190, Whitewood Creek Near Whitewood, SD non-stationarities identified for gage/stage height (ft.) for years 1982-2020. A variance non-stationarity was detected with the Lombard Mood method for the year 2015. The Bayesian Changepoint Test was not applied as the assumption of normality was not met. The segment variance from 1982-2014 was 1.4 ft. and 2016-2020 was 17 ft. The segment standard deviation for the period 1982-2014 was 1.2 ft. and 2016-2020 was 4.1 ft.

Variance Nonstationarities Detected with Lombard Mood



Variance Nonstationarities Detected with Lombard Mood

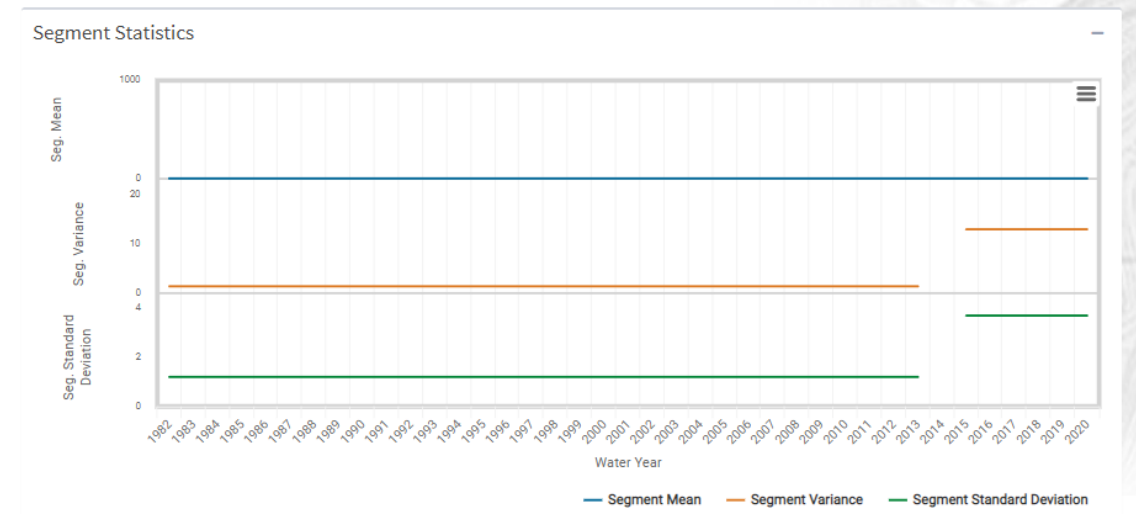


Figure 7.6.5. USGS Gage 06436190, Whitewood Creek Near Whitewood, plot of gage/stage height (ft.). The segment variance detected with Lombard Mood from 1982-2014 was 1.4 ft. and 2015-2020 was 13 ft. The segment standard deviation for the period 1982-2013 was 1.2 ft. and 2016-2020 was 3.7 ft.

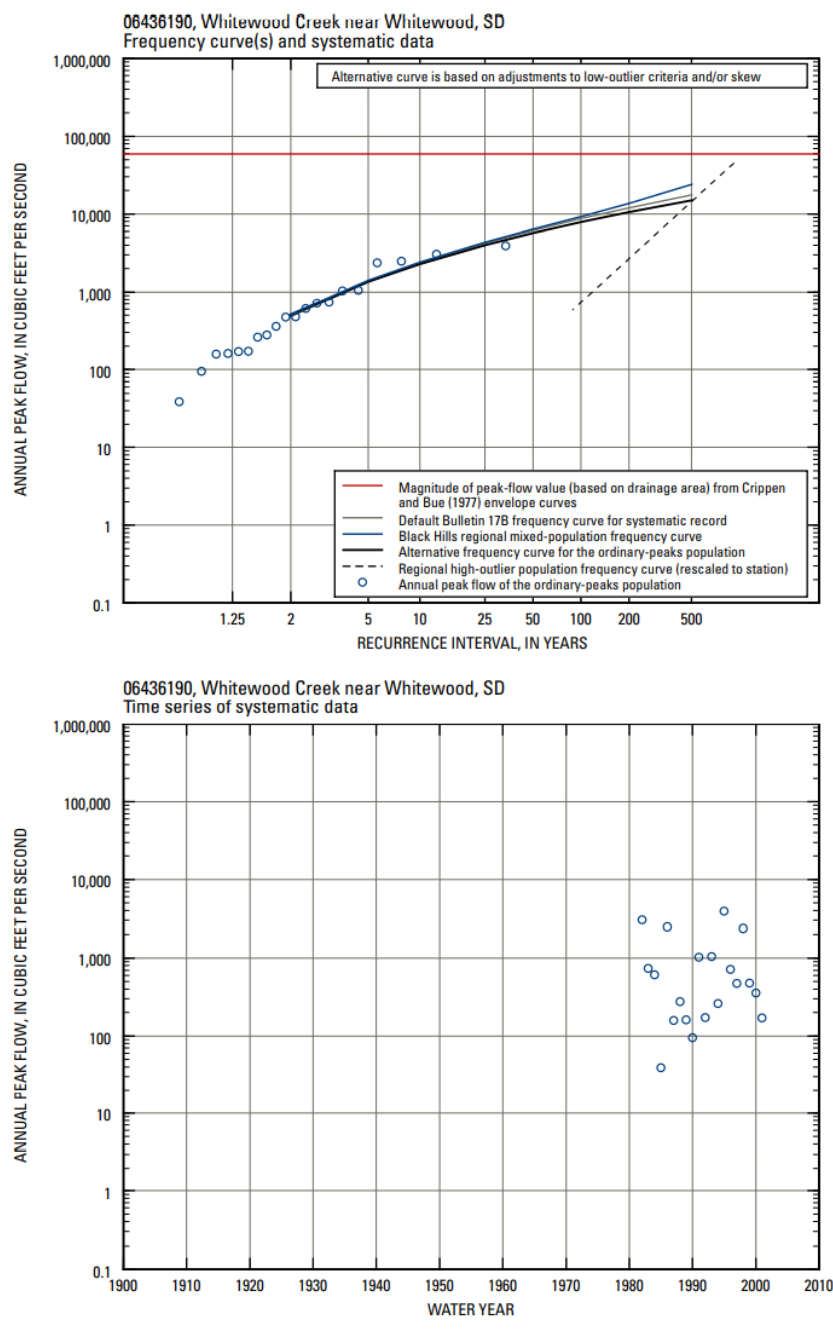
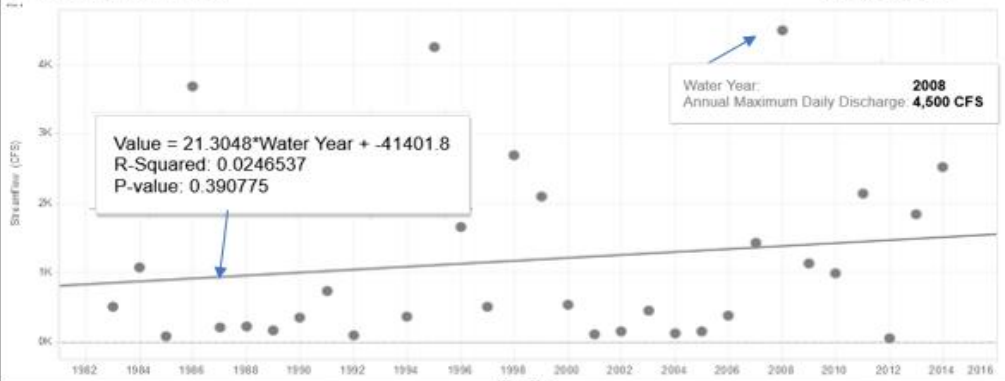
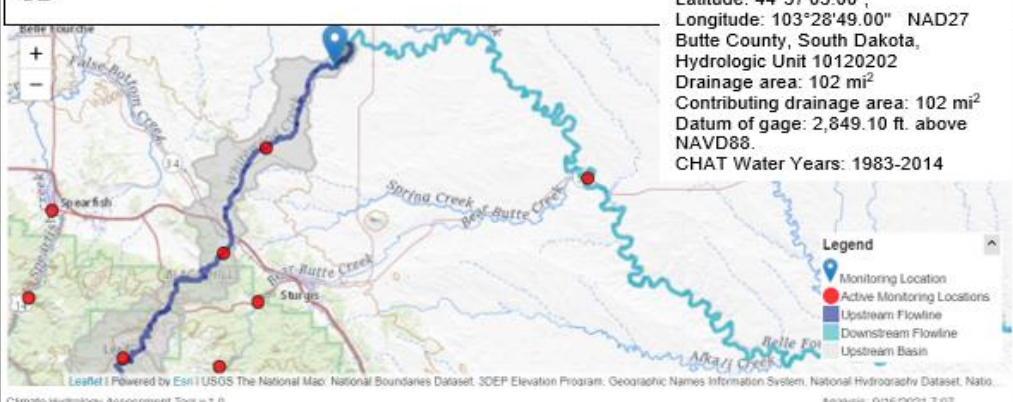


Figure 7.6.6. Peak-flow information for USGS gage station 06436190, Whitewood Creek near Whitewood, SD (Sando et al., 2008).

**Figure 7.7. HUC 4 CHAT Assessment 06436198-Whitewood Creek Above Vale, SD**



USGS Parameter Group	Data Types	Start Date	End Date
Information	Water-quality	1983-01-06	2021-08-23
Inorganics, Major, Metals	Water-quality	1983-01-06	2021-03-24
Inorganics, Major, Non-metals	Water-quality	1983-01-06	2021-07-06
Inorganics, Minor, Non-metals	Water-quality	1983-01-06	2021-03-24
Inorganics, Minor, metals	Water-quality	1983-01-06	2021-07-06
Nutrient	Water-quality	1986-02-26	1993-12-28
Organics, other	Water-quality	1985-06-07	1988-09-06
Organics, pesticide	Water-quality	2015-12-08	2015-12-08
Physical	Daily Values, Unit Values, Water-quality	1982-11-05	2021-09-16
Radiochemistry	Water-quality	1997-12-23	2021-03-24
Sediment	Water-quality	1983-01-06	2020-08-24

Nonstationarities Detected using Maximum Annual Flow



Figure 7.7.1. USGS Gage 06436198-Whitewood Creek Above Vale, SD plot of non-stationarities identified for Instantaneous Peak Streamflow (IPS) using annual peak streamflow in cfs, for years 1983-2020. The Bayesian Change-point Test was not applied as the assumption of normality was not met. No non-stationarities were detected.

Plot of Maximum Annual Flow/Height with Slope Fits (Traditional and Sen's Slope)

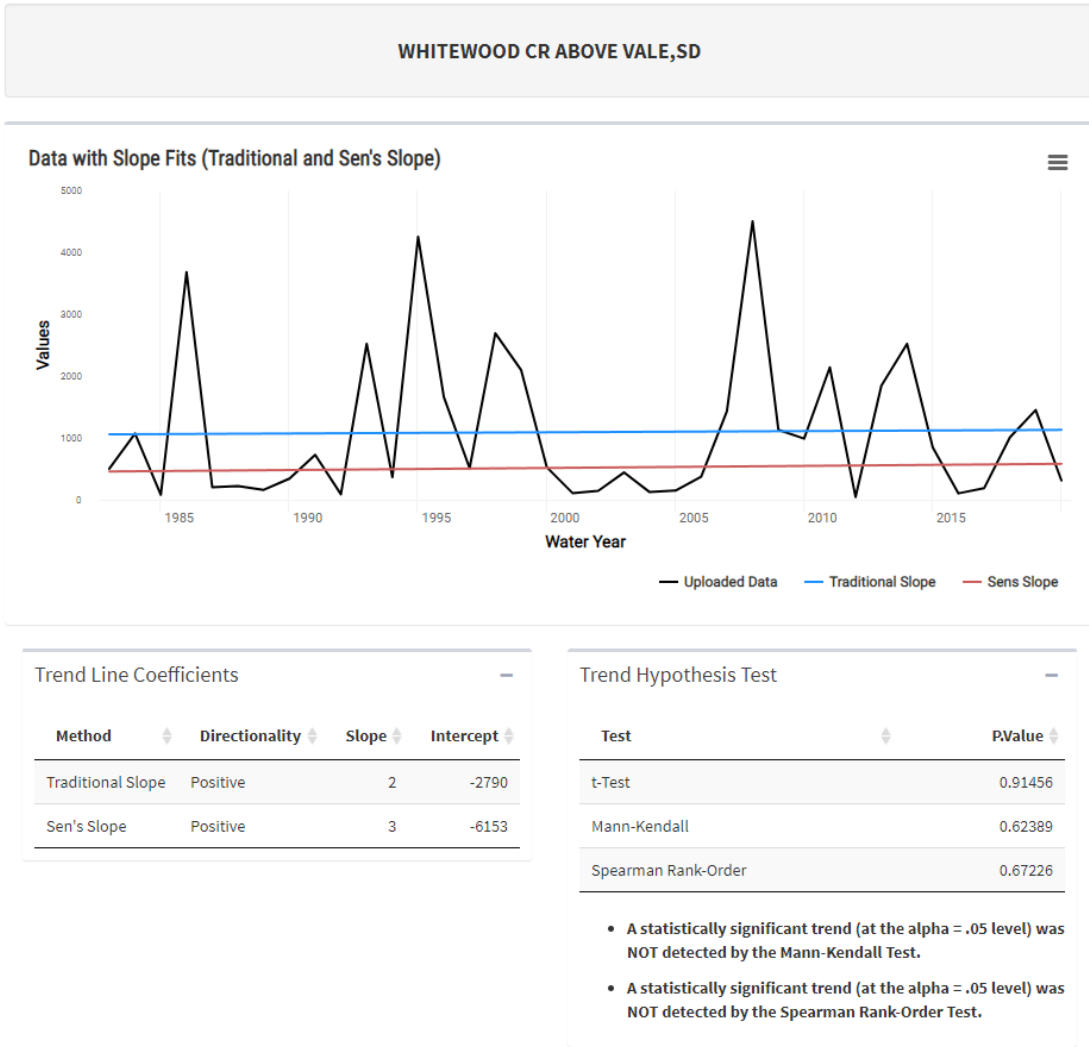
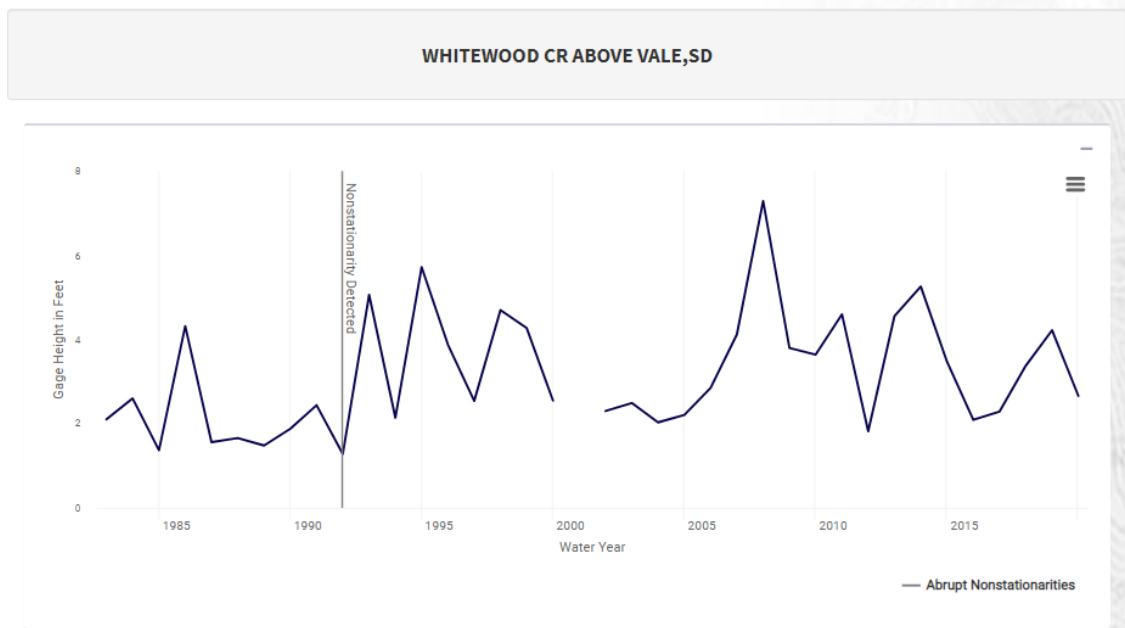


Figure 7.7.2. USGS Gage 06436198, Whitewood Creek Above Vale, plot of maximum annual flow (cfs) with slope fits (Traditional and Sen's Slope). No statistically significant trends (at the alpha = 0.05 level) were detected using the Mann-Kendall or the Spearman Rank-Order tests for the period 1983-2020.

Mean Nonstationarities Detected with Pettitt



Include Only Years



Mean Nonstationarities Detected with Pettitt

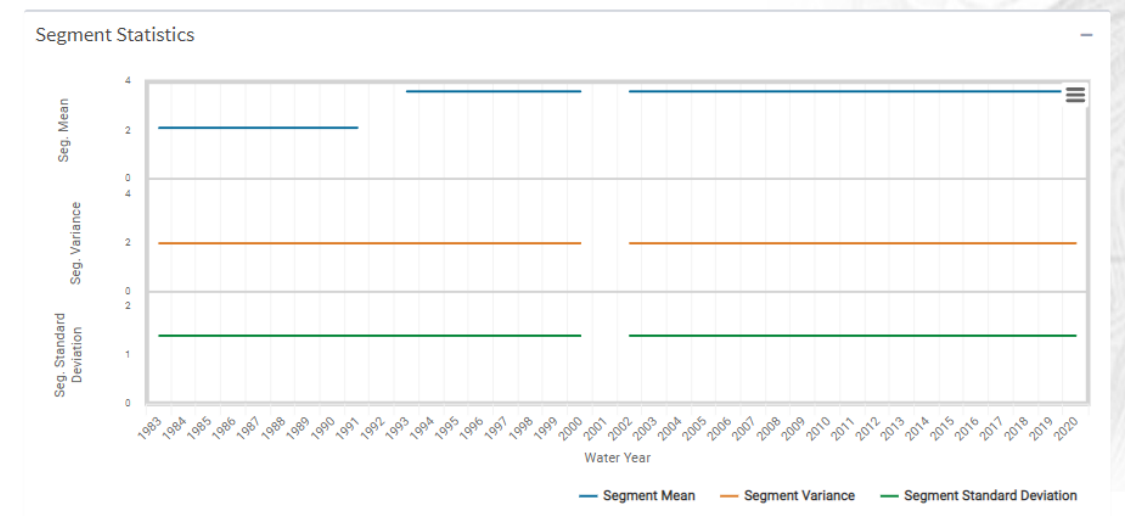


Figure 7.7.3. USGS Gage 06436198, Whitewood Creek Above Vale, mean nonstationarity was detected a non-parametric change with Pettitt in 1992. The northern Black Hills experienced significant winter storms during that year (NWS, 1992). Plot of the segment mean from 1983-1991 was 2.1 ft, from 1993-2000 was 3.6 ft. and from 2002-2020 was 3.6 feet. There was missing data from 2000-2002.

Plot of Maximum Annual Flow/Height with Slope Fits (Traditional and Sen's Slope)

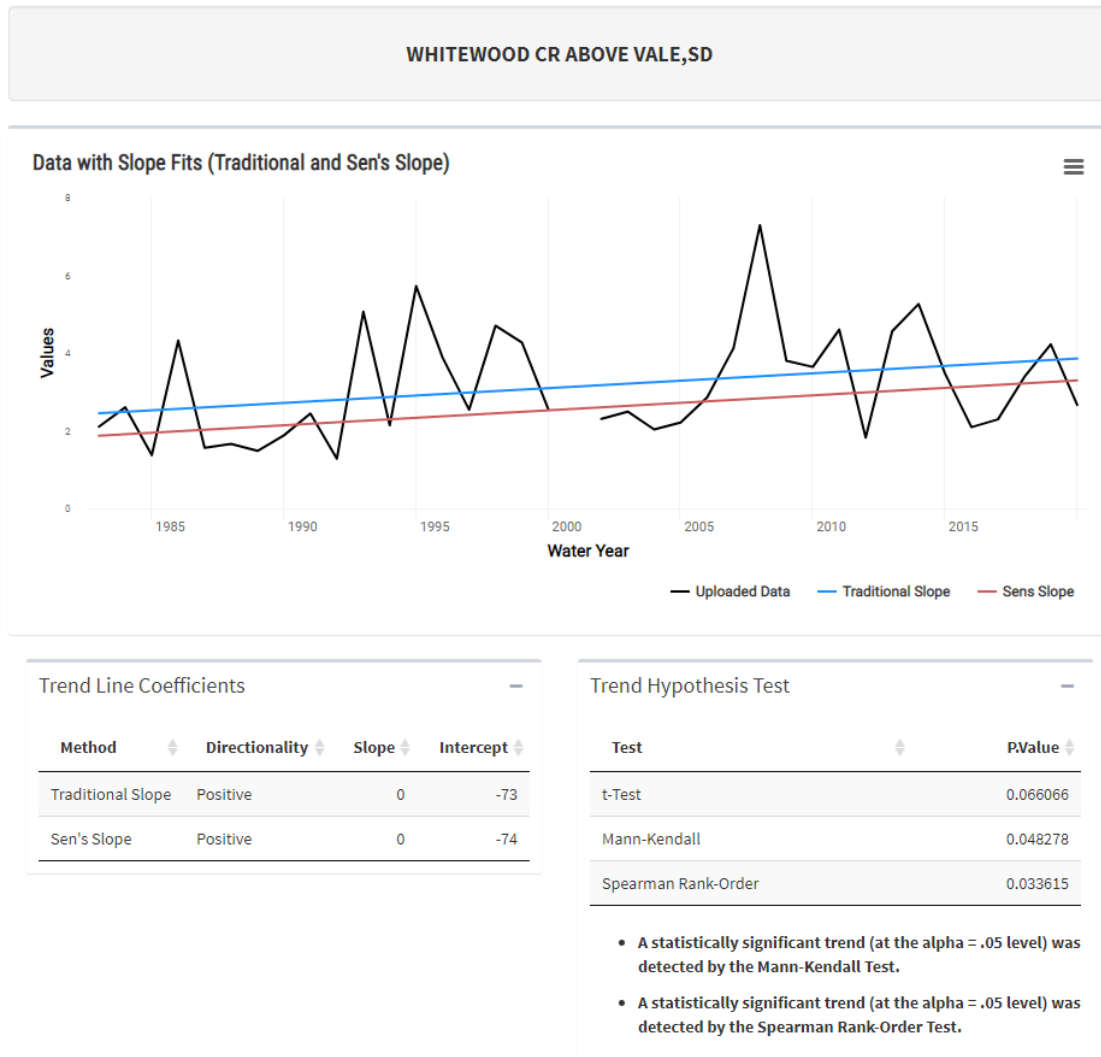


Figure 7.7.4. USGS Gage 06436198, Whitewood Creek Above Vale, SD, plot of gage/stage height (ft.) with slope fits (Traditional and Sen's Slope). Statistically significant trends (at the alpha =0.05 level) were detected using the Mann-Kendall or the Spearman Rank-Order tests for the period 1983-2020. There was missing data in 2000-2002.



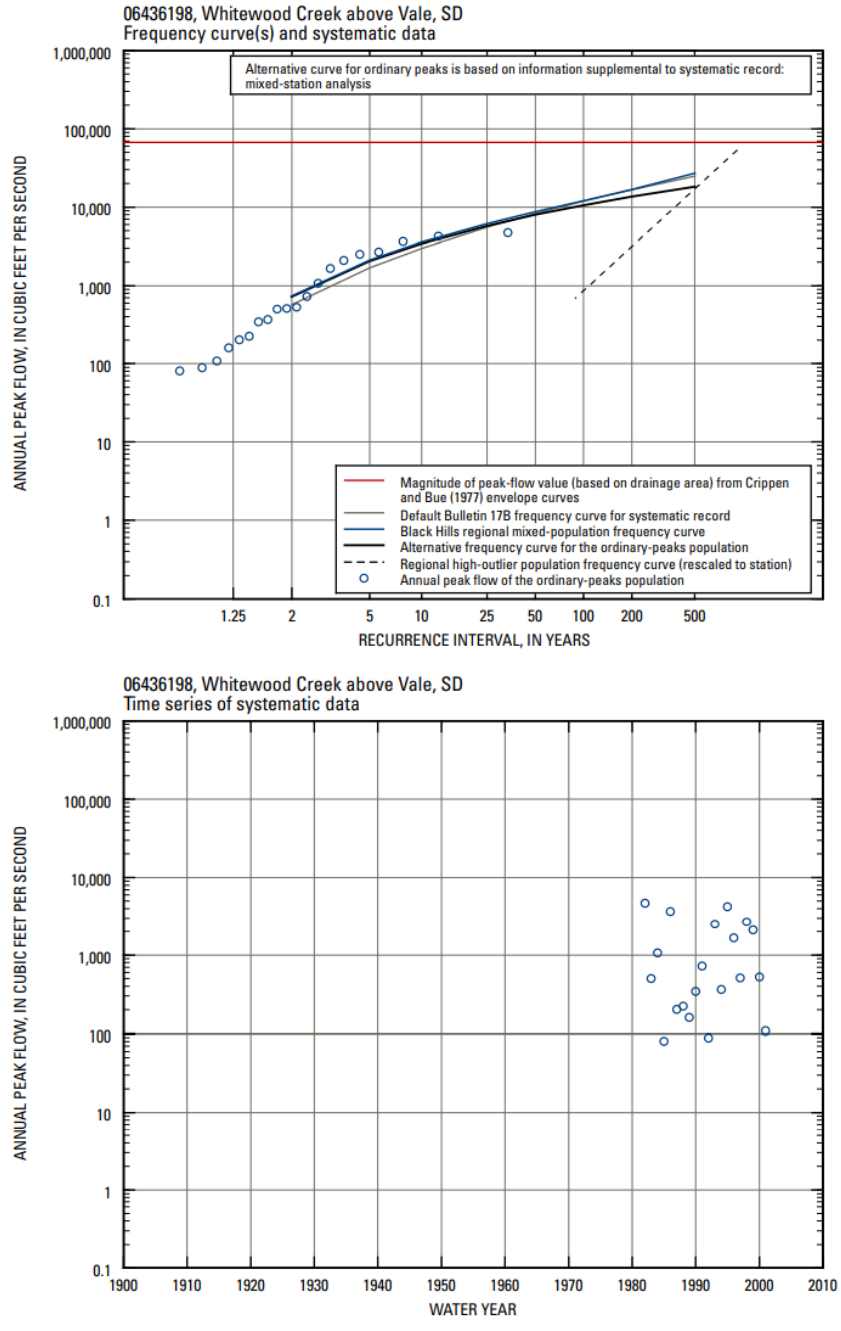
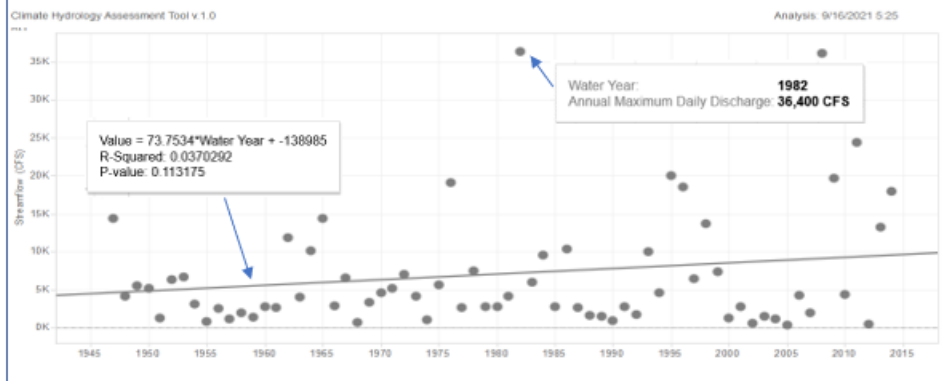
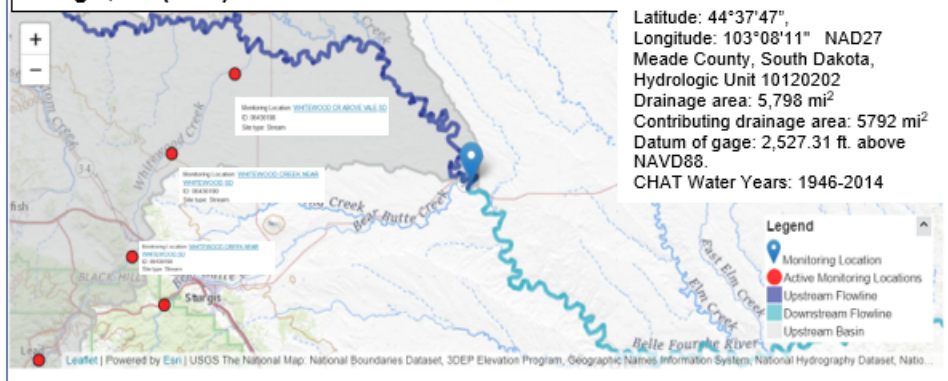


Figure 7.7.5. Peak-flow information for USGS gage station 06436198, Whitewood Creek above Vale, SD (Sando et al., 2008).

**Figure 7.8. HUC 4 CHAT Assessment 06437000-SBFS2-Belle Fourche Near Sturgis, SD (UNR)**



USGS Parameter Group	Data Types	Start Date	End Date
Information	Water-quality	1954-08-09	2002-11-14
Inorganics, Major, Metals	Water-quality	1954-08-09	2002-11-14
Inorganics, Major, Non-metals	Water-quality	1954-08-09	2010-10-07
Inorganics, Minor, Non-metals	Water-quality	1954-08-09	2002-11-14
Inorganics, Minor, metals	Water-quality	1954-08-09	2002-11-14
Microbiological	Water-quality	1969-01-22	1989-10-24
Nutrient	Water-quality	1954-08-09	1998-06-10
Organics, other	Water-quality	1985-06-10	1988-09-22
Organics, pesticide	Water-quality	1988-04-27	1988-10-26
Physical	Daily Values, Unit Values, Water-quality	1945-11-07	2021-09-16
Radiochemistry	Water-quality	1981-01-20	1994-09-06
Sediment	Water-quality	1955-10-31	2002-11-14

### Nonstationarities Detected using Maximum Annual Flow

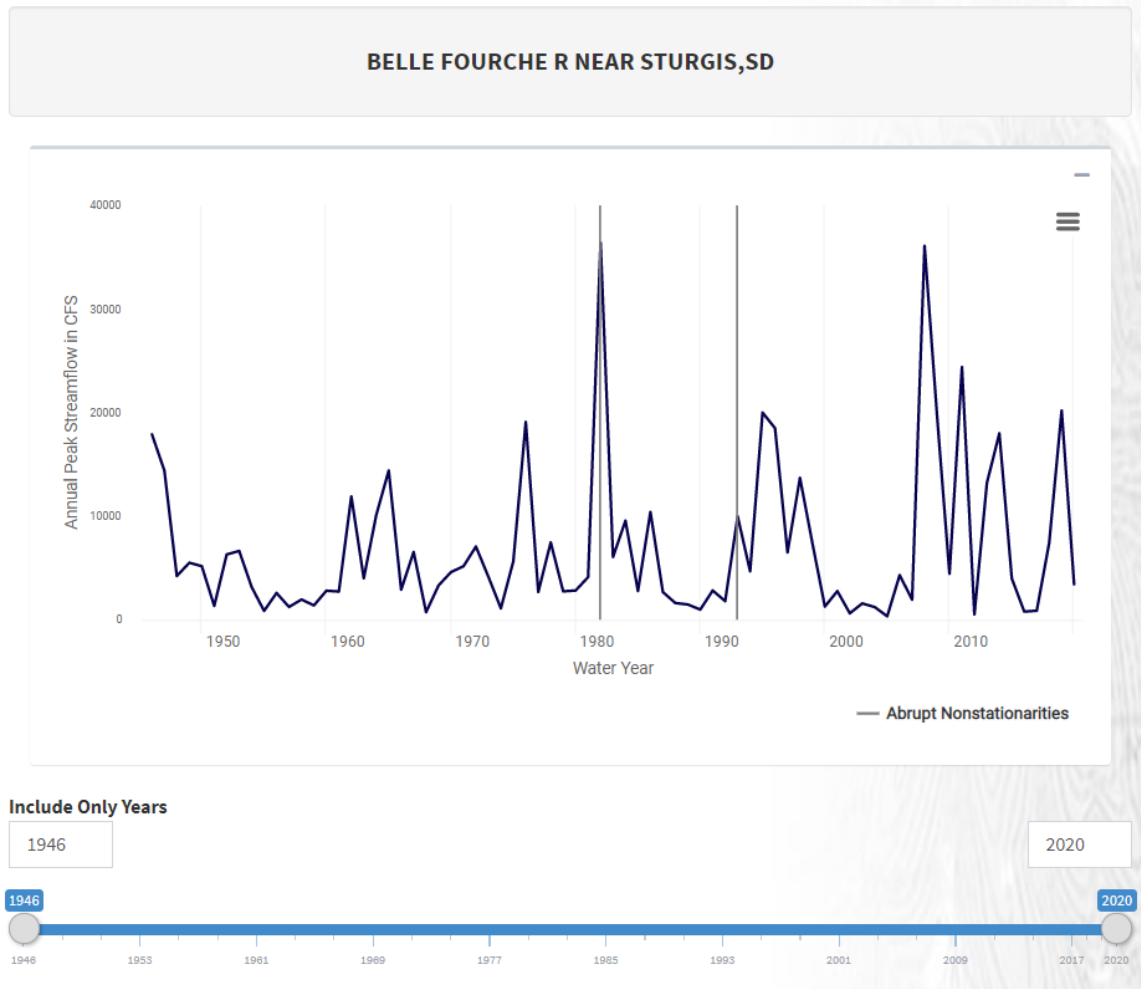


Figure 7.8.1. USGS Gage 06437000-Belle Fourche River Near Sturgis, SD, plot of non-stationarities identified for Instantaneous Peak Streamflow (IPS) using annual peak streamflow in cfs, for years 1946-2020 using NSD tool version 2.0. The Bayesian Changepoint Test was not applied as the assumption of normality was not met. Two non-stationarities were detected: Distribution-1982, Energy Divisive Method (Peak Flow, 36,400 cfs), and Variance-1993 Lombard Mood, (9,980 cfs) after a period of low-flow during 1987-1992.

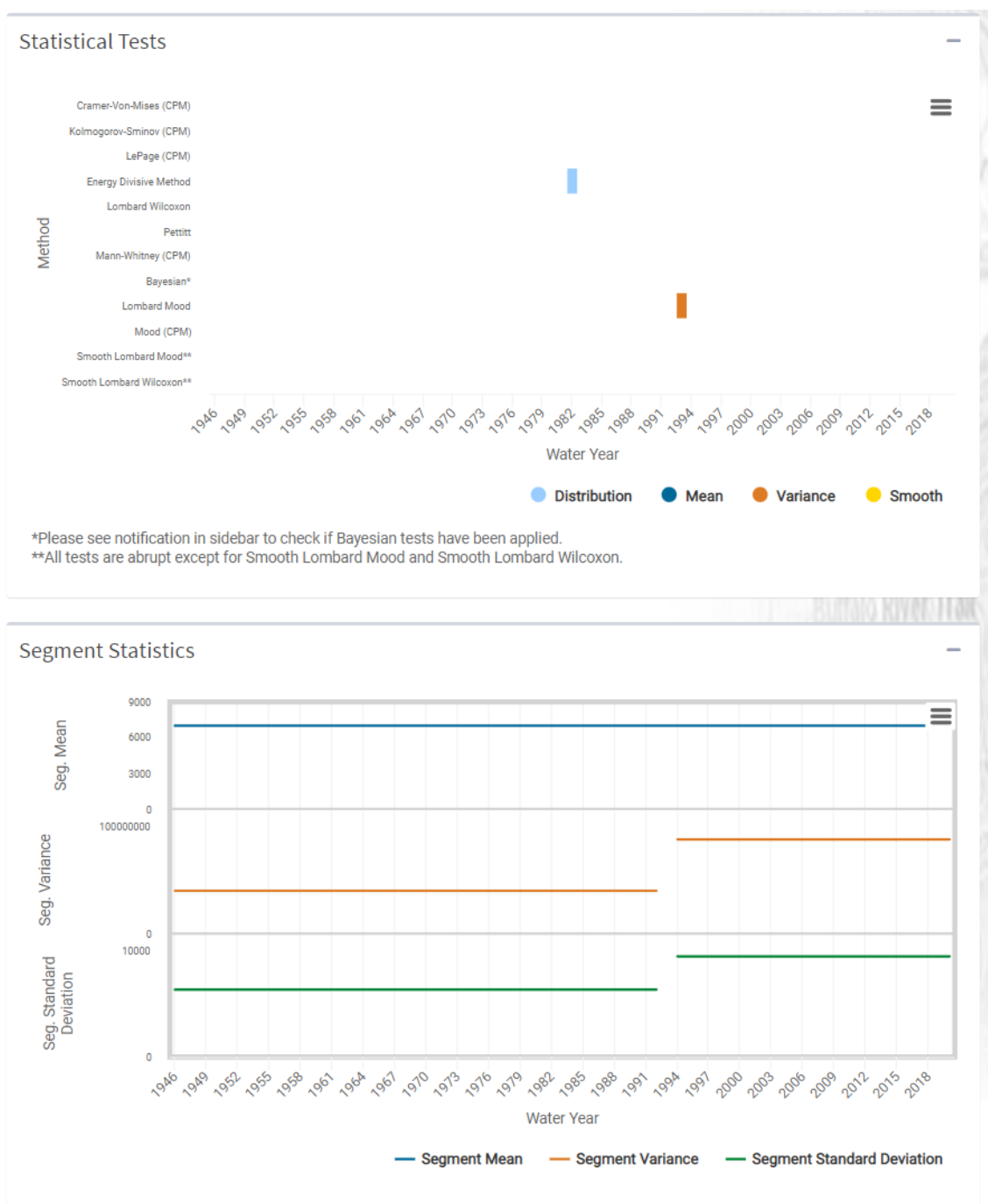


Figure 7.8.2. USGS Gage 06437000-Belle Fourche River Near Sturgis, SD, plots of non-stationarity identified with the NSD tool: Distribution, Energy Divisive Method in 1982 and the Variance, Lombard Mood in 1993.

Plot of Maximum Annual Flow/Height with Slope Fits (Traditional and Sen's Slope)

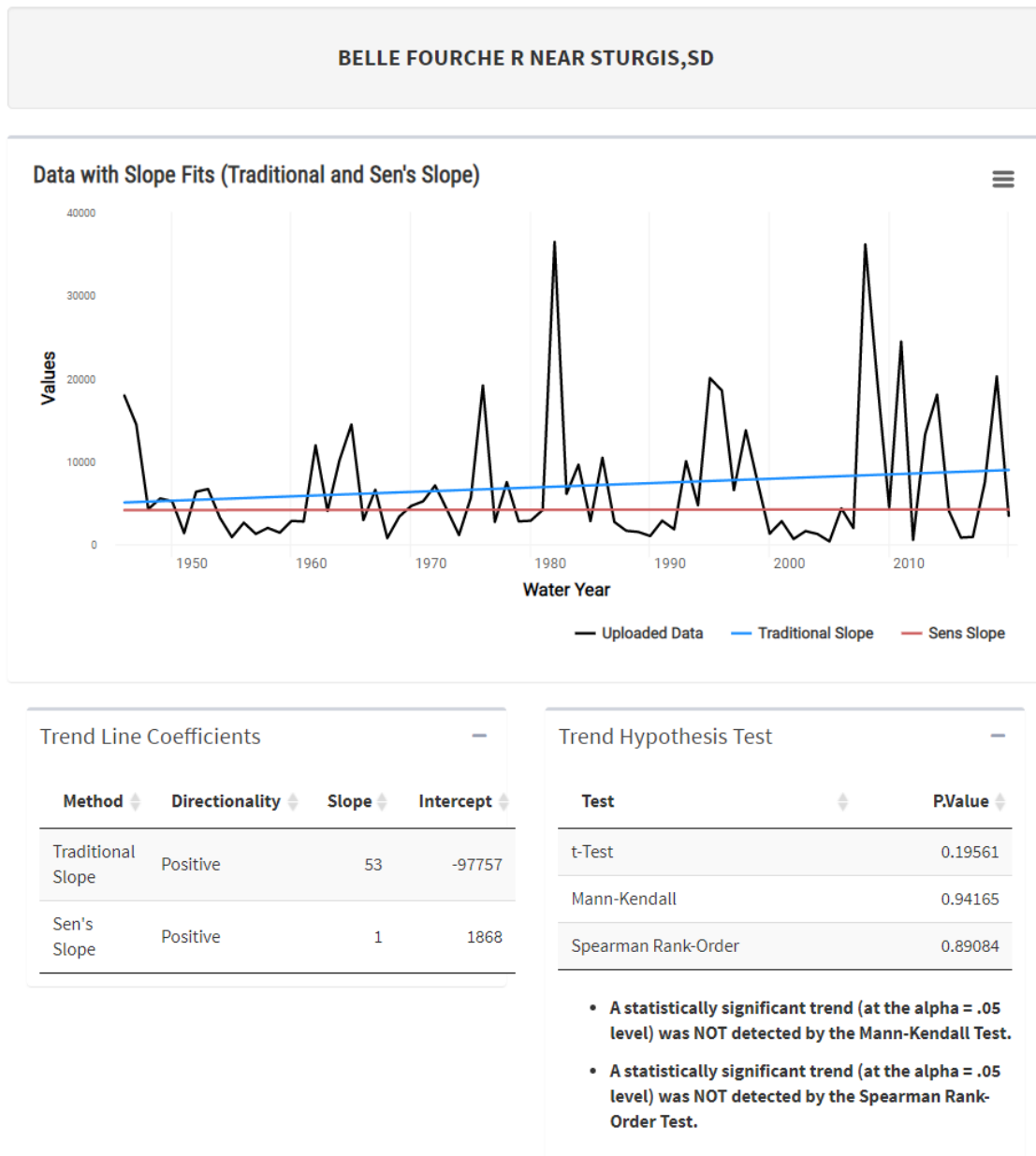
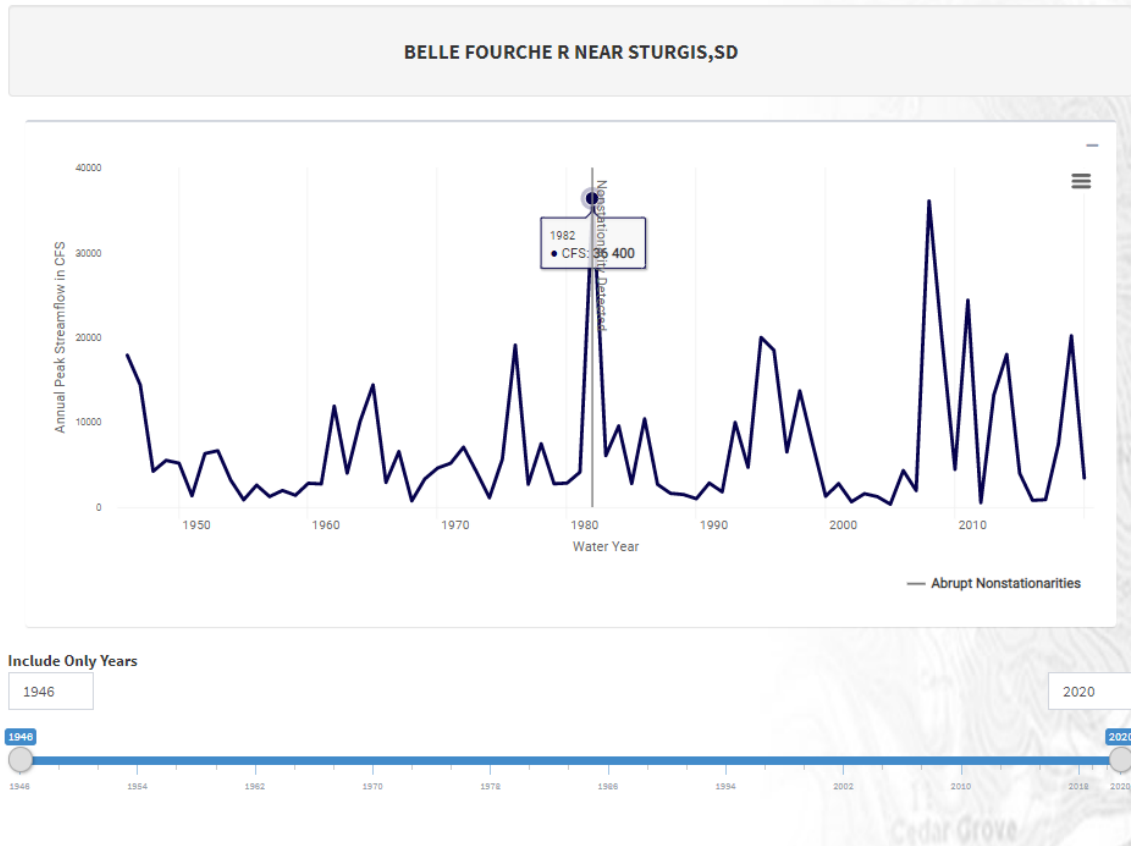


Figure 7.8.3. USGS Gage 06437000-Belle Fourche River Near Sturgis, SD, plot maximum annual flow with slope fits (Traditional and Sen's Slope). No statistically significant trends (at the alpha =0.05 level) were detected using the Mann-Kendall or the Spearman Rank-Order tests for the period 1946-2020.

Distribution Nonstationarities Detected with Energy Divisive Method



Distribution Nonstationarities Detected with Energy Divisive Method

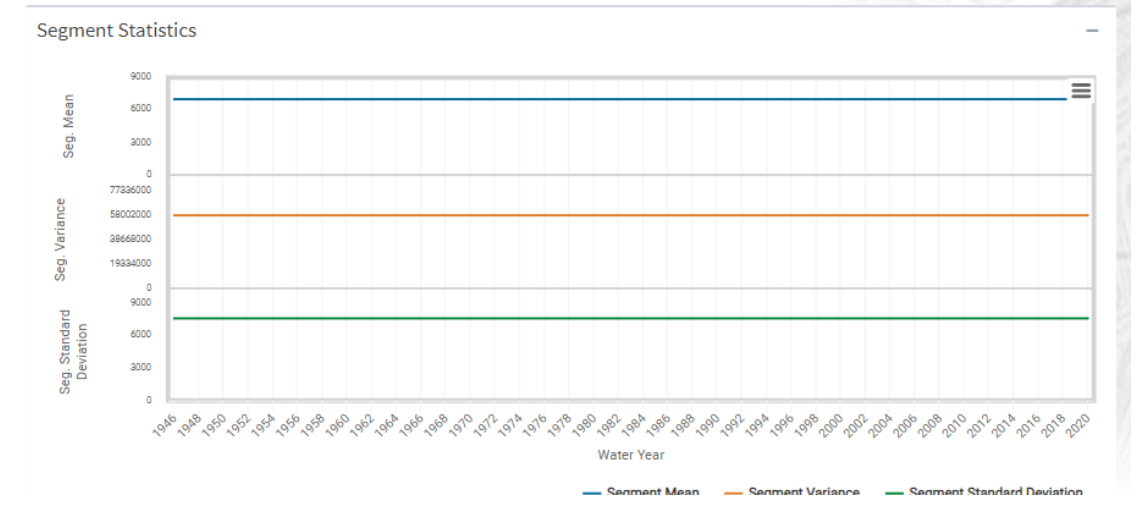
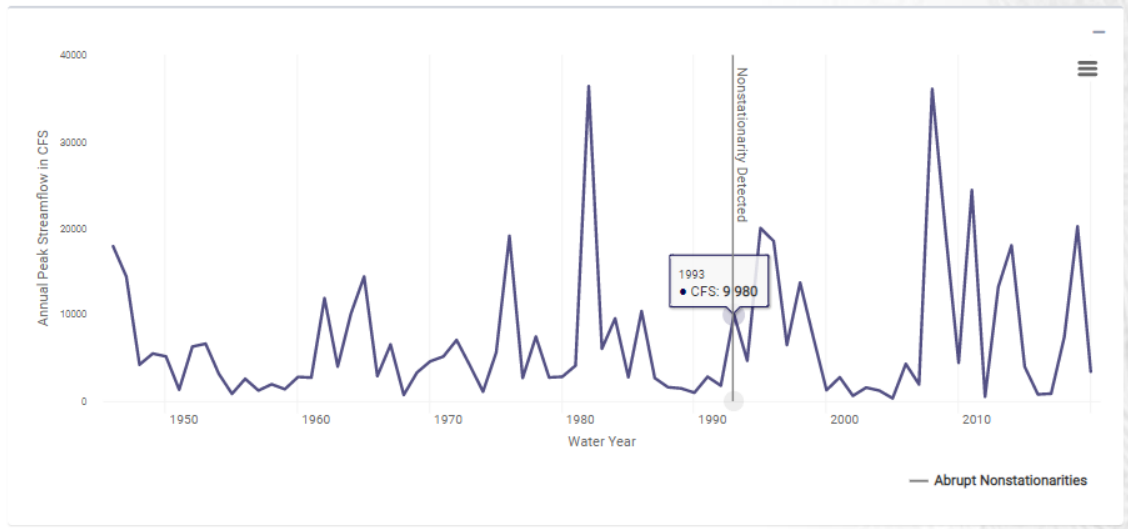


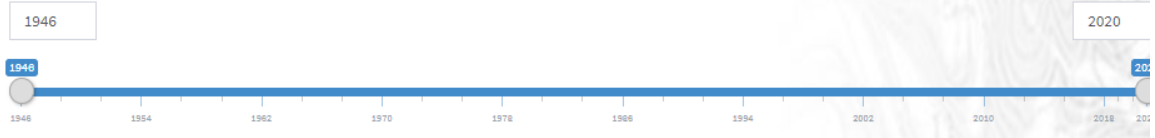
Figure 7.8.4. USGS Gage 06437000-Belle Fourche River Near Sturgis, SD, plot of distribution non-stationarities detected with the Energy Divisive Method in 1982, a peak annual discharge of 36,400 cfs.

Variance Nonstationarities Detected with Lombard Mood

BELLE FOURCHE R NEAR STURGIS,SD



Include Only Years



Variance Nonstationarities Detected with Lombard Mood

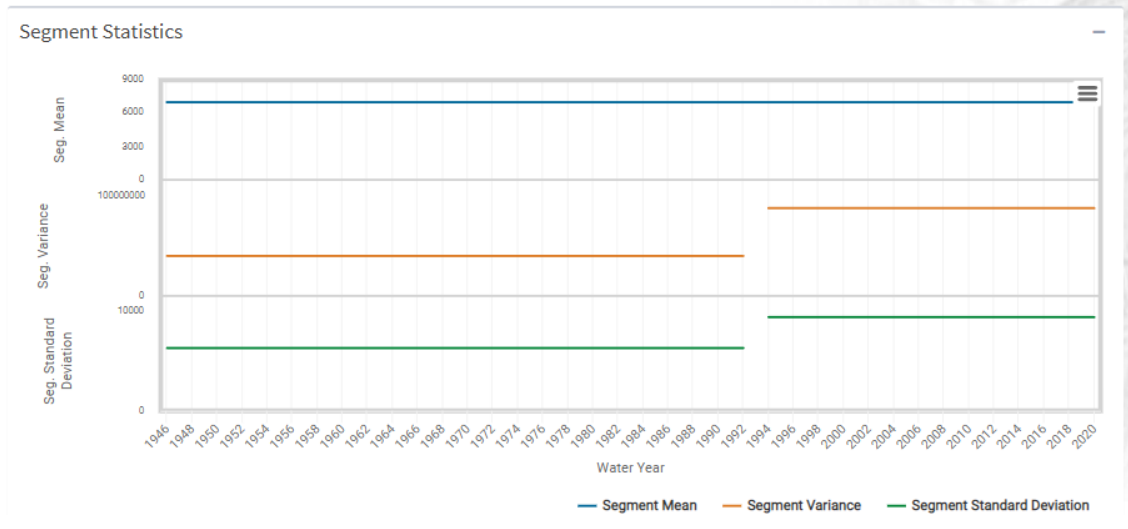


Figure 7.8.5. USGS Gage 06437000-Belle Fourche River Near Sturgis, SD, for the period 1946-2020. Plot of variance non-stationarities detected with Lombard Mood in 1993.

Nonstationarities Detected using Maximum Annual Height

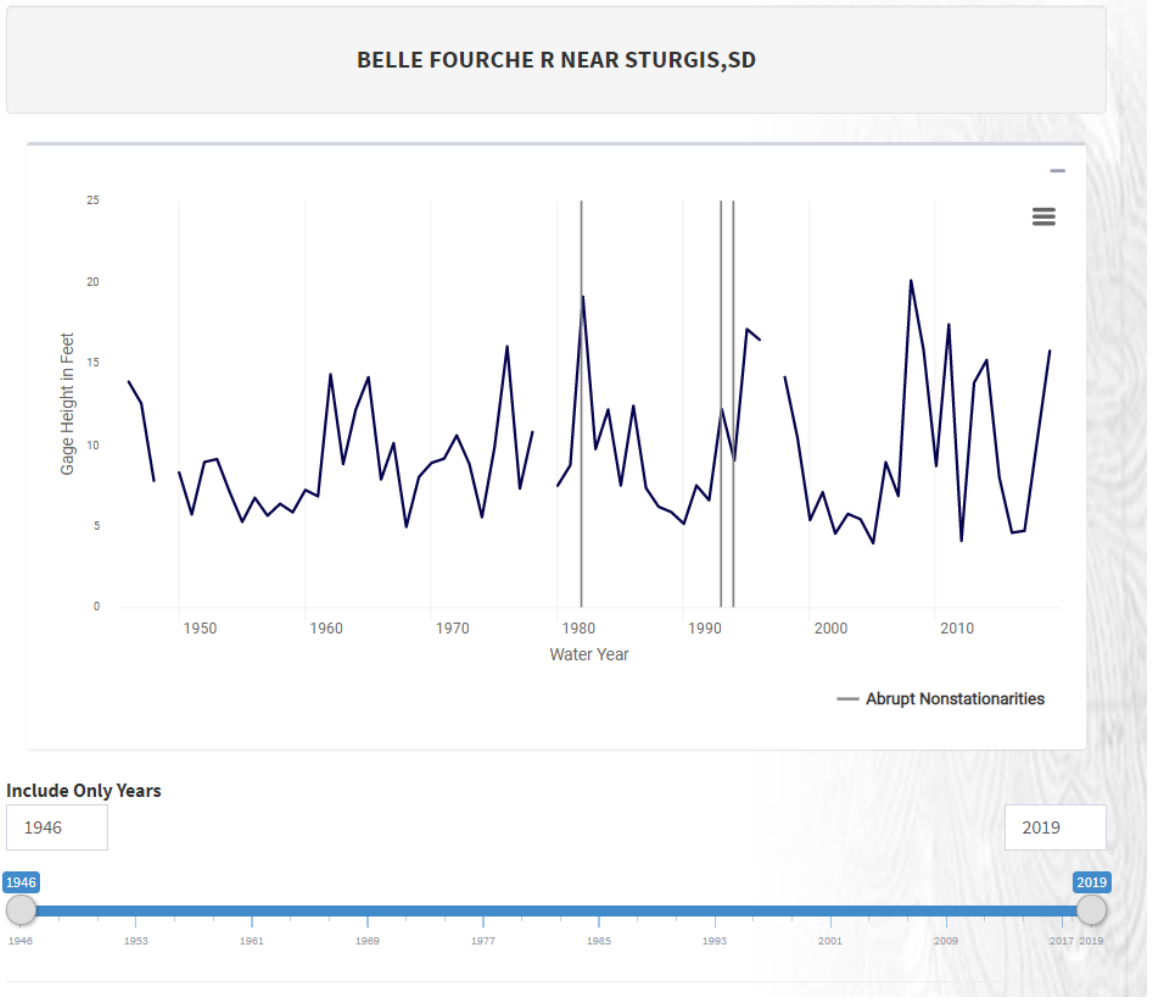


Figure 7.8.6. USGS Gage 06437000-Belle Fourche River Near Sturgis, SD plot of gage/stage height (ft.) for the period 1946-2020. Three non-stationarities were detected: the Distribution, Energy Divisive Method in 1982, and for Variance: Lombard Mood (1993) and Mood (1994). Data is missing for 1978-1980, and 1996-1998.





Figure 7.8.7. USGS Gage 06437000-Belle Fourche River Near Sturgis, SD, plot of statistical tests for gage/stage height (ft.) 1946-2020. The period of record has missing data points 1978-1980 and 1996-1998. Three NSDs detected: Distribution: Energy Divisive Method, 1982 (Peak Flow) Gage height 19.1 ft., and for Variance: Lombard Mood (12.18 ft.) in 1993 and Mood, (9.01) ft in 1994.

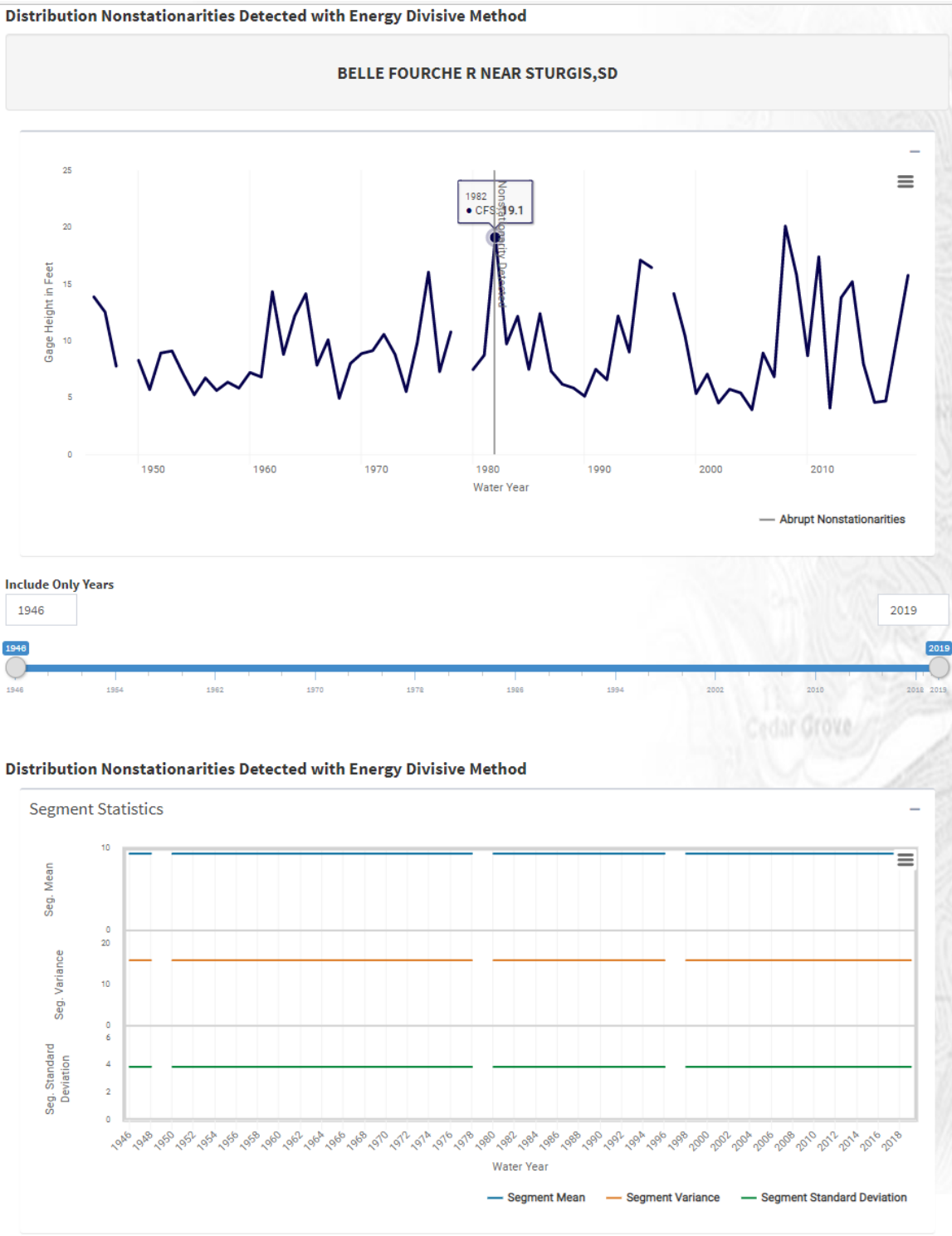
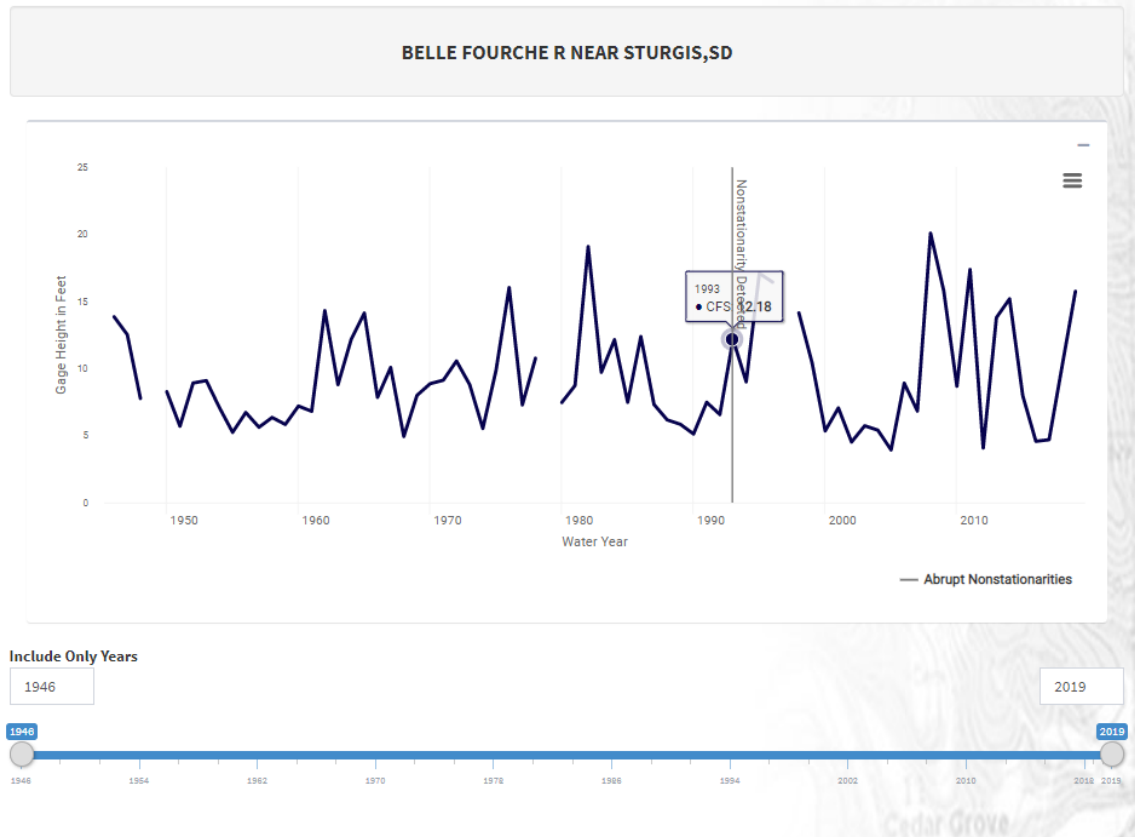


Figure 7.8.8. USGS Gage 06437000-Belle Fourche River Near Sturgis, SD plot of gage/stage height (ft.) 1946-2020. Distribution non-stationarities detected with the Energy Divisive Method in 1992.

Variance Nonstationarities Detected with Lombard Mood



Variance Nonstationarities Detected with Lombard Mood

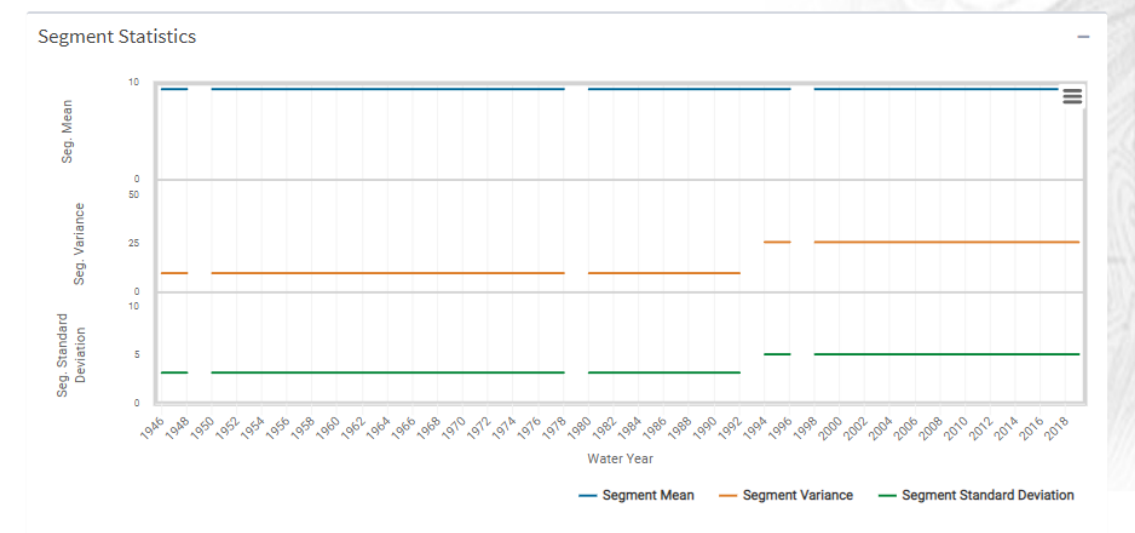


Figure 7.8.9. USGS Gage 06437000-Belle Fourche River Near Sturgis, SD plot of gage/stage height (ft.) non-stationarities identified during the years 1946-2020. Variance: Lombard Mood 1993 (12.18 ft.) (during a period with low-flow conditions) and Variance: Mood in 1994 (9.01 ft). Low-flow conditions recorded in 1989-1990.

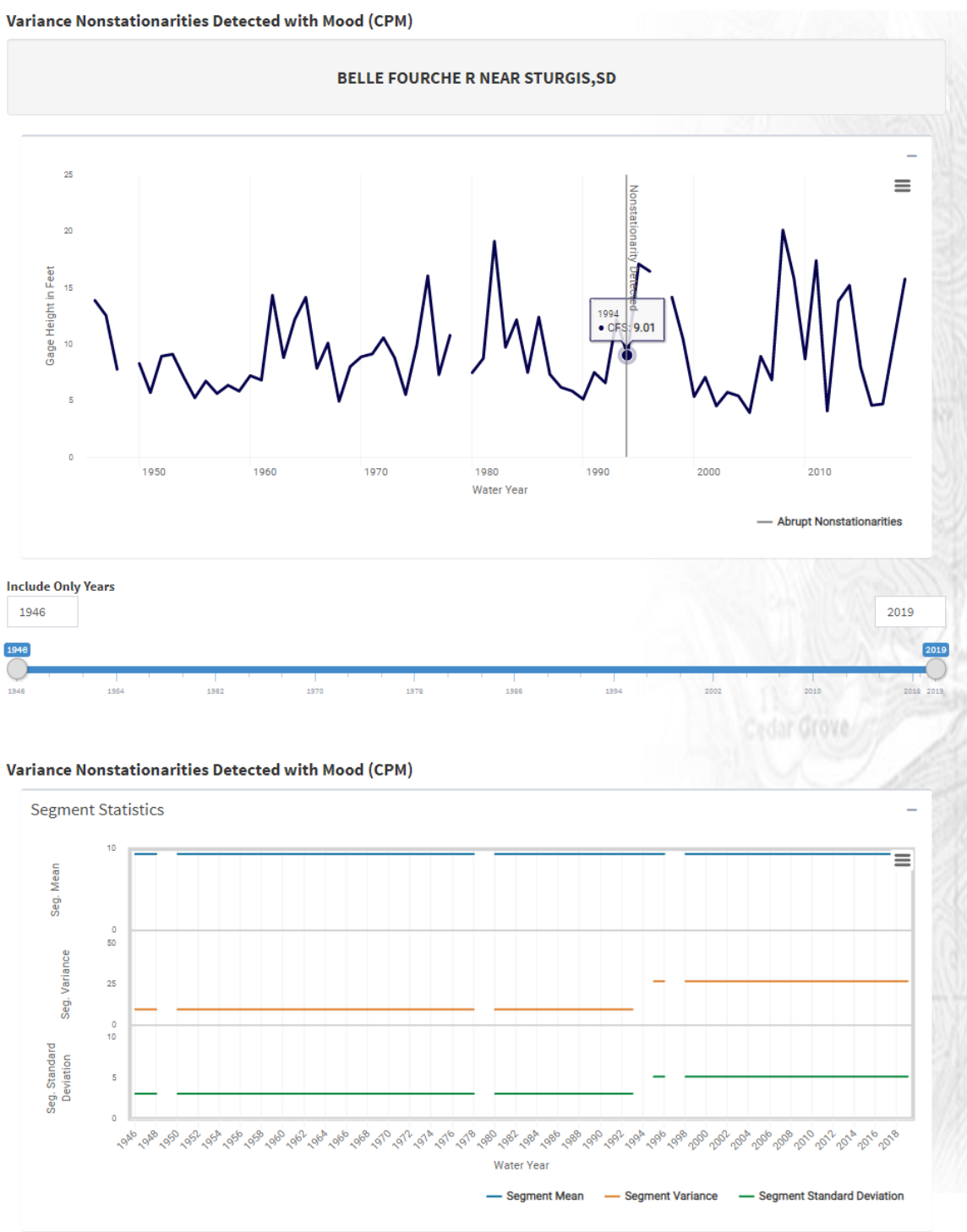


Figure 7.8.10. USGS Gage 06437000-Belle Fourche River Near Sturgis, SD plot of gage/stage height (ft.) the Variance Mood non-stationarity identified in 1994 for the period of record 1946-2020. Missing data occurs at: 1996-1998.

### Plot of Maximum Annual Flow/Height with Slope Fits (Traditional and Sen's Slope)

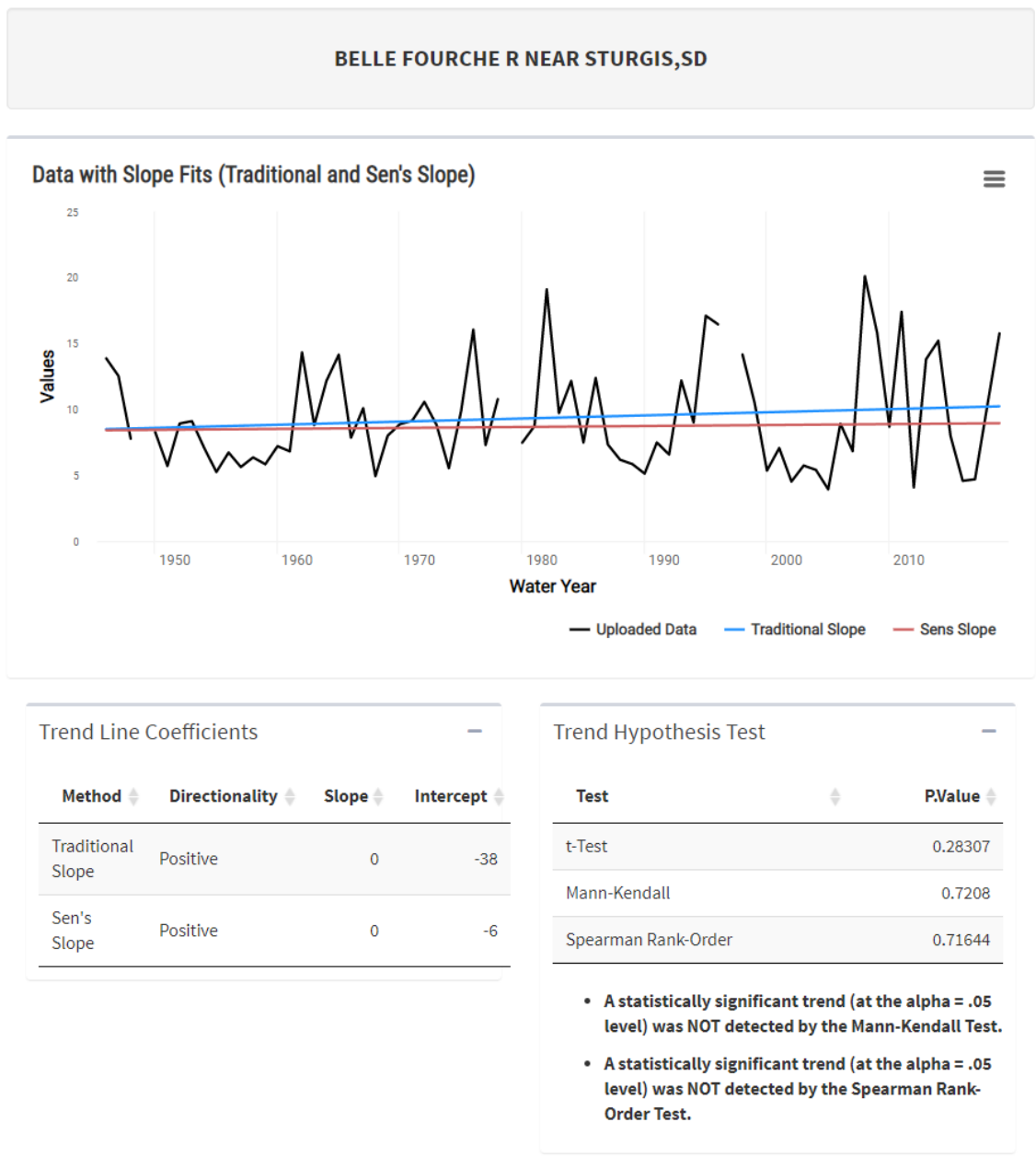


Figure 7.8.11. USGS Gage 06437000-Belle Fourche River Near Sturgis, plot of gage/stage height (ft.) with slope fits (Traditional and Sen's Slope). No statistically significant trends (at the alpha = 0.05 level) were detected using the Mann-Kendall or the Spearman Rank-Order tests for the period 1946-2020.

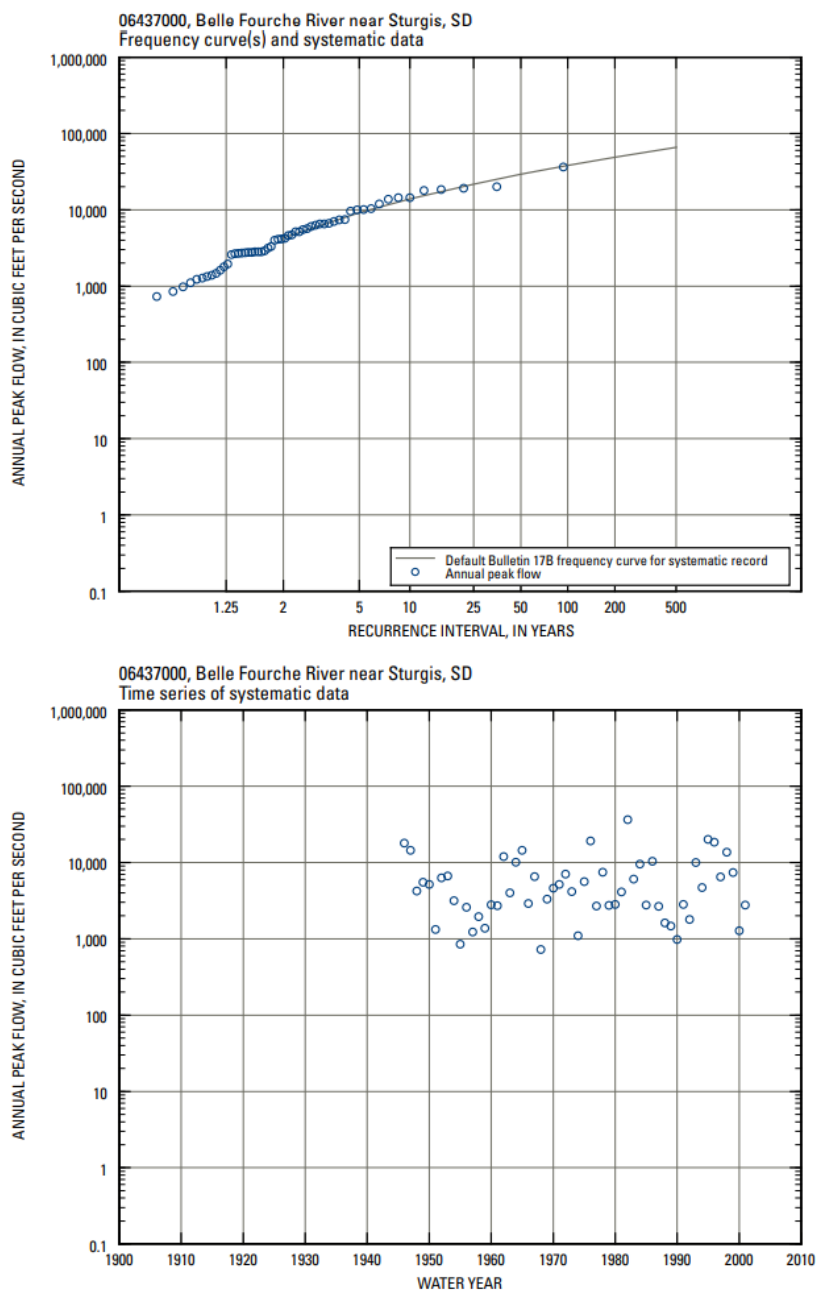


Figure 7.8.12. Peak-flow information for USGS gage station 06437000, Belle Fourche River near Sturgis, SD (Sando et al., 2008).

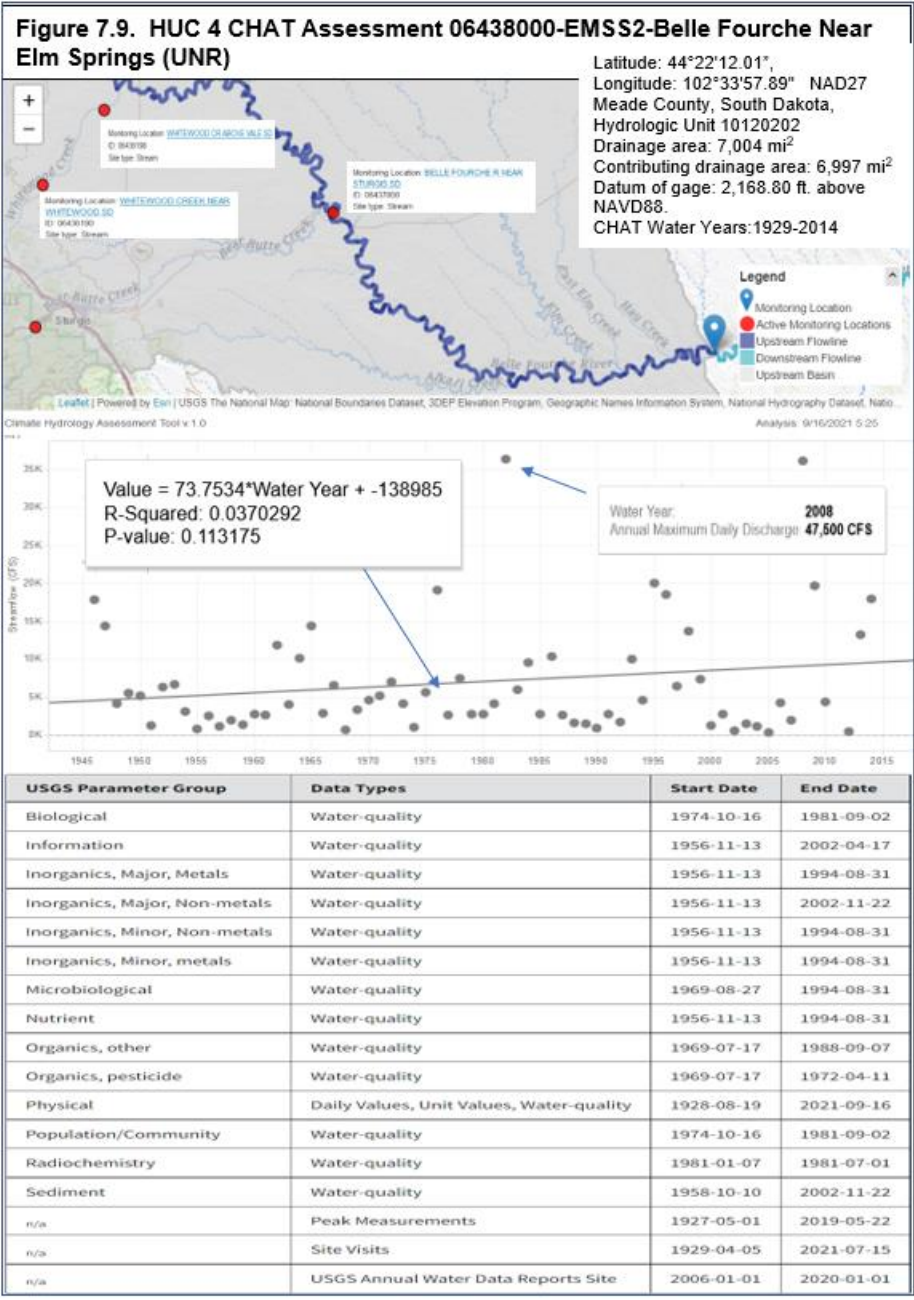


Figure 7.9. \*06438000 Belle Fourche River Near Elm Springs, SD, \*missing data points, 1932-1934.

Nonstationarities Detected using Maximum Annual Flow

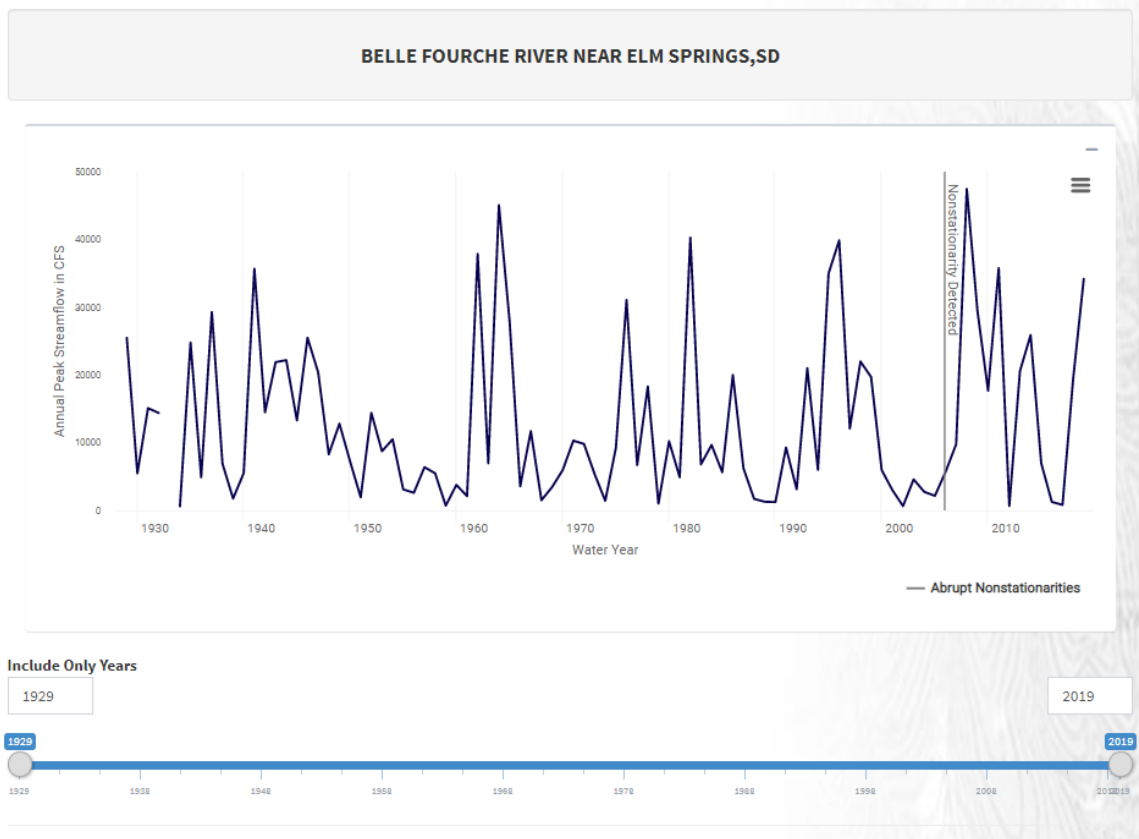


Figure 7.9.1. USGS Gage 06438000, Belle Fourche River Near Elm Springs, SD, non-stationarities identified for Instantaneous Peak Streamflow (IPS) using annual peak streamflow in cfs, for years 1929-2019 using NSD tool version 2.0. The Bayesian Changepoint Test was not applied as the assumption of normality was not met. A Variance: Lombard Mood non-stationarity was identified for the year 2006.





Figure 7.9.2. USGS Gage 06438000, Belle Fourche River Near Elm Springs, SD, plot of non-stationarity identified with the NSD tool identified for Instantaneous Peak Streamflow (IPS) using annual peak streamflow in cfs, for years 1929-2019 using NSD tool version 2.0.: Variance, Lombard Mood in 2006.

Plot of Maximum Annual Flow/Height with Slope Fits (Traditional and Sen's Slope)

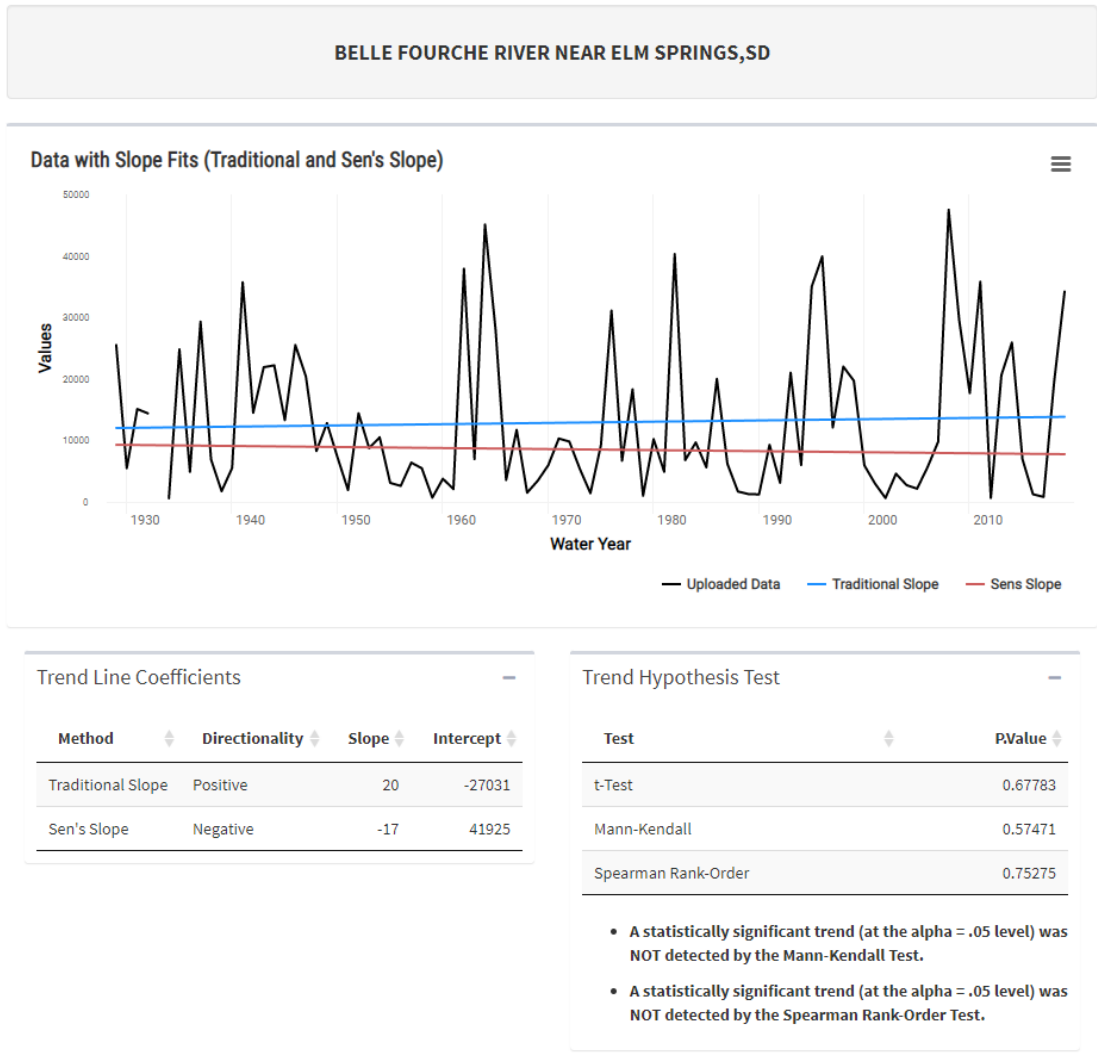


Figure 7.9.3. USGS Gage 06438000, Belle Fourche River Near Elm Springs, SD plot of maximum annual flow (cfs) with slope fits (Traditional and Sen's Slope). No statistically significant trends (at the alpha = 0.05 level) were detected using the Mann-Kendall or the Spearman Rank-Order tests for the period 1929-2019.

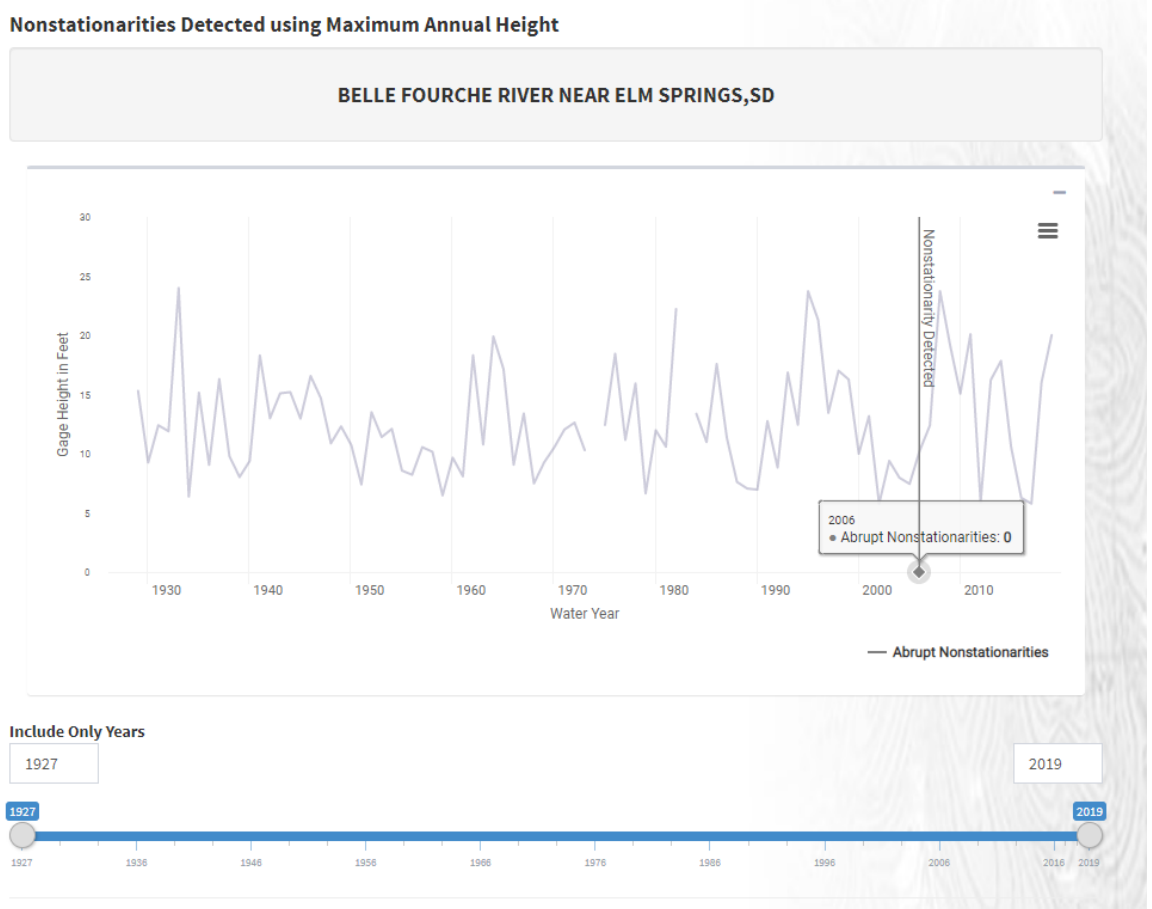


Figure 7.9.4. USGS Gage 06438000, Belle Fourche River Near Elm Springs, SD, one non-stationarity identified for gage/stage height (ft.) for years 1927-2019. A variance non stationarity was detected with the Lombard Mood method for the year 2006. The Bayesian Changepoint Test was not applied as the assumption of normality was not met.

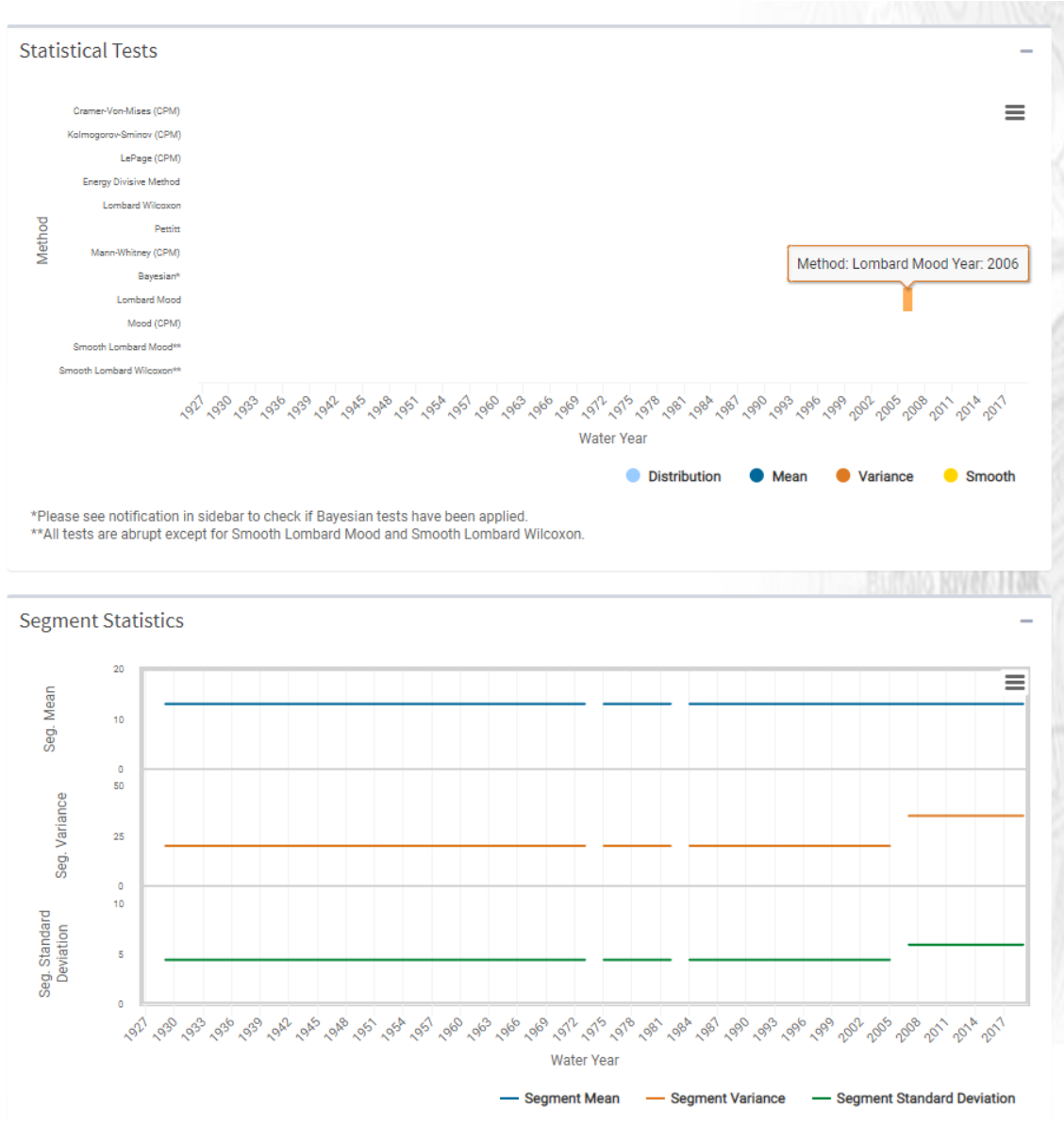
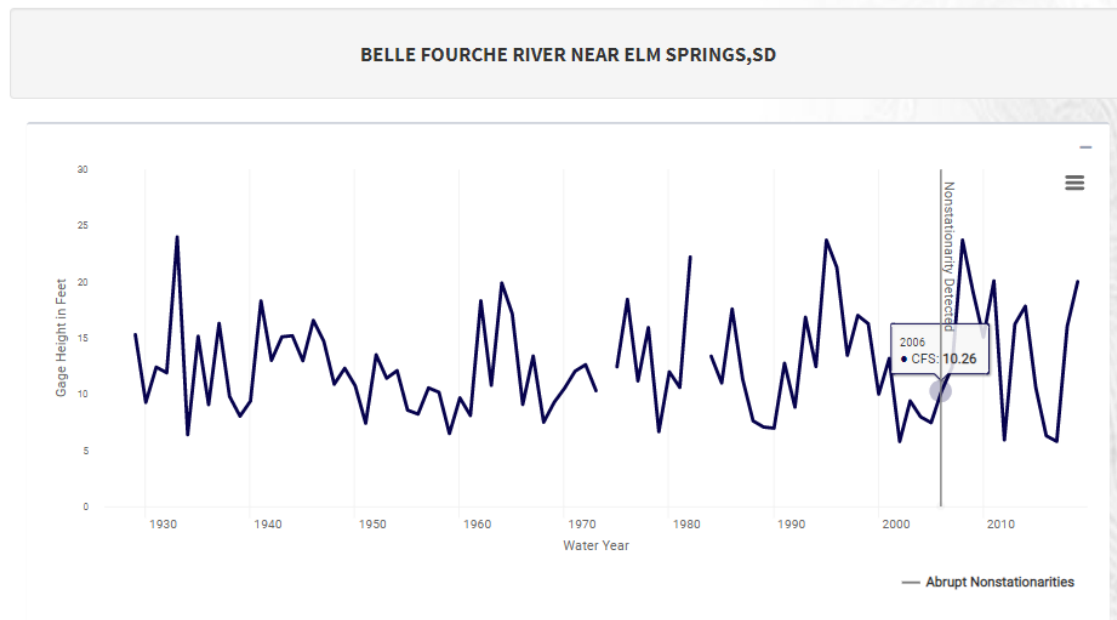
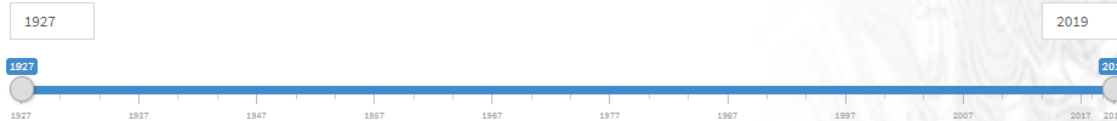


Figure 7.9.5. USGS Gage 06438000, Belle Fourche River Near Elm Springs, SD, the plot of non-stationarities identified for gage/stage height (ft.) for years 1927-2019. A variance non stationarity was detected with the Lombard Mood method for the year 2006.

Variance Nonstationarities Detected with Lombard Mood



Include Only Years



Variance Nonstationarities Detected with Lombard Mood

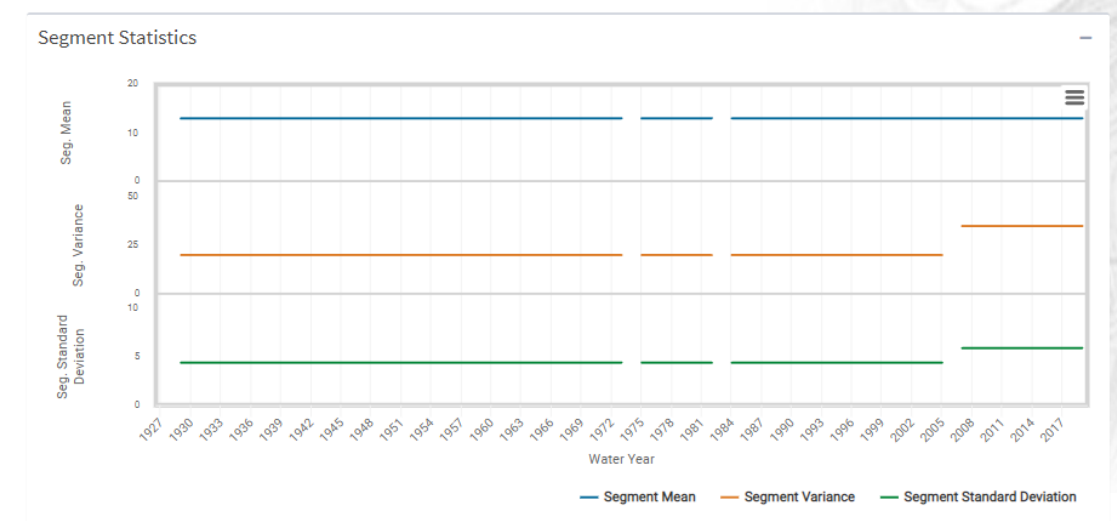
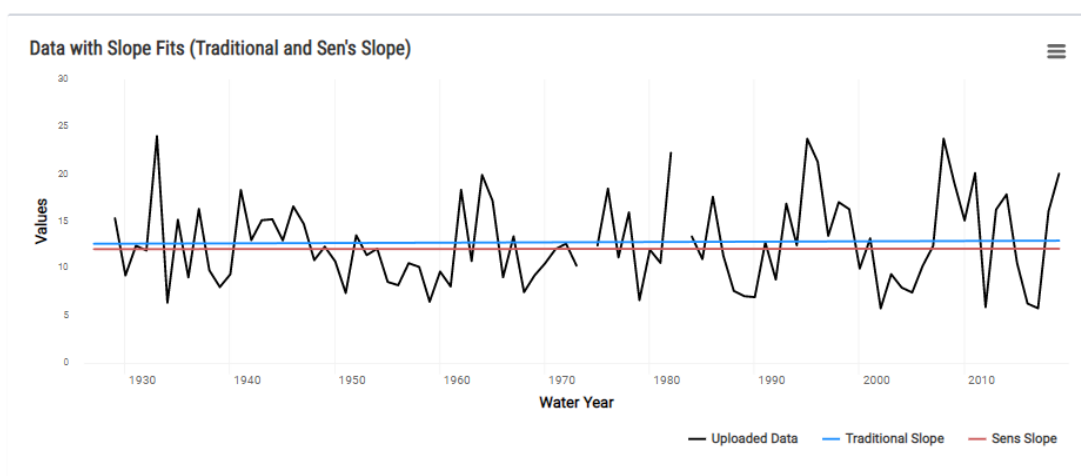


Figure 7.9.6. USGS Gage 06438000, Belle Fourche River Near Elm Springs, SD, USGS Gage 06438000, Belle Fourche River Near Elm Springs, SD, the plot of non-stationarities identified for gage/stage height (ft.) for years 1927-2019. A variance non stationarity was detected with the Lombard Mood method for the year 2006.

Plot of Maximum Annual Flow/Height with Slope Fits (Traditional and Sen's Slope)

BELLE FOURCHE RIVER NEAR ELM SPRINGS, SD



Trend Line Coefficients			
Method	Directionality	Slope	Intercept
Traditional Slope	Positive	0	6
Sen's Slope	Positive	0	11

Trend Hypothesis Test	
Test	PValue
t-Test	0.84827
Mann-Kendall	0.98054
Spearman Rank-Order	0.90207

- A statistically significant trend (at the alpha = .05 level) was NOT detected by the Mann-Kendall Test.
- A statistically significant trend (at the alpha = .05 level) was NOT detected by the Spearman Rank-Order Test.

Figure 7.9.7. USGS Gage 06438000, Belle Fourche River Near Elm Springs, SD, plot of stage/gage height (ft) with slope fits (Traditional and Sen's Slope). No statistically significant trends (at the alpha = 0.05 level) were detected using the Mann-Kendall or the Spearman Rank-Order tests for the period 1927-2019.

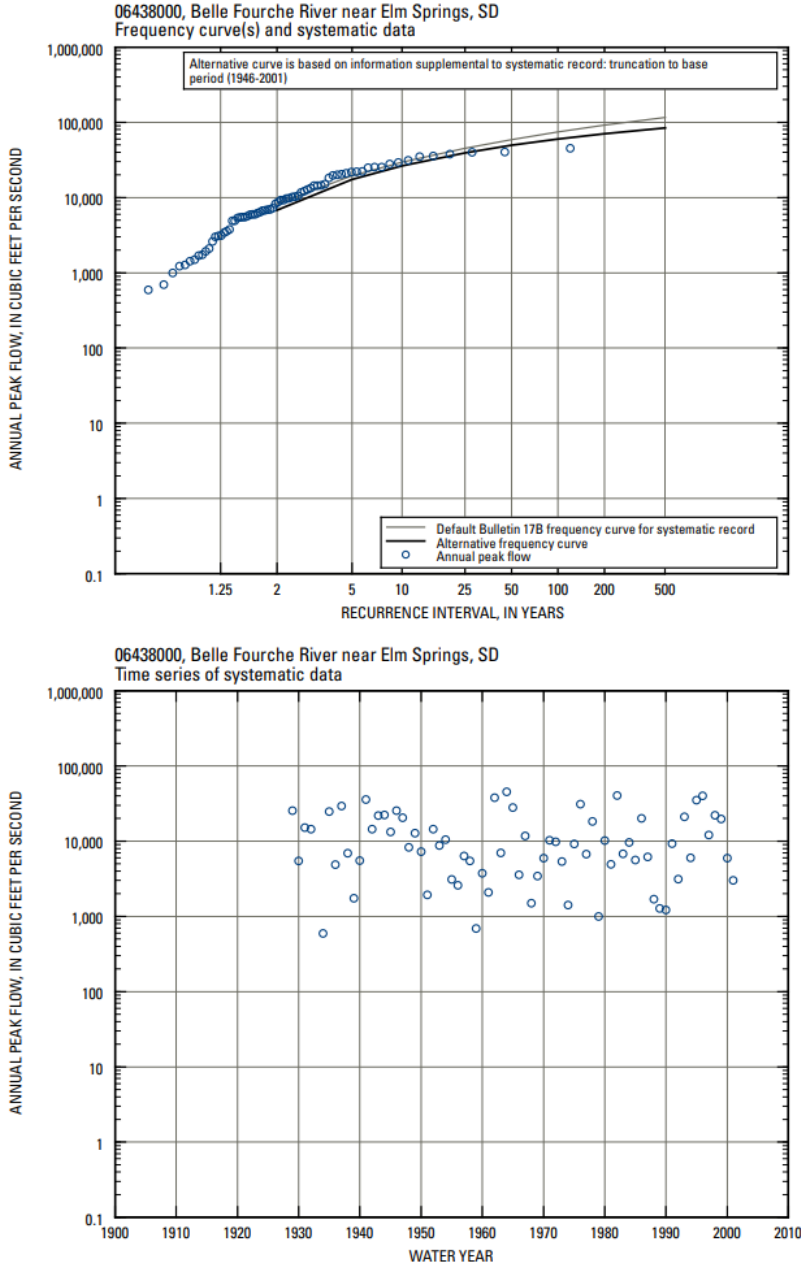
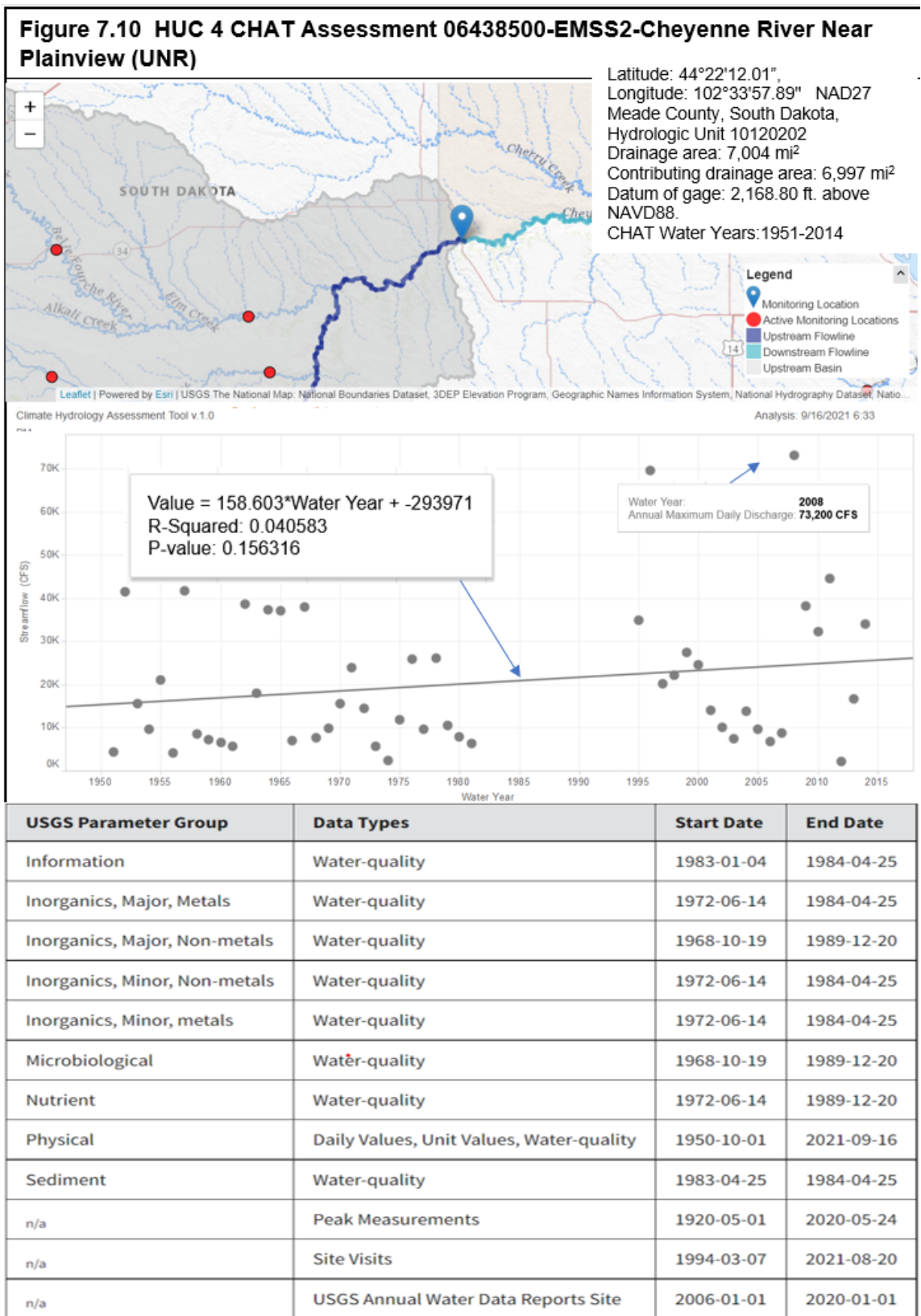


Figure 7.9.8. Peak-flow information for USGS gage station 06438000, Belle Fourche River near Elm Springs, SD (Sando et al., 2008).

Figure 7.10 USGS Gage 06438500 Cheyenne River Near Plainview, SD





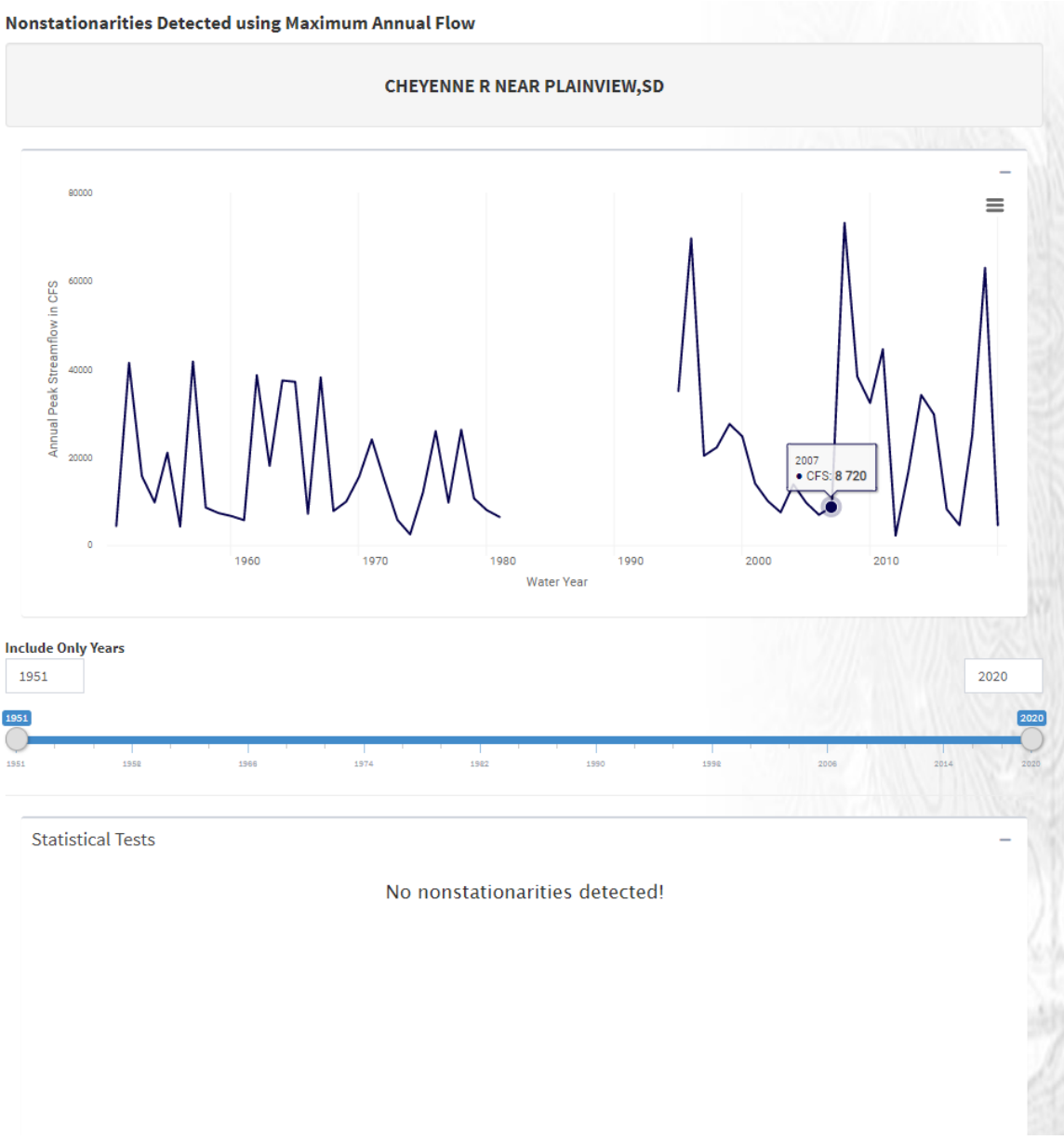


Figure 7.10.1 USGS Gage 06438500, Cheyenne River Near Plainview, SD, no non-stationarities identified for instantaneous peak streamflow for the period 1951-2020 using annual peak streamflow in cfs, using NSD tool version 2.0. The Bayesian Changepoint Test was not applied as the assumption of normality was not met. There is missing data at this gage from 1981-1995.

Plot of Maximum Annual Flow/Height with Slope Fits (Traditional and Sen's Slope)

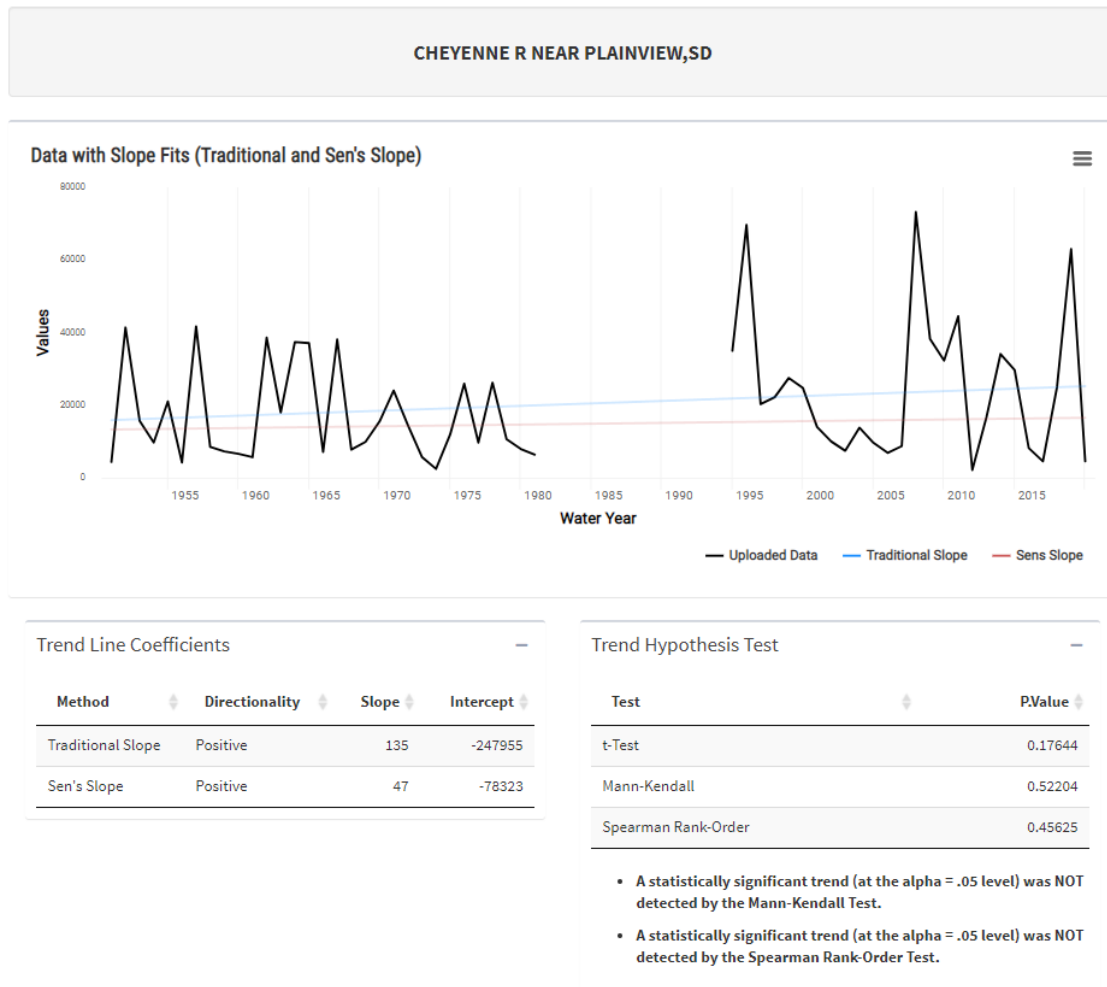


Figure 7.10.2 USGS Gage 06438500, Cheyenne River Near Plainview, SD, plot of maximum annual flow (cfs) with slope fits (Traditional and Sen’s Slope). No statistically significant trends (at the alpha = 0.05 level) were detected using the Mann-Kendall or the Spearman Rank-Order tests for the period 1951-2020. There is missing data at this gage from 1981-1995.

### Nonstationarities Detected using Maximum Annual Height

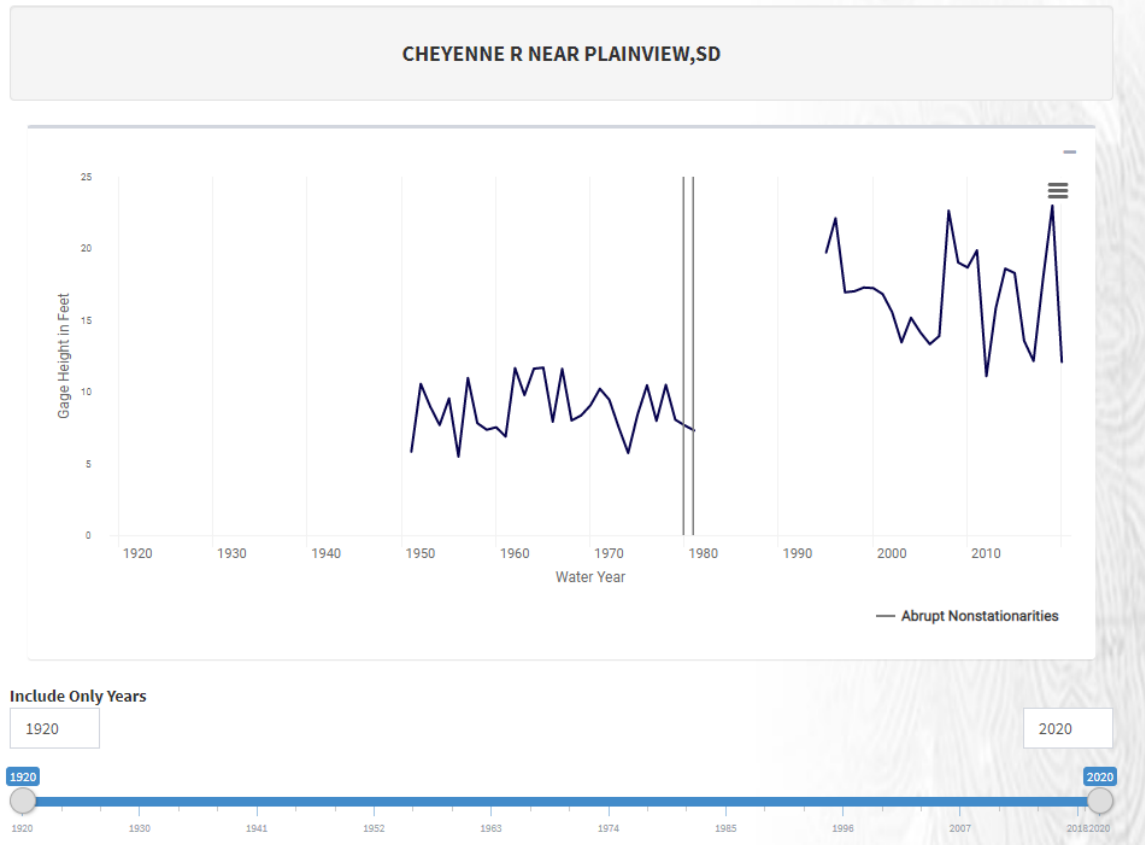


Figure 7.10.3 USGS Gage 06438500, Cheyenne River Near Plainview, SD, non-stationarities identified for gage/stage height (ft.) for years 1920-2020. The gage has missing data from 1981-1995 and as a result has multiple non-stationarities. The Bayesian Changepoint Test was not applied as the assumption of normality was not met.

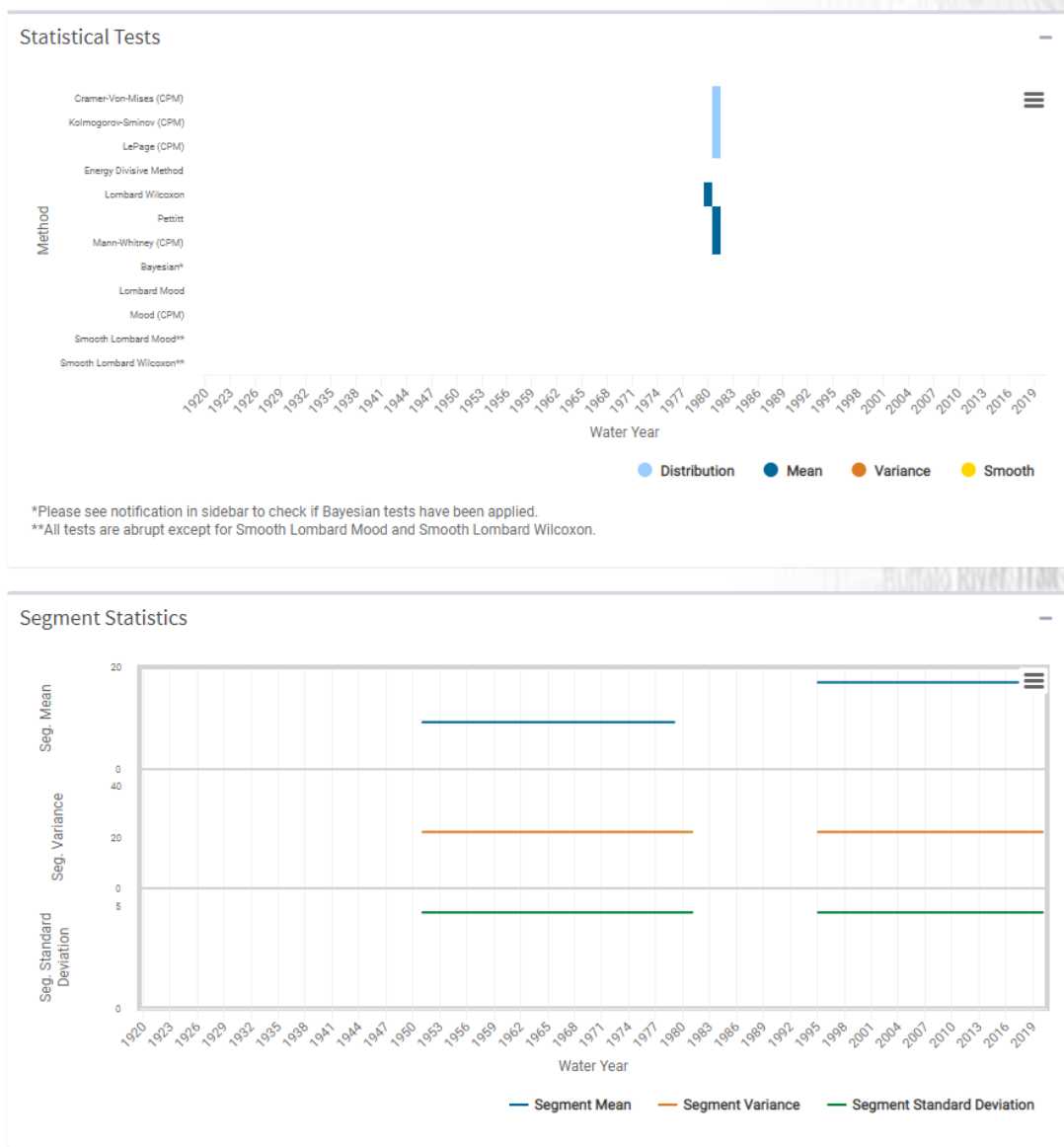


Figure 7.10.3 USGS Gage 06438500, Cheyenne River Near Plainview, SD. The gage has missing data from 1981-1995 and as a result has multiple non-stationarities.

Plot of Maximum Annual Flow/Height with Slope Fits (Traditional and Sen's Slope)

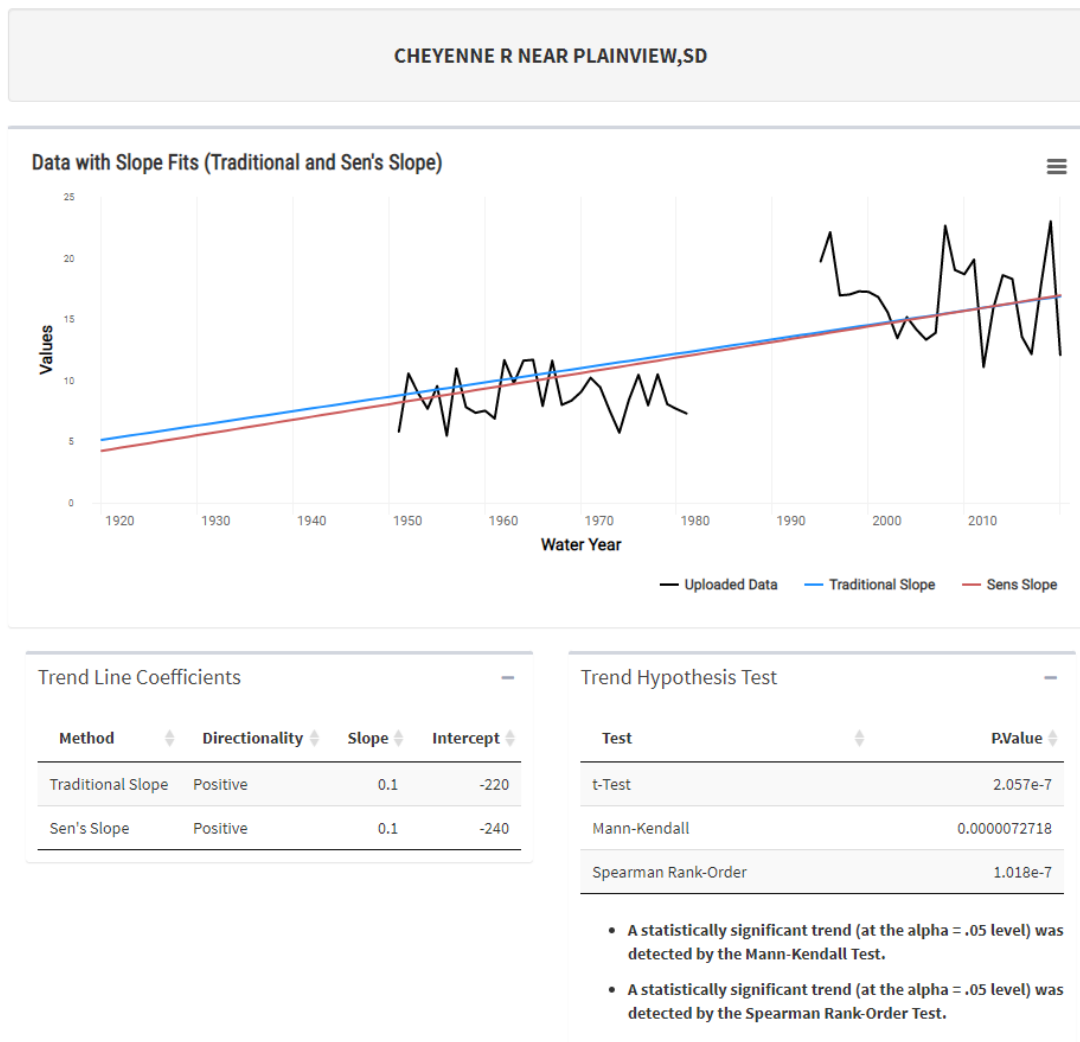


Figure 7.10.4 USGS Gage 06438500, Cheyenne River Near Plainview, SD, plot of gage/stage height (ft.) with slope fits (Traditional and Sen's Slope). Statistically significant trends (at the alpha = 0.05 level) were detected using the Mann-Kendall or the Spearman Rank-Order tests for the period 1951-2020. Data was missing from 1981-1995.

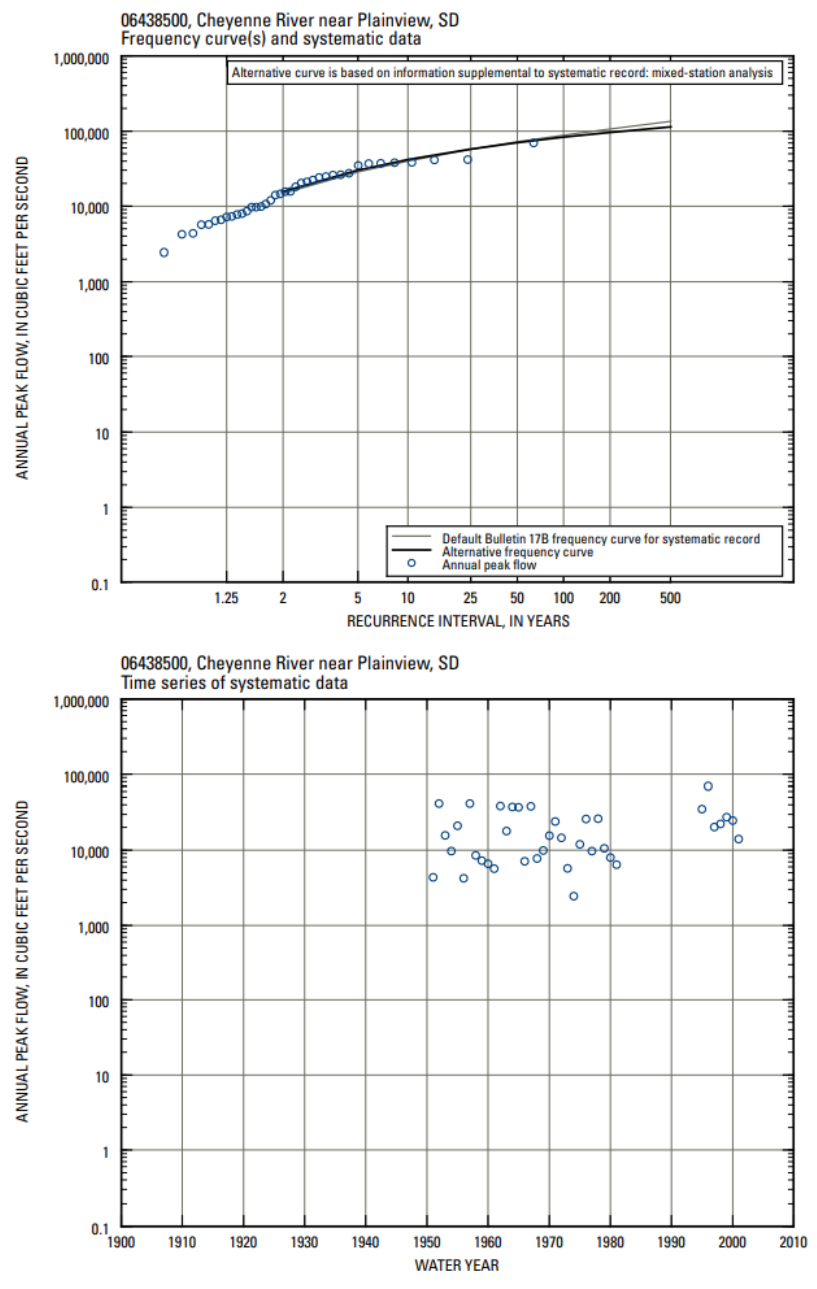
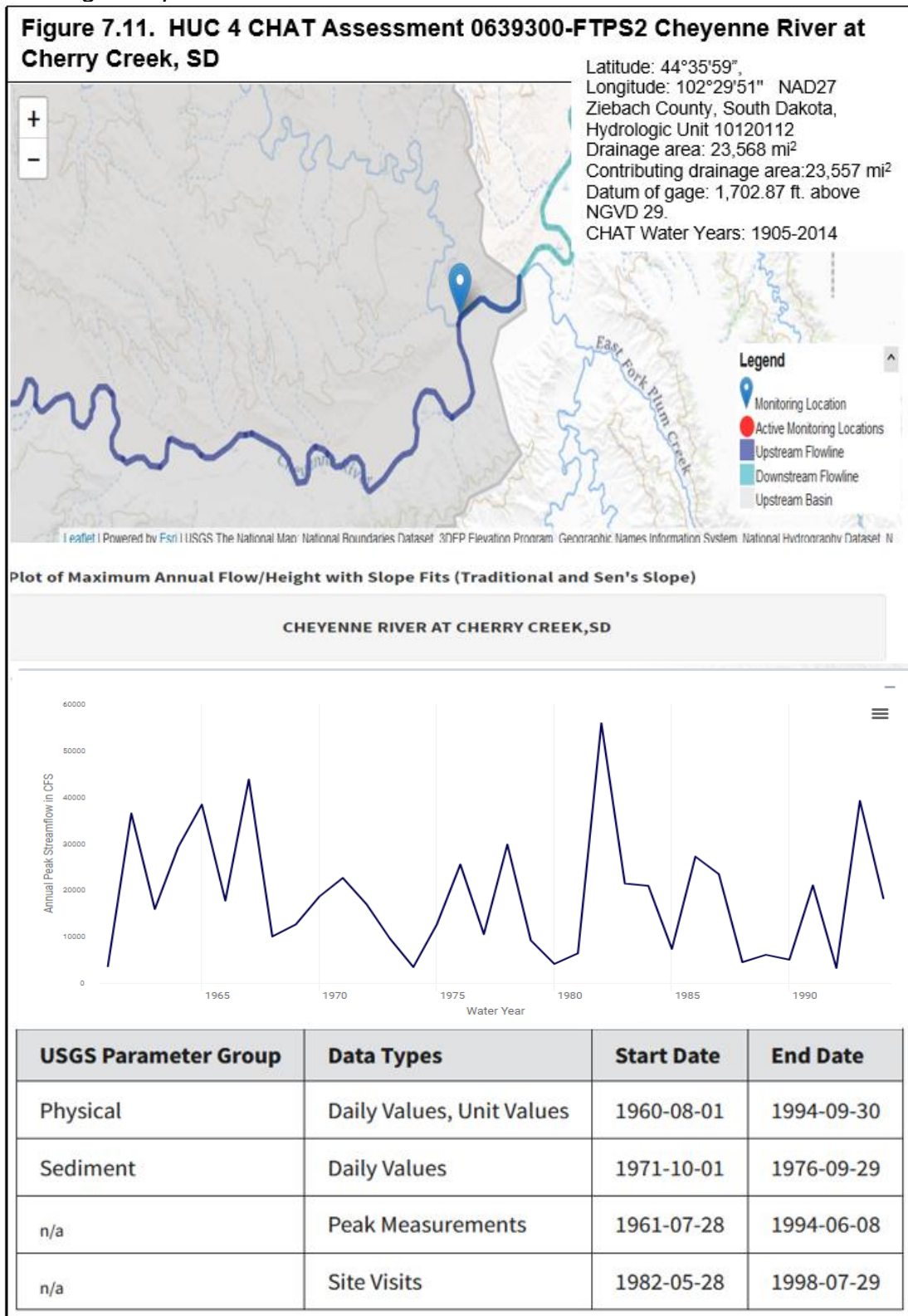


Figure 7.10.5. Peak-flow information for USGS gage station 06438500, Cheyenne River near Plainview, SD (from Sando et al., 2008).

**Figure 7.11 06439300 Cheyenne River at Cherry Creek**  
*\*missing data points 1981-1995*



### Nonstationarities Detected using Maximum Annual Flow

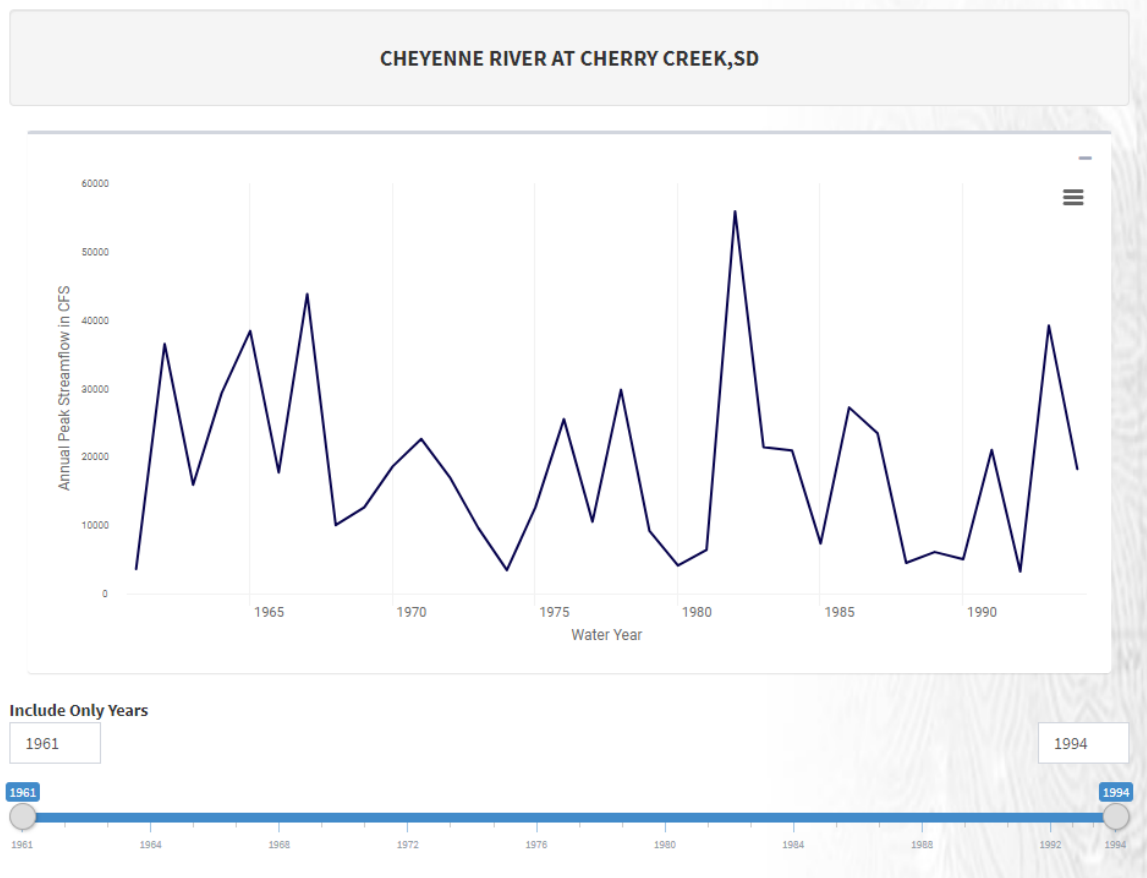


Figure 7.11.1. USGS Gage 0639300 Cheyenne River at Cherry Creek, SD, Instantaneous Peak Streamflow (IPS) using annual peak streamflow in cfs, for years 1961-1994 using NSD tool version 2.0. The Bayesian Change point Test was not applied as the assumption of normality was not met. There was not a sufficient dataset to be able to test for non-stationarity.



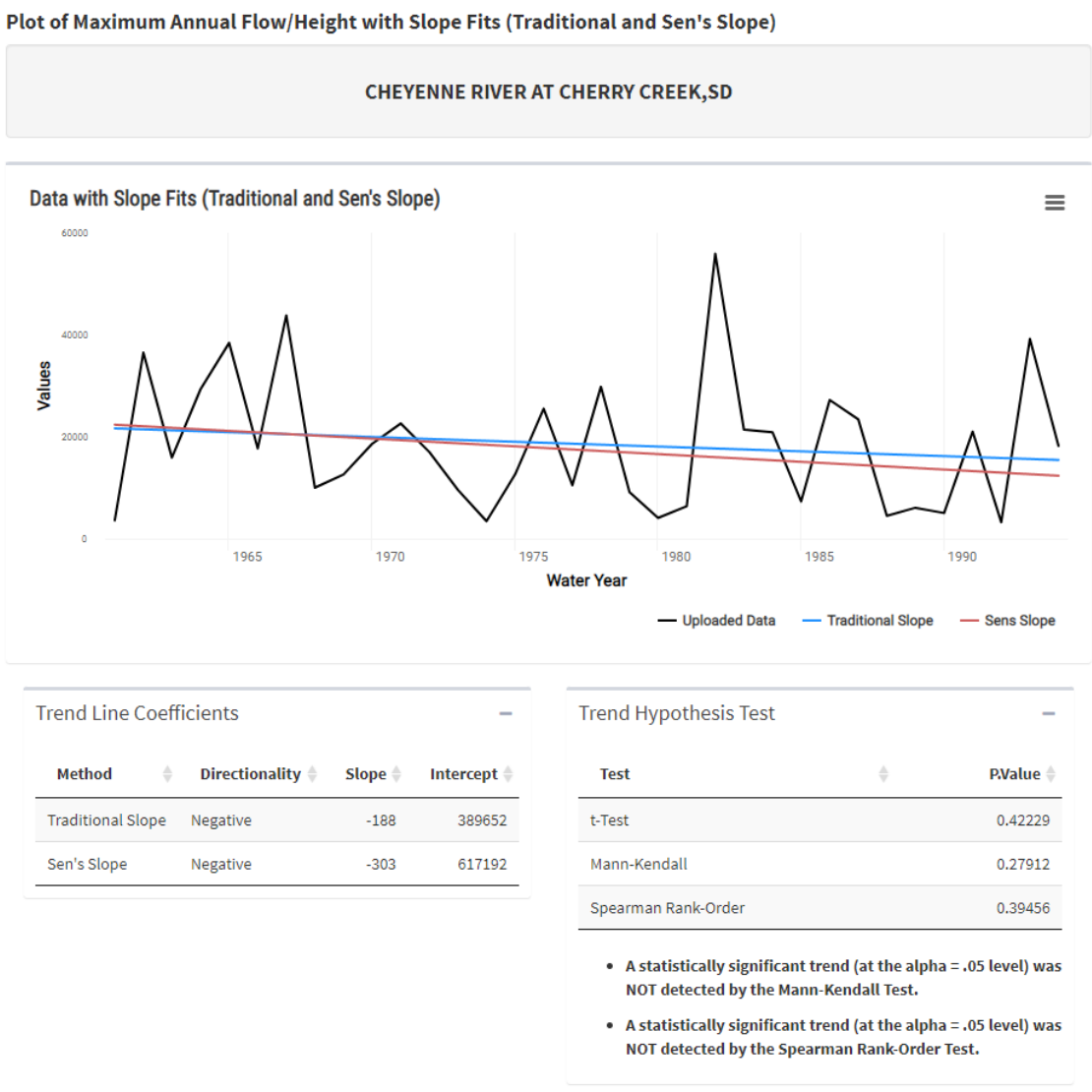


Figure 7.11.2. USGS Gage 0639300 Cheyenne River at Cherry Creek, SD, plot of maximum annual flow (cfs) with slope fits (Traditional and Sen's Slope). No statistically significant trends (at the alpha = 0.05 level) were detected using the Mann-Kendall or the Spearman Rank-Order tests for the period 1961-1994.

Plot of Maximum Annual Flow/Height with Slope Fits (Traditional and Sen's Slope)

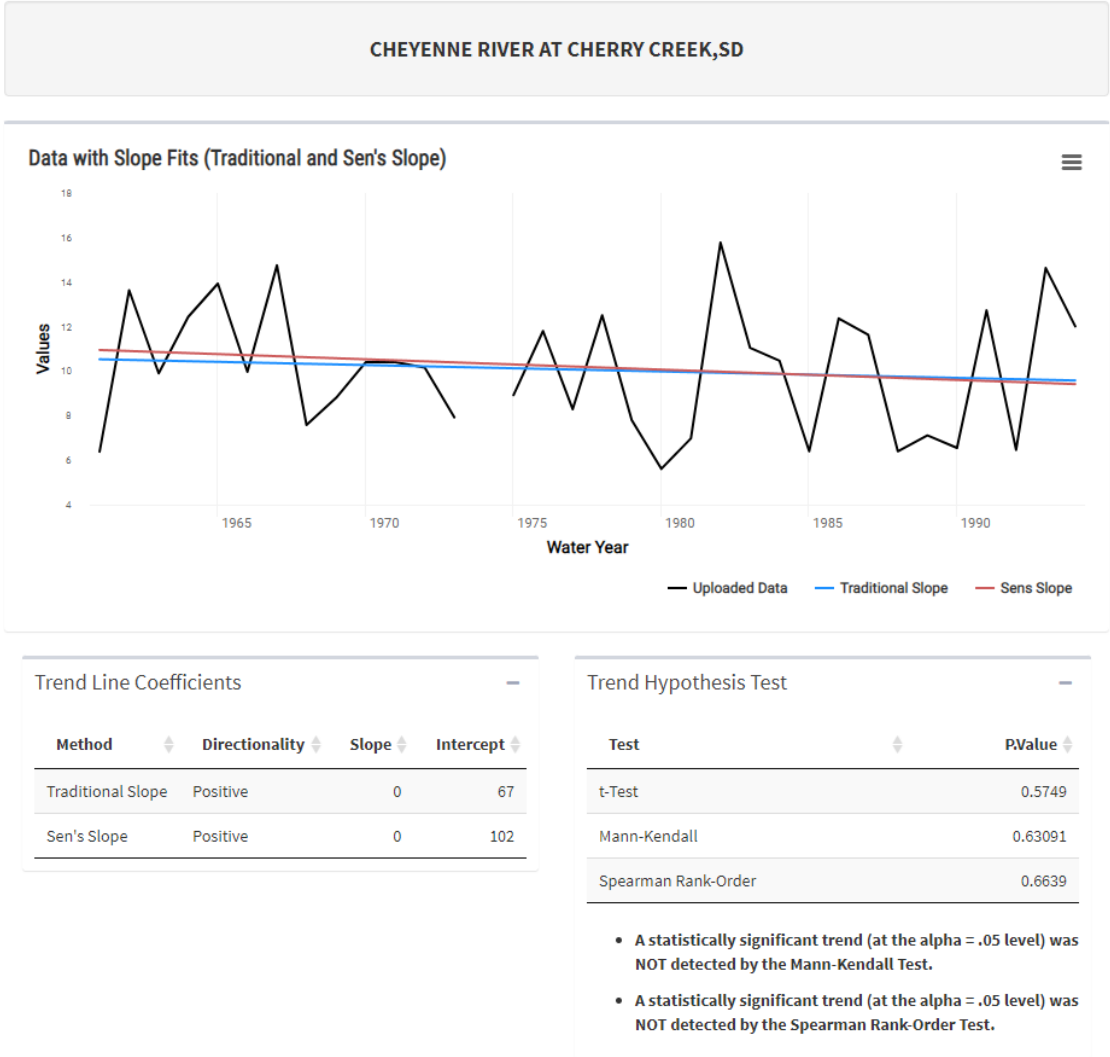


Figure 7.11.3. USGS Gage 0639300 Cheyenne River at Cherry Creek, SD, plot of gage/stage height (ft.) with slope fits (Traditional and Sen's Slope). No statistically significant trends (at the alpha = 0.05 level) were detected using the Mann-Kendall or the Spearman Rank-Order tests for the period 1961-1994. Data was missing from 1973-1979.

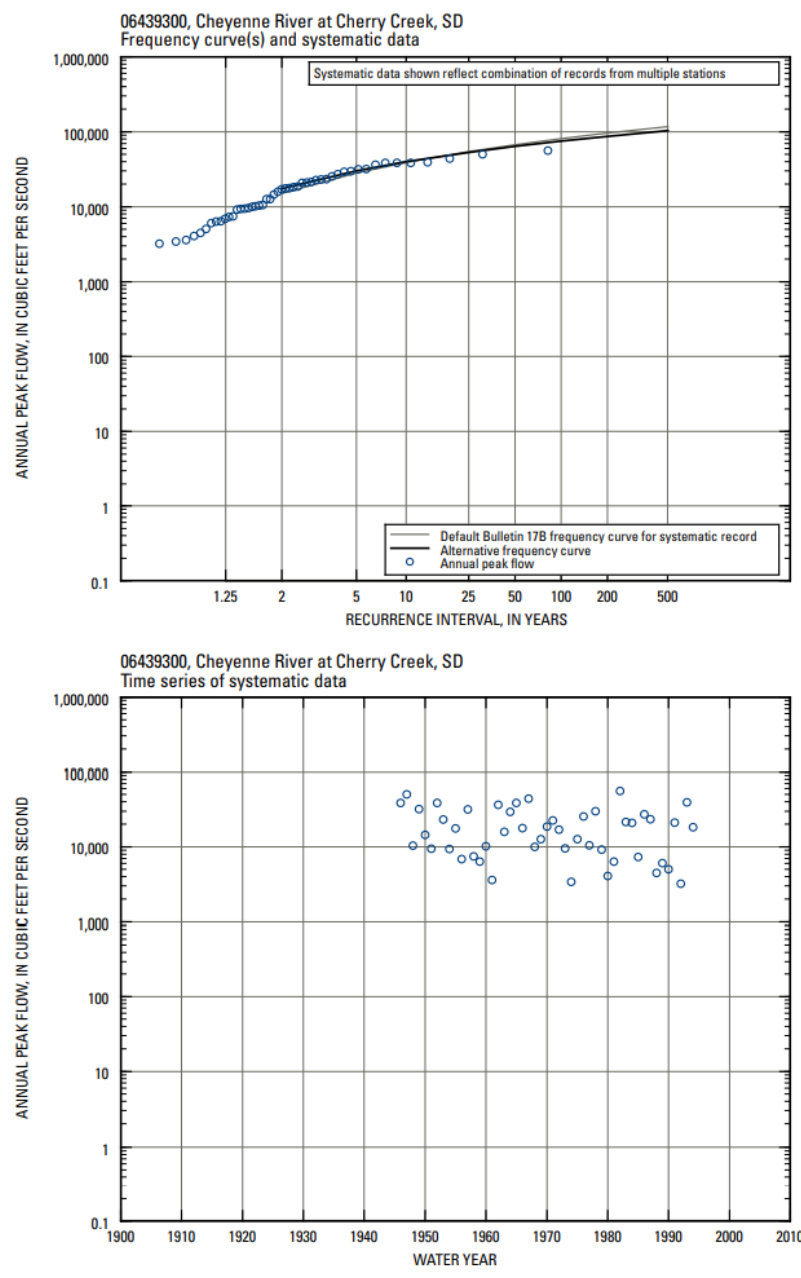


Figure 7.11.4. Peak-flow information for station 06439300, Cheyenne River at Cherry Creek, SD (Sando et al., 2008).

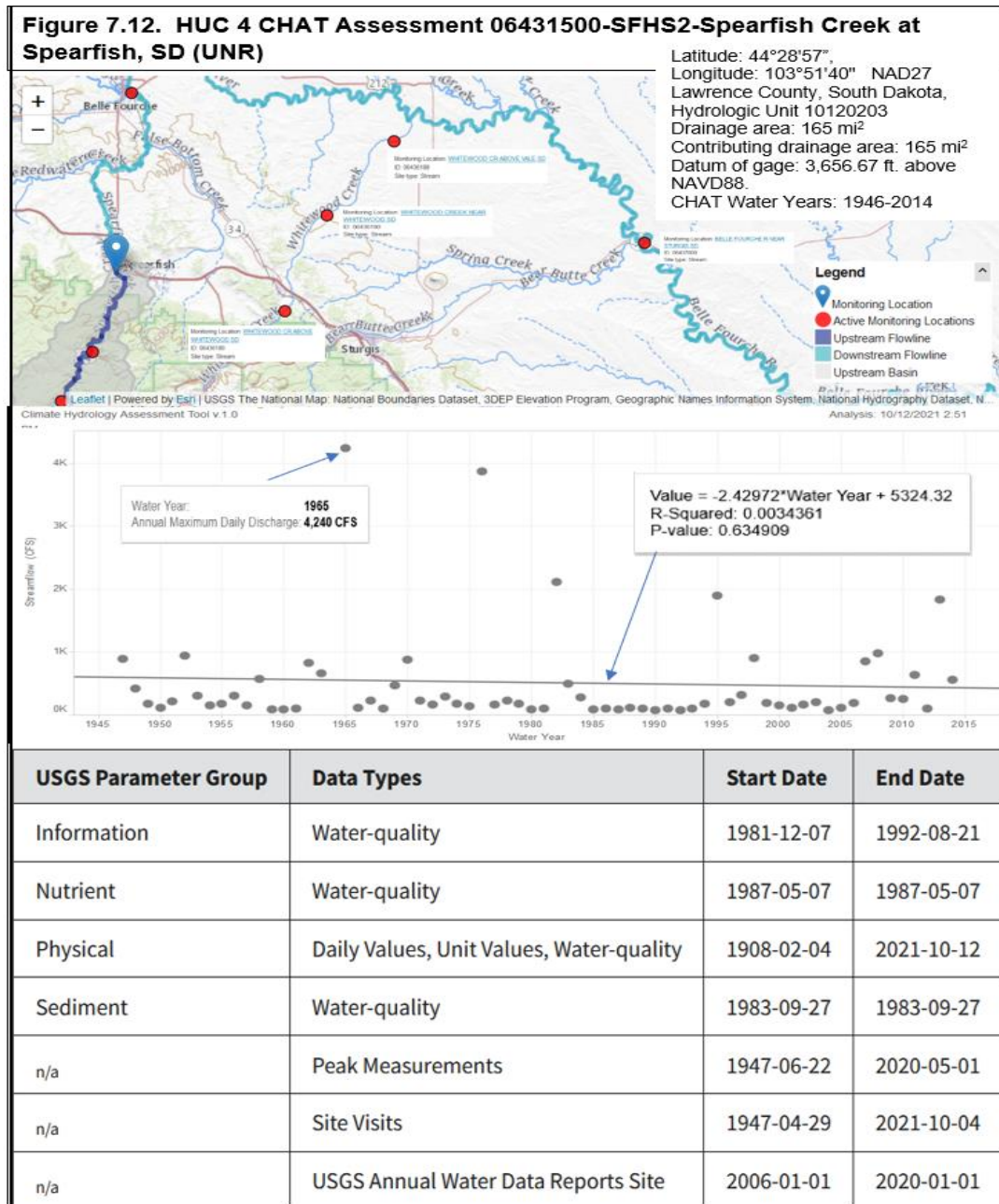


Figure 7.12. USGS Gage 06431500 Spearfish Creek at Spearfish, SD. Basin located west of Whitewood Creek. This area was not impacted by mine tailings. Gages evaluated in Western South Dakota. Initial evaluation of trends in streams in Western South Dakota and minimal diversions or regulations suggested they may be representative of climatic trends.

## Nonstationarities Detected using Maximum Annual Height

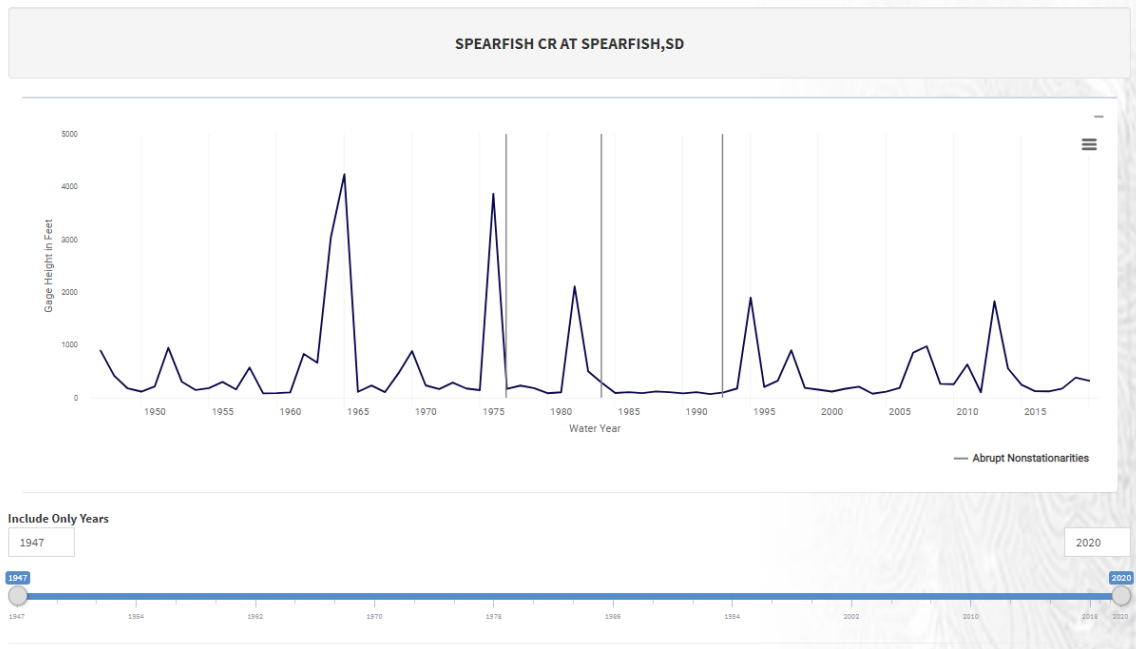


Figure 7.12.1. USGS Gage 06431500 Spearfish Creek at Spearfish SD, plot of maximum annual flow (cfs) using annual peak streamflow in cfs, for years 1947-2020 using NSD tool version 2.0. The Bayesian Changepoint Test was not applied as the assumption of normality was not met. Three non-stationarities were detected: Distribution: Energy Divisive Method,1977; Cramer-Von-Misses in 1984,1993 and Mean: Mann-Whitney in 1984,1993. Flow from this stream is regulated.

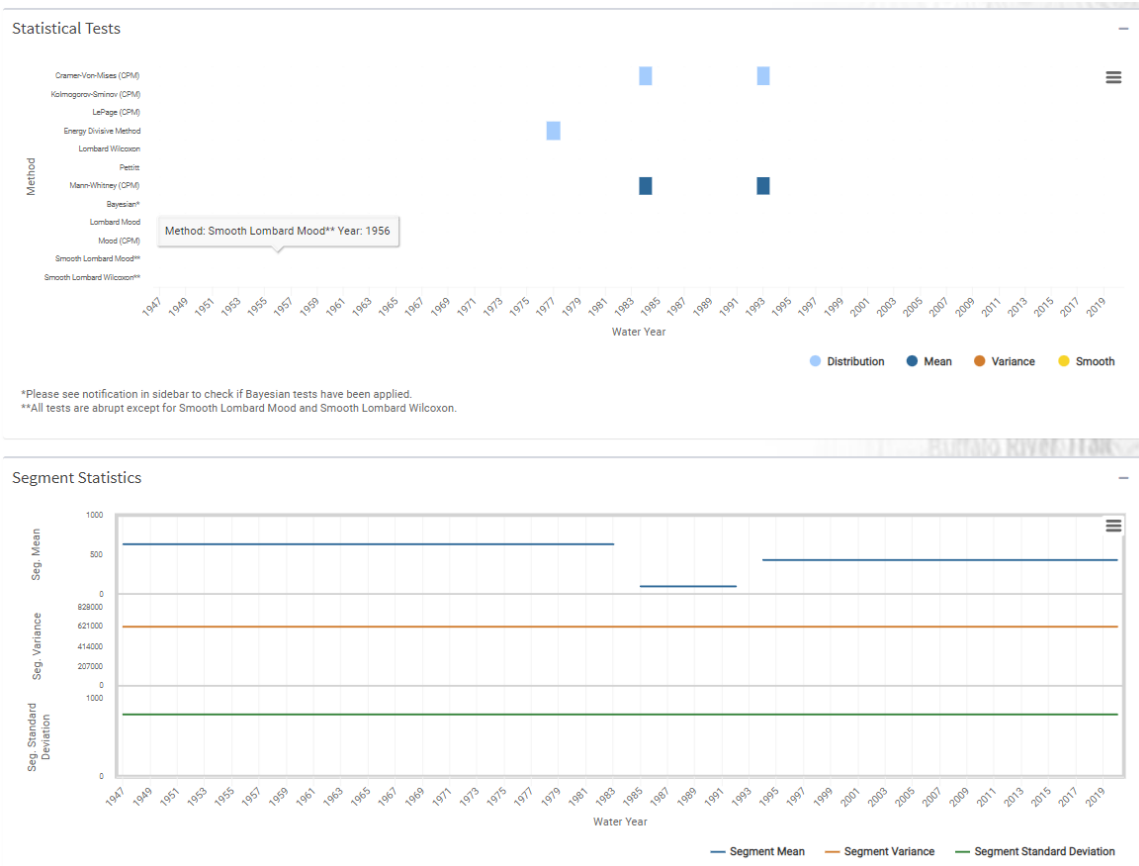


Figure 7.12.2. USGS Gage 06431500 Spearfish Creek at Spearfish SD, plot of maximum annual flow (cfs) using annual peak streamflow in cfs, for years 1947-2020 using NSD tool version 2.0. Three non-stationarities were detected: Distribution: Energy Divisive Method,1977; Cramer-Von-Misses in 1984,1993 and Mean: Mann-Whitney in 1984,1993. Flow from this stream is regulated.

## Plot of Maximum Annual Flow/Height with Slope Fits (Traditional and Sen's Slope)

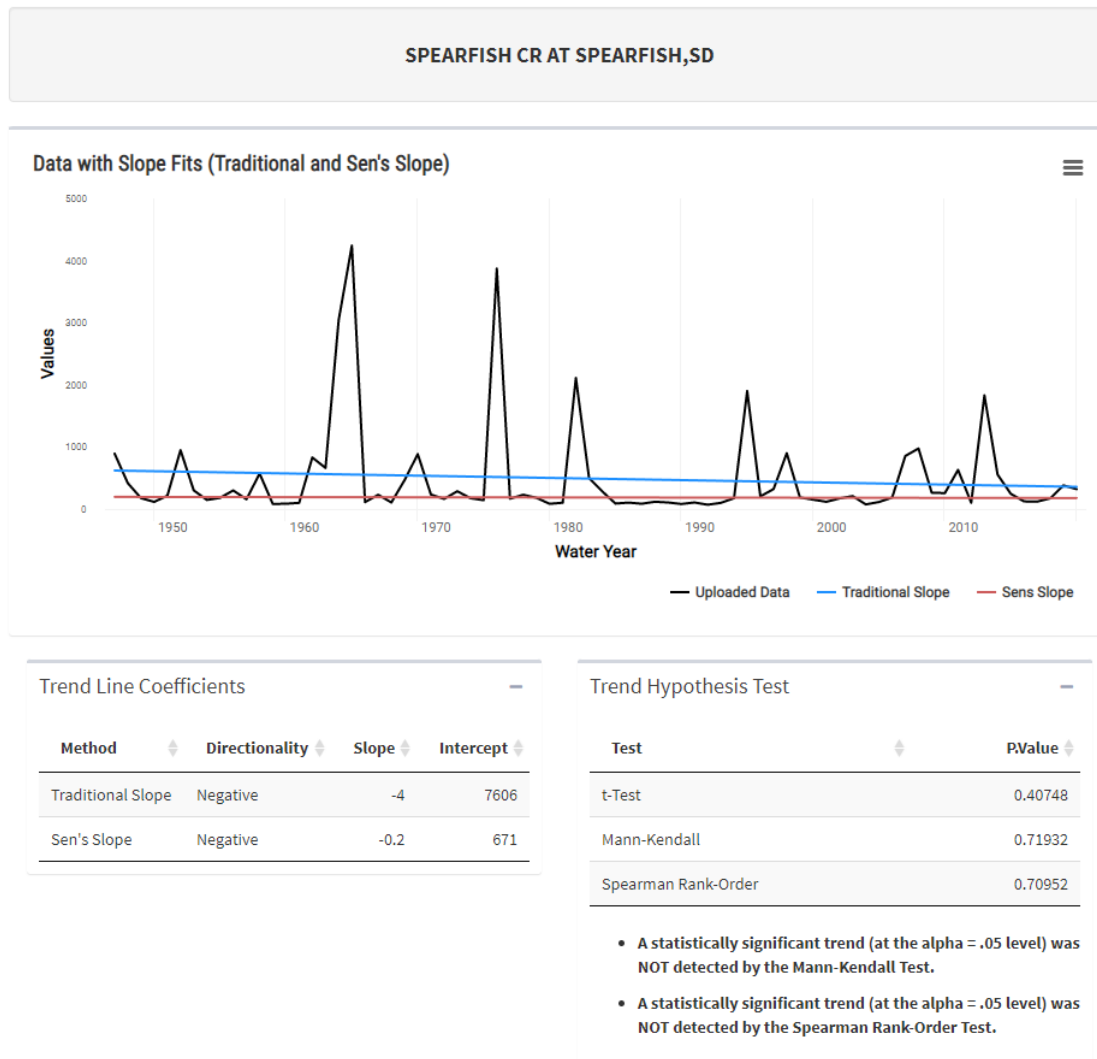


Figure 7.12.3. USGS Gage 06431500 Spearfish Creek at Spearfish, plot of maximum annual flow (cfs) with slope fits (Traditional and Sen's Slope). No statistically significant trends (at the alpha = 0.05 level) were detected using the Mann-Kendall or the Spearman Rank-Order tests for the period 1947-2020.

Nonstationarities Detected using Maximum Annual Height

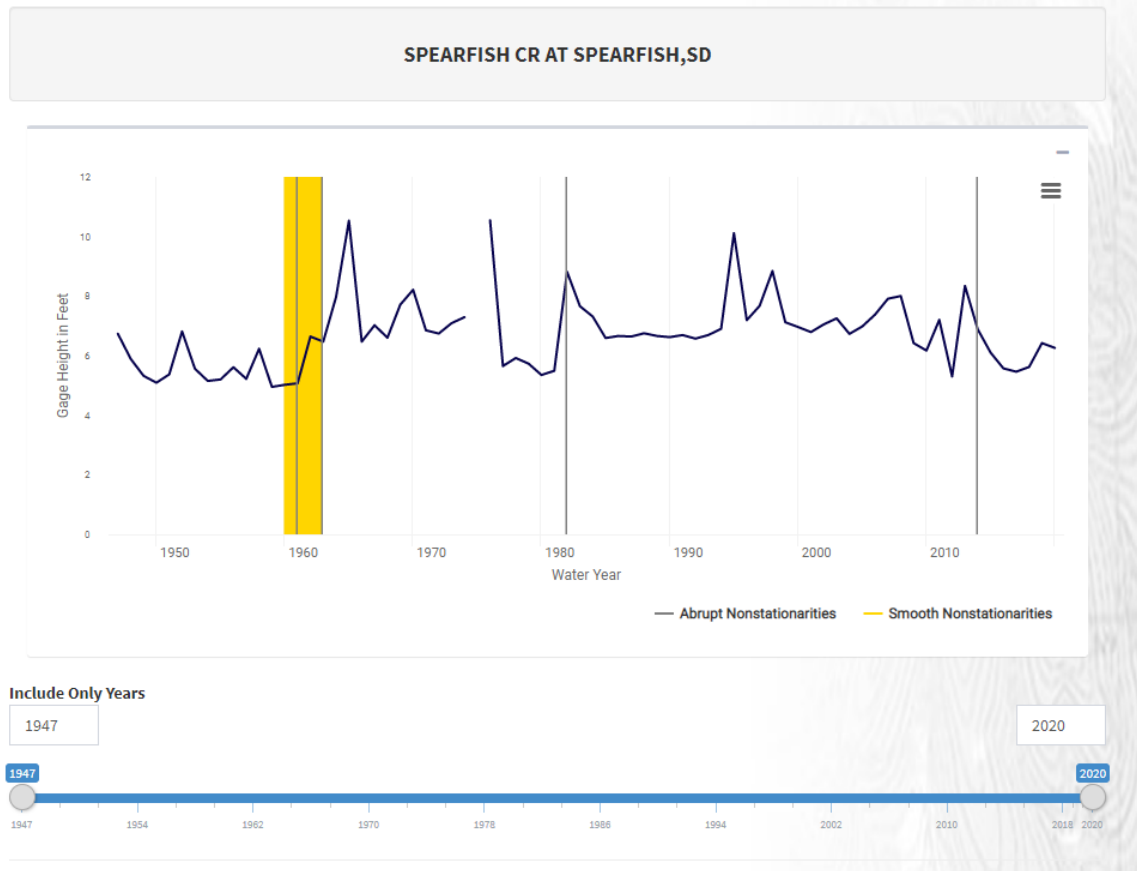


Figure 7.12.4 USGS Gage 06431500 Spearfish Creek at Spearfish, SD, non-stationarities identified for gage/stage height (ft.) for years 1947-2020.



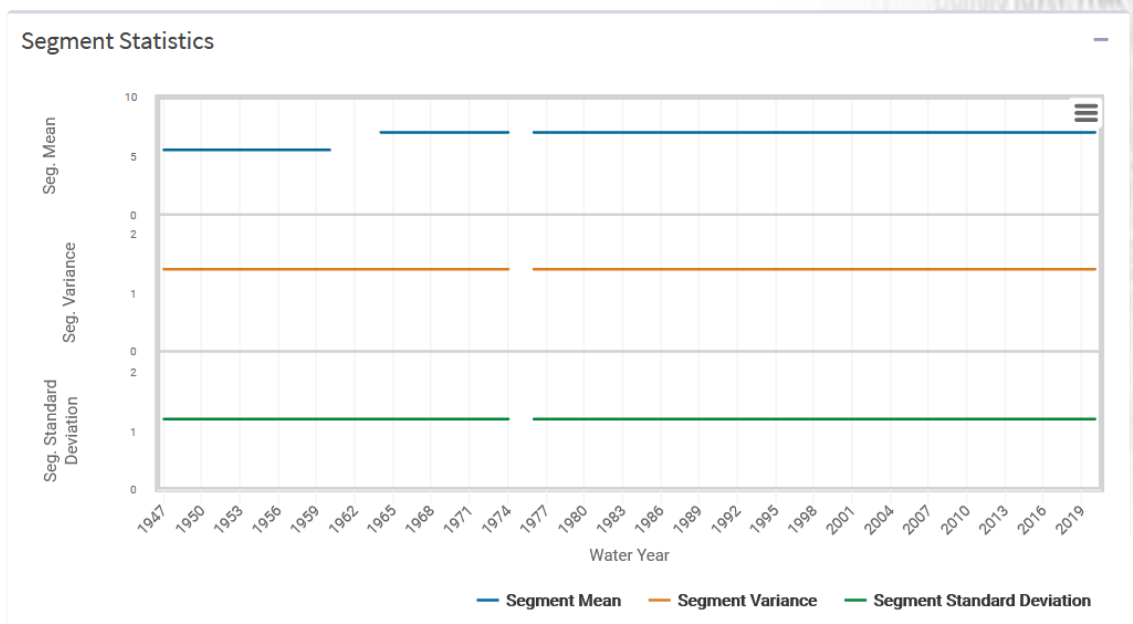
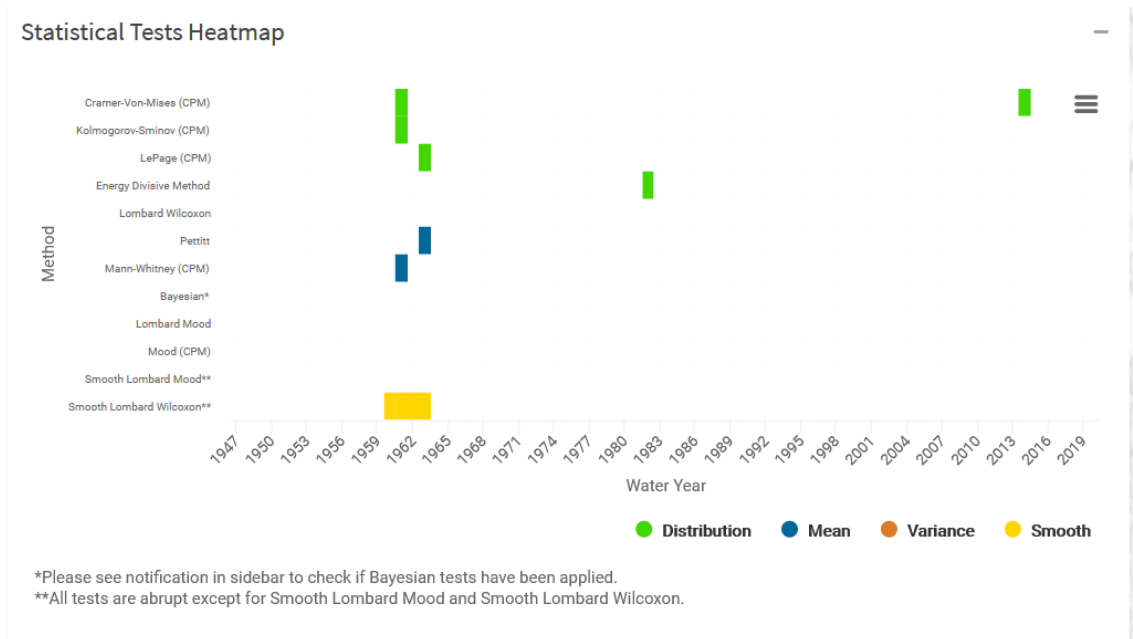
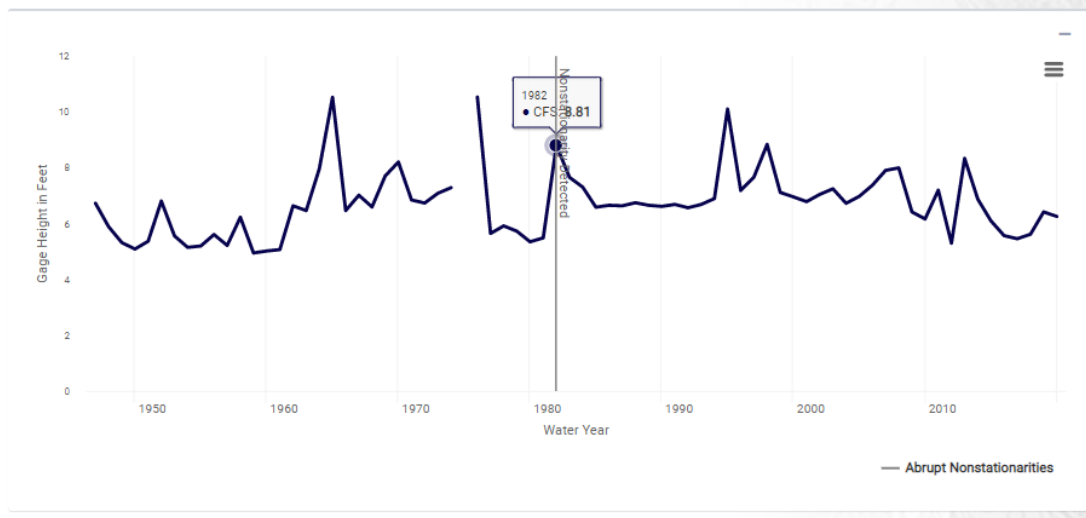


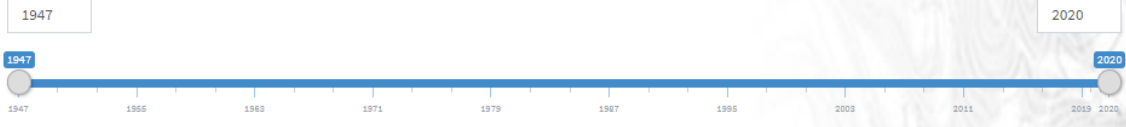
Figure 7.12.5 USGS Gage 06431500 Spearfish Creek at Spearfish, SD, four non-stationarities identified for gage/stage height (ft.) for years 1947-2020. Five Distribution with Cramer-Von-Mises in 1961 and 2014; One Kolmogorov-Sminov in 1961; One LePage in 1963 and one Energy Divisive Method in 1982. Two Mean non-stationarities: One Petit in 1963 and one Mann-Whitney in 1961. One Smooth Lombard Wilcoxon was detected from 1960-1963.

Distribution Nonstationarities Detected with Energy Divisive Method

SPEARFISH CR AT SPEARFISH,SD



Include Only Years



Distribution Nonstationarities Detected with Energy Divisive Method

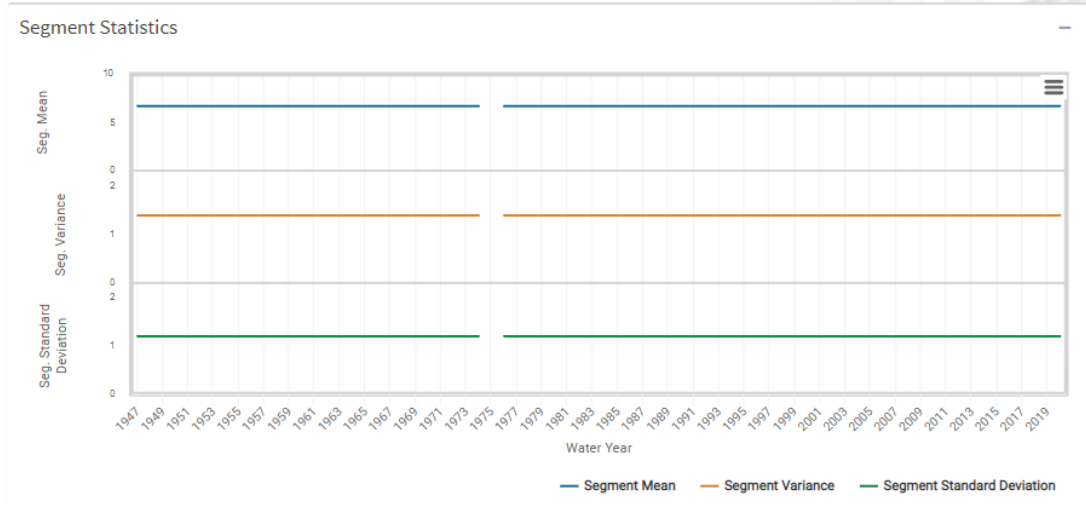


Figure 7.12.6 USGS Gage 06431500 Spearfish Creek at Spearfish, SD. A Distribution Non-stationarity was detected with the Distribution: Energy Divisive Method in 1982.

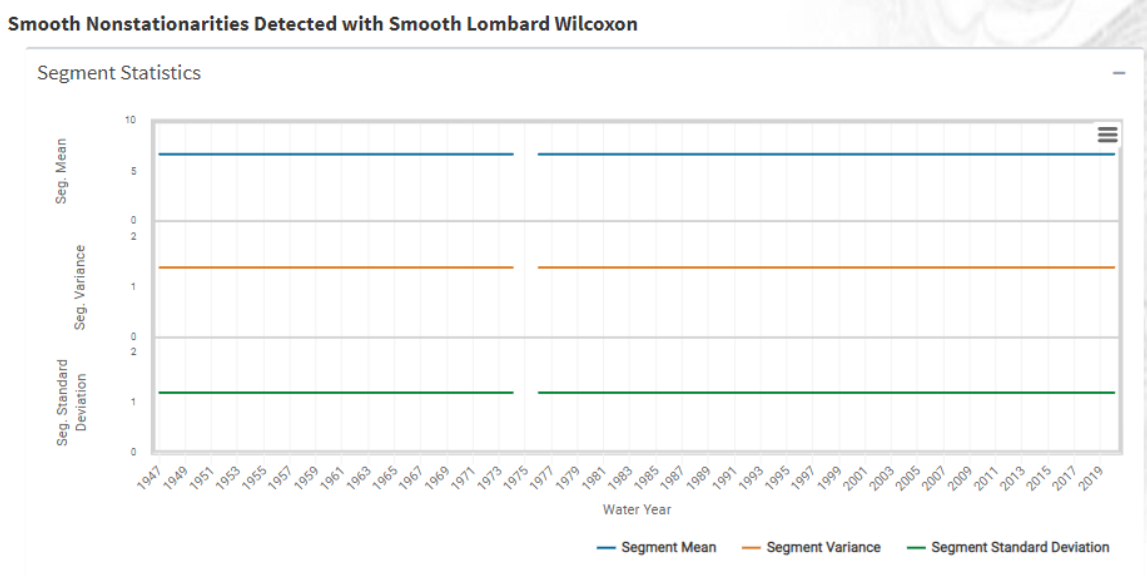
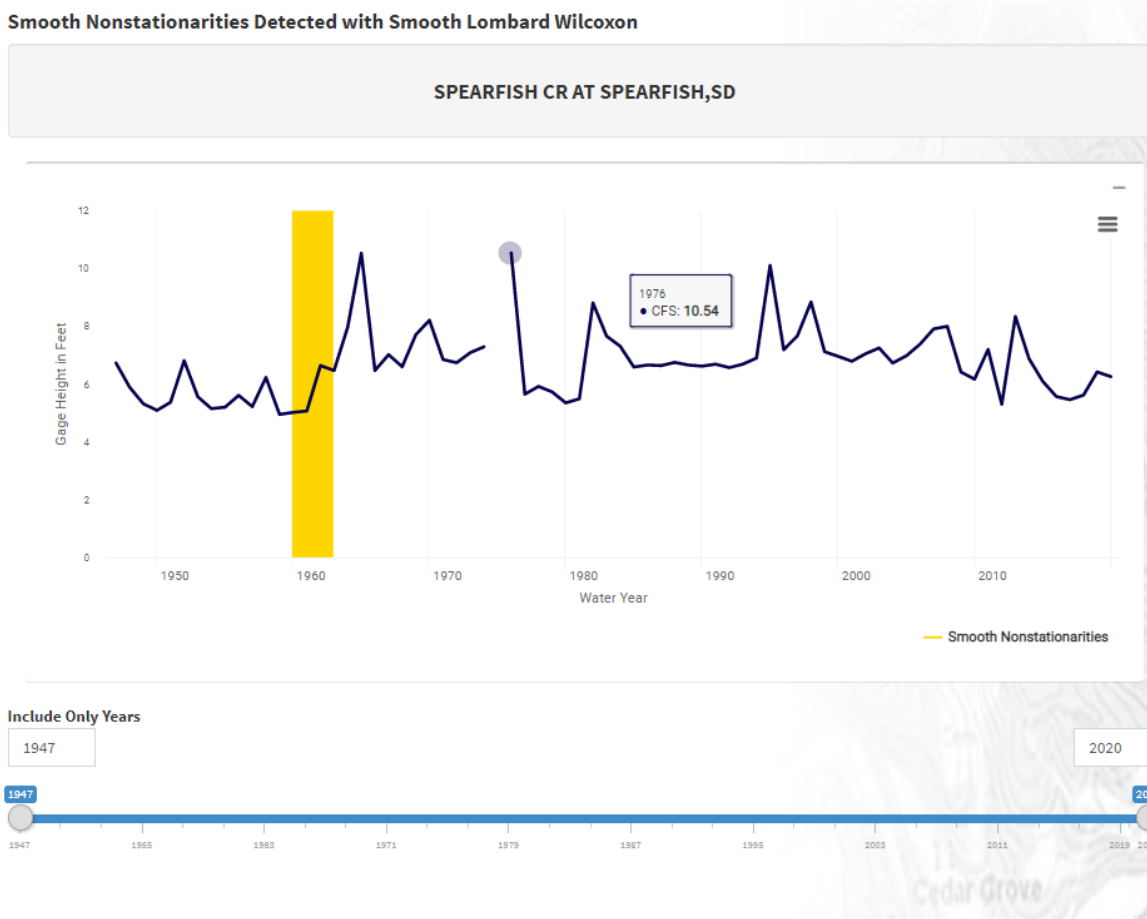
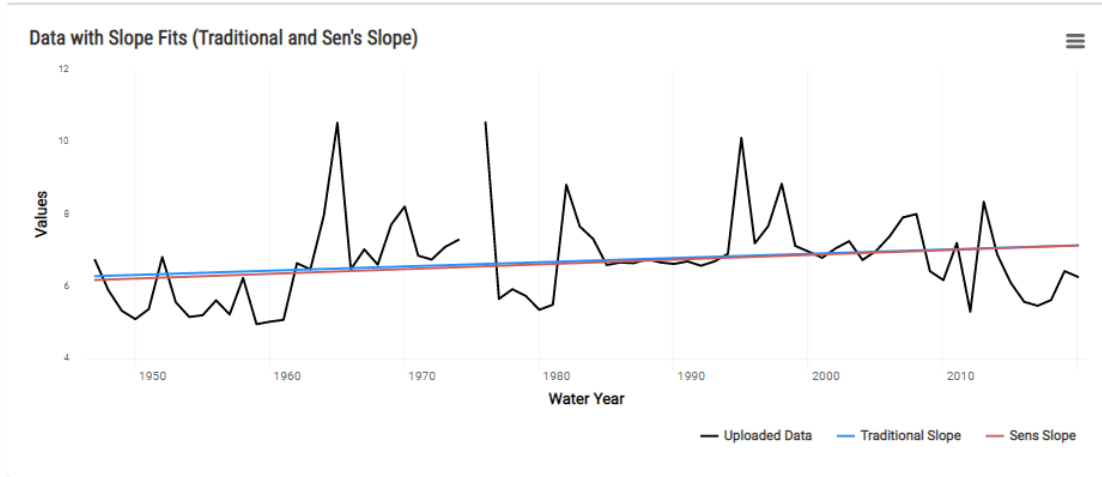


Figure 7.12.7 USGS Gage 06431500 Spearfish Creek at Spearfish, SD. Details of the segment statistics of the smooth Lombard Wilcoxon from 1960-1963.

Plot of Maximum Annual Flow/Height with Slope Fits (Traditional and Sen's Slope)

SPEARFISH CR AT SPEARFISH,SD



Method	Directionality	Slope	Intercept
Traditional Slope	Positive	0	-17
Sen's Slope	Positive	0	-19

Test	PValue
t-Test	0.073005
Mann-Kendall	0.016166
Spearman Rank-Order	0.014922

- A statistically significant trend (at the alpha = .05 level) was detected by the Mann-Kendall Test.
- A statistically significant trend (at the alpha = .05 level) was detected by the Spearman Rank-Order Test.

Figure 7.12.8 USGS Gage 06431500 Spearfish Creek at Spearfish, plot of gage/stage height (ft.) with slope fits (Traditional and Sen's Slope). Statistically significant trends (at the alpha = 0.05 level) were detected using the Mann-Kendall or the Spearman Rank-Order tests for the period 1947-2020.

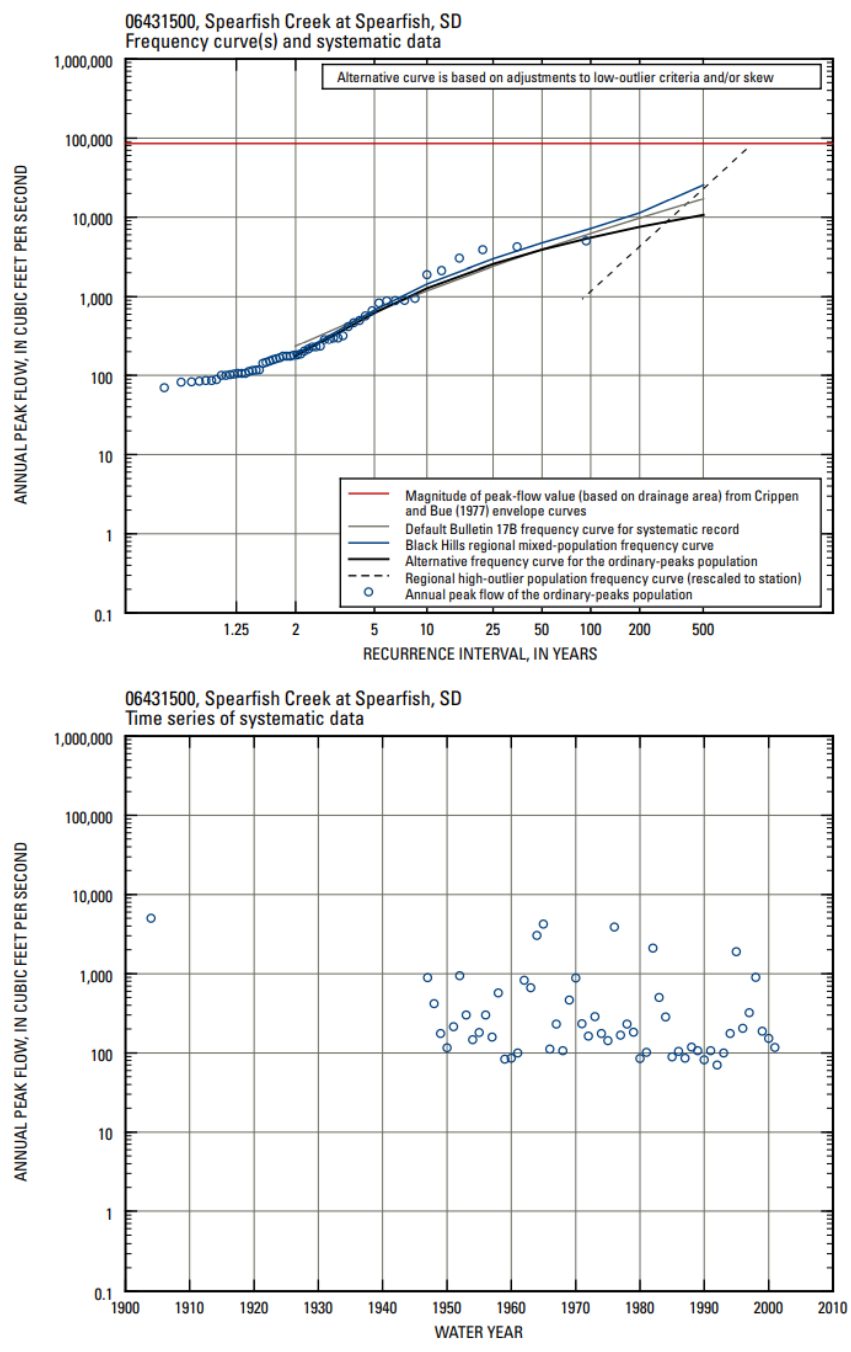
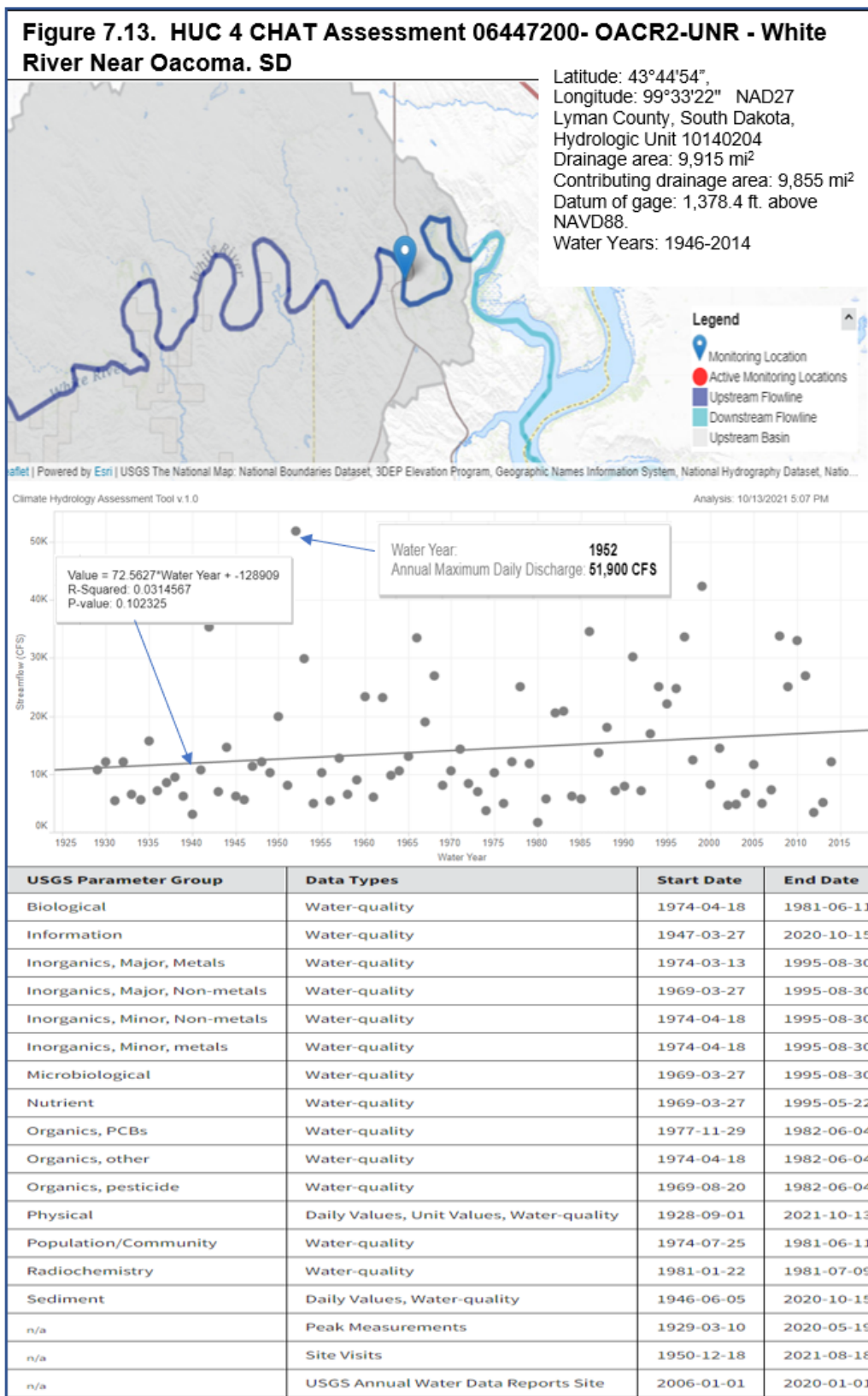


Figure 7.12.9. Peak-flow information for station 06431500, Spearfish Creek at Spearfish, SD (Sando et al., 2008).

Figure 7.13 USGS Gage 06452000 White River Near Oacoma, SD



### Nonstationarities Detected using Maximum Annual Flow

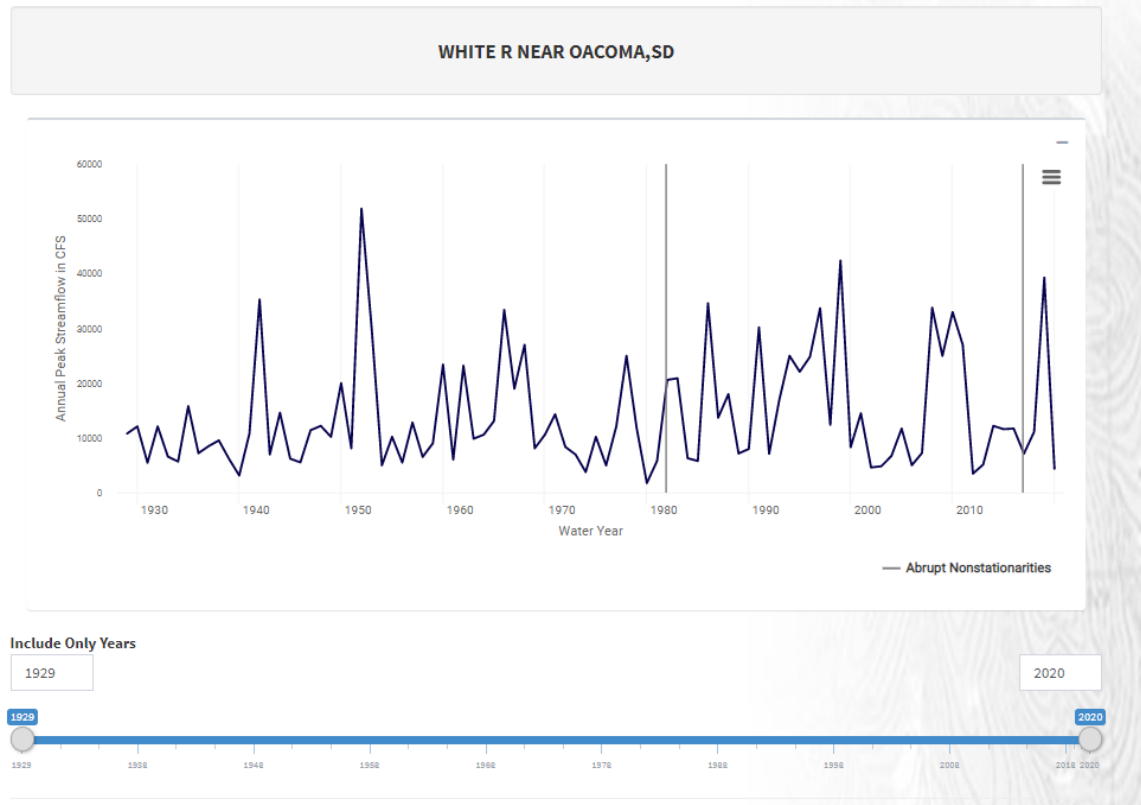


Figure 7.13.1. USGS Gage 06452000 White River Near Oacoma, SD, two non-stationarities identified for Instantaneous Peak Streamflow (IPS) using annual peak streamflow in cfs, for years 1929-2020 using NSD tool version 2.0. The Bayesian Changepoint Test was not applied as the assumption of normality was not met. A Smooth Lombard Wilcoxon was identified for the years 1929-1920.

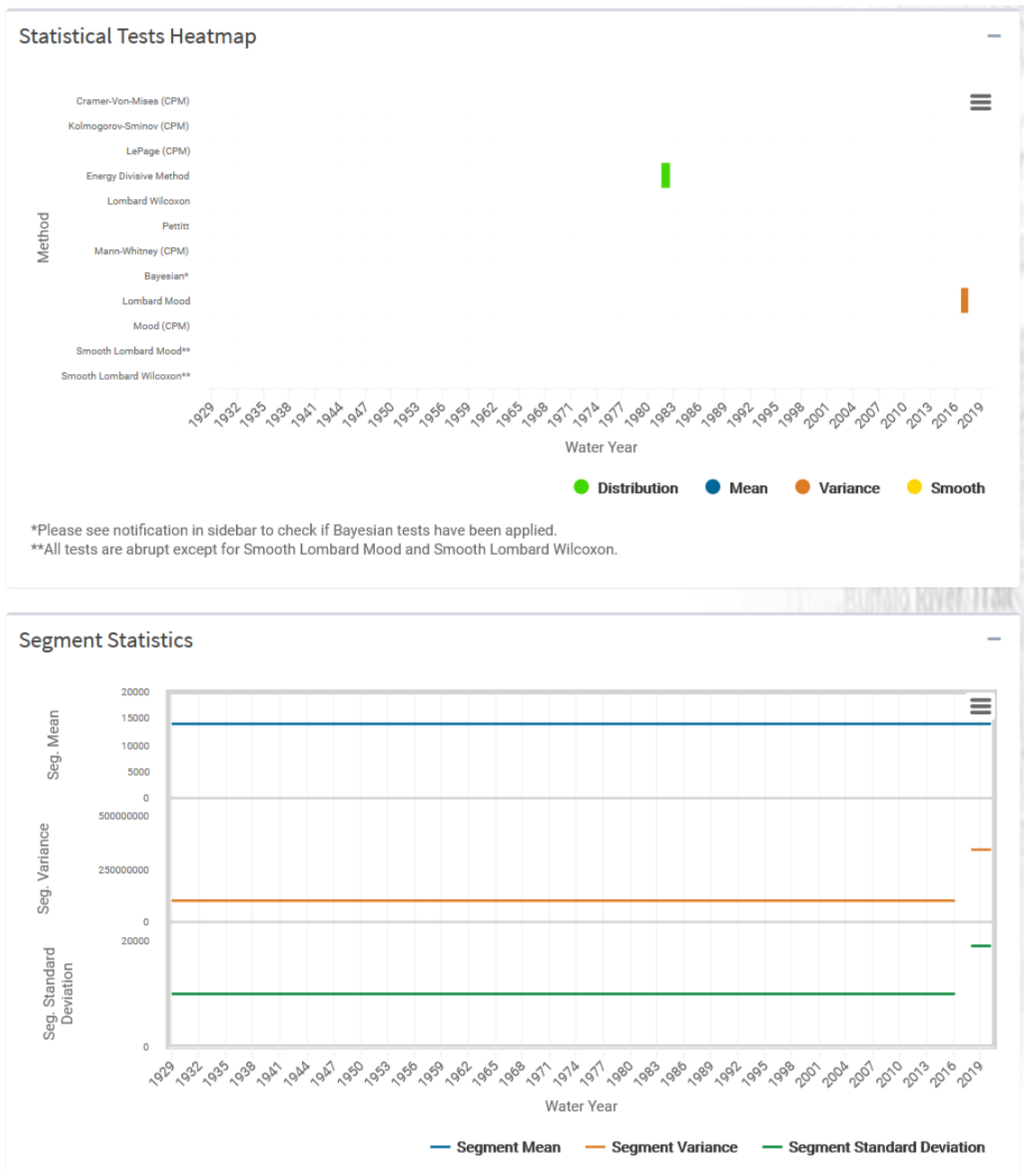


Figure 7.13.2. USGS Gage 06452000 White River Near Oacoma, SD, plot of non-stationarity identified with the NSD tool identified for Instantaneous Peak Streamflow (IPS) using annual peak streamflow in cfs, for years 1929-2019 using NSD tool version 2.0.: A Distribution non-stationarity for the Energy Divisive Method in 1982 and a Variance Lombard Mood in 2017.



Plot of Maximum Annual Flow/Height with Slope Fits (Traditional and Sen's Slope)

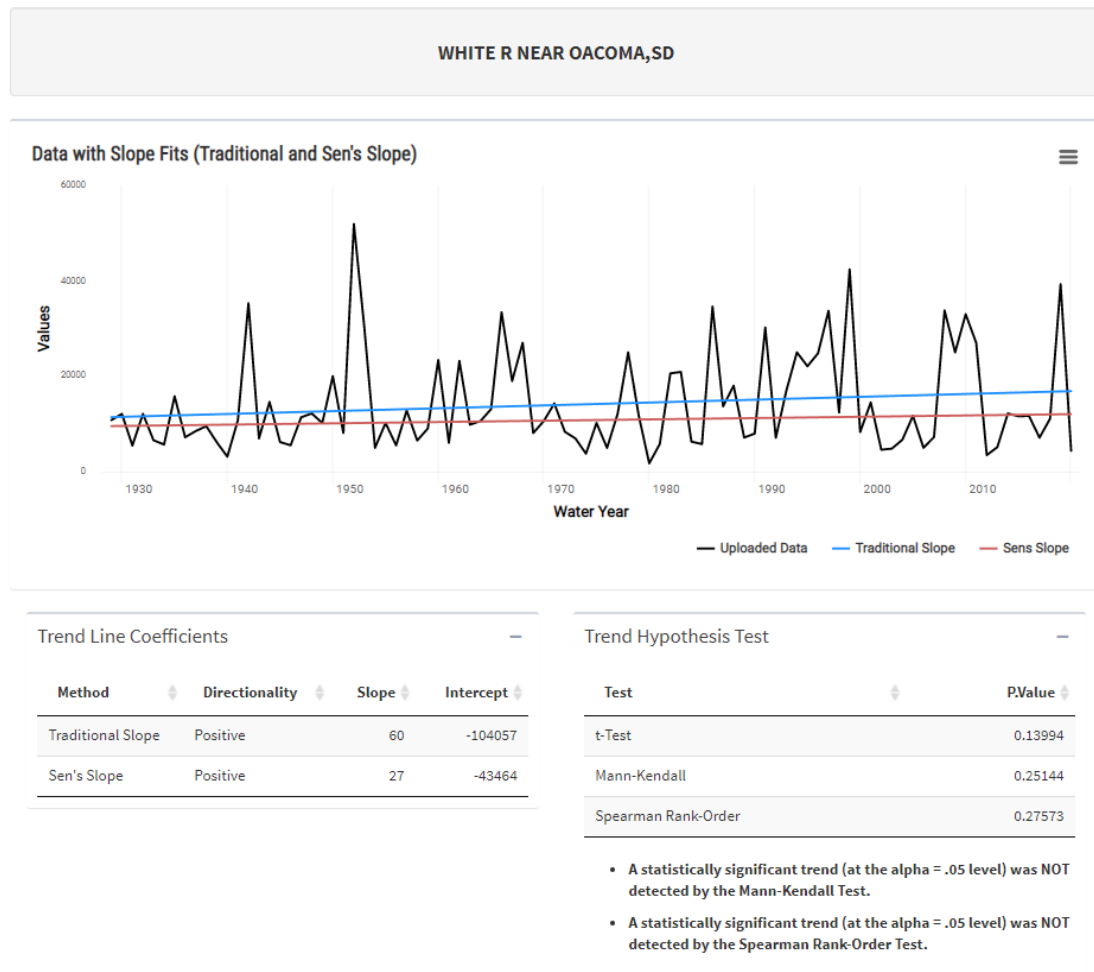
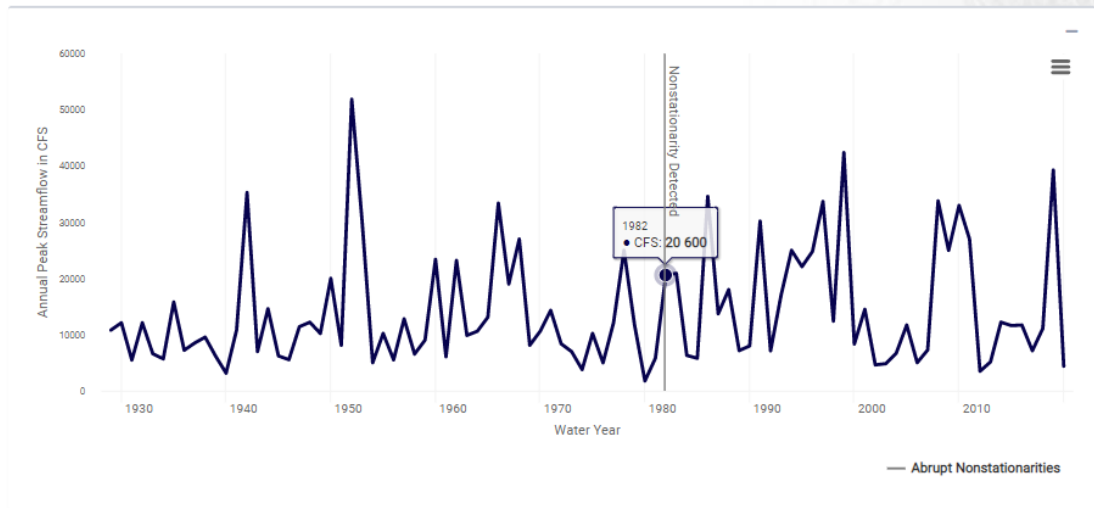


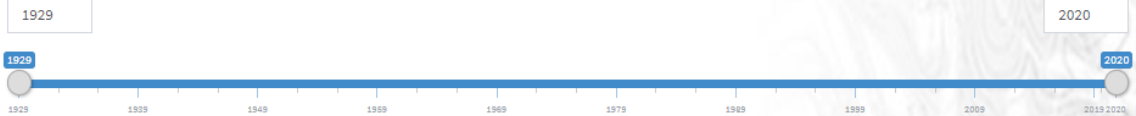
Figure 7.13.3. USGS Gage 06452000 White River Near Oacoma, SD, plot of maximum annual flow (cfs) with slope fits (Traditional and Sen's Slope). No statistically significant trends (at the alpha =0.05 level) were detected using the Mann-Kendall or the Spearman Rank-Order tests for the period 1929-2020.

Distribution Nonstationarities Detected with Energy Divisive Method

WHITE R NEAR OACOMA,SD



Include Only Years



Distribution Nonstationarities Detected with Energy Divisive Method

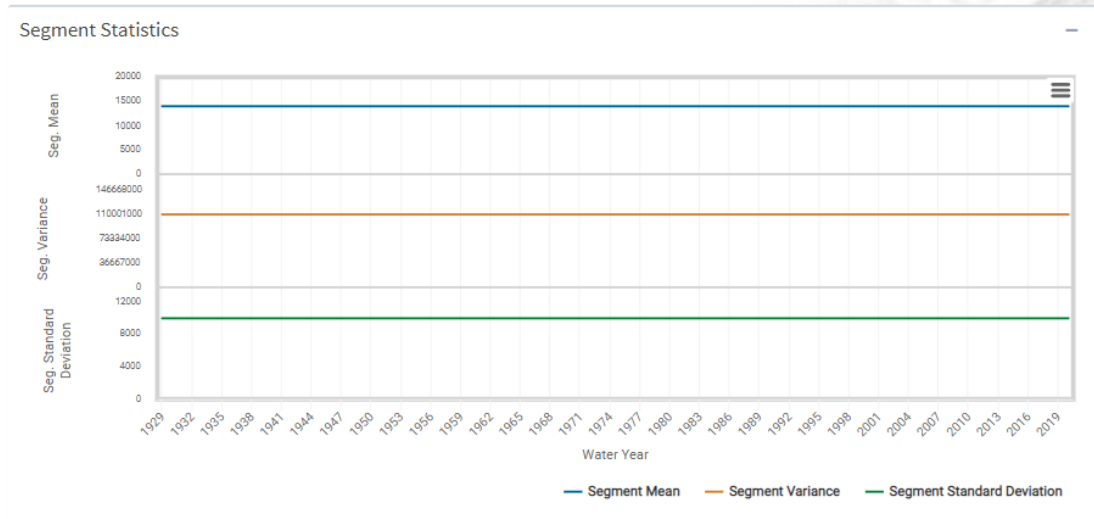
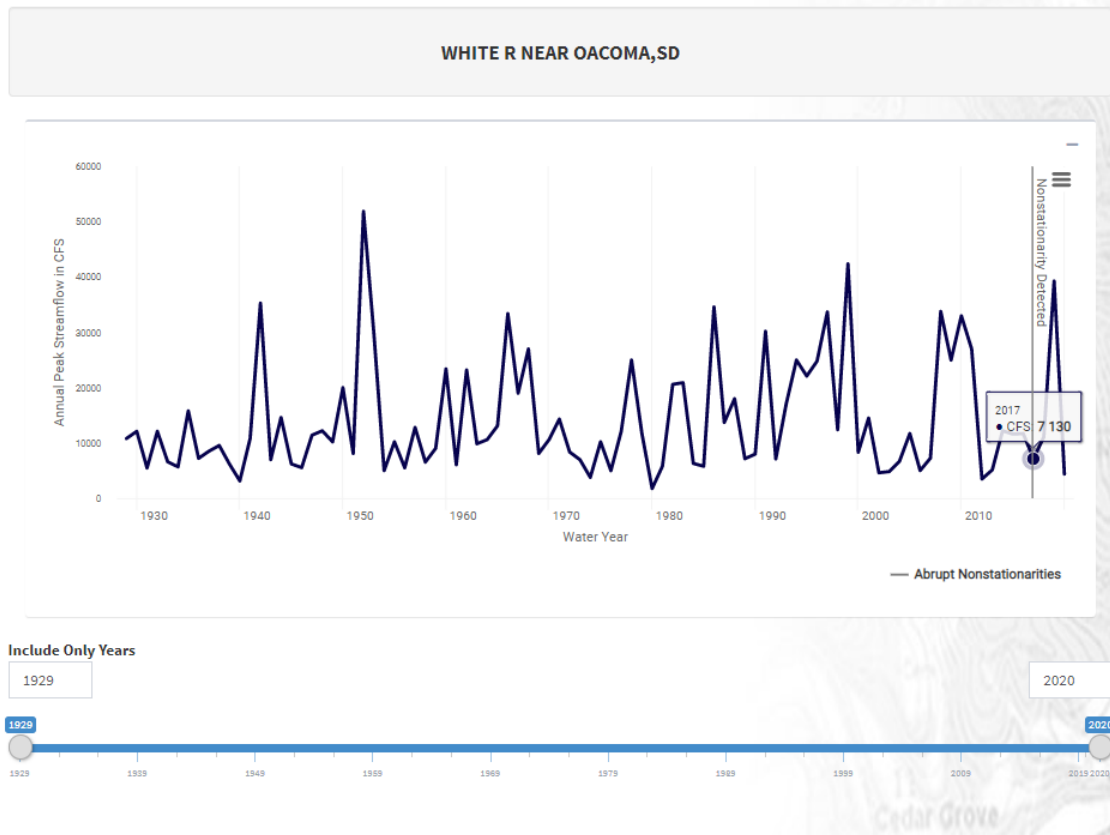


Figure 7.13.4. USGS Gage 06452000 White River Near Oacoma, SD, One Distribution non-stationarity for the Energy Divisive Method in 1982.

Variance Nonstationarities Detected with Lombard Mood



Variance Nonstationarities Detected with Lombard Mood

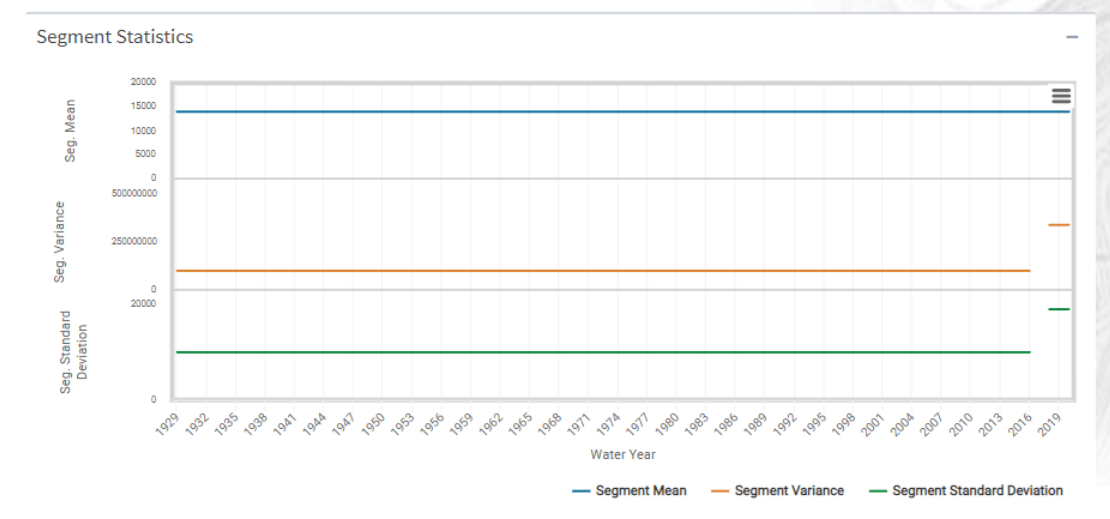


Figure 7.13.5. USGS Gage 06452000 White River Near Oacoma, SD, One Variance non-stationarity for the Lombard Mood in 2017.

Plot of Maximum Annual Flow/Height with Slope Fits (Traditional and Sen's Slope)

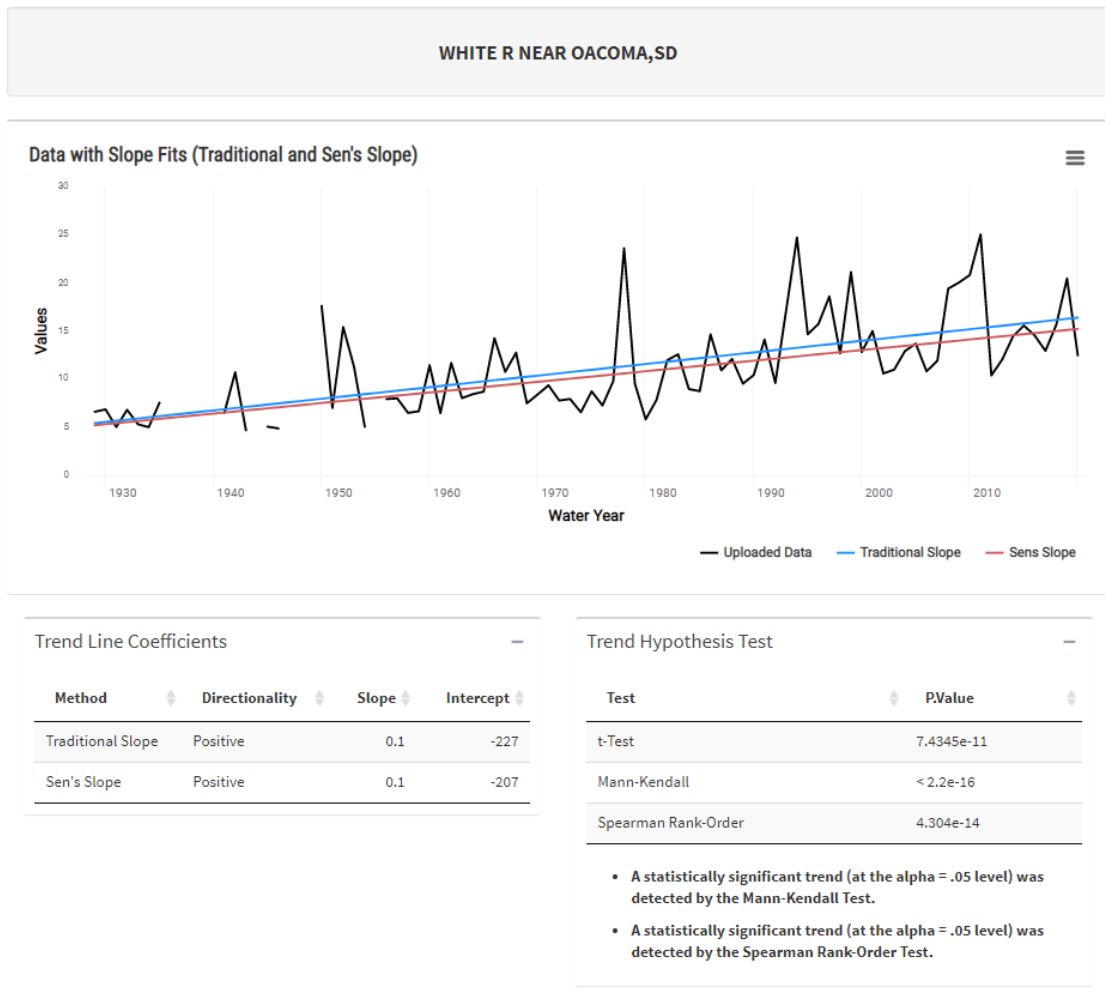


Figure 7.13.6. USGS Gage 06452000 White River Near Oacoma, SD, plot of gage/stage height (ft.) with slope fits (Traditional and Sen's Slope). Statistically significant trends (at the alpha =0.05 level) were detected using the Mann-Kendall and the Spearman Rank-Order tests for the period 1929-2020. There was missing data for the periods 1934-1949.

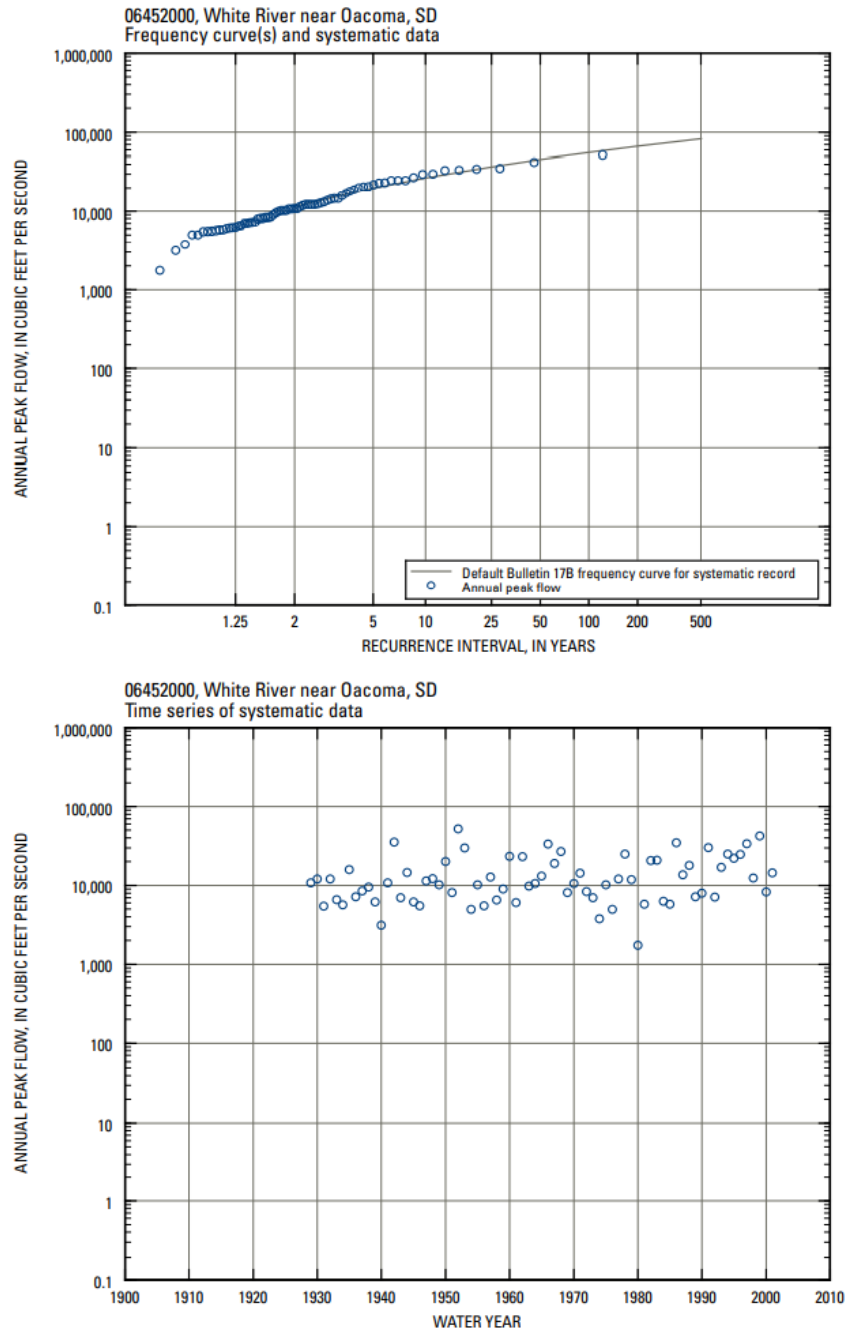
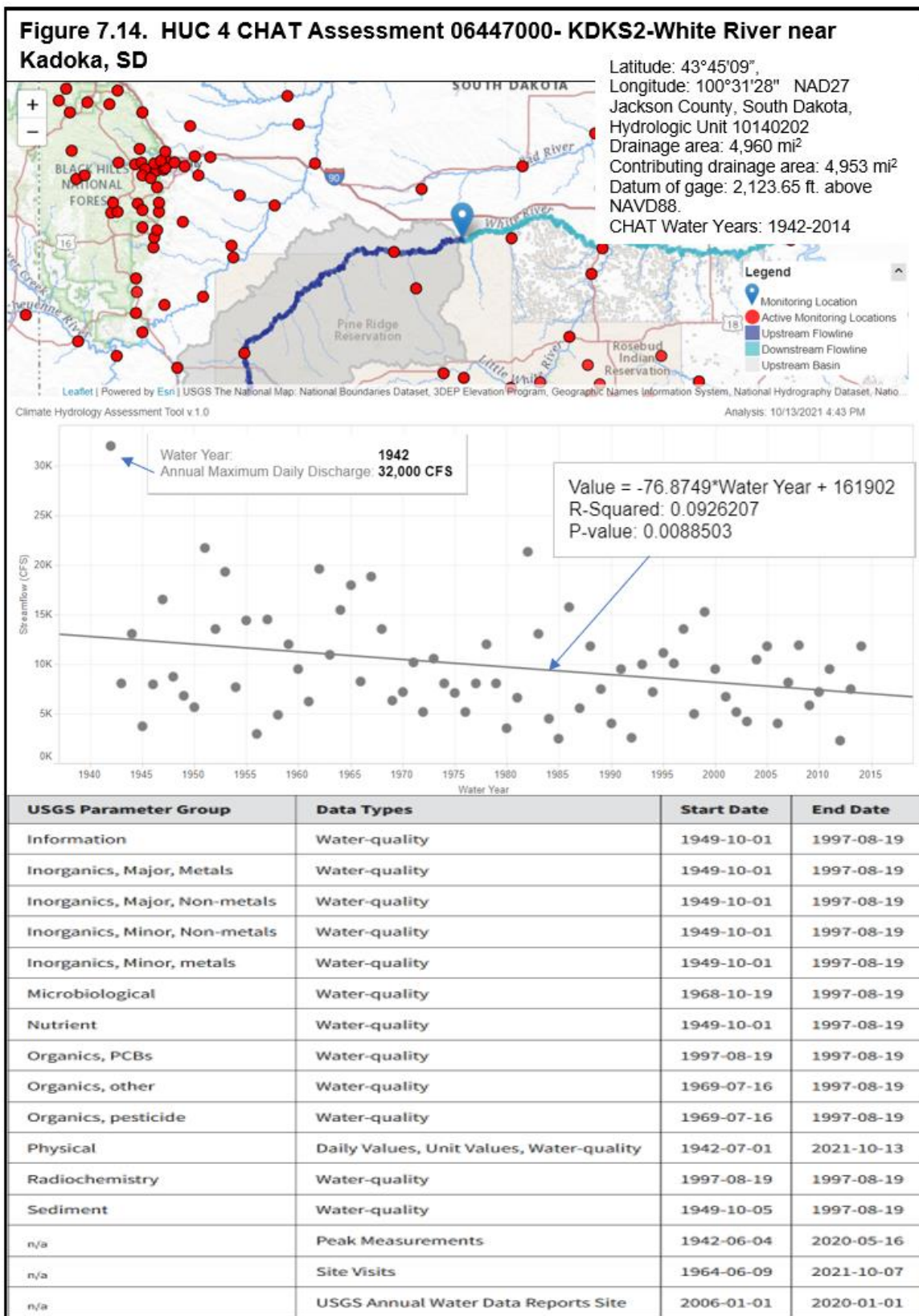


Figure 7.13.7. Peak-flow information for station 06452000, White River near Oacoma, SD (Sando et al., 2008).

Figure 7.14 06447000 White River Near Kadoka



Nonstationarities Detected using Maximum Annual Flow

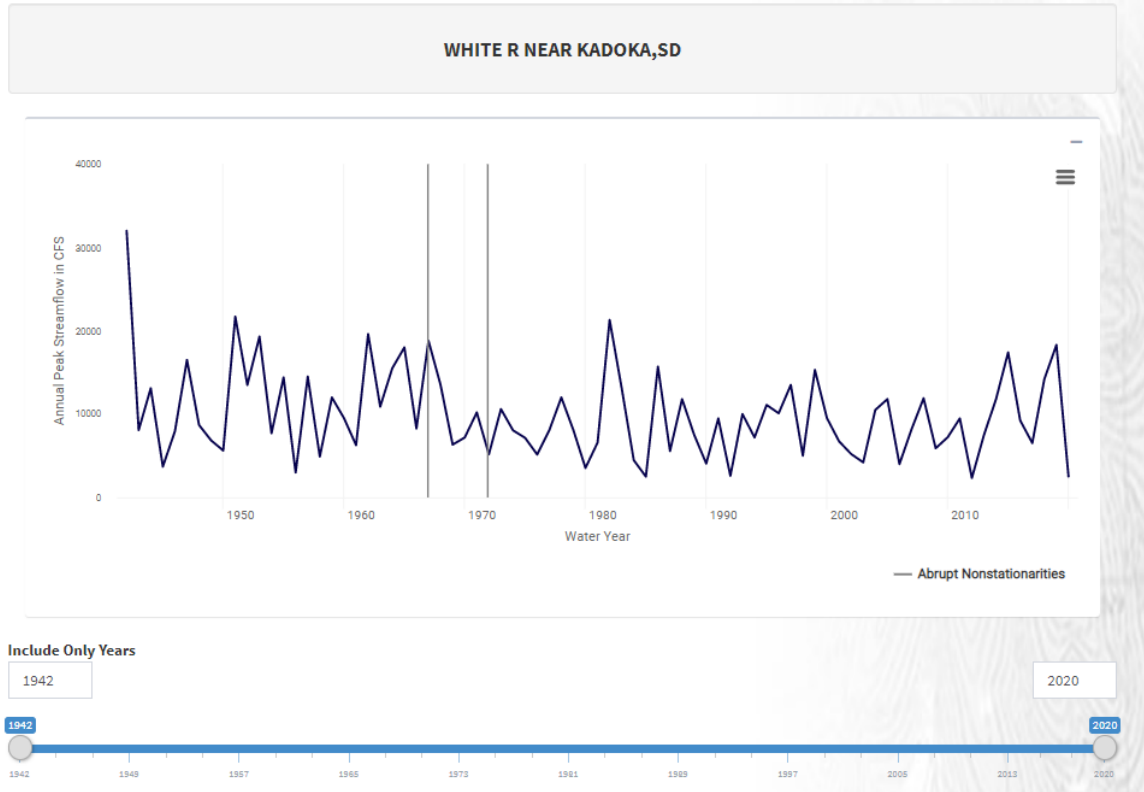


Figure 7.14.1. USGS Gage 06447000 White River Near Kadoka, SD. Two non-stationarities identified for Instantaneous Peak Streamflow (IPS) using annual peak streamflow in cfs, for years 1942-2020 using NSD tool version 2.0. The Bayesian Changepoint Test was not applied as the assumption of normality was not met. A Distribution: Energy Divisive Method in 1972 and a Mean: Lombard Wilcoxon in 1967.

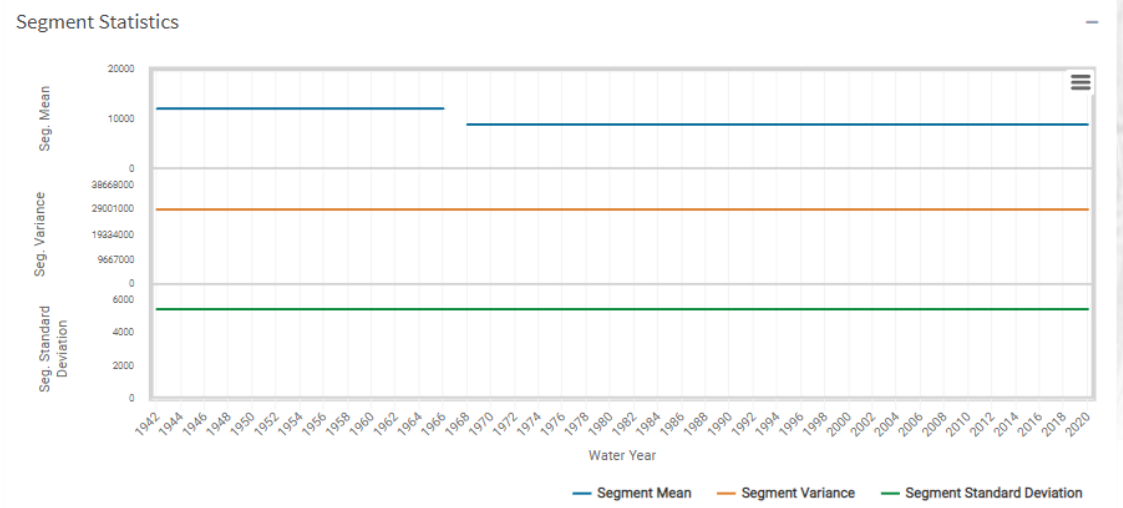
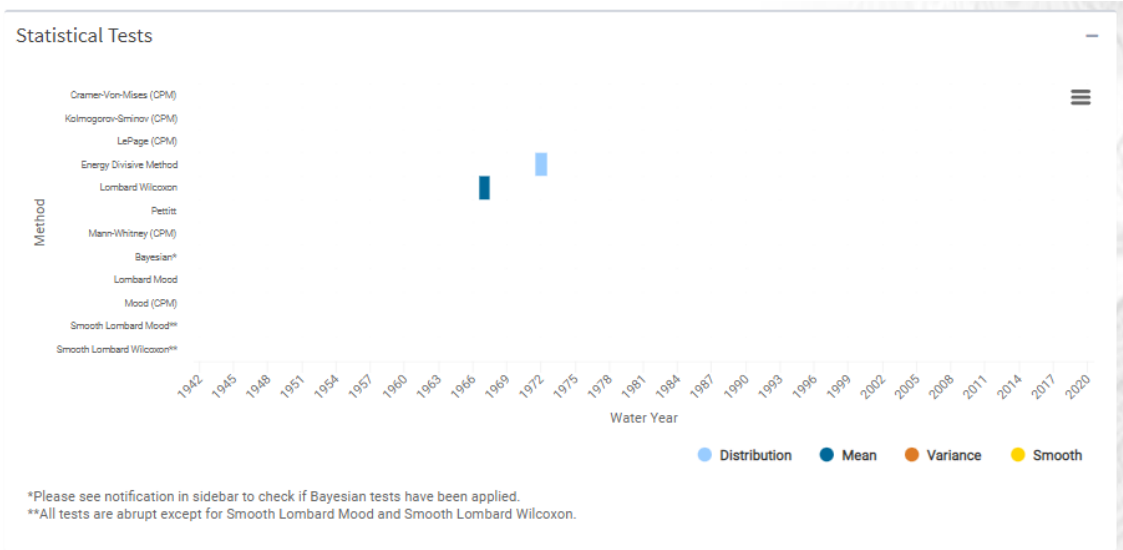
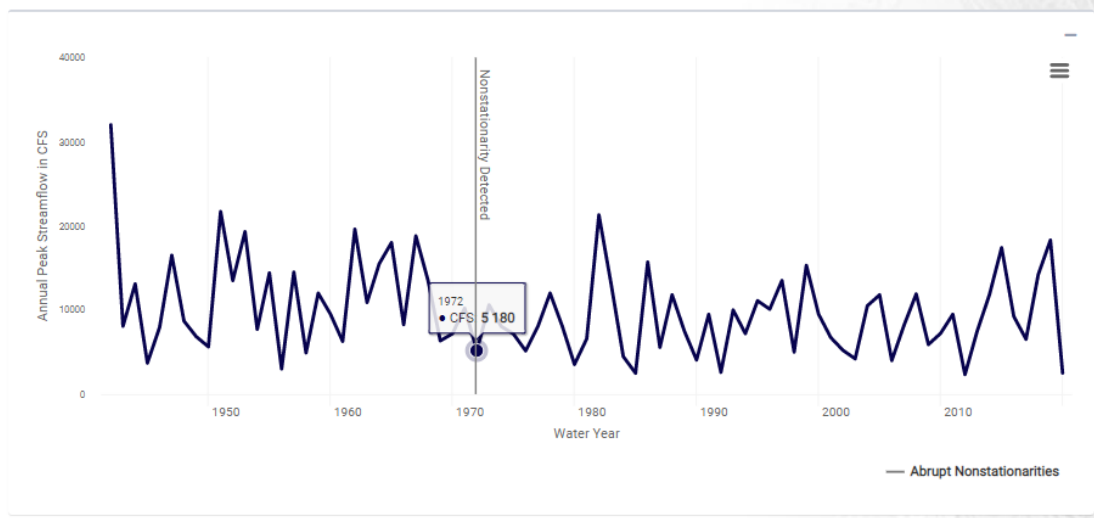


Figure 7.14.2. USGS Gage 06447000 White River Near Kadoka, SD. A Distribution: Energy Divisive Method in 1972 and a Mean: Lombard Wilcoxon in 1967.

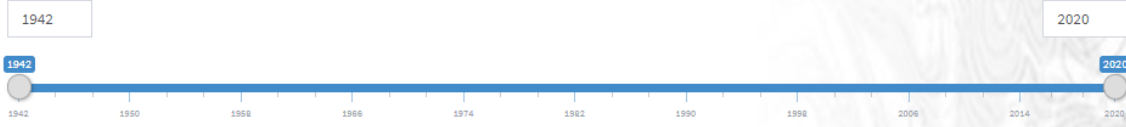


Distribution Nonstationarities Detected with Energy Divisive Method

WHITE R NEAR KADOKA,SD



Include Only Years



Distribution Nonstationarities Detected with Energy Divisive Method

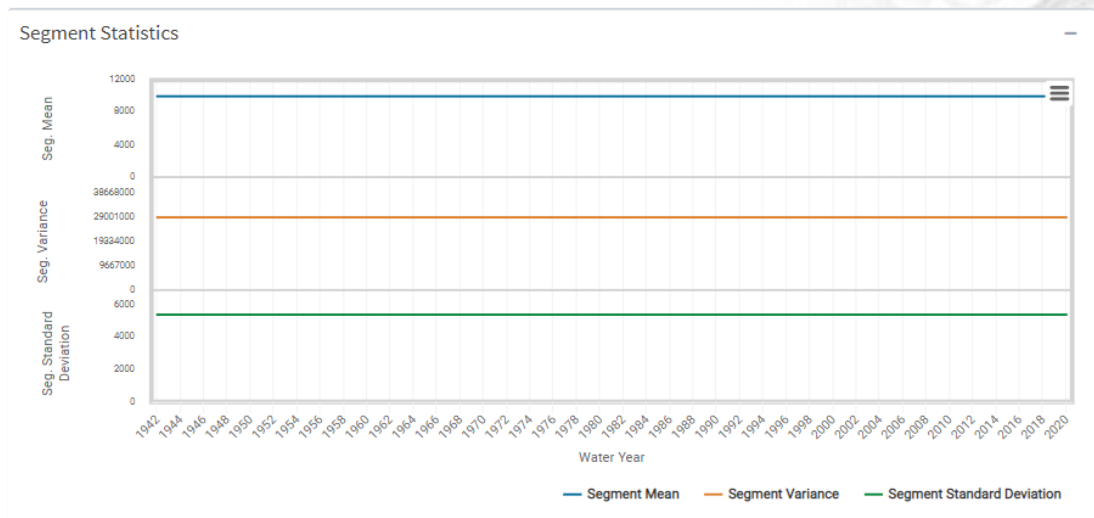
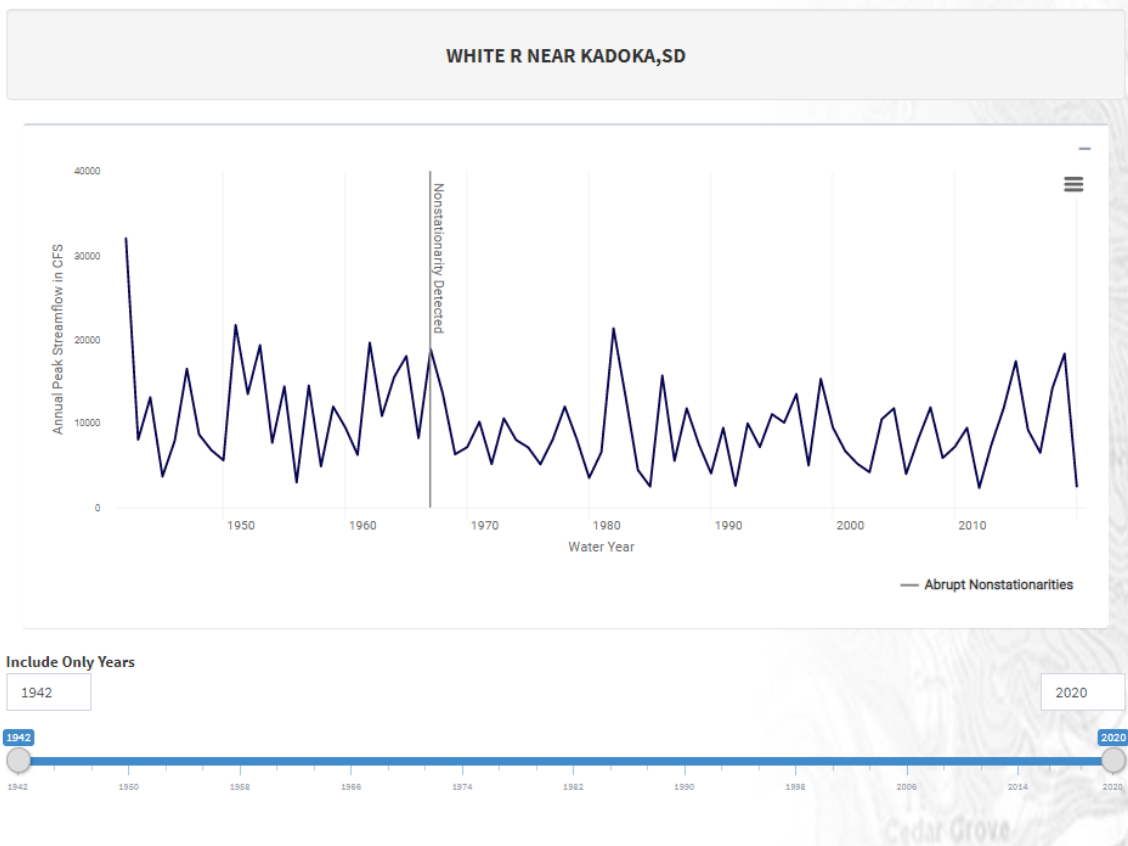


Figure 7.14.3. USGS Gage 06447000 White River Near Kadoka, SD. A non-stationarity Distribution was detected for maximum annual flow with the Energy Divisive Method in 1972.

Mean Nonstationarities Detected with Lombard Wilcoxon



Mean Nonstationarities Detected with Lombard Wilcoxon

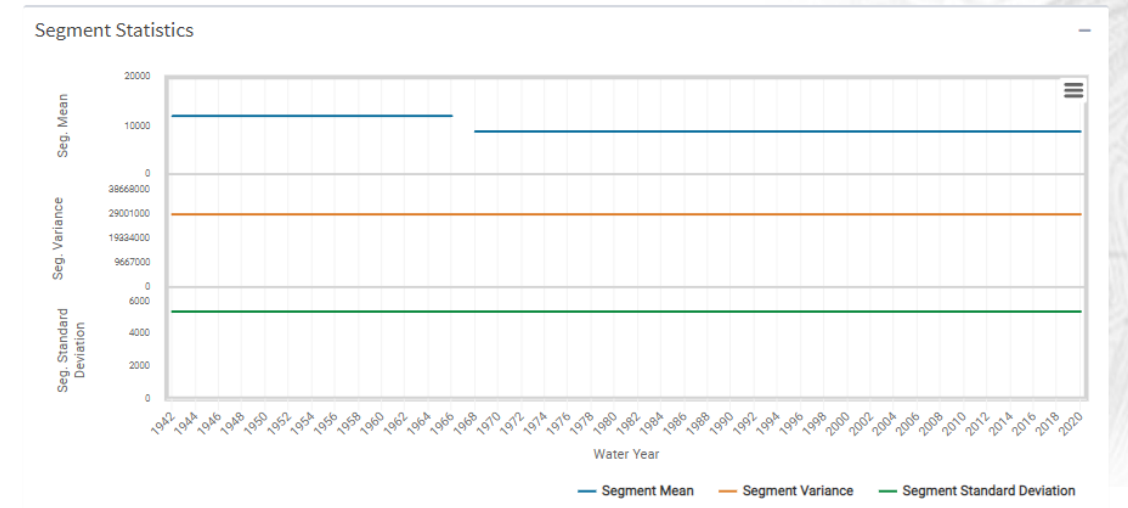


Figure 7.14.4. USGS Gage 06447000 White River Near Kadoka, SD. Mean nonstationarity detected with Lombard Wilcoxon in 1967.

Plot of Maximum Annual Flow/Height with Slope Fits (Traditional and Sen's Slope)

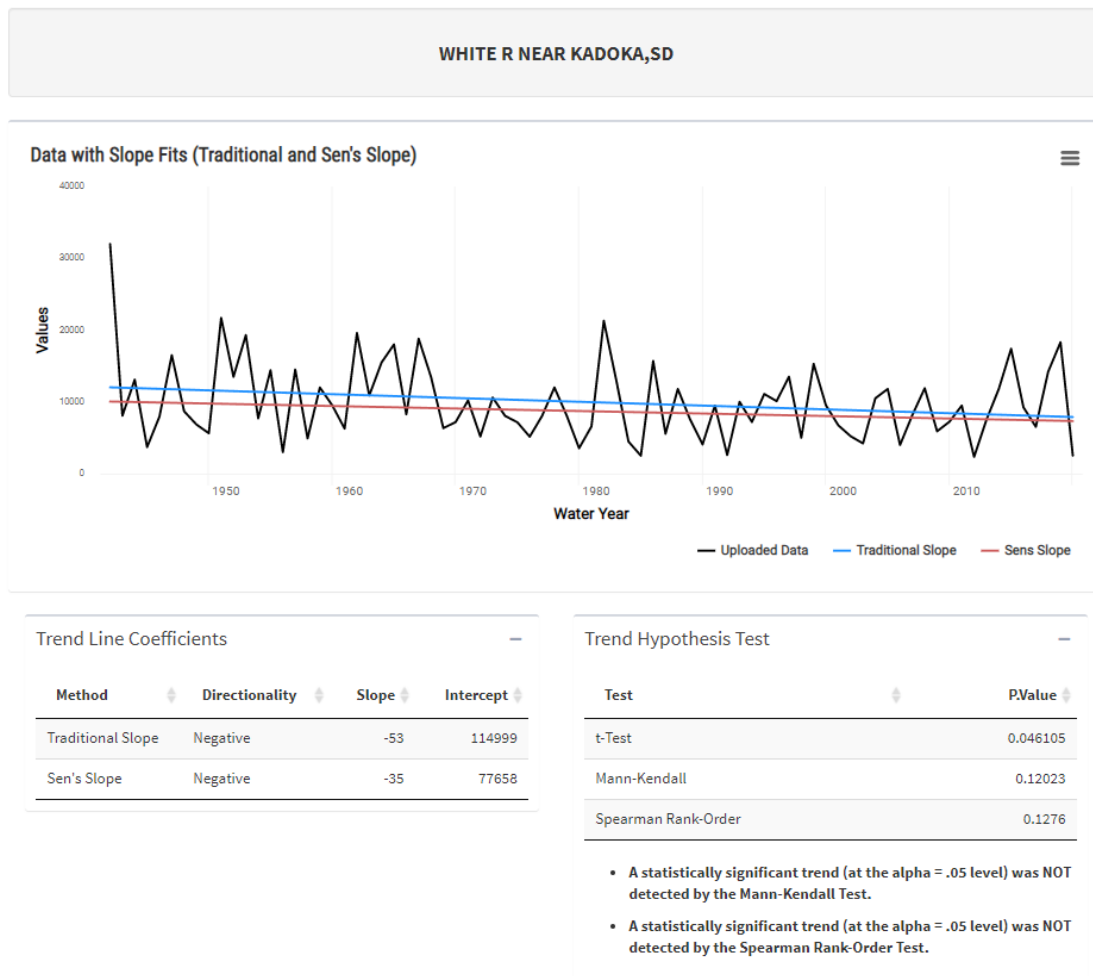


Figure 7.14.5. USGS Gage 06447000 White River Near Kadoka, SD plot of (cfs) with slope fits (Traditional and Sen's Slope) for Instantaneous Peak Streamflow (IPS) using annual peak streamflow in cfs, for years 1942-2020 using NSD tool version 2.0. No statistically significant trends (at the alpha =0.05 level) were detected using the Mann-Kendall or the Spearman Rank-Order tests for the period.

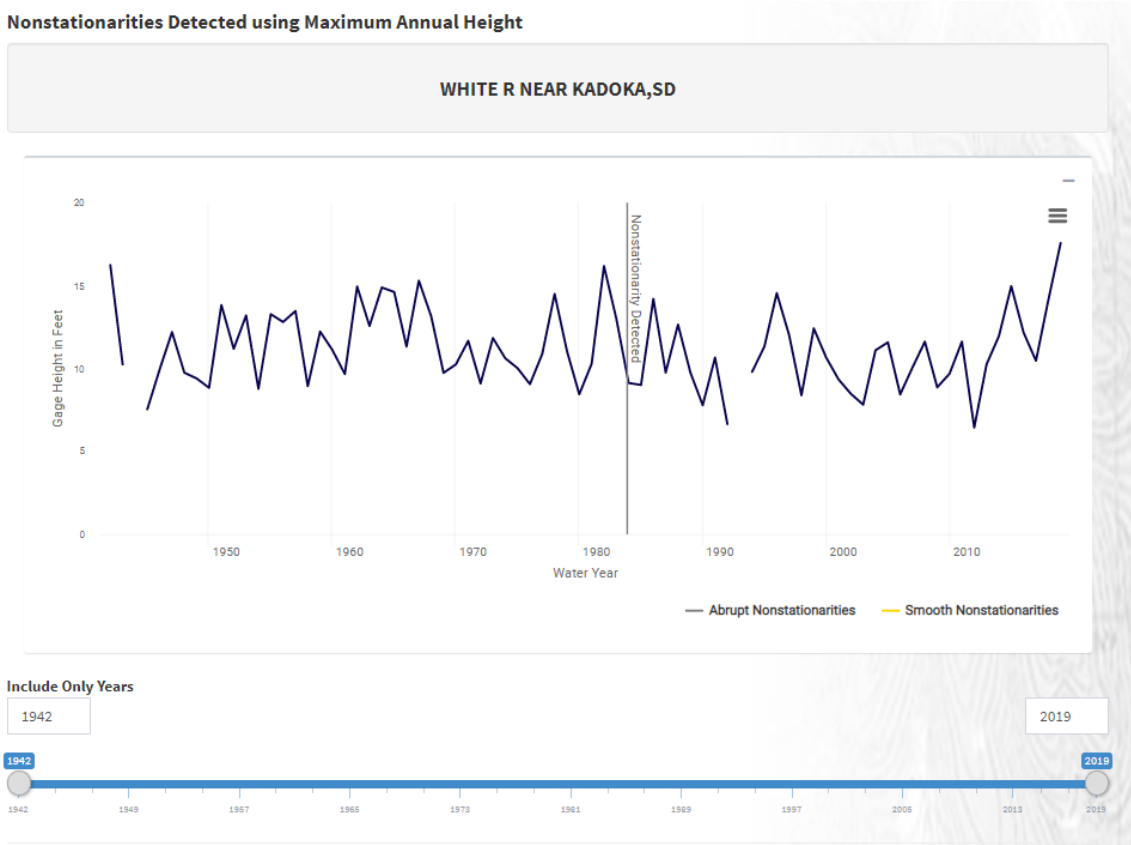


Figure 7.14.6. USGS Gage 06447000 White River Near Kadoka, SD. One nonstationarity was detected for the stage-gage height in 1984, for the Distribution: Energy Divisive Method for the period 1942-2019. Missing data points were identified in 1043-1945.

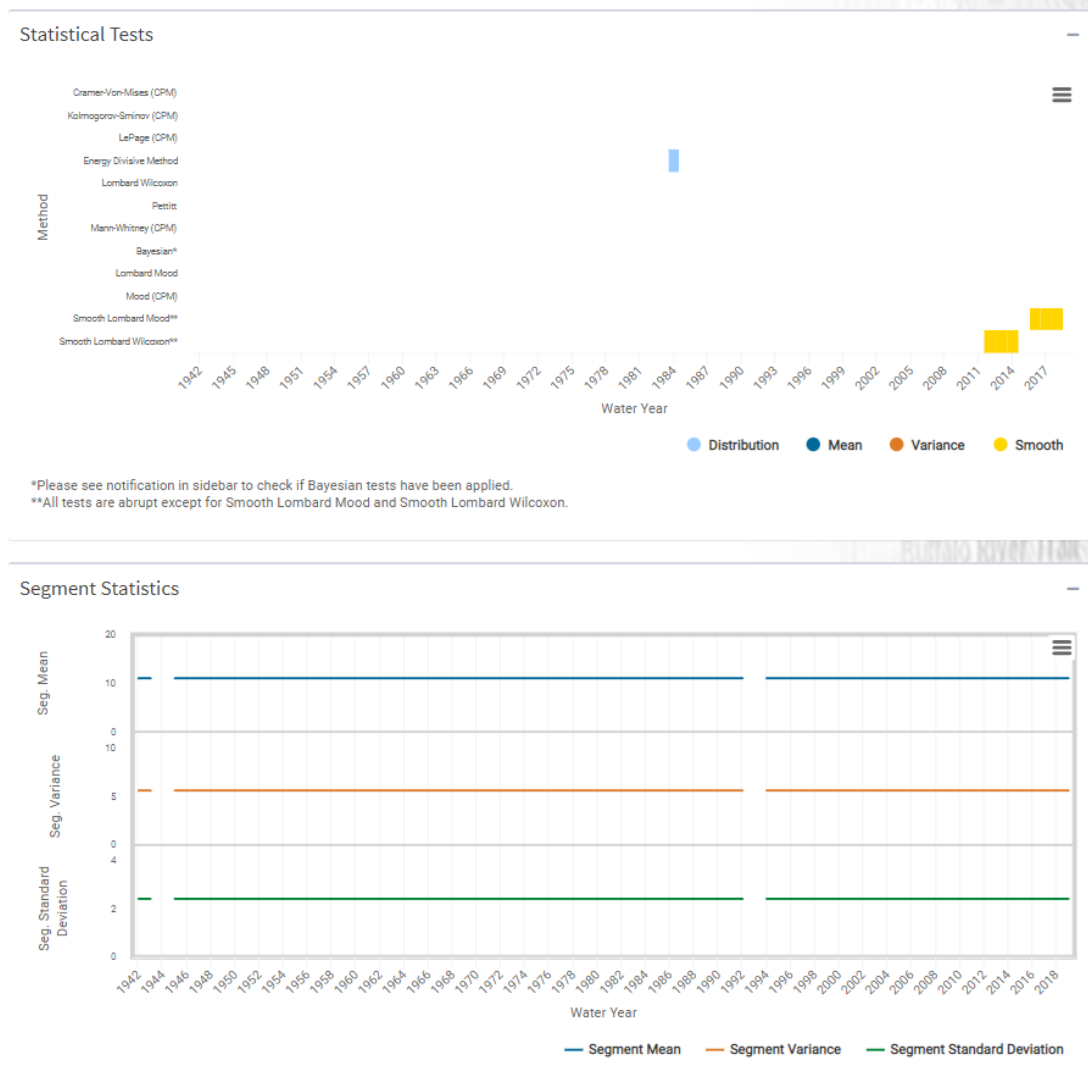
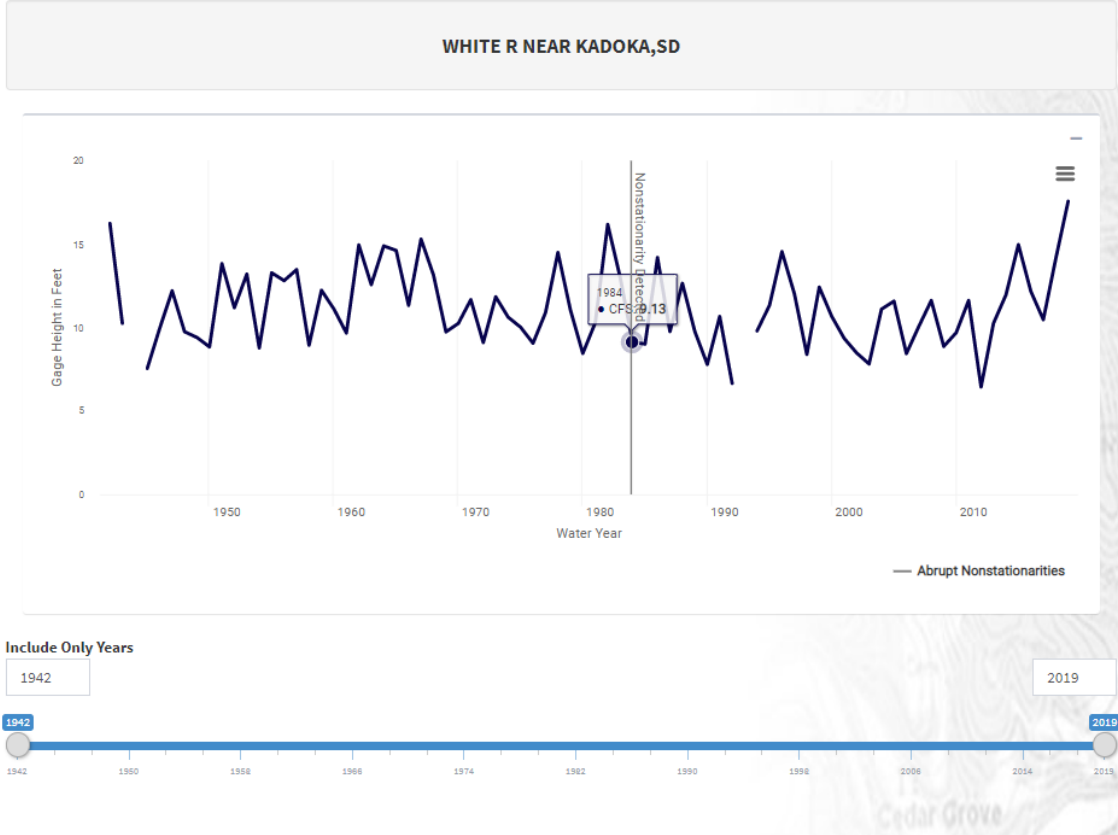


Figure 7.14.7. USGS Gage 06447000 White River Near Kadoka. Three non-stationarities were identified: one Distribution, Energy Divisive Method and two Smooth: Smooth Lombard Mood for the years 2016-2018, and a Smooth Lombard Wilcoxon, for the years 2012-2015.

Distribution Nonstationarities Detected with Energy Divisive Method



Distribution Nonstationarities Detected with Energy Divisive Method

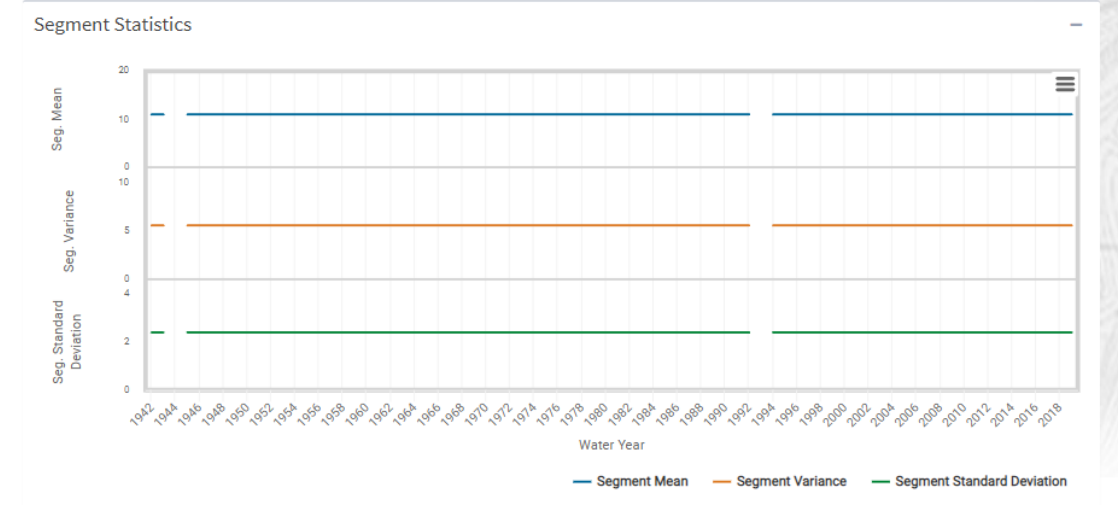
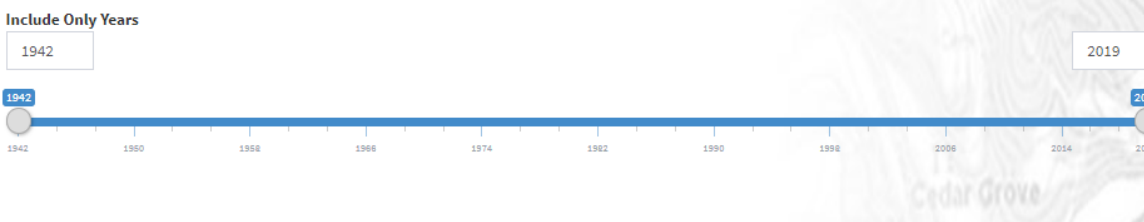
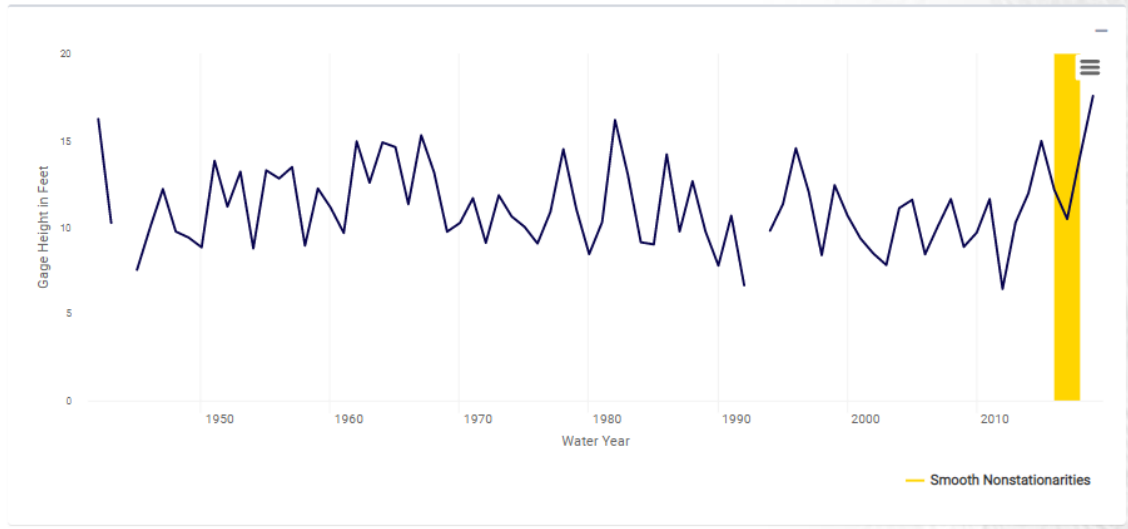


Figure 7.14.8. USGS Gage 06447000 White River Near Kadoka, SD a distribution non-stationarity was detected for the gage/stage height (ft) with the Energy Divisive Method in 1984.

Smooth Nonstationarities Detected with Smooth Lombard Mood

WHITE R NEAR KADOKA,SD



Smooth Nonstationarities Detected with Smooth Lombard Mood

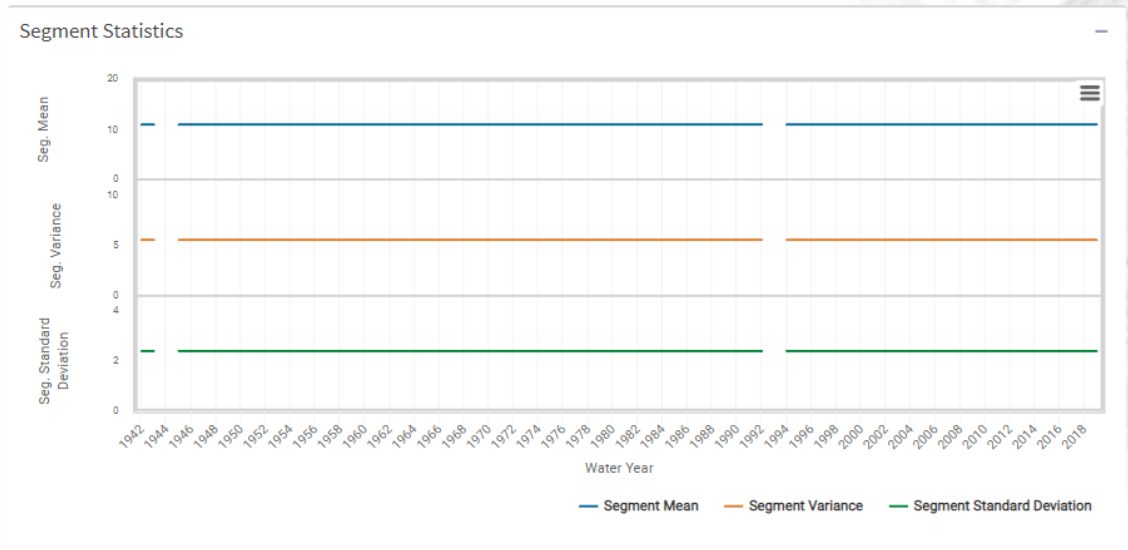


Figure 7.14.9. USGS Gage 06447000 White River Near Kadoka, SD. A Smooth Lombard Mood was detected for the years 2016-2018.

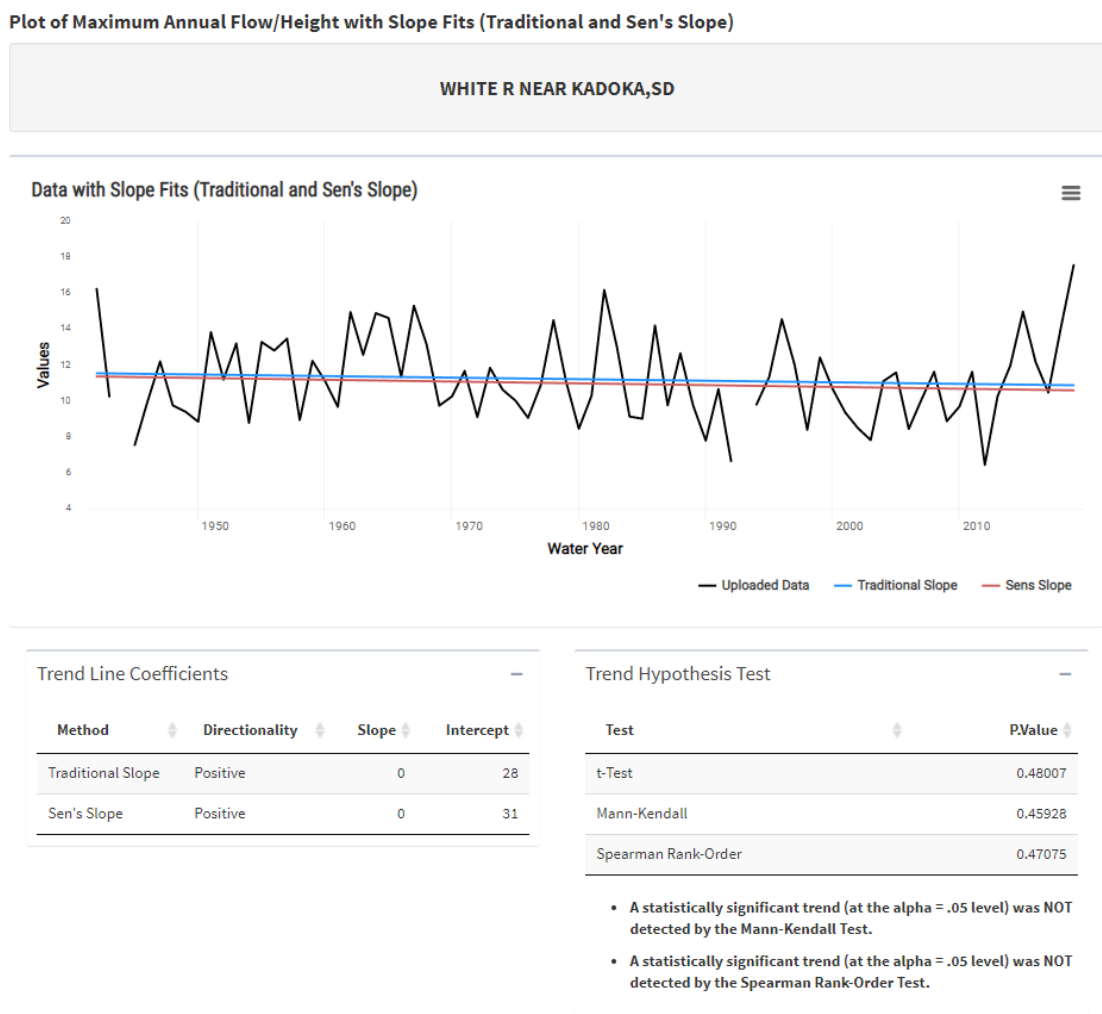


Figure 7.14.10. USGS Gage 06447000 White River Near Kadoka, SD plot of gage/stage height (ft.) with slope fits (Traditional and Sen's Slope). No statistically significant trends (at the alpha =0.05 level) were detected using the Mann-Kendall or the Spearman Rank-Order tests for the period.



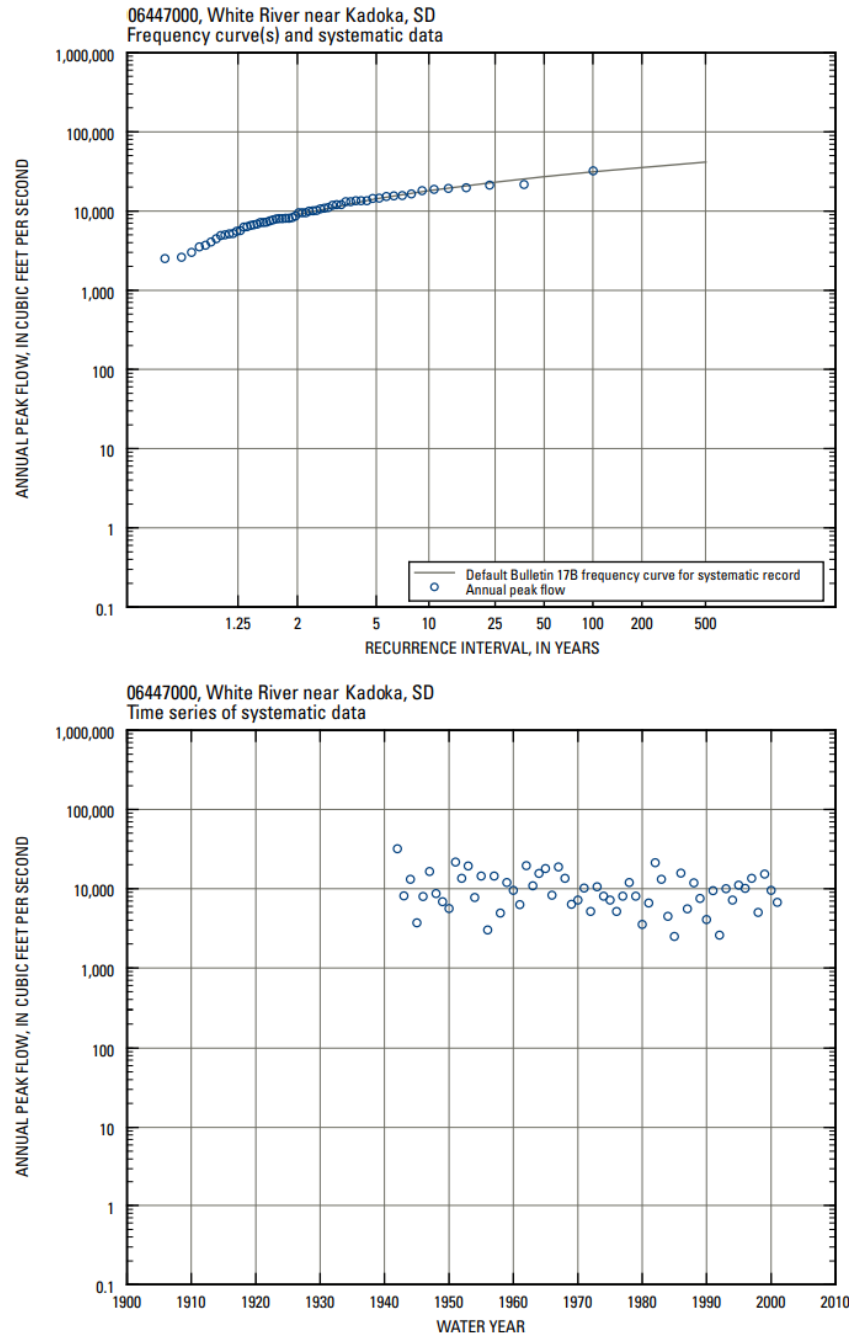


Figure 11.157 Peak-flow information for station 06447000, White River near Kadoka, SD.

Figure 7.14.11. Peak-flow information for station 06447000, White River near Kadoka, SD (from Sando et al., 2008).

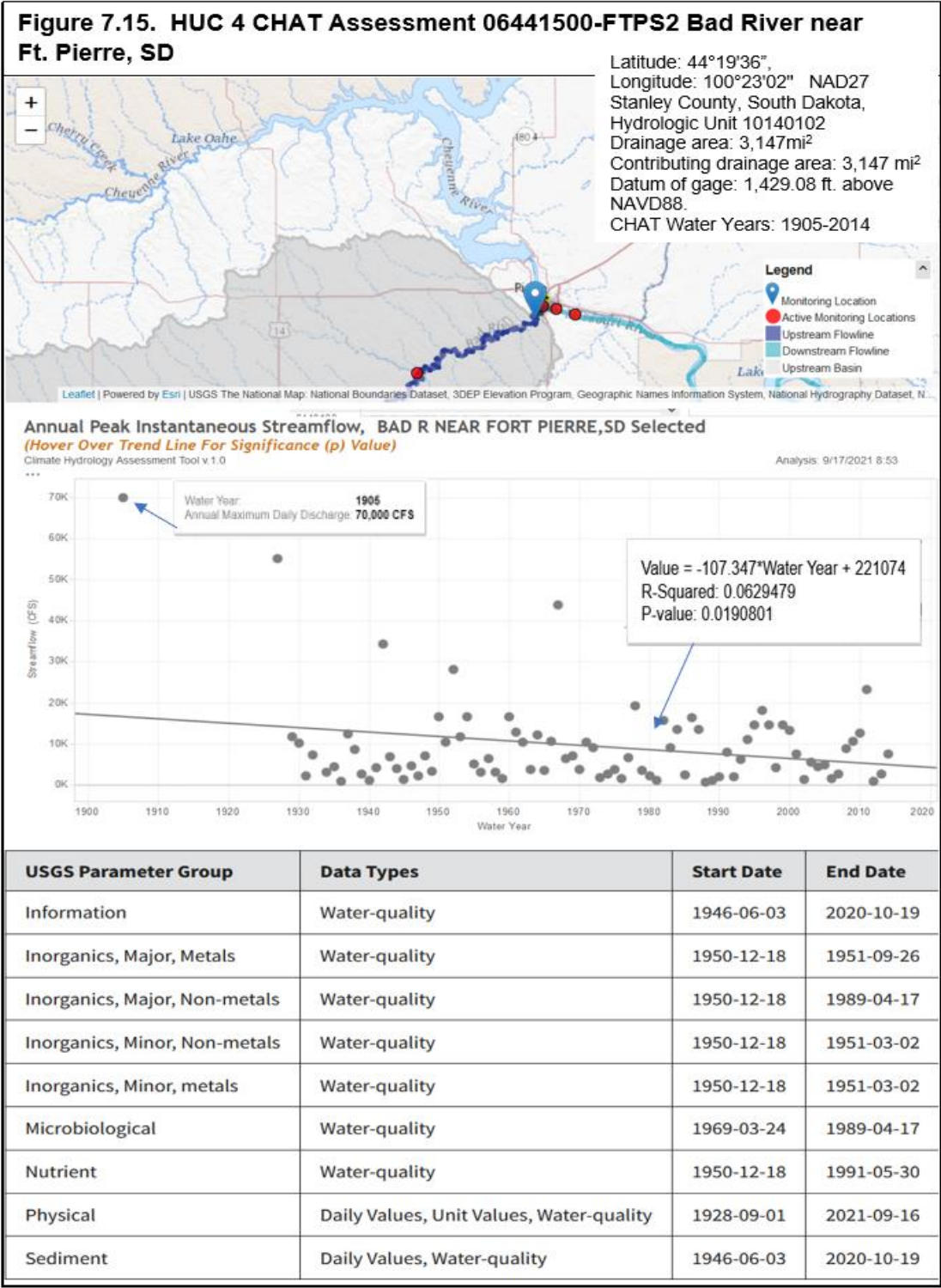


Figure 7.15 USGS Gage 06441500 Bad River Near Ft. Pierre

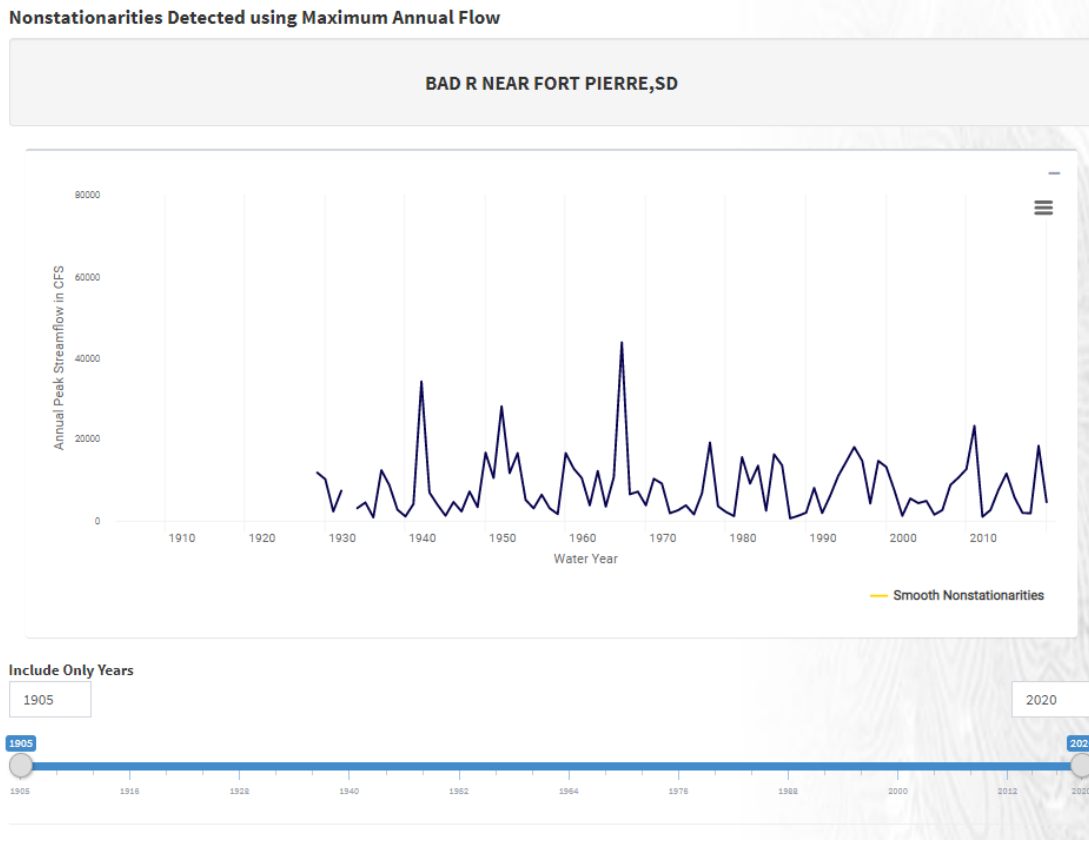


Figure 7.15.1. USGS Gage 06441500 Bad River Near Fort Pierre, SD. Figure 7.5.1. non-stationarities identified for Instantaneous Peak Streamflow (IPS) using annual peak streamflow in cfs, for years 1934-2020 using NSD tool version 2.0. The Bayesian Changepoint Test was not applied as the assumption of normality was not met. A Smooth Lombard Wilcoxon non-stationarity was identified for the years 1926-1929.

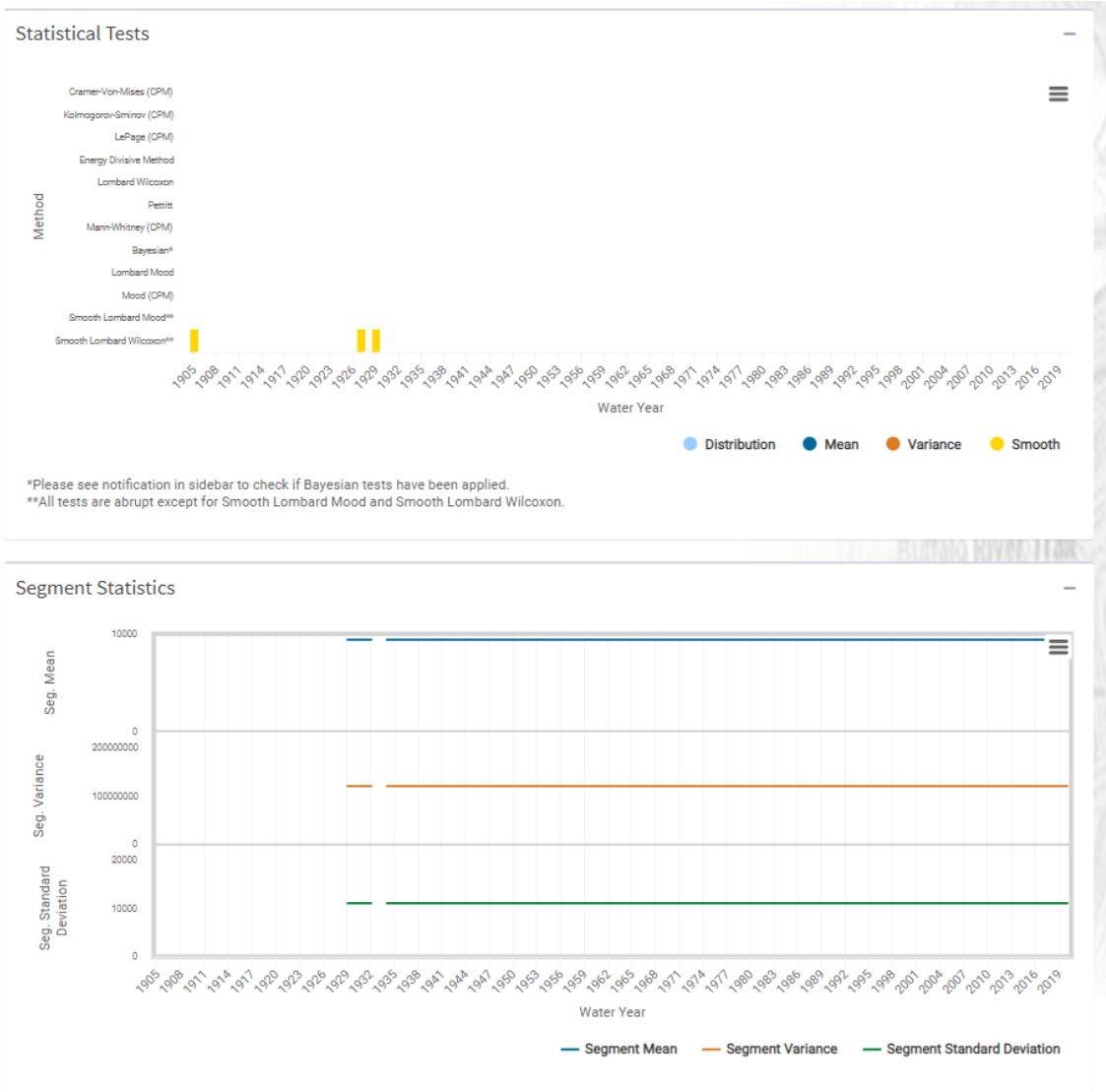
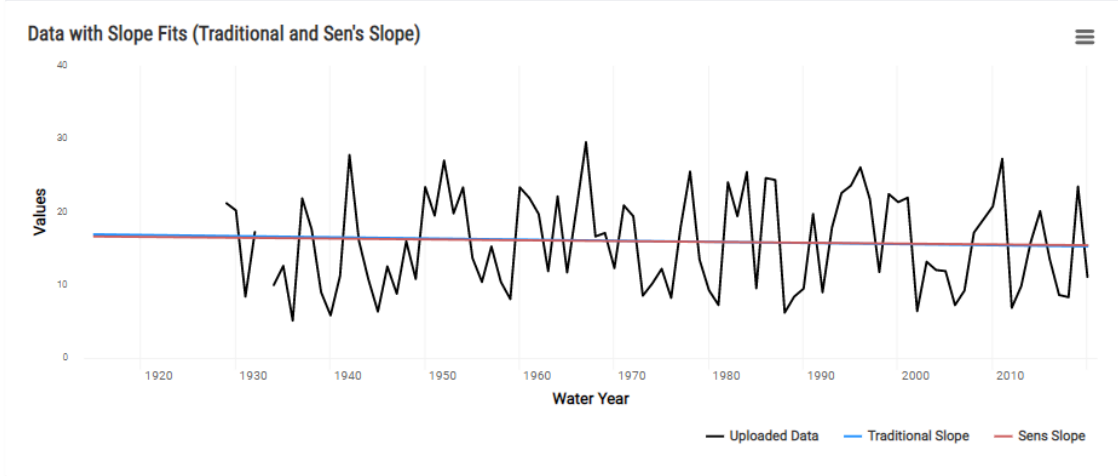


Figure 7.15.2. USGS Gage 06441500 Bad River Near Fort Pierre, SD. There is missing data for this period of record. A Smooth Lombard Wilcoxon non-stationarity was identified for the years 1926-1929.

Plot of Maximum Annual Flow/Height with Slope Fits (Traditional and Sen's Slope)

BAD R NEAR FORT PIERRE,SD



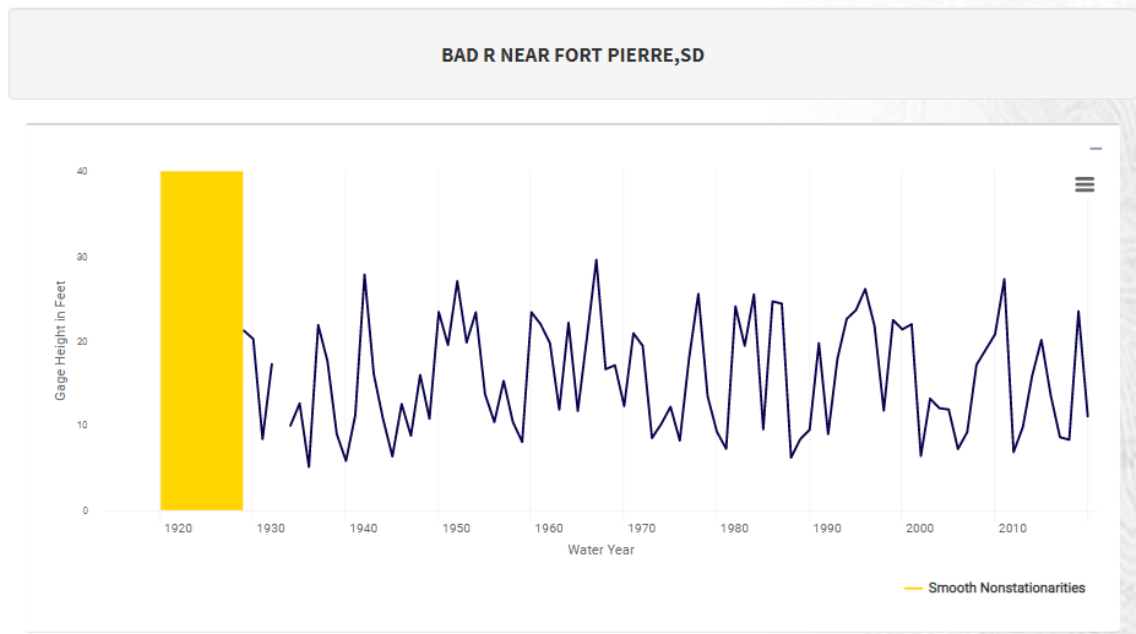
Trend Line Coefficients			
Method	Directionality	Slope	Intercept
Traditional Slope	Positive	0	47
Sen's Slope	Positive	0	39

Trend Hypothesis Test	
Test	PValue
t-Test	0.53452
Mann-Kendall	0.64695
Spearman Rank-Order	0.68945

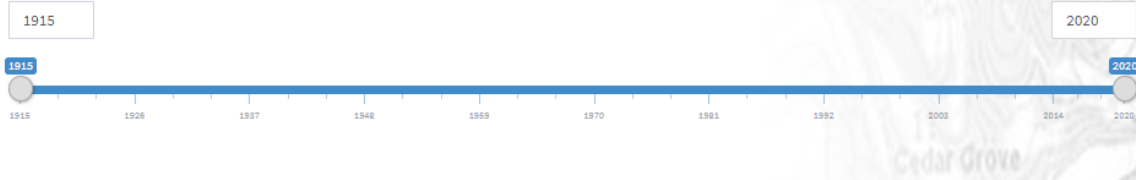
- A statistically significant trend (at the alpha = .05 level) was NOT detected by the Mann-Kendall Test.
- A statistically significant trend (at the alpha = .05 level) was NOT detected by the Spearman Rank-Order Test.

Figure 7.15.3. USGS Gage 06441500 Bad River Near Fort Pierre, SD. plot of gage/stage height (ft.) with slope fits (Traditional and Sen's Slope). No statistically significant trends (at the alpha = 0.05 level) were detected using the Mann-Kendall or the Spearman Rank-Order tests for the period 1934-2020.

Smooth Nonstationarities Detected with Smooth Lombard Wilcoxon



Include Only Years



Smooth Nonstationarities Detected with Smooth Lombard Wilcoxon

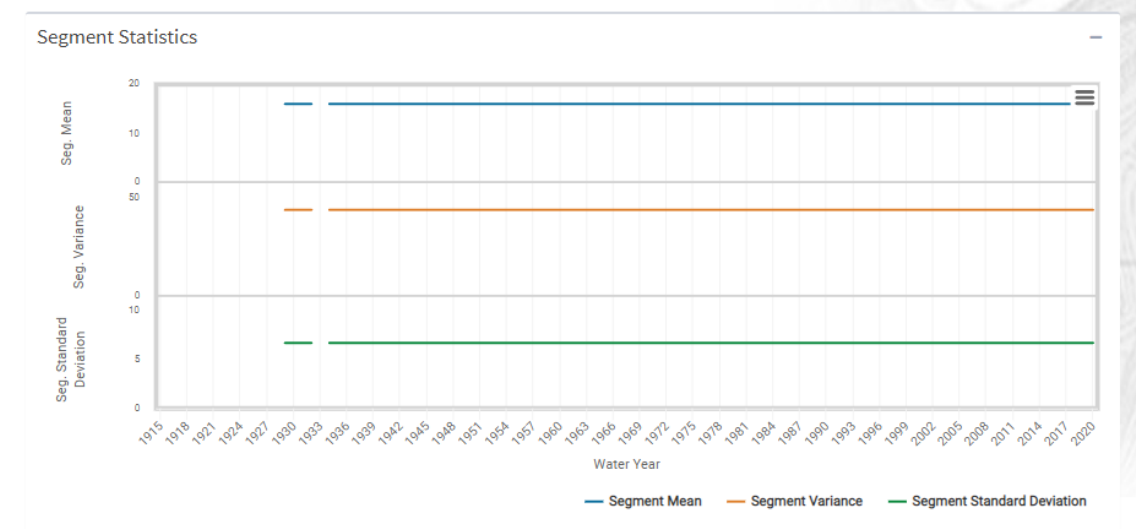


Figure 7.15.4. USGS Gage 06441500 Bad River Near Fort Pierre, SD. Smooth Lombard Wilcoxon was detected in stage/gage height (ft.) from 1918-1929.

Plot of Maximum Annual Flow/Height with Slope Fits (Traditional and Sen's Slope)

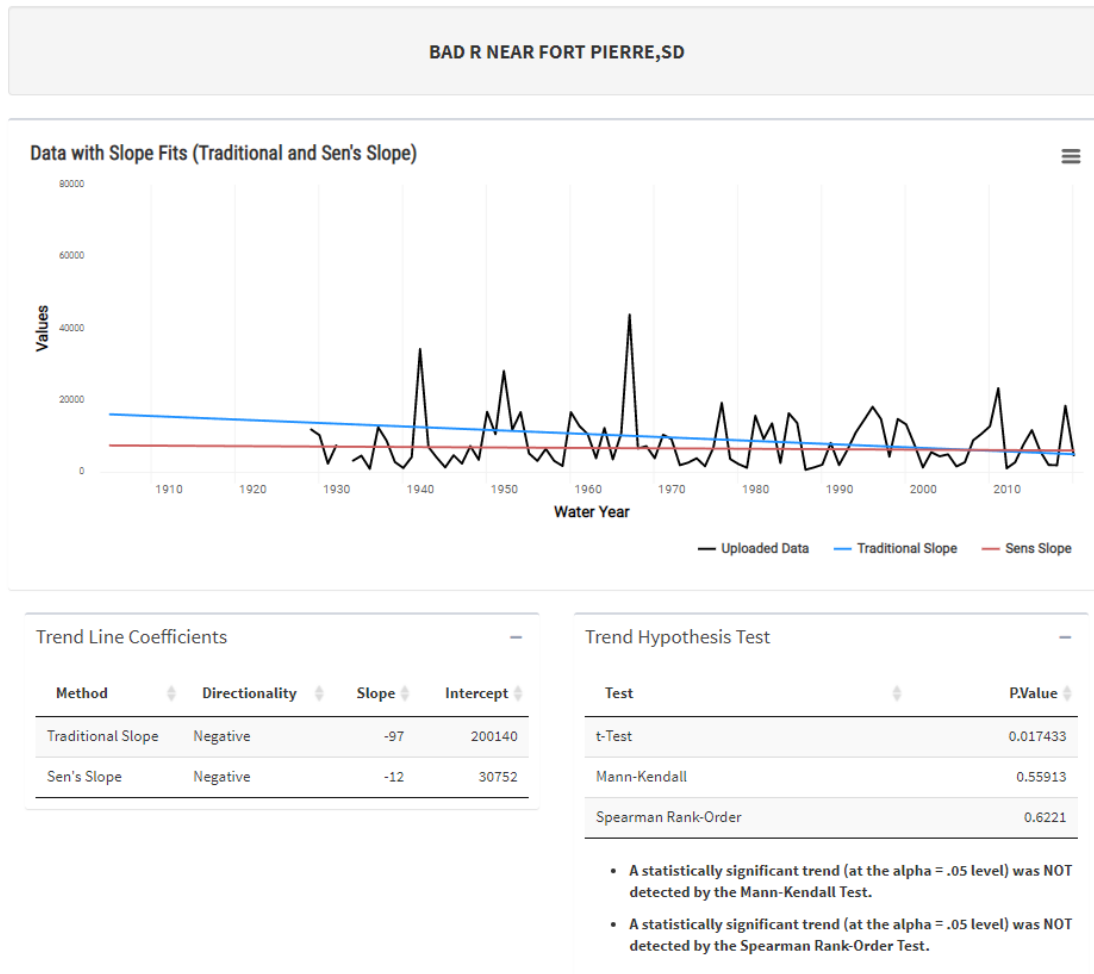


Figure 7.15.5. USGS Gage 06441500 Bad River Near Fort Pierre, SD. plot of gage/stage height (ft.) with slope fits (Traditional and Sen's Slope). No statistically significant trends (at the alpha = 0.05 level) were detected using the Mann-Kendall or the Spearman Rank-Order tests for the period 1905-2020.

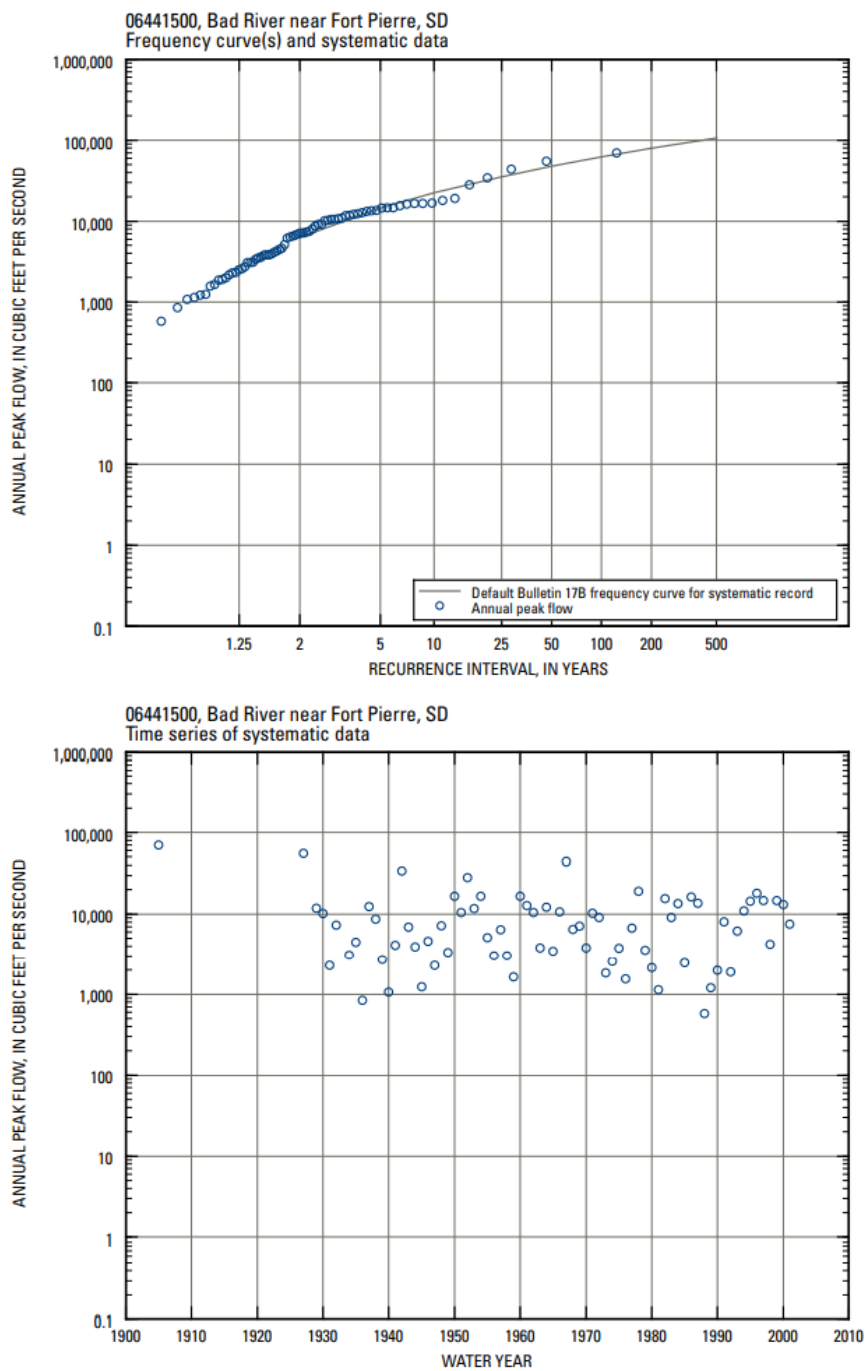
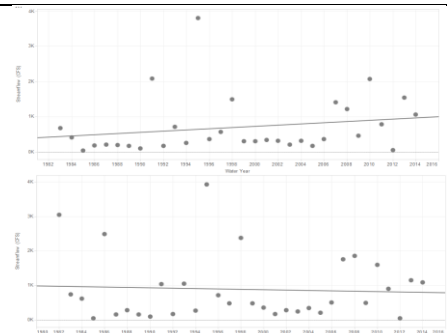
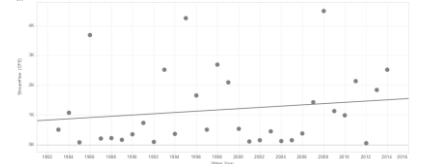


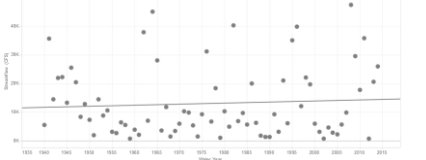
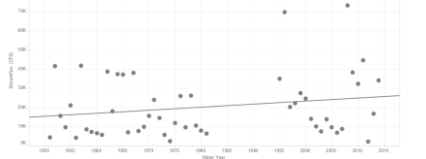
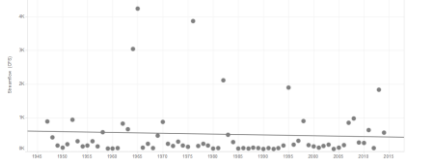
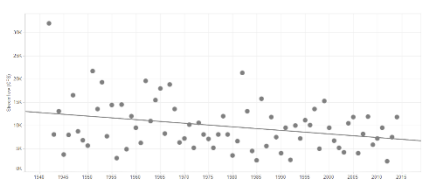
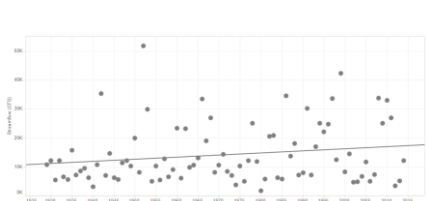


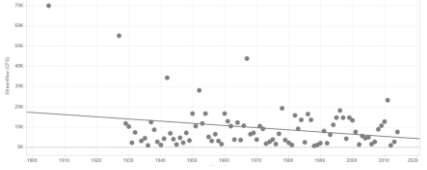
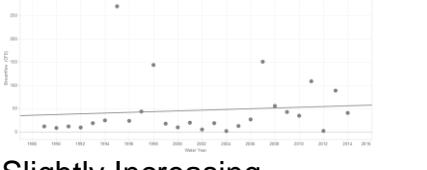

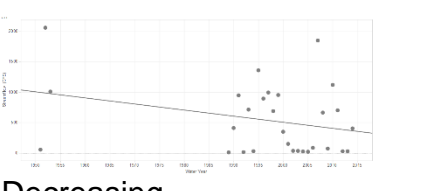
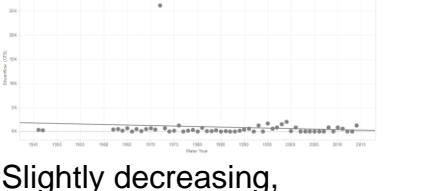
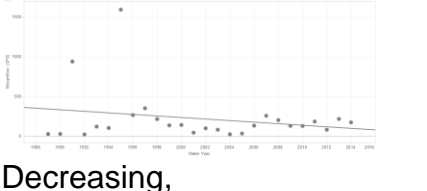
Figure 7.15.6. Peak-flow information for station 06441500, Bad River Near Ft. Pierre, SD (Sando, et al., 2008).

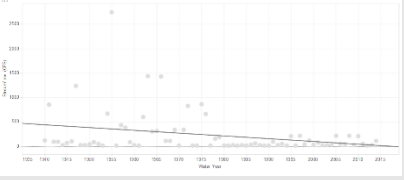
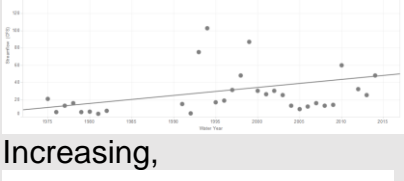
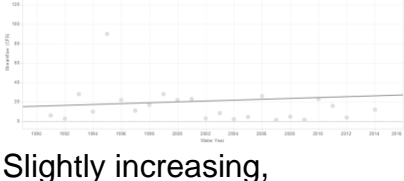
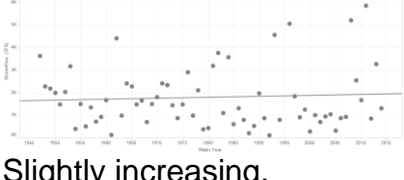
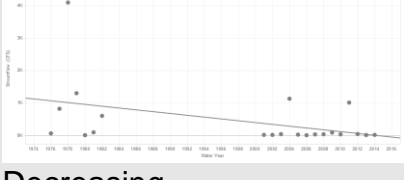
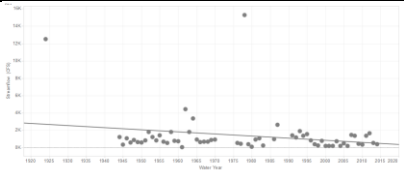


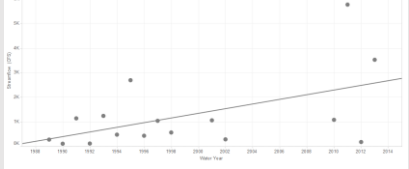

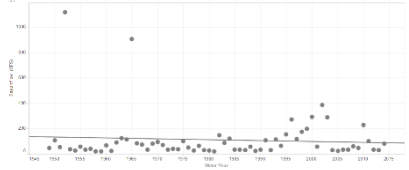
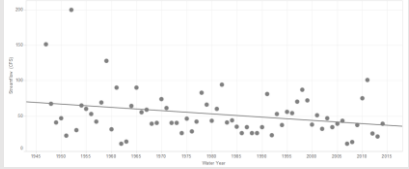
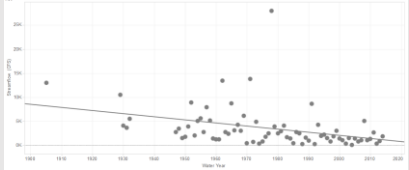
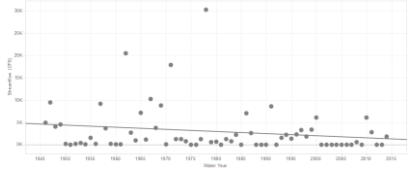
Table 7.2. CHAT Summary. USGS Gage Stations in the study area and those outside the area. Gages highlighted in gray have a p-value <0.05.

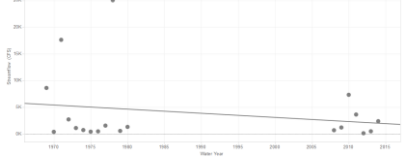
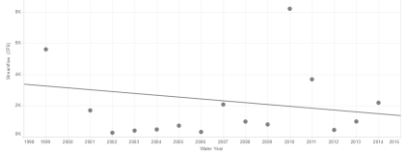
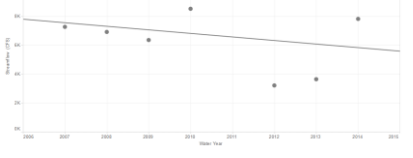
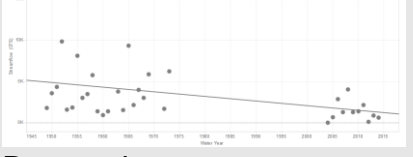
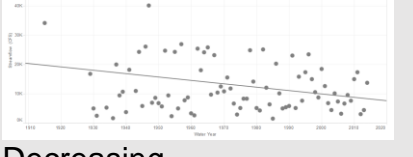
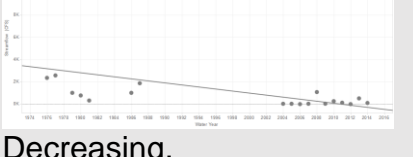
<b>Hydrologic Unit - 1012 Cheyenne</b>			
<b>USGS Gage Site Number Name</b>	<b>Water Year Trend Equation</b>	<b>Record Water Year used</b>	<b>R-squared (coefficient of determination), P-Value</b>
<b>06436190</b> Whitewood Creek Near Whitewood, SD	 Slightly Decreasing, Value = $-5.47393 * \text{Water Year} + 11818.1$	1982-2014	R <sup>2</sup> : 0.0031376  P-Value: 0.756854
<b>06436180</b> Whitewood Creek Above Whitewood, SD	Increasing, Value = $17.0035 * \text{Water Year} + -33277.5$	1983-2014	R <sup>2</sup> : 0.0396332  P-Value: 0.274681
<b>06436198</b> Whitewood Creek Above Vale, SD	 Increasing, Value = $21.3048 * \text{Water Year} + -41401.8$	1983-2014	R <sup>2</sup> : 0.0246537 P-Value: 0.390775
<b>06436000</b> Belle Fourche Near Fruitdale	 Slightly increasing, Value = $4.38933 * \text{Water Year} + -5994.75$	1946-2014	R <sup>2</sup> : 0.0007974 P-Value: 0.817843
<b>06437000</b> Belle Fourche Near Sturgis, SD	 Increasing, Value = $73.7534 * \text{Water Year} + -138985$	1946-2014	R <sup>2</sup> : 0.0370292 P-Value: 0.113175

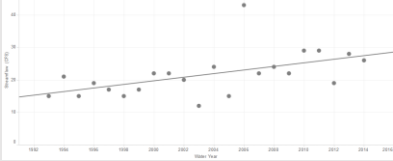
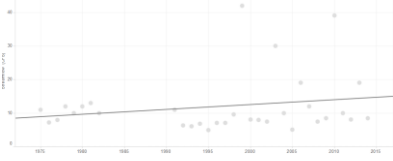
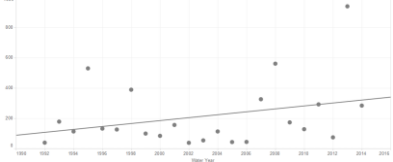
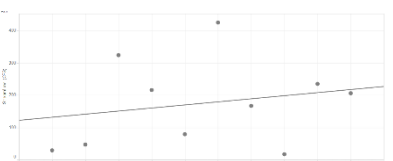
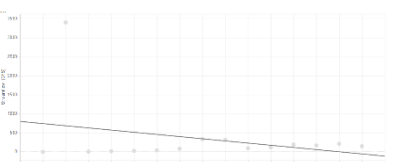
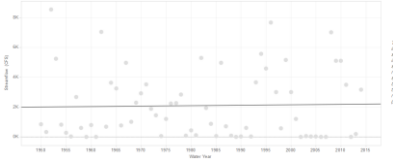
<b>06438000</b> Belle Fourche River Near Elm Springs, SD	 Slightly increasing, $\text{Value} = 24.3859 * \text{Water Year} + -35133.9$	1940-2014	0.004406 P-Value: 0.571519
06438500 Cheyenne River near Plainview, SD	 Slightly Increasing, $\text{Value} = 158.603 * \text{Water Year} + -293971$	1951-2014	0.040583 P-Value: 0.156316
Surrogate Basins Evaluated in the Region but outside the Cheyenne River Study Basin			
06431500 Spearfish Creek at Spearfish, SD	 Slightly Decreasing, $\text{Value} = -2.42972 * \text{Water Year} + 5324.32$	1947-2014	0.0034361 P-Value: 0.634909
06447000 White River near Kadoka, SD	 Decreasing, $\text{Value} = -76.8749 * \text{Water Year} + 161902$	1942-2014	R-Squared: 0.0926207  P-value: 0.0088503
06447200 White River near Oacoma, SD	 Slightly Increasing $\text{Value} = 72.5627 * \text{Water Year} + -128909$	1928-2014	R-Squared: 0.0314567  P-value: 0.102325


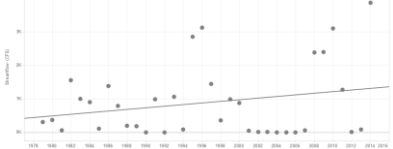
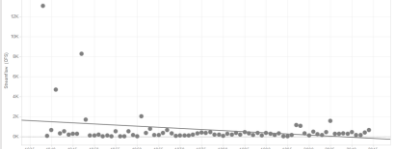
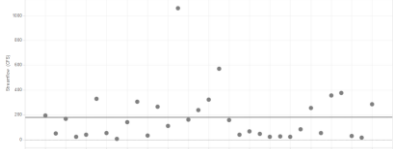
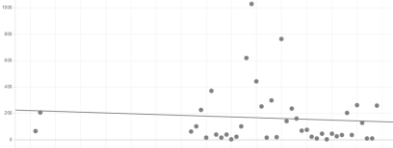
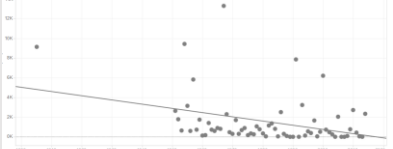
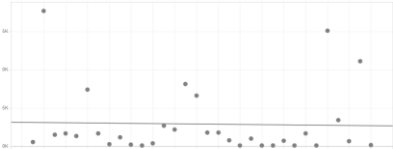
06441500 Bad River Near Fort Pierre, SD	 <p>Slightly Decreasing, Value = <math>-107.347 \cdot \text{Water Year} + 221074</math></p>	1928-2014	R-Squared: 0.0629479  P-Value: 0.0190801
<b>Regional Gages assessed with CHAT in the Cheyenne River HUC not directly associated with the Study</b>			
06430800 Anne Creek Near Lead, SD	 <p>Slightly Increasing Value = <math>0.778427 \cdot \text{Water Year} + -1511.51</math></p>	1989-2014	0.0094315 P-Value: 0.636955
06406000 Battle Creek at Hermosa, SD	 <p>Slightly Increasing, Value = <math>9.3792 \cdot \text{Water Year} + -17447.7</math></p>	1950-2014	0.002637 P-Value: 0.684563
06406500 Battle Creek Below Hermosa, SD	 <p>Decreasing, Value = <math>-10.0081 \cdot \text{Water Year} + 20522.3</math></p>	1951-2014	0.0869327 P-Value: 0.120498
06404000 Battle Creek Near Keystone, SD	 <p>Slightly decreasing, Value = <math>-21.033 \cdot \text{Water Year} + 42689.6</math></p>	1946-2014	0.0104806 P-Value: 0.457026
06437020 Bear Butte Creek Near Deadwood, SD	 <p>Decreasing, Value = <math>-9.74872 \cdot \text{Water Year} + 19731.1</math></p>	1989-2014	0.0504791 P-Value: 0.269826

<p>06402500 Beaver Creek Near Buffalo Gap, SD</p>	 <p>Decreasing, Value = <math>-16.5616 * \text{Water Year} + 33099.9</math></p>	<p>1940-2014</p>	<p>0.0816697 P-Value: 0.0129399</p>
<p>06392900 Beaver Creek at Mallo Camp, Near Four Corners, WY</p>	 <p>Increasing, Value = <math>0.929421 * \text{Water Year} + -1824.87</math></p>	<p>1975-2014</p>	<p>0.117496 P-Value: 0.054791</p>
<p>06402430 Beaver Creek Near Pringle, SD</p>	 <p>Slightly increasing, Value = <math>0.447913 * \text{Water Year} + -875.813</math></p>	<p>1991-2014</p>	<p>0.0103198 P-Value: 0.636693</p>
<p>06428500 Belle Fourche at WY-SD State Line</p>	 <p>Slightly increasing, Value = <math>4.2075 * \text{Water Year} + -6539.2</math></p>	<p>1947-2014</p>	<p>0.0034884 P-Value: 0.632345</p>
<p>06425720 Belle Fourche River Below Rattlesnake Creek, Near Piney, WY</p>	 <p>Decreasing, Value = <math>-28.0117 * \text{Water Year} + 56416.9</math></p>	<p>1976-2014</p>	<p>0.180275 P-Value: 0.0550511</p>
<p>06426500 Belle Fourche River Below Moorcroft, WY</p>	 <p>Decreasing, Value = <math>-24.264 * \text{Water Year} + 49372.3</math></p>	<p>1924-2014</p>	<p>0.0522741 P-Value: 0.0738736</p>

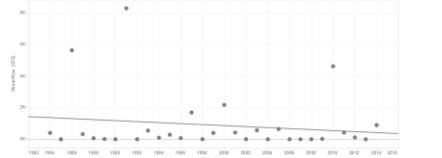
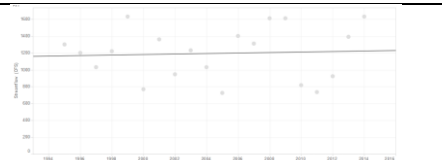

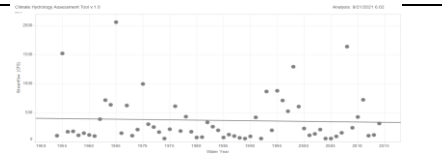
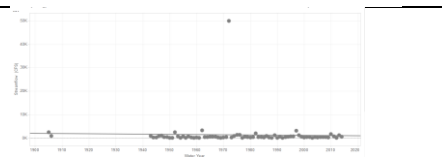
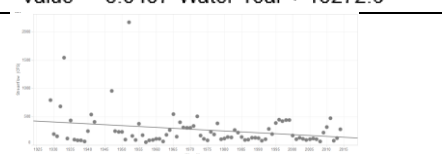
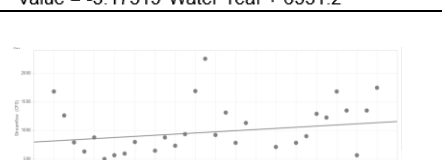
<p>06428200 Belle Fourche River Near Alva, WY</p>	 <p><b>Increasing,</b> Value = 94.7004*Water Year + -188058</p>	<p>1989-2013</p>	<p>0.263232 P-Value: 0.0421119</p>
<p>06422500 Box Elder Creek Near Nemo, SD</p>	 <p><b>Decreasing,</b> Value = -88.0656*Water Year + 176124</p>	<p>1907-2014</p>	<p>0.140268 P-Value: 0.0062302</p>
<p>06409000 Castle Creek Above Deerfield Reservoir Near Hill City, SD</p>	 <p><b>Decreasing,</b> Value = -0.703497*Water Year + 1504.39</p>	<p>1949-2014</p>	<p>0.0057536 P-Value: 0.544962</p>
<p>06410000 Castle Creek Below Deerfield Dam, SD</p>	 <p><b>Decreasing,</b> Value = -0.459938*Water Year + 963.496</p>	<p>1947-2014</p>	<p>0.0808426 P-Value: 0.0187791</p>
<p>06395000 Cheyenne River at Edgemont, SD</p>	 <p><b>Decreasing,</b> Value = -64.4781*Water Year + 131050</p>	<p>1905-2014</p>	<p>0.131815 P-Value: 0.0015943</p>
<p>06401500 Cheyenne River Below Angostura Dam, SD</p>	 <p><b>Decreasing,</b> Value = -47.497*Water Year + 97024.3</p>	<p>1946-2014</p>	<p>0.0336704 P-Value: 0.131242</p>

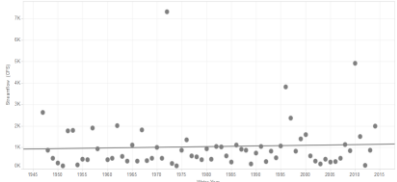
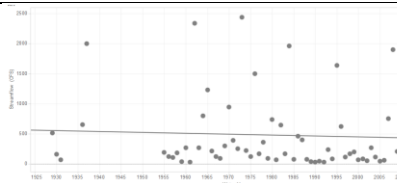
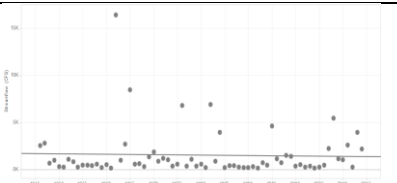
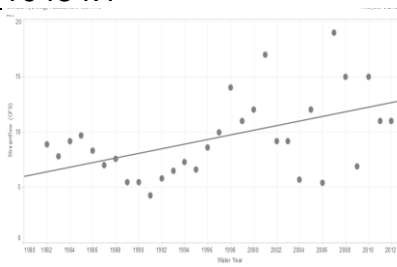
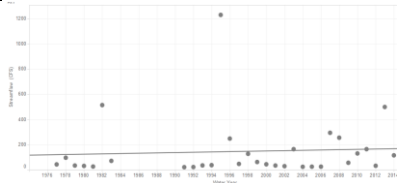
<p>06402600 Cheyenne River Near Buffalo Gap, SD</p>	 <p><b>Decreasing,</b> Value = <math>-77.1821 \cdot \text{Water Year} + 157481</math></p>	<p>1969-2014</p>	<p>0.0458127 P-Value: 0.378915</p>
<p>06403700 Cheyenne River at Red Shirt, SD</p>	 <p><b>Decreasing,</b> Value = <math>-118.376 \cdot \text{Water Year} + 239895</math></p>	<p>1999-2014</p>	<p>0.0395215 P-Value: 0.460447</p>
<p>06408650 Cheyenne River Near Scenic, SD</p>	 <p><b>Decreasing,</b> Value = <math>-245.714 \cdot \text{Water Year} + 500694</math></p>	<p>2007-2014</p>	<p>0.070285 P-Value: 0.525713</p>
<p>06386500 Cheyenne River Near Spencer, WY</p>	 <p><b>Decreasing,</b> Value = <math>-56.0887 \cdot \text{Water Year} + 114254</math></p>	<p>1949-2014</p>	<p>0.162016 P-Value: 0.0182728</p>
<p>06423500 Cheyenne River Near Wasta, SD</p>	 <p><b>Decreasing,</b> Value = <math>-115.457 \cdot \text{Water Year} + 240836</math></p>	<p>1915-2014</p>	<p>0.0838661 P-Value: 0.0068402</p>
<p>06365900 Cheyenne River Near Dull Center, WY</p>	 <p><b>Decreasing,</b> Value = <math>-91.0735 \cdot \text{Water Year} + 183133</math></p>	<p>1976-2014</p>	<p>0.256251 P-Value: 0.0270012</p>

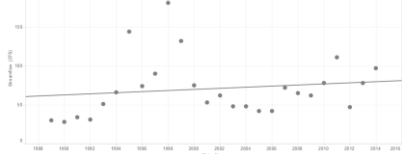
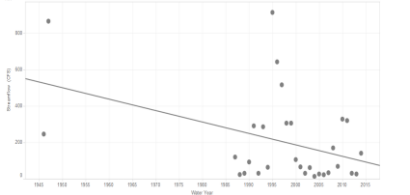
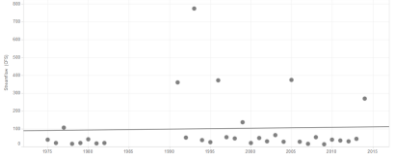
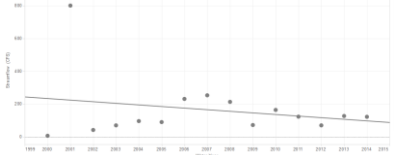
<p>06412810 Cleghorn Springs at Rapid City, SD</p>	 <p>Increasing, Value = 0.55336*Water Year + -1087.02</p>	<p>1993-2014</p>	<p>0.280954 P-Value: 0.0111684</p>
<p>06429500 Cold Springs Creek at Buckhorn, WY</p>	 <p>Increasing, Value = 0.144804*Water Year + -277.117</p>	<p>1975-2014</p>	<p>0.0393872 P-Value: 0.276207</p>
<p>06430532 Crow Creek Near Beulah, WY</p>	 <p>Increasing, Value = 9.69466*Water Year + -19204.7</p>	<p>1992-2014</p>	<p>0.091004 P-Value: 0.161839</p>
<p>06436165 Deadwood Creek at Central City, SD</p>	 <p>Increasing, Value = 9.53333*Water Year + -18982.7</p>	<p>2005-2014</p>	<p>0.0460324 P-Value: 0.551683</p>
<p>06426130 Donkey Creek Near Gillette, WY</p>	 <p>Decreasing, Value = -56.9494*Water Year + 114642</p>	<p>2000-2014</p>	<p>0.0893472 P-Value: 0.279152</p>
<p>06425500 Elk Creek Near Elm Springs, SD</p>	 <p>Slightly increasing, Value = 2.94681*Water Year + -3744.66</p>	<p>1950-2014</p>	<p>0.0006055 P-Value: 0.845728</p>

06424000 Elk Creek Near Roubaix, SD	 <p>Decreasing, Value = <math>-2.19029 \times \text{Water Year} + 4543.5</math></p>	1946-2014	0.111634 P-Value: 0.102604
06425100 Elk Creek Near Rapid City, SD	 <p>Increasing, Value = <math>24.1008 \times \text{Water Year} - 47227.2</math></p>	1979-2014	0.0558863 P-Value: 0.165099
06402000 Fall River at Hot Springs	 <p>Decreasing, Value = <math>-22.213 \times \text{Water Year} + 44587</math></p>	1938-2014	0.0764649 P-Value: 0.0149139
06403300 French Creek Above Fairburn, SD	 <p>Static Value = <math>0.0456551 \times \text{Water Year} + 87.6478</math></p>	1982-2014	0.00000493 P-Value: 0.990764
06404998 Grace Coolidge Creek Near Game Lodge Near Custer, SD	 <p>Slightly decreasing Value = <math>-1.20401 \times \text{Water Year} + 2562.27</math></p>	1945-2014	0.0069606 P-Value: 0.608775
06400000 Hat Creek Near Edgemont, SD	 <p>Decreasing, Value = <math>-42.7117 \times \text{Water Year} + 86176.8</math></p>	1905-2014	0.122966 P-Value:
06436760 Horse Creek Above Vale, SD	 <p>Static, Value = <math>-13.6972 \times \text{Water Year} + 30232.9</math></p>	1980-2014	0.0008398 P-Value: 0.874896



<p>06400875 Horsehead Creek at Oelrichs, SD</p>	 <p>Decreasing, Value = <math>-31.5947 \cdot \text{Water Year} + 64050.2</math></p>	<p>1984-2014</p>	<p>0.0231719 P-Value: 0.413646</p>
<p>06434505 Inlet Canal Above Belle Fourche Reservoir, SD</p>	 <p>Slight increase, Value = <math>3.00075 \cdot \text{Water Year} + -4821.76</math></p>	<p>1995-2014</p>	<p>0.0033201 P-Value: 0.809236</p>
<p>06412500 Rapid Creek Above Canyon Lake Near Rapid City, SD</p>	 <p>Slight decrease, Value = <math>-13.0787 \cdot \text{Water Year} + 26672.1</math></p>	<p>1947-2015</p>	<p>0.00471214 P-Value: 0.577682</p>
<p>06410500 Rapid Creek Above Pactola Reservoir at Silver City, SD</p>	 <p>Slight Decrease, Value = <math>-1.06843 \cdot \text{Water Year} + 2486.44</math></p>	<p>1954-2014</p>	<p>0.0020668 P-Value: 0.727914</p>
<p>06414000 Rapid Creek at Rapid City, SD</p>	 <p>Slight Decrease, Value = <math>-8.5457 \cdot \text{Water Year} + 18272.6</math></p>	<p>1905-2014</p>	<p>0.0012474 P-Value: 0.764132</p>
<p>06411500 Rapid Creek Below Pactola Dam, SD</p>	 <p>Decrease, Value = <math>-3.17319 \cdot \text{Water Year} + 6531.2</math></p>	<p>1929-2014</p>	<p>0.0646513 P-Value: 0.0211579</p>
<p>06418900 Rapid City Below Sewage Treatment Plant Near Rapid City, SD</p>	 <p>Increasing Value = <math>10.0013 \cdot \text{Water Year} + -19007.9</math></p>	<p>1982-2014</p>	<p>0.4265354 P-Value: 0.248953</p>

<p>06421500 Rapid Creek Near Farmingdale, SD</p>	 <p>Slight Increase, Value = <math>3.09798 \cdot \text{Water Year} + -5092.6</math></p>	<p>1947-2014</p>	<p>0.0028701 P-Value: 0.666777</p>
<p>06430500 Redwater Creek at WY-SD State Line</p>	 <p>Slight Decrease, Value = <math>-1.48371 \cdot \text{Water Year} + 3415.94</math></p>	<p>1929-2014</p>	<p>0.0028538 P-Value: 0.672561</p>
<p>06433000 Redwater River Above Belle Fourche, SD</p>	 <p>Static, Value = - <math>4.52079 \cdot \text{Water Year} + 10484.1</math></p>	<p>1946-2014</p>	<p>0.0013233 P-Value: 0.766662</p>
<p>06408700 Rhoads Fork Near Rochford, SD</p>	 <p>Increasing, Value = <math>0.20859 \cdot \text{Water Year} + -407.035</math></p>	<p>1982-2014</p>	<p>0.268854 P-Value: 0.0019927</p>
<p>06429905 Sand Creek Near Ranch A, Near Beulah, WY</p>	 <p>Slightly increased, Value = <math>1.28104 \cdot \text{Water Year} + -2412.51</math></p>	<p>1977-2014</p>	<p>0.0037539 P-Value: 0.743351</p>

<p>06430770 Spearfish Creek Near Lead, SD</p>	 <p>Slight increase, Value = <math>0.708034 * \text{Water Year} + -1346.32</math></p>	<p>1989-2014</p>	<p>0.0211458 P-Value: 0.478452</p>
<p>06407500 Spring Creek Near Keystone, SD</p>	 <p>Decreasing, Value = - <math>6.26813 * \text{Water Year} + 12722.9</math></p>	<p>1946-2014</p>	<p>0.166273 P-Value: 0.0253026</p>
<p>Stockade Beaver Creek Near Newcastle, WY</p>	 <p>slight increase Value = <math>0.506261 * \text{Water Year} + -909.193</math></p>	<p>1975-2014</p>	<p>0.0014566 P-Value: 0.83571</p>
<p>06426160 Stonepile Creek at Mouth Near Gillette, WY</p>	 <p>Decreasing, Value = - <math>9.72464 * \text{Water Year} + 19683.6</math></p>	<p>2000-2014</p>	<p>0.0530976 P-Value: 0.408673</p>

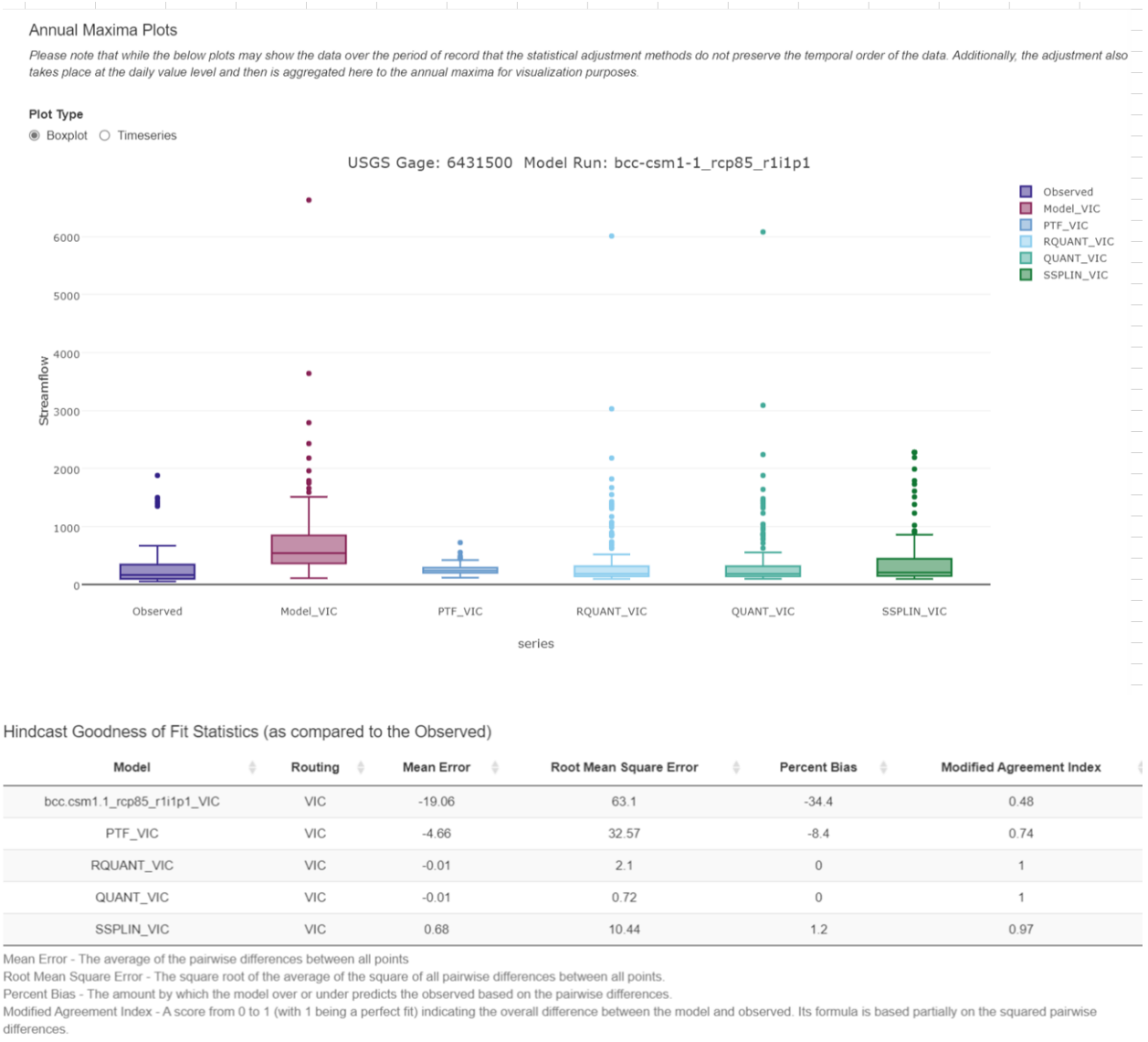
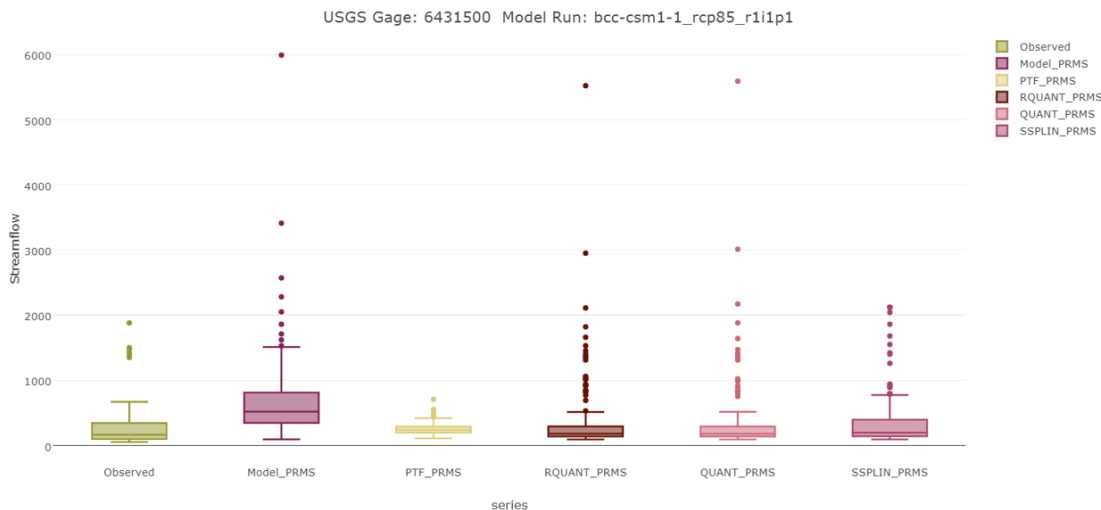


Figure 7.16. USGS Gage Spearfish Creek at Spearfish, SD; examples of downscaled GCM (BCC-csm101\_rcp85\_r1i1p1). The figure shows the different box plots for annual maxima and the hindcast fit compared to the observed data for the VIC hydrologic model.

Annual Maxima Plots

Please note that while the below plots may show the data over the period of record that the statistical adjustment methods do not preserve the temporal order of the data. Additionally, the adjustment also takes place at the daily value level and then is aggregated here to the annual maxima for visualization purposes.

Plot Type  
 Boxplot  Timeseries



You can zoom in on a set of data by holding down the left-mouse button and dragging, and you can zoom out by holding the Ctrl button and double clicking. All of the graphs shown are synchronized, so selecting values in one will select analogous values in all of them.

Hindcast Goodness of Fit Statistics (as compared to the Observed)

Model	Routing	Mean Error	Root Mean Square Error	Percent Bias	Modified Agreement Index
bcc.csm1.1_rcp85_r1i1p1_PRMS	PRMS	-19.1	62.2	-34.5	0.48
PTF_PRMS	PRMS	-4.67	32.44	-8.4	0.75
RQUANT_PRMS	PRMS	0	1.52	0	1
QUANT_PRMS	PRMS	-0.02	0.75	0	1
SSPLIN_PRMS	PRMS	0.52	8.85	0.9	0.97

Mean Error - The average of the pairwise differences between all points

Root Mean Square Error - The square root of the average of the square of all pairwise differences between all points.

Percent Bias - The amount by which the model over or under predicts the observed based on the pairwise differences.

Modified Agreement Index - A score from 0 to 1 (with 1 being a perfect fit) indicating the overall difference between the model and observed. Its formula is based partially on the squared pairwise differences.

Figure 7.17. USGS Gage Spearfish Creek at Spearfish, SD; examples of downscaled GCM (BCC-csm101\_rcp85\_r1i1p1). The figure shows the different box plots for annual maxima and the hindcast fit compared to the observed data for the PRMS hydrologic model.

### Annual Maxima Plots

Please note that while the below plots may show the data over the period of record that the statistical adjustment methods do not preserve the temporal order of the data. Additionally, the adjustment also takes place at the daily value level and then is aggregated here to the annual maxima for visualization purposes.

#### Plot Type

Boxplot  Timeseries



You can zoom in on a set of data by holding down the left-mouse button and dragging, and you can zoom out by holding the Ctrl button and double clicking. All of the graphs shown are synchronized, so selecting values in one will select analogous values in all of them.

Figure 7.18. USGS Gage Spearfish Creek at Spearfish, SD; examples of downscaled GCM (BCC-csm101\_rcp85\_r1i1p1). The figure shows the hindcast and scenario for future annual maxima plots for the VIC hydrological model. Quantile step size is 0.01%.

### Annual Maxima Plots

Please note that while the below plots may show the data over the period of record that the statistical adjustment methods do not preserve the temporal order of the data. Additionally, the adjustment also takes place at the daily value level and then is aggregated here to the annual maxima for visualization purposes.

#### Plot Type

Boxplot  Timeseries



You can zoom in on a set of data by holding down the left-mouse button and dragging, and you can zoom out by holding the Ctrl button and double clicking. All of the graphs shown are synchronized, so selecting values in one will select analogous values in all of them.

[About this model run](#)

Figure 7.19. USGS Gage Spearfish Creek at Spearfish, SD; examples of downscaled GCM (BCC-csm101\_rcp85\_r1i1p1). The figure shows the hindcast and scenario for future annual maxima plots for the PRMS hydrological model. Quantile step size is 0.01%.

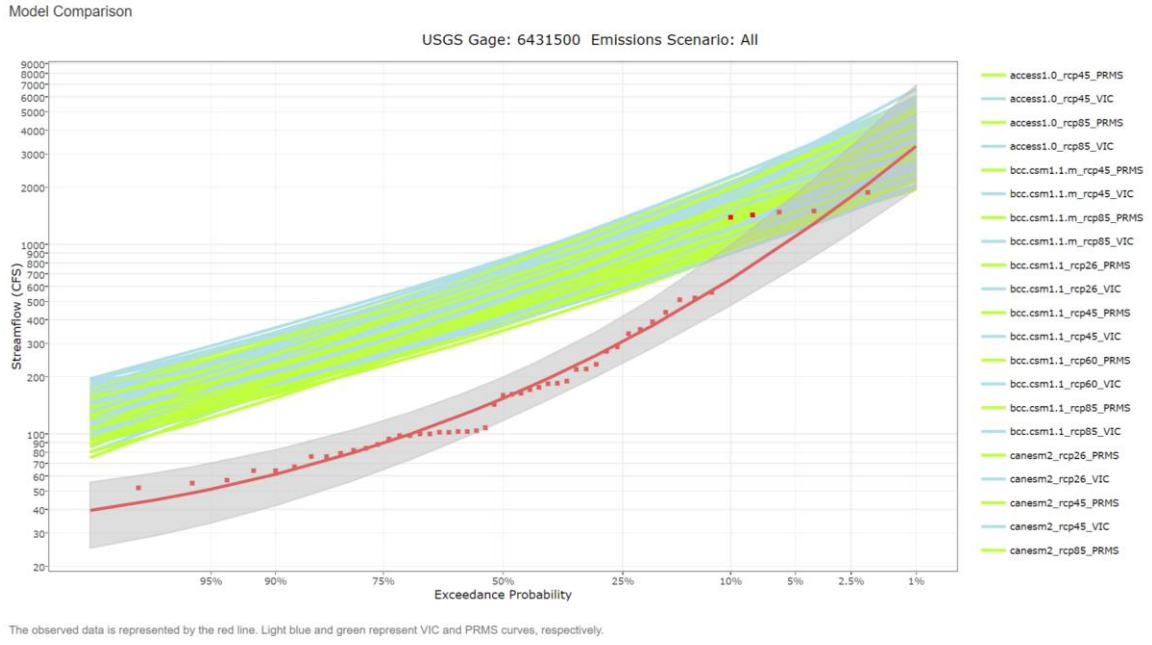


Figure 7.20. Pilot analysis of 17B curves representing model comparison scenario for all GCMs, all emission scenarios. Quantile step size is 0.01%, downscaled and populated with historical data from USGS Gage 0431500 Spearfish Creek at Spearfish, SD. Data then was input into both VIC and PRMS. Observed data is represented by the red line. Light blue and green represent VIC and PRMS curves, respectively. Annual Maxima Flow is in cfs. Confidence intervals are presented in gray. Plot of GCM model runs is unadjusted. No quantile mapping strategy is applied. For calculation, reported station skew was used.



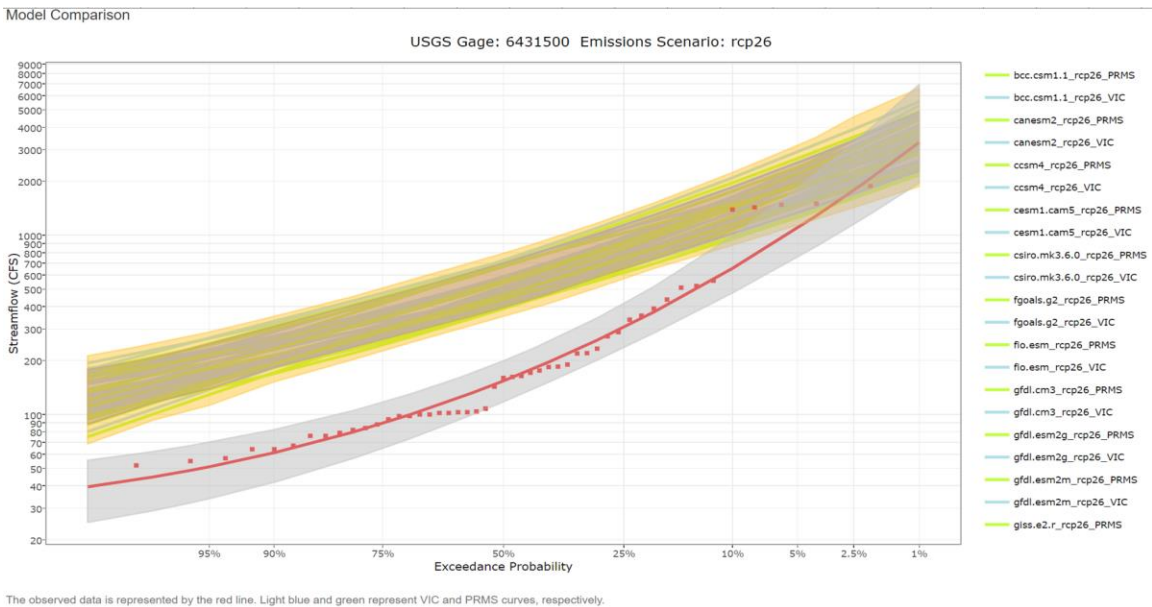


Figure 7.21. 17B curves representing daily statistical adjustment applied to annual maxima, with hindcast period. No quantile mapping strategy with station skew for USGS Gage 06413500 Spearfish Creek at Spearfish, SD.

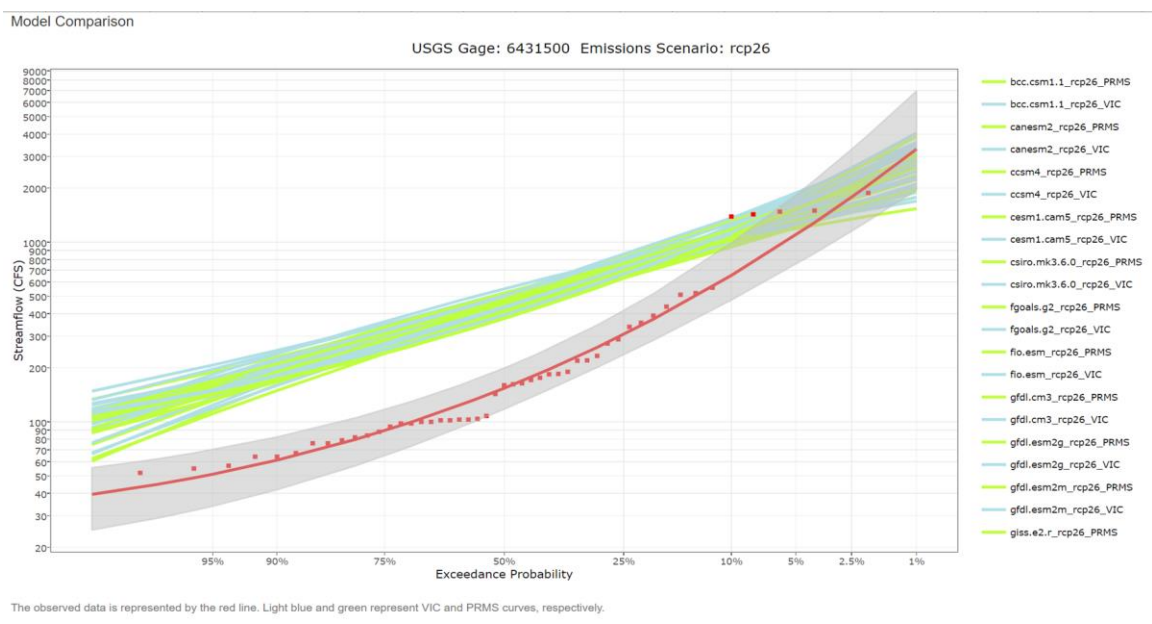


Figure 7.22. For a pilot assessment, annual maxima were used to determine observed confidence intervals, plot of unadjusted runs. Period in red reflects hindcast data from historical gage records.

Sediment transport is controlled by stream discharge. Sediment transport prediction refers to the methods and techniques to predict the equilibrium or steady rate of sediment transport in streams and rivers. This study found that there are non-stationarities in trend data when plotting the annual maximum of average monthly stream flow and gage/stage height discharge records at stream gages with time. This impacts the ability to create or modify representative sediment rating curves, which are fitted relationships between river discharge and suspended-sediment concentration, and are commonly used to assess patterns and trends in river water quality.

Because there is some evidence of potential increases to flood risk in the future based on projected datasets and basin conditions, it is suggested that flood risk continue to be monitored to see if a trend of increasing flow magnitudes begins to materialize within the basin. If a change of trend should begin to emerge, resilience measures should be considered. In addition to monitoring, the point where increases to flood risk would begin to critically undermine conditions should be identified.

Portions of this assessment indicate that flood risk has increased and may continue to increase in the future. Other information presented in this assessment, however, indicates that a great deal of uncertainty is associated with hydrologic parameters and their response to climate change. The use of surrogate GCM data for spatially downscaled, hydrologically simulated and routed statistically aggregated CMIP 5 GCM outputs at the HUC 8 watershed level indicates an increase for mean annual maximum of stage (representing

streamflow). However, simulated flows represented at individual stream gage sites generated from tools are not always in agreement.

Warmer air temperatures exert considerable control over numerous aquatic ecosystem processes, including lake and river ice dynamics. They can also have important implications for nuisance algal blooms and the stream ecological community structure. Elevated temperatures and enhanced biological mediated growth of algal blooms in the streams and reservoir could affect levels of dissolved oxygen concentration and the costs of treating water for potable supply.

In the event of climate change-induced higher precipitation in the Black Hills, the concentration of runoff during spring snowmelt, the descending elevation, and stream bedrock at/near the Whitewood Creek confluence with the Belle Fourche River should provide relatively efficient conditions for moving sediment in the lower reaches of Whitewood Creek. There is significant spatial and temporal variability in suspended sediment and associated trace element concentrations as they move toward their destination in the Oahe Reservoir. Information from this assessment, reviewed in the literature indicates an increase in precipitation in the future. This would create the potential for more erosion of the stream channels. With periods of sustained high flow, the potential for stream banks to become saturated increases, creating conditions for bank instability and discrete landslides that deliver sediment directly into the stream.

The study basin does not have homogenous geology. The contrasting color of tailings deposited among the natural alluvium is still evident in areas of

Whitewood Creek and the Belle Fourche River, providing a good visual indicator of the presence of tailings and distinction between pre-and post-mining alluvium. Arsenic is the primary tracer for mining contaminated sediment, and if post-mining alluvium is not distinguished by visual identification, tools can be used for mineral identification. Capable of detecting semiquantitative concentrations of arsenic in the stream bed, these tools include calibrated field portable-based X-ray fluorescence and laser-induced breakdown spectrometers (LIBS for elemental analysis; and visible and near infrared (Vis/NIR) spectrometer. Wuolo (1986), Goddard (1989), Marron (1992), and Pfeifle (2018) all provided minerology and chemistry of tailings sediment, which would be a tracer to identify areas where tailings may still be present. Horowitz and Elrick (2017) suggest that bed sediments can be used to address/identify certain types of water quality problems and could be employed more frequently for that purpose. Examples where bed sediments could be used include:

- Identifying new potential long-term monitoring sites/water quality “hot spots.”
- Building on established water quality/geochemical history available for a particular site/area.
- Use as a surrogate for establishing mean/median chemical values for suspended sediment.

Longer duration droughts are likely, even in areas where net annual precipitation does not change. During droughts, lower minimum flows may create less volume for dilution of ground water discharge and result in higher

concentrations of related constituents downstream of ground water seeps and inflow into the stream. Increased evaporation can also create very water-soluble effervescent sulfate salts which may be subject to transport by wind or rapid dissolution with future streamflow.

## Chapter 8: Summary and Recommendations

First and foremost, a large-scale, concerted effort to reduce greenhouse gas emissions is of primary importance in mitigating the effects of climate change. Though GHG levels will continue to rise in the foreseeable future even with immediate mitigating measures, no other action would likely have as much positive, long-range effect.

Based on the literature review, trend regression analysis, climate hydrology assessment, and non-stationarity analysis, it can be stated with certainty that a changing climate is a factor to consider in the Cheyenne River Basin, and likely a consideration that will persist well into the future. Climate change affects multiple hydroclimatic variables; however, the full extent of its impact is difficult to ascertain in a qualitative assessment with existing hydrologic data. Allen, et al. (2002) probably put it best: Climate change prediction is about quantifying risk and probabilities, and its effect on rainfall (precipitation) distributions could have greater impact than the risks posed by global warming. With water managers having more control over demand than over precipitation, water management practices responsive to this new reality and social changes affecting water use are the most realistic approaches to dealing with and mitigating the effects of either not enough or too much water as a consequence of climate change.

One obvious recommendation would be to improve the vertical datum in the entire Cheyenne River Basin, so that grids represent actual elevations (and digital elevation models) with the accuracy and precision needed for detailed

analysis. Various dynamic processes can impact elevations tied to geodetic and water level datums, and these processes would need to be monitored through development and use of common standard procedures. To meet the requirements of atmospheric models, hydrological data should be reported as point data of the highest possible temporal and spatial resolution. These data should also be collected in accordance with forthcoming new National Spatial Reference System standards to enable all entities – national, state, and local – to share consistent data sets. The NOAA National Geodetic Survey is developing a new reference frame, expected to be released in 2022, that will be based on measurements from the Global Navigation Satellite Systems (GNSS) and well-defined gravity models referred to as geoid models. This improved reference frame would provide for more consistent measurements across the basin, with better standardization between hydrologic and geodetic-based datums. Standard, high resolution data sets would enable more accurate long-term monitoring and analysis of hydrologic parameters such as flow, sediment flow, geomorphic activity, and land use patterns, for improved area watershed management. Drones could also be used to supplement these methods if consistent data reporting is available.

Employing advanced technology will be essential. Scientists and engineers need to develop new low-cost methods of collecting critical data from satellite observations, remotely sensed data, and sensors. In addition to space, this includes adoption of new and improved sensors deployed in the atmosphere, in the oceans, and on the Earth's surface. An example available today is NASA's

Gravity Recovery and Climate Change Experiment (GRACE), which provides information on changes in snow and groundwater and will assist in providing new insight into the quantity of water in rivers, with higher resolution. Another example is NASA's Soil Moisture Active Passive (SMAP) program, a mission to measure and map Earth's soil moisture and freeze/thaw state to better understand terrestrial water, carbon, and energy cycles. SMAP's direct measurements of soil moisture will be an important factor in accurately estimating water, energy, and carbon transfers between the land and atmosphere. Use of these and other tools depend on the correct characterization of these transfers. Methods and procedures for their use are directly applicable to flood assessment and drought monitoring. The use of new sensing and data analytics, operation and maintenance of long-term monitoring networks, and updated visualization tools can all increase understanding of which parameters are important in numerical models used in climate projections, weather prediction, and hydrologic modeling.

GCMs do not provide adequate scale for resolution when coupled with hydrologic models. GCM data are needed at the regional or local scale to make actionable decisions regarding climatologically impacted terrestrial conditions (for example, river discharge, water use, ground water, soil moisture, and precipitation). As the Federal Emergency Management Agency (FEMA) validates and verifies models for use in modeling floods and inundation mapping, a similar system should be established to verify which hydrologic models are acceptable for use with GCMs.



The hydrologic community of practice should also look to the advancement of models similar to the progression path of model development used in meteorology to forecast weather predictions. This could be improved with acceptable standards for the engineering and hydrologic community of practice. Once a diverse collection of observations, weather prediction is now a comprehensive ensemble of simulations and projections, with greatly increased forecast accuracy. Initial conditions are important to weather models, a concept that could be transferred and practiced in downscaling of GCMs with hydrologic models. Development should include new discharge derivation models calibrated with underlying hydraulic science and engineering principles, and used under improved community-of-practice standards to:

- Improve confidence in extrapolation (i.e., when applied to the range of known river channel geometries).
- Improve agreement on solutions (such as GCMs with standards for grid nesting or hydrologic models within larger domain simulations – verified by multiple hydrologists and engineers independently producing similar results).
- Improve results (such as by development or modification of existing rating curves and identification of the parameters supporting their development).
- Establish a standard unit of stream discharge – important for consistency and comparison for to better interpret and compare time-series trends.
- Determine if the NOAA Atlas Report 14 Precipitation-Frequency Atlas of the United States (2013) needs revision or adjustment for future climate scenarios.

- Act under the assumption that for hydrologic analyses, the climate is not stationary, or at equilibrium.

Unfortunately, many statistical models currently in use are based on a flawed premise of climatic stationarity, which diminishes their utility in a future of previously unseen climatic change. Based on this study, current approaches may not represent actual conditions. There is a strong effort to develop alternative methods, but development is in an early transitional state. The next generation of analytical tools to address non-stationarity need further development, then will need to be continuously improved. This will happen only if these capabilities are made a research-and-development funding priority.

Downscaling GCM model output and coupling it with hydrological models provides plausible scenarios of future climate conditions for further consideration in water resources planning. Historical records are grounded in recorded data but may not be representative of future conditions. Multiple drivers are changing hydrology; they include climate change, land use changes, and ground water depletions. Our response is evolving, with several efforts underway to start to document actions taken to improve methods and techniques to address trends and decadal shifts in time series for hydrologic data. A recommendation for the community of practice would be to feature examples of projects that are based on innovative tools, processes, and methods. Examples include the Red River of the North project, in which scientists and engineers are developing, applying, and evaluating a rigorous peer-reviewed methodology for computing the impact of climate change on flood frequency curves to the Red River of the North at Fargo,

North Dakota. Other examples would include the models under development to project inundation and flooding from coastal storms using high performance computing, learning algorithms, artificial intelligence, and machine learning for repetitive calculations. Noteworthy examples include those being developed for use in the Houston/Galveston area, and on the Carolina coasts.

Changes in hydrologic trends provide insight but do not predict the order of magnitude or intensity of changes that can occur. The risks associated with greater rainfall (and snow) are primarily related to changes in distribution (i.e., intensity). One of the key points of Brekke et al. (2009) is that climate change is but one of many challenges facing water resource managers, and a holistic approach to water resources management takes into account all significant drivers of change. Climate change is also occurring concurrently with increasing land use changes. The IPCC (2010) said that in order to assess climate change, the associated changes must be able to be detected. It defines attribution as the process of evaluation of the relative contribution of multiple causal factors to a change or event with an assignment of statistical confidence (IPCC 2010). Restoration of a riverine environment is most effective when focused on an understanding of all system processes that are contributing to the stream channel form.

Multiple challenges from the dynamic impacts of climate change and other factors in the Cheyenne River Basin include:

- Regional adjustment from isostatic rebound stemming from paraperiglacial events associated with continental glaciation and is reported to take centuries for landform readjustment.
- A new stream base level established with the construction of the Oahe Reservoir. Suspended sediments settle out of the Cheyenne River as deltaic and benthic sediments once the flow velocity of the river diminishes.
- The discharge of nearly a hundred-million tons of arsenic-laden mine tailing discharge over a century, which profoundly affected the equilibrium of sediments and the channel morphology, landforms, and slope within this fluvial system.
- Topographic and regional impacts that influence weather and resulting precipitation.
- Anthropogenic land use changes, dams, diversions, and water use.

The Cheyenne River Basin is a fluvial system not at equilibrium; it continues to adjust to many ongoing changes as vertical movement of the land surface and changes in water levels have occurred and will continue to do so. Continued erosion and sediment transport can also be expected, especially after spring snowmelt and during episodic thunderstorms, when high-velocity discharge can erode tailings-laden stream banks, causing arsenic-laden tailings to re-enter the stream. Any engineered approaches to mitigate future sediment exposure should recognize the need for and ensure that future designs act in concert with natural geomorphic adjustments occurring in the system.

The assimilative neutralization capacity of calcareous bedrock mixed with the post-mining tailings containing alluvium limits formation of acid from dissolution of sulfide minerals in mined tailings. The pH controls the speciation of arsenic, its affinity for sorption, and the tendency of arsenic to bind to surfaces. In the Cheyenne River Basin, the pH of the system is near-neutral, an important factor in the control of arsenic release and its potential attenuation and transport. Additional studies would be advantageous in areas with abundant tailings content to determine buffering capacity of the system, effect of iron on the chemistry of the system especially in light of projected climatic changes (temperature, drought, increased precipitation resulting in higher stream flows). Arsenic and phosphorous are chemically similar. With both increased land use and precipitation, the potential exists for increased flushing of phosphorus-containing fertilizers, animal wastes, and particulates into the watershed which also may influence arsenic chemistry and transport.

A major purpose of research in hydrological engineering is to collect data and discover and evaluate physical laws for use in calculating or predicting the stream conditions in a specific location under given conditions. Differentiation between long-term, natural trends and anthropogenic influences is needed to better understand system changes. Reliable, repetitive, and standardized methods and procedures are important to differentiating between the two.

There is a clear connection between climate change and stream discharge. Using the Clausius-Clapeyron relationship, researchers have identified that warmer air can hold more water vapor (7% per 1 degree C

temperature increase). This increased moisture content may in turn lead to increased intensity of precipitation events which contribute to increased streamflow.

Standard probabilistic statistical analysis plays an important role in how climate changes impact stream systems. In hydrology, statistical analysis of flood records relies on the annual peak discharge data. These probabilistic averages are important to validating models and analyzing hydrologic trends. Ironically, Keeling's identification of increases in atmospheric GHG arose from his curiosity and commitment to long-term sampling. Only with a commitment to long-term data collection can temporal and spatial changes to hydrologic systems be accurately studied.

As climate changes, annual average discharge data may exhibit non-stationarities. Improvements in methods to detect these non-stationarities are needed. Corresponding expert data interpretation in the context of local and regional conditions is equally important in assessing risk and developing mitigative responses. Climate change-related causal factors can drive conditions that amplify impacts from extreme events. These include antecedent and precedent soil conditions; localized conditions of compounding events (geology, geography, isostatic rebound from continental glaciation); subsidence changes from over-pumping of aquifers; and seasonal variation (frozen ground, ice/ice jams).

An understanding of limitations and uncertainty is important when merging models suited for different purposes, such as meteorological and hydrologic

models. GCMs were created to predict future climate conditions and use high-performance computing for climate and weather forecasting. They were not designed to downscale and inform hydrologic models. Results from climate-change scenarios depend heavily on a model's initial boundary conditions, emission scenarios, and the parameters used in its design

The present state of knowledge precludes the immediate capability of reaching an accepted method for determining climate change in hydrologic systems. It is important that scientists and engineers (particularly in the meteorological, hydrological, and information systems disciplines) integrate their specialized understanding to create analytical standards. Greater collaboration between multiple disciplines will be needed before satisfactory solutions or standard methods are identified. An example of successful interdisciplinary standardization is Bulletin 17B, Flood Frequency Guidelines, which is periodically updated in light of advances in understanding of and methods for hydrologic analysis. Government agencies, academic institutions, and other organizations collaborate to improve its contents. A recommendation for further improving Bulletin 17B would be to task the Hydrologic Frequency Analysis Work Group (HFAWG) to consider possible updates for specific use with GCMs.

Mined tailings-containing alluvium is made-up of metal and metalloid chemical constituents. This tailings-alluvium mixture remains in a system unless removed, which may not be feasible. The risk of exposure can be completely diminished only by removal. Mitigation action can be conducted to minimize

erosion, transportation, and dissolution/solubility. In physical chemistry, equilibrium conditions are used to determine solubility at standard conditions (one atmosphere at 25° C). With changing climate, it will be important to adapt assessment methods and chemical characterizations in response to these changes.



## Bibliography and References

Abatzoglou, J.T., 2013. "Development of gridded surface meteorological data for ecological applications and modelling." *International Journal of Climatology* Vol. 33 Issue 1, Jan. 2013, pp. 121-131. doi.org/10.1002/joc.3413

Abatzoglou, J.T. and Brown, T.J., 2012. "A comparison of statistical downscaling methods suited for wildfire applications." *International Journal of Climatology* Vol. 32 Issue 5, April 2012, pp. 772-780. doi.org/10.1002/joc.2312

Agency for Toxic Substances Disease Registry (ATSDR), 2011. "Toxic Substances Portal – Arsenic, Agency for Toxic Substances & Disease Registry." <https://www.atsdr.cdc.gov/toxprofiles/tp.asp?id=22&tid=3>

Aich, V., Zimmermann, A., Elsenbeer, H., 2014. "Quantification and interpretation of suspended-sediment discharge hysteresis patterns: How much data do we need?" *CATENA*, Vol. 122, pp. 120-129, 2014. doi.org/10.1016/j.catena.2014.06.020

Alder, J.R. and Hostetler, S.W., 2013. USGS National Climate Change Viewer. doi.org/10.5066/F7W9575T

Allen, M. and Ingram, W., 2002. "Constraints on future changes in climate and the hydrologic cycle." *Nature* 419: pp. 228–232. doi.org/10.1038/nature01092

Allison, J.D. and Allison, T.L., 2005. "Partition coefficients for metals in surface water, soil, and waste: Wash., D.C., U.S. EPA, July 2005, EPA/600/R-05-074", 93 p. Accessed Nov. 23, 2020 at: [https://iri.columbia.edu/~alesall/ouagaCILSS/articles/allen+ingram\\_nature2002.pdf](https://iri.columbia.edu/~alesall/ouagaCILSS/articles/allen+ingram_nature2002.pdf)

Andrew, A.S, Bernado, V., Warnke, L.A., Davey, J.C., Hampton, T., Mason, R.A., Thorpe, J.E., Ihnat, M.A., Hamilton, J.N., 2007. "Exposure to arsenic at levels found in U.S. drinking water modifies expression in the mouse lung." *Toxicology Science*, 100(1): 75-87, Nov.2007. doi.org/10.1093/toxsci/kfm200

Andrews, Edmund D., 1980. "Effective and Bankfull Discharges of Streams in the Yampa River Basin, Colorado and Wyoming." *Journal of Hydrology*, 46(1980) 311-330. doi.org/10.1016/0022-1694(80)90084-0

American Society of Testing Materials, 2014. ASTM E1689: "Standard Guide for Developing Conceptual Site Models for Contaminated Sites." doi:10.1520/E1689-20

Arai, Y., Sparks, D.L., Davis, J.A., 2005. "Arsenate: Adsorption Mechanisms at the Allophane-Water Interface." *Environ. Sci. Technol.* 2005, 39, 8, 2537-2544. <https://doi.org/10.1021/es0486770>

Archfield, S.A., Kennen, J.G., Carlisle, D.M., Wolock, D.M., 2014. "An Objective and Parsimonious Approach for Classifying Natural Flow Regimes at a Continental Scale." *River Research and Applications*, Vol.30, Issue 9, Nov. 2013, pp. 1155-1183.

Bailey, R.G., 1995. *Descriptions of the ecoregions of the United States*. Miscellaneous Publication 1391, U.S. Dept. of Agriculture, Forest Service, 108 p.

Baca, P., 2008. "Hysteresis effect in suspended sediment concentration in the Rybárik basin, Slovakia." *Hydrological Sciences Journal*, 53(1), 224–235. doi:10.1623/hysj.53.1.224

Blair, Edward, H., Dozier, Jeff, Davis, Robert E., Colee, Michael T., and Claffey, Keran J., 2015. "CUES—a study site for measuring snowpack energy balance in the Sierra Nevada." Technology Report Article, *Front. Earth Sci.*, 30 Sep.2015 <https://doi.org/10.3389/feart.2015.00058>

Barber, L.B., Paschke, S.S., Battaglin, W.A., Douville, C., Fitzgerald, K.C., Steffanie, H.K., Woodward, J.C., Walling, D.E., 2007. "Composite suspended sediment particles in river systems: their incidence, dynamics and physical characteristics." *Hydrological Processes*, 21, 3601-3614 (2007). doi:10.102/hyp.6586

Barber, L.B., Paschke, S.S., Battaglin, W.A., Douville, C., Fitzgerald, K.C., Keefe, S.H., Roth, D.A., Vajda, A.M., 2017. "Effects of an Extreme Flood on Trace Elements in River Water—From Urban Stream to Major River Basin." *Environmental Science Technology*, 2017, 51 (18), pp. 10344–10356. doi:10.1021/acs.est.7b01767

Barrick Gold Corporation Press Release, 2001. "Barrick Completes Merger with Homestake; Combination Creates World's Largest Gold Mining Company by Market Capitalization," Accessed Dec.14, 2001 at: [http://barrick.com/files/docs\\_pressrelease/PRe1\\_2001\\_12\\_14.pdf](http://barrick.com/files/docs_pressrelease/PRe1_2001_12_14.pdf)

Bates, B.C., Kundzewicz, Z.W., Wu, S., Palutikof, J.P., eds., 2008. "Climate Change and Water." Technical paper of the Intergovernmental Panel on Climate Change (IPCC), June 1, 2008, 210 p.

Belmont, Patrick, 2011. "Floodplain width adjustments in response to rapid base level fall and knickpoint migration." *Geomorphology*, vol 128, 2011, pp. 92-102.

Bencala, K.E., 1983. "Simulation of solute transport in a mountain pool and riffle stream with a kinetic mass transfer model for sorption." *Water Resources Research*, v. 19, no. 3, pp. 732-738. doi:10.1029/WR019i003p00732

- Bencala, K.E., 1984. "Interactions of solutes and streambed sediment—2. A dynamic analysis of coupled hydrologic and chemical processes that determine solute transport." *Water Resources Research*, v. 20, no. 12, pp. 1804-1814. doi:10.1029/WR020i012p01804
- Bencala, K.E., 1993. "A perspective on stream-catchment connections." *Journal of North American Benthological Society*, v. 12, pp. 44-47. doi:10.2307/1467684
- Bencala, K.E., 2000. "Invited Commentary—Hyporheic zone hydrological processes." *Hydrological Processes*, v. 14, no. 15, pp. 2797-2798. doi:10.1002/1099-1085(20001030)14:15, doi:2797:AID-HYP402>3.0.CO;2-6
- Bencala, K.E., Gooseff, M.N., Kimball, B.A., 2011. "Rethinking hyporheic flow and transient storage to advance understanding of stream-catchment connections." *Water Resources Research*, v. 47, no. 3. doi:10.1029/2010wr010066
- Bencala, K.E., Jackman, A.P., Kennedy, V.C., Avanzino, R.J., Zellweger, G.W., 1983. "Kinetic analysis of strontium and potassium sorption onto sands and gravels in a natural channel." *Water Resources Research*, v. 19, no. 3, p. 725-731. doi:10.1029/WR019i003p00725
- Bencala, K.E., Kennedy, V.C., Zellweger, G.W., Jackman, A.P., Avanzino, R.J., 1984. "Interactions of solutes and streambed sediments—1. An experimental analysis of cation and anion transport in a mountain stream." *Water Resources Research*, v. 20, no. 12, p. 1797-1803, 4W1200. doi:10.1029/WR020i012p01797
- Bennett, T.M.B., Maynard, N.G., Cochran P., Gough, R., Maldonado, J., Voggesser, G., Wotkyns, S., Cozzetto, K., 2014. "Ch. 12: Indigenous Peoples, Lands, and Resources." *Climate Change Impact in the United States: the Third National Climate Change Assessment*, Melillo, J.M., Richmond, T.C., Yohe, G.W., eds. GCRP publication, pp. 297–317.
- Bergeland, E.M., Ruth, G.R., Stack, R.L., and Emerick, R.J., 1977. "Arsenic toxicosis in cattle associated with soil and water contamination from mining operations." *American Association of Veterinary Laboratory Diagnosticians*, 19, pp. 311–316.
- Besser, J., Dwyer, J., Ingersoll, C., 1997. "Development and Application of Methods for Assessing Bioavailability of Contaminants Associated with Sediments II: Bioaccumulation and Toxicity Identification Procedures." *Proceedings of the USGS Sediment Workshop*, Feb. 4-7, 1997.
- Biedenharn, D.S. and Copeland, R.R., 2000. "Effective Discharge Calculation: A Practical Guide," 2000.

Bissen, M. and Frimmel, F.H, 2003. "Arsenic – a review. Part 1: Occurrence Toxicity, Speciation and Mobility." *Acta hydrochem. hydrobiol.* 31 (2003) 1, 9-18.

Blanchard, Peter E.R., Van Loon, L.L., Reid, J.W., Cutler, J.N., Rowson, J., Hughes, K.A., Brown, C.B., Mahoney, J.J., Xu, L., Bohan, M., Demopoulos, G.P., 2017. "Investigating arsenic speciation in the JEB Tailings Management Facility at McClean Lake, Saskatchewan using X-ray absorption spectroscopy." *Chemical Geology*, vol. 466, Sep.5, 2017, pp. 617-626.  
doi.org/10.1016/j.chemgeo.2017.07.014

Bodwell, J.E., Kingsley, L.A., Hamilton, J.W., 2004. "Arsenic at very low concentrations alters glucocorticoid receptor (GR)-mediated gene activation but not GR-mediated gene repression: complex dose-response effects are closely correlated with levels of activated GR and require a functional GR DNA binding domain." *Chem. Res. Toxicol.*, 2004, Aug 17 (8): 1064–1076.  
doi:10.1021/tx0499113

Bonfils, C., Santer, B.D., Pierce, D.W., Hidalgo, H.G., Bala, G., Das, T., Nozawa, T., 2008. "Detection and attribution of temperature changes in the mountainous western United States." *Journal of Climate* 21(23):6404–6424.

Borja, Angel, Dauer, Daniel M., and Gremare, Antoine, 2012. "The importance of setting targets and reference conditions in assessing marine ecosystem quality." *Ecological Indicators*, vol. 12, issue 1, Jan. 2012, pp. 1-7.  
doi.org/10.1016/j.econlind.2011.06.018

Boszke, L., Kowalski, A., Glosinska, G., Szarek, R., Siepak, J., 2003. "Environmental factors affecting speciation of mercury in the bottom sediments; an overview." *Policy Journal of Environmental Studies* 12:5–13

Bowell, R.J., 1994. "Sorptions of arsenic by iron oxides and oxyhydroxides in soils." *Applied Geochemistry* 9:279-286.

Brekke, L.D., Kiang, J.E., Olsen, J.R., Pulwarty, R.S., Raff, D.A., Turnipseed, D.P., Webb, R.S., White, K.D., 2009. *Climate change and water resources management—A federal perspective*. USGS Survey Circular 1331, 65 p.

Bruce, R.L., 1968. "Landslides in the Pierre Shale of South Dakota." *Record of the 2004 Highway Geology Symposium, Iowa State University, Transportation Research Board*, pp. 66-72. <http://trid.trb.org/view.aspx?id=121372>

Brunetti, M., Maugeri, M., Nanni, T., 2001. "Changes in total precipitation, rainy days, total precipitation and extreme events in northeastern Italy." *International Journal of Climatology*. Vol. 21, Issue 7, 15 June 2001, pp. 861-871.  
<https://doi.org/10.1002/joc.660>

Brunsdon, T. and Thornes, J.B., 1979. "Landscape sensitivity and changes." *Treatise on Geomorphology* (2013), vol. 9, pp. 768-793.

- Bunkers, M.J., Johnson, R.L., Miller, J.R., Hull Sieg, C., 1999. "Old Black Hills ponderosa pines tell story." *Proceedings of the South Dakota Academy of Science*. 78: 149-162
- Busby, J., Gullledge, J., Smith, T., White, K., 2011. "Of Climate Change and Crystal Balls: The Future Consequences of Climate, Change in Africa." University of Texas -Austin. Accessed at:  
[http://ccaps.strausscenter.org/system/research\\_items/pdfs/30/original.pdf?1283893878](http://ccaps.strausscenter.org/system/research_items/pdfs/30/original.pdf?1283893878)
- Cabrejo E., Phillips E., 2010. "In situ remediation and stabilization technologies for mercury in clay soils." U.S. Dept. of Energy Report ARC-2007-D2540-032-04
- Cain, D.J., Fend, S.V., Carter, J.L., 1989. "Temporal and spatial variability of arsenic in benthic insects from Whitewood Creek, South Dakota." *USGS Toxic Substances Hydrology Program—Proceedings of the Technical Meeting, Phoenix, AZ, Sep. 26-30, 1988*, Mallard, G.E and Raggone, S.E., eds. USGS Water-Resources Investigations Report 88-4220, pp. 257-268.
- Cain, D.J., Fend, S.V., Carter, J.L., 1988. "Arsenic concentrations of selected benthic insects in Whitewood Creek and the Belle Fourche River, South Dakota." *USGS Toxic Substances Hydrology Program—Surface-Water Contamination—Proceedings of the Technical Meeting, Denver, CO, Feb. 2-4, 1987*, Mallard, G.E., ed. USGS Open-File Report 87-764, pp. 55-60.
- California Institute of Technology, 2014. "From rivers to landslides: Charting the slopes of sediment transport." *ScienceDaily*, 29 Jan. 2014.  
[www.sciencedaily.com/releases/2014/01/140129165419.htm](http://www.sciencedaily.com/releases/2014/01/140129165419.htm).
- Callender, E. and Ficklin, W.H., 1987. "Remobilization of arsenic in sediments from the Cheyenne River area of Lake Oahe, South Dakota." *USGS Toxic Substances Hydrology Program--Surface-Water Contamination—Proceedings of the Technical Meeting, Denver, CO, Feb. 2-4, 1987*. USGS Open-File Report 87-764, pp. 41-48.
- Callender, E., Robbins, J.A., Morehead, N.R., 1988. "Records of fallout Cs-137 in the Oahe Reservoir System." *Proceedings of the 31<sup>st</sup> Conference on Great Lakes Research, Ontario, Canada, 1988*.
- Callender, E. and Robbins, J.A., 1993. "Transport and accumulation of radionuclides and stable elements in a Missouri River Reservoir." *Water Resources Research*, vol. 29, no. 6, pp. 1787–1804. doi:10.1029/93WR00387

- Canonica, S., Meunier, L., von Gunten, U., 2007. "Phototransformation of selected pharmaceuticals during UV treatment of drinking water." *Water Research*, Vol. 42, Issues 1-2, Jan. 2008, pp. 121-128.  
<https://doi.org/10.1016/j.watres.2007.07.026>
- Capel, P.D., McCarthy, K.A., Coupe, R.H., Grey, K.M., Amenumey, S.E., Baker, N.T., and Johnson, R.L., 2018. "Agriculture—A River runs through it—The connections between agriculture and water quality: USGS Circular 1433, 201 p.  
<https://doi.org/10.3133/cir1433>
- Carlisle, D.M., Wolock, D.M., Konrad, C.P., McCabe, G.J., Eng, K., Grantham, T.E., Mahler, B., 2019. *Flow modification in the nation's streams and rivers*. USGS Circular 1461," 75 p.
- Carpenter, S., Walker, B., Anderies, J., Abel, N., 2001. "From Metaphor to Measurement: Resilience of What to What?" *Ecosystems* 4, 765–781 (2001).  
[doi.org/10.1007/s10021-001-0045-9](https://doi.org/10.1007/s10021-001-0045-9)
- Carretier, S., Nievie're, B., Giamboni, M., Winters, T., 2006. "Do river profiles record along-stream variations of low uplift rate?" *Journal of Geophysical Research*, vol. III, F02024, 28 June 2006. doi:1029/2005JF000419, 200.
- Cavazos, T. and Arriaga-Ramírez, S., 2012. "Downscaled climate change scenarios for Baja California and the North American Monsoon during the twenty-first century." *J. Clim.* 25:5904-5915.
- Cayan, D.R., Kammerdiener, S.A., Dettinger, M.D., Caprio, J.M., and Peterson, D.H., 2001. "Changes in the onset of spring in the western United States." *Bulletin of the American Meteorological Society* 82:399–415.
- Cayan, D.R., Tyree, M., Kunkel, K.E., Castro, C., Gershunov, A., Barsugli, J., Ray, A.J., Overpeck, J.T., Anderson, M., Russell, J., Rajagopalan, B., Rangwala, I., Duffy, P., 2013. "Future climate: projected average." In *Assessment of Climate Change in the Southwest United States: A Report Prepared for the National Climate Assessment*, Garfin, G., Jardine, A., Merideth, R., Black, M., and LeRoy, S., eds., pp. 101-125.
- Cayan, D.R., Dettinger, M.D., Pierce, D., Das, T., Knowles, N., Ralph, F.M., and Sumargo, E., 2016. "Natural variability, anthropogenic climate change and impacts on water availability and flood extremes in the western United States." *Western Water Policy and Planning in a Variable and Changing Climate*, Miller, K., et al., eds. pp.17-42.
- Changnon, S.A., Jr., 1987. *Detecting Drought Conditions in Illinois*. State of Illinois Dept. of Energy and Natural Resources Circular 169, p. 3.  
[www.isws.illinois.edu/pubdoc/C/ISWSC-169.pdf](http://www.isws.illinois.edu/pubdoc/C/ISWSC-169.pdf)

- Chaudhry, M.H., 2009. *Open-Channel Flow*. 528 p. doi:10/1007/978-0-68648-6
- Cherry, J. A., Morel, F.M M., Rouse, J.V., Schnoor, J.L., Wolman, M.G., 1986. "Hydrogeochemistry of sulfide and arsenic-rich tailings and alluvium along Whitewood Creek, South Dakota (part 1 of 3 parts)." *Mineral and Energy Resources*, vol. 29(4), p. 12.
- Ciszewski, D. and Grygar, T.M., 2016. "A Review of Flood-Related Storage and Remobilization of Heavy Metal Pollutants in River Systems." *Water Air Soil Pollut.* 2016; 227(7): 239. doi:10.1007/s11270-016-2934-8
- Cleveland, W.S., 1979: "Robust locally-weighted regression and smoothing scatterplots." *Journal of the American Statistical Association*, 74, 829-836. doi:10.1080/01621459.1979.10481038
- Cohen, S., Praskievicz, S., Maidment, D., 2018. "Featured Collection Introduction: National Water Model." *Journal of the American Water Resources Association* 54: 767-769. doi:10.1111/1752-1688.12664
- Cohn, T.A., Barth, N.A., England, J.F., Jr., Faber, B.A., Mason, R.R., Jr., and Stedinger, J.R., 2019. *Evaluation of recommended revisions to Bulletin 17B*. USGS Open-File Report 2017–1064, 141 p. doi.org/10.3133/ofr20171064
- Colby, B.R., 1964. "Discharge of sands and mean velocity relations in sand-bed streams." USGS Professional Paper No. 462-A, pp. A1-A47.
- Collins, A.L., Pulley, S., Foster, D.L., Gellis, A., Horowitz, A.J., 2016. "Sediment source fingerprinting as an aid to catchment management: A review of the current state of knowledge and a methodological decision-tree for end-users." *Journal of Environmental Management*, Vol. 194, June 2017, pp. 86-108. <https://doi.org/10.1016/j.jenvman.2016.09.075>
- Colorado State University Workshop on Nonstationarity, Hydrologic Frequency Analysis, and Water Management, Jan.13-15, 2010, Boulder, CO. In *Water Institute Information Series No. 109*. [www.cwi.colostate.edu/publications/is/109.pdf](http://www.cwi.colostate.edu/publications/is/109.pdf)
- Conant, R.T., Kluck, D., Anderson, M., Badger, A., Boustead, B.M., Derner, J., Farris, L., Hayes, M., Livneh, B., McNeeley, S., Peck, D., Shulski, M., Small, V., 2018. "Chapter 22: Northern Great Plains." In *Impacts, Risks, and Adaptation in the United States: Fourth National Climate Assessment, Vol. II*, Reidmiller, D.R., Avery, C.W., Easterling, D.R., Kunkel, K.E., Lewis, K.L.M, Maycock, T.K., Stewart, B.C., eds. USGCRP publication, pp. 941–986. doi:10.7930/NCA4.2018.CH22
- Constantine, J.A., Dunne, T., Ahmed, J., Legleiter, C., Lazarus, E.D., 2014. "Sediment supply as a driver of river meandering and floodplain evaluation in the Amazon Basin." *Nature Geoscience*, vol. 7, Dec. 2014, pp. 899-903.

Coopersmith, E., Yager, M., Ye, S., Cheng, L., and Sivapalan, M., 2012. "Discussion of exploring the physical controls of regional patterns of flow duration curves Part 3: A catchment classification system based on seasonality and Runoff Regime." *Hydrol. Earth System Sci. Discuss.*, 9, pp. 7085-7129.

Coopersmith, E.J., Misker, B.S., and Sivapalan, M., 2014. "Patterns of regional hydroclimatic shift: an analysis of changing hydrologic regimes." *Water Resources Research*, vol. 50, issue 3, March 2014, pp. 960-1983.

Crane, M., Whitehouse, P., Comber, S., Ellis, J., Wilby, R.L., 2005. Climate Change Influences on Environmental and Human Health Chemical Standards." *Human and Ecol. Risk Assess.* 11, 289-318.

Culler, R.C. and Peterson, H.V., 1953. *Effect of Stock Reservoirs on Runoff in the Cheyenne Basin Above Angostura Dam*. USGS Circular 223, 33 p.

Dartmouth University-Hitchcock, 2006. "New study highlights arsenic Impacts." [www.dartmouth-hitchcock.org/news/newsdetail/42175/](http://www.dartmouth-hitchcock.org/news/newsdetail/42175/)

Darton, N.H., 1909. USGS Water Supply Paper 227, quoted in: Zaprowski, B.J., Evenson, E.B., Pazzaglia, F.J., Epstein, J.B., 2001, "Knickzone propagation in the Black Hills: A different perspective on the late Cenozoic exhumation of the Laramide Rocky Mountains." *Geology*, vol. 29, no. 6, pp. 547-550.

Dept. of Energy (DOE) Health and Safety Laboratory Group, 1977. "Final tabulation of monthly fallout data: 1954–1976." Environmental Quality HAS-329, 401 p.

DeVore, C.L., Rodriguez-Freire, L., Mehdi-Ali, A., Ducheneaux, C., Artyushkova, K., Zhou, Z., Latta, D.E., Lueth, V.W., Gonzales, M., Lewis, J., Cerrato, J.M., 2019, "Effect of bicarbonate and phosphate on arsenic release from mining-impacted sediments in the Cheyenne River watershed, South Dakota, USA." *Environ. Sci.: Processes & Impacts*, 2019, 21(6), pp. 456-468.  
doi:10.1039/C8EM00461G

Daly, C., Neilson, R., Phillips, D., 1992. "A Statistical-Topographic Model for Mapping Climatological Precipitation over Mountainous Terrain." *Journal of Applied Meteorology*, vol. 33, p. 140.

Daly, S.F., 2011. "Ice Formation in the Missouri River at Bismarck, North Dakota." Appendix A, USACE ERDC/CRREL, 11 p.  
[www.swc.nd.gov/pdfs/ice\\_formation\\_bismarck.pdf](http://www.swc.nd.gov/pdfs/ice_formation_bismarck.pdf)

Delpla, I., Jung, V., Baures, E., Clement, M., Thomas, O., 2009. "Impacts of climate change on surface water in relation to drinking water production." *Environment International* Vol. 35, Issue 8, Nov. 2009, pp. 1225-1233.  
doi.org/10.1016j.envint.2009.07.001



Deque, M., 2007. "Frequency of precipitation and temperature extremes over France in an anthropogenic scenario: Models results and statistical correction according to observed values." *Global Planet, Change* 57, 16-26.

DigitalGlobe Company imagery, 2015.

DiToro, D.M., Zarba, C.S., Hansen, D.J., Berry, W.J., Swartz, R.C., Cowan, C.E., Pavlou, S.P., Allen, H.E., Thomas, N.A., Paquin, P.R., 1991. "Technical basis for establishing sediment quality criteria for nonionic organic chemicals using equilibrium partitioning." *Environ. Toxicol. Chem.* doi:10:1541 1583

Dixit, S., Hering, J.G., 2003. "Comparison of arsenic(V) and arsenic(III) sorption onto iron oxide minerals: Implications for arsenic mobility." *Environmental Science & Technology*, 37(18): 4182–4189.

Dornelles, A.Z., Nunes, J.N., Boyd, E., Asquith, M., 2020. "Towards a bridging concept for undesirable resilience in social-ecological systems." *Global Sustainability* 3, July 2021, pp. 1-12. doi:10.1017/sus.2020.15

Driscoll, D.G. and Carter, J.M., 2001. *Hydrologic Conditions and Budgets for the Black Hills of South Dakota, Through Water Year 1998*. USGS Water Investigations Report 01-4226, 143 p.

Driscoll, D.G, Carter, J.M., Williamson, J., Putnam, L., 2002. *Hydrology of the Black Hills Area, South Dakota*. USGS Water-Resources Investigations Report 02-4094, 150 p.

Droppo, I.G and Ongley, E.D., 1992. "The state of suspended sediment in the freshwater fluvial environment: a method of analysis." *Water Research* 26: 65–72.

Droppo, I.G., Walling, D.E., Ongley, E.D., 1998. "Suspended sediment structure: implications for sediment and contaminant transport modelling." In *Modeling Soil Erosion, Sediment Transport and Closely Related Hydrological Processes*, International Association of Hydrological Sciences (IAHS) Publication No. 249, pp. 437–444.

Du Laing, I.G., Rinklebe, J., Vandecasteele, B., Meers, E., Tack, F.M.G., 2009. "Trace metal behaviour in estuarine and riverine floodplain soils and sediments: A review." *Science of the Total Environment*, Vol. 407, Issue 13, 15 June. 2009, pp. 3972-3985. <https://doi.org/10.1016/j.scitotenv.2008.07.025>

Durkin, T.V., Townsend, R.D., Cepak, M.D., 1998. "South Dakota Gold Mining: Regulations, Compliance and Environmental History." *Mining Engineering*, vol. 50, no. 4, pp. 27-32. <http://denr.sd.gov/documents/smepubsd.pdf>

Eberts, S.M., Woodside, M.D., Landers, M.N., Wagner, C.R., 2018. "Monitoring the pulse of our nation's rivers and streams—The U.S. Geological Survey Streamgaging Network." USGS Fact Sheet 2018–3081, 2 p. <https://doi.org/10.3133/fs20183081>

Einstein, H.A., 1950. "The Bed-Load Function for Sediment Transportation in Open Channel Flows." Technical Bulletin No. 1026, Sep.1950, USDA Soil Conservation Service.

Einstein, H.A., 1964. Quoted in Julien, P.Y., *Erosion and Sedimentation*. Cambridge University Press. 1998, p. 204.

Emett, M.T. and Khoe, G.H., 2001. "Photochemical oxidation of arsenic by oxygen and iron in acidic solutions." *Water Research*, 35(3), 649–656.

Esparza, L.E., 1988. "Minerals Yearbook, South Dakota." U.S. Dept. of the Interior, Bureau of Mines, p. 16. Accessed Dec. 12, 2013 at: [www.sdgs.usd.edu/pubs/pdf/ME-34%20-%2016%20pages.pdf](http://www.sdgs.usd.edu/pubs/pdf/ME-34%20-%2016%20pages.pdf) 16 p.

Eng, K., Carlisle, D.M., Wolock, D.M., Falcone, J.A., 2013. "Predicting the likelihood of altered streamflows at ungauged rivers across the conterminous United States." *River Research and Applications*, Vol. 29, No. 6, pp. 781–791. [doi.org/10.1002/rra.2565](https://doi.org/10.1002/rra.2565)

Eng, K., Carlisle, D.M., Grantham, T.E., Wolock, D.M., and Eng, R.L., 2019. "Severity and extent of alterations to natural streamflow regimes based on hydrologic metrics in the conterminous United States, 1980–2014." USGS Scientific Investigations Report 2019–5001, 25 p. [doi.org/10.3133/sir20195001](https://doi.org/10.3133/sir20195001)

Evans, C.D., Monteith, D.T., Cooper, D.M., 2005. "Long-Term Increases in Surface Water Dissolved Organic Carbon: Observations, Possible Causes and Environmental Impacts." *Environmental Pollution* 137(1):55-71, Oct. 2005. [doi:10.1016/j.envpol.2004.12.031](https://doi.org/10.1016/j.envpol.2004.12.031)

Fan, Y., Clark, M., Lawrence, D.M., Senson, S., Band, L.E., Brantley, S.L., et al., 2019. "Hillslope Hydrology in Global Change Research and Earth System Modeling." *Water Resources Research*, 55, 1737-1772. [doi.org/10.1029/2018WR023903](https://doi.org/10.1029/2018WR023903)

Fausch, K.D., Torgerson, C.E., Baxter, C.V., Li, H.W., 2002. "Landscapes to riverscapes: bridging the gap between research and conservation of stream fishes." *Bioscience* 52: 483-49.

Ferrari, R.L., 2007. "Belle Fourche Reservoir 2006 Sedimentation Survey." Prepared for the U.S. Dept. of Interior Bureau of Reclamation, 21 p. [Belle-Fourche-Reservoir-2006-Sedimentation-Survey.pdf \(fdlp.gov\)](https://www.fdlp.gov/Belle-Fourche-Reservoir-2006-Sedimentation-Survey.pdf)

Ficklin, W.H. and Callender, E., 1987. "Speciation of arsenic in sediments and interstitial water from the Cheyenne River arm of Lake Oahe, South Dakota." *USGS Toxic Substances Hydrology Program—Surface-Water Contamination—Proceedings of the Technical Meeting, Denver, CO, Feb. 2-4, 1987*, Mallard, G.E., ed. USGS Open-File Report 87-764, pp. 49-54.

Ficklin, W.H. and Ryder, J.L., 1988. "Arsenic species in ground water and pore water in stream sediments affected by mine drainage in Montana and Colorado." *USGS Program on Toxic Waste—Ground-Water Contamination—Proceedings of the second technical meeting, Cape Cod, MA, Oct,21-25, 1985*, Ragone, S.E., ed. USGS Open-File Report 86-481, pp. E-9-E-11.

Ficklin, W.H. and Callender, E., 1988. "Arsenic geochemistry of rapidly accumulating sediments, Lake Oahe, South Dakota." *USGS Toxic Substances Hydrology Program—Proceedings of the Technical Meeting, Phoenix, AZ, Sep. 26-30, 1988*, Mallard, G.E. and Ragone, S.E., eds. USGS Water-Resources Investigations Report 88-4220, pp. 217-222.

Fisher, J. C., Wallschlinger, D., Planer-Friedrich, B., Hollibaugh, J.T., 2007. "A new role for sulfur in arsenic cycling." *Environmental Science & Technology*, 42(1), 81–85.

Ficklin, W.H. and Callender, E., 1989. "Records of fallout CS-137 in Lake Oahe Reservoir, South Dakota." *USGS Toxic Substances Hydrology Program—Proceedings of the Technical Meeting, Phoenix, AZ, Sep.26-30, 1988*, Mallard, G.E. and Ragone, S.E., eds. USGS Water-Resources Investigations Report 88-4220, p. 611.

Fischenich, J.C., McKay, S.K., 2011. "Hydrologic analyses for stream restoration design." U.S. Army Engineer Research and Development Center (ERDC) Report TN-EMRRP-EBA-08.

Fischenich, J.C., Tripe, J., Meier, D., Pridal, D., Gibson, S., Hickley, J., Economouly, T., 2014. "Models, Data, and Literature to Support Habitat Analyses for the Missouri River Effects Analysis." ERDC/EL TR-14-X, April 2014, draft technical report.

Flint, R.F., 1955. "Pleistocene Geology of Eastern South Dakota." USGS Professional Paper 262, 173 p.

Ford, R.G., 2002. "Rates of Hydrous Ferric Oxide Crystallization and the Influence on Coprecipitated Arsenate." *Environ. Sci. Technol.* 36(11), 2459–2463.

Förstner U., Wittmann G., 1981. *Metal Pollution in the Aquatic Environment*. Berlin: Springer; 1981.

- Fovet, O., Ruiz, L., Hrachowitz, M., Faucheux, M., Gascuel-Oudou, C., 2005. "Hydrological hysteresis and its value for assessing process consistency in catchment conceptual models." *Hydrologic Earth Systems Science*, 9, pp.105–123, 2015. doi:10.5194/hess-19-105-2015
- Fox Consultants, Inc., 1984. "Whitewood Creek Study, Phase I and Phase II." Prepared for the South Dakota Department of Water and Natural Resources Office of Air Quality and Solid Waste, April 16, 1984.
- Frankson, R., Kunkel, K., Champion, S., Easterling, D., 2017. "South Dakota State Climate Summary." NOAA Technical Report NESDIS 149-SD, 4 p. South Dakota - State Summaries 2019 (ncics.org)
- Friedman, D.J., Schechter, B., Baker, C., Mueller, G., Villarini, G., and White, K.D., 2016. "USACE Nonstationarity Detection Tool User Guide."
- Fuller, C.C., Davis, J.A., Claypool-Frey, R., 1987. "Partitioning of arsenic by iron oxides in Whitewood Creek, South Dakota." *USGS Toxic Substances Hydrology Program—Surface-Water Contamination—Proceedings of the Technical Meeting, Denver, CO, Feb. 2-4, 1987*, Mallard, G.E., ed. USGS Open-File Report 87-764, pp. 19-22.
- Fuller, C.C. and Davis, J.A., 1989. "Influence of coupling of sorption and photosynthetic processes on trace element cycles in natural waters." *Nature*, Vol. 340, Issue 6228, pp. 52-57. doi:10.1038/340052a0
- Fuller, C.C., Davis, J.A., Zellweger, G.W., Goddard, K.E., 1989. "Coupled chemical, biological and physical processes in Whitewood Creek, South Dakota—evaluation of the controls of dissolved arsenic." *USGS Toxic Substances Hydrology Program—Proceedings of the Technical Meeting, Phoenix, AZ, Sep.26–30, 1988*. USGS Water-Resources Investigations Report 88-4220, pp. 235–246.
- Fuller, C.C. and Davis, J.A., 2003. "Section II: Evaluation of the processes controlling dissolved arsenic in Whitewood Creek, South Dakota." In "Toxic substances in surface waters and sediments—a study to assess the effects of arsenic-contaminated alluvial sediment in Whitewood Creek, South Dakota." USGS Professional Paper 1681.
- Gammonds, C.H., Grant, T.M., Nimick, D.A., Parker, S.R., De Grandpre, M.D., 2007. "Diel changes in water chemistry in arsenic-rich stream and treatment-pond system." *Science of the Total Environment*, Vol. 384, Issues 1-3, 1 Oct. 2007, pp. 433-451.

- Gandy, C.J., Smith, J.W.N., Jarvis, A.P., 2007. "Attenuation of mining-derived pollutants in the hyporheic zone: A review." *Sci. Total Environ.* 2007, 373, 435–446.
- Garrick, D., Jacobs, K., Garfin, G., 2008. "Models, Assumptions, and Stakeholders: Planning for Water Supply Variability in the Colorado River Basin." *Journal of the American Water Resources Association*, 44: 381-98.  
doi.org/10.1111/j.1752-1688.2007.00154.x
- Gharari, S., Razavi, S., 2018. "A review and synthesis of hysteresis in hydrology and hydrological modeling: Memory, path-dependency, or missing physics?" *Journal of Hydrology* Vol. 566, pp. 500-519.  
<https://doi.org/10.1016/j.jhydrol.2018.06.037>
- Glaser, M., Plass-Johnson, J., Ferse, S.C.A., Neil, M., Satari, D., Teichberg, M., Reuter, H., 2018. "Breaking Resilience for a Sustainable Future: Thoughts for the Anthropocene." *Front. Mar. Sci.*, 16 Feb. 2018, 34 p.  
doi.org/10.3389/fmars.2018.00034
- Goddard, K. E., 1987. *Composition, distribution, and hydrologic effects of contaminated sediments resulting from the discharge of gold milling wastes to Whitewood Creek at Lead and Deadwood, South Dakota*. USGS Water-Resources Investigations Report 87–4051, 76 p.
- Goddard, K. E., 1988. *USGS applied research studies of the Cheyenne River system, South Dakota: Description and collation of data, water years 1985–86*. USGS Open-File Report 88-484, 158 p.
- Goddard, K.E., 1988. "Gold-mill-tailings contamination of the Cheyenne River system, western South Dakota." *USGS Toxic Substances Hydrology Program--Surface-Water Contamination--Proceedings of the Technical Meeting, Denver, CO, Feb.2-4, 1987*, Mallard, G.E., ed. USGS Open-File Report 87-764, pp. 1-10.
- Goddard, K.E., 1989. "Overview of research activities on the Cheyenne River system, western South Dakota." *USGS Toxic Substances Hydrology Program--Proceedings of the Technical Meeting, Phoenix, AZ, Sep.26-30, 1988*, Mallard, G.E. and Ragone, S.E., eds. USGS Water-Resources Investigations Report 88-4220, pp. 199-202.
- Goddard, K.E., Horowitz, A.J., Shearer, C.K., 1988. "Distribution of solid-phase arsenic and trace elements in bottom and suspended sediments, Whitewood Creek and the Belle Fourche and Cheyenne Rivers, western South Dakota." *USGS Toxic Substances Hydrology Program--Surface-Water Contamination--Proceedings of the Technical Meeting, Denver, CO, Feb. 2-4, 1987*, Mallard G.E., ed. USGS Open-File Report 87-764, pp. 13-18.

Goddard, K.E. and Wuolo, R.W., 1988. "Processes controlling the concentration of dissolved arsenic in Whitewood Creek, South Dakota." *USGS Toxic Substances Hydrology Program--Surface-Water Contamination--Proceedings of the Technical Meeting, Denver, CO, Feb. 2-4, 1987*, Mallard G.E., ed. USGS Open-File Report 87-764, pp. 23-28.

Gomez, B. and Marron, D., 1991. "Neotectonic effects on sinuosity and channel migration, Belle Fourche River, western South Dakota." *Earth Surface Processes and Landforms*, vol. 16, pp. 227-235, doi:10.1002/esp.3290160304

Google Earth, 2014.

Google Earth, 2016. Imagery date is Sep. 20, 2013.

Graf, W.L., 2006. "Downstream hydrologic and geomorphic effects of large dams on American rivers." *Geomorphology*, vol. 79, issue 3-4, pp. 336-360

Grams, P.E., Topping, D.J., Schmidt, J.C., Hazel, J.E., Jr., Kaplinski, M., 2013. "Linking morphodynamic response with sediment mass balance on the Colorado River in Marble Canyon: Issues of scale, geomorphic setting, and sampling design." *Journal of Geophysical Research* Vol.118, Issue 2, June, 2013, pp. 361-381. doi.org/10.1002/jgrf.20050

Greene, S., no date given. "Eco-Geomorphic response to river flow regulation downstream of Gavins Pont Dam, Missouri River, South Dakota." <https://serc.carleton.edu/vignettes/collection/68169.html>

Gunn, A.M., Winnard, D.A., Hunt, D.T.E., 1988. "Trace metal speciation in sediments and soils." *In Metal Speciation: Theory, Analysis and Application*, Kramer, J.R., and Allen, H.E., eds., pp. 261-294, Lewis Publications.

Guo, J. and Julien, P.Y. (2008). "Application of Modified Log-Wake Law in Open-Channels." *Journal of Applied Fluid Mechanics* 1(2) 17-23.

Guo, H., Wen, D., Liu, Z., Jia, Y., Guo, Q., 2014. "A review of high arsenic groundwater in Mainland and Taiwan, China: distribution, characteristics and geochemical processes." *Appl. Geochem.*,41(2014), pp.196-217.

Hadley, R. F. and Rolfe, B.N, 1955. "Development and significance of seepage steps in slope erosion." *Trans.Am Geophys. Union* v 36, pp. 792-804.

Hadley, R. F. and Schumm, S. A., 1961. "Sediment sources and drainage basin characteristics in upper Cheyenne River Basin, USGS Water Supply Paper 1531-B, pp.137–146.

Hadley, R.F., Ongley, E.D., 1989. *Sediment and the Environment*. IAHS Publication no. 184, pp. 19-26.

Hagner, A.F., 1963. "Philosophical aspects of the geological sciences." *The Fabric of Geology*, Allbritton, C.C., ed., 372 p

Hains, D. and Zabilansky, L., 2004. "Laboratory test of scour under ice, Data and preliminary results." USACE ERDC/CRREL TR-04-09.

Hamilton, J., Dartmouth College, 2006. "Low Doses of Arsenic Can Have Broad Impact on Hormone Activity." *ScienceDaily*, 6 Dec. 2006. [www.sciencedaily.com/releases/2006/12/061204123351.htm](http://www.sciencedaily.com/releases/2006/12/061204123351.htm)2006.

Harden, T.M., O'Connor, J.E., Driscoll, D.G., Stamm, J.F., 2011. *Flood-frequency analyses from paleoflood investigations for Spring, Rapid, Boxelder, and Elk Creeks, Black Hills, western South Dakota*. USGS Scientific Investigations Report 2011–5131, 136 p.

Harvey J.W. and Bencala, K.E., 1993. "The effect of streambed topography on surface-subsurface water exchange in mountain catchments. *Water Resources Research* 29(1), pp. 89-98.

Hatch, T., 2002. *The Custer Companion: A Comprehensive Guide to the Life of George Armstrong Custer and the Plains Indian Wars*. Stackpole Books.

Hazelwood, K.T., 2019, "Late Cenozoic history of the Black Hills of South Dakota and Wyoming: a study of landscape evolution via stream profile analysis." Unpublished Ph.D. Dissertation, South Dakota School of Mines and Technology, Rapid City, SD.

Hazelwood, K.T. and Stetler, L.D., 2019. "New insights into the fluvial geomorphology and its effects on Paleofloods in the Black Hills, South Dakota." *Geomorphology* 327:80-92.

Hazelwood, K.T. and Stetler, L.D., 2016. "Watershed Decomposition: new GIS methods for watershed scale long valley profile analysis." *Western South Dakota Hydrology Conference, Abstracts with Program, April. 7, 2016, Rapid City, SD*.

He, F., Gao, J., Pierce, E., Strong, P.J., Wang, H., Li, L., 2015. "In situ remediation technologies for mercury-contaminated soil." *Environ Sci Pollut Res.* 22, pp. 8124-8147. doi.10.1007/s11356-015-4316-y

Helsel, D.R. and Hirsch, R.M., 2002. "Statistical methods in water resources": *U.S. Geological Survey Techniques of Water Resources Investigations*, book 4, chapter A3, 458 p. doi.org/10.3133/tm4a3

Hemond, H.F. and Benoit, Janina, 1988. "Cumulative impacts on water quality functions of wetlands." *Environmental Management*, Section III, Cumulative Impacts to Wetlands and Water Quality, Vol. 12, Issue 5, pp. 639-653.

Hesse, L.W., Brown, R.L., Heisinger J.F., 1975. "Mercury contamination of birds from a polluted watershed." *Journal of Wildlife Management*, Vol. 39, No. 2, April 1975, pp. 299–304.

Hicken, E.J., 1995. "River Geomorphology." Accessed Aug. 2014 at: [http://www.sfu.ca/~hickin/RIVERS/Rivers4\(Sediment%20transport\).pdf](http://www.sfu.ca/~hickin/RIVERS/Rivers4(Sediment%20transport).pdf)

Hirsch, R.M., Moyer, D.L., Archfield, S.A., 2010. "Weighted Regressions on Time, Discharge, and Season (WRTDS), With an Application to Chesapeake Bay River Inputs." *Journal of the American Water Resources Association* 46(5):857-880. doi:10.1111/j.1752-1688.2010.00482.x

Hoagstrom, C.W., 2006. "Fish Community Assembly in the Missouri River Basin." Ph.D. Dissertation, South Dakota State University, Brookings, SD.

Hochella, M.F., Moore, J.N., Putnis, C.V., Putnis, A., Kasama, T., Eberl, D.D., 2005. "Direct observation of heavy metal-mineral association from the Clark Fork River Superfund Complex: Implications for metal transport and bioavailability." *Geochimica et Cosmochimica Acta*, 69(7): 1651–1663.

Hoffman, F., 2015. "Black Swans and Pink Flamingos: Five Principles for Force Design." War on the Rocks, Aug. 19, 2015. <https://warontherocks.com/2015/08/black-swans-and-pink-flamingos-five-principles-for-force-design/>

Holdren, J.P. (of Harvard University), 2019. "National Hydrography Data Sets." June 6, 2019, lecture at Tsinghua University, Beijing, China. Accessed via Horizon Systems Corp. NHDPlusV2 online tool at: [www.horizon-systems.com/nhdplus/NHDPlusV2\\_home.php](http://www.horizon-systems.com/nhdplus/NHDPlusV2_home.php)

Holling, C.S., 1973. "Resilience and Stability of Ecological Systems." *Annual Review of Ecology and Systematics*, Vol. 4:1-23, Nov. 1975. doi.org/10.1146/annurev.es.04.110173000245

Holling, C.S. and Meffe, G.K., 1996. "Command and Control and the Pathology of Natural Resource Management." *Conservation Biology*, 10, 328-337. doi.org/10.1046/j.1523-1739.1996.10020328.x

Horowitz, A.J. and Elrick, K.A., 1987. "Arsenic geochemistry of sediment cores from the Cheyenne River arm of Lake Oahe, South Dakota - 1985 results." *USGS Toxic Substances Hydrology Program—Surface Water Contamination. Proceedings of technical meeting, Denver, CO, Feb. 2-4, 1987*, Mallard, G. ed. USGS Water-Resources Investigations Report 87-767, pp. 39-40



Horowitz, A.J., Elrick, K.A., Callender, E., 1988. "The effect of mining on the sediment - trace element geochemistry of cores from the Cheyenne River arm of Lake Oahe, South Dakota, USA." *Chemical Geology*, 67(1–2): 17–33. doi:10.1016/0009-2541(88)90003-4

Horowitz, A.J., Elrick, K.A., Cook, R.B., 1989. "Source and transport of arsenic in the Whitewood Creek-Belle Fourche-Cheyenne River-Lake Oahe system, South Dakota." *USGS Toxic Substances Hydrology Program—Proceedings of the Technical Meeting, Phoenix, AZ, Sep. 26-30, 1988*, Mallard, G.E. and Ragone, E.D., eds. USGS Water-Resources Investigations Report 88-4220, pp. 223-233.

Horowitz, A.J., 1991. *A Primer on Sediment-Trace Element Chemistry*, 136 p.

Horowitz, A.J., 2006. "The effect of the 'Great Flood of 1993' on subsequent suspended sediment concentrations and fluxes in the Mississippi River Basin, USA". In *Sediment Dynamics and the Hydromorphology of Fluvial Systems: Proceedings of a symposium held in Dundee, UK, July 2006*. IAHS Publ. 306, 2006. 110.

Horowitz, A.J., 2008. "Determining Annual Suspended Sediment and Sediment-Associated Trace Element and Nutrient Fluxes." *Science of the Total Environment*, 400 (1-3) p. 315-343. doi:10.1016/j.scitotenv.2008.04.022

Horowitz, A.J., 2013. "A Review of Selected Inorganic Surface Water-Quality Monitoring Practices: Are We Really Measuring What We Think, and If So, Are We Doing It Right?" *Environ. Sci. Technol.*, 2013, 47, 6, 2471-2486. doi:10.1021/es304058q

Horowitz, A.J., Stephens, V.C., Elrick, K.A., Smith, J.J., 2012. "Concentrations and annual fluxes of sediment-associated chemical constituents from conterminous US coastal rivers using bed sediment data." *Hydrological Processes*, 26, 1090–1114 (2012). doi:10.1002/hyp.8437

Horton, R.E., 1945. "Erosional development of streams and their drainage basins: Hydrophysical approach to quantitative morphology." *Geological Society of America Bulletin* 56: 275-370.

Hostetler, S.W. and Alder, J.R., 2016. "Implementation and evaluation of a monthly water balance model over the U.S. on an 800 m grid." *Water Resources Research* Vol. 52 Issue 10, pp. 9600-9620. doi.org/10.1002/2016WR018665

Hotchkiss, R.H, Jorgenson, S.F., Stone, M.C., Fontaine, T.A., 2000. "Regulated River Modeling for Climate Change Impact Assessment: The Missouri River." *Journal of the American Water Resources Association*, Vol. 36, No. 2, April 2000, pp. 375-386.

- Hsu-Kim, H., Kucharzyk, K.H., Zhang, T., Deshusses, M.A., 2013. "Mechanisms regulating mercury bioavailability for methylating microorganisms in the aquatic environment: a critical review." *Environ. Sci. Technol.*, 47 (2013), pp. 2441–2456.
- Hu, H., Lin, H., Zheng, W., Tomanicek, S.J., Johs, A., Feng, X., Elias, D.A., Liang, L., Gu, B., 2013. "Oxidation and methylation of dissolved elemental mercury by anaerobic bacteria." *Nat. Geosci.*, 6 (2013), pp. 751-754.
- Huggett, R.J., 1988. "Dissipative systems: implications for geomorphology." *Earth Surface Processes and Landforms* 13(1):45-49, Feb.1988.
- Huntington, T.G., Weiskel, P.K., Wolock, D.M., McCabe, G., 2018. "A new indicator framework for quantifying the intensity of the terrestrial water cycle." *Journal of Hydrology*. doi.org/10.1016/j.jhydrol.2018.02.048
- Iacobellis, V. and Fiorentino, M., 2000. "Derived distribution of floods based on the concept of partial area coverage with a climatic appeal." *Water Resources Research*, 36(2), 469–482. doi:10.1029/1999WR900287
- Inglis, C.C., 1949. *The behaviour and control of rivers and canals*. Research Publication 13, Central Waterpower Irrigation and Navigation Research Station, Poona, pp. 79-91.
- IPCC, 2012. "Managing the risks of extreme events and disasters to advance climate change adaptation." *Special report of the Intergovernmental Panel on Climate Change*, Field, C.B., Barros, V., Stocker, T.F., Qin, D., Dokken, K.L., Ebi, M.D., Mastandrea, K.J., Mach, G., Plattner, K., Allen, S.K., Tignor, M., Midgley, P.M., eds. Cambridge University Press, UK, 582 p.
- IPCC, 2013. *Climate Change 2013: The Physical Science Basis. Contribution of Working Group I to the Fifth Assessment Report of the Intergovernmental Panel on Climate Change*, Stocker, T.F., Qin, D., Plattner, G.K., Tignor, M., Allen, S.K., Boschung, J., Nauels, A., Xia, Y., Bex, V., Midgley, P.M., eds. Cambridge University Press, Cambridge, UK, and New York, NY, 1535 p.  
www.ipcc.ch/report/ar5/wg1/
- Ivancic, T.J. and Shaw, S.B., 2016. "A U.S.-based analysis of the ability of the Clausius-Clapeyron relationship to explain changes in extreme rainfall with changing temperature." *Journal of Geophysical Research Atmospheres* 121(7). doi:10.1002/2015JD024288
- Jaeger, K.L. and Olden, J.D., 2012. "Short Communication: Electrical Resistance Sensor Arrays as a Means to Quantify Longitudinal Connectivity of Rivers." *River Research and Applications*, 28: 1843-1852 (2012). doi:10.1002/rra.1554
- Jaquette, C., Wohl, E., Cooper, D., 2005. "Establishing a context for river rehabilitation, North Fork Gunnison River, Colorado." *Environmental Management*, 2005 May; 35(5):593-606. doi:10.1007/s00267-004-0101-2

- James, D.A., 2011. "The Influence of *Didymosphenia geminata* on Fisheries in the Black Hills of South Dakota." Ph.D. Dissertation, South Dakota State University, Brookings, SD. In *Electronic Theses and Dissertations*.  
<https://openprairie.sdstate.edu/etd/482>
- James, D.A., Mosel, K., Chipps, S.R., 2014. "The influence of light, stream gradient, and iron on *Didymosphenia geminata* bloom development in the Black Hills, SD." *Hydrobiologia* Vol. 721, Issue 1, Jan 2014, pp. 117-127.  
doi:10.1007/s10750-013-1654-y
- Jerenev, A. and Lann, H., 1971. "Mercury Accumulation in food chains." *Oikos* 22(3), pp. 403-406.
- Julien, P.Y., 1995. *Erosion and Sedimentation*. 280 p.
- Julien, P.Y. and Simons, D.B., 1985. "Sediment transport capacity of overland flow." *Transactions of the ASAE*, vol. 28 (3), May-June 1985, pp. 755-762.
- Jurgens, T.J., 1968. "A survey of pollution on selected streams in the Black Hills of South Dakota." Unpublished M.S. Thesis, South Dakota State University, Brookings, SD.
- Karna, R.R., Noerpel, M., Betts, A.R., Scheckel, K.G., 2017. "Lead and Arsenic Bioaccessibility and Speciation as a Function of Soil Particle Size." *Journal of Environmental Quality*, 46:1225-1235.
- Karner, D.B., Muller, R.A., 2000. "A Causality Problem for Milankovitch." *Science* 288: 2143-44.
- Keon, N.E., Swartz, C.H., Brabander, D.J., Harvey, C., Hemond, H.F., 2001. "Validation of an arsenic sequential extraction method for evaluating mobility in sediments." *Environmental Science & Technology*, 35(13), 2778–2784.
- Kibria, K.N., Ahiablame, L., Hay, C., Djira, G., 2015. "Streamflow Trends and Responses to Climate Variability and Land Cover Change in South Dakota." *Hydrology* 2016. 3(1):2. <https://doi.org/10.3390/hydrology3010002>
- Klimowski, B.A., Carpenter, D., Bunkers, M., 1996. South Dakota School of Mines and Technology: "Mesoscale convective systems over the northern Great Plains and Mid-Mississippi Valley."  
[https://www.comet.ucar.edu/outreach/abstract\\_final/9675669.htm](https://www.comet.ucar.edu/outreach/abstract_final/9675669.htm)
- Knowles, N. and Cayan, D.R., 2002. Potential effects of global warming on the Sacramento/San Joaquin watershed and the San Francisco estuary." *Geophysical Research Letters*, 29(18):1891
- Knowles, N., Dettinger, M.D., Cayan, D.R., 2006. "Trends in snowfall versus rainfall in the western United States." *Journal of Climate* 19:4545–4559.

- Kondolf, G. Mathais and Piegay, Herve, eds., 2003, *Tools in Fluvial Geomorphology*, 688 p. doi.10.1002/0470868333
- Koutsoyiannis, Demetris, 2006. "Nonstationarity versus scaling in hydrology." *Journal of Hydrology* 324 (2006) 239–254.
- Kröncke, I. and Reiss, H., 2010. "Influence of macrofauna long-term natural variability on benthic indices used in ecological quality assessment." *Marine Pollution Bulletin*, 60 (2010), pp. 58-68.
- Kumar V., 2011. "Hysteresis." In *Encyclopedia of Snow, Ice and Glaciers. Encyclopedia of Earth Sciences Series*, Singh, V.P., Singh, P., Haritashya, U.K., eds. Springer, Dordrecht. doi.org/10.1007/978-90-481-2642-2\_252
- Kunkel, K., Karl, T.R., Easterling, D.R., Redmond, K., Young, J., Yin, X., Hennon, P., 2013. "Probable maximum precipitation and climate change." *Geophys. Res. Lett.*, 40: 1402–1408. doi:10.1002/grl.50334
- Kuwabara, J.S., 1992. "Associations between benthic flora and diel changes in dissolved arsenic, phosphorus, and related physico-chemical parameters." *Journal of the North American Benthological Society*, vol. 11, pp. 218-228.
- Kuwabara, J.S., Cain, D.J., Carter, J.L., Fend, S.V., 1988. "Biological investigations—Surface Water Toxics Program, Whitewood Creek and the Belle Fourche and Cheyenne Rivers, South Dakota." *USGS Applied Research Studies of the Cheyenne River System, SD—Description and Collation of Data, Water Years 1985-86*, Goddard, K.E., ed. USGS Open-File Report 88-484, ch. J, pp. 148-158.
- Kuwabara, J.S., Chang, C.C.Y., Pasilis, S.P., 1988. "Effects of algal growth on arsenic transport in Whitewood Creek, South Dakota--Preliminary results." *USGS Toxic Substances Hydrology Program—Surface-Water Contamination—Proceedings of the Technical Meeting, Denver, CO, Feb. 2-4, 1987*, Mallard, G.E., ed. USGS Open-File Report 87-764, pp. 33-38.
- Kuwabara, J.S., Chang, C.C.Y., Pasilis, S.P., 1989. "Periphyton effects on arsenic transport in Whitewood Creek, South Dakota." *USGS Toxic substances Hydrology Program—Proceedings of the Technical Meeting, Phoenix, AZ, Sep.26-30, 1988*, pp. 247-256.
- Kuwabara, J.S., Chang, C.C.Y., Pasilis, S.P., 1990. "Effects of benthic flora on arsenic transport." *Journal of Environmental Engineering*, vol. 116, pp. 394-409.
- Kuwabara, J.S., Chang, C.C.Y., Pasilis, S. P., 2003. "Section I: Effects of benthic flora on arsenic transport in Whitewood Creek, South Dakota." In "Toxic substances in surface waters and sediments—a study to assess the effects of arsenic-contaminated alluvial sediment in Whitewood Creek, South Dakota." USGS Professional Paper 1681, 56 p.

Kunkel, K.E., Stevens, L.E., Stevens, S.E., Sun, L., Janssen, E., Wuebbles, D., Kruk, M.C., Thomas, D.P., Shulski, M., Umphlett, N., Hubbard, K., Robbins, K., Romolo, L., Akyuz, A., Pathak T., Bergantino, T., Dobson, J.G., 2013. "Regional Climate Trends and Scenarios for the U.S. National Climate Assessment, Part 4: Climate of the U.S. Great Plains." NOAA Technical Report NESDIS 142-4.

<http://scenarios.globalchange.gov/regions/great-plains>

Laidler, K.J., 1984. "The development of the Arrhenius equation." *J. Chem.Educ.* 1984, 61, 6, 494. doi.org/10.1021/ed061p494

Lamb, M.P., et al., 2014. "Incipient sediment motion across the river to debris-flow transition." *Geology*, Jan. 2014.

Lane, E.W., 1955. "The importance of fluvial morphology in hydraulic engineering." *Proceedings, American Society of Civil Engineers*, vol. 81, Paper 745, July.

Langmuir, D., 1997, *Aqueous Environmental Geochemistry*. Prentice Hall, 600 p.

Larson, L.N., Kipp, G.G., Mott, H.V., Stone, J.J., 2012. "Sediment pore-water interactions associated with arsenic and uranium transport from the North Cave Hills mining region, South Dakota, USA." *Applied Geochemistry*, 27(4), 879–891.

Lavery, J.M., Kurek, J., Rühland, K.M., Gillis, C.A., Pisaric, M.F.J., Smol, J.P., 2014. "Exploring the environmental context of recent *Didymosphenia geminata* proliferation in Gaspésie, Quebec, using paleolimnology." *Canadian Journal of Fisheries and Aquatic Sciences*. 71(4): 616-626. doi.org/10.1139/cjfas-2013-0442

Lebel, L., Anderies, J.M., Campbell, B., Folke, C., Hatfield-Dodds, S., Hughes, T.P., Wilson, J., 2006. "Governance and the Capacity to Manage Resilience in Regional Social-Ecological Systems." *Ecology and Society* Vol. 11, No. 1 (Jun 2006), 21 p. <https://www.jstor.org/stable/26267807>

Leopold, L.B. and Maddock, J.T., 1953. "The hydraulic geometry of stream channels and some physiographic implications." USGS Professional Paper 252.

Leopold, L.B., Wolman, M.G., Miller, J.P., 1964. "*Fluvial Processes in Geomorphology*." Referenced in "Models, the Establishment, and the Real World: Why Do So Many Flood Problems Remain in the UK?" *Journal of Geoscience and Environment Protection*, Vol.5 No.2, Feb.14, 2017

Leopold, L. and Bull, W. 1979. "Base Level, Aggradation and Grade." *Proceedings of the American Philosophical Society*, 123(3): 168-202.

Leopold, L.B., 1992. "Base level rise: Gradient of deposition." *Israel Journal of Earth Science*, vol. 41, pp. 57-64.

- Liang, X., Lettenmaier, D.P., Wood, E.F., Burges, J.J., 1994. "A Simple Hydrologically Based Model of Land Surface Water and Energy Fluxes for GSMs." *J. Geophys. Res.*, 99(D7), 14,415-14,428.
- Liu, G., Li, Y., Cai, Y., 2011. "Adsorption of mercury on solids in the aquatic environment." In *Environmental Chemistry and Toxicology of Mercury*, 2011 (Liu, G, Cai, Y., O'Driscoll, N., eds.), pp. 367-387
- Livneh, B., Rosenberg, E.A., Lin, C., Nijssen, B., Mishra, V., Andreadis, K.M., Maurer, E.P., Lettenmaier, D.P., 2013. "A Long-Term Hydrologically Based Dataset of Land Surface Fluxes and States for the Conterminous United States: Update and Extensions." *J. Climate*, 26, 9384– 9392. doi.org/10.1175/JCLI-D-12-00508.1
- Livneh, B., Bohn, T.J., Pierce, D.W., Munoz-Arriola, F., Nijssen, B., Vose, R., Cayan, D.R., Brekke, L., 2015. "A spatially comprehensive, hydrometeorological data set for Mexico, the US, and Southern Canada 1950–2013." "Scientific data, 2," 150042 p. doi:10.1038/sdata.2015.42
- Luminultra team, 2019. "Over-allocated: the Story of the Colorado River." Feb. 20, 2019 online blog at: <https://www.luminultra.com/blog/colorado-river-story/>
- Lynch, S., Batty, L., and Byrne, P., 2014. "Environmental Risk of Metal Mining Contaminated River Bank Sediment at Redox-Transitional Zones." *Minerals*, 2014, 4(1), p. 52-73. doi:10.3390/min4010052
- Lynch, S., Batty, L., and Byrne, P., 2017. "Critical control of flooding and draining sequences on the environmental risk of Zn-contaminated riverbank sediments." *Journal of Soils and Sediments* Nov. 2017, pp. 2691-2707. doi:1007/s11368-016-1646-4
- Macklin, M.G., Brewer, P.A., Hudson-Edwards, K.A., Bird, G., Coulthard, T.J., Dennis, I.A., Lechler, P.J., Miller, J.R., Turner, J.N., 2006. "A geomorphological approach to the management of rivers contaminated by metal mining." *Geomorphology*, vol. 79, Issues 3–4, pp. 423-447. doi.org/10.1016/j.geomorph.2006.06.024
- McCabe, G. and Wolock, D., 2020. "Multi-year hydroclimatic droughts and pluvials across the conterminous United States." *International Journal of Climatology*. 41. doi:10.1002/joc.6925
- Maidment, David R., 2002. *Arc Hydro: GIS for Water Resources*. Published by ESRI, Inc., pp. 70-72. Referenced in a 2012 UNL civil engineering class co-taught by Dr. Maidment, University of Texas, Dr. David Tarboton, Utah State University, and Dr. Ayse Kilic, UNL.

- Marcus, W.A., Meyer, G.A., Nimmo, D.W.R., 2001. "Geomorphic control of persistent mine impacts in a Yellowstone Park stream and implications for the recovery of fluvial systems." *Geology* 2001; 29, pp. 355-358. doi:10.1130/0091-7613
- Mallakpour, I., Villarini, G., 2015. "The Changing Nature of Flooding Across the Central United States." *Nature Climate Change*. Advanced online publication, Feb. 2015. doi:org.10.1038/nclimate2516
- Mallakpour, I., Agha Kouchak, A., Sadegh, M., 2019. "Climate-induced changes in the risk of hydrological failure of major dams in California." *Geophysical Research Letters*, 46, 2130–2139. doi.org/10.1029/2018GL081888
- Marron, D.C., 1986. "Floodplain storage of mine tailings near Lead, South Dakota." *Geological Society of America, Annual Meeting, Abstract Program*, San Antonio, Texas p.682.
- Marron, D.C., 1987. "Floodplain storage of metal-contaminated sediments downstream of gold mine at Lead, South Dakota." *Chemical Quality of Water and the Hydrologic Cycle*, Averett, R.C. and McKnight, D.M., eds., pp. 93–209.
- Marron, D.C., 1988. "Transport and flood-plain storage of metals associated with sediment downstream from Lead, South Dakota." *USGS Toxic Substances Hydrology Program—Surface-Water Contamination—Proceedings of the Technical Meeting, Denver, CO, Feb. 2-4, 1987*, Mallard, G.E., ed. USGS Open-File Report 87-764, pp. 11-12.
- Marron, D.C., 1988. *Field and laboratory data describing physical and chemical characteristics of metal-contaminated flood-plain deposits downstream from Lead, west-central South Dakota, USA*. USGS Open-File Report 88-349, p. 32.
- Marron, D.C., 1989. "Trends in arsenic concentration and grain-size distribution of metal-contaminated overbank sediments along the Belle Fourche River downstream from Whitewood Creek, South Dakota." *USGS Toxic Substances Hydrology Program—Proceedings of the Technical Meeting, Phoenix, AZ, Sep. 26–30, 1988*, Mallard, G.E. and Ragone, G.E., eds., USGS Water-Resources Investigations Report 88-4220, pp. 211–216.
- Marron, D.C., 1989. "Physical and chemical characteristics of a metal-contaminated overbank deposit, west-central South Dakota, USA." *Earth Surface Processes and Landforms*, vol. 14, pp. 419-432. doi:10.1002/esp.3290140507

Marron, D.C., 1992. "Floodplain storage of mine tailings in the Belle Fourche River system: a sediment budget approach." *Earth Surface Processes and Landforms*, vol. 17, issue 7, Nov.1, 1992, pp. 675-685.  
doi:10.1002/esp.3290170704

Martin, J.E., Foster, J.F., Fahrenbach, M.D., Tomhave, D.W., Schulz, L., 2004. *Geologic Map of South Dakota*.

Masson-Delmotte, V., Zhai, P., Pirani, A., Connors, S.L., Péan, C., Berger, S., Caud, N., Chen, Y., Goldfarb, L., Gomis, M.I., Huang, M., Leitzell, K., Lonnoy, E., Matthews, J.B.R., Maycock, T.K., Waterfield, T., Yelekçi, O., Yu, R., Zhou, B., eds., 2021. *Climate Change 2021: The Physical Science Basis. Contribution of Working Group I to the Sixth Assessment Report of the IPCC*. In press.

Matalas, N.C., 2017. *Note on the Assumption of Hydrologic Stationarity*.  
<http://opensiuc.ib.siu.edu/cgi/viewcontent.cgi?article=1242&context=jcwre>

May, T.W., Wiedmeyer, R.H., Gober, J., Larson, S., 2001. "Influence of Mining-Related Activities on Concentrations of Metals in Water and Sediment from Streams of the Black Hills, South Dakota." *Arch. Environ. Contam. Toxicol.* 40: 1–9. doi:10.1007/s002440010142

McCuen, R.H. and Galloway, K.E., 2010. "Record Length Requirements for Annual Maximum Flood Series." *Journal of Hydrologic Engineering* Vol. 15 issue 9. doi:10.1061/(ASCE)HE.1943-5584.0000223

McKallip, T.E., Goddard, K.E., and Horowitz, A.J., 1989. "Arsenic in the alluvial sediments of Whitewood Creek and the Belle Fourche and Cheyenne rivers in western South Dakota." *USGS Toxic Substances Hydrology Program—Proceedings of the Technical Meeting, Phoenix, AZ, Sep. 26-30, 1988*, Mallard, G.E., and Ragone, S.E., eds. USGS Water-Resources Investigations Report 88-4220, pp. 203-209.

McKay, L., Bondelid, T., Dewald, T., Johnston, J., Moore, R., Rea, A., 2021. "NHDPlus Version 2: User Guide", accessed Oct. 21, 2021 at:  
[https://s3.amazonaws.com/edap.nhdplus/NHDPlusV21/Documentation/NHDPlusV2\\_User\\_Guide.pdf](https://s3.amazonaws.com/edap.nhdplus/NHDPlusV21/Documentation/NHDPlusV2_User_Guide.pdf)

McRoberts, D.B. and Nielsen-Gammon, J.W., 2011. "A New Homogenized Climate Division Precipitation Dataset for Analysis of Climate Variability and Climate Change." *Journal of Applied Meteorology and Climatology*, Vol. 50: Issue 6, pp. 1187-1199. <https://doi.org/10.1175/2010JAMC2626.1>



- Meade, R.H. and Moody, J.A., 2009. "Causes for the decline of suspended-sediment discharge in the Mississippi River system, 1940-2007." *Hydrological Processes*, 24, 35-49. doi:10.1002/hyp.7477
- Melillo, J., Richmond, T.C., Yohe, G.W., eds., 2014. "Climate Change Impacts in the United States." *The Third National Climate Assessment*, USGCRP publication, 841 p. doi:10.7930/J0Z31WJ2
- Mellema, W.J. and Wei, T.C., 1986. "Missouri River aggradation and degradation trends." *Proceedings of the Fourth Federal Interagency Sedimentation Conference*, Wash., D.C.
- Miller, G.P., 2017. "Arsenic Partitioning: Making Predictions Using PHREEQC." [https://www.brr.cr.usgs.gov/projects/GWC\\_chemtherm/FinalAbsPDF/miller.pdf](https://www.brr.cr.usgs.gov/projects/GWC_chemtherm/FinalAbsPDF/miller.pdf)
- Miller, L.D. and Driscoll, D.G., 1993. "Streamflow characteristics for the Black Hills of South Dakota, through water year 1993." USGS Water-Resources Investigations Report 97-4288, 322 p.
- Milly, P., Betancourt, J., Falkenmark, M., Hirsch, R.M., Kundzewicz, Z., Lettenmaier, D., Stouffer, R., 2008. "Climate Change – Stationarity is Dead: Whither Water Management?" *Science*, Vol. 319 no. 5863, pp. 573-574. doi.10.1126/science.1151915
- Milly, P.C.D., Wetherald, R.T., Kunne, K.A., Delworth, T.L., 2002. "Increasing risk of great floods in a changing climate." *Nature* Vol. 415, 31 Jan.2002, pp. 514-517. doi.org/10.1038/415514a
- Mining History Association news release, 1993. "Discover Mining History." <http://www.mininghistoryassociation.org/BlackHills.htm>https
- Moe J., de Schampelaere, K., Clements, W.H., Sorensen, M., van den Brink, P., Liess, M., 2012. "Combined and interactive effects of global climate change and toxicants on populations and communities." *Environ Toxicol Chem* 32:49–61.
- Morel, F.M.M., Kraepiel, A.M.L., Amyot, M., 1998. "The chemical cycle and bioaccumulation of mercury." *Annu Rev Ecol Evol Syst* 29:543–566.
- Morlok, Brett A., 2010. "Water quality and physical habitat assessment relating to total suspended solids loadings in the lower Cheyenne River Watershed." Unpublished M.S. Thesis, South Dakota School of Mines and Technology, Rapid City, SD. <https://southdakotaschoolofminesandtechnology.on.worldcat.org/oclc/665089208>

Mote, P.W., 2003. "Trends in snow water equivalent in the Pacific Northwest and their climatic causes." *Geophysical Research Letters*, Vol. 30, Issue 12, June 2003. doi:org/10.1029/2003GL017258

Mujere, N. and Moyce, W., 2018. "Climate Change Impacts on Surface Water." *Hydrology and Water Resource Management: Breakthroughs in Research and Practice*, 19 p. doi:10.4018/978-1-5225-3427-3.ch004

Mukherjee, A., von Brömssen, M., Scanlon, B., Bhattacharya, P., Fryar, A., Hasan, M., Ahmed, K.M., Chatterjee, D., Jacks, G., Sracek, O., 2007. "Hydrogeochemical comparison and effects of overlapping redox zones on groundwater arsenic near the Western (Bhagirathi sub-basin, India) and Eastern (Meghna sub-basin, Bangladesh) margins of the Bengal Basin." *Journal of Contaminant Hydrology* 99: 31-48. doi:10.016/j.jconhyd.2007.10.005

Munoz, A., Chervona, Y., Hall, M., Kluz, T., Gamble, M.V., Costa, M., 2016. "Sex-specific patterns and deregulation of endocrine pathways in the gene expression profiles of Bangladeshi adults exposed to arsenic-contaminated drinking water." *Toxicology and Applied Pharmacology*, May 1, 2015; 284(3):330-8. doi:10.1016/j.taap.2015.02.025

Nace, R.L. and Pluhowski, E.J., 1956. "Drought of the 1950s with Special Reference to the Midcontinent." USGS Water Supply Paper 1804, 88 p.

Nanson, Gerald C., 1980. "A Regional Trend to Meander Migration." *The Journal of Geology* 88 no.1, Jan.1980: 100-108. doi:10.1086/628477

National Academies of Science, Engineering and Medicine, 2010. "Understanding the Changing Planet: Strategic Directions for the Geographical Sciences." <https://www.nap.edu/read/12860/chapter/6>

National Academies of Sciences, Engineering, and Medicine 2013. "Reference Guide for Applying Risk and Reliability-Based Approaches for Bridge Scour Prediction." Washington, DC: The National Academies Press, 164 p. <https://doi.org/10.17226/22477>

NASA, 2003. "Gateway to Astronaut Photography of the Earth, Photo ISS006-E-52932." <https://eol.jsc.nasa.gov/SearchPhotos/photo.pl?mission=ISS006&roll=E&frame=52932>

NASA, 2003. "Gateway to Astronaut Photography of the Earth, Photo ISS007-E-9267." <https://eol.jsc.nasa.gov/SearchPhotos/photo.pl?mission=ISS007&roll=E&frame=9267>

National Oceanic and Atmospheric Administration (NOAA), Earth System Research Laboratory (ESRL), Physical Sciences Division, no date given. "Rapid City AFB SD monthly anomalies" (temperature and precipitation), 1961-1990." Online data set. [www.esrl.noaa.gov/psd/cgi-bin/data/usclimate/city.pl?state=SD;lane=fast;itypea=4;loc.x=127;loc.y=188;.cgifields=itypea&City=444](http://www.esrl.noaa.gov/psd/cgi-bin/data/usclimate/city.pl?state=SD;lane=fast;itypea=4;loc.x=127;loc.y=188;.cgifields=itypea&City=444)

NOAA National Climate Data Center, no date given. "Climate Data Online." Online data set. <http://www.ncdc.noaa.gov/cdo-web/>

NOAA (formerly Weather Bureau, Rapid City), 1924. Historical records for April 6-9, 1924.

NOAA National Centers for Environmental Information, 2018. "Climate at a Glance: Statewide Time Series for South Dakota." [https://www.ncdc.noaa.gov/cag/statewide/time-series/39/tavg/12/12/1895-2018?base\\_prd=true&firstbaseyear=1901&lastbaseyear=2000&trend=true&trend\\_base=10&firsttrendyear=1895&lasttrendyear=2018&filter=true&filterType=loess](https://www.ncdc.noaa.gov/cag/statewide/time-series/39/tavg/12/12/1895-2018?base_prd=true&firstbaseyear=1901&lastbaseyear=2000&trend=true&trend_base=10&firsttrendyear=1895&lasttrendyear=2018&filter=true&filterType=loess)

NOAA National Climatic Data Center (NCDC), 2021. "Climate of South Dakota." Online data set. [https://www.ncdc.noaa.gov/climatenormals/clim60/states/Clim\\_SD\\_01.pdf](https://www.ncdc.noaa.gov/climatenormals/clim60/states/Clim_SD_01.pdf)

NOAA, 2021. Accessed May 2, 2021 from Science on a Sphere site. <https://sos.noaa.gov/catalog/datasets/climate-model-temperature-change-rcp-60-2006-2100/>

Image provided by the NOAA-ESRL Physical Sciences Division, Boulder, CO. <https://www.esrl.noaa.gov/psd/>

National Research Council, 1995. *Natural Climate Variability on Decade-to-Century Time Scales*. The National Academies Press, Wash., D.C. [doi.org/10.17226/5142](https://doi.org/10.17226/5142)

National Resource Conservation Service (NRCS) and RESPEC Consulting Services, 2007. "Lower Belle Fourche – HUC 10120202 South Dakota Portion of 8 Digit Hydrologic Unit Profile, Belle Fourche River Watershed Partnership." <http://bellefourchewatershed.org/media/bellefourchefactor360com/documents/reports/3%20-%20Final%20LBF%20RWA.pdf>

Neill, C.R., ed., 1973. *Guide to Bridge Hydraulics*. Univ. of Toronto Press, 191 p.

Newman, R.L., Berry, C.R., and Duffy, W., 1999. "A Biological Assessment of Four Black Hills Streams." *Proceedings of the South Dakota Academy of Science*, Vol. 8 (1999)

Noble, A.J., 1950. "Ore Mineralization in the Homestake Gold Mine, Lead, South Dakota." *Bulletin, Geological Society of America*, vol. 61, pp. 221-252.

Nomikos, A., Bodwell, J., Hamilton, J., Gosse, J., 2006. Dartmouth College researchers cited in "Low Doses Of Arsenic Can Have Broad Impact." *Science Daily*, Dec.6, 2016 online publication.  
<https://www.sciencedaily.com/releases/2006/12/061204123351.htm>

Nordstrom, K., 2009. "Acid rock drainage and climate change." *Journal of Geochemical Exploration*, Vol. 100, Issues 2-3, Feb.-Mar. 2009, pp. 97-104., Vol.100, Issues 2–3, Feb.–Mar. 2009, pp. 97-104.  
<https://doi.org/10.1016/j.gexplo.2008.08.002>

North Carolina Institute for Climatic Studies (CICS-NC) online data set.  
<https://ncics.org/data/>

North Dakota State University, 2016. Graph: "Meade County South Dakota annual first and last frost dates data."  
[https://www.ndsu.edu/climate/South%20Dakota/Homepage/First\\_last\\_frost/Meade.html](https://www.ndsu.edu/climate/South%20Dakota/Homepage/First_last_frost/Meade.html)

Norton, P.A., Anderson, M.T., Stamm, J.F., 2014. "Trends in Annual, Seasonal, and Monthly Streamflow Characteristics at 227 Streamgages in the Missouri River Watershed, Water Years 1960–2011." USGS Scientific Investigations Report 2014-5053, 128 p.

O'Brien, K. and Sygna, L., et al., 2004. "Vulnerable or Resilient? A Multi-Scale Assessment of Climate Impacts and Vulnerability in Norway." *Climatic Change* 64: 193-225.

O'Connor, J.E. and Costa, J.E., 1959. *Large Floods in the United States: Where They Happen and Why*. USGS Circular 1245, 13 p.

O'Day, P. and Illera, V., 2010. "Final Report Addendum, Environmental Fate and Exposure Assessment for Arsenic in Groundwater." U.S. Dept. of Defense Strategic Environmental Research and Development Program (SERDP) Project ER01374, University of California, Merced, pp.1-38.

O'Day, P.A., Vlassopoulos, D., Root, R., Rivera, N., 2004. "The influence of sulfur and iron on dissolved arsenic concentrations in the shallow subsurface under changing redox conditions." *Proceedings of the National Academy of Sciences*, 101(38), 13703–13708.

Olson, S., Sant-Miller, A., White, K., 2019. "U.S. Army Corps of Engineers Time Series Toolbox User Guide."

- Ollson, C.J., Smith, E., Scheckel, K.G., Betts, A.R., Juhasza, A.L., 2016. "Assessment of arsenic speciation and bioaccessibility in mine-impacted materials." *Journal of Hazardous Materials*, vol. 313, Aug. 5, 2016, pp. 130-137. doi.org/10.1016/j.jhazmat.2016.03.090
- Ombaba, J.M., 1996. "Total Mercury Determination in Biological and Environmental Standard Samples by Gold Amalgamation Followed by Cold Vapor Atomic Absorption Spectrometry." *Microchemical Journal*, Vol. 53, Issue 2, Feb. 1996, pp. 195–200.
- Owens, P.N., Batalla, R.J., Collins, A.J., Gomez, B., Hicks, D.M., Horowitz, A.J., Kondolf, G.M., Marden, M., Page, M.J., Peacock, D.H., Petticrew, E.L., Salomonsk, W., Trustrum, N.A., 2005. "Fine-Grained Sediment in River Systems: Environmental Significance and Management issues." *River Research and Applications* 21: 693–717 (2005). doi:10.1002/rra.878
- Parks, J.M., Johs, A., Podar, M., Bridou, R., Hurt, R.A., Jr., Smith, S.D., Tomanicek, S.J., Qian, Y., Brown, S.D., Brandt, C.C., Palumbo, A.V., Smith, J.C., Wall, J.D., Elias, D.A., Liang, L., 2013. "The genetic basis for bacterial mercury methylation." *Science* 339:1332–1335.
- Palecki, M.A., Angel J.R., Hollinger S.E., 2005. "Storm precipitation in the United States. Part I: Meteorological characteristics." *Journal of Applied Meteorology* 44:933-946.
- Pall, P., Allen, M.R., Stone, D.A, 2007. "Testing the Clausius–Clapeyron constraint on changes in extreme precipitation under CO<sub>2</sub> warming." *Clim Dyn* 28, 351–363 (2007). <https://doi.org/10.1007/s00382-006-0180-2>
- Patceg, Andrew J., 2006. "Physical Habitat Assessment of the Lower Cheyenne River Watershed." Unpublished M.S. Thesis, South Dakota School of Mines and Technology, Rapid City, SD.
- Pfeifle, B.D., Stamm, J.F., Stone, J.J., 2018. "Arsenic Geochemistry of Alluvial Sediments and Pore Waters Affected by Mine Tailings along the Belle Fourche and Cheyenne River Floodplains." *Water Air Soil Pollut* 229, p. 183. <https://doi.org/10.1007/s11270-018-3836-8>
- Pedersen, H.D., Postma, D., Jakobsen, R., 2006. "Release of arsenic associated with the reduction and transformation of iron oxides." *Geochimica et Cosmochimica Acta* 70(16), 4116–4129.

- Peltier, Louis C., 1950. "The Geographic Cycle in Periglacial Regions as It is Related to Climatic Geomorphology." *Annals of the Association of American Geographers* Vol. 40, No. 2 (Sep., 1950), pp. 214-236.
- Pew Center on Global Climate Change (Smith, J.B., Stratus Consulting), 2004. 505-New/Piz (pewtrusts.org)
- Pew Center on Global Climate Change (Postel, S.), 2019. "The Water Cycle is Broken but We can Fix it." <https://www.pewtrusts.org/en/trend/archive/spring-2019/the-water-cycle-is-broken-but-we-can-fix-it>
- Pfeifle, B.D., Stamm, J.F., Stone, J.J., 2018. "Arsenic Geochemistry of Alluvial Sediments and Pore Waters Affected by Mine Tailings along the Belle Fourche and Cheyenne River Floodplains." *Water Air Soil Pollut* 229, p. 183. <https://doi.org/10.1007/s11270-018-3836-8>
- Phillips, G.R., Medvick, P.A., Skaar, D.R., Knight, D.E., 1984. "Factors affecting mobilization, transport, and bio-availability of mercury in reservoirs of the upper Missouri River basin." Contract report prepared for the U.S. EPA.
- Pierce, D.W., Cayan, D.R., Thrasher, B.L., 2014. "Statistical Downscaling Using Localized Constructed Analogs (LOCA)" *Journal of Hydrometeorology*, 15(6), 2558- 2585. doi:10.1175/JHM-D-14-0082.1
- Plumley, W.J., 1948. "Black Hills terrace gravels: a study in sediment transport." *Journal of Geology* 56:526-577.
- Poff, N.L., Allan, J.D., Bain, M.B., Karr, J.R., Prestegard, K.L., Richter, B.D., Sparks, R.E., Stromberg, J.C., 1997. "The natural flow regime." *Bioscience* 47: 769-784.
- Ponce, V.M. and Simons, D.B., 1977. "Shallow wave propagation in open channel flow." *American Society of Civil Engineers Journal of the Hydraulics Division*, Vol. 103, No. HY 12, December.
- Ponce, V.M., 2007. "The Lane Relation Revisited." Accessed Feb. 2, 2014 at Dr. Ponce's San Diego State University website: [http://ponce.sdsu.edu/lane\\_relation\\_revisited.html](http://ponce.sdsu.edu/lane_relation_revisited.html)
- Porterfield, G., 1977. "Computation of fluvial-sediment discharge." *Techniques of Water-Resources Investigations of the U.S. Geological Survey*, Chap. C3, Book 3.

Prein, A., Rasmussen, R., Ikeda, K., et al., 2017. "The future intensification of hourly precipitation extremes." *Nature Climate Change* 7, 48–52 (2017). <https://doi.org/10.1038/nclimate3168>

Prentice, I.C., Farquhar, G.D, Fasham, M.J.R, Goulden, M.L., Heimann, M., Jaramillo, V.J., Kheshgi, H.S., Le Quéré, C., Scholes, R.J., Wallace, D.W.R, 2018. *The Carbon Cycle and Atmospheric Carbon Dioxide*. IPCC publication, 237 p. <https://www.ipcc.ch/site/assets/uploads/2018/02/TAR-03.pdf> and <https://archive.ipcc.ch/ipccreports/tar/wg1/096.htm>

Pryor, S.C., Scavia, D., Downer, C., Gaden, M., Iverson, L.N., Patz J., Robertson, G.P., 2014. "Chapter 18: Midwest climate change impacts in the United States." In *Climate Change Impacts in the United States. The Third National Climate Assessment*, Melillo, J.M., Richmond, T.C., Yohe, G.W., eds. USGCRP publication, pp. 418-440. <https://doi.org/10.7930/J0J1012N>

Rahn, P.H., Davis, A.D., Webb, C.J., Nichols, A.D., 1996. "Water quality impacts from mining in the Black Hills, South Dakota, USA." *Environ Geol* 27:38–53

Rahn, P.H., 1996. "Terrace Chronology for Rapid Creek in Rapid City, South Dakota." Geological Society of America Abstracts with Program 28:35.

Rajith, M., Pradhanang, S.M., Schneiderman, E.M., Pierson, D.C., Anandhi, A., Zion, M.S., Matonse, A.H., Lounsbury, D.G., Steenhuis, T.S., 2013. "Suspended sediment source areas and future climate impact on soil erosion and sediment yield in a New York City water supply watershed, USA." *Geomorphology*, vol. 183, Feb. 1, 2013, pp. 110-119. [doi.org/10.1016/j.geomorph.2012.06.021](https://doi.org/10.1016/j.geomorph.2012.06.021)

Ravenscroft, P., Brammer, H., Richards, K., 2009. *Arsenic Pollution: a Global Synthesis*. [doi:10.1002/9781444308785](https://doi.org/10.1002/9781444308785)

Razavi, T. and Coulibaly, P., 2013. "Streamflow Prediction in Ungauged Basins: Review of Regionalization Methods." *J. Hydrol. Eng.*, 2013, 18(8): 958-975

Rees, T.F. and Ranville, J.F., 1988. "Identification of colloids present at Sheeler Seeps, Whitewood Creek, South Dakota." *USGS Toxic Substances Hydrology Program—Surface-Water Contamination—Proceedings of the Technical Meeting, Denver, CO, Feb. 2-4, 1987*, Mallard, G.E., ed. USGS Open-File Report 87-764, pp. 29-32.

Renaie, S.L., Drakos, P.G., Katzman, D., Malmon, D.V., McDonald, E.V., and Rytel, R.T., 2004. "Geomorphic controls on contaminant distribution along an ephemeral stream." *Earth Surface Processes and Landforms*, Vol. 29, No. 10, Sep. 2004, pp. 1209-1223.

- Reidmiller, D.R., Avery, C.W., Easterling, D.R., Kunkel, K.E., Lewis, K.L.M., Maycock, T.K., Stewart, B.C., eds., 2018. *Impacts, Risks, and Adaptation in the United States: Fourth National Climate Assessment, Vol.II.* USGCRP publication, 1,515 p. doi:10.7930/NCA4.2018
- Ritchie, J.C., Cooper, C.M., McHenry, J.C., 1986. "Sediment accumulation rates in lakes and reservoirs in the Mississippi River Valley." *Proceedings of the Third International Symposium on River Sedimentation*, Wang, S.Y., Shen, H.W., Ding, L.Z., eds., University of Mississippi, pp. 122-137.
- Roddy, W.R., Green, E.A., Sowards, C.L., 1991. *Reconnaissance Investigation of Water Quality, Bottom Sediment, and Biota Associated with Irrigation Drainage in the Belle Fourche Reclamation Project, Western South Dakota, 1988-1989.* USGS Water-Resources Investigations Report 90-4192, 113 p.
- Rohr, J.R., Johnson, P., Hickey, C.W., Helm, R.C., Fritz, A.R., Brasfield, S., 2012. "Implications of global climate change for natural resource damage assessment, restoration, and rehabilitation." *Environ Toxicol Chem* 32:93–101.
- Rolfe, B.N. and Hadley, R.F., 1964. "Weathering and Transport of Sediment in the Cheyenne River Basin, Eastern Wyoming." *Proceedings of the 12<sup>th</sup> National Conference on Clays and Clay Minerals, Atlanta, GA, Sep./Oct. 1963.* Pergamon Press, NY, pp. 649-670.
- Roman, D., Vogel, R.M., Schwarz, G.E., 2012. "Regional Regression Models of Watershed Suspended-Sediment Discharge for the Eastern United States." *Journal of Hydrology* (472-473):53-62.
- Root, R.A., Dixit, S., Campbell, K.M., Jew, A.D., Hering, J.G., O'Day, P.A., 2007. "Arsenic sequestration by sorption processes in high-iron sediments." *Geochimica et Cosmochimica Acta*, 71(23), 5782–5803.
- Root, R.A., Vlassopoulos, D., Rivera, N.A., Rafferty, M.T., Andrews, C., O'Day, P.A., 2009. "Speciation and natural attenuation of arsenic and iron in a tidally influenced shallow aquifer." *Geochimica et Cosmochimica Acta*, 73(19), 5528–5553.
- Romero-Mujalli, G., Hartmann, J., Börker, J., Gaillardet, J., Calmels, D., 2019. "Temperature and CO<sub>2</sub> dependency of global carbonate weathering fluxes – Implications for future carbonate weathering research." *Chemical Geology*, Vol. 527. doi.org/10.1016/j.chemgeo.2018.08.010
- Rosgen, D.L., 1994. "A classification of natural rivers." *CATENA* 22 (1994), 169-199. [https://doi.org/10.1016/0341-8162\(94\)90001-9](https://doi.org/10.1016/0341-8162(94)90001-9)
- Rovira, A. and Batalla, R.J., 2006. "Temporal distribution of suspended sediment transport in a Mediterranean basin: The Lower Rordera (NE Spain)." *Geomorphology*, Vol. 79, Issues 1-2, 15 Sep. 2006, pp. 58-71.



- Samuels, R., Rimmer, A., Hartmann, A., Krichak, S., Alpert, P., 2010. "Climate Change Impacts on Jordan River Flow: Downscaling Application from a Regional Climate Model." *Journal of Hydrometeorology*, 11(4), 860-879.  
[https://journals.ametsoc.org/view/journals/hydr/11/4/2010jhm1177\\_1.xml](https://journals.ametsoc.org/view/journals/hydr/11/4/2010jhm1177_1.xml)
- Sanford Underground Research Facility, 2013. Press release, June 19, 2013.  
<http://sanfordlab.org/article/one-more-clean-water-award>
- Salomons, W., 1995. "Environmental impact of metals derived from mining activities: Processes, predictions, prevention." *Journal of Geochemical Exploration*, v. 52, pp. 5-23.
- Sando, S.K., Driscoll, D.G., Parrett, C., 2008. *Peak-flow frequency estimates based on data through water year 2001 for selected streamflow-gaging stations in South Dakota*. USGS Scientific Investigations Report 2008–5104, 367 p.
- Sadiq, M., 1997. "Arsenic chemistry in soils: an overview of thermodynamic predictions and field observations." *Water, Air, and Soil Pollution* 93:117-136.
- Sankarasubramanian, A. and Vogel, R., 2001. "Climate elasticity of streamflow in the United States." *Water Resources Research* 37(6), pp.1771–1781.  
doi:10.1029/2000WR900330
- Saunders, J.A., Lee, M.K., Shamsudduha, M., Dhakal, P., Uddin, A., Chowdury, M.T., Ahmed, K.M., 2008. "Geochemistry and mineralogy of arsenic in (natural) anaerobic groundwaters." *Applied Geochemistry* 23(11): 3205–3214.
- Schultz, P., ed. 1996. *Engineering Within Ecological Constraints*. National Academy of Engineering, 224 p. doi.org/10.17226/4919
- Schumm, S.A., 1977. *The Fluvial System*. John Wiley and Sons, New York, NY, 338 p.
- Schumm, S.A., 1991. *To Interpret the Earth: Ten Ways to Be Wrong*. Cambridge University Press, 133 p.
- Schumm, S.A., 1993. "River Response to Baselevel Change: Implications for Sequence Stratigraphy. The Journal of Geology Vol. 101 No. 2, March 1993, pp. 279-294. Accessed Jan. 15, 2013, at [www.jstor.org/stable.30081141](http://www.jstor.org/stable.30081141)
- Schumm, S.A., 2005. *River Variability and Complexity*. Cambridge University Press, pp. 64-65.
- Schumm, S.A., Harvey, M.D., Watson, C.C., 1984. *Incised Channels: Morphology, Dynamics, and Control*. Water Resources Publications, Littleton, CO, 200 p.
- Schumm, S.A. and Winkley, B.R., 1994. *The Variability of Large Alluvial Rivers*, ASCE Press, 467 p.

- Schwarz, G.E., 2008. *A Preliminary SPARROW model of suspended sediment for the conterminous United States*. USGS Open-File Report 2008–1205, 8 p. <https://pubs.usgs.gov/of/2008/1205>
- Scully, J. 1975. "Landslides in the Pierre Shale in Central South Dakota." Technical Report, Executive Summary Report for the Federal Highway Administration and SD Dept. of Transportation, 28 p.
- Seaber, P.R., Kapinos, F.P., Knapp, G.L., 1987. "Hydrologic Unit Maps." USGS Water Supply Paper 2294, 63 p.
- Searcy, J.K., 1959. USGS Water Supply Paper 1542-A, "Flow-Duration Curves," 33 p., in *Manual of Hydrology: Part 2*. doi.org/10.3133/wsp1542A
- Shafer, M., Ojima, D., Antle, J.M., Kluck, D., McPherson, R.A., Petersen, S., Scanlon, B., Sherman, K., 2014. "Chapter 19: Great Plains." In *Climate Change Impacts in the United States. The Third National Climate Assessment*, Melillo, J.M., Terese, T.C., Richmond, T., Yohe, G.W., eds., pp. 441-461. USGCRP publication. doi:10.7930/J0D798BC.
- Sharples, J. and Sharples, D., 1986. "The Rebirth of Whitewood Creek." Cottonwood Productions video.
- Shockley, J.C., 1989, "The occurrence and spatial distribution of trace elements in bottom sediments of the Whitewood Creek, Belle Fourche River, and Cheyenne River system, Western South Dakota." Unpublished M.S. Thesis, South Dakota School of Mines and Technology, Rapid City, SD.
- Smith, K.G., 1958. "Erosional processes and landforms in Badlands National Monument, South Dakota." *Geological Society of America Bulletin* 69, pp. 975–1000, 1958.
- So, H.U., Postma, D., Jakobsen, R., Larsen, F., 2008. "Sorption and desorption of arsenate and arsenite on calcite." *Geochim. Cosmochim. Acta*, 72 (2008), pp.5871-5884
- Smedley, P.L. and Kinniburgh, D.G., 2002. "A review of the source, behaviour and distribution of arsenic in natural waters." *Applied Geochemistry*, 17(5): 517–568.
- Soh, Y.C., Roddick, F., van Leeuwen, J., 2007. "The Future of Water in Australia: The potential effects of climate change and ozone depletion on Australian water quality, quantity, and treatability." *The Environmentalist* 28, 158-165 (2008).

South Dakota Dept. of Health, 1960. Two reports: 1960a: "Report on gold recovery wastes, Homestake Mining Company, Lead, South Dakota," 35 p.; and 1960b: "Report on water pollution studies, Gold Run Creek, Whitewood Creek, Belle Fourche River, Cheyenne River, South Dakota," 42 p.

South Dakota Dept. of Environment and Natural Resources (DENR), 2014. "Belle Fourche River Watershed Management and Project Implementation Plan, Segment 7.

<https://denr.sd.gov/dfta/wp/319apps/2014/documents/bellefourcheseq7.pdf>

South Dakota DENR, 2016. "The 2016 South Dakota Integrated Report for Surface Water-Quality Assessment."

<http://denr.sd.gov/dfta/wp/319apps/2016/bellefourcheseqsegment8.pdf>

South Dakota DENR, 2020, "The 2020 South Dakota Integrated Report for Surface Water Quality Assessment, Water Years 2014-2019." <http://denr.sd.gov>

Spaulding, S.A. and Elwell, L., 2007. "Increase in nuisance blooms and geographic expansion of the freshwater diatom *Didymosphenia geminate*." USGS Open-File Report 2007-1425, 38 p.

Stach, R.L., Helgerson, R.N., Bretz, R.F., Tipton, M.J., Beissel, D.R., Harksen, J.C., 1978. "Arsenic levels in the surface and ground waters along Whitewood Creek, Belle Fourche River, and a portion of Cheyenne River, South Dakota." South Dakota Geological Survey Completion Report Number A-0540-South Dakota, 42 p.

Stahl, R.G., Jr., Hooper, M.J., Balbus, J.M., Clements, W., Fritz, A., Gouin, T., Helm, R., Hickey, C., Landis, W., Moe, S.J., 2013. "The influence of global climate change on the scientific foundations and applications of environmental toxicology and chemistry: introduction to a SETAC international workshop." *Environmental Toxicology and Chemistry*, 32: 13-19. doi.org/10.1002/etc.2037

Strahler, A.N., 1992, "Quantitative-dynamic geomorphology at Columbia 1945-1960: A retrospective." *Progress in Physical Geography* 16:65-84.

Stamm, J.F. and Hoogenstratt, G.K., 2012. "Concentrations of selected metals in Quaternary-Age fluvial deposits along the Lower Cheyenne River and middle Belle Fourche Rivers, western South Dakota, 2009-2010." USGS Data Series 695, 29 p.

Stamm, J.F., Hendricks, R.R., Sawyer, J.F., Mahan, S.A., Zaprowski, B.J., Geibel, N.M., Azzolini, D.C., 2013. "Late Quaternary stream piracy and strath terrace formation along the Belle Fourche and lower Cheyenne Rivers, South Dakota and Wyoming." *Geomorphology*, Vol. 197, Sep.1, 2013, pp.10-20. doi.org/10.1016/j.geomorph.2013.03.028

- Stetler, L.D. and Hazelwood, K.T., 2020. "Cenozoic Geomorphic Evolution of the Fluvial Landscapes in the Black Hills, SD. *Proceedings of the South Dakota Academy of Science*, Vol. 99: 57-67.
- Stewart, I.T., Cayan, D.R., Dettinger, M.D., 2005. "Changes towards earlier streamflow timing across western North America." *Journal of Climate* 18(8):1136–1155.
- Stoltenberg, M., Oswald, J., Walter, E. of RESPEC, 2017. "Topical report RSI 2736: Belle Fourche River Watershed Management and Project Implementation Plan Segment 7, Watershed Project Final Report Section 319, Nonpoint source pollution control program." Prepared for the Belle Fourche River Watershed Partnership.  
[www.bellefourchewatershed.org/media/bellefourchefactor360com/documents/reports/Segment%207%20compressed.pdf](http://www.bellefourchewatershed.org/media/bellefourchefactor360com/documents/reports/Segment%207%20compressed.pdf)
- Sun, HongGuang, Yong Zhang, Dumitru Baleanu, Wen Chen, YangQuan Chen, 2018. "A new collection of real-world applications of fractional calculus in science and engineering." *Communications in Nonlinear Science and Numerical Simulation*, vol. 64, pp. 213-231. doi.org/10.1016/j.cnsns.2018.04.019
- Swennen, R. and Van der Sluys, J., 1998. "Zn, Pb, Cu, and As distribution patterns in overbank and medium-order stream sediment samples: their use in exploration and environmental geochemistry." *Journal of Geochemical Exploration*, 65, pp. 27-46.
- Taleb, N.M., 2010. *The Black Swan: The Impact of the Highly Improbable*. Random House, 444 p.
- Thomas, A.N., Root, R.A., Lantz, R.C., Saez, A.E., Chorover, J., 2018. "Oxidative weathering decreases bioaccessibility of toxic metal(oids) in PM<sub>10</sub> emissions from sulfide mine tailings." *GeoHealth*, 2, 118-138.  
 doi.org.10.1002/2017GH000118
- Todd, J.E., 1914. "The Pleistocene history of the Missouri River." *Science* 39(39): 263-74.
- Todd, J.E., 1923. "Glacial diversion of the Missouri River." *Pan-American Geologist* 39(3) 169-184.
- Todd, J.E., 1923. "Is the channel of the Missouri River through North Dakota of Tertiary origin?" *Geol. Soc. America Bull.*, v. 34, pp. 469-494.

- Tourtelot, H.A., 1962. "Preliminary investigation of the geologic setting and chemical composition of the Pierre Shale great plains region." USGS Professional Paper 390, 74 p.
- Thurman, E.M. and Fallon, J.D., 2006. "The Deethylatrazine/Atrazine Ratio as an Indicator of the Onset of the Spring Flush of Herbicides into Surface Water of the Midwestern United States." *International Journal of Environmental Analytical Chemistry*, 65:1-4, 203-214. doi:10.1080/03067319608045555
- Trenberth, K.E., Dai, A., Rasmussen, R.M., Parsons, D.B., 2003. "The changing character of precipitation." *Bull. Am. Meteorol. Soc.* 84, 1205–1217.
- Tung, Y-K, Wong, C-L, 2016. "Sensitivity and Uncertainty Analysis of Hydrologic/Hydraulic Model for the Shenzhen River and Northern New Territory Basin In Hong Kong." 12<sup>th</sup> International Conference on Hydroinformatics, 2016 [https://www.dsd.gov.hk/EN/Files/Technical\\_Manual/technical\\_papers/LD1602.pdf](https://www.dsd.gov.hk/EN/Files/Technical_Manual/technical_papers/LD1602.pdf)
- University of Mississippi Stream Solute Workshop, 1990. "Concepts and methods for assessing solute dynamics in stream ecosystems." *Journal of the North American Benthological Society*, vol. 9, pp. 95-119.
- U.S. Climate Data, 2019. "U.S. Climate Data: Temperature – Precipitation – Sunshine – Snowfall." [www.usclimatedata.com/climate/denver/colorado/united-states/usco0105](http://www.usclimatedata.com/climate/denver/colorado/united-states/usco0105)
- U.S. Army Corps of Engineers (USACE), 1965. "Report on sedimentation, John Martin Reservoir, Arkansas River Basin, Colorado."
- USACE, 1966. "Report on sedimentation, Conchas Reservoir, Canadian River Basin, New Mexico."
- USACE, Omaha District, 1972. "Flood Report Cheyenne River Basin, South Dakota Black Hills Area, Flood of 9-10 June, 1972."
- USACE, 1982. "Missouri River, Lake Sakakawea, North Dakota, Reservoir Water Quality Data Report."
- USACE, 1999. "Sedimentation Impacts in the Cheyenne River Arm, Lake Oahe, Phase II, Projected to 2058." Sedimentation and Channel Stabilization Section, Hydrologic Engineering Branch, Engineering Division, Nov. 1999, MRD Sediment Memorandum No. 20.
- USACE Engineer Research and Development Center (ERDC), 2000. "Effective Discharge Calculation." ERDC/CHL TR-00-15, Aug. 2000. [www.dtic.mil/get-tr-doc/pdf?AD=ADA383261](http://www.dtic.mil/get-tr-doc/pdf?AD=ADA383261)

USACE, Omaha District, 2010. "Final Oahe/Lake Oahe Master Plan, Missouri River, South Dakota and North Dakota." Design Memorandum MO-224, Sep. 2010. Accessed at:

<http://survey.swc.nd.gov/4dlink9/4dcgi/GetSubContentPDF/PB-2810/Oahe%20Dam-Lake%20Master%20Plan.pdf>

USACE, Hydrologic Engineering Center River Analysis System website, 2014. Online software for computing/calculating/modeling water flow and sediment transport. [www.hec.usace.army.mil/software/hec-ras/](http://www.hec.usace.army.mil/software/hec-ras/)

USACE, 2014. "USACE Strategic Sustainability Performance Plan, 30 Jun 2014." [Fhessa4\\_USACE\\_Sustainability\\_Plan.pdf](#)

USACE, 2014. Personal communication.

USACE. 2014. Engineering and Construction Bulletin 2014-10: "Guidance for Incorporating Climate Change Impacts to Inland Hydrology in Civil Works Studies, Designs, and Projects."

USACE, Hydrologic Engineering Center River Analysis System website, 2014. Online software for computing/calculating/modeling water flow and sediment transport. [www.hec.usace.army.mil/software/hec-ras/](http://www.hec.usace.army.mil/software/hec-ras/)

USACE, 2015. "Civil Works Technical Report, CWTS-2015-04: "Recent US Climate Change and Hydrology Literature Applicable to USACE Missions – Missouri River Region 10." In USACE Climate Preparedness and Resilience User Guide."

USACE, 2016. Engineering and Construction Bulletin 2016-25: "Guidance for Incorporating Climate Change Impacts to Inland Hydrology in Civil Works Studies, Designs, and Projects."

USACE, 2017. "U.S. Army Corps of Engineers Nonstationarity Detection Tool User Guide." Version 1.1, Jan. 2017, pp. 1-58. USACE Climate Preparedness and Resilience Community of Practice. Accessed at <http://corpsclimate.us/ptcih.cfm>

USACE, 2017. Engineering Technical Letter 1100-2-3: "Guidance for Detection of Non-stationarities in Annual Maximum Discharges," April 2017.

USACE, 2018. "National Inventory of Dams." Accessed at: [http://nid.usace.army.mil/cm\\_apex/f?p=838:3:0::NO::P3\\_STATES:SD](http://nid.usace.army.mil/cm_apex/f?p=838:3:0::NO::P3_STATES:SD)

USACE, 2019. "Climate Preparedness and Resilience Community of Practice Applications Portal: Hydrology Tools (Climate Hydrology Assessment Tool, Nonstationarity Detection Tool, and Vulnerability Assessment Tool)." Accessed March 2019 at: <https://maps.crrel.usace.army.mil/projects/rcc/portal.html>

USACE, 2020. "Engineering and Construction Bulletin 2018-14: "Guidance for Incorporating Climate Change Impacts to Inland Hydrology in Civil Works Studies, Designs, And Projects." Published Sep.10, 2018; revised Sep.10, 2020. [www.wbdg.org/ffc/dod/engineering-and-construction-bulletins-ecb/usace-ecb-2018-14](http://www.wbdg.org/ffc/dod/engineering-and-construction-bulletins-ecb/usace-ecb-2018-14)

USACE, 2020. "Engineering With Nature," online collaborative site. <https://ewn.el.erdc.dren.mil/about.html>

USACE, 2021. "Climate Hydrology Assessment Tool." Accessed at: <https://climate.sec.usace.army.mil/chat/>

USDA, 1993. "Soil Survey Manual," USDA Handbook 18.

USDA Natural Resources Conservation Service (NRCS), 2009. "Phase II Sedimentation Assessment for the Upper Missouri Basin." June 2009, 51 p. <http://msaconline.com/wp-content/uploads/2015/01/Missouri-River-Phase-II-Report.pdf>

USDA, 2019. Technical Release 2010-60: "Earth Dams and Reservoirs." USDA Natural Resources Conservation Service.

U.S. EPA, 1971. Unpublished data later reported by Hesse, L.W., Brown, R.L. and Heisinger, J.F. (1975) in "Mercury Contamination of Birds from a Polluted Watershed," *The Journal of Wildlife Management*, 39 (2).

U.S. EPA, 1973. "Mercury, zinc, copper, arsenic, selenium, and cyanide content of selected waters and sediment collected along Whitewood Creek, the Belle Fourche River, and the Cheyenne River in western South Dakota, December 1971–October 1972."

U.S. EPA, 1994. "Institutional Controls for Whitewood Creek, Superfund Site: EPA ID: SDD980717136 Section C, County Building Permit Handbook, (Including Approved County Ordinances) and County Commission Meeting Minutes, SDMS Document ID: 1065317, Lawrence County, Whitewood Creek Tailings Area." *Building Permit Handbook: A Guide to Building in the Whitewood Creek Tailings Area, Jan. 10, 1994.*

U.S. EPA, 2001. "Drinking Water Requirements for States and Public Water Systems." At online informational site: <https://www.epa.gov/dwreginfo/chemical-contaminant-rules>

U.S. EPA, 2002. "What are EPA's drinking water regulations for arsenic?" Accessed at informational site: <https://safewater.zendesk.com/hc/en-us/articles/212077897-4-What-are-EPA-s-drinking-water-regulations-for-arsenic->

U.S. EPA, 2003. "Sediment quality guidelines."

- U.S. EPA, 2005. "Ecological risk assessment for the Cheyenne River, South Dakota."
- U.S. EPA, 2006. "Guidance on Systematic Planning Using the Data Quality Objectives Process." (EPA QA/G-4), EPA/240/B-06/001
- U. S. EPA, 2007, "Five-Year Review of the Whitewood Creek Superfund Site Lead, South Dakota, Aug. 2007."
- U.S. EPA, 2011. "Environmental Cleanup Best Management Practices: Effective Use of the Project Life Cycle Conceptual Site Model." (EPA 542-F-11-011)
- U.S. EPA, 2012. "Third Five-Year Review Report for Whitewood Creek Superfund Site, EPA ID: SDD980717136, Lawrence, Meade, and Butte Counties, South Dakota." Prepared by Seko Solutions, Sep. 2012, for the US EPA. Accessed Dec.10, 2013 at:  
[www.epa.gov/ictssw07/public/export/08/SDD980717136/1065317.pdf](http://www.epa.gov/ictssw07/public/export/08/SDD980717136/1065317.pdf)
- US EPA, 2013. "Hg Remediation in Aquatic Environments" webinar held Sep.26, 2013. <http://trainex.org/Hg>
- U.S. EPA Superfund website, 2016. Information for Whitewood Creek Superfund site. Accessed April 19, 2016 at:  
<https://cumulis.epa.gov/supercpad/cursites/csinfo.cfm?id=0800570>
- USGS, 1983. USGS Circular 953, *Proceedings of the Advanced Seminar on Sedimentation, Aug.15-19, 1983, Denver, CO*, Glysson, G.D., ed., 41 p.
- USGS, 2016, The National Map Spot Elevation tool.  
[http://viewer.nationalmap.gov/theme/elevation/###bottom, 3DEP, 1/3 arc-second](http://viewer.nationalmap.gov/theme/elevation/###bottom,3DEP,1/3arc-second)
- USGS, 2017. "South Dakota Water Science Center 2017, "Black Hills Area Floods - 1911 to 1920." <https://sd.water.usgs.gov/projects/FloodHistory/1911-1920/FH1911.html>
- USGS. Hydrologic Unit Maps at <http://water.usgs.gov/GIS/huc.html>
- USGS, 2013. "Photo gallery: Arsenic Contamination from Hard Rock Mining - Whitewood Creek - Belle Fourche River - Cheyenne River System, Western South Dakota." Image accessed at:  
[http://toxics.usgs.gov/photo\\_gallery/whitewood\\_creek.html](http://toxics.usgs.gov/photo_gallery/whitewood_creek.html)
- USGS, 2014. Water data. <https://waterdata.usgs.gov/nwis/rt>
- USGS, 2018. USGS water data for the Nation: USGS National Water Information System database. [doi.org/10.5066/F7P55KJN](https://doi.org/10.5066/F7P55KJN)



USGS Streamer, 2018. Online hydrology information site. Accessed at:  
<https://txpub.usgs.gov/DSS/streamer/web/>

U.S. Government Printing Office, 2000. "Water Resources Development Act of 2000, Public Law 106-541." Accessed at:  
<https://www.gpo.gov/fdsys/pkg/PLAW-106publ541/html/PLAW-106publ541.htm>

U.S. Interagency Advisory Committee on Water Data, 2002. "Guidelines for determining flood flow frequency." Bulletin 17-B of the Hydrology Subcommittee, Hydrologic Analysis Work Group. (As-amended version dated Oct, 10, 2002; first version published in 1982.). [www.fema.gov/mit/tsd/dl\\_flow.htm](http://www.fema.gov/mit/tsd/dl_flow.htm)

U.S. Interagency Committee on Water Resources, 1957. "Report No. 12: Some Fundamentals of Particle Size Analysis – A Study of Methods Used in Measurement and Analysis of Sediment Loads in Streams," 56 p.  
[https://water.usgs.gov/fisp/docs/Report\\_12.pdf](https://water.usgs.gov/fisp/docs/Report_12.pdf)

University of California, San Diego (UCSD), Scripps Institute of Oceanography, 2013. "History of the Keeling Curve."  
<https://keelingcurve.ucsd.edu/2013/04/03/the-history-of-the-keeling-curve/>

UCSD, Scripps Institute of Oceanography, 2021: Current CO<sub>2</sub> reading as of Sep, 27, 2021. <https://keelingcurve.ucsd.edu/>

Vannote R.L., Minshall, G.W., Cummins, K.W., Sedell, J.R., Cushing, C.E., 1982. "The River Continuum Concept." *Canadian Journal of Fisheries and Aquatic Sciences*, 37: 130-137.

Vano, J., Hamman, J., Gutmann, E., Wood, A., Mizukami, N., Clark, M., Pierce, D.W., Cayan, D.R., Wobus, C., Nowak, K., Arnold, J., June 2020. "Comparing Downscaled LOCA and BCSD CMIP5 Climate and Hydrology Projections - Release of Downscaled LOCA CMIP5 Hydrology," 96 p. Accessed at:  
[https://gdo.dcp.ucllnl.org/downscaled\\_cmip\\_projections/techmemo/LOCA\\_BCSD\\_hydrology\\_tech\\_memo\\_Pdf](https://gdo.dcp.ucllnl.org/downscaled_cmip_projections/techmemo/LOCA_BCSD_hydrology_tech_memo_Pdf)

Villarini, G., Serinaldi, F., Smith, J.A., Krajewski, W.F., 2009. "On the stationarity of annual flood peaks in the continental United States during the 20th century." *Water Resour. Res.*, 45, W08417, doi:10.1029/2008WR007645

Vogel, R.M., Yaindl, C., Walter, M., 2011. "Nonstationarity: Flood magnification and recurrence reduction factors in the United States." *Journal of the American Water Resources Association* 47(3):464-474.

- Walsh, J., Wuebbles, D., Hayhoe, K., Kossin, J., Kunkel, K., Stephens, G., Thorne, P., Vose, R., Wehner, M., Willis, J., Anderson, D., Doney, S., Feely, R., Hennon, P., Kharin, V., Knutson, T., Landerer, F., Lenton, T., Kennedy, J., Somerville, R., 2014. "Chapter 2: Our Changing Climate." In *Climate Change Impacts in the United States. The Third National Climate Assessment*, Melillo, J.M., Richmond, T.C, Yohe, G.W., eds. USGCRP publication, pp. 19-67.
- Walter, C.M., June, F.C., Brown, H.G., 1973. "Mercury in Fish, Sediments, and Water in Lake Oahe, South Dakota." *Journal (Water Pollution Control Federation)* Vol. 45, No. 10 (Oct. 1973), pp. 2203-2210. [www.jstor.org/stable/25038018](http://www.jstor.org/stable/25038018)
- Walter, R.C. and Merritts, D.J, 2008. "Natural streams and the legacy of water-powered mills." *Science* 319 (5861): 299-304.
- Wang, H., Schubert, S., Suarez, M., Chen, J., Hoerling, M., Kumar, A., Pegion, P., 2009. "Attribution of the seasonality and regionality in climate trends over the United States during 1950-2000." *Journal of Climate* 22:2571-2590.
- Wang, J. and Zhang X., 2008. "Downscaling and projection of winter extreme daily precipitation over North America." *Journal of Climate* 21:923-937. <https://doi.org/10.1175/2007JCLI1671.1>
- Wentz, D.A., Brigham, M.E., Chasar, L.C., Lutz, M.A., Krabbenhoft, D.P., 2014. *Mercury in the Nation's Streams—Levels, Trends, and Implications*. USGS Circular 1395, 90 p. [doi.org/10.3133/cir1395](https://doi.org/10.3133/cir1395)
- White, Kathleen D. and Arnold, Jeffrey R., 2015. "Recent U.S. Climate Change and Hydrology Literature Applicable to USACE Missions-Missouri River Region." CWTS-2015-05, Institute for Water Resources, CDM Smith, Contract # 2912HQ-10-D-0004, Task Order 147. <https://usace.contentdm.ocic.org>
- White, S., 2006. "Sediment Yield Prediction and Modeling." *Encyclopedia of Hydrological Sciences*. doi:10.1002/0470848944.hsa089
- Whitehead, P.G., Wilby, R.L., Battarbee, R.W., Kernan, M., Wade, A.J., 2009. "A Review of the Potential Impacts of Climate Change on Surface Water Quality." *Hydrological Research Journal* Vol. 54, 2009 – Issue 1. <https://doi.org/10.1623/hysj.54.1.101>
- Whitewood Development Corporation (WDC), 1994. "Whitewood Creek Institutional Controls Completion Report," July 27, 1994.
- Wikipedia, 2017. Definition of stationarity.
- Wilkin, R., Wallschläger, D., and Ford, R., 2003. "Speciation of arsenic in sulfidic waters." *Geochemical Transactions*, 4(1):1.

- Wilkie, J. and Hering, J., 1998. "Rapid oxidation of geothermal arsenic (III) in streamwaters of the eastern Sierra Nevada." *Environmental Science Technology* 32: 657-666.
- Wilbanks, T.J., Kates, R.W., 1999. "Global Change in Local Places: How Scale Matters." *Climatic Change* 43: 601-628.
- Wuebbles, D.J., Fahey, D.W., Hibbard, K.A., Dokken, D.J., Stewart, B.C., Maycock, T.K., eds., 2017. *Climate Science Special Report: Fourth National Climate Assessment, Vol. I*. USGCRP publication, 470 p. doi:10.7930/J0J964J6.
- Vose, R.S., Easterling, D.R., Kunkel, K.E., LeGrande, A.N., Wehner, M.F., 2017. "Chapter 6: Temperature changes in the United States." *Climate Science Special Report: Fourth National Climate Assessment, Vol. 1*. USGRCP publication, pp. 185-206. doi:10.7930/J0N29V45.
- Wuolo, R., 1986. "Laboratory Studies of Arsenic Adsorption in Alluvium Contaminated with Gold-Mine Tailings Along Whitewood Creek, Black Hills, South Dakota". Unpublished M.S. Thesis, South Dakota School of Mines and Technology, Rapid City, SD.
- Wolman, M.G. and Miller, J.P., 1960. "Magnitude and frequency of forces in geomorphic processes." *The Journal of Geology*, Vol. 68, No. 1, pp. 54-74.
- Woodward, J.C. and Walling, D.E., 2007. "Composite suspended sediment particles in river systems: their incidence, dynamics and physical characteristics." *Hydrological Processes*, 21, 3601-3614 (2007). doi:10.102/hyp.6586
- Zabilansky, L.J., Ettema, R., Wuebben, J., Yankielun, N., 2002. "Survey of river ice influences on channel bathymetry along the Fort Peck reach of the Missouri River, winter 1998-1999." USACE ERDC/CRREL TR-02-14.
- Zaprowski, B.J., Evenson, E.B., Pazzaglia, F.J., Epstein, J.B., 2001. "Knickzone propagation in the Black Hills: A different perspective on the late Cenozoic exhumation of the Laramide Rocky Mountains." *Geology*, vol. 29, no. 6, pp. 547-550. doi 10.1130/0091-7613(2001)029<0547:KPITBH>2.0.CO;2
- Zaprowski, B.J., Pazzaglia, F.J., Evenson, E.B., 2005. "Climatic influences on profile concavity and river incision." *Journal of Geophysical Research*, 110, F03004. doi:10.1029/2004JF000138
- Zeng, Feng, Ming-Guo Ma, Dong-Rui Di, and Wei-Yu Shi, 2020: "Review Separating the Impacts of Climate Change and Human Activities on Runoff: A Review of Method and Application." (Affiliated with Southwest University, Chongqing, China, and Sophia University, Tokyo, Japan.)

Zingari, P.C., 2010. "Building Co-operations, Coalitions and Governance on Mountain Catchments Sustainability." *Integrated Watershed Management: Perspectives and Problems*, Beheim, E., ed., p. 51.  
doi:10.1007/978-90-48

## Appendix A: USGS NCCV 2021 Climate Summary

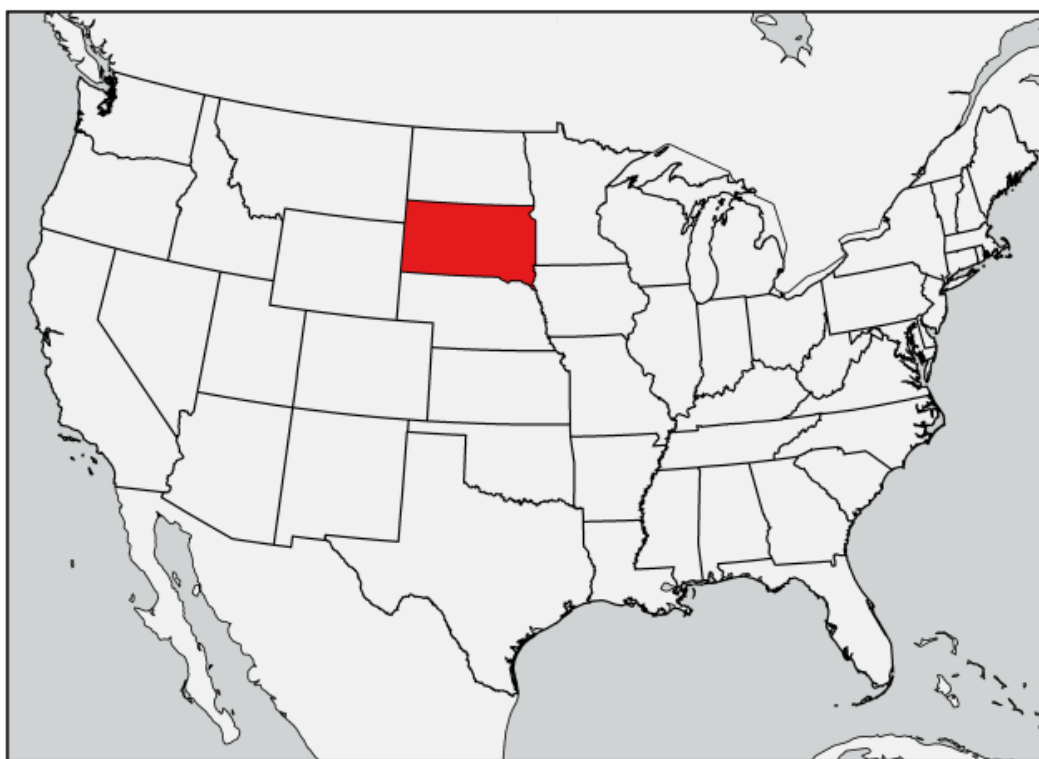
Summary of Cheyenne HUC 1012

A1 – A38



U.S. Geological Survey - National Climate Change Viewer

### Summary of South Dakota



May 5, 2021

# 1 Mean temperature

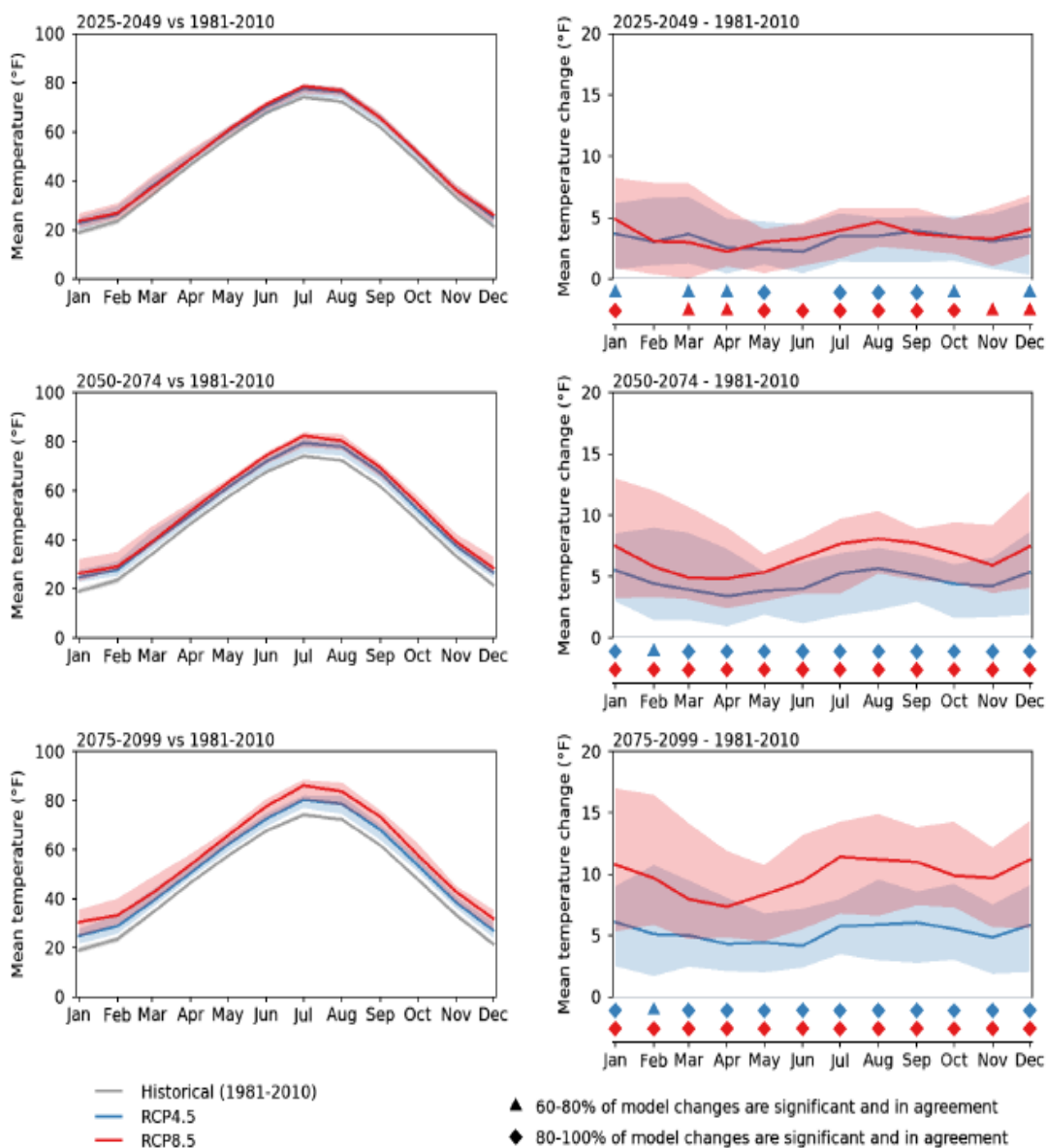


Figure 1: Monthly averages of mean temperature for the three future time periods for the RCP4.5 and RCP8.5 simulations. The median of 20 CMIP5 models is indicated by the solid lines and the ensemble 10th to 90th percentile range is indicated by the respective shaded envelopes. Raw values relative to the historical simulation (1981-2010) are shown in the left column and future minus historical changes are shown in the right column. Triangle and diamond symbols indicate the percent of models that simulate future minus present changes that are of the same sign and significant. A Mann-Whitney rank test is used to establish significance ( $\rho < 0.05$ ).

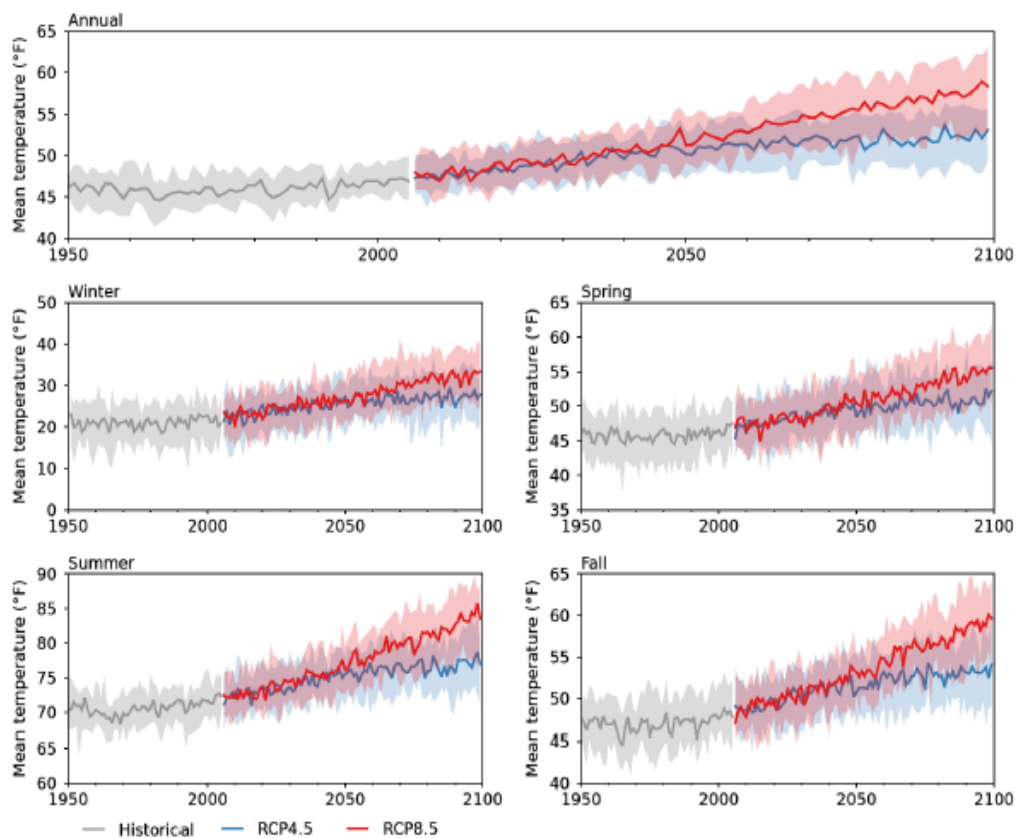


Figure 2: Annual and seasonal time series of mean temperature for historical (gray), RCP4.5 (blue) and RCP8.5 (red). The historical period ends in 2005 and the future periods begin in 2006. The median of 20 CMIP5 models is indicated by the solid lines and the ensemble 10th to 90th percentile range is indicated by the respective shaded envelopes.

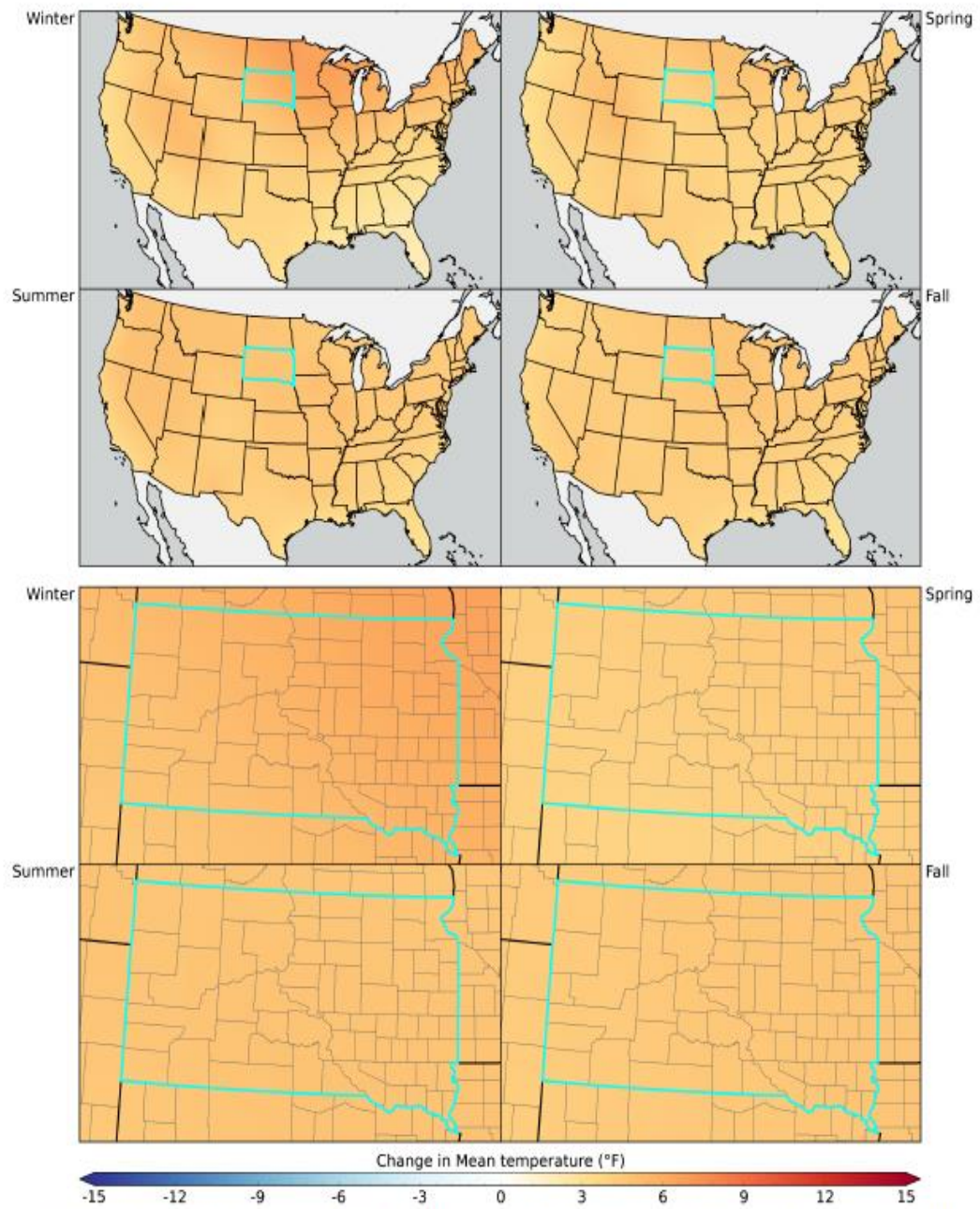


Figure 3: Seasonal maps of mean temperature for RCP4.5 2050-2074 minus 1981-2010 for the ensemble mean model.



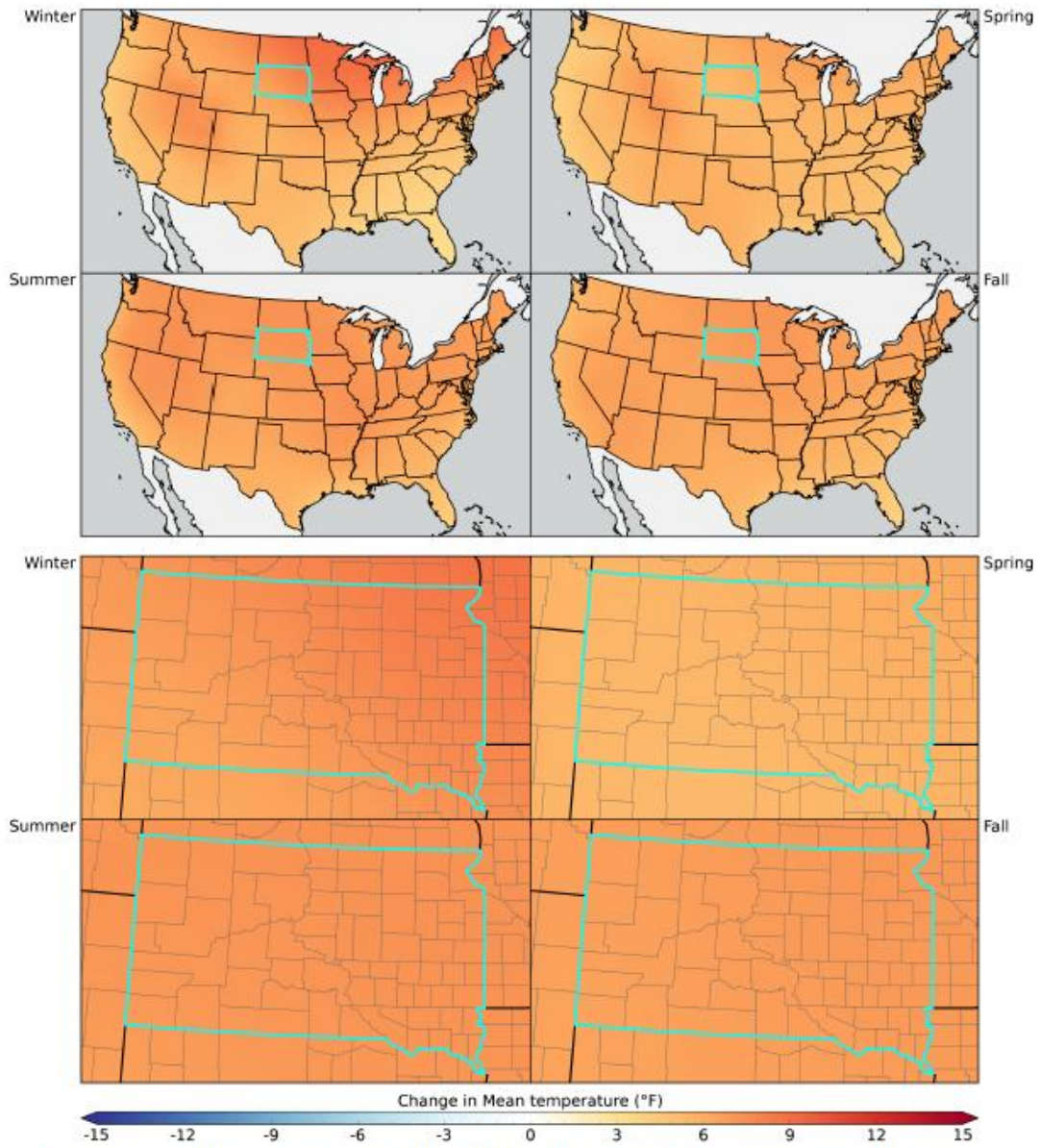


Figure 4: Seasonal maps of mean temperature for RCP8.5 2050-2074 minus 1981-2010 for the ensemble mean model.

2 Maximum temperature

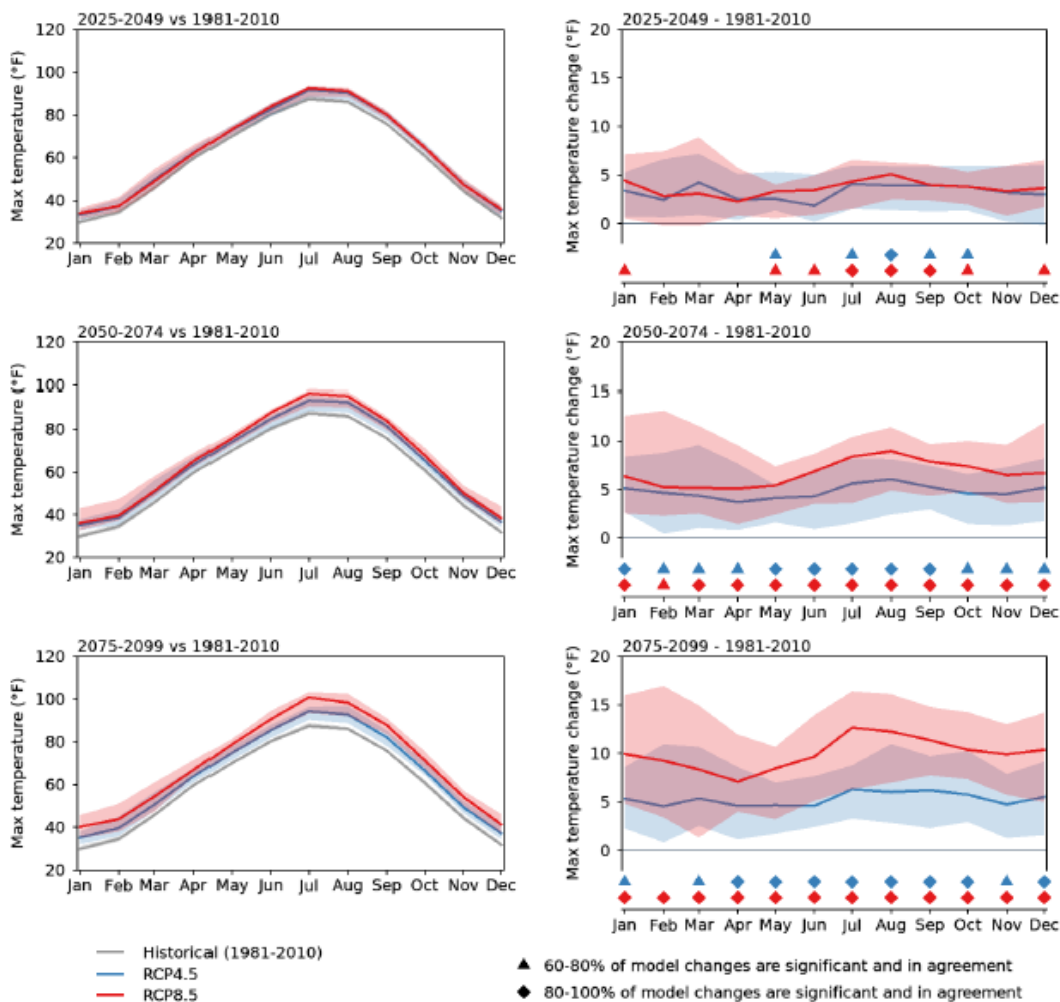


Figure 5: Monthly averages of maximum temperature for the three future time periods for the RCP4.5 and RCP8.5 simulations. The median of 20 CMIP5 models is indicated by the solid lines and the ensemble 10th to 90th percentile range is indicated by the respective shaded envelopes. Raw values relative to the historical simulation (1981-2010) are shown in the left column and future minus historical changes are shown in the right column. Triangle and diamond symbols indicate the percent of models that simulate future minus present changes that are of the same sign and significant. A Mann-Whitney rank test is used to establish significance ( $p < 0.05$ ).

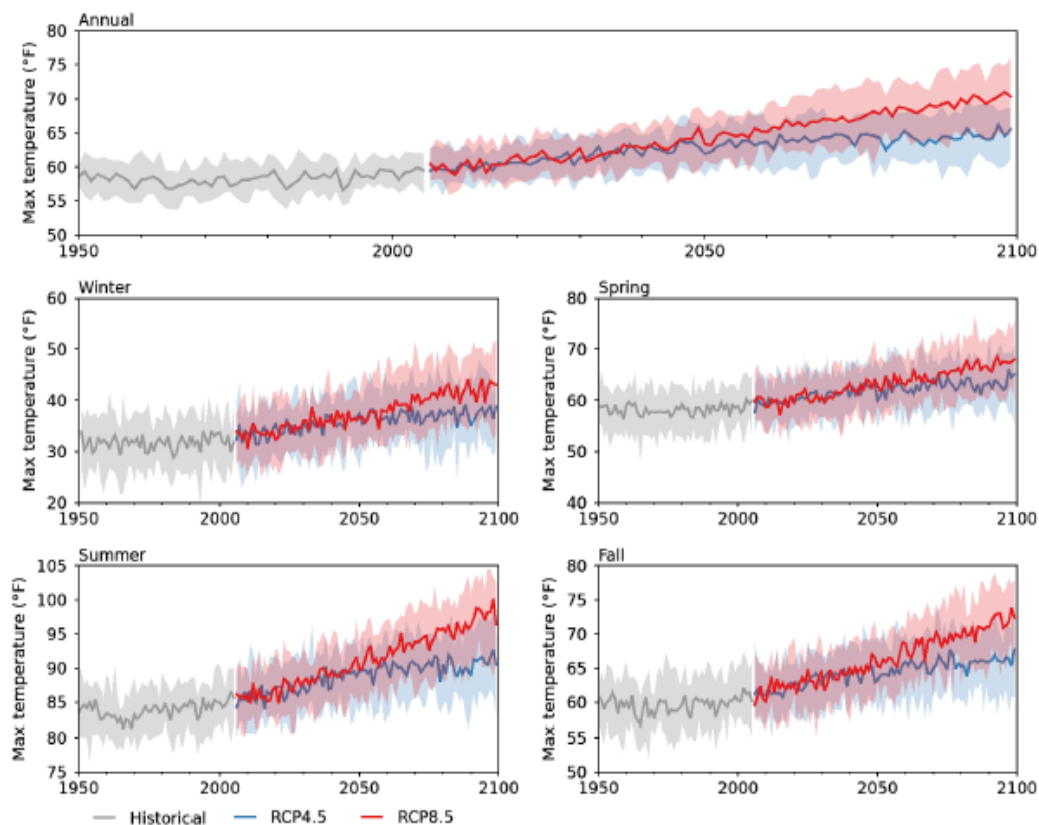


Figure 6: Annual and seasonal time series of maximum temperature for historical (gray), RCP4.5 (blue) and RCP8.5 (red). The historical period ends in 2005 and the future periods begin in 2006. The median of 20 CMIP5 models is indicated by the solid lines and the ensemble 10th to 90th percentile range is indicated by the respective shaded envelopes.

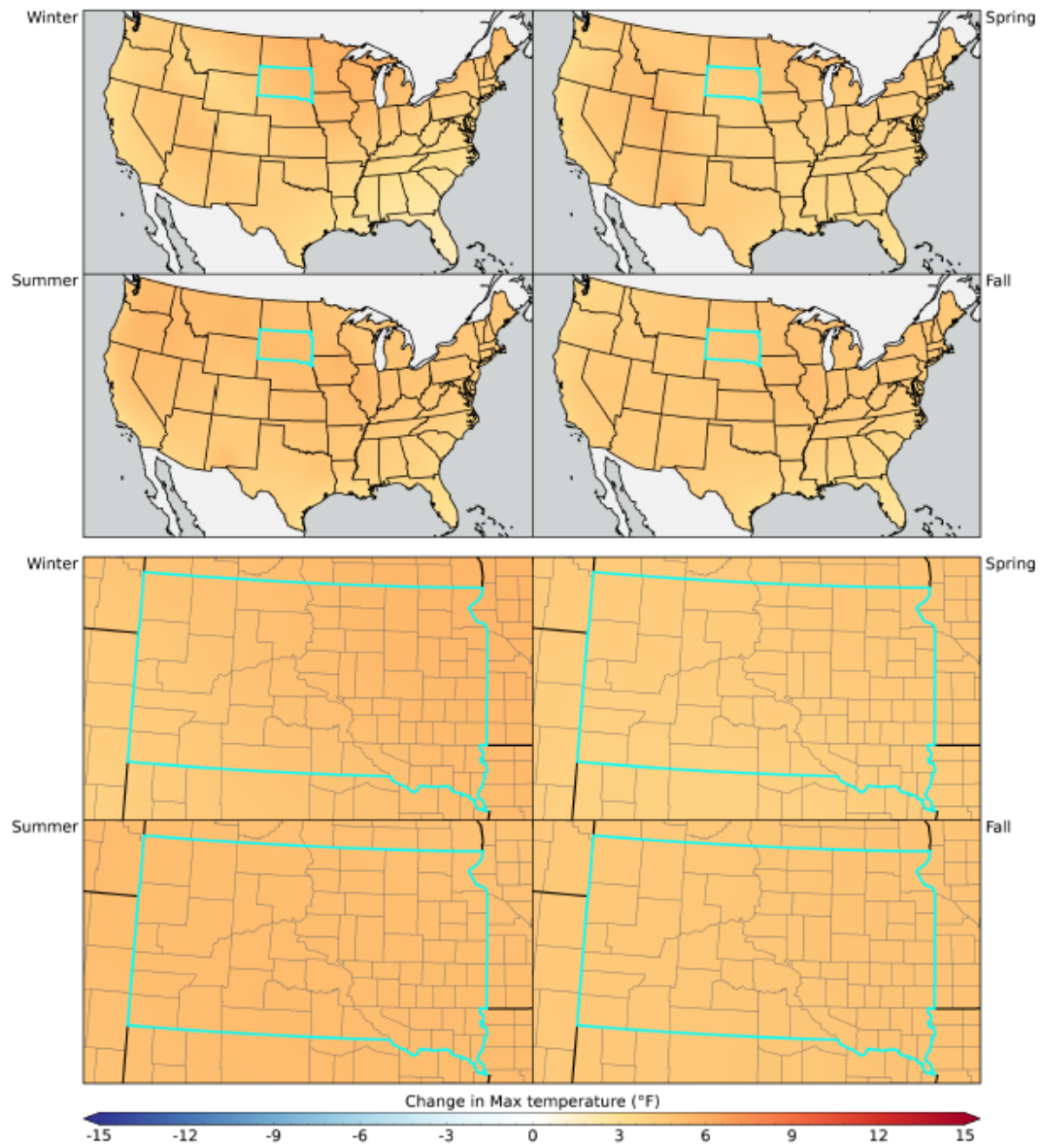


Figure 7: Seasonal maps of maximum temperature for RCP4.5 2050-2074 minus 1981-2010 for the ensemble mean model.



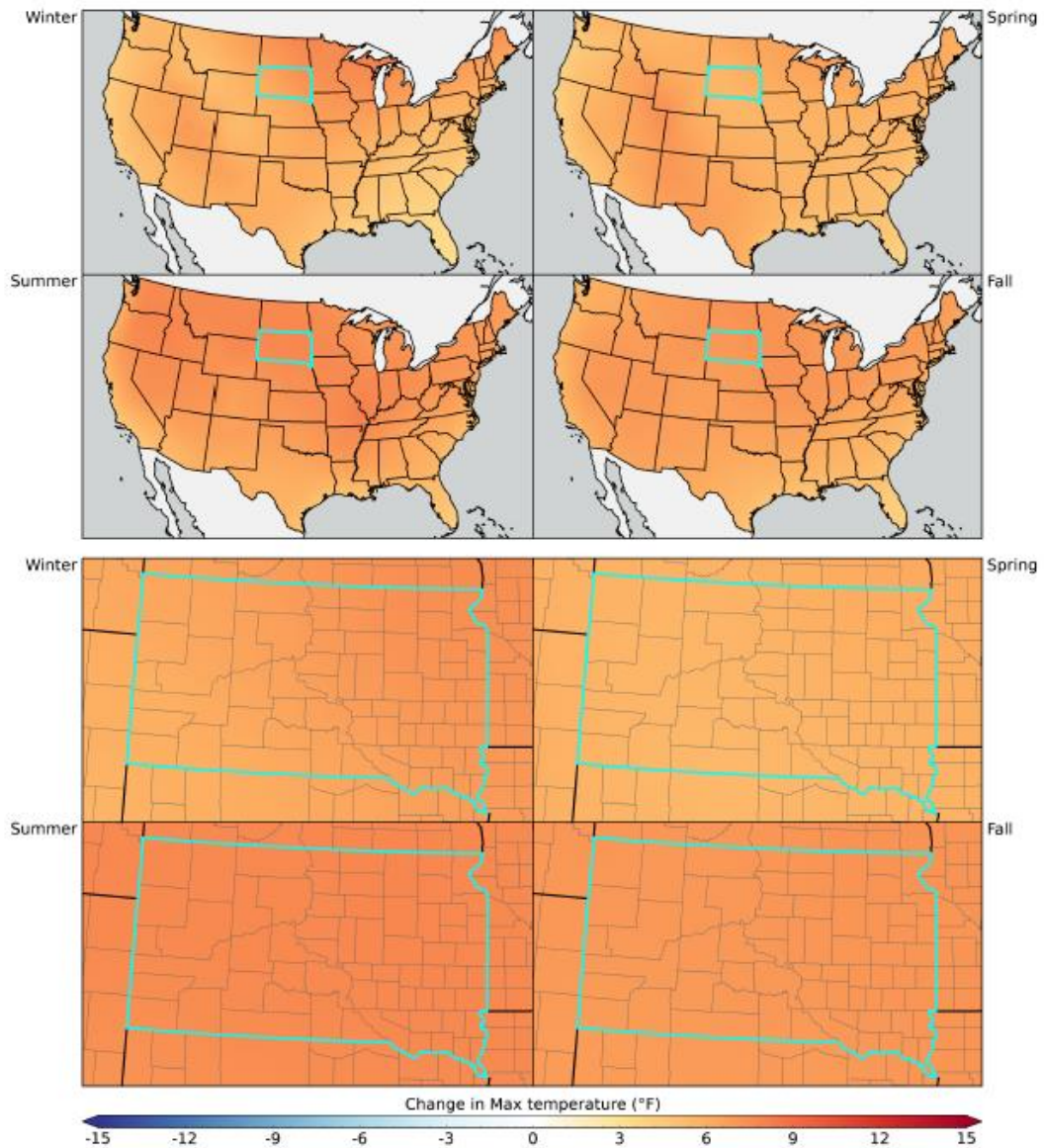


Figure 8: Seasonal maps of maximum temperature for RCP8.5 2050-2074 minus 1981-2010 for the ensemble mean model.

### 3 Minimum temperature

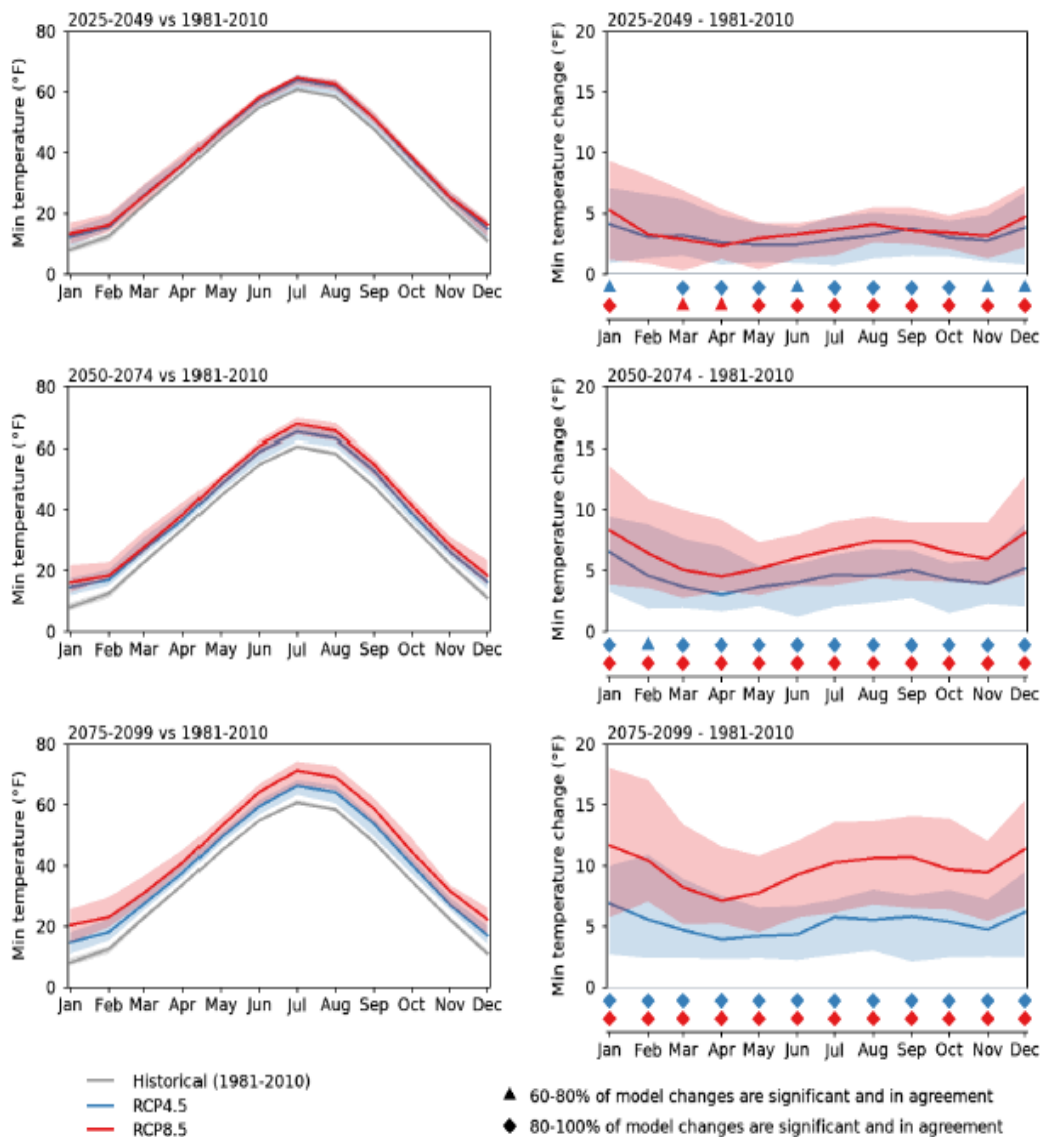


Figure 9: Monthly averages of minimum temperature for the three future time periods for the RCP4.5 and RCP8.5 simulations. The median of 20 CMIP5 models is indicated by the solid lines and the ensemble 10th to 90th percentile range is indicated by the respective shaded envelopes. Raw values relative to the historical simulation (1981-2010) are shown in the left column and future minus historical changes are shown in the right column. Triangle and diamond symbols indicate the percent of models that simulate future minus present changes that are of the same sign and significant. A Mann-Whitney rank test is used to establish significance ( $p < 0.05$ ).

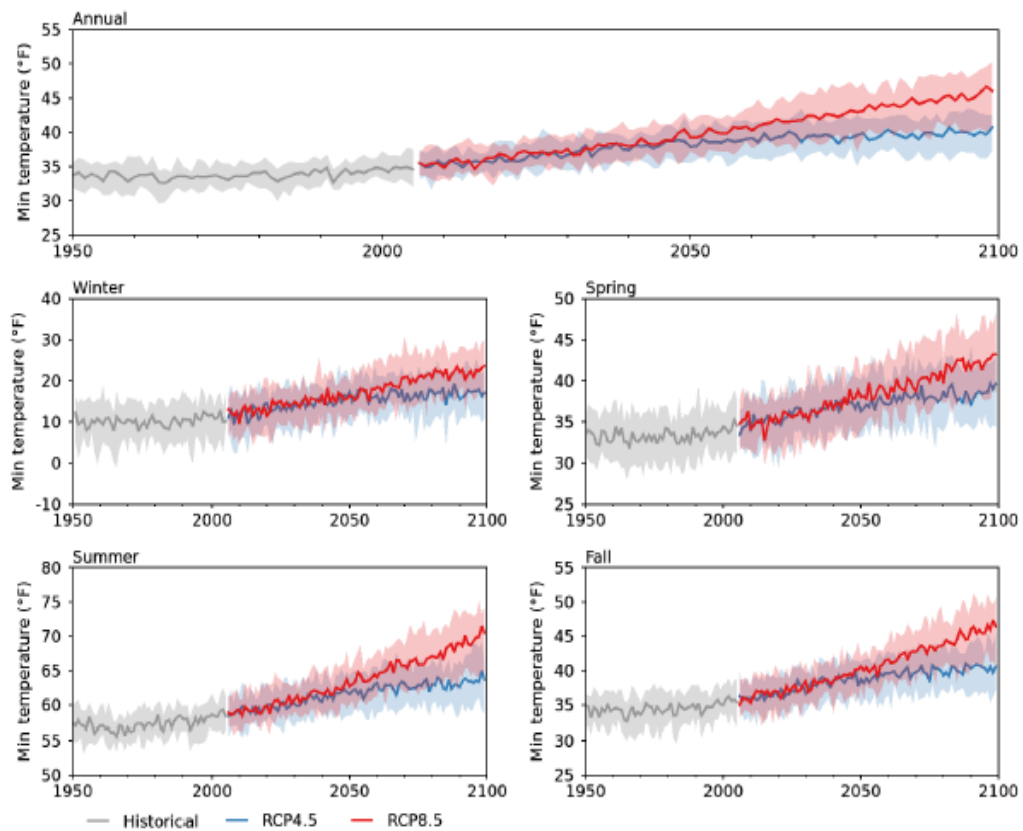


Figure 10: Annual and seasonal time series of minimum temperature for historical (gray), RCP4.5 (blue) and RCP8.5 (red). The historical period ends in 2005 and the future periods begin in 2006. The median of 20 CMIP5 models is indicated by the solid lines and the ensemble 10th to 90th percentile range is indicated by the respective shaded envelopes.

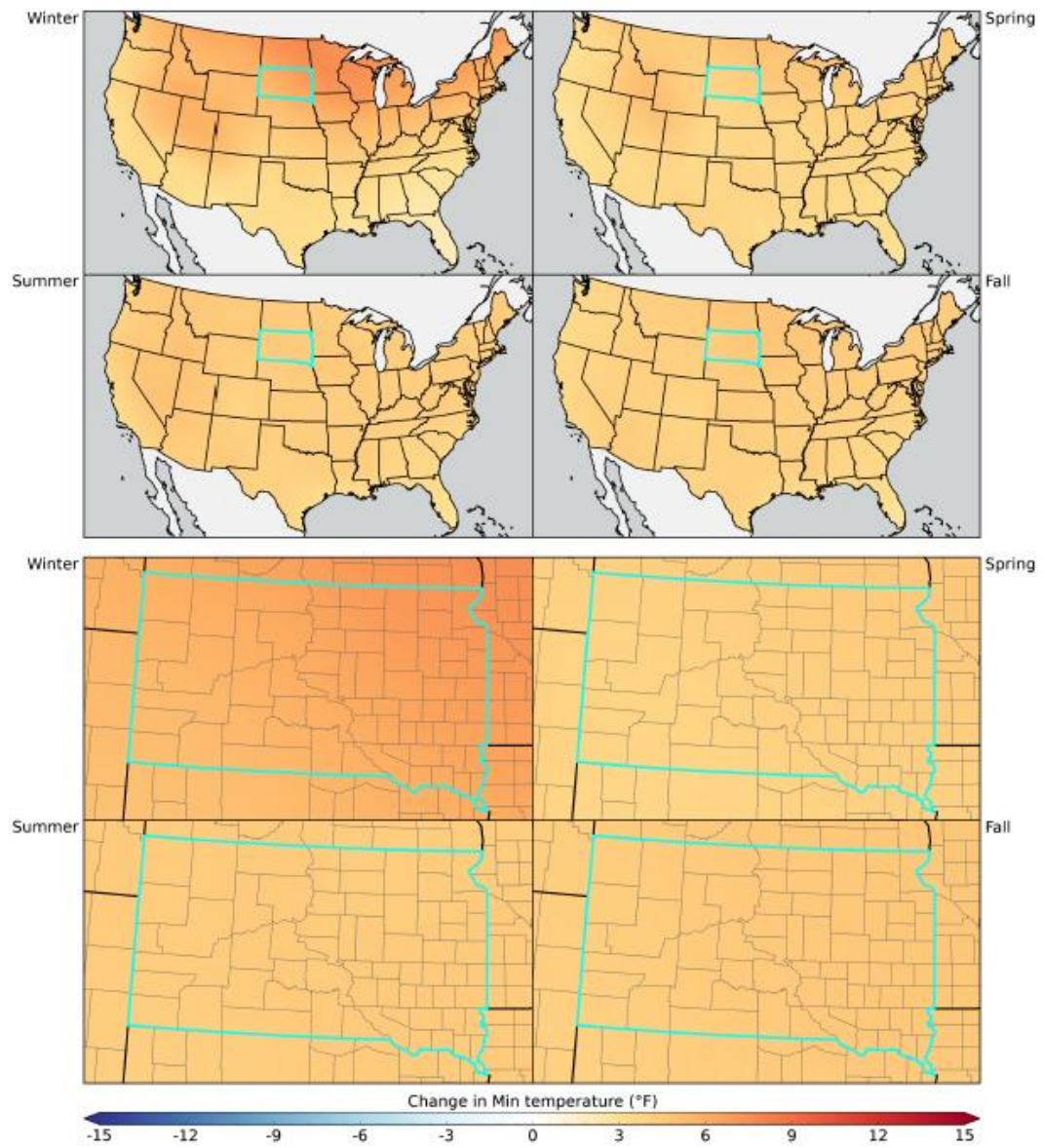


Figure 11: Seasonal maps of minimum temperature for RCP4.5 2050-2074 minus 1981-2010 for the ensemble mean model.



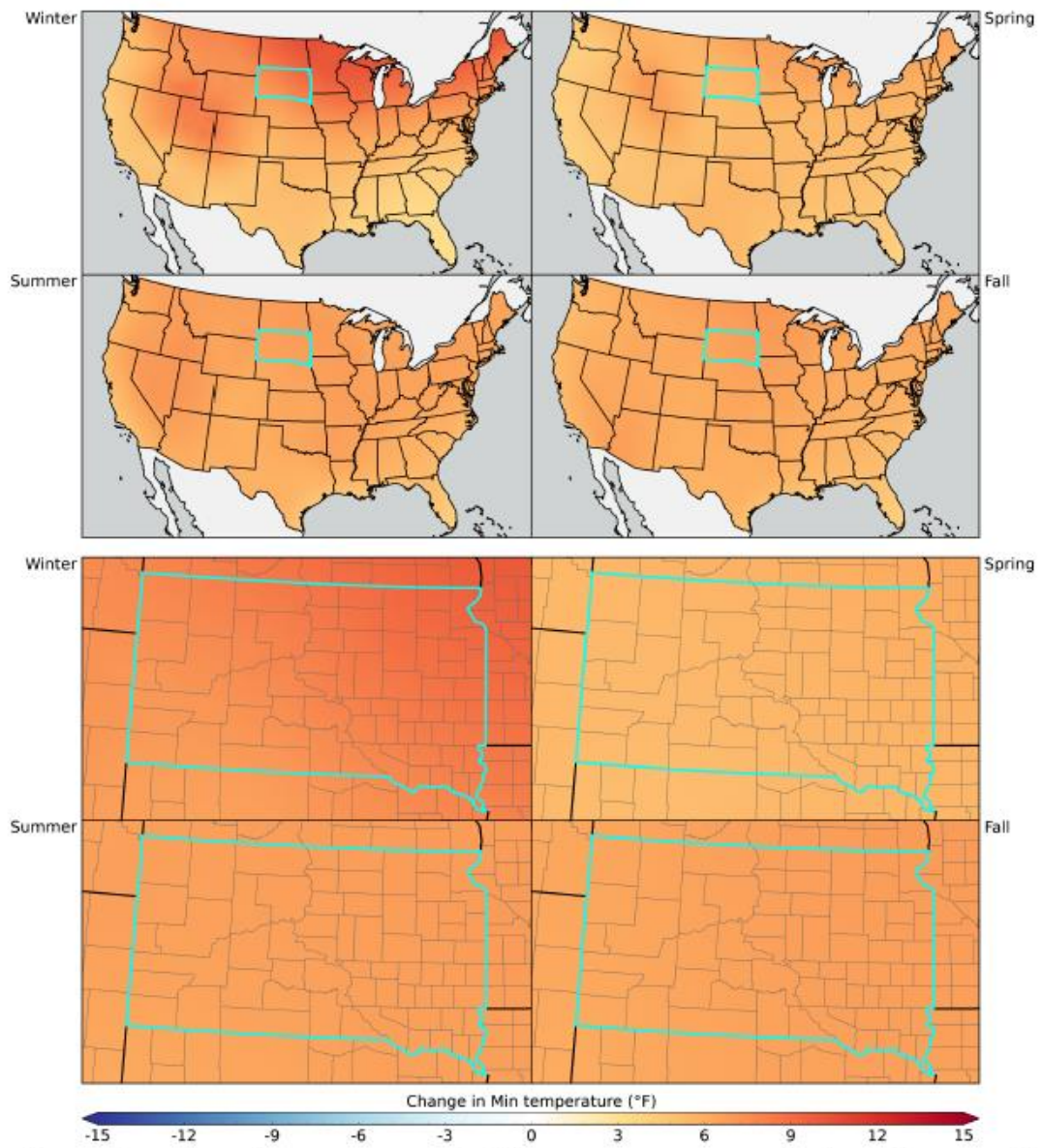


Figure 12: Seasonal maps of minimum temperature for RCP8.5 2050-2074 minus 1981-2010 for the ensemble mean model.

## 4 Precipitation

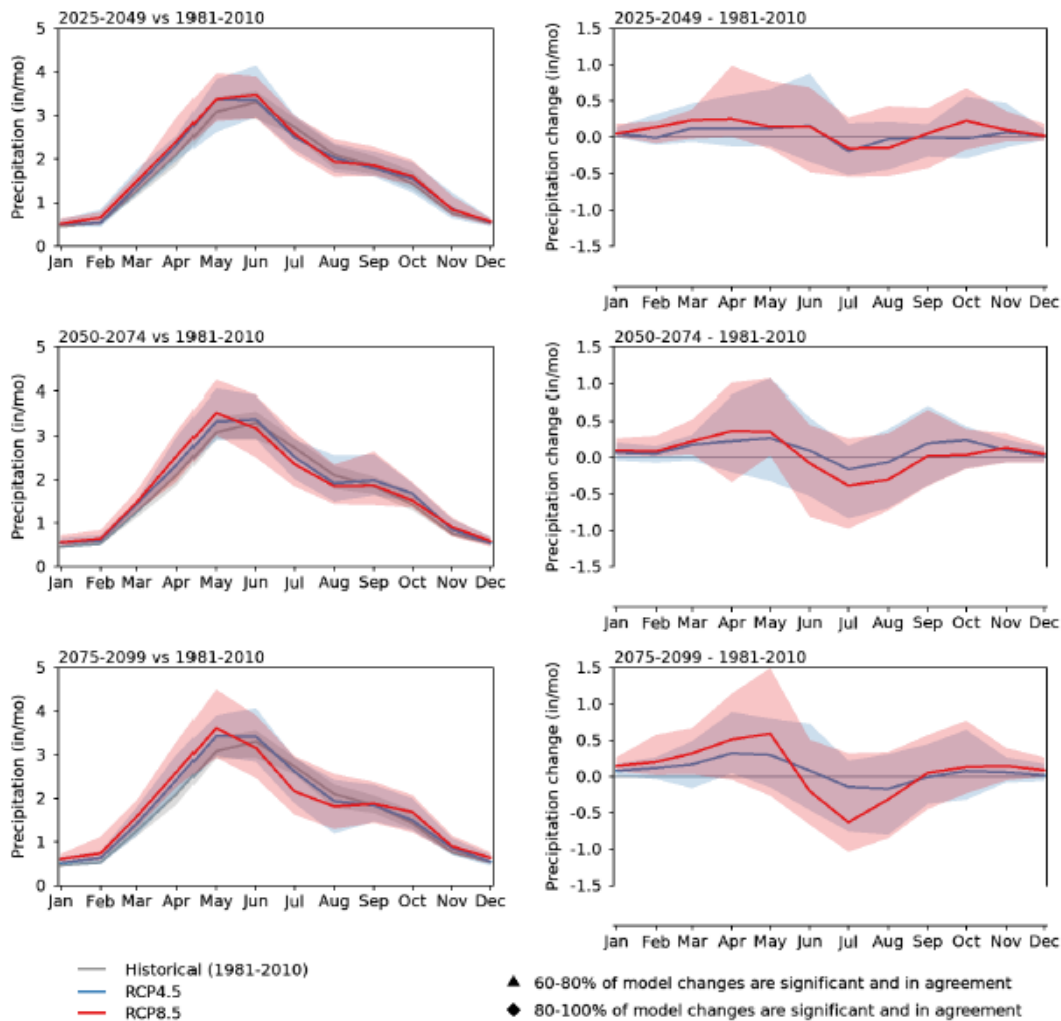


Figure 13: Monthly averages of precipitation for the three future time periods for the RCP4.5 and RCP8.5 simulations. The median of 20 CMIP5 models is indicated by the solid lines and the ensemble 10th to 90th percentile range is indicated by the respective shaded envelopes. Raw values relative to the historical simulation (1981-2010) are shown in the left column and future minus historical changes are shown in the right column. Triangle and diamond symbols indicate the percent of models that simulate future minus present changes that are of the same sign and significant. A Mann-Whitney rank test is used to establish significance ( $\rho < 0.05$ ).

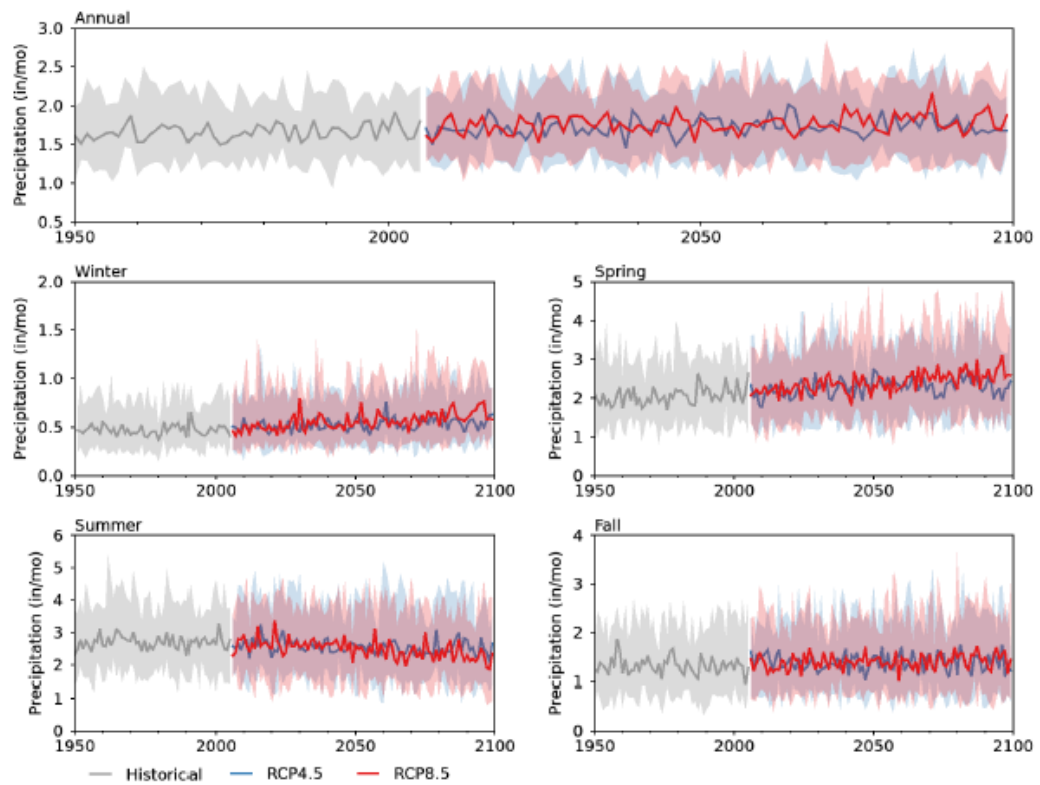


Figure 14: Annual and seasonal time series of precipitation for historical (gray), RCP4.5 (blue) and RCP8.5 (red). The historical period ends in 2005 and the future periods begin in 2006. The median of 20 CMIP5 models is indicated by the solid lines and the ensemble 10th to 90th percentile range is indicated by the respective shaded envelopes.

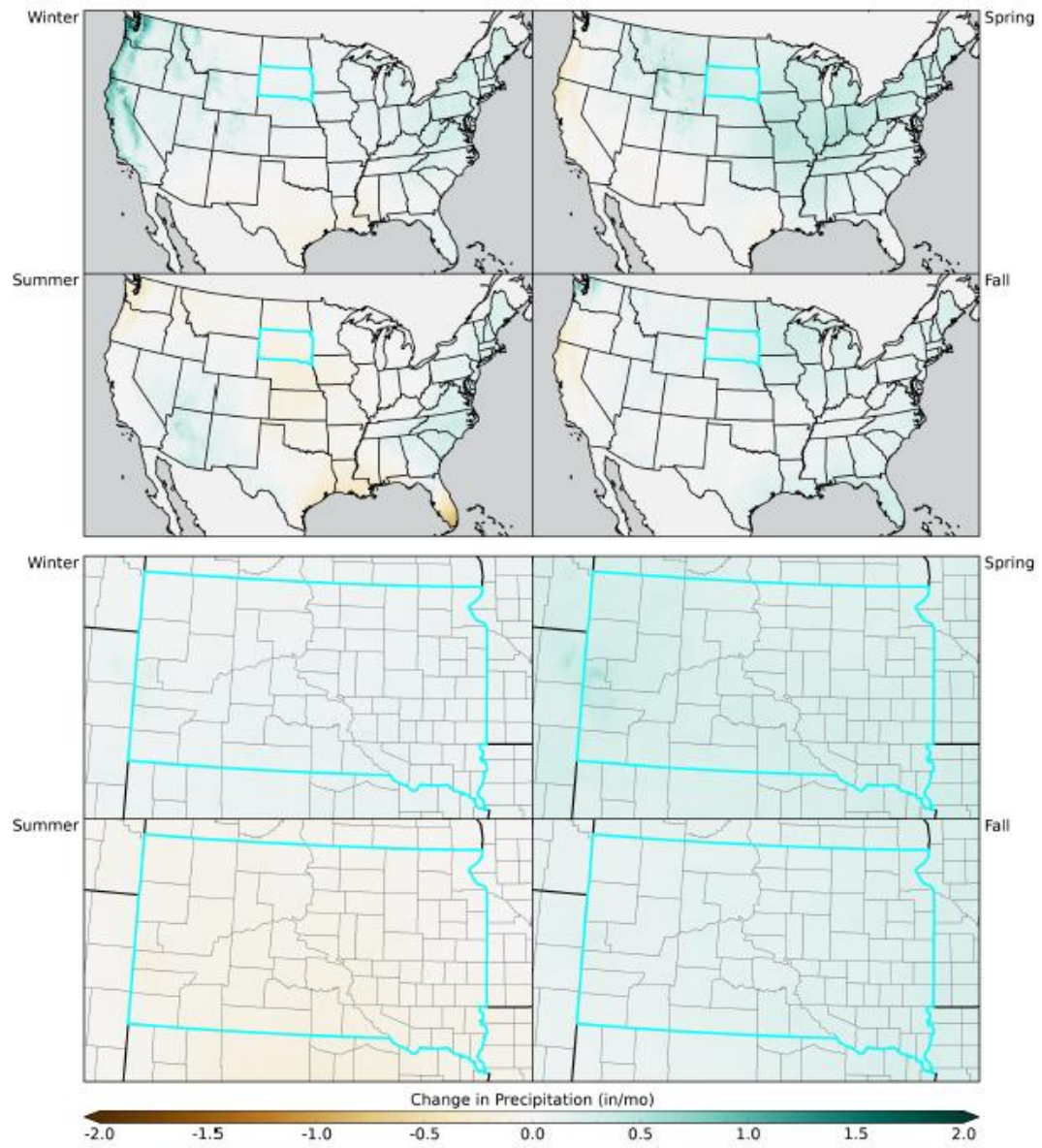


Figure 15: Seasonal maps of precipitation for RCP4.5 2050-2074 minus 1981-2010 for the ensemble mean model.



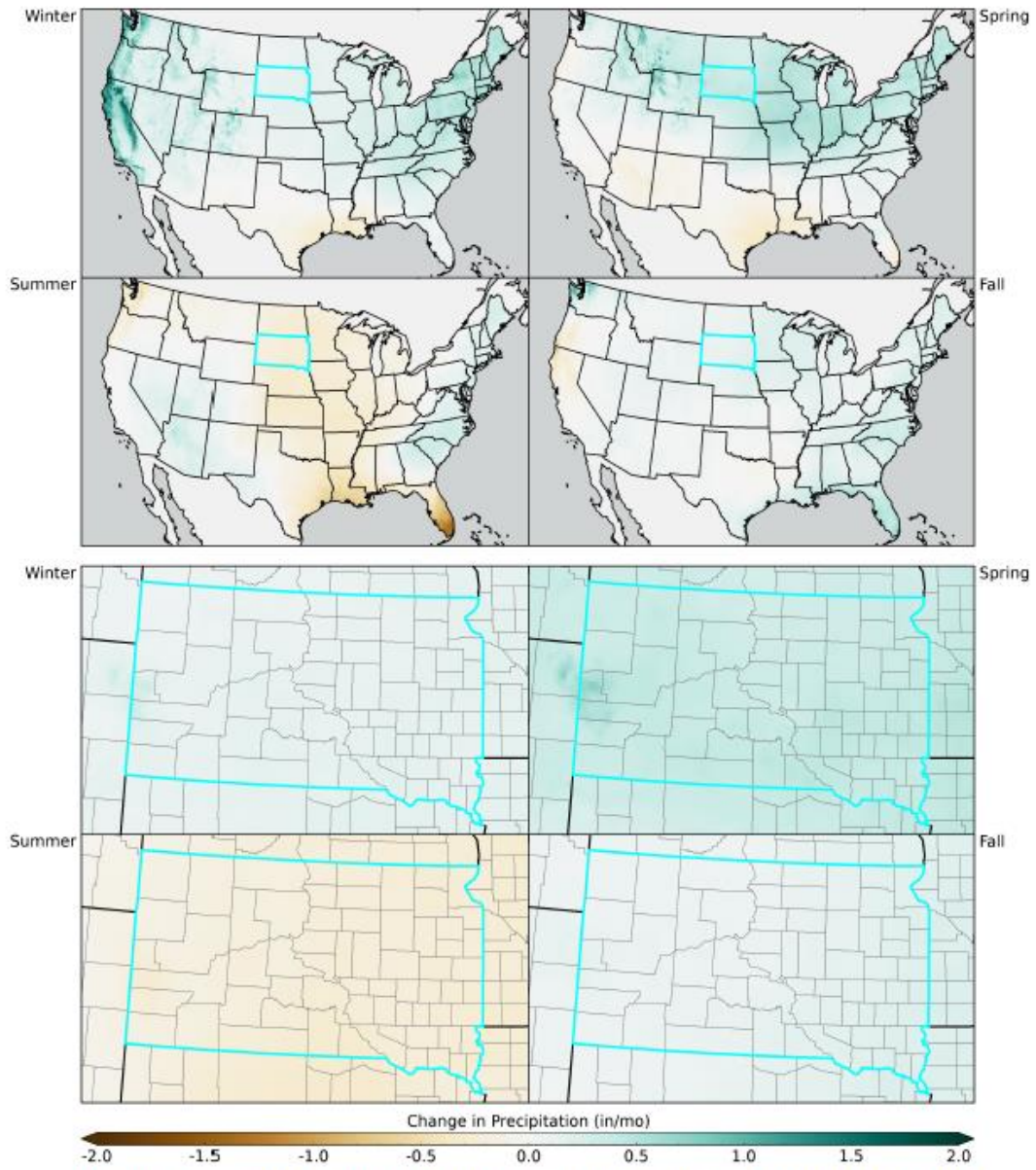


Figure 16: Seasonal maps of precipitation for RCP8.5 2050-2074 minus 1981-2010 for the ensemble mean model.

### 5 Vapor pressure deficit

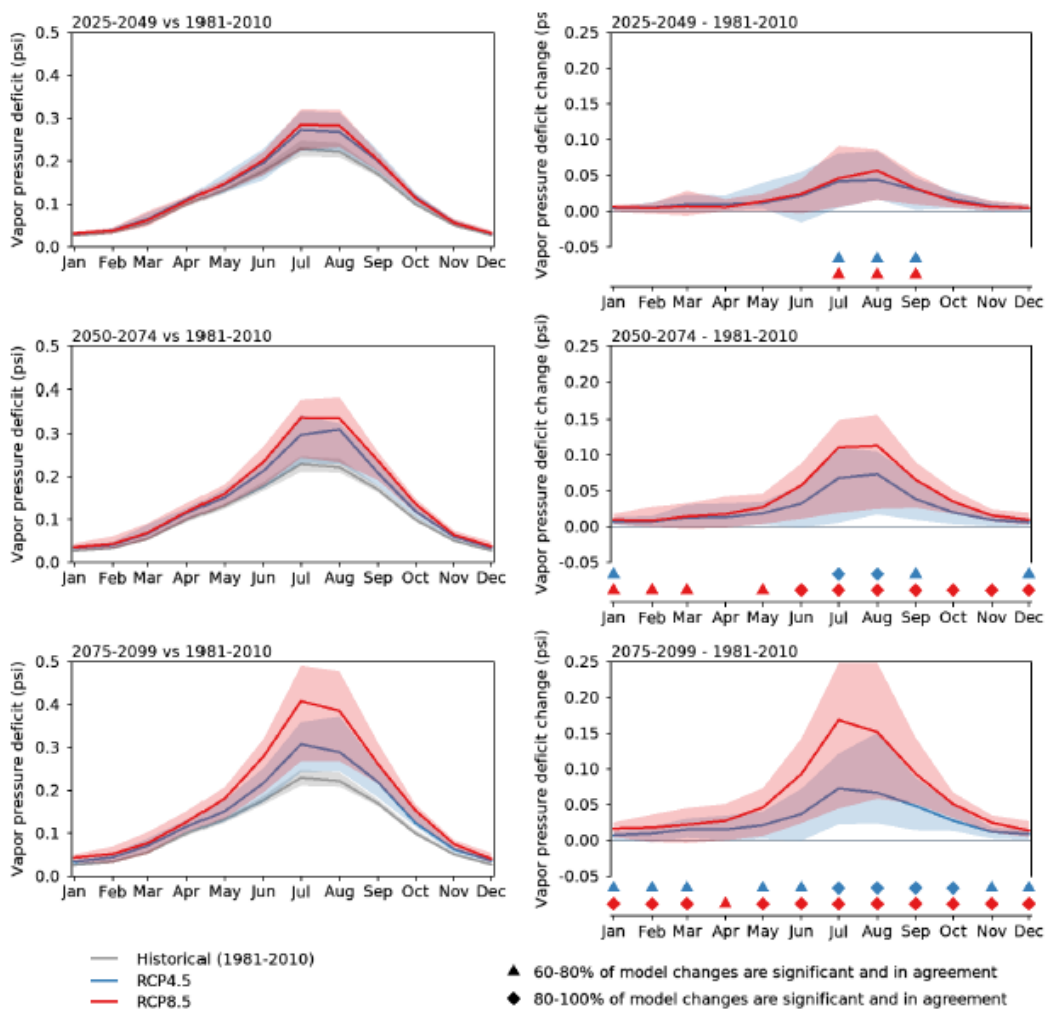


Figure 17: Monthly averages of vapor pressure deficit for the three future time periods for the RCP4.5 and RCP8.5 simulations. The median of 20 CMIP5 models is indicated by the solid lines and the ensemble 10th to 90th percentile range is indicated by the respective shaded envelopes. Raw values relative to the historical simulation (1981-2010) are shown in the left column and future minus historical changes are shown in the right column. Triangle and diamond symbols indicate the percent of models that simulate future minus present changes that are of the same sign and significant. A Mann-Whitney rank test is used to establish significance ( $p < 0.05$ ).

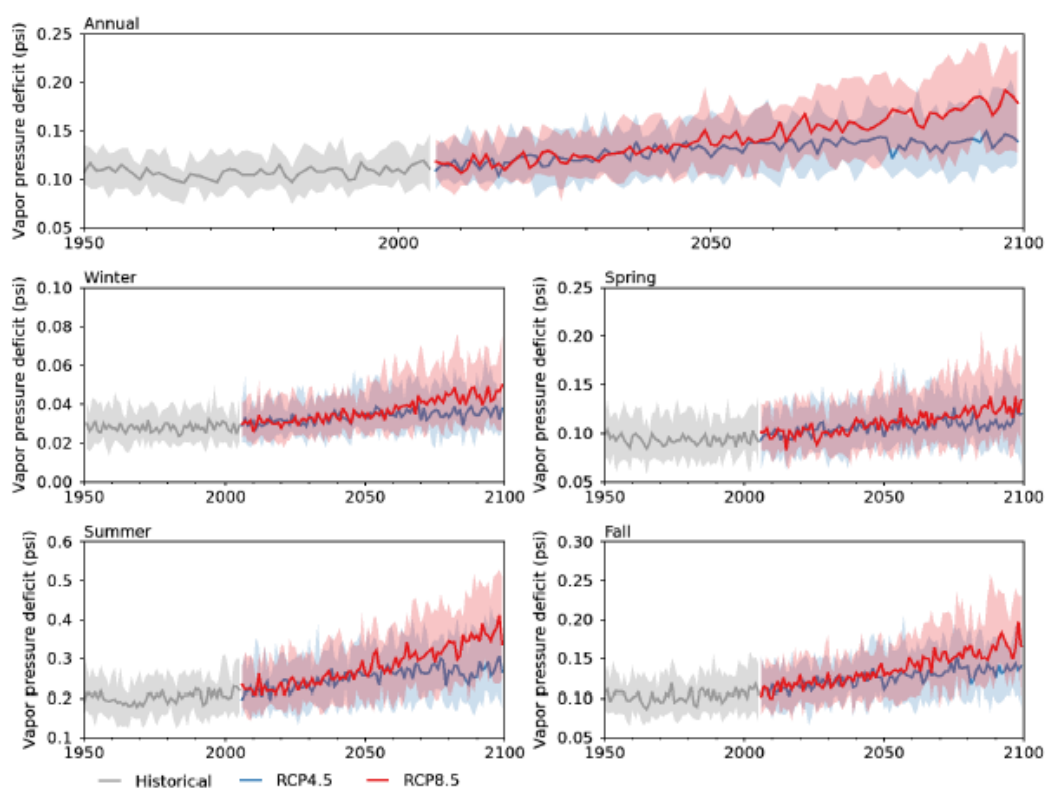


Figure 18: Annual and seasonal time series of vapor pressure deficit for historical (gray), RCP4.5 (blue) and RCP8.5 (red). The historical period ends in 2005 and the future periods begin in 2006. The median of 20 CMIP5 models is indicated by the solid lines and the ensemble 10th to 90th percentile range is indicated by the respective shaded envelopes.

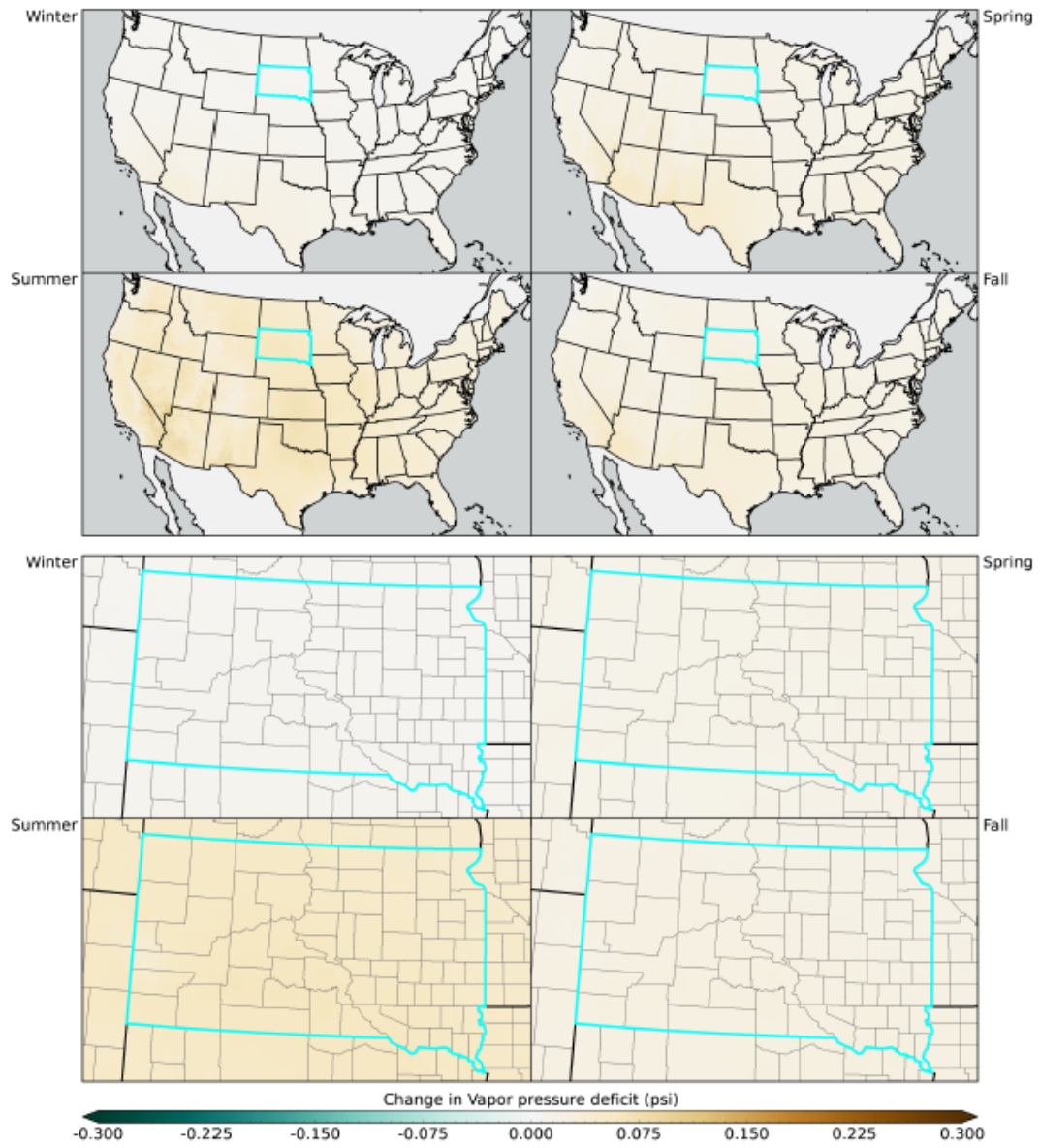


Figure 19: Seasonal maps of vapor pressure deficit for RCP4.5 2050-2074 minus 1981-2010 for the ensemble mean model.



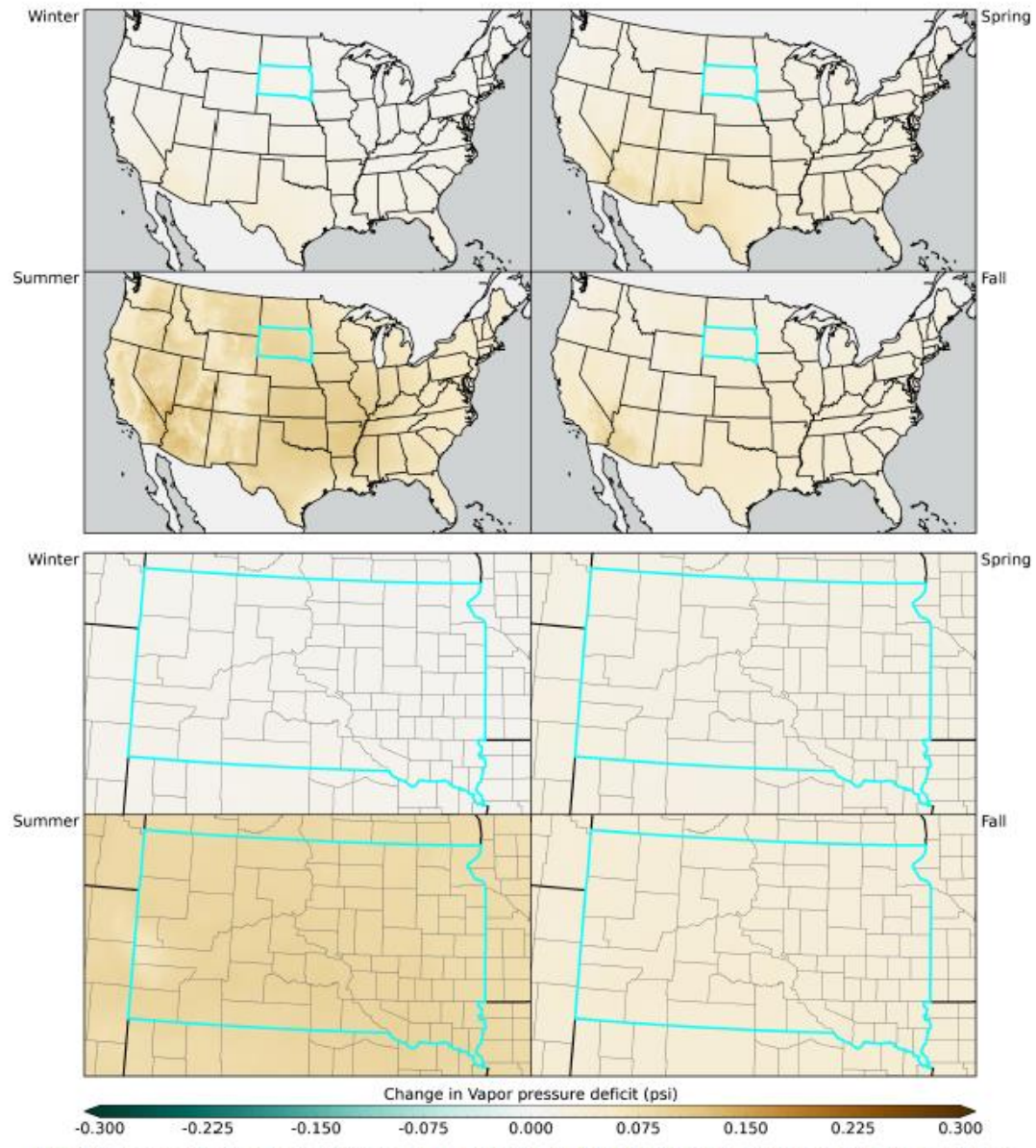


Figure 20: Seasonal maps of vapor pressure deficit for RCP8.5 2050-2074 minus 1981-2010 for the ensemble mean model.

### 6 Snow Water Equivalent

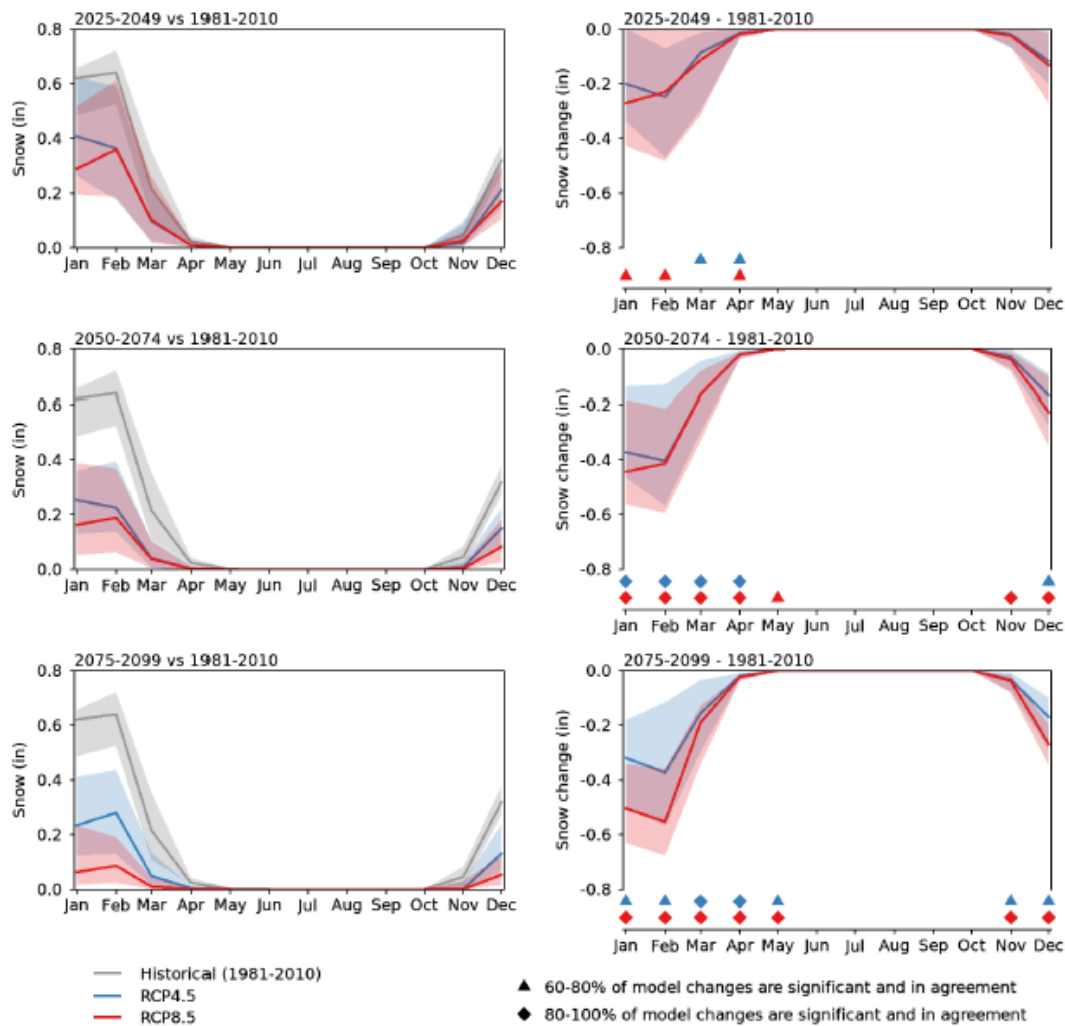


Figure 21: Monthly averages of snow water equivalent for the three future time periods for the RCP4.5 and RCP8.5 simulations. The median of 20 CMIP5 models is indicated by the solid lines and the ensemble 10th to 90th percentile range is indicated by the respective shaded envelopes. Raw values relative to the historical simulation (1981-2010) are shown in the left column and future minus historical changes are shown in the right column. Triangle and diamond symbols indicate the percent of models that simulate future minus present changes that are of the same sign and significant. A Mann-Whitney rank test is used to establish significance ( $p < 0.05$ ).

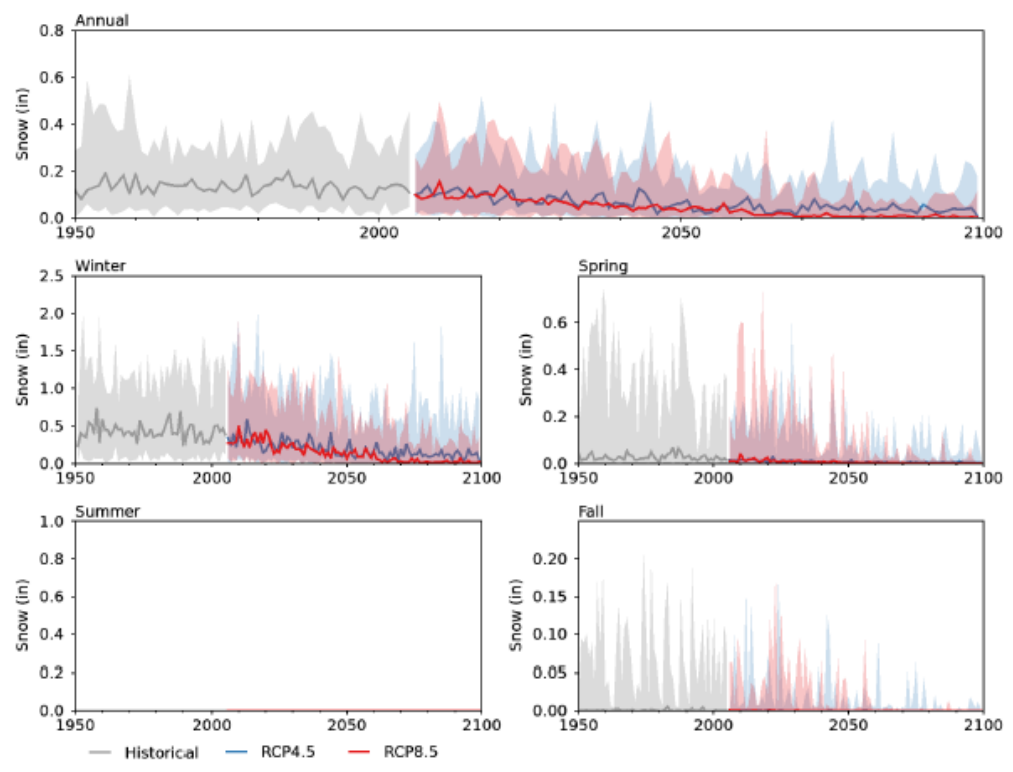


Figure 22: Annual and seasonal time series of snow water equivalent for historical (gray), RCP4.5 (blue) and RCP8.5 (red). The historical period ends in 2005 and the future periods begin in 2006. The median of 20 CMIP5 models is indicated by the solid lines and the ensemble 10th to 90th percentile range is indicated by the respective shaded envelopes.

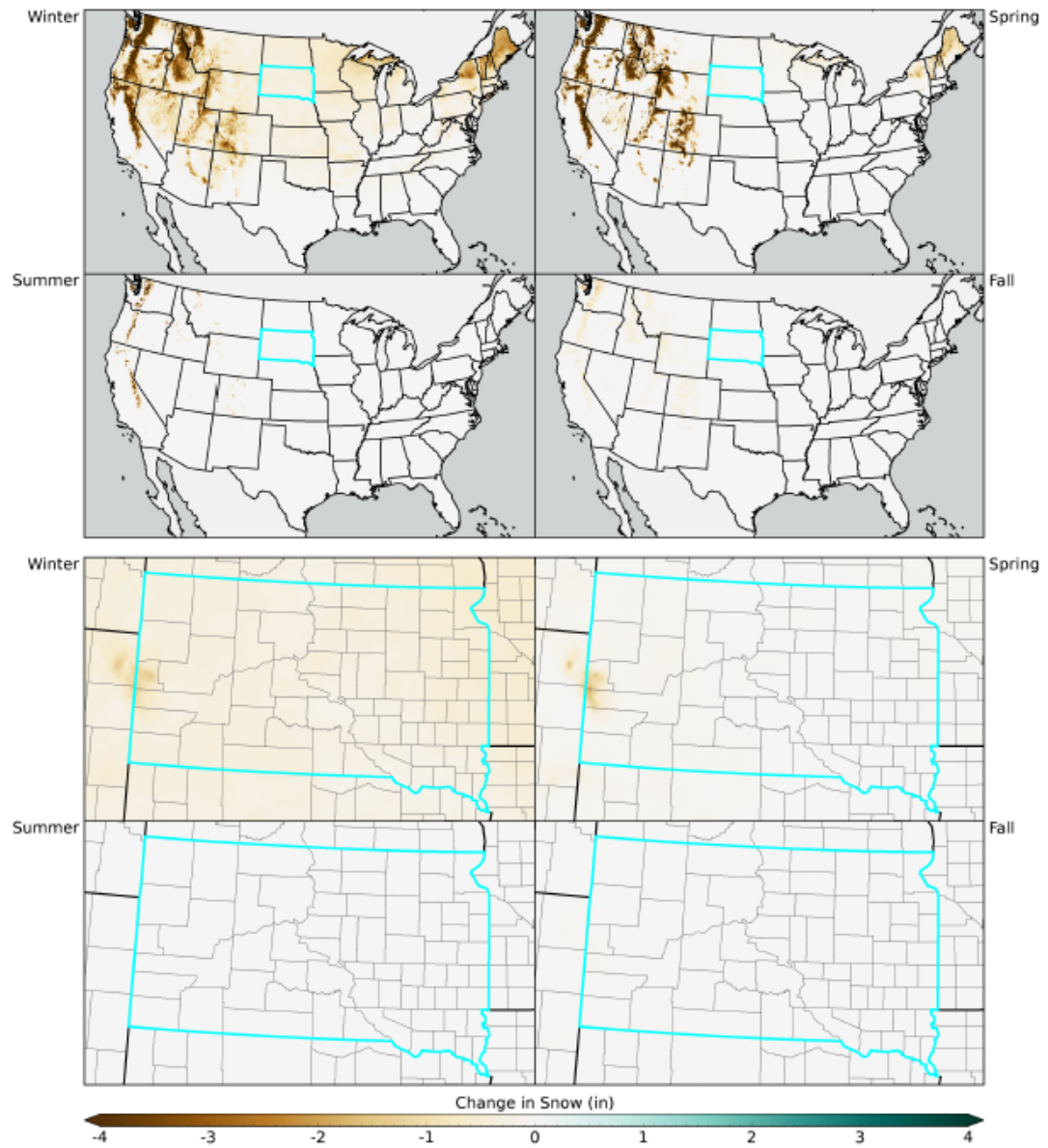


Figure 23: Seasonal maps of snow water equivalent for RCP4.5 2050-2074 minus 1981-2010 for the ensemble mean model.

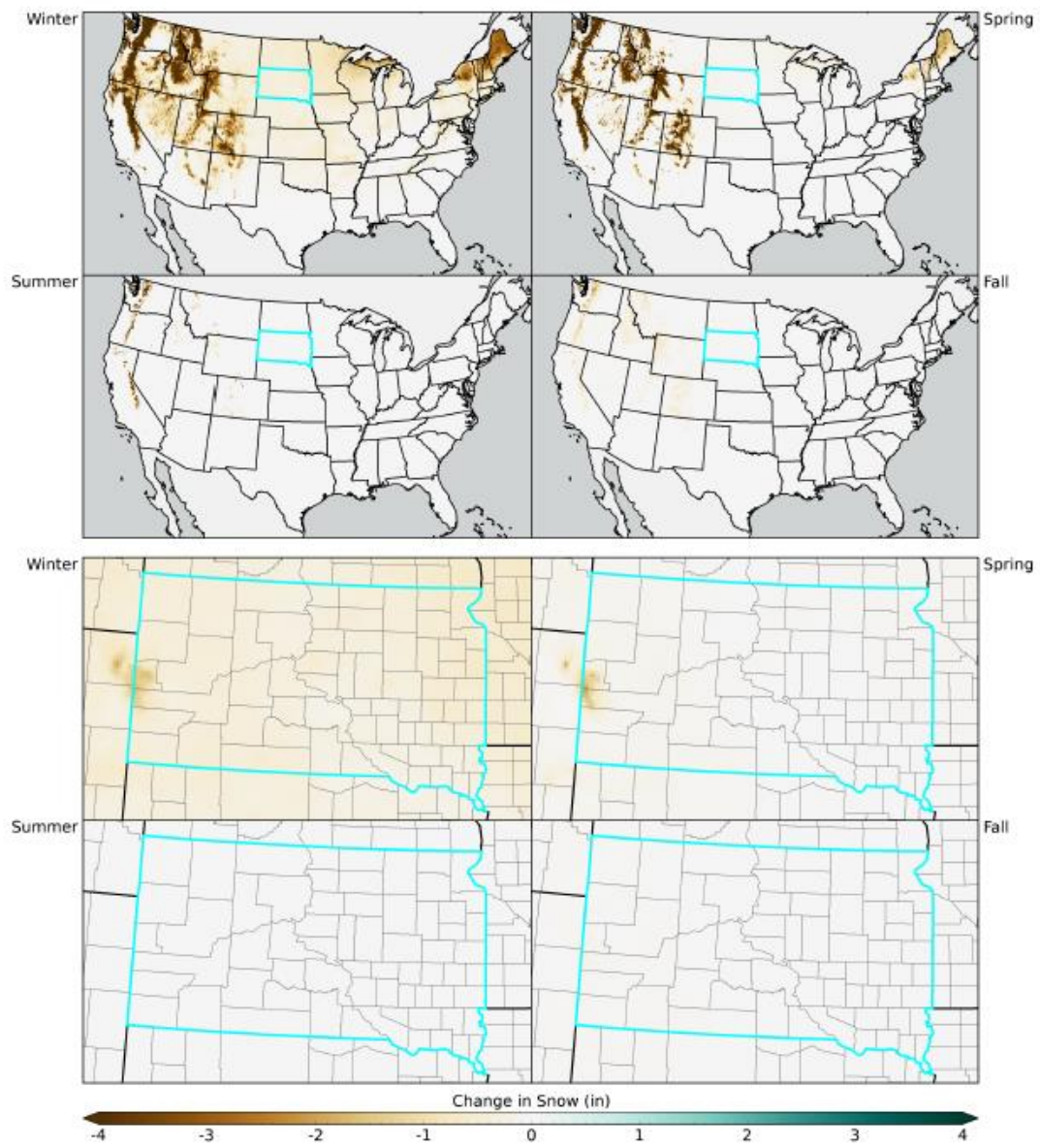


Figure 24: Seasonal maps of snow water equivalent for RCP8.5 2050-2074 minus 1981-2010 for the ensemble mean model.



7 Runoff

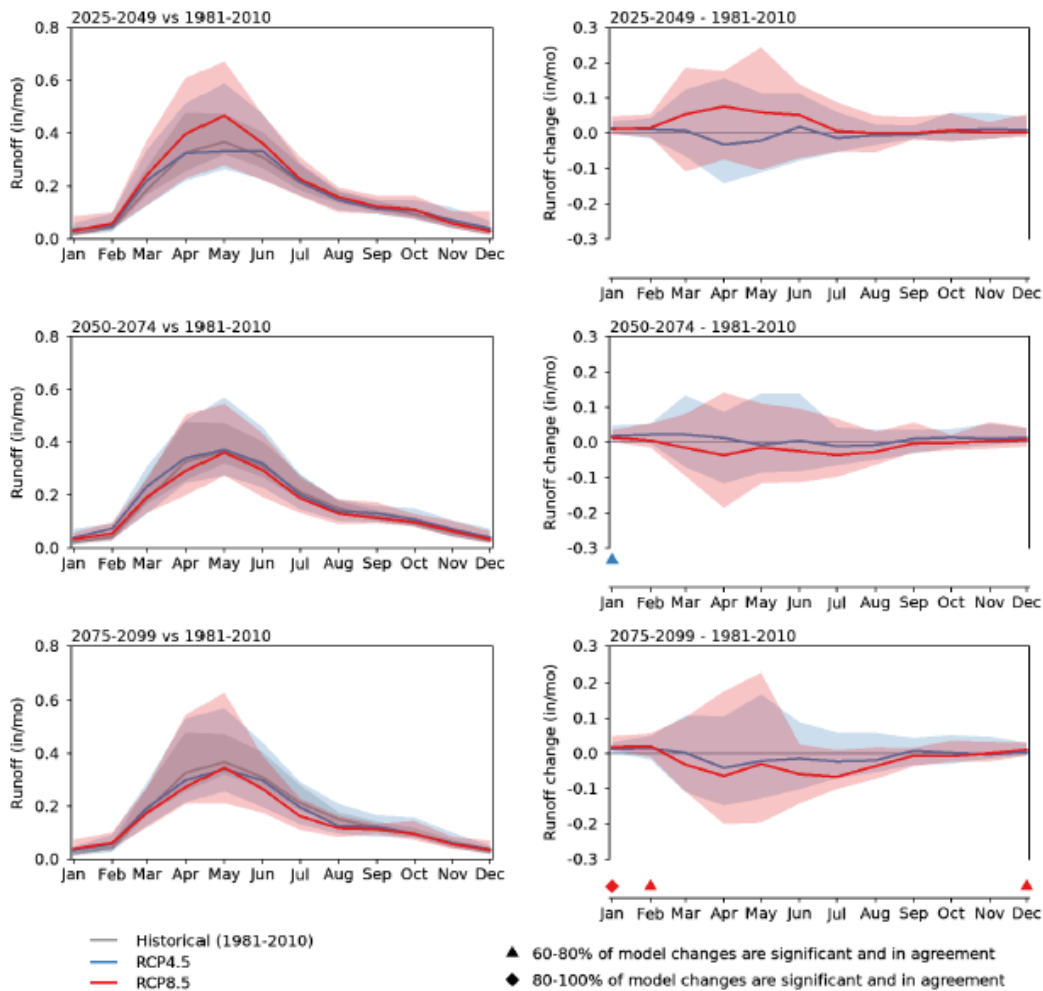


Figure 25: Monthly averages of runoff for the three future time periods for the RCP4.5 and RCP8.5 simulations. The median of 20 CMIP5 models is indicated by the solid lines and the ensemble 10th to 90th percentile range is indicated by the respective shaded envelopes. Raw values relative to the historical simulation (1981-2010) are shown in the left column and future minus historical changes are shown in the right column. Triangle and diamond symbols indicate the percent of models that simulate future minus present changes that are of the same sign and significant. A Mann-Whitney rank test is used to establish significance ( $p < 0.05$ ).

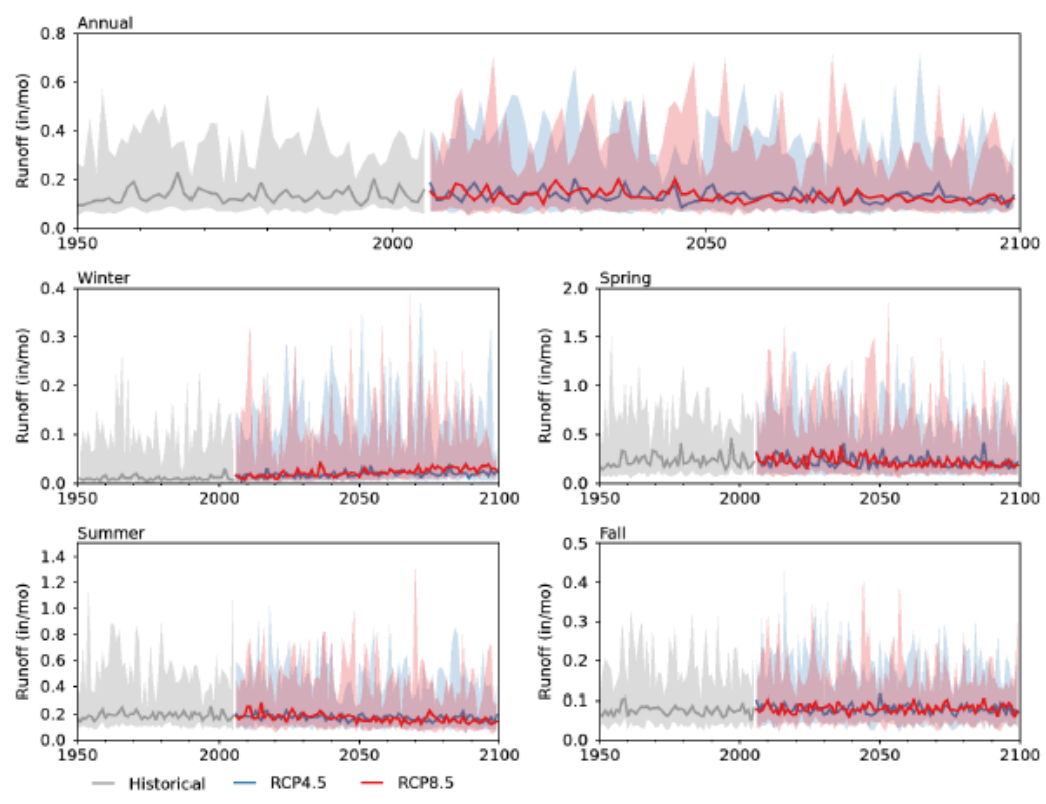


Figure 26: Annual and seasonal time series of runoff for historical (gray), RCP4.5 (blue) and RCP8.5 (red). The historical period ends in 2005 and the future periods begin in 2006. The median of 20 CMIP5 models is indicated by the solid lines and the ensemble 10th to 90th percentile range is indicated by the respective shaded envelopes.

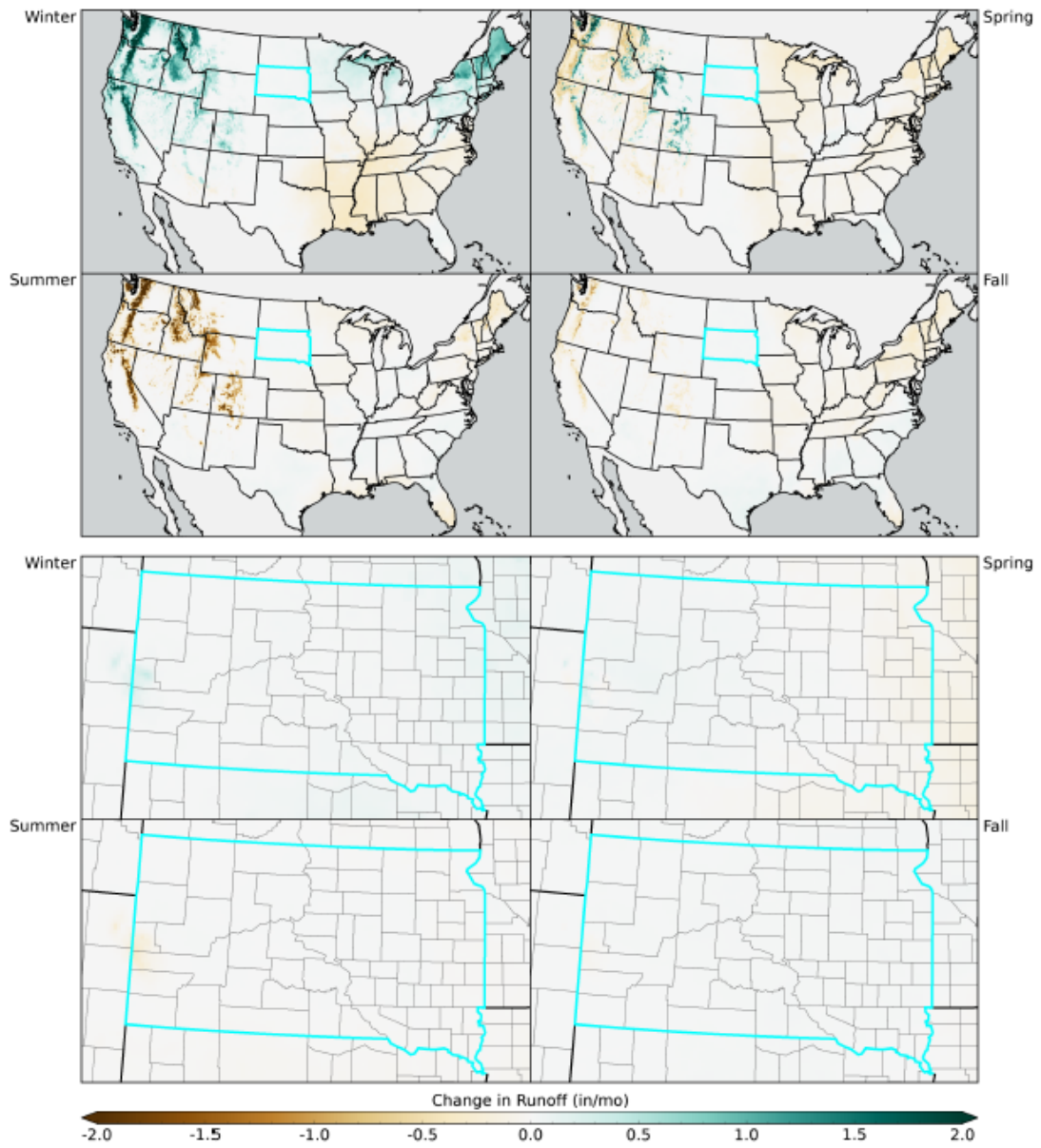


Figure 27: Seasonal maps of runoff for RCP4.5 2050-2074 minus 1981-2010 for the ensemble mean model.



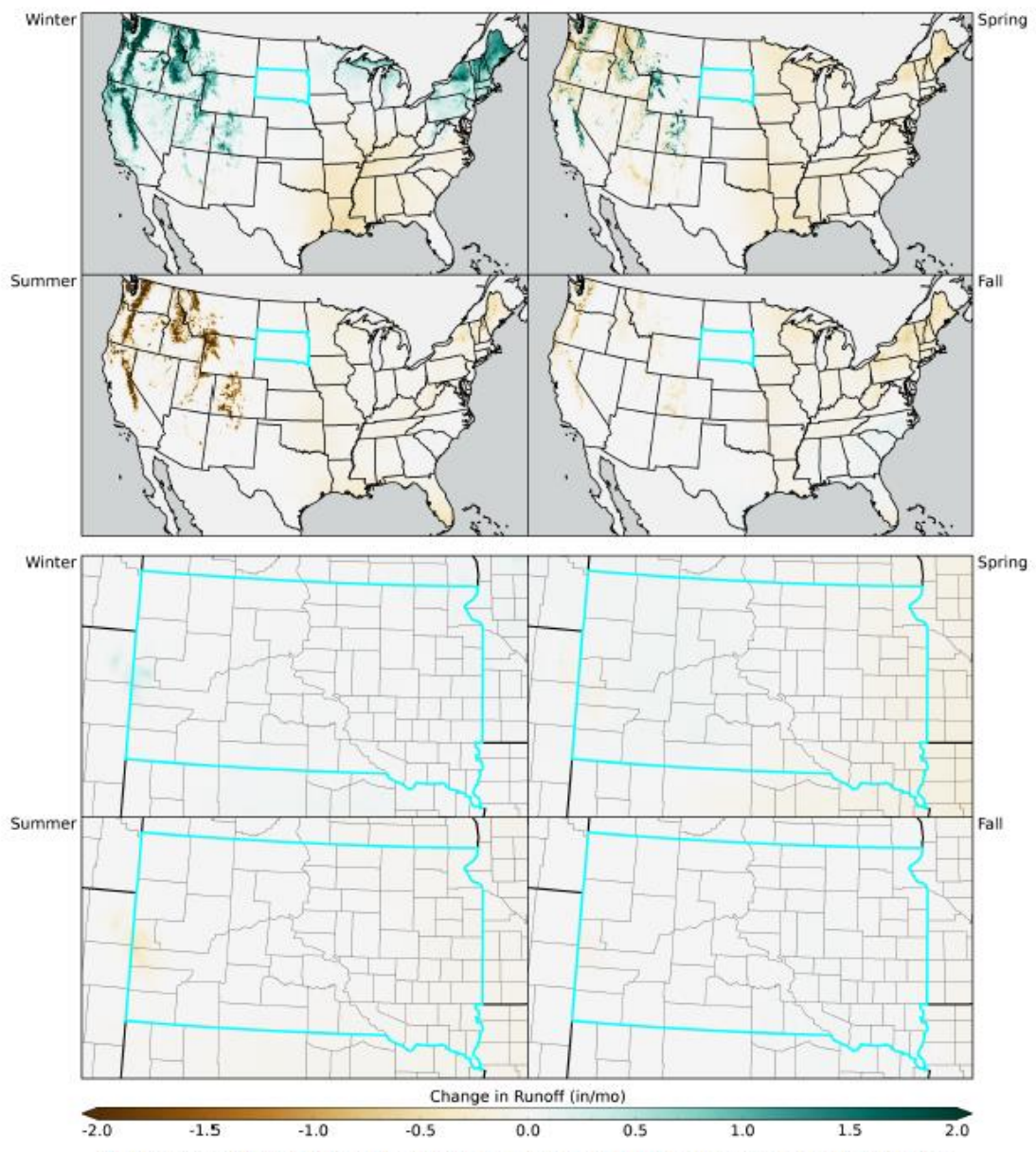


Figure 28: Seasonal maps of runoff for RCP8.5 2050-2074 minus 1981-2010 for the ensemble mean model.

### 8 Soil Water Storage

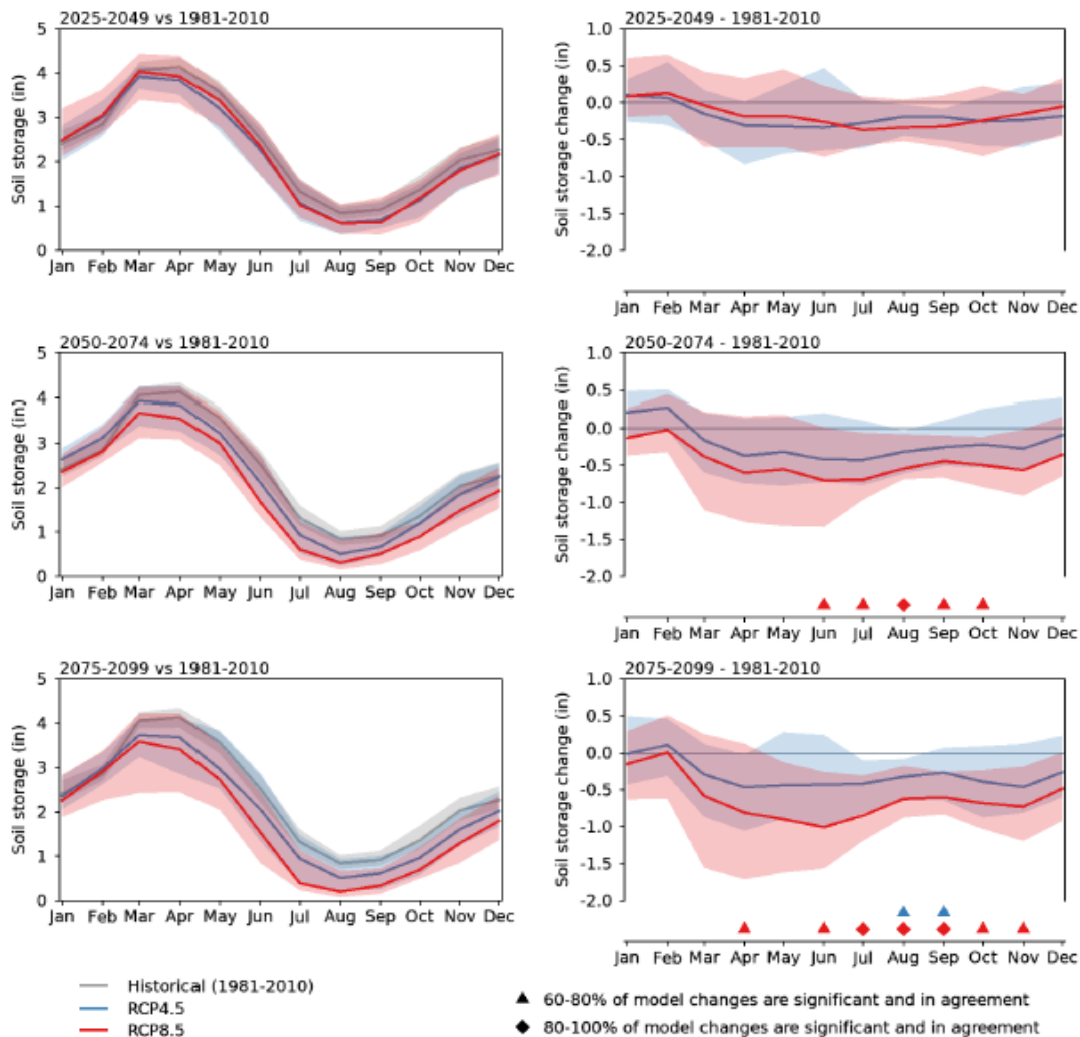


Figure 29: Monthly averages of soil water storage for the three future time periods for the RCP4.5 and RCP8.5 simulations. The median of 20 CMIP5 models is indicated by the solid lines and the ensemble 10th to 90th percentile range is indicated by the respective shaded envelopes. Raw values relative to the historical simulation (1981-2010) are shown in the left column and future minus historical changes are shown in the right column. Triangle and diamond symbols indicate the percent of models that simulate future minus present changes that are of the same sign and significant. A Mann-Whitney rank test is used to establish significance ( $p < 0.05$ ).

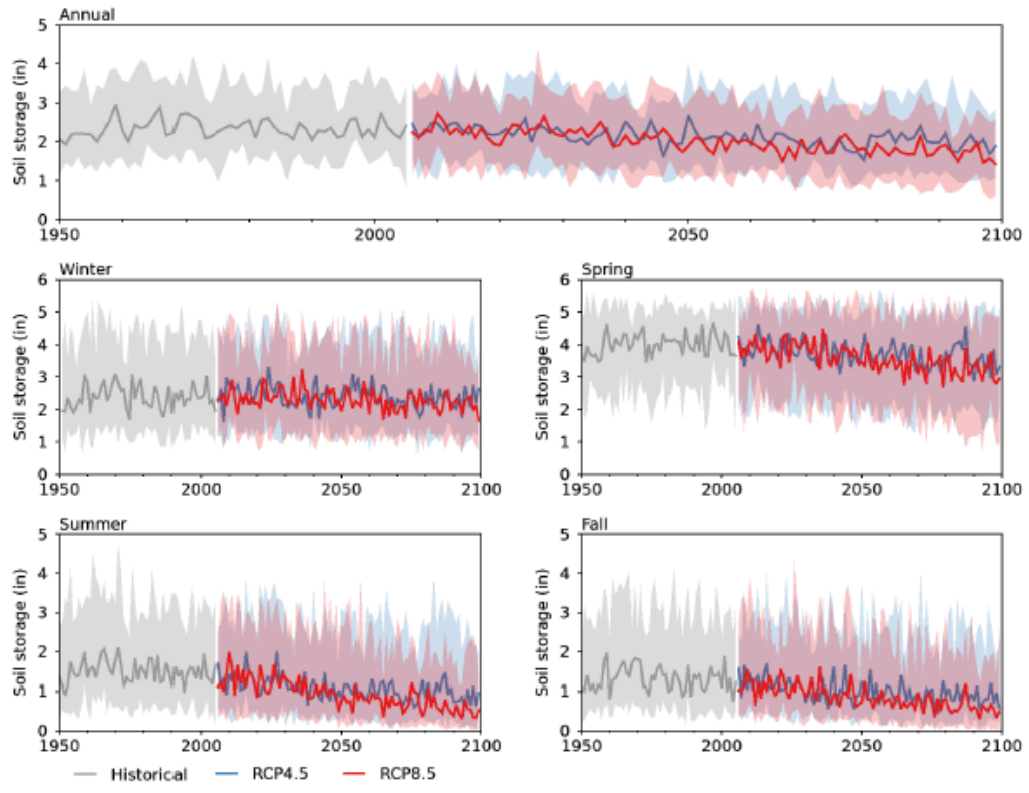


Figure 30: Annual and seasonal time series of soil water storage for historical (gray), RCP4.5 (blue) and RCP8.5 (red). The historical period ends in 2005 and the future periods begin in 2006. The median of 20 CMIP5 models is indicated by the solid lines and the ensemble 10th to 90th percentile range is indicated by the respective shaded envelopes.

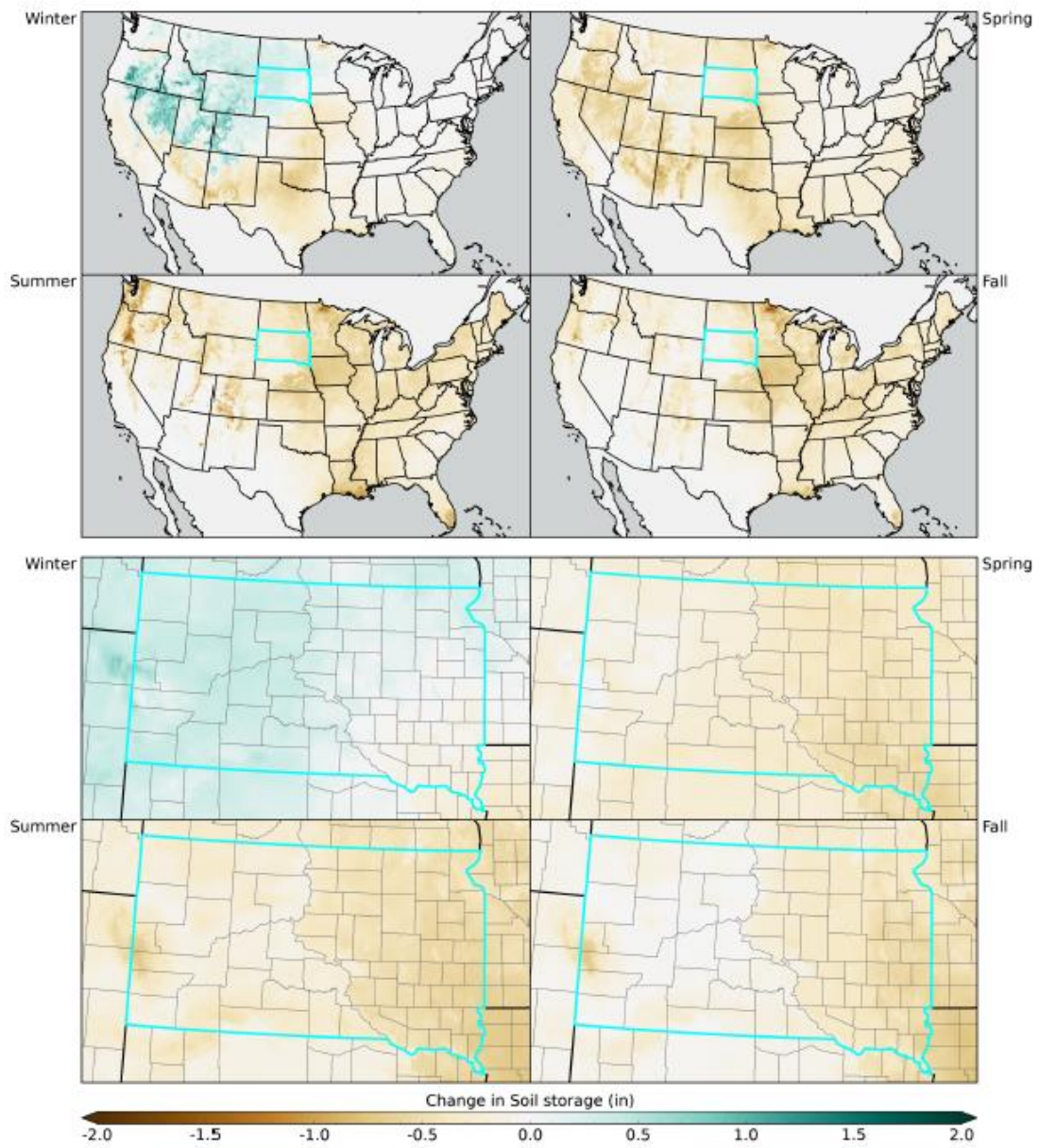


Figure 31: Seasonal maps of soil water storage for RCP4.5 2050-2074 minus 1981-2010 for the ensemble mean model.



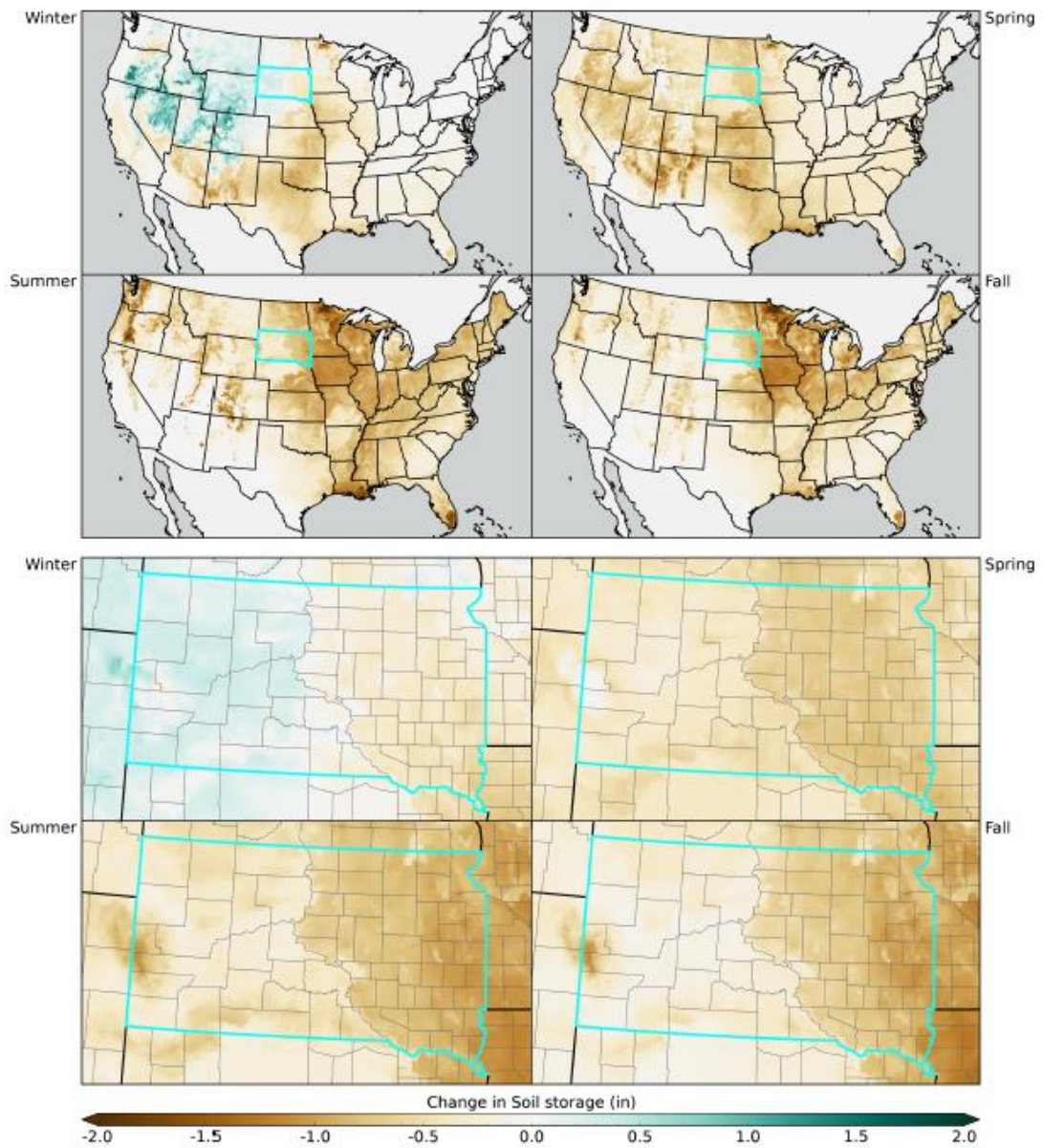


Figure 32: Seasonal maps of soil water storage for RCP8.5 2050-2074 minus 1981-2010 for the ensemble mean model.

### 9 Evaporative Deficit

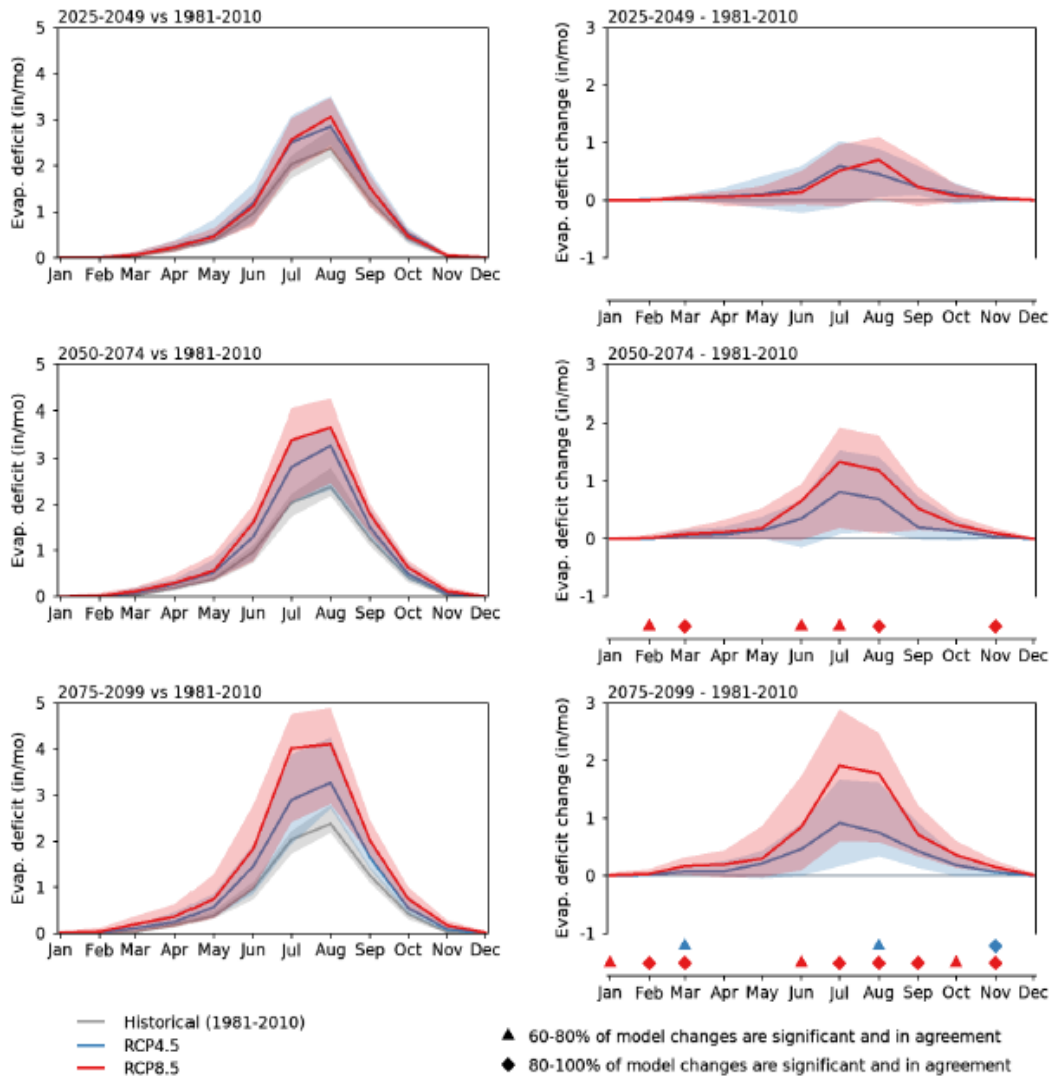


Figure 33: Monthly averages of evaporative deficit for the three future time periods for the RCP4.5 and RCP8.5 simulations. The median of 20 CMIP5 models is indicated by the solid lines and the ensemble 10th to 90th percentile range is indicated by the respective shaded envelopes. Raw values relative to the historical simulation (1981-2010) are shown in the left column and future minus historical changes are shown in the right column. Triangle and diamond symbols indicate the percent of models that simulate future minus present changes that are of the same sign and significant. A Mann-Whitney rank test is used to establish significance ( $\rho < 0.05$ ).

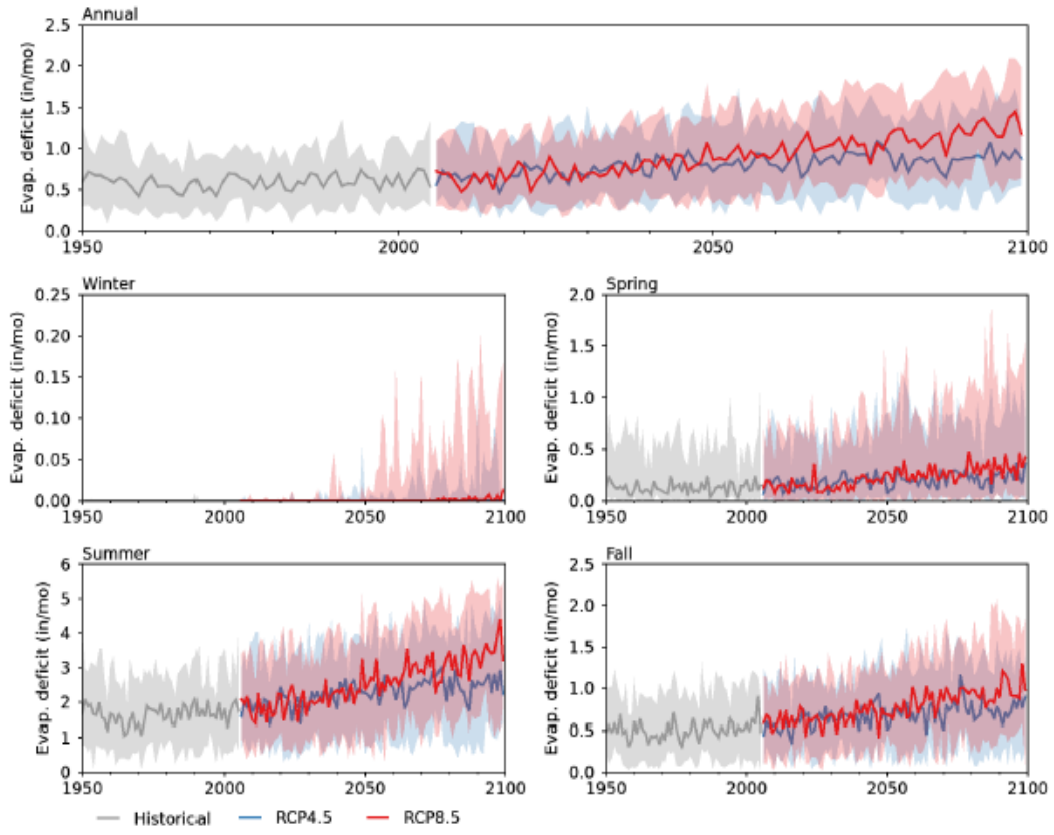


Figure 34: Annual and seasonal time series of evaporative deficit for historical (gray), RCP4.5 (blue) and RCP8.5 (red). The historical period ends in 2005 and the future periods begin in 2006. The median of 20 CMIP5 models is indicated by the solid lines and the ensemble 10th to 90th percentile range is indicated by the respective shaded envelopes.

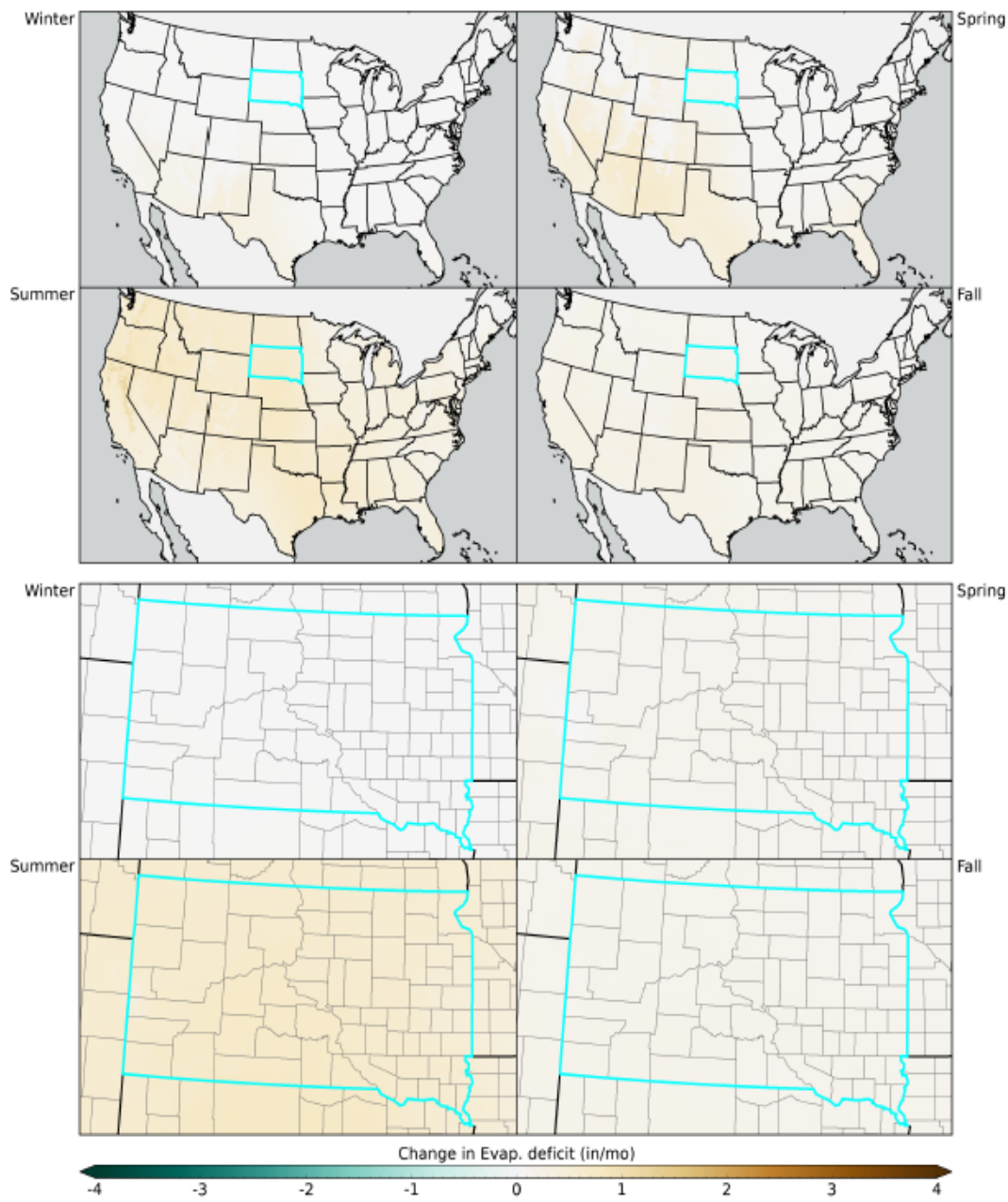


Figure 35: Seasonal maps of evaporative deficit for RCP4.5 2050-2074 minus 1981-2010 for the ensemble mean model.



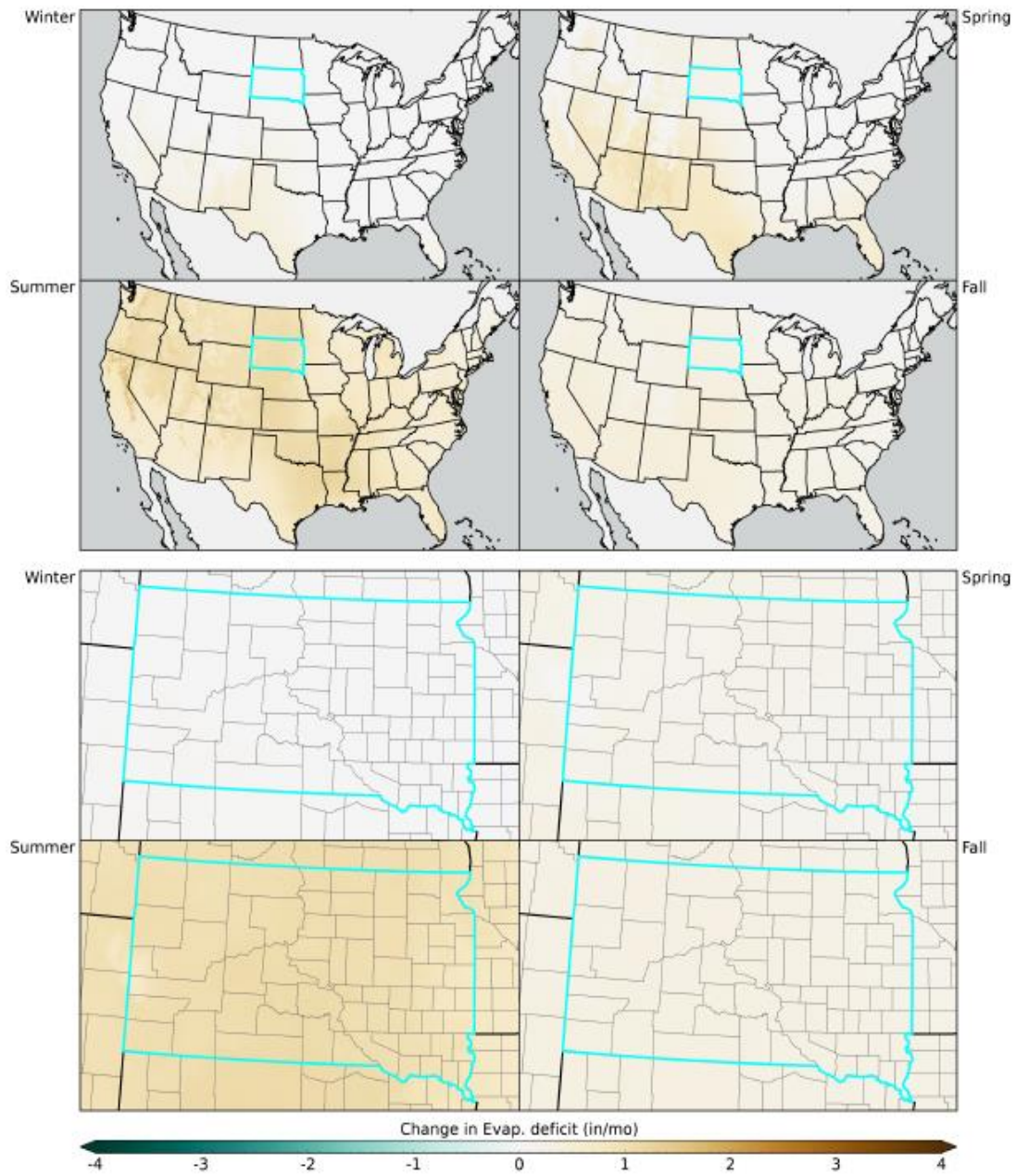


Figure 36: Seasonal maps of evaporative deficit for RCP8.5 2050-2074 minus 1981-2010 for the ensemble mean model.

SUMMARY OF SOUTH DAKOTA

---

## 10 Data

The temperature, precipitation, and vapor pressure deficit summaries are created by spatially averaging the MACAv2-METDATA data set (Abatzoglou and Brown, 2012). The water-balance variables snow water equivalent, runoff, soil water storage and evaporative deficit are simulated by using the MACAv2-METDATA temperature and precipitation as input to a simple model (McCabe and Wolock, 2007). The water-balance model accounts for the partitioning of water through the various components of the hydrologic system, but does not account for groundwater, diversions or regulation by impoundments.

## 11 Models

MeanModel	bcc-csm1-1-m	bcc-csm1-1	BNU-ESM	CanESM2
CCSM4	CNRM-CM5	CSIRO-Mk3-6-0	GFDL-ESM2G	GFDL-ESM2M
HadGEM2-CC365	HadGEM2-ES365	inmcm4	IPSL-CM5A-LR	IPSL-CM5A-MR
IPSL-CM5B-LR	MIROC5	MIROC-ESM	MIROC-ESM-CHEM	MRI-CGCM3

## 12 Citation Information

Abatzoglou, J.T., 2011. Development of gridded surface meteorological data for ecological applications and modelling. *International Journal of Climatology*, doi: 10.1002/joc.3413.

Abatzoglou, J.T., and Brown T.J., 2012. A comparison of statistical downscaling methods suited for wildfire applications. *International Journal of Climatology*, doi: 10.1002/joc.2312.

Alder, J. R. and S. W. Hostetler, 2013. USGS National Climate Change Viewer. US Geological Survey <https://doi.org/10.5066/F7W9575T>.

Hostetler, S.W. and Alder, J.R., 2016. Implementation and evaluation of a monthly water balance model over the U.S. on an 800 m grid. *Water Resources Research*, 52, doi:10.1002/2016WR018665.

## 13 Disclaimer

These freely available, derived data sets were produced by J. Alder and S. Hostetler, US Geological Survey (Alder, J. R. and S. W. Hostetler, 2013. USGS National Climate Change Viewer. US Geological Survey <https://doi.org/10.5066/F7W9575T>). Climate forcings in the MACAv2-METDATA were drawn from a statistical downscaling of global climate model (GCM) data from the Coupled Model Intercomparison Project 5 (CMIP5, Taylor et al. 2010) utilizing a modification of the Multivariate Adaptive Constructed Analogs (MACA, Abatzoglou and Brown, 2012) method with the METDATA (Abatzoglou, 2011) observational dataset as training data. No warranty expressed or implied is made by the USGS regarding the display or utility of the derived data on any other system, or for general or scientific purposes, nor shall the act of distribution constitute any such warranty. The USGS shall not be held liable for improper or incorrect use of the data described and/or contained herein.